

https://dspace.org/

Improving the separation efficiency of hematite from slimes through selective flocculation

Da Corte, Carla

2019

https://hdl.handle.net/10539/28068

da Corte, Carla Fatima De Abreu, (2019). Improving the separation efficiency of hematite from slimes through selective flocculation, University of the Witwatersrand, https://hdl.handle.net/10539/28068

Downloaded from a DSpace repository. https://dspace.org/

FACULTY OF ENGINEERING AND THE BUILT ENVIRONMENT
School of Chemical and Metallurgical Engineering



IMPROVING THE SEPARATION EFFICIENCY OF HEMATITE FROM SLIMES THROUGH SELECTIVE FLOCCULATION

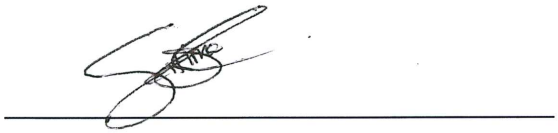
CARLA DA CORTE
0609335J

30 January 2019

A dissertation submitted to the faculty of Engineering and the Built Environment University of Witwatersrand, Johannesburg, in fulfilment of the requirements for the degree of Master of Science in Engineering

DECLARATION

I declare that the dissertation, **Improving the separation efficiency of hematite from slimes through selective flocculation**, is my own unaided work and that each source of information used has been acknowledged by means of a complete reference. This dissertation is being submitted for the Degree of Master of Science in Engineering at the University of the Witwatersrand, Johannesburg. It has not been submitted before for any degree or examination at any other university.



Carla Da Corte

30th day of January 2019 at Randburg, South Africa

ABSTRACT

The prevalence and treatment of low grade, finely disseminated iron ore has resulted in the production of primary and secondary slimes that constitute potential resources. Slimes processing is hindered by the particle size limits of current process equipment and this dissertation explores the potential of coupling selective flocculation with magnetic and gravity separation to improve separation efficiencies.

Base case tests (without selective flocculation) were conducted on the SLon-100 (laboratory scale pulsating Wet High Intensity Magnetic Separator) and the laboratory scale Reflux Classifier (RC). The base case tests were conducted to determine the optimal intensity for the SLon-100 and a semi-batch test was done on the RC to determine the effect of increasing water fluidisation rates on the response variables namely Fe concentrate grade, Fe concentrate recovery and separation efficiency. Thereafter selective flocculation conditions were optimised by coupling the process with magnetic separation in order to determine the effect of the operating variables on the response variables mentioned above. A Box-Behnken design was utilised and the ANOVA models developed for the significant response variables were used to optimise the selective flocculation process by simultaneously maximising the response variables whilst minimising the three factors (sodium oleate, paraffin dosage and conditioning time). The optimised selective flocculation conditions were then coupled with the RC in order to compare magnetic and gravity separation with and without selective flocculation.

The optimised selective flocculation conditions (1 kg/ton sodium silicate; pH 10; 500g/t sodium oleate; 1431.1g/t paraffin and 4.6 min conditioning time) coupled with magnetic separation showed improved metallurgical performance when compared to the base case test. Selective flocculation coupled with magnetic separation improved the magnetic product Fe grade from 52.28±0.38% to 59.21±0.42% Fe whilst simultaneously improving the separation efficiency from 40±1.46% to 56.8±2.0% and maintaining the Fe concentrate recovery within the 95% confidence limits (69.9% to 72.1%). These results were achieved under laboratory and ideal conditions and may differ from industrial scale results. Inconclusive results were achieved with selective flocculation coupled with the RC and additional testwork is recommended.

TECHNICAL SUMMARY

The prevalence and treatment of low grade, finely disseminated iron ore has resulted in the production of primary and secondary slimes that constitute potential resources. The beneficiation of slimes is difficult mainly due to particle size limitations of current equipment and the poor process efficiencies associated with treating slimes. The potential to improve the recovery of hematite from slimes by gravity and magnetic separation is available by increasing particle size through selective flocculation. Selective flocculation involves the aggregation of a desired mineral from a mixture of minerals by the bridging mechanism using either surfactants (collectors) or polymers and comprises of four stages namely dispersion of particles, selective adsorption of flocculent on the desired mineral surface with the subsequent formation of flocs, growth of flocs through conditioning at low shear and finally solid-solid separation.

In addressing the objective of the study, to determine if selective flocculation improves the metallurgical performance of magnetic and gravity separators in the treatment of hematite slimes, various technical aspects needed to be investigated. Due to the complexity of the process, some aspects were linked.

The first step of the process is to select a sample of suitable characteristics namely low Fe head grade, simple mineralogy and fine particle size distribution. Iron ore from Angola grading at 37.34±0.47%Fe was crushed and milled to a grind of 80% passing 35µm to generate artificial slimes for this study. The simple mineralogy of the ore with the principal mineral hematite well liberated from the dominant gangue quartz makes this sample well suited to this study.

The second step of the process is to ensure that the sample is well dispersed before flocculation to prevent heteroflocculation. Rheology testwork was conducted on the sample without selective flocculation at various sodium silicate (dispersant) dosages and pulp densities. At a pulp density of 45% solids, which is shown in literature to reduce the flocculation residence times and thus costs, a sodium silicate dosage of 1kg/ton achieved lower viscosities and a calculated yield stress of 0.558Pa. The low yield stress indicates that a force of small magnitude is required to overcome the attractive forces between the solids thereby allowing for adequate dispersion. During the first stage of the flocculation process, namely the dispersion stage, conducted in

a 1L flotation cell and stirring speed of 1200 rpm would provide sufficient force to overcome the attractive forces to ensure dispersion occurs.

The third step of the process was to determine the pH that achieved the best floc size since literature had indicated a correlation between these two parameters. The bigger the floc, the larger the magnetic and gravity separation forces become against the competing and dominant force for slimes namely the hydrodynamic drag force. The pH was varied from 9 to 11 at increments of 0.5 while the selective flocculation conditions remained fixed. The flocculated material at each pH was subjected to the Malvern Mastersizer to determine the particle size distribution. The laser diffraction results from the Malvern Mastersizer indicated increasing floc size with increasing pH with the Dv (0.5) of the feed (15.9µm) doubling at a pH of 11. However to determine the effect of pH on the response variables (separation efficiency, concentrate Fe grade and recovery) a solid-solid separator would be required after the flocculation process. Due to the small mass requirements per test, magnetic separation (SLon-100) was selected as the solid-solid separator. It was important to first optimise the magnetic separation conditions on the sample without selective flocculation (the base case). For the base case test the magnetic field intensity was varied from 3 000 Gauss to 6000 Gauss with results on the sample, without selective flocculation, showing that increasing the magnetic field intensity improved both the separation efficiency and Fe recovery (maximum 40±1.46% and 72.1±3.15% respectively) whilst maintaining the Fe grade at 52-54%. At the best intensity the effect of pH on the response variables could be determined. The selectively flocculated material at each of the five pHs was subjected to magnetic separation at a magnetic field intensity of 6 000 Gauss. Despite increased floc sizes with increasing pH, magnetic separation coupled with selective flocculation showed that a similar separation efficiency, concentrate Fe grade and recoveries was achieved across the pH range of 10-11 with the least deviation occurring at a pH of 10. The latter pH was selected for the next aspect namely optimisation of the selective flocculation conditions.

Optimisation of the selective flocculation conditions was the fourth step in the process. To determine the influence of the selective flocculation conditions on the response variables the process was coupled with magnetic separation. At the optimal sodium silicate dispersant dosage and pH a Box-Behnken design matrix with seventeen runs

in triplicate was employed to study the effect of three factors (sodium oleate dosage, paraffin dosage and conditioning time each at three levels) on the response variables separation efficiency, concentrate Fe grade and recovery. The ANOVA models developed for the significant response variables (separation efficiency and concentrate Fe grade) were used to optimise the three factors by simultaneously maximising the response variables whilst minimising the three factors. At a background magnetic field intensity of 6000 Gauss, optimised selective flocculation improved the magnetic product Fe grade from 52.28±0.38% to 59.21±0.42% Fe whilst simultaneously improving the separation efficiency from 40±1.46% to 56.8±2.0% and maintaining the Fe concentrate recovery within the 95% confidence limits (69.9% to 72.1%). These results were achieved at the optimised factors of 500g/t sodium oleate; 1431.1g/t paraffin and 4.6 min conditioning time. Assuming a demand for the two magnetic products a simple reagent operating cost study indicated the optimised Floc Magnetic Separation (FMS) process would generate 39% more revenue after reagent costs were deducted when compared to magnetic separation as is. Preconcentration before the FMS process may reduce reagent costs further, and although the FMS process shows potential, a pilot scale run and thorough techno-economic study are recommended to account for all the costs involved in this process.

At a similar recovery to the FMS process the base case semi-batch Reflux Classifier (RC) test, without selective flocculation, achieved the best Fe grade of 46.85±1.71% at a dismal separation efficiency of 25.3±1.6%. Potential reasons for the poor performance on the RC could be attributed to the long residence times for the test and pH of the fluidisation water affecting the floc's characteristics and its selectivity. In addition, the optimised floc conditions for the SLon may not be the best floc conditions for the RC. The low solids concentration in the semi-batch RC tests facilitate a size separation as opposed to density separation and it is expected that a continuous run would improve the results through the activation of the autogenous media separation zone as demonstrated in literature. It is recommended that should sufficient feed be available a continuous run with and without flocculation be conducted with a smaller gap spacing of 3mm to validate these findings before the RC is conclusively ruled out.

ACKNOWLEDGEMENTS

I am greatly indebted to Mintek for funding my research project and for providing the necessary facilities and resources to successfully complete my research project.

I would like to express my heartfelt appreciation to my two supervisors, Professor Lorenzo Woollacott and Carl Bergmann, for their guidance and useful critiques during the planning, development and execution of this project. Their willingness to share their knowledge as well as encouraging, stimulating and developing my thinking and writing abilities have made me a better engineer.

This research project consisted of various aspects that could not be achieved without the assistance of Mintek's various divisions namely, Mineralogy and Analytical Services Division for feed characterisation and chemical analysis; Plastic Workshop for constructing the Polyvinyl chloride Reflux Classifier; as well as the chief investigators, operators, technicians and students at the Minerals Processing Division. A special thanks goes to Sipho Mabuza for assisting with the testwork and sample preparation during the project, your attention to detail and accuracy have made this complex research project a success.

I wish to thank my parents for their support and encouragement throughout my educational career. My love and appreciation also go to Thabiso Christopher, thank you for your continued support, encouragement and inspiration especially towards the end when writing became cumbersome and you re-energised me.

LIST OF PRESENTATIONS AND PUBLICATIONS

Da Corte, C., 2016, *Recovery of hematite from slimes through selective flocculation.* Presentation for the SAMMRI (South African Minerals to Metals Research Institute) workshop 31 October-01 November 2016. Cape Town, South Africa

A paper has been submitted to SAIMM and is currently awaiting to be assigned.

TABLE OF CONTENTS

DECLARATION I
ABSTRACT II
TECHNICAL SUMMARY III
ACKNOWLEDGEMENTS VI
LIST OF PRESENTATIONS AND PUBLICATIONS VII
TABLE OF CONTENTS VIII
LIST OF FIGURES XIII
LIST OF TABLES XIX
LIST OF ACRONYMNS AND ABBREVIATIONS XXV
GLOSSARY XXVI
CHAPTER 1 : INTRODUCTION 1
1.1 Background Information 1
1.2 Problem Statement 4
1.3 Limits of Present Concentration Processes and Equipment 6
1.4 Previous Work Conducted on Selective Flocculation 8
1.5 Thesis Statement and Research Objectives 10
1.6 Significance 11
CHAPTER 2 : LITERATURE REVIEW 12
2.1 The Problematic Nature of Slimes 12
2.2 The principle of Magnetic Separation 16
2.3 The principle of Classification 20
2.3.1 The principle of Classification 20
2.3.2 Hindered Settling 21
2.4 Increasing Particle Size through Hydrophobic Flocculation 22
2.4.1 Oil-based methods 23
2.4.2 Hydrophobic association 24
2.4.2.1 Shear Flocculation 26
2.4.2.2 Carrier Flotation 27
2.4.2.3 Selective Magnetic Aggregation with or without the aid of hydrophobicity 28
2.4.3 Challenges with Hydrophobic association 29
2.5 Selective flocculation 29
2.5.1 Selective flocculation using Microorganisms 33
2.5.2 Selective flocculation using polymers 34
2.5.2.1 Starch 35
2.5.2.2 Adsorption of Polymers and the process of Flocculation 37
2.5.2.3 Factors affecting Selective Polymer Flocculation 41
2.5.2.3.1 Dispersion 42
2.5.2.3.2 pH and Electrolyte Concentration 42

2.5.2.3.3 Type of flocculent 44
2.5.2.3.4 Effect of Reagent Sequence Addition 47
2.5.2.3.5 Particle Size Effects 48
2.5.2.3.6 Effect of Solids Concentration 49
2.5.2.3.7 Effect of Water Quality 50
2.5.2.4 Disadvantages of Polymer Flocculation 52
2.5.3 Selective flocculation using sodium oleate 53
2.5.3.1 Factors affecting Selective Flocculation with Sodium Oleate as the flocculent 56
2.5.3.1.1 Effect of Stirring Speed and Time 56
2.5.3.1.2 Effect of pH 57
2.5.3.1.3 Effect of % Solids 59
2.5.3.1.4 Effect of Dosage 59
2.6 Application of Selective Flocculation to Magnetic Separation 62
2.7 Conclusion 65
CHAPTER 3 : RESEARCH DESIGN, SAMPLE SELECTIION AND FEED CHARACTERISATION 67
3.1 Introduction 67
3.2 Research Design 70
3.2.1 Response Variables 74
3.2.2 Limitations of the Study 75
3.3 Sample Preparation 77
3.3.1 Methodology 77
3.3.1.1 Crushing 77
3.3.1.2 Milling 78
3.3.2 Results and Discussions 80
3.4 Feed Characterisation 81
3.4.1 Methodology 81
3.4.1.1 Chemical Analysis 81
3.4.1.2 Mineralogy 83
3.4.1.2.1 Electron Microprobe Analysis (EMPA) 83
3.4.1.2.2 Particle Tracking Analysis (PTA) 84
3.4.1.3 Size-By-Assay 84
3.4.2 Results and Discussion 85
3.4.2.1 Chemical Analysis 85
3.4.2.2 Mineralogy 86
3.4.2.2.1 Electron Microprobe Analysis (EMPA) 86
3.4.2.2.2 Particle Tracking Analysis (PTA) 87
3.4.2.3 Size-By-Assay 92
3.4.2.3.1 SBA from Sieving 92
3.4.2.3.2 SBA from Particle Tracking Analysis 95

3.4.2.3.3 Comparative SBA results 97
3.5 Conclusion 99
CHAPTER 4 : BASELINE TESTS 101
4.1 Introduction 101
4.2 Base Case SLon-100 Intensity Variation Testwork 102
4.2.1 Methodology 102
4.2.1.1 Selection of Equipment 102
4.2.1.2 Working Principle of the SLon-100 Pulsating WHIMS 104
4.2.1.3 Selection of Operating Parameters 107
4.2.1.4 Tests 112
4.2.1.5 Precautions 112
4.2.1.6 Limitation of the SLon-100 Testwork 113
4.2.2 Results and Discussion 114
4.3 Selection of Dispersant Dosage at Various Pulp Densities 115
4.3.1 Methodology 115
4.3.1.1 Selection of Dispersant 115
4.3.1.2 Selection of Equipment 116
4.3.1.3 Working Principle of the Rheometer 117
4.3.1.4 Selection of Operating Parameters 118
4.3.1.5 Tests 124
4.3.1.6 Precautions 125
4.3.1.7 Limitation of the Physica Rheolab QC rheometer 125
4.3.2 Results and Discussion 126
4.4 pH Selection for optimum flocculation 131
4.4.1 Methodology 131
4.4.1.1 Tests 131
4.4.1.2 Reagent Preparation 135
4.4.1.3 Particle Size Distribution by Laser Diffraction 136
4.4.1.3.1 Selection of Equipment 137
4.4.1.3.2 Working Principle of the Malvern Mastersizer 137
4.4.1.3.3 Selection of Operating Parameters 140
4.4.1.3.4 Tests 141
4.4.1.3.5 Precautions 142
4.4.1.3.6 Limitations of the Malvern Mastersizer Testwork 142
4.4.1.4 Precautions for pH Selection 143
4.4.1.5 Assumptions/Limitation of this aspect 144
4.4.2 Results and Discussion 145
4.5 Conclusion 152
CHAPTER 5 : OPTIMISING SELECTIVE FLOCCULATION COUPLED WITH MAGNETIC SEPARATION 154

5.1 Introduction 154
5.2 Methodology 155
5.2.1 Selection of Experimental Design 155
5.2.2 Selection of Operating Parameters 160
5.2.3 Tests 160
5.2.4 Analysis of Results 162
5.2.4.1 Design Evaluation 162
5.2.4.2 Analysis of Variance 162
5.3 Results and Discussion 166
5.3.1 Outlier Determination 166
5.3.2 Design Evaluation 168
5.3.3 Evaluating the models 170
5.3.4 Analysis of Variance 176
5.3.5 Optimisation 187
5.4 Conclusion 193
CHAPTER 6 : OPTIMISED SELECTIVE FLOCCULATION COUPLED WITH THE REFLUX CLASSIFIER 195
6.1 Introduction 195
6.2 Methodology 195
6.2.1 Selection of Equipment 195
6.2.2 Working Principle of the Reflux Classifier 202
6.2.3 Design of Mintek's PVC Reflux Classifier 205
6.2.4 Selection of Operating Approach 214
6.2.5 Selection of Operating Parameters 216
6.2.6 Tests 218
6.2.7 Precautions 220
6.2.8 Limitations of the Reflux Classifier Testwork 221
6.3 Results and Discussion 221
6.4 Conclusion 227
CHAPTER 7 : COMPARISON OF SELECTIVE FLOCCULATION COUPLED WITH MAGNETIC SEPARATION AND THE RC 228
7.1 Introduction 228
7.2 Comparative Results 228
7.3 Conclusion 230
CHAPTER 8 : IMPLICATIONS OF THE FINDINGS FROM THE STUDY 232
8.1 Introduction 232
8.2 Price of Fine Iron Ore 232
8.3 Reagent Operating Costs 235
8.4 Conclusion 239
CHAPTER 9 : CONCLUSIONS 240
REFERENCES 246
APPENDIX A: RAW DATA FOR SAMPLE PREPARATION AND FEED CHARACTERISATION 262
APPENDIX B: RAW DATA FOR THE BASELINE TESTS 277

APPENDIX C: RAW DATA FOR OPTIMISING SELECTIVE FLOCCULATION COUPLED WITH MAGNETIC SEPARATION 311

APPENDIX D: RAW DATA FOR OPTIMISED SELECTIVE FLOCCULATION COUPLED WITH REFLUX CLASSIFIER 326

LIST OF FIGURES

Figure 1.1: Iron Ore's value chain from raw material to end customer (Allwood et al., 2011) 2

Figure 1.2: Iron ore production for the financial year 2016 (Creamer Media, 2017) ... 3

Figure 1.3: Typical Hematite Beneficiation Options 4

Figure 1.4: Effective range of application of conventional processing techniques (Wills, 2006) 7

Figure 1.5: The processing circuit for Tilden Mines (Keranen 1986 cited in Haselhuhn et al., 2012) 9

Figure 2.1: The relationship between magnetic force and liquid drag force in a Jones WHIMS for a hematite particle of various particle sizes (Roy, 2012) 19

Figure 2.2: Particles settling when conditions prevail for (a) free and (b) hindered settling (Wills, 2006) 22

Figure 2.3: Schematic representation of surface-based concentration methods (physiochemical methods): a = froth flotation; b, d-f = oil extraction and or spherical agglomeration; c = carrier separation; d = selective flocculation/hydrophobic association; d-e = aggregate flotation; c-h,c-j,c-j-i = ultra flotation; b-i, d-f-i=oil flotation (Fuerstenau et al., 1979 cited by Sivamohan, 1990) 26

Figure 2.4: The structure of hematite and starch interaction (Kar et al., 2013) 37

Figure 2.5: Flocculation Stages (Hoggs et al., 1993 as cited in Abro, 2009) 38

Figure 2.6: Possible polymer conformations subsequent to adsorption (Alagha et al., 2013 cited in Wang et al., 2014) 39

Figure 2.7: (a) High Molecular Weight (MW) polymer in the absence (a) and presence (b) of a site blocking low MW polymer (Brotherson and Deng (2008) cited in Gregory and Barany (2011)) 40

Figure 2.8: Inactive and active adsorbed polymers on a charged particle (Pelssers et al. 1990 cited in Gregory and Barany 2011). The dotted line indicates the diffuse part of the double layer. 49

Figure 2.9: Molecular structure of Sodium Oleate (Bulatovic, 2007) 54

Figure 2.10: Flocculation stages of hematite with sodium oleate as the flocculent (a) adsorption of oleate ions onto hematite surface (b) oleic acid droplets form on hematite surface and in the slurry (c) floc formation due to particle collisions (Pascoe and Doherty, 1997) 55

Figure 2.11: Zeta Potential of concentrated Hematite (68% Fe) from Qidashan Mine as a function of pH (Yin et al., 2011) 58

Figure 2.12: Hematite floc size as a function of insoluble oleic acid concentration (Pascoe and Doherty, 1997) 61

Figure 2.13: Solubility curve of oleic acid in relation to the minimum pH required for hematite flocculation (Pascoe and Doherty, 1997) 62

Figure 2.14: Schematic representation of the Floc Magnetic Separation (FMS) process applied to hematite (Song et al., 2002) 63
Figure 3.1: Schematic representation of the Floc Magnetic Separation (FMS) process applied to hematite (Song et al., 2002) 67
Figure 3.2: A graphical overview of the research design applied to this study using the Angolan Fe Ore Sample..... 71
Figure 3.3: Polysius Labwal HPGR 77
Figure 3.4: Milling Curve on the -1.18mm material targeting a grind of 80% -38 µm 80
Figure 3.5: Data reconciliation check for chemical analysis of testwork products 86
Figure 3.6: Proportion of the dominant minerals in the greater than 80% liberated class (liberation by area) 88
Figure 3.7: Proportion of the dominant minerals in the completely (100%) liberated class (liberation by area) 89
Figure 3.8: False Colour Images of the feed showing hematite and quartz attachments for various particle sizes (100 µm scale bar included for reference purposes).. 90
Figure 3.9: The cumulative mass per cent liberated by size for Hematite 91
Figure 3.10: Data reconciliation check for mineralogical and chemical analysis 92
Figure 3.11: Discrete Mass and Fe Grade Distribution of the Feed 94
Figure 3.12: Discrete Fe Deportment of the Feed 94
Figure 3.13: Cumulative Fe Grade of the Feed 94
Figure 3.14: Cumulative Mass and Fe Deportment of the Feed 94
Figure 3.15: PTA Discrete Mass and Grade Distribution of the Feed..... 96
Figure 3.16: PTA Discrete Grade Deportment of the Feed 96
Figure 3.17: PTA Cumulative Grade Distribution of the Feed 96
Figure 3.18: PTA Cumulative Mass and Deportment of the Feed 96
Figure 3.19: Comparative Discrete Mass and Fe Grade Distribution of the Feed via Sieving and PTA 98
Figure 3.20: Comparative Discrete Fe Deportment of the Feed via Sieving and PTA..... 98
Figure 3.21: Comparative Cumulative Fe Grade Distribution of the Feed via Sieving and PTA..... 98
Figure 3.22: Comparative Cumulative Mass and Fe Deportment of the Feed via Sieving and PTA 98
Figure 3.23: Section preparation and the reduction in particle size during measurement on the MLA..... 99
Figure 4.1: Schematic representation of the Floc Magnetic Separation (FMS) process applied to hematite (Song et al., 2002) 101
Figure 4.2: SLon-100 Pulsating WHIMS..... 103
Figure 4.3: Eriez Laboratory scale L4 WHIMS (Eriez, 2016)..... 104

Figure 4.4: Cross-sectional view of the SLon-100 (Adapted from Outotec, 2012).. 105
Figure 4.5: Pulsating Mechanism for the SLon-100 (Adapted from Outotec, 2012) 106
Figure 4.6: Rod Matrices with rod diameter indicated. The outer plates and handle of the matrices are a 300 series stainless (not magnetic) while rods are 400 series stainless (magnetic) 108
Figure 4.7: Yoke Holes in Feed Chamber and below Matrix 113
Figure 4.8: The Average Mass Pull, Fe Grade, Fe Recovery and Separation Efficiency in the Magnetic Product at three Background Magnetic Field Intensities (2 Standard deviations are depicted by the error bars) 114
Figure 4.9: Physica Rheolab QC Rheometer 117
Figure 4.10: Schematic diagram of the basic tool geometries for the rotational rheometer (Hackley & Ferraris, 2001) 119
Figure 4.11: Double Gap tool for the Physica Rheolab QC Rheometer 120
Figure 4.12: Identification of flow curves based on their characteristic shapes (Hackley & Ferraris, 2001) 121
Figure 4.13: Shear Stress vs Shear Rate at 0g/t Sodium Silicate for various pulp densities 127
Figure 4.14: Shear Stress vs Shear Rate at 500g/t Sodium Silicate for various pulp densities 127
Figure 4.15: Shear Stress vs Shear Rate at 1000g/t Sodium Silicate for various pulp densities 127
Figure 4.16: Shear Stress vs Shear Rate at 1500g/t Sodium Silicate for various pulp densities 127
Figure 4.17: Apparent Viscosity vs Shear Rate at 0g/t Sodium Silicate for various pulp densities 128
Figure 4.18: Apparent Viscosity vs Shear Rate at 500g/t Sodium Silicate for various pulp densities 128
Figure 4.19: Apparent Viscosity vs Shear Rate at 1000g/t Sodium Silicate for various pulp densities 128
Figure 4.20: Apparent Viscosity vs Shear Rate at 1500g/t Sodium Silicate for various pulp densities 128
Figure 4.21: Apparent Viscosity vs Shear Rate at various Sodium Silicate Dosages for a fixed pulp density of 45% solids 131
Figure 4.22: Flocculation step for pH screening tests showing (A) the Denver Float Cell with pulp at 45% solids and (B) reagents used during flocculation 133
Figure 4.23: Knick pH meter used during the flocculation 133
Figure 4.24: Flocculated pulp at each pH subsequent to the flocculation step and prior to magnetic separation 134
Figure 4.25: Schematic diagram of the Malvern Mastersizer 2000E with the Hydro-2000 MU as the sample dispersion unit, figure adapted from Malvern Instruments Ltd. (2007 and 2007a) 139

Figure 4.26: Cumulative Volume % Passing without ultrasonic displacement at a pump/stirring speed of 600 rpm..... 146
Figure 4.27: Cumulative Volume % passing with and without ultrasonic displacement at a pump/stirring speed of 600 rpm..... 146
Figure 4.28: Cumulative Volume % Passing without ultrasonic displacement at a pH of 9.5 and pump/stirring speed of 600rpm..... 148
Figure 4.29: Cumulative Volume % Passing without ultrasonic displacement at a pH of 10 and pump/stirring speed of 600rpm..... 148
Figure 4.30: Cumulative Volume % Passing without ultrasonic displacement at a pH of 10.5 and pump/stirring speed of 600rpm..... 148
Figure 4.31: Cumulative Volume % Passing without ultrasonic displacement at a pH of 11 and pump/stirring speed of 600rpm..... 148
Figure 4.32: The average Cumulative Volume % Passing without ultrasonic displacement at a pH of 9.5 -11 and pump/stirring speed of 600rpm..... 149
Figure 4.33: The Average Mass Pull, Fe Grade, Fe Recovery and Separation Efficiency in the Magnetic Product at three Background Magnetic Field Intensities (2 Standard deviations are depicted by the error bars) 151
Figure 4.34: Fe Recovery-Grade Curve at the various pH conditions tested (2 Standard deviations are depicted by the error bars) 152
Figure 5.1: Schematic representation of the Floc Magnetic Separation (FMS) process applied to hematite (Song et al., 2002) 154
Figure 5.2: A Box-Behnken design for three factors (NIST, 2012) 160
Figure 5.3: The standard error for the design for the AB interaction with the split factor C at a coded value of -1 168
Figure 5.4: The standard error for the design for the AC interaction with the split factor B at a coded value of -1 169
Figure 5.5: The standard error for the design for the AC interaction with the split factor B at a coded value of -1 169
Figure 5.6: Fraction of Design Space (FDS) as a function of the standard error mean..... 170
Figure 5.7: The relationship between the actual and predicted separation efficiency for the 2Fl and Quadratic Models..... 172
Figure 5.8: The relationship between the actual and predicted concentrate Fe grade for the linear and 2Fl Quadratic Models 172
Figure 5.9: The actual and predicted separation efficiency using the Quadratic Model at 95% Confidence limits..... 173
Figure 5.10: The actual and predicted concentrate Fe Grade using the 2Fl Model at 95% Confidence limits..... 174
Figure 5.11: Normal plot of residuals for the response variable: Separation Efficiency..... 175

Figure 5.12: Externally studentized residuals for the response variable: Separation Efficiency 175
Figure 5.13: Normal plot of residuals for the response variable: concentrate Fe Grade 175
Figure 5.14: Externally studentized residuals for the response variable: concentrate Fe Grade 175
Figure 5.15: Perturbation plot for Separation Efficiency at the centre point 178
Figure 5.16: Separation efficiency as a function of paraffin and sodium oleate dosage within the range of levels tested 179
Figure 5.17: Separation efficiency as a function of sodium oleate dosage for the current study as compared to the findings of Roy (2012) 179
Figure 5.18: Interactive effect of sodium oleate dosage and conditioning time on separation efficiency – View A 180
Figure 5.19: Interactive effect of sodium oleate dosage and conditioning time on separation efficiency – View B 181
Figure 5.20: Perturbation plot for Concentrate Fe grade at the centre point 184
Figure 5.21: Concentrate Fe grade as a function of conditioning time for the current study as compared to the findings of Song et al. (2002) 185
Figure 5.22: Concentrate Fe grade as a function of sodium oleate dosage for the current study as compared to the findings of Roy (2012) and Song et al. (2002) 186
Figure 5.23: The actual and predicted separation efficiency for the optimisation runs using the Quadratic Model at 95% Confidence limits 189
Figure 5.24: The actual and predicted concentrate Fe Grade for the optimisation runs using the 2Fl Model at 95% Confidence limits 190
Figure 5.25: Perturbation plot for Separation Efficiency for Run 17 (un-optimised) 191
Figure 5.26: Perturbation plot for Concentrate Fe Grade for Run 17 (un-optimised) 191
Figure 5.27: Perturbation plot for Separation Efficiency for Optimisation Run 24 ... 192
Figure 5.28: Perturbation plot for Concentrate Fe Grade for Optimisation Run 24 . 192
Figure 6.1: Hydraulic classifiers with their optimum particle size range (Tripathy et al., 2015) 197
Figure 6.2: The development and applications of the Reflux Classifier until 2012, figure adapted from Tripathy et al. (2015, p. 215) 198
Figure 6.3: RCTM2000 Reflux Classifier (Orupold et al., 2014) 199
Figure 6.4: RC^{TM}300 Pilot Scale Reflux Classifier (Orupold et al., 2014) 199
Figure 6.5: Dependence of the actual throughput advantage on the aspect ratio of the inclined channels for different particle Reynolds numbers. The angle of inclination is fixed at 70° for all the data (Zhou et al., 2006) 201
Figure 6.6: Schematic diagram of a Reflux Classifier-100 (Amariei et al., 2014) ... 203

Figure 6.7: Flow conditions within an inclined channel between two parallel plates, reproduced from Nguyentranlam and Galvin (2004, p. 85) 204

Figure 6.8: The lamellae plates of the RC-100 extending past the overflow weir to ensure equal flow velocities in each channel 209

Figure 6.9: Fluidisation water distributor for the first RC built at Mintek 209

Figure 6.10: Schematic diagram of the angles of holes in the distributor for the fluidisation water 210

Figure 6.11: Angles of holes in the distributor for the fluidisation water..... 211

Figure 6.12: Fluidisation water distributor for the RC-100 212

Figure 6.13: Reflux Classifier employed for this study which was made from PVC plastic..... 213

Figure 6.14: Lamellae plates made from 316 Stainless Steel with PVC plastic used to achieve a gap spacing of 5mm..... 213

Figure 6.15: Experimental set-up for the PVC RC testwork at Mintek..... 219

Figure 6.16: Effect of Water Fluidisation rate on the Cumulative Fe Grade of the RC U/F with and without selective flocculation (at 95% Confidence limits) 223

Figure 6.17: Effect of Water Fluidisation rate on the Cumulative Fe Recovery of the RC U/F with and without selective flocculation (at 95% Confidence limits)..... 223

Figure 6.18: Effect of Water Fluidisation rate on the Cumulative Separation Efficiency of the RC U/F with and without selective flocculation (at 95% Confidence limits)..... 224

Figure 6.19: Discrete Fe and Si Deportment of the RC U/F with and without selective flocculation 225

Figure 6.20: Fe grade-recovery curve for the current semi-batch study and the continuous run conducted by Hunter et al. (2015) on fine Fe ore of similar head grade..... 226

Figure 7.1: Fe Grade-Recovery curve for the SLon and RC concentrates with and without selective flocculation (at 95% Confidence limits) 229

Figure 7.2: A plot of the two significant factors for the SLon product at 6 000 Gauss with and without selective flocculation (at 95% Confidence limits)..... 230

Figure 8.1: Historical and forecasted prices for iron ore fines C.F.R (cost and freight) to China at a grade of 62% Fe (World Bank Group, 2017)..... 233

Figure 8.2: Historical Prices for iron ore fines [C.F.R China at a grade of 62% Fe] and base metals over the last 10 years (World Bank Group, 2017) 234

Figure 9.1: A graphical representation of the interrelationships between ore characteristics, selective flocculation and the solid-solid separator..... 245

LIST OF TABLES

Table 1.1: Commonly exploited iron-bearing minerals (Astrup et al., 1998) 1

Table 1.2: Fines classification according to Ansari (1997) 5

Table 2.1: Process Difficulties experienced in the Flotation of Slimes (Ansari, 1997) 13

Table 2.2: Slimes processes and their ability to overcome slimes problems numbered in Table 2.1 (Ansari, 1997) 15

Table 2.3: Competing forces in Magnetic Separation (Svoboda & Fujita, 2003) 17

Table 2.4: Effect of particle size on magnetic separation (Svoboda & Fujita, 2003). 18

Table 2.5: Oil/Water Emulsification techniques for the treatment of Slimes (Ansari, 1997) 24

Table 2.6: Industrial Application of Selective flocculation to Iron Ore (as cited by Abro et al., 2013) 31

Table 2.7: Problems associated with the industrial application of selective flocculation 32

Table 2.8: List of polymers used in flocculation (Bulatovic, 2007) 34

Table 2.9: Types of Polymers (Sivamohan, 1990) 35

Table 2.10: Effect of pH and electrolyte concentration on polymer adsorption (Abro, 2009) 43

Table 2.11: Selective flocculation separation achieved with various mineral combinations (Sivamohan, 1990) 46

Table 2.12: Anionic collectors used in Iron Ore Flotation (Filippov et al., 2014) 54

Table 2.13: Selective Flocculation applied to Magnetic Separation 64

Table 3.1: Experimental Design for optimising magnetic separation, gravity separation as well as selective flocculation 72

Table 3.2: Size Fractions 78

Table 3.3: Ball Milling Conditions 79

Table 3.4: Chemical Analysis Breakdown 82

Table 3.5: Size Analyses Fractions 85

Table 3.6: Chemical analysis of the feed sample 85

Table 3.7: EPMA results of 100 randomly selected Fe oxide grains (15 kV, 20 nA, spot size 5 µm) 87

Table 3.8: Mineral Abundances of the two polished sections of the Feed Sample ... 87

Table 3.9: Analysis of feed sample by chemical and mineralogical methods 92

Table 4.1: Rod Matrices available (Outotec, 2012) 108

Table 4.2: Comparison of the mineralogy and grade of the samples used in the Da Corte et al. (2015) study and the current study 109

Table 4.3: Variation of Intensity, Pulsation Frequency and Pulse Amplitude for each Size Fraction (Da Corte et al., 2015) 110

Table 4.4: Significant Factors affecting Fe Grade and Recovery for the -1.18mm+38 µm & -38 µm size fractions (Da Corte et al., 2015) 111

Table 4.5: The combination of parameters that achieve the best Fe grade and recovery at the rougher stage for the -38 µm size fraction (Da Corte et al., 2015) 111

Table 4.6: SLon-100 Operating Conditions for -38 µm sample as-is 112

Table 4.7: Various models for suspensions, gels and pastes that exhibit pseudoplastic flow curves 123

Table 4.8: Matrix of Tests for Sodium Silicate at various dosages and pulp densities 124

Table 4.9: Interpolated Yield Stress at Various Sodium Silicate Dosages and Pulp Densities 130

Table 4.10: Operating conditions for the pH screening tests 132

Table 4.11: Technical Specifications for the Malvern Mastersizer 2000E (Malvern Instruments Ltd., 2007) 139

Table 4.12: Matrix of Tests conducted on the Malvern Mastersizer 2000 E with the Hydro-2000 MU 141

Table 4.13: Summary of hydrodynamic conditions used by various researchers ... 144

Table 4.14: The average Dv (0.5) for each of the pHs tested compared to that of the feed (all obtained by laser diffraction) 150

Table 5.1: Design selection guide outline by NIST (2012) 157

Table 5.2: Summary of properties of the Classical Response Surface Designs (NIST,2012) 159

Table 5.3: Factors and their respective levels employed in the Box-Behnken design 160

Table 5.4: Matrix of tests for Block 1 of the Box-Behnken Design 161

Table 5.5: Determination of outliers in the data set obtained 167

Table 5.6: Model evaluation for the Response Variable: Separation Efficiency 171

Table 5.7: Model evaluation for the Response Variable: concentrate Fe Grade 171

Table 5.8: Model evaluation for the Response Variable: concentrate Fe Recovery 171

Table 5.9: ANOVA Table for the Quadratic model for the response variable: separation efficiency 177

Table 5.10: ANOVA Table for the Quadratic model for the response variable: Concentrate Fe Grade 183

Table 5.11: Constraints and objectives for optimisation of the selective flocculation process 187

Table 5.12: Optimised solutions within the defined constraints 188

Table 6.1: Capital and Operating Costs for the RC, TBS and TBS combined with spirals for a capacity of 100 t/h (Da Corte et al., 2016) 202

Table 6.2: Design and Process Variables for the RC (Tripathy et al., 2015) 205
Table 6.3: Separation efficiencies at varying inclination angles and similar design and operating variables (Data extracted from Laskovski et al., 2006)..... 206
Table 6.4: Process Variables for the TBS and RC (Tripathy et al., 2015) 216
Table 6.5: Summary of semi-batch operating conditions and sample characteristics for coal and ilmenite 217
Table 6.6: RC Operating Conditions for the -38 µm sample as-is and for the flocculated sample 220
Table 8.1: Historical and forecasted prices for iron ore fines C.F.R (cost and freight) to China at a grade of 62% Fe (World Bank Group, 2017)..... 233
Table 8.2: Price of 52%Fe and 58%Fe iron ore fines [C.F.R China] in June 2016 (Platts, 2016)..... 235
Table 8.3: Reagent operating costs for magnetic separation coupled with selective flocculation assuming a plant capacity of 100t/hr (Protea Chemicals, 2017) .. 238
Table 8.4: Revenue for magnetic separation with and without selective flocculation using reagent Option B and excluding all other operating costs 238
Table A.1: Particle size distribution of the HPGR product (-1.18mm)..... 262
Table A.2: Milling Curve Raw Data 262
Table A.3: Data reconciliation check for Fe and SiO_2 chemical analysis of testwork products 263
Table A.4: EPMA raw data of 100 randomly selected Fe oxide grains (15 kV, 20 nA, spot size 5 µm)..... 265
Table A.5: PTA raw data – Density Distribution of Section A and B..... 267
Table A.6: PTA raw data – Mineral Abundance for Section A and B..... 268
Table A.7: Raw Data for the average hematite cumulative mass per cent liberated by size..... 269
Table A.8: Proportion of the dominant minerals in the greater than 80% liberated class and the completely (100%) liberated class (liberation by area)..... 269
Table A.9: PTA Size-By-Assay for Section A 270
Table A.10: PTA Size-By-Assay for Section B 271
Table A.11: PTA Average Size-By-Assay for Section A and B..... 272
Table A.12: Fe and SiO_2 Data reconciliation check for mineralogical analysis..... 273
Table A.13: Sieving Size-By-Assay for Aliquot 1..... 274
Table A.14: Sieving Size-By-Assay for Aliquot 2..... 275
Table A.15: Sieving Average Size-By-Assay for Aliquot 1 and 2..... 276
Table B.1: Raw Data for the SLon-100 Baseline Tests without Selective Flocculation..... 277
Table B.2: Summary of the Raw Data for SLon-100 Baseline Tests without Selective Flocculation..... 279

Table B.3: The experimental and modelled yield stress as well as apparent viscosity as a function of shear rate for 0 g/t Sodium Silicate at 0% solids (w/w) [Sample 3] 280

Table B.4: The experimental and modelled yield stress as well as apparent viscosity as a function of shear rate for 0 g/t Sodium Silicate at 20% solids (w/w) [Sample 11] 281

Table B.5: The experimental and modelled yield stress as well as apparent viscosity as a function of shear rate for 500 g/t Sodium Silicate at 20% solids (w/w) [Sample 8] 282

Table B.6: The experimental and modelled yield stress as well as apparent viscosity as a function of shear rate for 1 000 g/t Sodium Silicate at 20% solids (w/w) [Sample 10] 283

Table B.7: The experimental and modelled yield stress as well as apparent viscosity as a function of shear rate for 1 500 g/t Sodium Silicate at 20% solids (w/w) [Sample 7] 284

Table B.8: The experimental and modelled yield stress as well as apparent viscosity as a function of shear rate for 0 g/t Sodium Silicate at 30% solids (w/w) [Sample 1] 285

Table B.9: The experimental and modelled yield stress as well as apparent viscosity as a function of shear rate for 500 g/t Sodium Silicate at 30% solids (w/w) [Sample 4] 286

Table B.10: The experimental and modelled yield stress as well as apparent viscosity as a function of shear rate for 1 000 g/t Sodium Silicate at 30% solids (w/w) [Sample 2] 287

Table B.11: The experimental and modelled yield stress as well as apparent viscosity as a function of shear rate for 1 500 g/t Sodium Silicate at 30% solids (w/w) [Sample 9] 288

Table B.12: The experimental and modelled yield stress as well as apparent viscosity as a function of shear rate for 0 g/t Sodium Silicate at 45% solids (w/w) [Sample 5] 289

Table B.13: The experimental and modelled yield stress as well as apparent viscosity as a function of shear rate for 500 g/t Sodium Silicate at 45% solids (w/w) [Sample 13] 290

Table B.14: The experimental and modelled yield stress as well as apparent viscosity as a function of shear rate for 1 000 g/t Sodium Silicate at 45% solids (w/w) [Sample 6] 291

Table B.15: The experimental and modelled yield stress as well as apparent viscosity as a function of shear rate for 1 500 g/t Sodium Silicate at 45% solids (w/w) [Sample 12] 292

Table B.16: Malvern Mastersizer sizing results for the as-is feed in slurry form with and without ultrasonic displacement 293

Table B.17: Malvern Mastersizer sizing results at the Box-Behnken centre points for Selective Flocculation and at a pH of 9.5 295

Table B.18: Malvern Mastersizer sizing results at the Box-Behnken centre points for Selective Flocculation and at a pH of 10 297

Table B.19: Malvern Mastersizer sizing results at the Box-Behnken centre points for Selective Flocculation and at a pH of 10.5 299

Table B.20: Malvern Mastersizer sizing results at the Box-Behnken centre points for Selective Flocculation and at a pH of 11 301

Table B.21: Raw Data of the SLon-100 tests at the Box-Behnken centre points for Selective Flocculation and at a pH of 9.5; 6 000 Gauss and 261.2 rpm..... 303

Table B.22: The average raw data of the SLon-100 Mags at the Box-Behnken centre points for Selective Flocculation and at a pH of 9.5; 6 000 Gauss and 261.2 rpm..... 304

Table B.23: Raw Data of the SLon-100 tests at the Box-Behnken centre points for Selective Flocculation and at a pH of 10; 6 000 Gauss and 261.2 rpm..... 305

Table B.24: The average raw data of the SLon-100 Mags at the Box-Behnken centre points for Selective Flocculation and at a pH of 10; 6 000 Gauss and 261.2 rpm..... 306

Table B.25: Raw Data of the SLon-100 tests at the Box-Behnken centre points for Selective Flocculation and at a pH of 10.5; 6 000 Gauss and 261.2 rpm..... 307

Table B.26: The average raw data of the SLon-100 Mags at the Box-Behnken centre points for Selective Flocculation and at a pH of 10.5; 6 000 Gauss and 261.2 rpm 308

Table B.27: Raw Data of the SLon-100 tests at the Box-Behnken centre points for Selective Flocculation and at a pH of 11; 6 000 Gauss and 261.2 rpm..... 309

Table B.28: The average raw data of the SLon-100 Mags at the Box-Behnken centre points for Selective Flocculation and at a pH of 11; 6 000 Gauss and 261.2 rpm..... 310

Table C.1: Raw Data for Block 1 results of the SLon-100 coupled with Selective Flocculation using the Box-Behnken experimental Design 311

Table C.2: Raw Data for Block 2 results of the SLon-100 coupled with Selective Flocculation using the Box-Behnken experimental Design 314

Table C.3: Raw Data for Block 3 results of the SLon-100 coupled with Selective Flocculation using the Box-Behnken experimental Design 317

Table C.4: Raw Data for Block 1-3 Mags Average results of the SLon-100 coupled with Selective Flocculation using the Box-Behnken experimental Design..... 320

Table C.5: Raw Data of the Optimisation Validation Tests for Run 11, 23, 24 and 25 of the SLon-100 coupled with the Optimal Selective Flocculation conditions.. 322

Table C.6: Average Raw Data of the Optimisation Validation Tests for Run 11, 23, 24 and 25 of the SLon-100 coupled with the Optimal Selective Flocculation conditions..... 325

Table D.1: Raw Data for the Base case Reflux Classifier testwork without selective flocculation (Test 1)..... 326

Table D.2: Raw Data for the Base case Reflux Classifier testwork without selective flocculation (Test 2) 328

Table D.3: Raw Data for the Base case Reflux Classifier testwork without selective flocculation (Test 3) 330

Table D.4: Raw Data for the Average Base case Reflux Classifier testwork without selective flocculation (Test 1-3) 332

Table D.5: Raw Data for Optimised Selective Flocculation coupled with the Reflux Classifier (Test 4) 334

Table D.6: Raw Data for Optimised Selective Flocculation coupled with the Reflux Classifier (Test 5) 335

Table D.7: Raw Data for Optimised Selective Flocculation coupled with the Reflux Classifier (Test 6) 337

Table D.8: Raw Data for the Average Test for Optimised Selective Flocculation coupled with the Reflux Classifier (Test 4-6) 339

Table D.9: PTA raw data – Density Distribution of the RC Underflow with and without selective flocculation 341

Table D.10: PTA raw data – Mineral Abundance of the RC Underflow with and without selective flocculation 341

Table D.11: PTA Size-By-Assay for the RC Underflow without selective flocculation 342

Table D.12: PTA Size-By-Assay for the RC Underflow with selective flocculation . 344

LIST OF ACRONYMNS AND ABBREVIATIONS

2FI	Two-level factorial model
ANOVA	ANalysis Of VAriance
ASD	Analytical Services Division
C.F.R.	Cost and freight to China
CMC	Critical Micelle Concentration
D(v,0.50)	50% of the sample passing a specific size fraction by volume
EPMA	Electron Microprobe Analysis
F test	Fisher's test
FDS	Fraction of Design Space
FHS	FerroHydrostatic Separators
FMS	Floc Magnetic Separation
HPGR	High Pressure Grinding Rolls
LOI	Loss On Ignition
Mags	Magnetic Product
MLA	Mineral Liberation Analyser
MNL	Mineralogy
N-Mags	Non-Magnetics Product
O/F	Overflow
PAA	PolyAcrylic Acid
PTA	Particle Tracking Analysis
p-value	Probability value
PVC	Polyvinyl chloride
RC	Reflux Classifier
RSM	Response Surface Method Design
SE	Separation Efficiency
SF	Selective Flocculation
SLon	Laboratory scale pulsating Wet High Intensity Magnetic Separator
Std Dev	Standard Deviation
U/F	Underflow
WHIMS	Wet High Intensity Magnetic Separation
XRF	X-Ray Fluorescence

GLOSSARY

• **Aliases (also referred to as Confounding)**	When two or more variables vary together, and the effect of each variable cannot be separated from each other.
• **Amorphous**	Having no crystalline form, i.e. having no ordered shape or structure.
• **ANOVA**	A statistical technique used to investigate and model the relationship between a response variable and one or more independent variables also referred to as factors.
• **Apparent viscosity**	Viscosity at a value of shear rate and temperature and is defined as the shear stress applied divided by the shear rate.
• **Aspect ratio:**	The length of inclined plates in the Reflux Classifier divided by the spacing between the inclined plates.
• **Autogenous dense media zone**	The fine heavy particles that settle on the inclined plates of the Reflux Classifier creates a sediment layer that slides down the inclined plates and creates a suspension underneath the plates. This suspension also serves to facilitate the movement of coarse light particles in the feed into the overflow. The multiple times the fine heavy particles are circulated through the inclined planes and back into the suspension is also referred to as the Reflux Action.
• **Blocking**	An experimental approach in which a combination of several factors at specific levels are grouped and tested such that any changes in the variables outside the experiment are concentrated in the levels (NIST, 2012). The groups or blocks are similar.
• **Box-Behnken**	An experimental design for response surface modelling which only requires three levels of each factor. The combinations of factors and levels lies in the centre of the experiment region and at the midpoint of the edges of the experiment region (NIST, 2012). This design is typically used for optimisation studies.
• **Bridging mechanism**	When a polymer adsorbs onto the surface of two particles, with either the head attached to one particle and the tail to another or through loops.

- **Carrier flotation** — Ultrafines of the desirable mineral coat a coarse particle of a different mineral whilst under shear conditions to facilitate agglomeration of the desirable ultrafine mineral.
- **Causticisize** — Solubilising corn starch by using sodium hydroxide (caustic soda). This method of solubilising cornstarch is also referred to as alkali gelatinisation.
- **Charge neutralisation** — The use of polymer flocculents/polyelectrolytes to reduce the charge density at the surfaces of particles.
- **Chemisorption** — Chemical adsorption. A chemical bond is created between the polymer and particle surface and is irreversible (IUPAC, 2002).
- **Conformation** — The shape or structure of the polymer
- **Contour plots** — A contour plot graphically represents a 3-D surface in a 2-D form. For a given z value, lines are drawn on the x-y plot connecting the x and y coordinates for the given z-value (NIST, 2012).
- **Covariate** — A control variable that is observed and not changed by the investigator during an experiment or study but the variable can affect the results of the experiment or study.
- **Critical micelle concentration** — When the concentration of surfactant in solution is exceeded, and any further surfactant addition will form micelles.
- **Depressants** — A compound that depresses or reduces the floatability of the selected mineral during the flotation process.
- **Design Expert** — A statistical software created by Stat-Ease Inc that is typically used for the design of experiments.
- **Dispersion** — The process of keeping particles in a slurry separate from each other thereby preventing aggregation from occurring.

- **Double fractionation:** A sample is placed in the Reflux Classifier which is operated in semi-batch mode. In this mode, a sample of a specific mass is charged into the unit, and the fluidisation water flowrate is varied from low to high. No additional feed sample is introduced during the run. The overflow collected at each fluidisation water flowrate is dried, weighed and sized.
- **Electro-coagulation (electrolytic coagulation)** The process of agglomerating particles using a highly charged polymer with the addition of an electrical current to the solution.
- **Electrolyte** A chemical compound that dissolves into ions when in solution and through the movement of ions it can conduct electricity.
- **Electron microprobe analysis** A laboratory instrument used to determine the chemical composition of minerals.
- **Emulsification** The dispersion of one liquid in another liquid that are typically incapable of mixing in the attempt to achieve a more homogenous solution.
- **Entrainment** The entrapment of liberated desired mineral(s) with liberated gangue/undesired mineral(s) in the products of process units.
- **Ferruginous** Containing iron oxides
- **Floc** A mass of fine particles that have aggregated either naturally or through the addition of a flocculant. Flocs are also referred to as an aggregate.
- **Flocculant** A compound that causes flocculation or aggregation to occur.
- **Flocculation** The process of reducing the repulsive forces between particles such that smaller particles are attracted to each other to form a floc. This is also referred to as aggregation.
- **Free settling** The settling of particles in a dilute slurry in which the fall of particles is unaffected by the other well dispersed particles.
- **Functional groups** A specific arrangement of bonded atoms that give a compound certain physical and chemical characteristics (Lumen, n.d.)

- **Gelatinisation** — In this study, gelatinisation refers to starch gelatinisation where the intermolecular bonds in the starch molecules are broken either by water and heat referred to as thermal gelatinisation or by adding sodium hydroxide referred to as alkali gelatinisation.
- **Heteroflocculation** — The simultaneous flocculation of the target mineral and undesirable minerals.
- **Hindered settling** — The settling of particles in a thick slurry in which the settling rate of particles are reduced due to the water rising through the slurry and due to the interactions/crowing effect of nearby particles.
- **Hydrogen bonding** — The attractive force between a hydrogen atom attached to an O, N, F atom of one molecule and the hydrogen atom attached to an O, N, F atom of another molecule (Elmhurst College, 2003).
- **Hydrophobic association** — Various methods of selectively making one mineral hydrophobic and in the process creating flocs of the desired mineral. This study covers four methods namely shear flocculation, carrier flotation, selective magnetic aggregation and selective flocculation.
- **Hydrophobic interaction** — The interaction between non-polar molecules in water.
- **Inertial force** — The resistance to the change in the velocity of an object and is typically equal in magnitude to the applied force expect in the reverse direction.
- **Interfacial area** — The contact area between two liquids.
- **Intermolecular forces** — The total of all forces that act between two molecules and usually consist of London dispersion forces, dipole-dipole interaction (under which hydrogen bonding falls) and ion-dipole interaction (Helmenstine, 2017).
- **Leaching** — The use of an aqueous medium to facilitate the conversion of metals, contained within ores, into a soluble salt.
- **Liquid-liquid extraction** — A process of transferring a compound from one liquid/solvent to another whereby both liquids/solvents are immiscible.
- **Magnetic field gradient** — The rate at which the magnetic field intensity increases towards the surface of the magnet (Wills & Napier-Munn, 2006).

- **Magnetic field intensity** — The magnetic force that generates lines of force through a material (Wills & Napier-Munn, 2006).
- **Magnetic susceptibility** — The degree to which a material is magnetised when a magnetic force is applied.
- **Metabolites** — Products generated from the chemical processes necessary for life in living organisms
- **Micelle** — Molecules that possess both polar (charged) and non-polar groups that aggregate in an aqueous solution. The polar groups form the outer shell of the aggregate whilst the non-polar groups align to the centre of the aggregate with the aggregate having a similar appearance to oil drops (University "Federico II" of Naples, n.d)
- **Null hypothesis** — A statement that there is no statistical or significant difference between a) the factor/variable and the mean of its population and b) factors or variables, and thus there is no relationship between the factors or group of factors.
- **Orthogonal blocking** — Occurs when the effects of the blocking can be separated from the effects of individual factors or interaction factors (NIST, 2012).
- **Particle tracking analysis** — The data obtained for each particle from the Mineral Liberation Analyser (MLA). Particle data such as the mineral types/compositions, particle size, density, weight per cent of the particle population, area of particle, shape factor, circularity, and perimeter can be obtained from the MLA. The particle data is useful in modelling and simulating gravity separation processes and circuits and can be used to track where particles of certain characteristics reported to in the circuit.
- **Perturbation (trace) plots** — Silhouette views of the response surfaces for all the factors at a given value for each factor (Stat-ease, 2016).
- **Physisorption** — Physical adsorption. Intermolecular forces such as the van der Waals forces are responsible for adsorption of the polymer onto the particle surface and is reversible (IUPAC, 2002).
- **Point of zero charge** — When the surface charge density of a material or mineral is zero.

- **Polyelectrolyte** — An electrolyte with high molecular weight and many repeating ionising groups.
- **Polymer** — A chemical compound of a chain like structure which is made up of smaller repeating units throughout the chain.
- **Polymer flocculation** — The aggregation of particles of the desired mineral through the use of water-soluble polymers resulting in flocs of the desired mineral.
- **Precipitation** — The creation of a solid phase from a solution by either making the substance insoluble or by changing the composition of the solution such that the substance becomes insoluble.
- **Pulse amplitude** — The distance the slurry or water in the feeding box (of the SLon-100) moves from the rest position.
- **Pulse frequency** — The number of pulses generated in a second by the pulsating mechanism of the SLon-100.
- **Residual plots** — A graph with residuals on the y-axis and the independent variable on the x-axis. The way the residuals that are dispersed around the x-axis indicates what regression model is most appropriate for the data.
- **Residuals** — Residuals are the estimation of the experimental error. It is calculated as the difference between the actual response and predicted response obtained from a fitted model (NIST, 2012).
- **Response surface method design** — A design for experiments that models the response variables within a defined operating range.
- **Response variables** — The dependent variables in this study, namely concentrate Fe grade, Fe recovery, and separation efficiency.
- **Rheogram** — A graphical plot of the shear rate of a fluid on the x-axis and shear stress on the y-axis.
- **Rheology** — The study of the deformation and flow of fluids in response to applied forces.
- **Rheometer** — A laboratory instrument that measures the rheological properties of the fluid (how the fluid flows in response to a force) over a varied and extended range of conditions.

- **Selective flocculation**: The aggregation of the desired mineral from a mixture of minerals using the bridging mechanism. Surfactants are typically added to aggregate or flocculate the desired mineral with the generated flocs being hydrophobic.
- **Separation by particle rotation**: The ability to magnetically separate ferromagnetic minerals (or particles with ferromagnetic inclusions) from each other provided the minerals have different magnetic properties when rotated along different molecular axes or directions.
- **Separation efficiency**: In this study, the efficiency of the separation units is determined as the difference between the recovery of the desirable mineral in the product (concentrate) and the recovery of the gangue mineral in the product (concentrate). Separation efficiency is also referred to as collection efficiency by other researchers.
- **Shear flocculation**: A mineral particle is made hydrophobic and allowed to flocculate with other hydrophobic particles by the adsorption of collectors (surfactants) under high shear conditions.
- **Shear stress**: The stress experienced by a material when a force is applied parallel to its surface and a change in the material's shape occurs as a result of the applied force.
- **Site blocking agents**: Low molecular weight polymers that adsorb onto the surfaces of all the minerals to prevent adsorption of the flocculent onto gangue minerals (Forbes, 2011). The objective of this approach is to improve the selectivity of the flocculation process.
- **Slimes**: For the purposes of this dissertation, slimes is classified as material finer than 45 µm.
- **SLon**: A laboratory scale pulsating wet high intensity magnetic separator
- **Smearing**: Coatings of contaminants or other fine minerals, such as slimes, on the surfaces of particles.
- **Steric stabilisation**: The prevention of agglomeration through the firm adsorption of polymers onto the surface of a particle such that there are sites for further attachment.

- **Studentized residuals**

  Studentized residuals represent the standard deviation of an individual residual in relation to the standard deviation of the entire residual distribution (NIST, 2012). Internally studentized residuals include all residuals while externally studentized residuals exclude residuals which are improbably large and not normally distributed.

- **Surface modification**

  Changing the surface of a material to tailor the material to a specific application without affecting the bulk characteristics of the material

- **Surfactant**

  Surfactant is an abbreviation for SURFace ACTive AgeNT. Surfactants are compounds that have both lyophilic (liquid loving) and lyophobic (liquid adverse) groups (Zhao et al., 2004). Defoamers, dispersants, foaming agents and collectors used in flotation can be considered surfactants (Zhao et al., 2004).

- **Temperature responsive polymers**

  Polymers that are capable of changing from hydrophobic to hydrophilic when the temperature of the solution is below or exceeds the critical solution temperature.

- **Terminal velocity**

  The constant velocity a particle will fall at once the gravitational and fluid resistance counterbalance each other.

- **Transformation**

  Changing the data to make it easier to understand, obtain a normal distribution or obtain a linear relationship between variables, e.g. plotting on a log scale, subtracting a fixed number from all data points, squaring or cubing all data points etcetera.

- **van der Waals forces**

  “The attractive or repulsive forces between molecules (or between groups within a molecule) that cannot be attributed to bond formation or the electrostatic interaction between ions or ionic groups” (Chemicool Dictionary, 2017).

- **Viscosity**

  The resistance of a fluid to changes in shape and movement when shear stress is applied.

CHAPTER 1 : INTRODUCTION

“You need to let the little things that would ordinarily bore you suddenly thrill you.” Andy Warhol succinctly describes the purpose of this dissertation. Metallurgists across the world have negative connotations of slimes due to the adverse effects it has on minerals processing. Rather than viewing slimes, particularly iron ore slimes, as a hindrance this dissertation serves to show its potential as a resource.

1.1 Background Information

The average mass % of iron in the earth's crust is 5% making iron one of the most abundant elements in the earth's crust (Astrup et al., 1998). Creamer Media (2017) reports that the world contains approximately 800 billion tonnes of crude iron ore reserves with the iron ore commodity market the third largest after oil and gas. The commonly exploited iron-bearing minerals with their compositions and iron content are presented in Table 1.1. This investigation will focus on hematite.

Table 1.1: Commonly exploited iron-bearing minerals (Astrup et al., 1998)

Iron Bearing Mineral	Composition	Fe Content (%)
Magnetite	$FeO.Fe_2O_3$	72
Hematite	Fe_2O_3	70
Goethite	FeO.OH	61
Lepidocrocite	FeO.OH	61
Siderite	$FeO.CO_2$	48
Chamosite	$3FeO.Al_2O_3.2SiO_2.6H_2O$	35

An overwhelming proportion (98%) of the iron produced across the world is used in steelmaking. A graphical representation of iron ore's value chain is presented in Figure 1.1 and indicates that two-thirds of liquid steel is produced from iron ore with the remainder from recovered scrap.

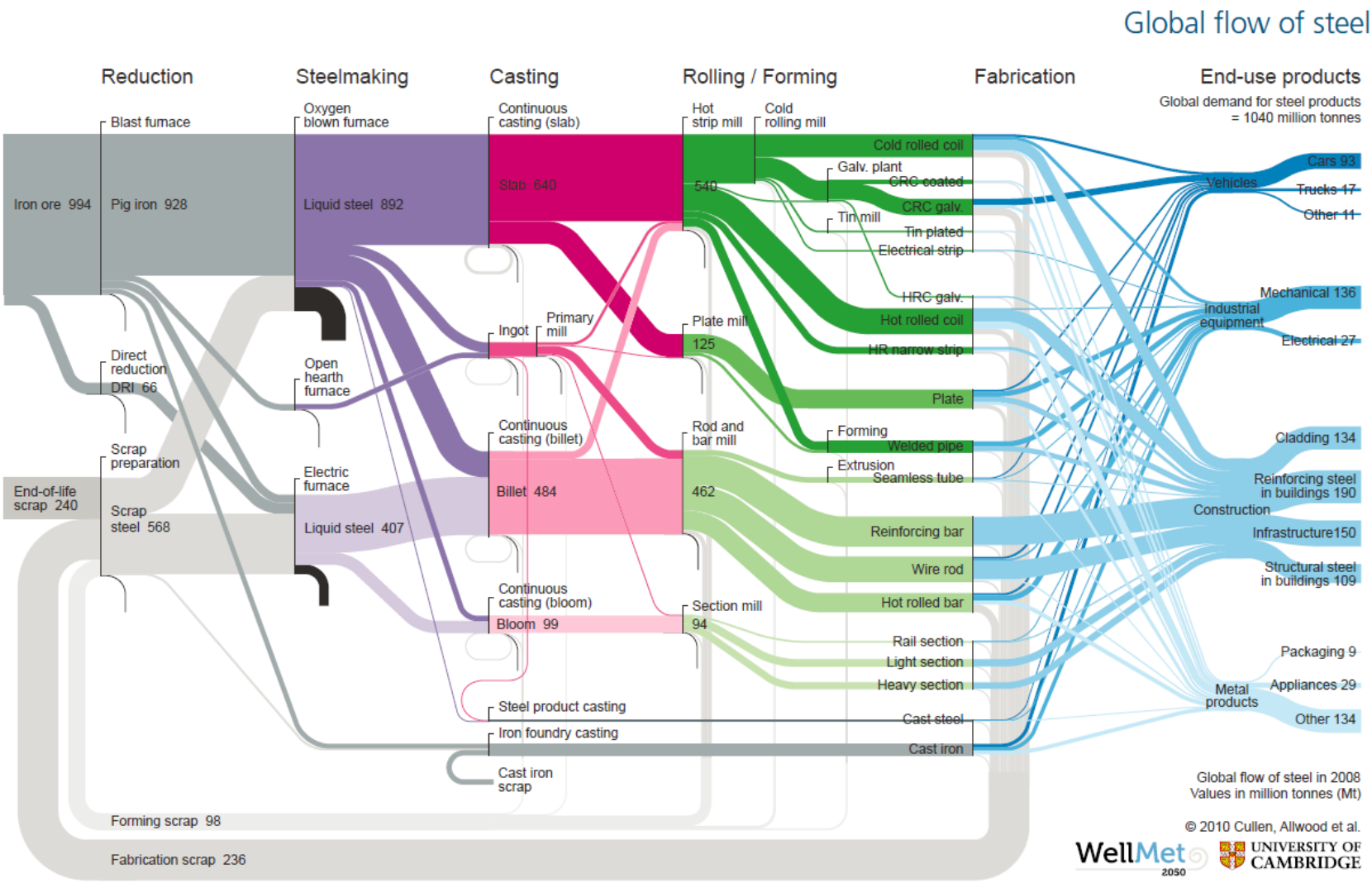


Figure 1.1: Iron Ore's value chain from raw material to end customer (Allwood et al., 2011)

South Africa produces 55 million tons of iron ore a year making it the seventh largest producer in the world. The major iron ore producers in South Africa are presented in Figure 1.2 indicating Kumba as the major producer at 41.48 million tonnes in 2016 followed by Assmang with Evraz Highveld Steel and Vanadium placed under business rescue. An estimated 58 million tonnes is expected to be exported from South Africa for the year 2017.

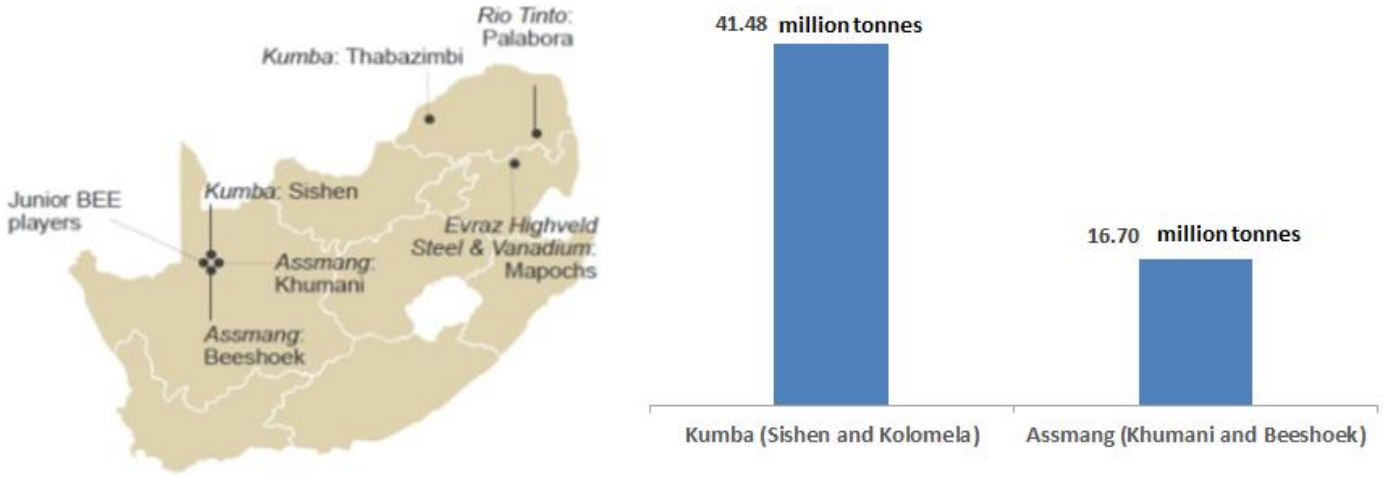


Figure 1.2: Iron ore production for the financial year 2016 (Creamer Media, 2017)

Hematite is typically beneficiated as illustrated in Figure 1.3, with lumpy and fine direct shipping ore requiring no beneficiation. The vast majority of operations require either coarse and/or fines processing. Coarse processing involves dense media separation and jigging with multiple fines processing options and configurations available. The unit operations for fines processing vary from gravity (spirals, teeter bed separation and reflux classifiers) to magnetic separation and flotation.

Li et al. (2010) reveals that approximately 50.7 billion tonnes of iron ore tailings have been discarded as waste in China. The annual generation of iron ore tailings in China totals 130 million tons and contains on average 11% Fe. These tailings represent a potential lost resource of 1.41 million tons of Fe annually. Dworzanowski (2014) reports that Kumba Iron Ore's Sishen mine discards approximately 3 Mt/a of -200 µm material as tails. These tails contain ~60% -10 µm material.

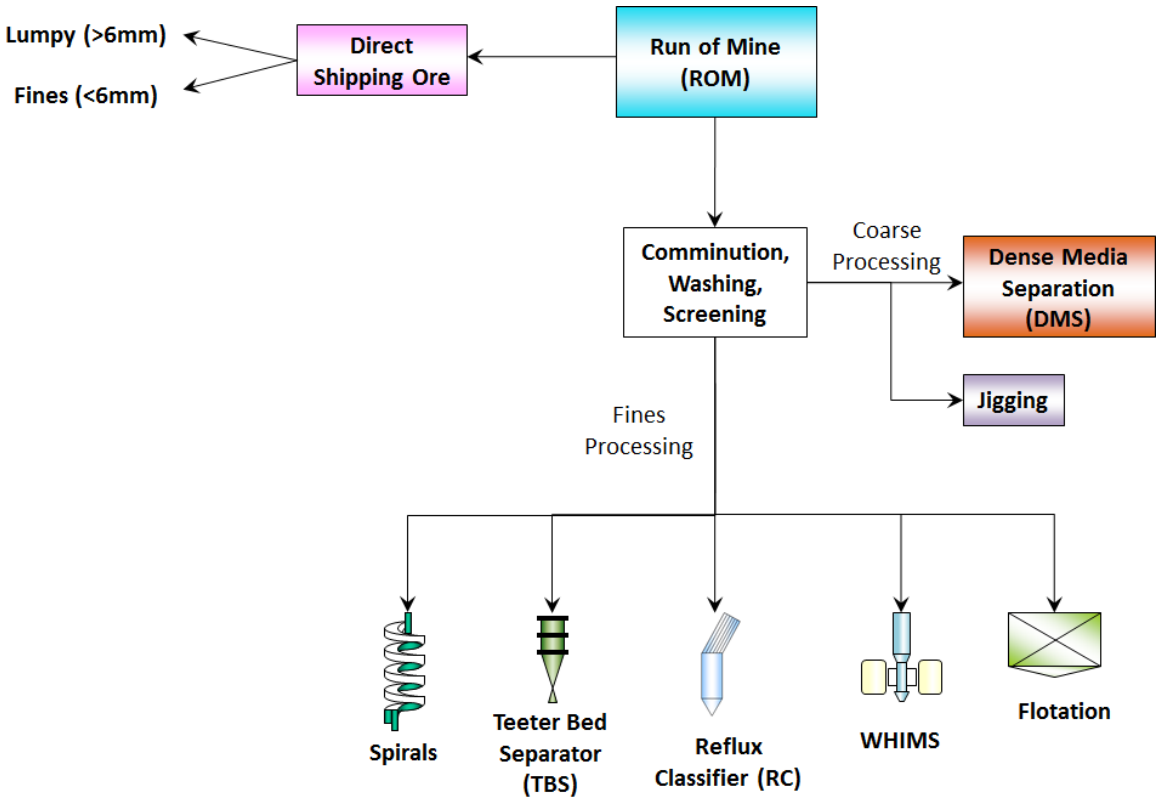


Figure 1.3: Typical Hematite Beneficiation Options

1.2 Problem Statement

As the mining of oxidised iron ore increases and reserves of rich iron ores decreases, the mineral processing industry is facing problems with treating low grade and finely disseminated iron ore. Exacerbating the problems of low-grade ores is a variety of other considerations such as the less than desirable process efficiencies for fine particles and the high proportion of mineral and metal values lost as slime in many of the mineral recovery operations.

The recovery of iron ore from tailings is currently achieved through two main processes namely magnetising roasting and direct reduction (Li et al., 2010). Roasting reduces paramagnetic hematite to ferromagnetic magnetite enabling the recovery via Wet Low Intensity Magnetic Separation. However, both options are energy intensive with temperatures ranging between 700°C to 900 °C for magnetising roasting and >1000

°C for direct reduction. As the drive towards less energy intensive processes become more critical, alternative approaches to slimes treatment are required.

Ansari (1997) claims that there is no universal description of slimes although a generally accepted description for slimes is that portion of the ore which is too fine to be economically processed through the processes developed for coarser particles. Ansari (1997) makes an important distinction between primary slimes and secondary slimes. Primary slimes are generated by the natural weathering processes, and decomposition of certain rock components while secondary slimes are generated through the comminution of ore to its liberation size. The proportion of secondary slimes that are generated can be attributed to the ore's inherent characteristics such as liberation and breakage pattern as well as the comminution methods employed for ore liberation. Although secondary slimes generation can be somewhat reduced by appropriate comminution methods to generate fewer fines, the presence of primary slimes cannot be avoided.

Interest in developing suitable process technologies for recovery of fines is growing and becoming critical as low grade and finely disseminated ores are mined. In Ansari's (1997) review of fine processing, he classified fines as particles below 100 µm and went further to categorise fines into five size fractions as per Table 1.2. For this dissertation, slimes was classified as material finer than 45 µm.

Table 1.2: Fines classification according to Ansari (1997)

Size class	**Fines Classification**
<100 µm	Fines
<20 µm	Very fine
<5 µm	Ultrafines
<1 µm	Colloids
<0.2 µm	Supercolloids

In addition to energy and process inefficiencies is the environmental consequences of developing large volumes of waste resulting from the mining of finely dispersed, low-grade ore. Verma et al. (2013) investigated the ground-water quality of an iron ore mine in India and reported the presence of heavy metals (Cu, Cr, Mn and Fe). In

addition to these elements, Wong (1981) also reported Pb and Zinc in iron ore tailings disposed along the shores of Hong Kong. These heavy metals may leach out and pollute water bodies and ground-water as a result of seepage from tailings dams. Tailings comprising of sulphide-bearing minerals exacerbates acid mine drainage and the leaching of heavy metals. In their review of fine tailings treatment, Wang et al. (2014) suggests erosion and evaporation as other environmental concerns of tailings dams. In addition to the problems of water and air contamination, is the physical stability of the tailings dam. Franks et al. (2011) contend that the majority of mining-related environmental incidents are a result of structural failures of tailings dams causing flooding and destruction of nearby environments. One such current incident is the dam failure at Samarco's iron ore tailings dam in the Bento Rodrigues district of Brazil on the 5th November 2015 claiming 17 lives, injuring 16 people and causing significant environmental damage (BBC, 2015 and Aljazeera, 2015). If the mass percentage of Fe in the tailings could be reduced by increasing the efficiency of resource utilisation the benefits would include the mitigation:

- of tailings generated,
- land requirements and
- of Fe leaching into ground-water.

1.3 Limits of Present Concentration Processes and Equipment

The treatment of ultrafines (slimes) is difficult due to a number of factors such as small mass, high surface area and high surface energy of particles. These factors will be further expounded in the following chapter. In addition to inefficient separation is the lack of development in ultrafine technology (Wills, 2006). As a result, a large amount of valuable fines that report to the tailings or slimes fraction are commonly discarded by the processing industry. However, it should be noted that the mineralogy of the ore will also dictate the separation efficiency of the various units.

The applicability of various unit processes according to the particle size range limit is presented in Figure 1.4. The upper size limit is governed by the dominance of gravitational forces which begin to interfere with the separation process at coarse

sizes. The lower limit is determined by the principles of separation on which the process under consideration operates. Below 20 µm only tilting frames, Mozley tables, matrix magnets and froth flotation are effective with matrix magnets the only effective unit operation below 5 µm. Although tilting frames and Mozley tables are potential slimes processing equipment, their low capacities limit their practical use in industry.

Despite the effectiveness of matrix magnets in the sub 5 µm range some researchers (Dey et al., 2012; Umadevi et al., 2013) deslime prior to magnetic separation for improved grades. Contradicting this work Dworzanowski (2014) showed that a greater yield at similar grades could be achieved if the entire feed is treated as-is rather than in discrete size fractions. He attributes this finding to the high probability of the +10 µm particles adhering to the matrix and tending to behave as magnets themselves and increasing the probability of -10 µm particles collecting on the matrix. Of the physical separation processes, matrix magnets show the most potential for the treatment of slimes however these units are typically operated at high intensities of 10 000 Gauss requiring considerable energy.

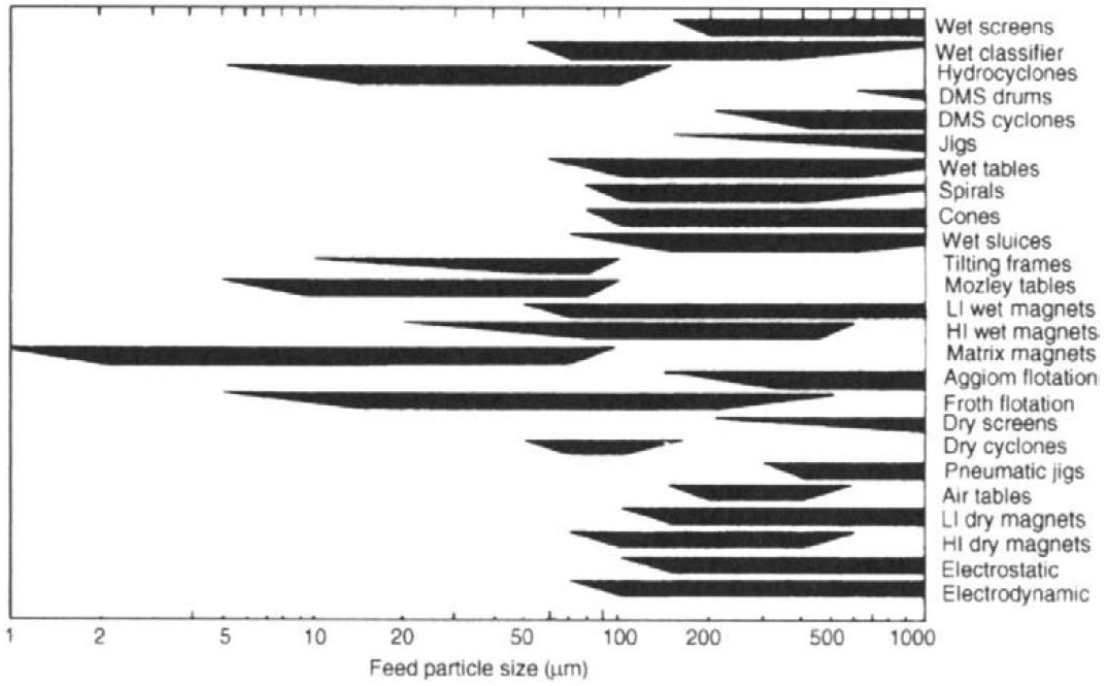


Figure 1.4: Effective range of application of conventional processing techniques (Wills, 2006)

1.4 Previous Work Conducted on Selective Flocculation

Literature focusing on the processing of iron ore slimes using selective flocculation is dominated by the flocculents starch and hydrolysed polyacrylamides. Starch-based polymers have been used over the last 80 years with extensive research conducted on selective polymer flocculation and its adsorption mechanisms (Abro et al., 2013). Weissenborn et al. (1994) claim that polyacrylamides are selective for synthetic mixtures of hematite and quartz in deionised water but are not effective on slimes where they behave as bulk flocculents.

Paananen and Turcotte (1980) cited in Haselhuhn et al. (2012) reported that Tilden Mines in the USA has been using selective flocculation coupled with flotation to recover fine hematite in the -25 µm size range since 1974. The beneficiation circuit used is presented in Figure 1.5. After primary comminution using autogenous mills, Glass-H® (sodium hexametaphosphate) is added to precipitate calcium and magnesium metaphosphates. This addition ensures that the $CaOH^+$ and $MgOH^+$ are removed from the particle surfaces thereby maintaining dispersion. Pebble mills further reduce the grind size to the liberation size of 25 µm. Subsequently, starch is added to the cyclone overflow with the latter entering a thickener. The thickener underflow is subjected to flotation with the concentrate filtered in vacuum disc filters.

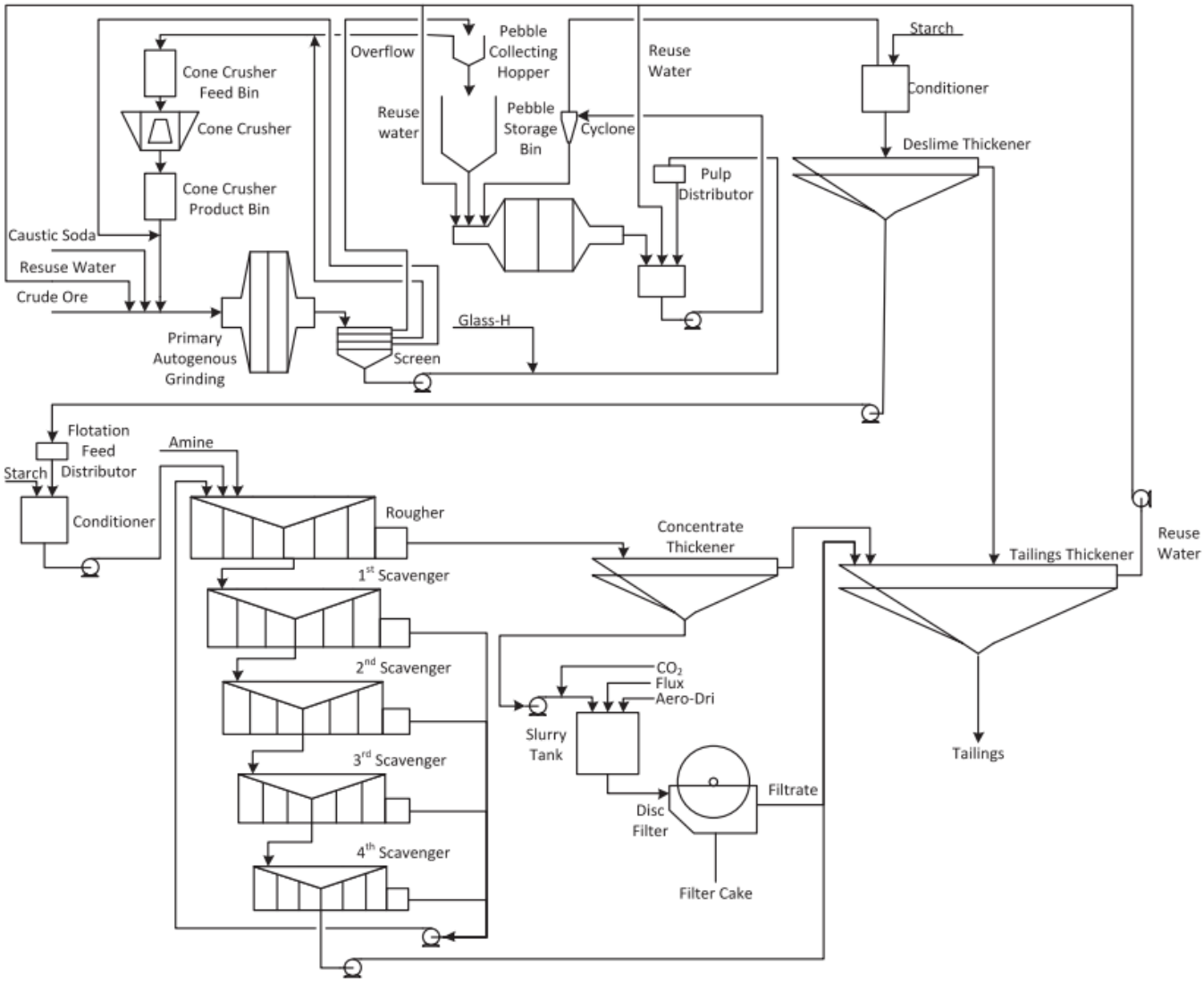


Figure 1.5: The processing circuit for Tilden Mines (Keranen 1986 cited in Haselhuhn et al., 2012)

Although the Tilden mine has successfully applied selective flocculation, applications to other iron ore mines have proved challenging due to poor selectivity. Poor selectivity can be attributed to the following factors:

- Complex ore mineralogy
- Poor liberation or smearing (slime coating) of minerals during the grinding
- Difficulties in controlling surface properties of minerals and preventing heteroflocculation (the flocculation of the target mineral and undesirable minerals)
- Water quality

- Entrainment and physical entrapment of gangue minerals in the voids of the flocculated mineral
- Reagent preparation
- High reagent costs

These factors and potential solutions are explored in the following chapter. In most applications flotation has been selected as the solid-solid separator. Very few researchers have applied selective flocculation to magnetic separation (Roy, 2012; Arol and Aydogan, 2004; Song et al., 2002) and currently the application of selective flocculation to gravity separation methods has not been published in literature.

1.5 Thesis Statement and Research Objectives

In the beneficiation of hematite-bearing slimes, the separation efficiency of conventional gravity and magnetic separators can be improved by coupling these processes with selective flocculation. The focus of this investigation is on selective flocculation and its application to alternative solid-solid separators to flotation, such as gravity and magnetic separation compared to the use of flotation for slimes processing.

The research objectives of this investigation are summarised as follows:

- To investigate the extent to which the separation efficiency of the selected types of solid-solid separators can be improved through the use of selective flocculation. Should slimes be efficiently recovered, processing plants already employing gravity and magnetic separation techniques and who encounter more slimes as their good resources are depleted have an option to retrofit their current plants to include selective flocculation rather than investing in equipment upgrades or new technology.
- To investigate the impact of selective flocculation on the product Fe grade and recovery achieved on the SLon (a pulsating wet high intensity magnetic separator) and the Reflux Classifier (a gravity separator also referred to as a fluidised bed).

- To ascertain the optimal range of operating parameters for selective flocculation for the particular ore studied whilst simultaneously maximising the three response variables namely: separation efficiency, Fe grade and Fe recovery.
- To determine if the additional reagent costs for the optimised selective flocculation process is justified based on the yield and grade of the concentrate produced since reagent costs form a substantial proportion of plant operating costs.

1.6 Significance

The investigation will indicate the potential for improving slimes beneficiation by employing gravity and magnetic separation units which are typically not applied to ultra-fines.

The point of departure of this study from previous work conducted is the use of gravity separators and pulsating magnetic separators for the solid-solid separation stage.

The literature review in Chapter Two details the principles of gravity and magnetic separation, the typical problems associated with slimes beneficiation and how this can be addressed by applying selective flocculation.

CHAPTER 2 : LITERATURE REVIEW

The beneficiation of slimes is associated with processing and handling difficulties and these pose barriers to efficient separation. These barriers need to be understood, and the possibility of addressing these barriers by the application of flocculation will be discussed in this chapter. The principles of magnetic and gravity separation are also explained in terms of how selective flocculation could improve the separation efficiency of both these separation mechanisms. Lastly, the application of magnetic and gravity separation mechanisms as solid-solid separators in selective flocculation is highlighted as an alternative to conventional flotation methods.

2.1 The Problematic Nature of Slimes

Processing difficulties involving the handling and treatment of slimes can be attributed to three physical properties namely small mass, high surface area and high surface energy. These three physical properties reduce process efficiencies with the common difficulties experienced being heteroflocculation (the flocculation of the target mineral and undesirable minerals), high reagent consumption combined with poor selectivity, increased pulp viscosity and coatings. In addition to these common difficulties Table 2.1 provides a more exhaustive list of difficulties experienced with the flotation of slimes.

Table 2.1: Process Difficulties experienced in the Flotation of Slimes (Ansari, 1997)

Nature of Slimes	Process Difficulties
Small Mass	• Low particle momentum • Heteroflocculation • Particle Entrainment in concentrates • Low probability of collision with a bubble • Difficulty in overcoming the energy barrier between particle and particle; and particle and bubble
High Surface Area	• High dissolution rate in water • Adsorption of a large quantity of chemicals • Rigidity of froth • High pulp viscosity • Undesirable coating of valuable particles by ultrafine gangue particles
High Surface Energy (Due to imperfect crystallisation, increased cracks, dislocations, edges; and high energy sites)	• Nonspecific adsorption of reagents • Increased hydration • Rapid surface reaction • Increased solubility (Not significant above 0.1 µm)

In addition to the three physical factors hindering process efficiency, Somasundaran (1983, 1984) as cited in Sivamohan (1990) identified three factors that influence the behaviour of fine particles and hence process efficiency. The three factors namely morphology, mineralogy and surface chemical composition are defined below.

a) Morphology

Fractionation (size reduction) and variation in the mineralogical composition within a particle changes the angularity or roughness (morphology) of particles' surfaces. The morphology has a significant effect on the wettability of particles.

In his doctoral thesis, Lidstrom (1968) as cited by Sivamohan (1990) showed that the surface of a mineral is changed by grinding. Wet grinding and especially dry grinding, to different grinds, resulted in varying levels of amorphousness and disorder (angularity or roughness) at the particle surfaces. Surfaces that are amorphous and or disordered have been shown to have a greater degree of dissolution than that of undisturbed surfaces. The method of grinding in

conjunction with the duration of grinding affects the severity of the change. For instance, Lidstrom (1968) suggested dry grinding produced the most changes with the most reactive surfaces whilst certain grinding conditions increased the solubility of quartz due to increased disrupted surfaces and amorphousness.

b) Mineralogy

Despite mineralogical compositions within particles varying, the effect of grinding and particle sizes on some minerals is surprising. Regarding particle sizes the minerals apatite and wavellite ($Ca_5(PO_4)_3(OH, F, Cl)$ and $Al_3(PO_4)_2(OH, F)_3•5(H_2O)$) although both phosphates differ in particle sizes with the former typically coarser than the latter. Prolonged grinding of calcite converts this mineral into aragonite while quartz tends to assume an amorphous structure with prolonged grinding.

c) Surface chemical composition

The chemical composition of particles' surfaces can change based on various factors ranging from

- surface oxidation common in sulphide ores,
- high concentration of foreign elements on the mineral surface;
- interactions on the surface resulting in precipitation on the surface;
- coating of the surface by bulk precipitates as observed with surface pollution by iron hydroxide when iron grinding media is used in wet grinding.

Despite these challenges, researchers have developed several slimes processes to reduce the detrimental effects listed in Table 2.1. Ansari (1997) summarised these processes and their ability to reduce or eliminate the effects as documented in Table 2.2.

Table 2.2: Slimes processes and their ability to overcome slimes problems numbered in Table 2.1 (Ansari, 1997)

Process	Aspects of the slimes problem with which the process				Present scale of operation
	Eliminates	Reduces	Has no effect	Not relevant	
Column Flotation	3	4; 8	1; 2; 5-7; 9-14		Limited Plant Trials
Mozley Table		1; 2; 9		6-8; 10; 8	Limited Commercial Plant
Electrostatic separation (with pulsed corona)		1; 3		2; 4-5; 6-14	Laboratory Trials
Liquid Liquid Extraction (spherical agglomeration etc.)		1; 3-5	2; 6-7; 9-10; 11-14	8	Pilot Plant Trials
Selective Flocculation	1	2-3; 7; 10	9-14	4-5; 8	Pilot Plant Trials
Electrophoresis (non-aqueous)	1; 6; 14	2; 3	7; 9-13	4; 5; 8	Laboratory Trials

Although the Mozley table and electrostatic separation are capable of treating slimes, the low capacity of these units limits their application to low-value high throughput commodities such as iron ore. Also, the high costs of liquid-liquid extraction makes this an uneconomical option for iron ore. Of the remaining processes, selective flocculation and column flotation have both been tested at pilot scale and show potential for slimes treatment.

Since Ansari's (1997) paper there has been a significant advancement in the treatment of fines with the pulsating Wet High Intensity Magnetic Separator, widely referred to as the SLon. This unit reportedly enhances the recovery of -10 µm particles through the pulsation mechanism. Skosana (2011) compared two process routes for the upgrading of a thickener underflow at a particle size of 80% passing 45 µm and Fe grade of 53%. A two-stage SLon process achieved a product grade of 66.5% Fe at a yield of 40%. The complicated alternative process comprising of classification, two stages of wet high intensity magnetic separation and finally five stages of flotation was unable to achieve the product grade specifications at pilot scale.

Of the three factors mentioned above Ansari (1997) believes that surface properties and particularly electrical phenomena dominate fines behaviour. By exploiting the

differences in these properties between the gangue and valuable minerals, selective flocculation can improve the separation efficiency of other processing units such as gravity and magnetic separation.

2.2 The principle of Magnetic Separation

Magnetic separators separate valuable minerals from non-magnetic gangue or other valuables by exploiting differences in their magnetic properties. All materials are affected by a magnetic field. The response of the materials is categorised into two groups, diamagnetics and paramagnetics. The orbital shells of diamagnetic particles are all filled, and there are no unpaired electrons. However, when placed in a magnetic field they are repelled to a point with a smaller field intensity. Quartz and calcite exhibit these characteristics. Paramagnetic materials have unpaired electrons in their orbital shells making them attracted to points of greater field intensity. When the field is removed, the magnetisation is zero. Ilmenite, monazite and hematite are examples of paramagnetics and are concentrated in high intensity magnetic separators. Ferromagnetic materials are a special form of paramagnetism. They are highly susceptible to magnetic forces. Ferromagnetics retain some magnetism when removed from the field and thus require low intensity separators. Magnetite is a ferromagnetic material.

When paramagnetic or ferromagnetic material particles are placed in a non-homogenous magnetic field, they are acted upon by the magnetic force given by Equation 2.1.

$$\overrightarrow{F_m} = \frac{\kappa}{\mu_0} V B \overrightarrow{\nabla \mathrm{B}}$$

Equation 2.1

Where κ = volumetric magnetic susceptibility of the particle;

μ_0 = magnetic permeability of vacuum;

V = volume of a particle;

B= external magnetic field;

$\overrightarrow{\nabla \mathrm{B}}$= gradient of the magnetic field;

In a homogenous magnetic field, in which $\overrightarrow{\nabla \mathrm{B}}$ =0, the force on a particle would be zero.

Several competing forces exist in magnetic separators namely gravity, inertial force, hydrodynamic drag, surface and inter-particle forces (Svoboda & Fujita, 2003). The major competing forces are described mathematically in Table 2.3.

Table 2.3: Competing forces in Magnetic Separation (Svoboda & Fujita, 2003)

Force	Equation	Symbols
Gravity	$\overrightarrow{F_g} = \rho V \vec{g}$	ρ = particle density g = gravitational acceleration
Hydrodynamic Drag	$\overrightarrow{F_d} = 6\pi\eta b\overrightarrow{v_p}v_p$	η = fluid viscosity b = particle radius v_p = The relative velocity of a particle with respect to the fluid

For magnetic separation to be efficient the magnetic force for the magnetic particles must exceed the competing forces while the reverse must hold for the non-magnetic particles. Svoboda & Fujita (2003) however caution against the use of high magnetic forces. With high magnetic forces, particles of various magnetic susceptibility cannot be selectively separated from each other as all the particles respond to the high magnetic force. The magnitude of these forces is dependent on the particle size. Hydrodynamic drag forces are proportional to the diameter of particles while gravity and magnetic forces are proportional to the second and third power of the particle diameter ($F_d \propto b$ while $F_g \propto b^2$ and $F_m \propto b^3$). Arol & Aydogan (2004) reveal that hydrodynamic drag forces dominate at fine particle sizes, gravity forces dominate at coarse particle sizes and magnetic forces at intermediate size ranges.

Table 2.4 illustrates the non-selective nature of magnetic separators. A coarse weakly magnetic particle reports to the same product as a small highly magnetic particle. Thus for efficient separation, the competing forces must be manipulated such that the competing forces affect particles of different sizes differently.

Table 2.4: Effect of particle size on magnetic separation (Svoboda & Fujita, 2003)

Particle Size [a.u.]	**Magnetic Susceptibility [a.u.]**	**Magnetic Force [a.u.]**
10	1	1000
1	1000	1000

The effect of magnetic force and liquid (hydrodynamic) drag on hematite particles at different sizes is presented in Figure 2.1. At 1.06 Tesla hematite particles smaller than 25 µm cannot be recovered as the drag forces dominate magnetic forces. However, increasing the intensity to 1.40 Tesla and 1.52 Tesla decreases the particle size limit threshold to 22 µm and 21 µm respectively, similar to that reported by Song et al., (2002).

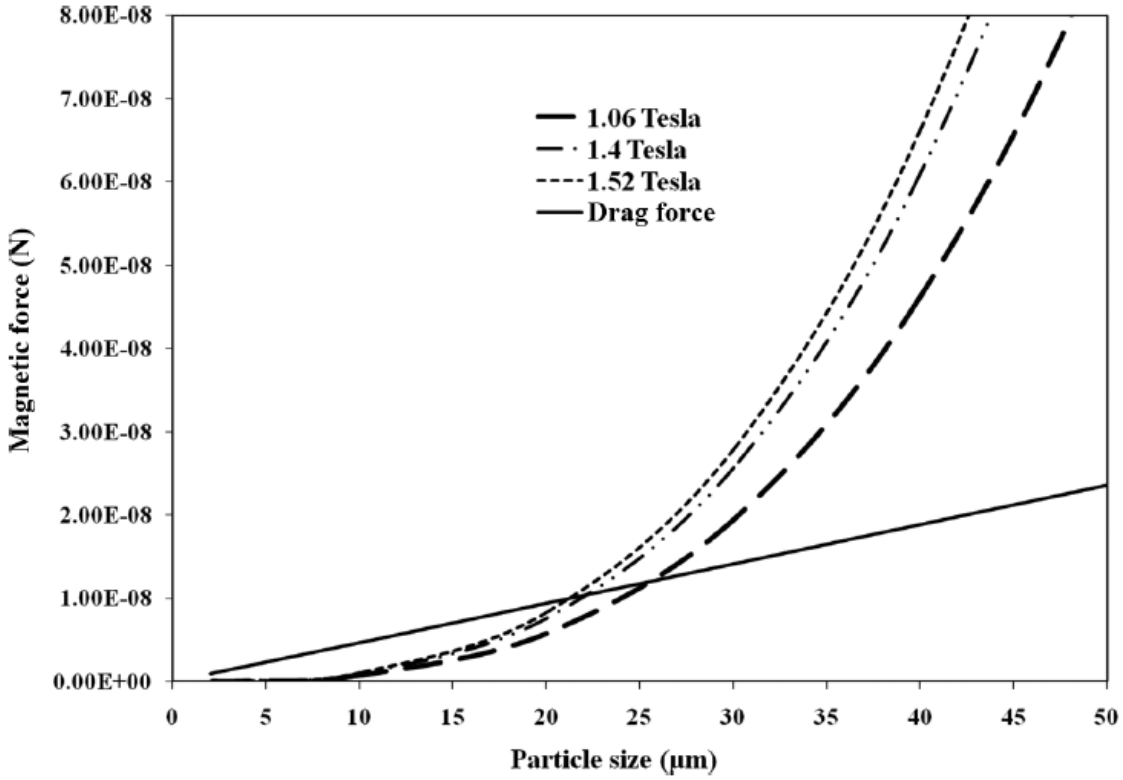


Figure 2.1: The relationship between magnetic force and liquid drag force in a Jones WHIMS for a hematite particle of various particle sizes (Roy, 2012)

The efficiency of treating weakly magnetic particles by magnetic separation can be improved by increasing the magnetic field gradient, field intensity and particle size. The two former ways can be achieved through high gradient magnetic separators and superconducting magnetic separators respectively.

Svoboda & Fujita (2003) reported novel magnetic methods such as magnetic flocculation of fine weakly magnetic material, separation by particle rotation, magnetic flotation (whereby reverse flotation of silica in a magnetic field is conducted) and magnetism assisted gravity separation. Of the various methods mentioned selective flocculation of the desired mineral (thereby increasing the particle size) before magnetic separation will be further discussed since this method can easily be retrofitted into existing magnetic separation plants.

2.3 The principle of Classification

Classification is a technique of separating particles of different shapes, sizes and density into two or more products based on their settling velocities in a fluid medium, which in the minerals processing industry is typically water (Heiskanen, 1993 as cited by Wills, 2006).

A particle falling in a vacuum will reach a constant acceleration, and its velocity will increase indefinitely regardless of its size and density. In a fluid medium such as air or water, resistance increases with velocity until a terminal velocity is achieved in which equilibrium between gravitational and fluid resistance is established, and the particle will fall at a constant velocity.

A particle settling in a fluid medium can either undergo free or hindered settling depending on the fluid's pulp density.

2.3.1 The principle of Classification

Particles falling freely and unobstructed by other particles in a fluid medium will undergo free settling. Free settling occurs in well-dispersed slurries with a pulp density below 15% (Wills, 2006).

Stokes showed that the terminal settling velocity for spherical particles, assuming the drag force to be laminar, can be expressed as:

$$v = \frac{g d^2 \left(D_s - D_f\right)}{18\mu}$$

Equation 2.2

Where v = terminal velocity;

g = gravitational force;

d = particle diameter;

D_s = particle density;

D_f =fluid density;

μ = fluid viscosity;

When a laminar flow prevails but the drag force is dominated by turbulent resistance Newton's equation for terminal velocity, Equation 2.3, can be used:

$$v = \left[\frac{3gd(D_s - D_f)}{D_f}\right]^{0.5}$$

Equation 2.3

Wills (2006), states that Stokes' law is valid for particles with a diameter less than 50 µm and Newton's law is valid for particles with diameters exceeding 5000 µm (0.5 cm). Stokes and Newton's law both indicate that terminal settling velocity is a function of only the particle size and density. However, at coarser particle size ranges (applying Newton's Law) density has a more profound effect on terminal velocity than at finer particle size ranges (applying Stokes' law). Thus for finer particles sizes, specifically slimes, increasing the particle size significantly increases the terminal velocity.

2.3.2 Hindered Settling

With increasing pulp density, the effect of particle crowding becomes more pronounced and decreases the falling settling rate of particles and hindered settling arises. An approximation of the terminal velocity when hindered settling prevails can be developed by modifying Newton's law and taking the increase in turbulent resistance into consideration. The modified Newton's law is given by Wills (2006) as

$$v = k\left[d\left(D_s - D_p\right)\right]^{0.5}$$

Equation 2.4

Where D_p is the pulp density.

Hindered settling reduces the effect of particle size and increases the effect of density on classification. The differences in the separation of particles under either free or hindered settling conditions are illustrated in Figure 2.2.

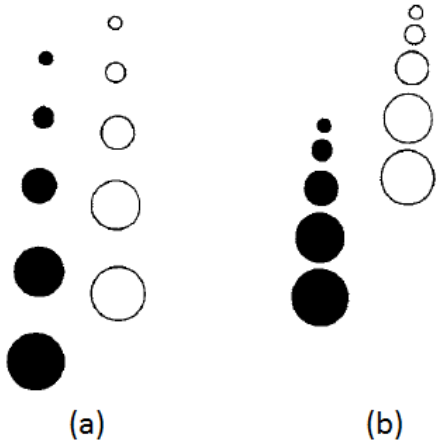


Figure 2.2: Particles settling when conditions prevail for (a) free and (b) hindered settling (Wills, 2006)

Hindered settling classifiers such as teeter bed separators and hydrosizers are used to increase the effect of density on the separation whereas free-settling classifiers use dilute suspensions to ensure particle size dominates the separation (Wills, 2006).

The equations for free and hindered settling all show an increase in terminal settling velocity with increasing particle size. One way of increasing particle size is by flocculation or aggregation which will be explored in the following section.

2.4 Increasing Particle Size through Hydrophobic Flocculation

The preceding sections confirm that increasing particle size will be beneficial for both magnetic separation and classification. One method of increasing particle size that will be explored in this dissertation is flocculation.

Bulatovic (2007) suggests the flocculation process is opposite to that of dispersion. In a dispersed solution, particles of all species can be aggregated into larger particles (flocs) by reducing the inter-particle repulsion forces which can be achieved by several

mechanisms. The aggregation of mineral fines in aqueous suspensions can be achieved by numerous methods such as electrolytic coagulation, polymer flocculation, electro-coagulation, hydrophobic flocculation and magnetic flocculation. Song et al. (2002) report that of all these methods, hydrophobic flocculation creates the most compact flocs that are better able to withstand floc rupturing forces. This is an important issue because compact flocs able to withstand shearing forces during pumping or desliming are critical for flocculation to be applied to gravity and magnetic separation. Thus hydrophobic methods of flocculation such as oil agglomeration, shear flocculation, carrier flotation, selective magnetic aggregation and selective flocculation will be further explored.

2.4.1 Oil-based methods

The intermolecular forces between oil and solid are much larger than those between air and solid. Oil was used in flotation before the use of air flotation with the former not as widespread as the latter due to high cost and environmental pollution (Sivamohan, 1990).

In his review of fines processing Ansari (1997) recommended the use of oil/water emulsions for the treatment of slimes due to their large interfacial areas. Separation of the oil and water phases after emulsification can be done by screening, liquid-liquid extraction or flotation. Table 2.5 lists the techniques for oil /water emulsification and the separation methods of the oil and water phases.

Table 2.5: Oil/Water Emulsification techniques for the treatment of Slimes (Ansari, 1997)

Technique	Description of Technique	Ionic Collector	Oily Collector	Oil Consumption	Conditioning	Method of Separation
Extender Flotation	Oil added with usual collectors. Increases size range of floated particles.	Yes	Yes	0.05-0.5 kg/t	Regular	Flotation
Agglomeration Flotation	High oil addition required for particles with large surface areas. . Oil increases hydrophobic nature of the particles, induces agglomeration and improves collector dispersion. Not efficient at pulp densities above 5%.	Yes	Yes	A few kg/t	Intense	Flotation
Emulsion	Appropriate collectors and fuel oil added to induce aggregation of valuable mineral fines whilst strong stirring is applied.	No	Yes	Up to a few kg/t	Regular	Flotation
Oil Agglomeration	Stable emulsion is not used. Hydrophobic particles concentrated in oil phase with agglomerates as big as 2-5mm in diameter. Agglomerates screened out of aqueous phase.	No	Yes	5-10%	Slow/intense shearing to prevent emulsification	Sizing
Liquid-liquid extraction	No air bubbles required. Oil collects particles themselves with particles as fine as 0.1um extractable. Disadvantage is the loss of the collector to the oil phase.	Yes	Yes	High consumption	Intense	Phase Separation

In addition to oil/water emulsions, an emerging slimes treatment process is selective flocculation (categorised under hydrophobic association) for the particles below 20 microns. The factors that determine the success of selective flocculation is ensuring that the desired mineral is well dispersed in the slurry and it possesses different surface properties to the other minerals present in the sample (Ansari, 1997).

2.4.2 Hydrophobic association

Hydrophobic association is a term Sivamohan (1990) used to categorise various methods of selectively making a specific mineral hydrophobic resulting in flocs of the

desired mineral. Hydrophobic methods of flocculation are shear flocculation, carrier flotation, magnetic surfactant flocculation and hydrophobic selective flocculation. Each of these methods is described below and graphically presented in Figure 2.3.

Hydrophobic flocculation consists of three steps namely, dispersion, selective hydrophobic flocculation and the separation of the flocs from the dispersed particles.

- Dispersion is achieved through the use of dispersants and pH adjustment to prevent mineral fines from heteroflocculation which is detrimental to separation efficiency.
- Selective hydrophobization is achieved by the addition of collectors which adsorb onto the desired mineral resulting in hydrophobic particles. During selective hydrophobization the kinetic energy required to overcome the energy barrier separating particles is mechanically imparted by stirring, thereby facilitating the collision and growth of flocs.
- The separation of the flocs from the dispersed slurry is achieved by various methods such as screening, magnetic separation and flotation (Song and Lu, 2000). Flotation is the most common separation method as the hydrophobic surfaces are already present. Screening and magnetic separation require big compact flocs and magnetic flocs respectively.

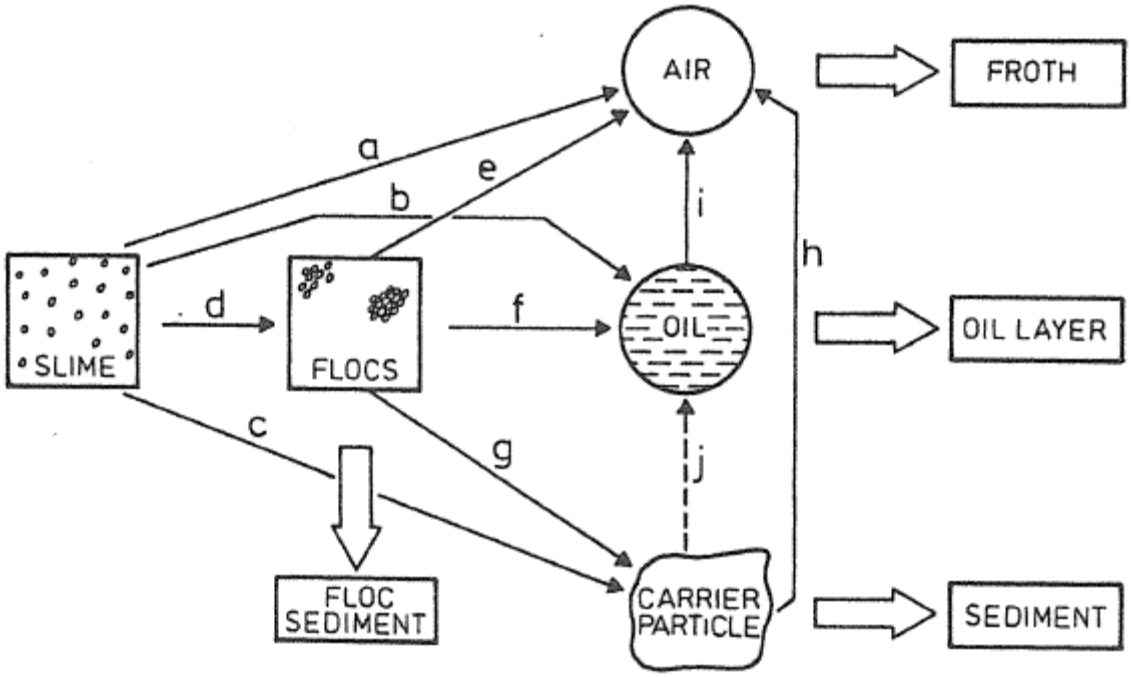


Figure 2.3: Schematic representation of surface-based concentration methods (physiochemical methods): a = froth flotation; b, d-f = oil extraction and or spherical agglomeration; c = carrier separation; d = selective flocculation/hydrophobic association; d-e = aggregate flotation; c-h,c-j,c-j-i = ultra flotation; b-i, d-f-i=oil flotation (Fuerstenau et al., 1979 cited by Sivamohan, 1990)

2.4.2.1 Shear Flocculation

In shear flocculation, a mineral particle is made hydrophobic by the adsorption of collectors under high shear conditions. Important factors that affect shear flocculation are particle size, hydrophobicity, surface charges and intensity of agitation. The advantages of shear flocculation as cited by Sivamohan (1990) are listed below:

- Aggregates are stable and can withstand the disruptive turbulent energies at high shear rates due to the strong hydrophobic energy. The aggregates created by a polymer are weaker and easily broken up by intense agitation.
- The collector can be used as both an aggregating and flotation reagent. The flotation of shear flocs has been successfully achieved in industry.

- Shear flocs can be easily separated from the slurry by sedimentation as shown by the work of Read and Hollick (1976) as cited in Sivamohan (1990)
- The surfactant addition may not be high, and even at high dosages the suspension remains dispersed
- High dosages of pH regulators, modifiers and depressants are not required to cause shear flocculation
- Flotation after shear flocculation is possible due to foam prevention, increasing flotation rate and increasing recovery without loss in grade.

For any surface-based methods, including hydrophobic association, to be successful selectivity between the different minerals which possess similar surface responses is critical (Sivamohan, 1990). This can be achieved by creating a difference in the surface charge by the addition of modifying agents. Dispersion of the suspension is also critical, and hence it is important to select a dispersant that has no chemical affinity towards the mineral to be aggregated or separated.

2.4.2.2 Carrier Flotation

Carrier flotation is similar to shear flocculation except in the case whereby the carrier particles (the coarser particle) are of a different mineral from that of the finer particles. The ultrafine coating of coarser particles results in the increased rate of aggregation while the shear rate required to cause aggregation is also much less compared to that of ultrafine aggregation. The improvement can be attributed to the increased probability of adhesion and collision. The addition of oils such as tall oil and kerosene to strengthen the aggregates is also common in carrier flotation. If the carrier particle is of a different mineral to the ultrafine material, separation of the carrier particle from the ultrafines will be necessary.

Song et al. (2002) report that carrier flotation was commercially applied to the purification of kaolin by removing anatase fines. This was achieved by the adhesion of anatase fines on coarse calcite thorough hydrophobic flocculation followed by flotation of the coated calcite.

2.4.2.3 *Selective Magnetic Aggregation with or without the aid of hydrophobicity*

Magnetic induction can achieve the aggregation of ultrafine ferromagnetic and paramagnetic minerals under high intensity and super conducting systems respectively (Collins and Read, 1971; Lawver and Hopstock, 1974 as cited by Sivamohan, 1990). Without the use of an appropriate dispersant, entrainment of non-magnetic particles will occur. In addition, the flocs created are weak and unable to withstand disruptive forces.

The work of Parsonage (1977) and cited in Sivamohan (1990) indicated the potential to concentrate non-magnetic minerals from each other by exploiting the differences in their densities. In this approach, paramagnetic and ferromagnetic liquids under a magnetic field will have a density different from its natural density. The density of the liquid changes with the intensity of the field. This method can be used to separate non-magnetic minerals with density differences as low as 0.1g/cm^3, although +20 µm particles are required. Sivamohan (1990) suggests that upscaling would be problematic. Svoboda (2003) reports that numerous ferrohydrostatic separators (FHS) using this principle have been designed for the separation of non-ferrous metals from automobile scrap and for the recovery of gold, PGMs and diamonds. Although the FHS has been used industrially, wide-scale implementation has not occurred. The availability of cost-effective environmentally and user-friendly magnetic liquids that can easily be recycled could potentially improve its implementation.

Further to his research Parsonage (1984a) as cited by Sivamohan (1990) developed a selective magnetic aggregation technique by incorporating hydrophobic association. The non-magnetic minerals and metallic particles were coated with a specially prepared magnetite colloid and thereafter separated by magnetic separation. Selectivity was achieved by controlling the zeta potential and hydrophobicity of the minerals. Singh et al. (2015) also applied a similar approach with the addition of a colloidal magnetite and oleate colloidal coating. The effect of the concentration of colloidal magnetite, pH and magnetic field strength were investigated. At the optimal parameters, the recovery of -100 µm particles was increased from 61.6% to 72% whilst maintaining the product grade at 62% Fe. Disadvantages of this process are the

treatment of +75 µm particles and the excessive adsorption of the surfactant by the magnetite colloids.

In addition to the hydrophobic association mechanisms described above for increasing particle size, selective flocculation coupled with shear flocculation appeared to be the most suitable method applicable to gravity and magnetic separation. These solid-solid separators would require dense and compact flocs capable of withstanding the large shearing forces expected in these units as well as pumping systems.

2.4.3 Challenges with Hydrophobic association

Although each method described above has its benefits, there are concerns regarding their implementation. Oil-based methods are expensive and raise environmental pollution concerns. The other hydrophobic processes such as carrier flotation would require at least two processing steps namely the separation of the carrier particles from the gangue and thereafter separation of the carrier particle from the desired mineral. This introduces complexities and costs into the beneficiation process especially if magnetic and gravity units are to be considered as solid-solid separators. Magnetic flocculation and hydrophobic association with magnetite colloids have restrictions regarding particle sizes with the former requiring +20 µm particles and the latter +75 µm particles. The size restrictions in conjunction with the weak flocs produced by magnetic flocculation limits the application of these two methods. The lack of process selectivity and high energy costs required for the sufficient hydrodynamic conditions in shear flocculation have limited the application of this method (Bakker et al., 2002 as cited by Forbes, 2011). Although selective flocculation is favoured, it is a sensitive process with various parameters affecting its efficiency. This approach with its sensitivities is discussed in the following section.

2.5 Selective flocculation

Selective flocculation utilises the differences between physical and chemical properties of the various mineral species in a mixed suspension. It involves the

aggregation of the desired mineral from a mixture of minerals using the bridging mechanism. Surfactants (collectors) or polymers are typically used to aggregate the desired minerals with polymers possessing higher molecular weights compared to the former. The selective flocculation process comprises of four stages namely dispersion of particles, selective adsorption of flocculent on the desired mineral surface with the subsequent formation of flocs, the growth of flocs through conditioning at low shear and finally solid-solid separation (Mathur et al., 2000).

Selective flocculation is an industrially established process for the concentration of non-magnetic taconites and copper-bearing minerals. Ansari (1997) reports that a three-stage selective flocculation process applied to a Cu ore from the Democratic Republic of the Congo, on which flotation was almost completely ineffective, about 20% Cu grade at 65% recovery was attained. Selective flocculation has also been applied to the beneficiation of potash ore in Cominco Limited, Saskatchewan (Yu and Attia, 1987 as cited by Forbes, 2011). In the beneficiation of potash ore at Cominco Limited, the undesirable clay minerals are selectively flocculated, and the valuable dispersed sylvite particles are removed from the flocculated clay by flotation. The flocculation of gangue minerals reduces gangue entrainment in the sylvite flotation concentrate.

Selective flocculation has been applied to slimes from mines across the world at a laboratory scale as presented in Table 2.6. The flocculent, separation technique and final product grades and recoveries are specified. In most cases, improved grades and recoveries were achieved, but besides the good results, it is unclear if these mines have applied these processes industrially as in the case of Tilden (Haselhuhn et al. (2012).

Although selective flocculation has been successfully applied at industrial scale, certain factors have prohibited its widespread application. A few of these factors are presented in Table 2.7 with potential solutions cited by some researchers.

Table 2.6: Industrial Application of Selective flocculation to Iron Ore (as cited by Abro et al., 2013)

Mine	Location	Main minerals	Method of Selective flocculation	Reference
Tilden Mines*	USA	Hematite, Martite, Goethite, Magnetite, Siderite Gangue: Chert, Ankerite, Feldspar, Chlorite	Flocculation by starch followed by reverse flotation. Upgrades feed from ~35%Fe to 44%Fe at a recovery of 85-90%	Colombo (1986)
Wadi Sawawin Mines* (Investigated by Bureau's Pilot plant in the USA but it is unclear if it has been implemented)	Saudi Arabia	Hematite; Magnetite; Quartz; Chlorite; Calcite; Apatite	Fine Grinding with STPP (0.15-0.2kg/ton) to 75% -75µm and starch addition of 0.15-0.2kg/ton Reverse Flotation of silica. Feed upgraded from 42.5% Fe to 59.4% at 61.5% recovery.	Subramanian and Natarahan (1991)
Camdag Mines	Turkey	Hematite Gangue: calcite, ankerite. clinochlore, quartz	Selective flocculation (1kg/ton sodium silicate; 50g/ton Cornstarch) followed by flotation. Upgraded from 46.6% Fe to 53.7%. Recovery not specified.	Kafali et al. (1988)
Goldsworthy Mining Ltd*	Finucane Island, Port Hedland in Australia	Hematite, Goethite, quartz, kaolinite	Lab scale STPP (10ppm); Wheat starch (50ppm)	Weissenborn (1993)
Kudremukh Iron Ore Mines (shut down in 2005 for environmental conservation)	Karnataka, India	Goethite, Hematite, Magnetite, Quartz	Lab: Anionic PAA (0.2kg/ton) Dispersant: Unspecified	Khangoankar and Balasubramani (1993)

*Still active

Table 2.7: Problems associated with the industrial application of selective flocculation

Problem	Potential Solution
Complex ore mineralogy	-
Poor liberation or smearing (slime coating) of minerals during the grinding effect	Use selective dispersants. The addition of a dispersant in the mill has been shown to reduce cross-contamination (Frommer and Colombo, 1966 as cited in Drzymala & Fuerstenau, 2014). However, Moudgil and Mehta, 1994 cited in Mathur et al. (2000) showed wet grinding with sodium silicate and NaHMP did not benefit selectivity. Mathur et al. (2000) report the effect of grinding on selectivity is the least understood parameter in selective flocculation.
Difficulties in controlling surface properties of minerals and preventing heteroflocculation.	Lower polymer dosages to prevent adsorption onto surfaces of gangue minerals. However, lower dosages affects floc properties and separation efficiencies (Mathur et al., 2000) Use site blocking agents aka dual polymer flocculation (Abro et al., 2013). These are lower molecular weight versions of the same polymer used to induce flocculation. These site blocking agents adsorb onto all the mineral surfaces thereby preventing adsorption of the flocculent on gangue minerals. (Forbes, 2011) Design flocculent molecules with a configuration compatible with the surface molecular structure of the desired mineral (Mathur et al., 2000).
High reagent costs	Use temperature responsive polymers that can change from hydrophobic to hydrophilic at temperatures above and below their critical solution temperature. These polymers can be used as a flocculent and flotation collector. The hindrance to the application of temperature responsive polymers is the energy costs required to heat up water, although pumping and flotation pulps temperatures can easily reach 37°C and 28°C respectively (Forbes, 2011).

Table 2.7: Problems associated with the industrial application of selective flocculation (Contd.)

Problem	Potential Solution
Water quality (dissolved ion interferences) - affects surface properties of particles (Haselhuhn et al., 2012; Drzymala & Fuerstenau, 2014)	Temperature responsive flocculation is less sensitive to solution chemistry and shear (Forbes, 2011). Requires more work to determine its efficacy and commercial viability.
Entrainment and physical entrapment of gangue minerals in the voids of the flocculated mineral (Mathur et al., 2000)	Mechanical agitation by stirring or ultrasound. The flocs are sheared to re-disperse them and thereafter re-flocculated.
Flocculent preparation. Hanumantha Rao & Narasimhan (1985) and Gururaj et al. (1983), as cited in Hanumantha Rao & Narasimhan (1985), conducted similar selective flocculation tests on the same material. The former prepared starch by a rapid heating and cooling method and achieved good results whilst the latter prepared starch through the causticizing method followed by homogenisation with a blender at 16 000rpm and achieved poor results.	Ensure a standard preparation method is applied to the specific flocculent being used.

2.5.1 Selective flocculation using Microorganisms

Poorni and Natarajan (2013) successfully flocculated hematite from an artificial hematite kaolinite mixture using bacteria. The bacteria are grown in the presence of each mineral such that the metabolic products selectively flocculate the hematite and disperse the kaolinite. A number of other investigators have used this approach in selective flocculation and flotation of other mineral mixtures such as pyrite and chalcopyrite, pyrite and sphalerite; galena and sphalerite; pyrite, quartz and calcite amongst others (Patra and Natarajan, 2003, 2004, 2008; Chandraprabha and Natarajan, 2004; Santhiya et al., 2000, 2001). Although successful with artificial binary mineral mixtures this approach has yet to be tested on slimes from industry where

multi-mineral samples may complicate selective flocculation. In addition, deionised double distilled water is commonly used in these experiments with the effect of process water on the flocculation and flotation process neglected. However, should this approach be successful it has great practical relevance due to its cost-effectiveness and minimal environmental impact.

2.5.2 Selective flocculation using polymers

The aggregation of fine particles employing polymers is utilised in a wide variety of industries including paper making, water treatment, biotechnology and minerals processing such as hematite, phosphate (Parsaei et al., 2006), bauxite (Wang et al., 2011) and chromite (Panda et al., 2014).

Bulatovic (2007) reveals that organic polymers used as depressants are also used as flocculents when their chemical structure is altered. Bulatovic (2007) lists hydrolysed starch and modified polysaccharides as polymers used in flocculation. An extract from his list is presented in Table 2.8. He also reports that selective flocculation of iron oxides is achieved using starch and caustic soda (a silica dispersant) at pH 10.5 with the flocs separated from fine silica using a thickener.

Table 2.8: List of polymers used in flocculation (Bulatovic, 2007)

Category	Chemical/polymer	Class
Flocculants	1. Polyacrylamides	Non-ionic
	2. Acrylamide/sodium acrylate co-polymers	Anionic
	3. Sodium or ammonium polyacrylates	Anionic
	4. Acrylamide DMAEM[a] or DMEA[a] quat co-polymers	Cationic
	5. Acrylamide DADMAC co-polymers	Cationic
	6. Polyethylene oxide	Non-ionic
	7. Guar gum	–
	8. Hydrolyzed starch	–
	9. Acrylamide/sodium 2-amps co-polymers (sulfonate)	Anionic
	10. Modified polysaccharides	–
	11. Ferro salts	–

Sivamohan (1990) further classifies polymers as physisorbing and chemisorbing. In chemisorption (chemical adsorption) a chemical bond is created between the polymer

and particle surface which is an irreversible process. In physisorption (physical adsorption) intermolecular forces such as the van der Waals forces are responsible for adsorption of the polymer onto the particle surface. Physisorption is thus reversible (IUPAC, 2002).

The advantages and disadvantages of physisorbing and chemisorbing polymers are described in Table 2.9 below.

Table 2.9: Types of Polymers (Sivamohan, 1990)

Type of Polymer	**Main Examples**	**The interaction between the polymer and the mineral surface**	**Advantage/Disadvantage**
Physisorbing	Non-ionic and ionic Polyacrylamide type polymers Non-ionic polymers, eg polyvinyl alcohol and polyethylene oxide	• Electrostatic forces • Hydrogen bonding forces	**Disadvantage:** • Acts on many mineral surfaces and thus not selective unless surface properties carefully controlled. • Unsuccessful application at pilot level for different mineral applications
Chemisorbing (Incorporates functional groups capable of covalent bonding with specific cations)	Carboxylate, Iminodiacetate, diethanolamine, xanthate		**Advantage:** • More selective • Successful application at pilot scale

2.5.2.1 Starch

According to Sivamohan (1990), starch and polyacrylamide have been shown to flocculate iron oxide minerals selectively. Weissenborn et al. (1994) claim polyacrylamides are selective for synthetic mixtures of hematite and quartz in deionised water but are not effective on slimes where they behave as bulk flocculents. Extensive research has been undertaken in polymer flocculation using starch to flocculate hematite selectively and this concept will be further explored in this section.

Cornstarch is typically used in industry as an iron ore depressant due to its wide availability. However, starches derived from vegetables such as cassava, potato, wheat, rice and arrowroot have also been used as depressants.

Starches comprise mainly of amylase and amylopectin (98-99%) with the balance being fibres, mineral matter, oil and protein. The amylase and amylopectin ratios are important factors during polymer flocculation. Cornstarch is insoluble in water due to the hydrogen bonds connecting amylase and amylopectin. Two approaches can be taken to solubilise the cornstarch, namely heating it in water at 56°C or adding NaOH (Araujo et al., 2005). Filippov et al. (2014) refer to these two methods as thermal gelatinisation and alkali gelatinisation. Araujo et al. (2005) indicate that the alkali approach is preferred industrially due to the hazards of hot water. The effectiveness of alkali gelatinisation is strongly dependent on the starch to NaOH ratio and the dissolution method (Broome et al., 1951& Iwasaki and Lai, 1965 as cited in Filippov et al. 2014).

The maximum adsorption of all starches (soluble starch, corn starch, potato starch and rice starch) tested by Kar et al. (2013) occurs between a pH of 5 to 9. Starch can depress both quartz and iron oxides. Kar et al. (2013) attribute the depressant action of starch to the coating of a hydrophobic surface with a hydrophilic film to prevent the attachment of air bubbles in flotation. The high electronegativity and large size of amines make starch ionise easily in water and react with the silica particles at slightly alkaline pHs. At alkaline pHs the starch adsorbed on the quartz particles, desorb in the presence of a suitable collector concentration.

Different adsorption mechanisms of starch adsorption onto oxide surfaces are reported in literature with Pinto et al. (1992 as cited in Filippov et al. 2014) stating hydrogen bonding as a mechanism of starch adsorption on hematite, calcite, apatite and quartz. Kar et al. (2013) purport both hydrogen bonding and chemical interaction as the adsorption technique. The depressing ability of starch on hematite is attributed to the interaction of the hydroxyl groups in starch with the OH group on the hematite surface as illustrated in Figure 2.4.

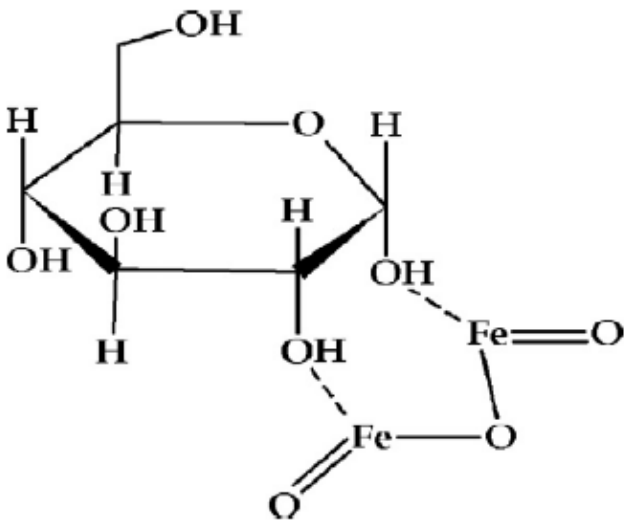


Figure 2.4: The structure of hematite and starch interaction (Kar et al., 2013)

While the depressing mechanism of starch on hematite has been explained in literature, the mechanism of flocculation of ultrafine hematite particles using starch is not clear.

2.5.2.2 Adsorption of Polymers and the process of Flocculation

Upon introduction of the polymer into the slurry the polymer will either selectively or non-selectively attach to solids. In cases where the adsorption is complete and no polymer remains in solution, the attachment is irreversible, and desorption will not occur. However, if the solution contains other potential sources for adsorption, competitive adsorption may cause detachment of the polymer chains previously adsorbed (Gregory and Barany, 2011).

According to Hoggs et al. (1993 as cited in Abro, 2009), the process of polymer flocculation is characterised by three stages as graphically illustrated in Figure 2.5. The polymer introduced into the solution will disperse and loosely binds a number of particles into highly porous aggregates with a large effective radius and thus settles rapidly (Figure 2.5a). Subsequent to further mixing, particles become entrapped to create compact aggregates with smaller effective radius thereby extending settling

time (Figure 2.5b). Continued agitation will rupture developed flocs yielding smaller flocs (Figure 2.5c).

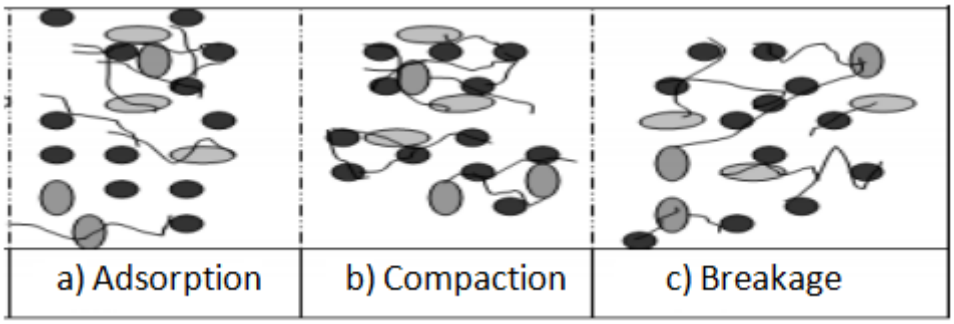


Figure 2.5: Flocculation Stages (Hoggs et al., 1993 as cited in Abro, 2009)

The mechanism governing the attachment of a polymer to a solid surface has been described in literature by many researchers. Various mechanisms have been proposed including the electrostatic patch mechanism, hydrogen bonding, hydrophobic interaction, ion binding, surface modification and bridging mechanisms (Gregory and Barany, 2011; Wang et al., 2014; Somasundaran and Runkana, 2003).

Charge neutralisation, whether simple or patch, reduces the charge density of the particle surfaces by using polymeric flocculents such as polyelectrolytes. The reduction in the surface charge density enables particles to approach one another and attract by the van der Waals forces. In simple charge neutralisation, flocculation is not sensitive to the molecular weight of the polymer. Patch neutralisation usually refers to cationic polyelectrolytes of high charge density that once adsorbed onto particle surfaces results in regions on the particle surface of positive charge spaced with regions of bare or negative charges. Attraction between approaching particles with adsorbed polyelectrolyte results when these positive and negative regions are aligned (Birdi, 2002; Gregory and Barany, 2011).

The rate of flocculation by the bridging mechanism is magnitudes higher than charge patch neutralisation or simple neutralisation. The rate of flocculation by these methods is described by Somasundaran and Runkana (2003) as:

Bridging mechanism>>charge patch neutralisation>>simple charge neutralisation

The mechanism governing the interactions between the polymer and solids is greatly influenced by the conformation of the polymer before and after adsorption. Polymers with a stretched and linear chain have a conformation that is termed extended thereby aiding the bridging mechanism. Polymers with flattened or coiled conformations agglomerate particles by either charge patch neutralisation mechanism or surface modification mechanisms. (Mathur et al., 2000; Weissenborn, 1993 cited in Abro, 2009). In surface modification mechanisms the surface of a particle is entirely covered by the flocculent and agglomeration of particles occurs due to the interaction between the adsorbed flocculent molecules.

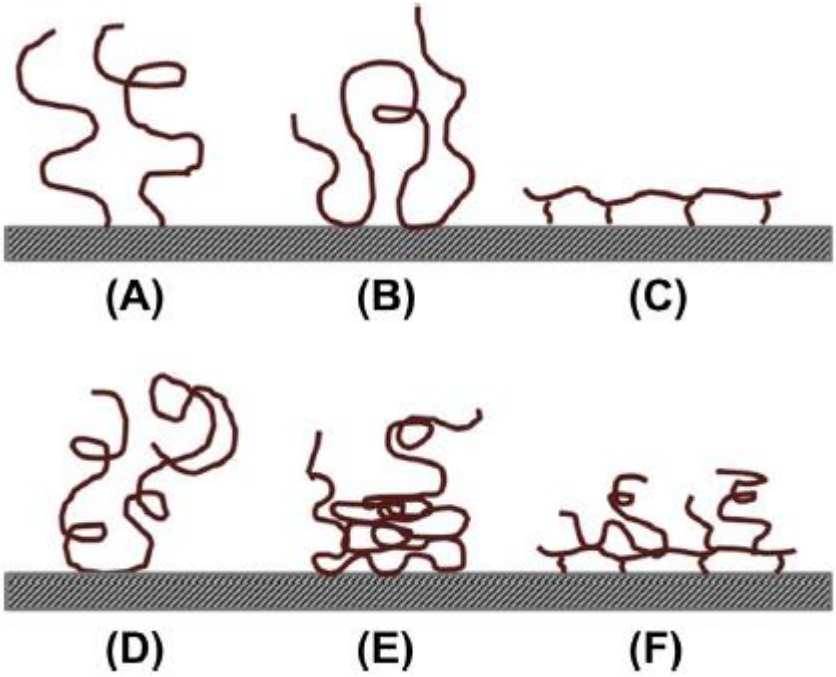


Figure 2.6: Possible polymer conformations subsequent to adsorption (Alagha et al., 2013 cited in Wang et al., 2014)

The interactions between the polymers, solids and water are graphically described above in Figure 2.6 by Alagha et al. (2013) cited in Wang et al. (2014). Polymers strongly attracted to the solid surface will collapse on the surface of the solid (Figure 2.6 c and f). A weak attraction between the solid and polymer encourages the polymer to extend away from the attachment site (Figure 2.6 a, b and d). Polymers with a stronger affinity for water than for the particle surface will extend into the water maximising its surface contact (Figure 2.6 a, b and d). Conversely hydrophobic polymers reduce their exposure to water by creating mushroom-like conformations

(Figure 2.6 f). The excessive attraction of the functional groups within the polymer chain will create loops and coils yielding a collapsed conformation (Figure 2.6 e). Highly charged polymers are resistant to changes in their polymer conformations (Figure 2.6 a and c).

Polymer bridging can be improved by:

- Using linear chained polymers with high molecular weights
- Using appropriate polymer dosages as excess polymer causes restabilisation
- Using certain metal ions at an appropriate ionic strength
- Using site blocking polymers. In site blocking a low molecular weight polymer or nanoparticles are introduced prior to the polymer and limit the number of adsorption sites on the solid surface thereby encouraging the polymer to take on a more extended conformation, as in (b) in Figure 2.7, as opposed to the less extended conformation (a) in Figure 2.7 (Gregory and Barany, 2011).

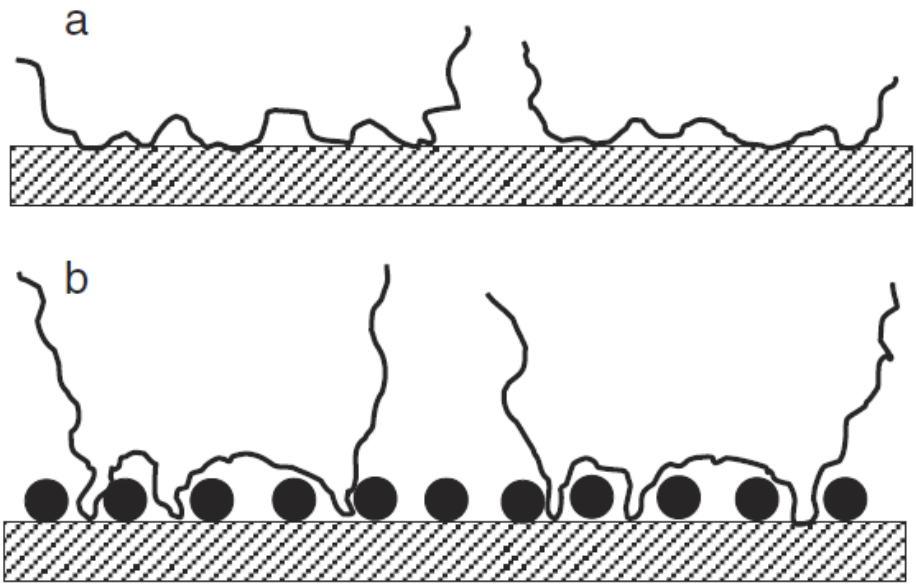


Figure 2.7: (a) High Molecular Weight (MW) polymer in the absence (a) and presence (b) of a site blocking low MW polymer (Brotherson and Deng (2008) cited in Gregory and Barany (2011))

2.5.2.3 Factors affecting Selective Polymer Flocculation

Numerous studies have been conducted on starch selective flocculation to determine the effect of process variables such as pH, concentration of dispersants, types and concentration of polymers, stirrer speeds and times, ratio of amylopectin to amylose, molecular weights and chain structures or conformation of polymers, sequence of reagent addition and water chemistry (Abro et al., 2013, Haselhuhn et al., 2012; Ma, 2012; Gregory & Barany, 2011; Mathur et al., 2000; Weissenborn, 1996; Hanumantha Rao & Narasimhan, 1985). In most cases, selective polymer flocculation was tested on artificial mineral mixtures and in a few cases successfully applied to tailings at a laboratory scale. Roy (2012), Yin et al. (2011), Arol and Aydogan (2004) and Pascoe & Doherty (1997) also studied the effect of these parameters on hematite flocculation using sodium oleate.

The rate of adsorption of polymers onto mineral surfaces is dependent on the polymer properties such as dosage; molecular weight; nature and concentration of functional groups; and configuration. The properties of the mineral such as surface charge and oxidation state and solution properties such as ionic strength, temperature and intensity of agitation also affect the kinetics of adsorption (Somasundaran, 1978).

Warren (1992) as cited by Pascoe and Doherty (1997) and Song et al., (2002) suggest flocs produced by polymer flocculation are weaker than flocs produced using flotation collectors such as sodium oleate. Sodium oleate will be explored in Section 2.5.3, and thus the factors that affect both polymer flocculation and selective flocculation using sodium oleate will be further discussed, namely:

- Dispersion
- pH and Electrolyte Concentration
- Type of Flocculent
- Effect of Reagent Sequence Addition
- Particle Size Effects
- Effect of Solids Concentration
- Effect of Water Quality

2.5.2.3.1 Dispersion

Dispersion of particles in an aqueous solution can be achieved in one of two ways, through either electrostatic and /or steric stabilisation. The former is usually achieved through the use of sodium silicate or sodium hexametaphosphate. These dispersants induce a high negative surface charge on the particles. Steric stabilisation on the other hand, occurs with polymeric dispersants such as polyethylene oxide and polyvinyl pyrrolidone which adsorb at the interface and prevent coagulation. Polymeric additives that are charged, such as polyacrylates, exhibit both methods of stabilisation (Mathur et al.,2000).

The effect of dispersion on selective flocculation with addition into a mill and after the mill has yielded conflicting results among researchers. Mathur et al. (2000) reveal the change in the surface properties of particles during grinding is not clear and requires further research. Since slimes generated from a hematite processing plant is typically treated by selective flocculation, the effect of grinding and sequence of dispersant addition will not be discussed here.

Sodium silicate is widely used in the iron ore industry for dispersing siliceous gangue minerals. However, for alumina bearing gangue minerals such as kaolinite Ma (2011) determined sodium hexametaphosphate as a more effective dispersant.

Zhan (1999) claims polymers used as flocculents can also be used as dispersants depending on the molecular weight (MW). Polymer flocculants are characterised as linear conformations with high MW (10^6) while dispersing polymers are branched and low MW (10^4). However, at high concentrations polymers may cause dispersion.

2.5.2.3.2 pH and Electrolyte Concentration

The major process parameters affecting polymer conformation (and hence successful flocculation) is pH and electrolyte concentration (Abro, 2009 and Mathur et al., 2000). These variables affect the affinity of the polymer for solids and solutions. The range in these parameters and the effect on polymers are presented in Table 2.10.

Table 2.10: Effect of pH and electrolyte concentration on polymer adsorption (Abro, 2009)

Parameter	**Effect on polymer**
High anionic concentration (addition of NaOH or polyacrylate)	Higher repulsive forces in segments of polymer chain facilitating extension of the polymer chain and dispersion of the polymer
The decrease in cationic concentration (addition of copolymers or decrease in ionic strength)	Repulsive forces decrease and dispersion of polymer decreases
High pH	The solubility of the polymer increases and adsorption decreases

The surface charge of particles, the surface of hydroxyl groups and flocculent conformation can be altered with variation in pH. Rivashanker et al. (1995) cited in Zhan (1999) reports selective adsorption of starch onto hematite in a quartz-hematite system by controlling the pH at 10.5. At this pH, quartz particles have a higher negative charge as compared to hematite due to the difference in their point of zero charge. Starch experiences less repulsion from hematite and thus preferentially adsorbs onto the hematite particles.

Somasundaran and Ramachandaran (1988) cited in Mathur et al. (2000) indicated that the flocculation of alumina was enhanced by raising the pH of the solution from 4 to 10 compared to flocculation starting and controlled at a pH of 10. They attributed the improvement to the stretching of the adsorbed polymer chains in PAA, i.e. altering the polymer conformation.

2.5.2.3.3 Type of flocculent

The choice of flocculent to use in selective flocculation is influenced by three factors (Mathur et al., 2000):

- constituent minerals,
- the desired nature of the flocs such as their size, strength and density
- the separation of flocs from the slurry.

The solid-solid separation processes associated with selective flocculation requires flocs to be large, strong and in some instances dense depending on the solid-solid separator. For example, flocs subjected to magnetic separation will need to be large whilst gravity separation requires dense and large flocs. In addition, the flocs would need to be compact in order to withstand shearing forces that will be experienced during process handling such as pumping and desliming.

The use of anionic polyacrylamides to flocculate various minerals are presented in Table 2.11. Tapioca flour, polyacrylamides and polystyrene sulfonate have been successfully used at a laboratory scale to selectively flocculate hematite from quartz.

The selection between high and low molecular weight polymers remains undecided with high molecular polymers (5 x10^4 to 9 x 10^5) producing stronger and fast settling flocs, but Sivamohan (1990) indicates these polymers are inherently unsuitable for selective flocculation. Hoggs (1993) as cited in Abro (2009) revealed increased flocculation rates of 10-100 times upon doubling the mean molecular mass. Higher molecular masses results in longer chains that can penetrate the double repulsive layer of particles and increase the collision radius. Polymers of low molecular mass <10^5 are better suited as dispersants rather than flocculents (Mathur et al., 2000). Khan (1985) as cited by Abro (2009) states the efficacy of polymer bridging to be dependent on particle size and polymer molecular weights. Khan (1985) recommends the use of low molecular weight polymers for small particles and high molecular weight polymers for coarse particles.

Entrainment of non-flocculated particles has been observed by Yarar and Kitchener (1970 a, b) as cited by Sivamohan (1990). Fortunately, this problem can be overcome by

- slurry dilution
- sufficient dosage to ensure minimum floc strength is achieved
- gentle agitation of flocs to release entrained particles
- repeated dispersion and re-flocculation

Table 2.11: Selective flocculation separation achieved with various mineral combinations (Sivamohan, 1990)

Flocculent	Mineral Combinations	Mineral Flocculated	Pulp Density (%)	Recovery (%)	Grade (%)	Stages
Tapioca Flour (cooked at 90°C with NaOH)	Hematite; Quartz	Hematite	10-20	82	67	Sel Floc; two stage desliming; flotation of quartz
Polyacrylamide types A100, A130, A150, A70, A80, P250	Quartz; Calcite	Calcite	3-5	89	15	Two Stage
	Quartz; Galena	Galena		100	65	One Stage
	Calite; Galena	Galena		92	67	
	Quartz; Galena; Calcite	Galena		98	69	One Stage
Polyacryl amide types A100, A130, A150, A70, A80	Hematite; Quartz	Hematite	16	79	83	Four Stages
Tapioca Flour (cooked at 90°C with NaOH)	Hematite; Quartz coground	Hematite	10	91	67	Three Stages
	Non-magnetic Fe ore	Hematite		69	55	
Modified chelating polyacryl amide	Copper Ore	Cu minerals	10	62	20	Four Stages
Poly(ethylene oxide) + surfactants	Copper Ore	Cu minerals	10	74	27	More than 1 stage
Polyacryl amide A100	Quartz; Galena	Galena		68	50	4 Stages; Flotation after flocculation
	Quartz; Chalco	Chalco		68	26	
	Quartz; Sphalerite; Calcite	Sphalerite		68	40	
Polystyrene sulfonate	Hematite; Quartz	Hematite	5	90	70	Two Stage
Hydroxypropy cellulose	Quartz; Chalco	Chalco		95		
Ionic polymers + collectors	Baryte; Sphalerite	Sphalerite		86	54	One Stage
Anionic polyacryl amide	Apatite; Calcite; Quartz	Apatite	4	73	25	Elutriation

An improvement to the purely polymer flocculation method is the combination of both surfactants and polymers. The desired mineral is made hydrophobic with the addition of a surfactant before the addition of the polymer for flocculation of the hydrophobic mineral. The key is keeping all the undesired minerals hydrophilic. The use of both surfactants and polymers makes this process less sensitive to water quality, pH and other chemicals than the use of surfactants only. However, if the desired level of selectivity depends on the fine control of the ionic environment, then this process is not recommended by Sivamohan (1990).

Ansari (1997) recommends the treatment of minerals with a conventional flotation collector before addition of flocculent. The selective adsorption on specific minerals provides the differentiation in surface properties required for successful selective flocculation. The flocculent will then only adsorb on the hydrophobic surfaces resulting from the addition of the collector. This technique would be simpler, cheaper and more widely applicable than using specially prepared polymers.

In a system where pure mineral components are inert to the selected polymer Mathur et al. (2000) interestingly revealed the possibility of inducing selective flocculation by coating the desired mineral with another mineral known to interact with the polymer. They cited the work of Mathur (1996) in which flocculation of dolomite was possible due to the coating of palygorskite. This clay mineral coated the surfaces of the dolomite and adsorbed onto the flocculent polyethylene oxide inducing flocculation.

2.5.2.3.4 Effect of Reagent Sequence Addition

Ma (2012) investigated the sequence of starch and dispersant addition and found that for an artificial mineral mixture of quartz and hematite that flocculation of hematite is not affected by pre-conditioning with starch prior to dispersant addition. Dispersant addition before that of starch resulted in fewer adsorption sites on the hematite thereby limiting the starch adsorption and thus flocculation. However, the testwork was conducted on a pure hematite sample making the extrapolation to multi-mineral samples invalid. It is likely with more complex ores that dispersant addition before

starch addition will be required to prevent heteroflocculation and reduce starch dosages.

2.5.2.3.5 Particle Size Effects

Testwork conducted by Arol and Aydogan (2004) indicated the potential to effectively recover ultrafine magnetite particles after size enlargement by polymer flocculation using cornstarch. Since natural corn starch is widely known for its selectivity for iron minerals, natural corn starch was used. Without starch addition, the recovery of magnetite particles in a Davis tube was poor at 50% for particles less than 7.5 µm due to the dominant hydrodynamic drag force. The addition of starch increased the recovery by 20% for the -7.5 µm fraction. Minimal recovery improvement (5%) was observed for the coarser fraction (-23+16 µm) when flocculent was added. To increase the efficiency of selective flocculation for coarser particles higher molecular weight polymers would be required (Mathur et al., 2000). The reduced efficiency with variation in particle size indicates polymer flocculation is not robust for samples with a wide particle size distribution.

In addition, fine particles have larger surface areas compared to coarser particles necessitating high flocculent dosages. Caution should be taken regarding starch addition as high concentrations (such as 5 g/l in the work conducted by Arol and Aydogan, 2004) adversely affected recovery due to re-dispersion of the pulp. Redispersion occurs due to the complete coverage of particle surfaces by the flocculent leading to the loss of bridging sites on individual particles which behave as single particles rather than as aggregates. In addition, Arol and Aydogan (2004) conducted the tests at the natural pH of the ore and did not take the point of zero charge into consideration to maximise the efficiency of selective flocculation and reduce the dosage of starch required.

Suspensions with coarse particles and without polymer addition will result in destabilisation due to settling by gravity. Khan (1985) cited by Abro (2009) found that destabilisation of a suspension purely due to flocculation will occur for coal and

metalliferous particles smaller than 40 µm. Thus selective flocculation is suited to particles less than 40 µm.

2.5.2.3.6 Effect of Solids Concentration

Gregory and Barany (2011) found that for charged particles bridging polymers need to extend beyond the range of the double layer indicated by the dotted line in Figure 2.8. Extension beyond this layer is more likely to happen with extended conformations. Polymers with extended conformations are deemed active polymers as the extensions increase the effective collision radius of a particle allowing for greater opportunities for contact to occur. If the re-conformation rate of the polymers is faster than the rate of particle collisions, then the polymers will have sufficient time to achieve their relaxed equilibrium conformations. In this latter case, the polymer is deemed inactive as it is situated within the double layer allowing electrical repulsion to prevail and preventing bridging flocculation. At higher solid concentrations, a greater probability for particle collisions exists thereby ensuring active polymers are present for polymer bridging to occur resulting in larger and stronger flocs (Abro, 2009).

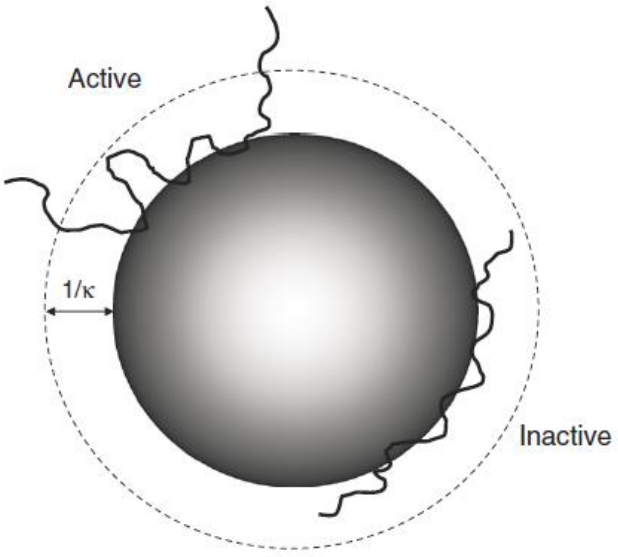


Figure 2.8: Inactive and active adsorbed polymers on a charged particle (Pelssers et al. 1990 cited in Gregory and Barany 2011). The dotted line indicates the diffuse part of the double layer.

Various researchers have conducted their selective polymer flocculation tests at dilute pulp densities of 0.5-5% (Hanumantha Rao and Narasimhan, 1985; Weissenborn et al., 1994; Ahmed and Mahran, 2013; Arol and Aydogan, 2004). Weissenborn (1993) cited in Abro (2009) revealed a marginal decrease in the Fe grade of flocs when increasing pulp densities from 2% to 20% and attributed the degradation in grade to entrapment of kaolin in the hematite flocs.

According to Jones (1998), at high pulp densities, sufficient mixing of flocculents is difficult with local overdosing occurring resulting in re-dispersion of the flocculated particles.

2.5.2.3.7 Effect of Water Quality

As mentioned in Chapter 1 the surface chemistry of flocculation depends largely on the water chemistry. Treatment of process water prior to successful selective flocculation may be required.

With stringent regulations on freshwater usage, the mining and minerals processing industry is obliged to recycle process water. Process water is classified by Levay and Schumann (2006) into recycled water streams and make-up water. The make-up water originates from various sources such as surface (rivers, lakes, reservoirs and dams), groundwater (wells and springs), potable water, treated and untreated sewage waters and industrial effluents. Recycled water typically comprises of concentrate thickener overflows, filtrate from concentrate filtration plant and tailings dam return water. The deterioration in the quality of process water due to recycling can be caused by:

- Accumulation of organic compounds (residual reagents, reaction and decomposition by-products of chemical reagents due to interactions between reagents like collectors, frothers, flocculents) and inorganic (acids, alkalis, inorganic salts and heavy metals)
- By-products of microbiological activities which are supported by conditions during mineral processing

- Impurities in the reagents used in the processing plant
- Dissolution of soluble mineral phases in the ore (e.g., metal chlorides, nitrates, phosphates, sulfates, hydroxides and carbonates)

The effects of poor water quality on mineral processing operations range from process efficiency, reagent dosages and efficacy, and increased maintenance of process equipment. These effects are detailed below by Levay and Schumann (2006):

- Acceleration of corrosion and scale deposition, thereby increasing maintenance and replacement of plant equipment
- Increased reagent consumption due to :
    - metabolites from micro-organisms reacting with and adsorbing onto surfaces of mineral particles.
    - Adsorption of reagents onto the surface of microbial cells
    - Changes in pH and Eh due to microbiological activities
- Adsorption and/or precipitation of dissolved species or colloidal species onto the surface of mineral particles thereby interfering with selective flotation
- Inefficient dewatering of tailings and concentrates
- Accumulation of very fine suspended particles creating viscosity problems.

Haselhuhn et al. (2012) investigated the effect of water quality on the selective flocculation process at Tilden Mines and found that the pH of the process water is the most important factor in selective flocculation and dispersion as it affects the surface properties of the particles. At high pH values, some minerals may dissolve adding metallic cations such as magnesium and calcium into the slurry. Iwasaki (1989) cited in Haselhuhn et al. (2012) explains that these cations adsorb onto the negatively charged surfaces as $CaOH^+$ and $MgOH^+$ and disrupt the sign and magnitude of the surface charge thereby inhibiting dispersion. Besides Ca and Mg polyvalent ions, Abro et al. (2013) also mentioned that Fe ions interfere with dispersion. Drzymala and Fuerstenau (2014) support this statement with Fe^{3+} and Al^{3+} cations activating quartz in the 3-9 pH range thus creating heterogeneous flocs. Ferric ion activation of quartz can be overcome by adding Ethylenediaminetetraacetic acid (EDTA) and fluoride ions. A good indication of the calcium and magnesium content in the process is water

hardness, the higher the content of these elements the greater the hardness. In addition to inhibiting dispersion higher water hardness affects downstream processes and the re-use of the water in the system.

2.5.2.4 Disadvantages of Polymer Flocculation

Although the use of starch for selective hematite flocculation has been successful at Tilden mines, the industrial application and success of polymer flocculation have been limited. A few disadvantages of this approach are outlined below.

- Although flocs produced by polymer flocculation may be resistant to breakage by high shear, when they are broken they may not easily reform when the shear is reduced. The irreversible breakage could be due to scission of the polymer chains under turbulent conditions or the detachment of adsorbed polymer (Gregory & Barany, 2011).
- The work of Hogg (1984) as cited by Zhan (1999) revealed optimal flocculation occurred when more than 50% of the particle surface is exposed. Increased polymer coverage could lead to steric stabilisation, a process in which the adsorbed polymers create a strong repulsion between particles thereby inhibiting flocculation. This is supported by Gregory & Barany (2011) where overdosing resulted in poor flocculation performance.
- Weissenborn et al. (1994) recommend that starch solutions be prepared daily as the use of starch solutions for more than one day may lead to deterioration in the performance of selective flocculation. For industrial applications it is necessary to ensure reagents are not wasted on a daily basis, leading to unnecessary expenditure, and thus sufficient quantities will need to be prepared and ageing monitored.
- Flocs created by polymers are stronger than those produced with salts because the strength of the polymer surface bond is high and the polymer chain has attachments at multiple sites on the surface (Somasundaran and Runkana, 2003).

Ravishankar et al. (1989) as cited by Mathur et al. (2000) compared the flocculation separation efficiency of iron oxides from clays using PolyAcrylic Acid (PAA) and starch. The latter produced flocs that were smaller but more compact and resistant to shear. However, Warren (1992) as cited by Pascoe and Doherty (1997) claim that flocs produced by flotation collectors are stronger than those produced by polymers with long chains. It is essential that flocs generated can withstand high shear rates that will be encountered during materials handling and processing. Song et al. (2002) concurs with this statement and is doubtful that loose flocs generated by polymer flocculation can withstand the strong floc rupturing forces generated from feeding flows and wash water in magnetic separators.

Considering these disadvantages and particularly the findings of Warren (1992) an alternative flocculent such as a flotation collector was reviewed and is presented in the next section.

2.5.3 Selective flocculation using sodium oleate

Achieving selectivity during flocculation is a major challenge when flocculating ultrafine particles. The use of flotation collectors as mineral flocculents have been investigated by researchers with success achieved for various minerals such as hematite, sulphides, scheelite, apatite, cassiterite, quartz (Wang and Heiskanen, 1992; Blackwell et al, 1002; Koh et al, 1986; Bilgen et al, 1994; Raju et al, 1991; as cited in Pascoe and Doherty, 1997) and colemanite (Ucbeyiay Sahinkaya and Ozkan, 2011).

Sodium oleate is a heteropolar anionic collector, meaning it has both polar and non-polar groups. When sodium oleate adsorbs onto the particle surface of the mineral of interest, the polar group adsorbs onto the particle surface whilst the non-polar group is positioned towards the water thereby making the particle hydrophobic. The molecular structure of sodium oleate showing the polar group, non-polar groups as well as the solidophilic (which has an affinity for solid particles) and hydrophilic groups is illustrated in Figure 2.9.

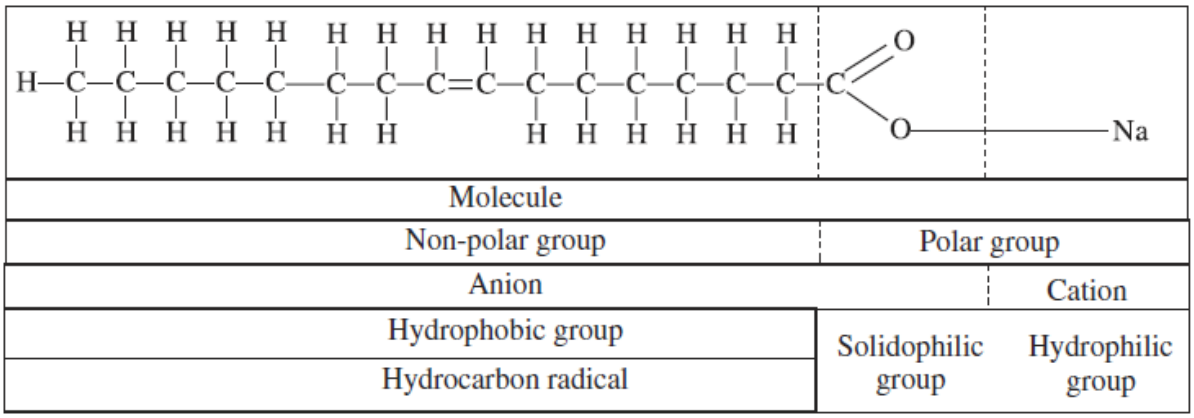


Figure 2.9: Molecular structure of Sodium Oleate (Bulatovic, 2007)

Filippov et al. (2014) summarised the anionic collectors used during Fe ore flotation as shown in Table 2.12. It should be noted that sodium oleate can also float quartz. It is assumed that the addition of sodium silicate as a dispersant in the FMS (Floc Magnetic Separation) process could also have a depressing effect on the quartz improving selectivity.

Table 2.12: Anionic collectors used in Iron Ore Flotation (Filippov et al., 2014)

Mineral Floated	**Collector**
Hematite	Lauric acid
	Hydroxamates
	Sodium alkyl sulphate
	Sodium alkyl benzyl sulphonate
	Sodium Oleate
	Oleic acid
	C6-C18 saturated fatty acids
Apatite	A mixture of ethoxylated tall oil ester of maleic acid and maleic anhydride
Quartz	Sodium oleate
	Alkyl sulphate

Pascoe and Doherty (1997) believe that the stages in the flocculation of hematite with sodium oleate can be described as follows with a graphical representation in Figure 2.10:

a. The oleate ion chemically adsorbs onto the hematite surface
b. Oleic acid droplets form both on the mineral surface and in the bulk solution
c. Floc formation occurs when particles coated with oleic acid/oleate collide with one another and with oleic acid droplets
d. Flocs break and grow until equilibrium is reached

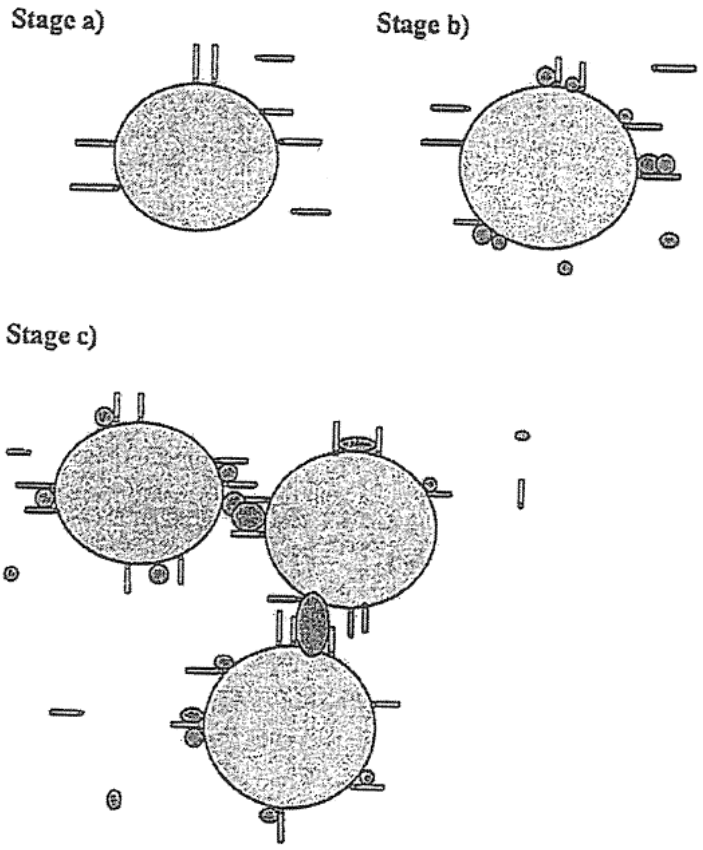


Figure 2.10: Flocculation stages of hematite with sodium oleate as the flocculent (a) adsorption of oleate ions onto hematite surface (b) oleic acid droplets form on hematite surface and in the slurry (c) floc formation due to particle collisions (Pascoe and Doherty, 1997)

2.5.3.1 *Factors affecting Selective Flocculation with Sodium Oleate as the flocculent*

Song et al. (2002) purport that the most critical parameters for hydrophobic flocculation in the FMS process are particle hydrophobicity, kinetic energy input and non-polar oil addition. In their work on selective flocculation of hematite slimes, Pascoe and Doherty (1997) found that sodium oleate concentration, pH, shear rate and agitation time were the main factors that affected floc size.

To understand the effect of various parameters on the kinetics of flocculation Patil et al. (2001) cited by Yin et al. (2011) used a lumped population balance model. The model indicated decreased flocculation rates with increasing shear rate. Higher concentrations of sodium oleate reduced the floc strength, and the use of dispersants such as sodium carbonate and sodium silicate reduced the flocculation rate.

2.5.3.1.1 Effect of Stirring Speed and Time

Successful hydrophobic flocculation is dependent on sufficient kinetic energy to overcome the energy barrier between particles. The amount of kinetic energy imparted into a conditioning tank is dependent on two main factors: stirring speed and stirring time. In the former factor, the stirring speed, tank size, impeller size and slurry volume have an impact. To avoid froth formation during stirring due to the presence of oleate ions, Song et al. (2002) fixed the stirring speed to 1200rpm and varied the stirring time. Iron grade and recovery increased with stirring time and reached a plateau at about 20 minutes indicating sufficient kinetic energy had been imparted for successful hydrophobic flocculation.

At a pH of 9, sodium oleate concentration of 0.394 mmol/L, 6% solids and stirring time of 20 minutes Yin et al. (2011) observed the formation of hematite flocs when the stirring speed increased from 800 rpm to 1000 rpm. The flocs continued to grow when speeds up to 1400 rpm were achieved with floc rupture observed at speeds exceeding 1400 rpm. They found that to ensure an increase in floc size the floc strength must exceed the floc rupturing forces. At an optimal stirring speed of 1400 rpm, Yin et al.

(2011) determined that flocculation commenced after 10 minutes of stirring with increasing floc size observed after 20 minutes. Increasing the residence time to 25 min resulted in the rupture of flocs. This indicates that both an optimal stirring speed and residence time exists to maximise floc size. Yin et al. (2011) found that the factors that influence the optimal stirring speed to be the electric potential of particle surfaces and the original size of the particles. Flocs are stronger with decreasing particle size and thus require higher shear rates for further flocculation. On the other hand particles with lower surface charges will require lower shear rates and less flocculation time. The optimal flocculation time is also affected by the stirring speed with lower stirring speeds requiring lower longer flocculation time.

Pascoe and Doherty (1997) investigated the effect of stirring speed and time on the flocculation of fine hematite at two pH values of 6 and 8. The fixed operating variables were 0.7% solids and 1 x 10^{-3} M sodium oleate. At a pH of 6, increasing the stirrer speed and time had negligible effects on the floc size (the volume median or volume average particle size (Dv 50) of 30-35µm). However, a positive correlation between floc size and increasing stirring speed and time was observed at a pH of 8. The biggest floc size (Dv 50) of 30µm was achieved at a stirring speed and time of 1200rpm and 20 minutes respectively.

2.5.3.1.2 Effect of pH

Yin et al (2011) investigated the effect of pH on the floc size and established that flocculation occurred over a wide pH range (2.5-11) at a fixed stirring speed (1400rpm), flocculation time (20 minutes) and sodium oleate concentration of and 0.394 mmol/L. The flocculation rate was observed to be faster in the acid pH range of 2.3-3 than that of the intermediate pH range of 5-8. This is supported by Pascoe and Doherty (1997) findings in which hematite flocculation was favoured by neutral to acidic conditions. However, in contrast to Pascoe and Doherty's (1997) findings, Yin et al. (2011) observed a dramatic increase in floc size when the pH was above 8 but decreased in strongly alkaline conditions (pH>10). The discrepancy between Pascoe and Doherty's (1997) findings to that of Yin et al (2011) is that in the work of the former researchers stirring speed in the 400-1600 rpm range had no effect on floc size at a

pH of 6 whilst an increase in stirring speed increased the floc size at a pH of 8. It is anticipated that when determining the effect of pH on floc size Pascoe and Doherty (1997) selected a sub-optimal stirring speed of 800rpm that distorted their results.

Yin et al. (2011) determined the optimal pH to be 9. Yin et al. (2011) attributed the increase in flocs size when the pH exceeds 8 to the increase in particle hydrophobicity supported by the increase in the hematite zeta potential with pH as observed in Figure 2.11.

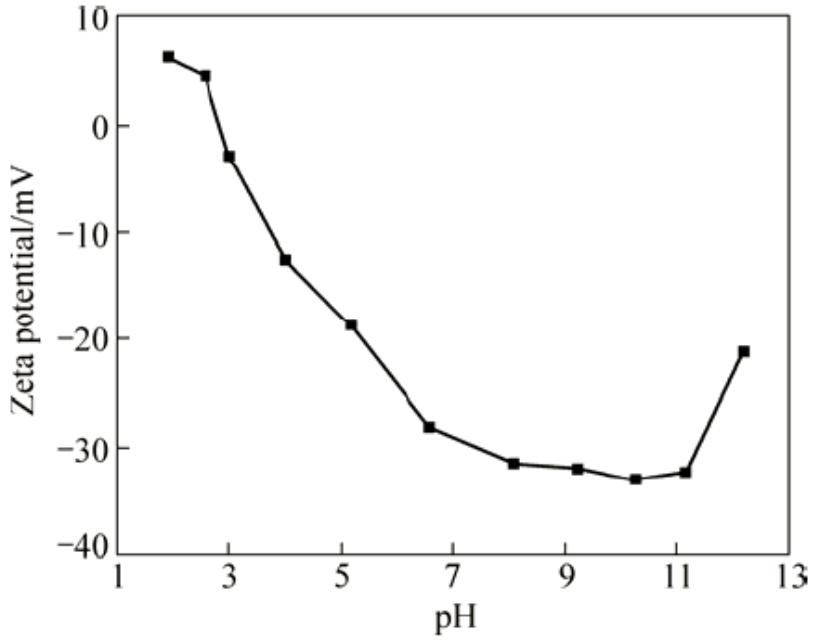


Figure 2.11: Zeta Potential of concentrated Hematite (68% Fe) from Qidashan Mine as a function of pH (Yin et al., 2011)

Zhou (2008) as cited in Yin et al. (2011) explained the solution chemistry of sodium oleate as a function of pH. At a pH of 8.6, an equilibrium between the molecules of oleic acid and oleate ions exist in solution. At lower pH, the sodium oleate exists primarily as oleic acid. At a pH exceeding 8.6, the sodium oleate exists mainly in the form of oleate ions with theory indicating a maximum concentration of oleate ions at a pH of 8.6. This explains why the hydrophobicity and thus floc size was at a maximum at a pH of 9. The decreased floc size at strong alkaline conditions (pH >10) can be attributed to increased concentrations of OH^- that competes with $RCOO^-$ for adsorption onto the surfaces of hematite particles thereby reducing the hydrophobicity of the particle surfaces.

2.5.3.1.3 Effect of % Solids

As in the case of polymer flocculation, most researchers employing sodium oleate as a flocculent conducted their tests in dilute pulp densities of 0.7-3% solids (Pascoe and Doherty, 1997; Arol and Ayodogan, 2004). Roy (2012) investigated the effect of sodium oleate dosages at a higher pulp density of 10%, pH of 9.5, sodium silicate dosage of 1kg/ton and a stirring speed of 800 rpm. At the time of this thesis and based on the articles reviewed, Song et al. (2002) were the only researchers to have investigated the effect of higher pulp densities on hematite flocculation.

To determine the effect of pulp density on hydrophobic flocculation Song et al. (2002) investigated two pulp densities of 20% and 45% at the optimal sodium oleate and kerosene dosage. Higher pulp densities achieved the same iron grade and recovery but in half the conditioning time (10 minutes) of the dilute slurry. It is anticipated that higher pulp densities increase the collision probability of particles. The reduced residence time at higher pulp densities would have an advantage of increased throughput, but Song et al. (2002) admitted that it might not necessarily reduce power consumption as higher torques are required to maintain the same speed in a conditioner with higher percentage solids.

2.5.3.1.4 Effect of Dosage

Roy (2012) found that the Fe recovery increased sharply with small increments in the sodium oleate concentration. At lower dosages in the 1-2 mg/L range, the grade of the flocs remained the same and decreased at higher dosages of 3.5 mg/L. Higher dosages caused stronger adsorption and flocculation of not only hematite and goethite but also ferruginous clay minerals with Fe, Al and Si components.

On the other hand, Song et al. (2002) did not observe a decrease in grade as the sodium oleate dosage increased. A sharp increase in grade was observed as the dosage increased and thereafter remained constant at dosages higher than 2 kg/ton (the ore contained no clays but did have chlorite and limonite). The recovery also increased with increased sodium oleate dosage. Since sodium oleate is an expensive

collector, Song et al. (2002) also investigated the effect of reducing the sodium oleate dosage with the addition of kerosene (a non-polar oil) which would assist with hydrophobic flocculation. Although the concentrate grade did not vary with kerosene dosage, the recovery significantly increased with increased kerosene dosages until it reached a plateau at 4kg/ton. Song et al. (2002) successfully demonstrated that similar results could be achieved by substituting sodium oleate with kerosene, a considerably cheaper reagent. This would significantly reduce reagent costs. The enhancement of hydrophobic flocculation through the addition of a non-polar oil is attributed to the oil bridge that forms between particles which:

- Increases the strength of flocs enabling them to withstand higher shear forces
- Reduces the porosity of the flocs making them more compact. In addition, less porous flocs reduce the probability of entrapment of gangue within the floc structure.

Using the optimal conditions determined experimentally Yin et al. (2011) varied the sodium oleate dosage from 0.197 mmol/L to 0.591 mmol/L while fixing the stirring speed, flocculation time and pH to 1400 rpm, 20 min and 9 respectively. In the dosage range selected, flocculation of fine hematite was observed with a maximum floc size attained at 0.394 mmol/L. Yin et al. (2011) explained that flocculation occurred in the range tested due to the dosages exceeding the Critical Micelle Concentration (CMC). As the concentration of sodium oleate increases the oleate adsorbs onto the mineral surfaces sequentially as a monolayer, aggregates and then micelles. The concentration at which these micelles begin to form is termed the CMC, and for sodium oleate it is 0.187 mmol/L.

Pascoe and Doherty (1997) also investigated the effect of sodium oleate dosage (1 mmol/L to $1x10^{-3}$ mmol/L) on the hydrophobic flocculation of ultrafine hematite. Hematite flocs were produced only when the solubility of oleic acid was exceeded, and an oil-in-water emulsion was created. Figure 2.12 indicates that the floc size increased as the concentration of insoluble oleic acid increased. In Figure 2.13 Pascoe and Doherty (1997) compared the pH at which flocculation commences to the pH required to produce insoluble oleic acid for a range of oleate concentrations. The figure indicates that once the oleic acid solubility has been exceeded, then flocculation

commences. As the concentration of insoluble oleic acid increases so did the floc size indicating that oleic acid droplets can form directly on the mineral surfaces. Although the formation of droplets is an important factor in hydrophobic flocculation Yin et al. (2011) discovered that overly oil-in-water emulsions would reduce floc size and that an optimal dosage exists.

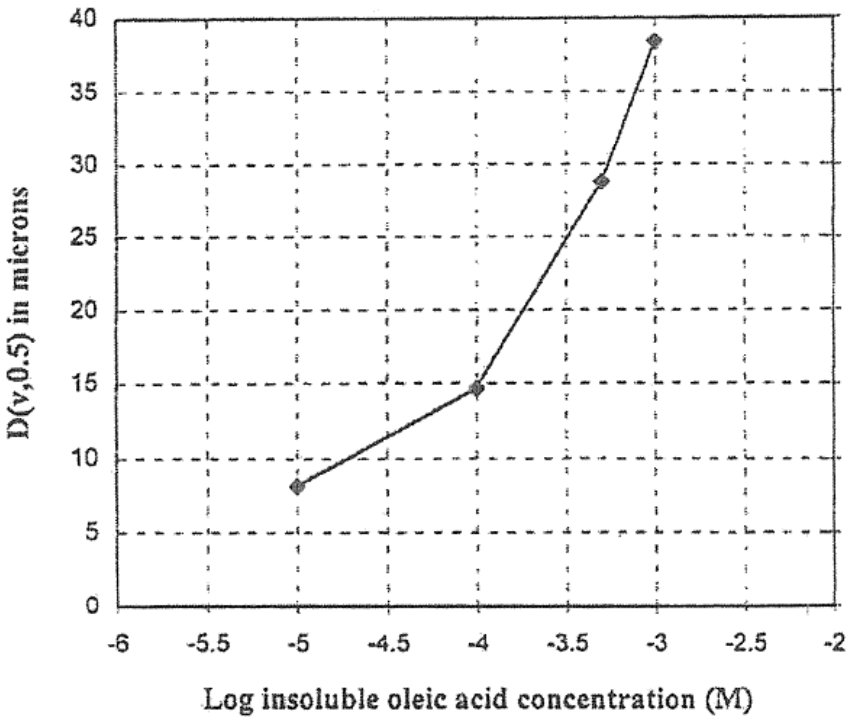


Figure 2.12: Hematite floc size as a function of insoluble oleic acid concentration (Pascoe and Doherty, 1997)

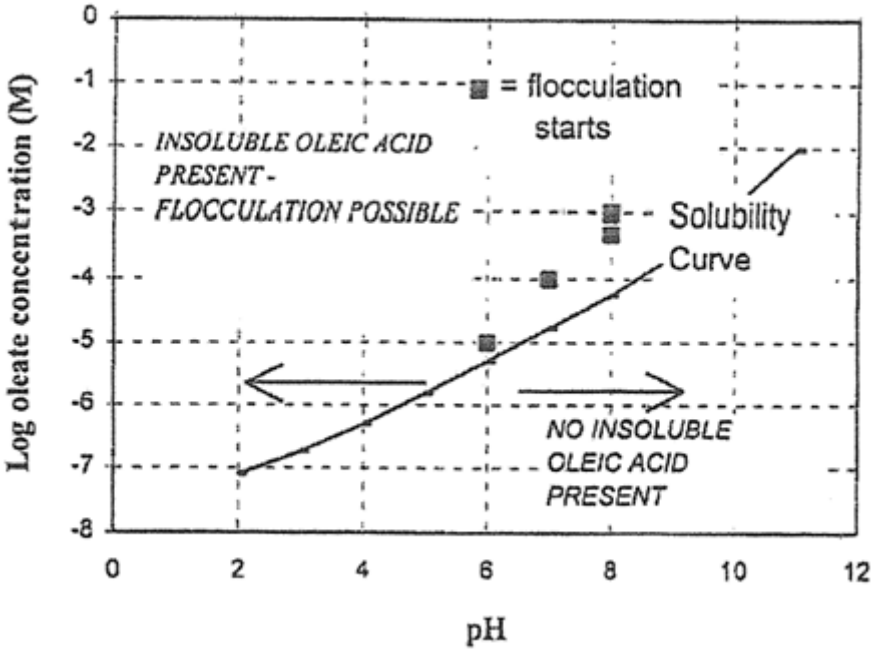


Figure 2.13: Solubility curve of oleic acid in relation to the minimum pH required for hematite flocculation (Pascoe and Doherty, 1997)

2.6 Application of Selective Flocculation to Magnetic Separation

Song et al. (2002) applied the principle of selective flocculation to the treatment of hematite slimes with magnetic separation used as the solid-solid separator. Hematite fines were first selectively flocculated followed by a magnetic separation at a middle field intensity rather than high intensity or high-gradient magnetic separations which are energy intensive. They termed this process Floc Magnetic Separation (FMS) which consists of four steps namely dispersion, selective hydrophobization, hydrophobic flocculation and magnetic separation. This process is schematically presented in Figure 2.14.

- **Dispersion**

  Appropriate dispersant with pH adjusters are added to eliminate hetero-coagulation of magnetic and non-magnetic fines in suspensions which is detrimental to separation efficiency

- **Selective hydrophobization**

  Achieved by the addition of appropriate surfactants and the adsorption of these surfactants by the magnetic fines

- **Hydrophobic flocculation**

  Supply mechanical conditioning to ensure particles have sufficient kinetic energy to overcome the energy barrier (repulsive forces) between particles. Non-polar oils are typically added to enhance this process by the creation of an oil bridge and increasing particle hydrophobicity.

- **Magnetic Separation**

  The flocculated hematite particles would be introduced into a magnetic separator (the solid-solid separator) to separate hematite from quartz (or other non-magnetic gangue).

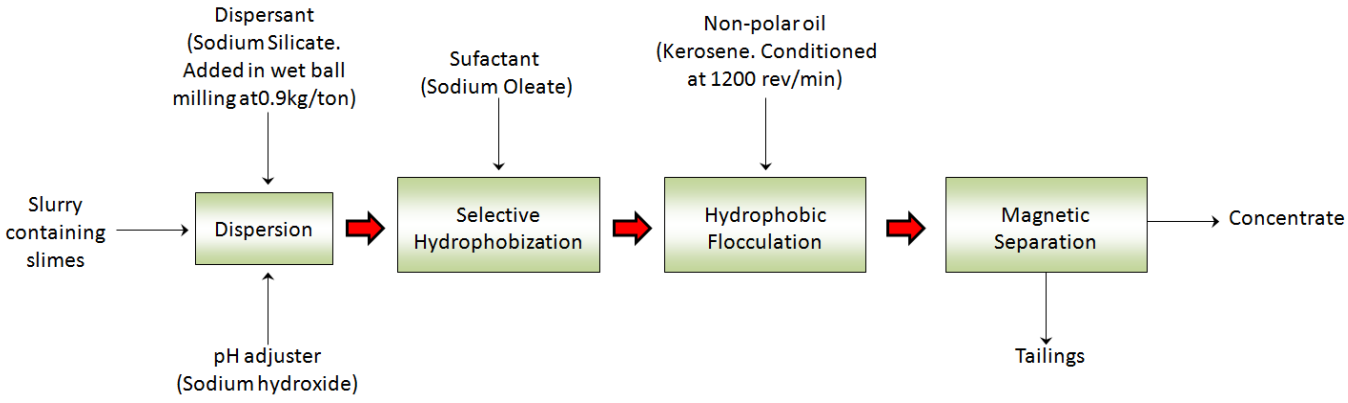


Figure 2.14: Schematic representation of the Floc Magnetic Separation (FMS) process applied to hematite (Song et al., 2002)

Song et al. (2002) claim that hydrophobic flocs generated by the FMS process are better able to withstand floc rupturing forces such as feeding flows, washing flows and pulsation that are present in magnetic separators than those created by polymer flocculation. Thus the approach taken by Song et al. (2002) in the FMS process will be investigated in this thesis. Table 2.13 summaries the testwork conditions and results obtained by each researcher who applied the FMS process and polymer flocculation to magnetic separation.

Table 2.13: Selective Flocculation applied to Magnetic Separation

Reference	Feed Characteristics	Flocculent & Flocculation conditions	Magnetic Separation Conditions	Concentrate Fe Grades & Recovery
Roy, 2012	Fe ore slimes (source unidentified); **Head Grade:** 59.58% Fe; 4.57% SiO2; 3.78% Al_2O_3 **PSD:** D_{80} 16µm; **Mineralogy:** Limonitic kaolinite	Dispersant: Sodium silicate (1kg/ton) pH: 9.5 Conditioning speed: 800rpm; Sodium oleate (1.5-3.5kg/ton with latter optimal)	**Jones WHIMS lab unit** 5-10% solids; Grooved Plate; Slurry feed rate: 500mL/min; Wash water: 250mL/min; Intensity: 1.52 Tesla	**Without flocculation:** Fe grade: 67.06% Fe Recovery: 37.4% **With flocculation**: Fe grade: 65.14% Fe Recovery: 79.6%
Arol and Aydogan, 2004	Magnetite (Turkey)-Quartz artificial mixture. **Head Grade:** Pure Magnetite: 97.6% Fe_2O_3	Corn starch (0-20 mg/L with 5 mg/L optimal), Natural Pulp pH, Distilled water	**Davis Tube:** Slurry Velocity: 8.5 cm/s; 3% solids; Intensity: 1000 Gauss	**-23+16µm:** Fe_2O_3 Grade: 93.7%; Fe_2O_3 Recovery: 89.3% **-7.5µm:** Fe_2O_3 Grade: 85%; Fe_2O_3 Recovery: 65%
Song et al., 2002	1. Hematite (China) **Head Grade:** 30.5% Fe **Mineralogy:** Hematite, Limonite, Magnetite, Quartz, Chlorite **Mill PSD:** D_{50} 4.1 µm;	Sodium Silicate (added in ball mill: 0.9-1.0 kg/ton) Sodium Oleate (0-8 kg/ton; optimal: 1 kg/ton) Kerosene (0-5 kg/ton, optimal: 3 kg/ton) Tap water Conditioning speed: 1200 rpm pH: 9.5	**Jones WHIMS lab unit** 15% solids; Grooved Plate; Slurry feed rate: 200 ml/min Intensity: 1.0 Tesla	**Without flocculation:** Fe grade: 41.0% Fe Recovery: 42.0% **With flocculation:** Fe grade: 63.95% Fe Recovery: 82.03%
	2. Limonite (China) **Head Grade:** 38.11% Fe **Mineralogy:** Limonite, Hematite, Quartz, Chlorite, Calcite **Mill PSD:** D_{50} 7.3 µm;			**Without flocculation:** Fe grade: 51.04% Fe Recovery: 48.2% **With flocculation:** Fe grade: 50.78% Fe Recovery: 81.7%

The majority of research investigating polymer flocculation was conducted on binary synthetic or artificial mixtures of hematite and quartz or kaolinite. The success of selective flocculation coupled with magnetic separation on actual slimes sample from industry was demonstrated by Roy (2012) and Song et al. (2002) using tap water. In

their investigations on Fe ore slimes, Song et al. (2002) and Roy (2012) both show that flocculation drastically increases Fe recovery whilst maintaining grade. The exception is the hematite sample for Song et al. (2002) in which flocculation improved both grade and recovery compared to conventional magnetic separation. Both investigators investigated grinds below ~20 µm, and it is unclear if selective flocculation is better suited to certain size classes. Advanced magnetic separation and gravity devices such as the pulsating WHIMS and the Reflux Classifier have not been investigated as alternative solid-solid separation units. It is anticipated that elutriation in the Reflux Classifier and the pulsating mechanism on the pulsating WHIMS will reduce entrainment and physical entrapment of gangue minerals within the floc structure improving the concentrate grade.

Although Roy (2012) and Song et al. (2002) achieved good recoveries and grades, both researchers conducted the magnetic separation testwork at high intensities of 1.52 Tesla and 1 Tesla respectively. These intensities were selected based on WHIMS intensity variation testwork on the slimes as-is. With flocculation increasing the hematite size this intensity and thus energy consumption could be reduced.

2.7 Conclusion

The prevalence and treatment of low grade, finely disseminated iron ore has resulted in the production of primary and secondary slimes that constitute potential resources. The beneficiation of slimes is difficult mainly due to particle size limitations of current equipment and the poor process efficiencies associated with treating slimes. The potential to improve the recovery of hematite from slimes by gravity and magnetic separation is available by increasing particle sizes through hydrophobic flocculation. Methods of hydrophobic flocculation include oil agglomeration, shear flocculation, carrier flotation, magnetic aggregation and selective flocculation. Each method is faced with disadvantages that have limited its commercial applicability namely that oil agglomeration is expensive and poses environmental hazards. High energy costs for shear flocculation and the challenges with increased complexity in separating the carrier particles from the desired mineral in carrier flotation have limited its application to industry. Weak magnetic flocs and feed particle size requirements of +20µm in

magnetic aggregation and poor selectivity in selective flocculation have also limited its application.

Improved selectivity in selective flocculation can be achieved by varying many parameters with the main parameters investigated by researchers being dispersant dosage, pH and electrolyte concentration, reagent sequence, particle sizes, water quality, flocculant dosage, % solids, kinetic energy (stirring speed and duration) and lastly type of flocculent.

Selective flocculation using polymers (mostly starch) as the flocculent has received much attention from researchers in the past, with the most successful commercial application of polymer flocculation being the flocculation of hematite using starch at Tilden Mines. Of concern in polymer flocculation using starch is the requirement to prepare the starch on a daily basis, polymers breaking under high shear and not being able to reform and increased dosages causing steric stabilisation thereby inhibiting flocculation. These concerns along with flotation collectors (such as sodium oleate) producing stronger flocs compared to those of polymer flocculation have made selective flocculation using sodium oleate the focal point of this thesis. The work of Song et al. (2002) applying the Floc Magnetic Separation (FMS) process was critical in determining the parameters that affect selective flocculation using sodium oleate as the collector/surfactant. Yin et al. (2011) also contributed to understanding these parameters with four critical parameters investigated by both sets of researchers namely: pH, stirring speed and time, % solids and dosages of dispersants, collectors and non-polar oils. Screening tests will be required to define appropriate ranges of each parameter with previous work conducted in this field to be used as a guideline.

Should selective flocculation with sodium oleate be successful at increasing the particles size of hematite, alternative solid-solid separators to flotation can be investigated. Provided large, competent flocs can be generated improved recoveries of hematite on magnetic and gravity separators are anticipated. Although large flocs are desired in magnetic and gravity separators, the increase in floc size correlates to increased floc porosity and thus reduced floc densities that may counteract the benefit of increased size when applied to gravity separators such as elutriators.

CHAPTER 3 : RESEARCH DESIGN, SAMPLE SELECTIION AND FEED CHARACTERISATION

3.1 Introduction

The purpose of this study is to establish if selective flocculation of hematite from slimes improves the separation efficiency of selected magnetic and gravity separators. To address this research question, two outcomes need to be addressed namely:

- To determine the optimal conditions for selective flocculation and
- To test the impact of selective flocculation on beneficiation

Literature indicates that Song et al. 's (2002) Floc Magnetic Separation (FMS) process, on which this thesis is based, comprises of four stages namely dispersion, selective hydrophobization, hydrophobic flocculation and a solid-solid separator (magnetic separation) as illustrated in Figure 3.1. Figure 3.1 is Figure 2.14 from Chapter 2 and is repeated here for convenient reference. In order to address the first outcome mentioned above, numerous factors have to be taken into consideration to optimise these four stages of selective flocculation.

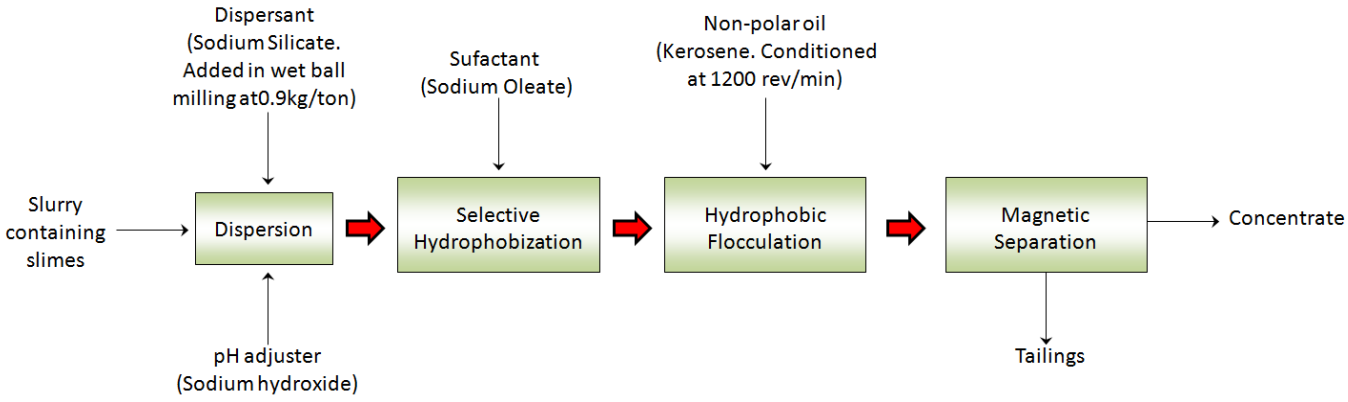


Figure 3.1: Schematic representation of the Floc Magnetic Separation (FMS) process applied to hematite (Song et al., 2002)

To optimise the selective flocculation conditions it is important to establish the optimal dispersant dosage, pH, collector (sodium oleate) and non-polar oil (paraffin) dosage along with conditioning time. The sequence of tests to address the first outcome is

determined by the selective flocculation stages. Due to the complexity of the study some stages were coupled together namely, the optimal magnetic separation conditions (without selective flocculation) were coupled firstly with the pH optimisation stage and secondly the reagent dosage and conditioning optimisation stages. The coupling of magnetic separation with these stages was required to determine the effect of these variables on the response variables (separation efficiency, Fe grade and recovery). Thus the sequence of steps for the study are outlined below:

1. Determining the optimal intensity for the magnetic separator, without selective flocculation.

   To establish the optimum magnetic field intensity that would achieve the maximum range for each of the response variables (separation efficiency, Fe grade and recovery) without selective flocculation intensity variation testwork was required. Intensity variation testwork involves determining the response variables over a range of magnetic field intensities. The response variables at the optimum magnetic field intensity was used as a baseline for comparison to the results achieved by coupling magnetic separation with selective flocculation. The coupling of magnetic separation at the optimum intensity whilst varying (i) selective flocculation pH will be reported in Chapter 4 and (ii) selective flocculation variables (reagent dosage and conditioning time) will be reported in Chapter 5.

2. Determining the optimal dispersant dosage and pulp density that would result in adequate dispersion of hematite from silicates.
   Dispersion is critical in ensuring the selectivity of the flocculation process. In order to determine if dispersion was achieved rheology tests with the slimes as-is (without flocculation) must be conducted to determine the yield stress. The yield stress indicates the amount of force required to overcome the attractive forces between the solids thereby allowing for adequate dispersion.

3. Determining the optimal pH for selective flocculation.
   Once the optimal dispersant dosage and pulp density are established the next step is to determine the optimum pH. pH affects the hydrophobicity of particles (critical in selective flocculation) as well as the size of the flocs generated. The

bigger the flocs, the more dominant the magnetic and gravity separation forces become over the hydrodynamic drag force. It is thus necessary to determine the particle size distribution of the sample before and after selective flocculation at various pHs to determine the effect of pH on floc size. The flocculation conditions used for this stage will be the centre point conditions for the second and third stages of the FMS process. However to determine the effect of pH on the response variables separation efficiency, Fe grade and recovery a solid-solid separator is required after selective flocculation. Due to the small mass requirements per a test, the SLon-100 (magnetic separator) was selected as the solid-solid separator.

Steps 1-3 define the pre-conditions for selective flocculation and are defined as the baseline tests which are reported in Chapter 4. Once the optimum pre-conditions for selective flocculation were established the variables influencing the selective flocculation stage itself can be determined. The effect of sodium oleate dosage, paraffin dosage and conditioning time on selective flocculation is reported in Chapter 5. This latter optimisation stage was also coupled with the magnetic separator (SLon-100) to determine the effect of these operating variables on the response variables. Thereafter the optimal selective flocculation conditions was applied to the Reflux Classifier and compared to the Reflux Classifier without selective flocculation to establish the benefit of selective flocculation on a gravity separator (Chapter 6).

Before conducting these steps, it was imperative to select a sample that would be amenable to selective flocculation. Literature has shown that poor selectivity in the flocculation stage can be attributed to complex mineralogy and thus a sample of simple mineralogy would be better suited to address the purpose of the study. Thus feed characterisation of the sample comprising of chemical analysis, mineralogy and size-by-assay was conducted to ensure that these requirements were achieved prior to commencing with selective flocculation.

This chapter will explain the research design selected and feed characterisation of the sample employed in the study. The limitation of the study, the research instruments used and the analysis of the data acquired during feed characterisation will also be identified and expanded upon.

The raw data pertaining to this chapter is presented in Appendix A.

3.2 Research Design

A graphical illustration presenting the approach followed for the study is given in Figure 3.2. Fe ore from Angola at a top size of 30 mm was stage crushed, using a jaw crusher to reduce the top size from 30 mm to 100% -12 mm in preparation for the Labwal High Pressure Grinding Rolls (HPGR). The Labwal HPGR reduced the top size to 100% -1.18 mm which was subsequently blended with a mechanical blender and five 25 kg sub-samples removed for milling using the cross-cut method. The samples were milled to a target grind of 80% passing 38µm. The mill discharge was subjected to feed characterisation entailing head analysis, mineralogy and size-by-assay.

Base case magnetic separation (SLon described in Chapter 4 Section 4.2) and gravity separation tests (Reflux Classifier described in Chapter 6 Section 6.2) were conducted to determine the response of the material before selective flocculation. Parameters such as magnetic field intensity and fluidisation water were varied for magnetic separation and gravity separation respectively to achieve the best Fe grade, Fe recovery and separation efficiency.

Thereafter the various parameters that influence selective flocculation were investigated. The experimental design for the study is presented in Table 3.1 and summarises the various aspects that needed to be determined, what response variable was being measured and how it was measured. Table 3.1 also shows the inter-dependence between stages and the large number of variables in the study.

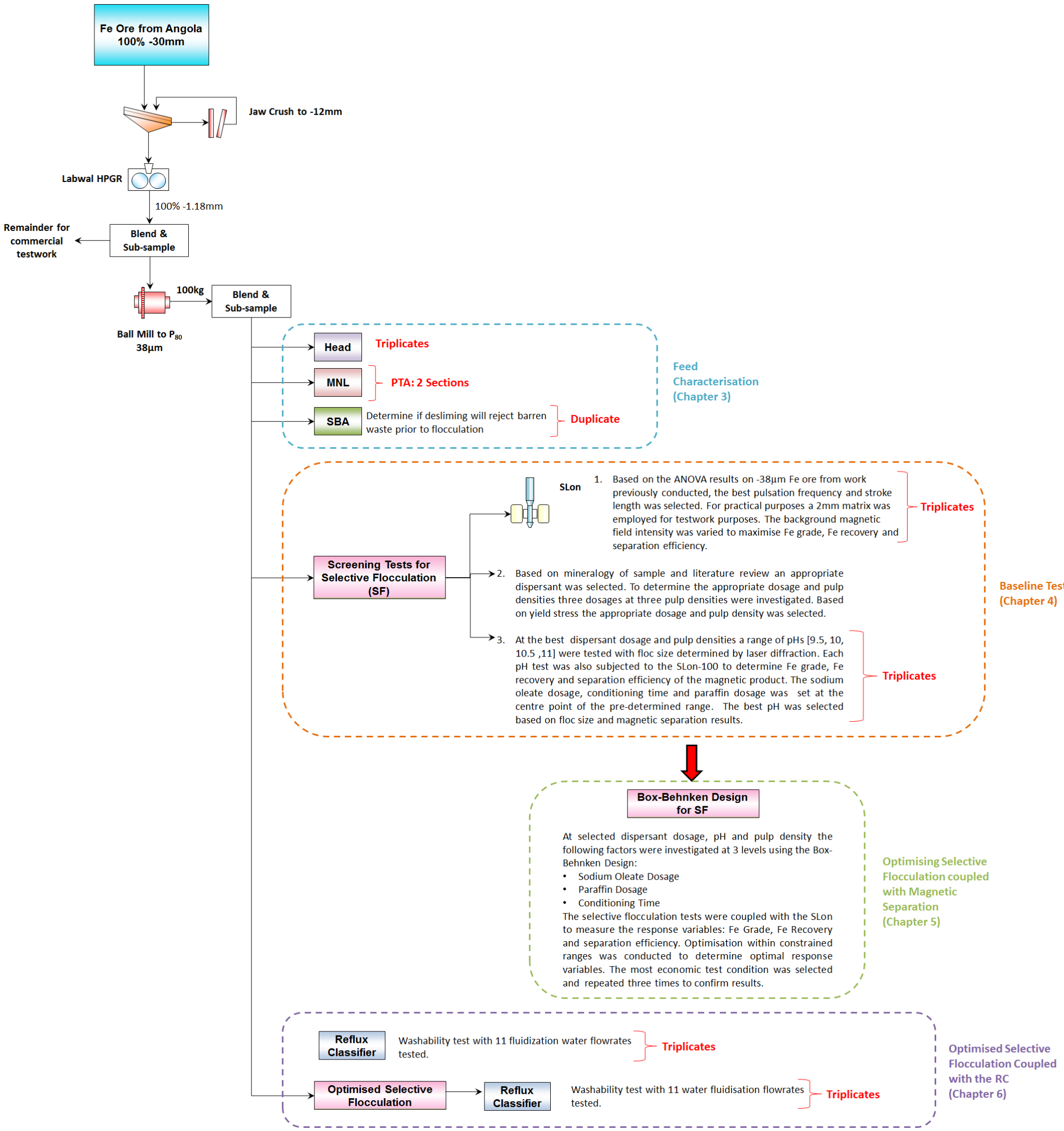


Figure 3.2: A graphical overview of the research design applied to this study using the Angolan Fe Ore Sample

Table 3.1: Experimental Design for optimising magnetic separation, gravity separation as well as selective flocculation

	Aspect Investigated	Operating Parameters	Response Variable Measured	Measurement Technique	Measurement Instrument
Base-line Tests: Magnetic Separation Without Selective Flocculation	Magnetic Field Intensity	**Fixed Conditions:** Rod Matrix (2mm rods); Pulsation Frequency (250rpm); Pulsation Amplitude (5mm) **Variable Conditions:** Magnetic Field Intensity (3 kGauss; 4 kGauss; 6 kGauss)	Concentrate Fe grade; recovery and separation efficiency	Magnetic separation	SLon-100
Base-line Tests: Reflux Classifier Without Selective Flocculation	Water fluidisation rate	**Fixed Conditions:** Semi-batch mode operation; Feed Mass (3.3kg) **Variable Conditions:** Water fluidisation rate (8.2 kg/h; 12.5 kg/h; 16.8kg/h; 21.0 kg/h; 25.3 kg/h; 31.5 kg/h; 50.5 kg/h; 67.3 kg/h; 100.9 kg/h; 121.1 kg/h; 146.4 kg/h)	Concentrate Fe grade; recovery and separation efficiency	Gravity separation	PVC Reflux Classifier
Screening Tests (set preconditions for selective flocculation)	Dipsersion	Sodium silicate dosage (0 kg/t; 0.5 kg/ton; 1 kg/ton; 1.5 kg/ton) Pulp Density (0%; 20%; 30%; 45%)	Yield stress	Rheology	Physica Rheolab QC rheometer
	pH	**Fixed Conditions:** Pulp Density (45%); Sodium silicate (1 kg/ton); Sodium Oleate (1 kg/ton); Paraffin (3 kg/ton); Stirring Speed (1200 rpm); Stirring Time (10 min); Magnetic field intensity (6 kGauss) **Variable Conditions:** pH (9.5; 10.0; 10.5; 11.0)	Floc Size	Laser diffraction (digital particle size analysis)	Malvern Mastersizer 2000E with sample dispersion unit Hydro-2000 MU
			Concentrate Fe grade; recovery and separation efficiency	Magnetic separation	SLon-100
FMS Process Optimisation	Selective Flocculation Conditions (Sodium Oleate dosge; Paraffin dosage; Conditioning Time)	**Fixed Conditions:** Pulp Density (45%); Sodium silicate (1 kg/ton); pH (10); Stirring Speed (1200 rpm); Magnetic field intensity (6 kGauss) **Variable Conditions:** Sodium Oleate (0.5 kg/ton, 1 kg/ton, 2 kg/ton); Paraffin (2kg/ton, 3 kg/ton, 4kg/ton); Stirring Time (5 min, 10 min, 20 min)	Concentrate Fe grade; recovery and separation efficiency	Magnetic separation	SLon-100
Reflux Classifier coupled with the Optimal Selective Flocculation conditions	Water fluidisation rate	**Fixed Conditions for Selective Flocculation:** Pulp Density (45%); Sodium silicate (1 kg/ton); pH 10; Sodium Oleate (0.5 kg/ton); Paraffin (1.43 kg/ton); Stirring Speed (1200 rpm); Stirring Time (4.6 min); **Fixed Conditions for the RC:** Semi-batch mode operation; Feed Mass (3.3kg) **Variable Conditions:** Water fluidisation rate (8.2 kg/h; 12.5 kg/h; 16.8kg/h; 21.0 kg/h; 25.3 kg/h; 31.5 kg/h; 50.5 kg/h; 67.3 kg/h; 100.9 kg/h; 121.1 kg/h; 146.4 kg/h)	Concentrate Fe grade; recovery and separation efficiency	Gravity separation	PVC Reflux Classifier

The literature review of the selected Floc Magnetic Separation (FMS) process revealed several parameters were important in the selective flocculation process namely pH, conditioning time, pulp density and dosages of dispersants, collectors and

non-polar oils. Therefore it is necessary to establish the optimum conditions for each of these parameters.

To simplify this process, the testwork was conducted in two stages. The first stage labelled as baseline tests described in Chapter 4 focused on

a) intensity variation testwork on the magnetic separator (SLon) without selective flocculation to establish the intensity that would achieve the maximum separation efficiency, Fe grade and recovery. These results would be used in the pH tests (Chapter 4) and selective flocculation optimisation tests (Chapter 5) to follow.
b) Rheology testwork was conducted on the sample without selective flocculation to determine the yield stress at various dispersant dosages and pulp densities. The yield stress indicates the amount of force required to overcome the attractive forces between the solids thereby allowing for adequate dispersion, the first critical step in selective flocculation.
c) Yin et al. (2011) showed that pH affected the equilibrium between the molecules of oleic acid and oleate ions in solution thereby affecting hydrophobicity and floc size. Thus the effect of pH variation on the floc size was investigated at the best dispersant dosage and pulp density with the selective flocculation conditions at the centre point of the study (sodium oleate dosage 1000 g/ton; paraffin dosage 3000 g/ton and conditioning time of 10 min). To determine the effect of pH variation on the response variables separation efficiency, Fe grade and recovery; magnetic separation tests were coupled with the selective flocculation stage.

The second stage, reported in Chapter 5, focused on the effect of the three operating variables (also referred to as factors) namely, dosages of sodium oleate and paraffin; and the conditioning time on the response variables separation efficiency, Fe grade and recovery. For this aspect, the Box-Behnken design was employed whereby selective flocculation was coupled with magnetic separation. Based on the relationship between the factors and response variables optimisation of the operating variables (factors) was conducted to attain maximum separation efficiency, Fe grade and

recovery. After the optimisation study, the most economical conditions were selected and repeated three times for statistical confidence in the results.

Once the optimal conditions were selected from selective flocculation coupled with magnetic separation, only the optimal conditions were subjected to gravity separation (Reflux Classifier). This approach was taken because selective flocculation coupled with magnetic separation required less sample, was quicker to run and obtain results compared to using the Reflux Classifier asa the solid-solid separator.

3.2.1 Response Variables

Three response variables namely, Fe grade, Fe recovery, and separation efficiency also referred to as collection efficiency were reported for each process unit tested. Holland-Batt (1985) cited by Amariei et al. (2014) proposed the following equations for selectivity indexes and collection efficiency

$$S_{v_{(product)}} = \frac{R_{v_{(product)}} - R_{g_{(product)}}}{R_{v_{(product)}}}$$

Equation 3.1

$$S_{g_{(discard)}} = \frac{R_{g_{(discard)}} - R_{v_{(discard)}}}{R_{g_{(discard)}}}$$

Equation 3.2

$$Ec = S.E. = R_{v_{(product)}} - R_{g_{(product)}}$$

Equation 3.3

Where $S_{v_{(product)}}$ = selectivity index for valuables (total Fe) in the product;

$S_{g_{(discard)}}$ = selectivity index for gangue (SiO_2) in the discard;

$R_{v_{(product)}}$ = valuables (total Fe) recovery in the product;

$R_{v_{(discard)}}$ = valuables (total Fe) recovery in the discard;

$R_{g_{(product)}}$ = gangue (SiO_2) recovery in the product;

$R_{g_{(discard)}}$ = gangue (SiO_2) recovery in the discard;

Ec = collection efficiency;

$S.E.$ = separation efficiency;

Pascoe and Doherty (1997) used separation efficiency (defined as collection efficiency by Holland-Batt (1985)) to provide a single index for metallurgical separation efficiency. Thus for the surface response modelling, utilizing the Box-Behnken design, the three response variables selected were concentrate Fe grade, concentrate Fe recovery and separation efficiency.

3.2.2 Limitations of the Study

The investigation will be limited to hematite slimes in the -45 µm size fraction. Natural slimes from a thickener underflow would have been preferred but could not be obtained, and thus artificial slimes were generated through ball milling.

The literature review in the previous chapter describes the various methods of hydrophobic flocculation such as shear flocculation, carrier flotation, magnetic aggregation and selective flocculation. Selective flocculation can be achieved by many approaches with polymers being the most commonly used flocculent. This investigation will consider selective flocculation using sodium oleate as the surfactant or flocculent. The reasons for this approach are outlined in the literature review. The potential for selective flocculation is limited to the reagents selected for the investigation, the ore mineralogy and water chemistry.

One separation device for gravity and magnetic separation was used as the solid-solid separator. The laboratory scale elutriator (Reflux Classifier) and pulsating Wet High Intensity Magnetic Separator (SLon) were employed in the investigation with other types of separators omitted. As mentioned in Chapter 2 Section 2.6, these two units have been selected as it is envisaged that elutriation and the pulsation mechanism respectively will reduce entrainment and entrapment of gangue minerals in the floc structure, thereby improving the concentrate grade.

The methodological limitations of each of the research instruments are listed in the preceding sections. Additional limitations of the investigation are listed below:

- Samples from thickener underflows or tailings dams will not be investigated as weathering and ageing will change the surface chemistry thereby necessitating a different approach. Artificial slimes were generated through ball milling. The extrapolation of positive results to actual slimes will be limited. The approach will need to be confirmed on plant slimes where mineralogy, surface chemistry and water chemistry may vary considerably.
- The results are specific to the sample tested as mineralogy of each sample will dictate the appropriate approach to be taken.
  For example, complex Fe ores with Fe bearing silicates will reduce the separation efficiency of magnetic separation. For gravity processes, high-density gangue minerals present in the ore will interfere with the efficiency of separation in terms of sedimentation.

- Rand water was used for all tests conducted with the effect of water quality and ageing neglected. Selective flocculation is dependent on surface chemistry and hydrodynamics. Water chemistry plays an important role in the effectiveness of selective flocculation in industry, and the effect of process water and ageing on flocculation was not investigated in this study.
- The potential for selective flocculation coupled with other gravity and magnetic separation units cannot be extrapolated from this investigation.
- Laboratory scale tests indicate the potential for the approach and do not define what can be achieved at a pilot scale.

3.3 Sample Preparation

3.3.1 Methodology

3.3.1.1 Crushing

Approximately 2.6 tons of Fe ore from Angola at a top size of 30 mm was stage crushed to 100% -12 mm using a jaw crusher. The -12 mm material was subsequently processed through the Labwal HPGR illustrated in Figure 3.3. The applied grinding pressure was arbitrarily set at 30 bar and no optimisation was conducted. After each pass the +1.70 mm fraction was combined with the -12 mm feed until the entire sample was crushed to 100% passing 1.70 mm.



Figure 3.3: Polysius Labwal HPGR

The HPGR discharge at -1.70 mm was blended and one kilogram removed for sizing and another 100 kg removed for testwork purposes.

The 100 kg aliquot was blended and prepared into 25 kg batches for ball milling whilst the one-kilogram aliquot was wet screened into the size fractions listed in Table 3.2 to determine the particle size distribution. The -25 µm size fraction was subjected to ultrasonic bath sizing at 10 µm.

Table 3.2: Size Fractions

Size Fraction (µm)
-1700+1180
-1180+850
-850+600
-600+425
-425+300
-300+212
-212+150
-150+106
-106+75
-75+53
-53+38
-38+25
-25+10
-10

3.3.1.2 Milling

The -1.70 mm fraction prepared into 25 kg batches was ball milled at 50% solids targeting a grind of 80% passing 38 µm to generate artificial slimes for SLon tests, RC tests and selective flocculation. The mill dimensions, ball charge and sample charge are presented in Table 3.3.

Table 3.3: Ball Milling Conditions

Mill	Grey Mill
% Grinding media in mill	35.0
Specific gravity of balls	7.85
Mill diameter (inside liners (m))	0.6
Mill length (inside liners (m))	0.6
Specific gravity of ore	3.63
Sample Mass per Batch	25
% Solids	50

Ball Size (mm)	Size %	Mass (kg)
30	33.3	93.211
25	33.3	93.211
15	33.3	93.211
Total	**100.0**	**279.633**

The size of the balls selected for the ball charge is dependent on the top size of the mill feed, the target grind of the mill discharge and the hardness of the ore.

Milling Curve

One 25 kg aliquot was batch milled. After each milling time, a representative sub-sample was taken and screened at 38 µm to determine the percentage passing. The process was repeated several times in order to construct a milling curve (milling time versus % passing 38 µm) and the time required to achieve the target grind was determined.

Mill to Grind

After establishing the correct time for milling one 25 kg aliquot to the target grind, the remaining batches were milled for the time determined from the milling curve to achieve the target grind.

The mill discharges were combined, filtered, dried and the lumps broken prior to blending and sub-sampling for feed characterisation entailing head analysis, mineralogy, Size-By-Assay (SBA) and laser diffraction.

3.3.2 Results and Discussions

The milling curve for wet milling one 25 kg batch of -1.18 mm material to 80% passing 38 µm is presented in Figure 3.4. The target grind was achieved at a milling time of 45 minutes. All the remaining batches were milled for this duration.

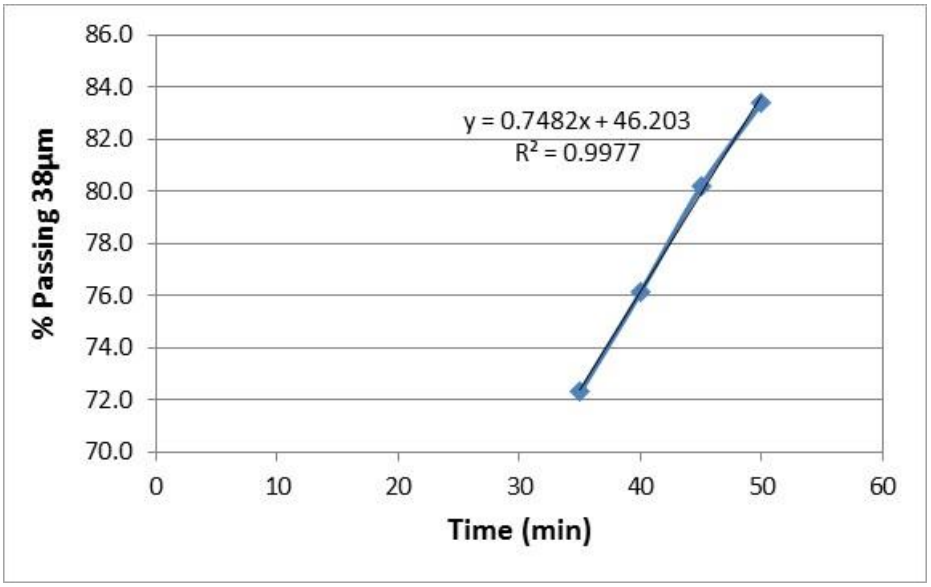


Figure 3.4: Milling Curve on the -1.18mm material targeting a grind of 80% -38 µm

To prevent smearing of minerals during the milling stage, it is recommended that in future a dispersant is added into the mill as indicated by Frommer and Colombo (1966) cited in Drzymala & Fuerstenau (2014). It is envisaged that smearing of the minerals would adversely affect the selective flocculation stage as a very thin layer of contaminant can affect the surface properties and response of the particle to any of the stages of selective flocculation. In this study it is unlikely that smearing would occur for the following reasons:

- The simple mineralogy of the ore with the dominant minerals being hematite and quartz with minor proportions of goethite

- The slimes were artificially generated from coarse ore
- The long milling times (45 minutes) would assist in cleaning the surfaces of the particles

3.4 Feed Characterisation

To determine if selective flocculation can improve the separation efficiencies of conventional gravity and magnetic separation units in the treatment of slimes, the sample employed should be low grade, well liberated and have simple mineralogy (dominant minerals that are easy to separate from each other in terms of gravity and magnetic based separations). The former can be determined by chemical analysis whilst the latter two aspects can be determined mineralogically. Since selective flocculation is typically applied to slimes (< 45 µm), it is important to determine if the artificially generated slimes meets this criterion. This criterion can be determined by sizing the sample. In addition, chemical analysis of the produced size fractions referred to as size-by-assay will also indicate the potential for barren waste rejection.

3.4.1 Methodology

3.4.1.1 Chemical Analysis

All samples submitted for chemical analysis, namely the head samples and products from each process unit were pulverised in a tungsten bowl until a powder of similar consistency to baby powder was obtained. The samples would be analysed for Loss On Ignition (LOI) and X-Ray Fluorescence (XRF) analysis by Mintek's Analytical

Services Division. The analytical techniques and their detection limits are presented in Table 3.4.

Table 3.4: Chemical Analysis Breakdown

Method	Description	Analytes	Detection Limit
LOI: Loss On Ignition	Loss on ignition is determined gravimetrically by weighing a sample before and after heating at 900°C until a constant mass is reported.	LOI	N/A
XRF12: Hematite Ref: Sarm 11	Fusion method for iron ore (hematite) samples	Al_2O_3; CaO; Cr_2O_3; Fe (total); MgO; MnO; SiO_2; TiO_2; K_2O; P_2O_5	Al_2O_3= 500ppm; CaO = 500ppm; Cr_2O_3 = 2%;Fe (total)= 9%; MgO= 500ppm; MnO= 0.2%; $SiO_{2=}$ 0.2%; $TiO_{2=}$ 0.1%; V_2O_5= 0.1%; ; $P_2O_{5=}$ 500ppm; K_2O= 600ppm

A grind of 90% passing 75 µm and 20 µm are required for Loss On Ignition (LOI) and X-Ray Fluorescence (XRF) analysis respectively. Since one sample would be submitted for chemical analysis a grind of 90% passing 20 µm was targeted. Should the samples be too coarse Mintek's Analytical Services Division would return the samples for further pulverising prior to analysis.

For quality control purposes the following measures were taken:

- Tungsten bowls were used to pulverise samples to prevent Fe contamination of the sample. In addition, the bowls were cleaned with water and dried prior to pulverising each sample.
- Three aliquots of the head sample were subjected for chemical analysis to obtain confidence in the head analysis.
- The LOI results in combination with the XRF results were used to determine the sum of oxides for each sample. Sum of oxides ranging between 96% and 100% were deemed acceptable.
- The relative error between the measured and calculated head analyses was also calculated to identify assay outliers.
- The analysis obtained from mineralogy was compared to the chemical analyses to ensure precise results were obtained.

- A calibration curve of Fe vs SiO_2 was plotted using chemical analysis results to determine assay outliers. From experience, it has been observed that XRF measures Fe results accurately but in some instances low levels of SiO_2 cannot be accurately measured. In these instances, the Fe value would be assumed to be correct (indicated by low Fe relative errors compared to SiO_2) and the calibration curve would be used to calculate the SiO_2 value.

Initial mineralogical results of the sample selected indicated that hematite and quartz were the dominant minerals at 51% and 45% by mass respectively. The other Fe bearing mineral in the sample was identified as goethite and only represented 2.6% of the sample. Since hematite represented the majority of the Fe bearing minerals in the sample, the Fe reported by XRF was assumed to be hematite, and thus the selectivity between hematite and siliceous gangue using Fe and SiO_2 grades and recoveries were justified. If the sample had contained significant proportions of other Fe bearing minerals such as ferruginous clays, then X-Ray Diffraction (XRD) of the products would be required to determine the selectivity between hematite and quartz.

3.4.1.2 Mineralogy

A 500 g aliquot of the feed at 80% passing 38 µm was subjected to Electron Microprobe Analysis (EPMA) to determine the hematite mineral chemical composition, and Particle Tracking Analysis (PTA) to determine the modal abundances, hematite liberation and association with other minerals.

3.4.1.2.1 Electron Microprobe Analysis (EMPA)

A representative normal mount polished section of the sample was analysed on the Cameca SX 50 electron microprobe using wavelength dispersive spectrometry. The system was calibrated using pure oxide reference standards and cross-referenced to hematite standards during measurement to ensure reproducibility and quality of

results. Oxygen content was calculated by stoichiometry. An accelerating voltage of 15 kV was used with a beam current of 20 nA and a probe diameter of 10 µm.

3.4.1.2.2 Particle Tracking Analysis (PTA)

Two polished sections of the feed sample, the underflow of the Reflux Classifier from the base case test and selectively flocculated tests were prepared, carbon coated and analysed using the Mineral Liberation Analyser (MLA). During the measurement, the MLA generated an X-ray analysis for each grey level region within a particle. The measurement mode employed in this study was chosen on the basis of the ore type, runtime, purpose of the study, particle size and the successful ability to delineate mineral grain boundaries in particles. During the investigation, >10000 particles per polished section were analysed and processed via AutoSEM. A larger number of particles aids in the acquisition of a statistically representative dataset of the overall sample. Particle characterisation data pertaining to mineral types/compositions, particle size, density, weight per cent of the particle population, the particle area, shape factor, circularity, and perimeter of each particle were ascertained during offline processing.

3.4.1.3 Size-By-Assay

The feed at 80% passing 38 µm was subjected to a standard root 2 wet sizing analysis to determine the particle size distribution. Table 3.5 presents the size classes that were analysed, with a sub-sample of the -25 µm fraction submitted for ultrasonic sizing at 10 µm.

Table 3.5: Size Analyses Fractions

Size Fraction (µm)
+600
-600+425
-425+300
-300+212
-212+150
-150+106
-106+75
-75+53
-53+38
-38+25
-25+10
-10

Each of the size fractions produced was weighed and submitted for chemical analyses to determine the occurrence of Fe and SiO_2 within each size class. These results were compared with that obtained from PTA.

3.4.2 Results and Discussion

3.4.2.1 Chemical Analysis

Head Analysis

The sample milled to 80% passing 38 µm has a head grade of 37.34±0.47% at 95% confidence with silicates a major diluent at 41.78±0.21% as shown in Table 3.6. The Loss On Ignition (LOI) is low indicating low volatile content, and the sum of oxides are within the acceptable range indicating good assay accountability.

Table 3.6: Chemical analysis of the feed sample

Sample	Discrete Grade (%)										∑ Oxides
	Fe	SiO_2	Al_2O_3	MnO	K_2O	CaO	P_2O_5	Na_2O	MgO	LOI	
Aliquot 1	37.41	41.75	1.05	0.05	0.07	0.39	0.26	0.10	0.32	0.58	98.07
Aliquot 2	37.54	41.90	0.99	0.05	0.07	0.39	0.27	0.10	0.33	0.69	98.45
Aliquot 3	37.08	41.70	0.90	0.05	0.07	0.37	0.26	0.10	0.28	1.31	98.06
Average	**37.34**	**41.78**	**0.98**	**0.05**	**0.07**	**0.38**	**0.26**	**0.10**	**0.31**	**0.86**	**98.19**
Std Dev @ 95% Confidence	**0.47**	**0.21**	**0.15**	**0.00**	**0.00**	**0.02**	**0.01**	**0.00**	**0.05**	**0.79**	

Data Reconciliation Check

The Fe to SiO_2 grade relationship for the testwork products presented in Figure 3.5 indicates a good correlation with more scatter observed at lower Fe grades. Thus higher certainty can be attributed to the concentrate grades.

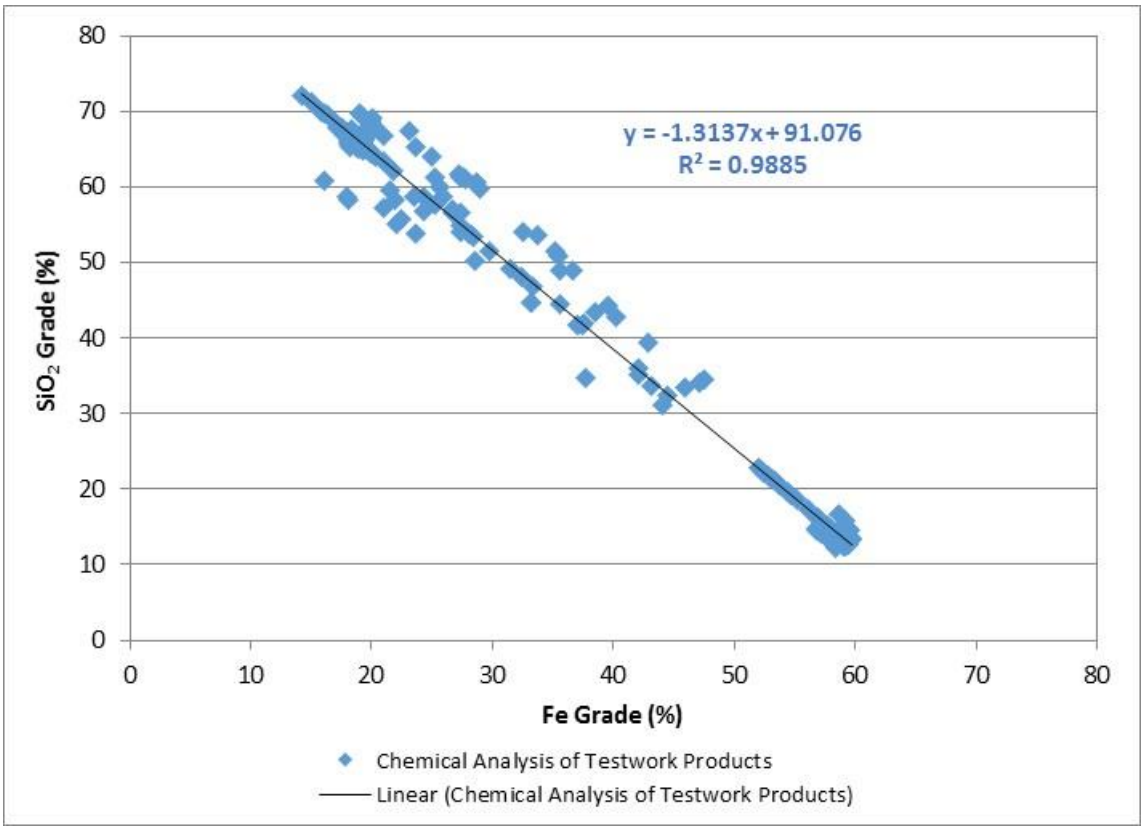


Figure 3.5: Data reconciliation check for chemical analysis of testwork products

3.4.2.2 Mineralogy

3.4.2.2.1 Electron Microprobe Analysis (EMPA)

The average Fe composition of hematite in the sample is lower than the theoretical composition indicating fine inclusions or dissemination of silicates within the hematite (Table 3.7). The theoretical composition is calculated using the molecular weights from the empirical formula for hematite (Fe_2O_3). The average hematite composition was used for PTA (Particle Tracking Analysis).

Table 3.7: EPMA results of 100 randomly selected Fe oxide grains (15 kV, 20 nA, spot size 5 µm)

Point	O	Mg	Al	Si	Fe	MgO	Al2O3	SiO2	Fe2O3	Total
Min	29.68	-	-	0.03	67.95	-	-	0.07	97.15	98.36
Max	30.69	0.12	0.24	0.73	70.67	0.20	0.45	1.56	101.03	101.43
Average	30.24	0.04	0.09	0.24	69.65	0.07	0.17	0.52	99.57	100.18
Std. Dev.	0.19	0.03	0.06	0.16	0.56	0.05	0.12	0.34	0.80	0.62
Theoretical Hematite Composition	30.06	0.00	0.00	0.00	69.94	0.00	0.00	0.00	100.00	100.00

3.4.2.2.2 Particle Tracking Analysis (PTA)

Mineral Abundances

The feed sample was selected for this study due to its simple mineralogy as indicated in Table 3.8. Hematite and quartz are the dominant minerals with minimal proportions of goethite and clay present in the sample. Since hematite is the dominant Fe bearing mineral the use of Fe assays via XRF analysis to represent hematite is acceptable.

Table 3.8: Mineral Abundances of the two polished sections of the Feed Sample

			Sample		Average	2 Std Dev
			A	B		
Mineral Name	**Chemical Formula**	**S.G.**	**Mass %**	**Mass %**	**Mass %**	**Mass %**
Hematite	Fe_2O_3	5.30	51.2	51.5	51.3	0.5
Quartz	SiO_2	2.71	45.5	44.8	45.1	1.1
Goethite	FeO(OH)	5.30	2.1	2.6	2.4	0.7
Apatite	$Ca_5(PO_4)_3(OH,F,Cl)$	2.60	0.4	0.5	0.5	0.1
Clay (Kaolinite and Boehmite)	$Al_2Si_2O_5(OH)_4$ and AlO(OH)	3.04	0.2	0.3	0.2	0.0
Ilmenite	$FeTiO_3$	4.55	0.1	0.0	0.1	0.1
Dolomite	$CaMg(CO_3)_2$	2.63	0.1	0.1	0.1	0.0
Rutile	TiO_2	4.25	0.1	0.1	0.1	0.0
Other	-	2.62	0.2	0.2	0.2	0.0
Total			**100.0**	**100.0**		

Mineral Liberation Characteristics

Liberation of the dominant minerals hematite, quartz and goethite are discussed using the liberation classes described below. These were based on the degree of liberation of the mineral, i.e., the portion of the grain that was exposed and therefore did not share a boundary with another mineral.

- Liberated: More than 80% of the surface of the particle
- Completely liberated: 100% of the surface of the particle

Figure 3.6 indicates that the sample at 80% passing 38 µm is well liberated with similar proportions (89% to 91.5%) of the dominant minerals (hematite and quartz) in the greater than 80% liberated class. However, Figure 3.7 indicates the proportion of completely liberated hematite and quartz drops by ~20% to ~69% whilst only a slight drop is noticed for goethite. The difference in the two liberation by area classes indicates a quartz and hematite association with quartz expected to dilute the concentrate grade due to incomplete liberation.

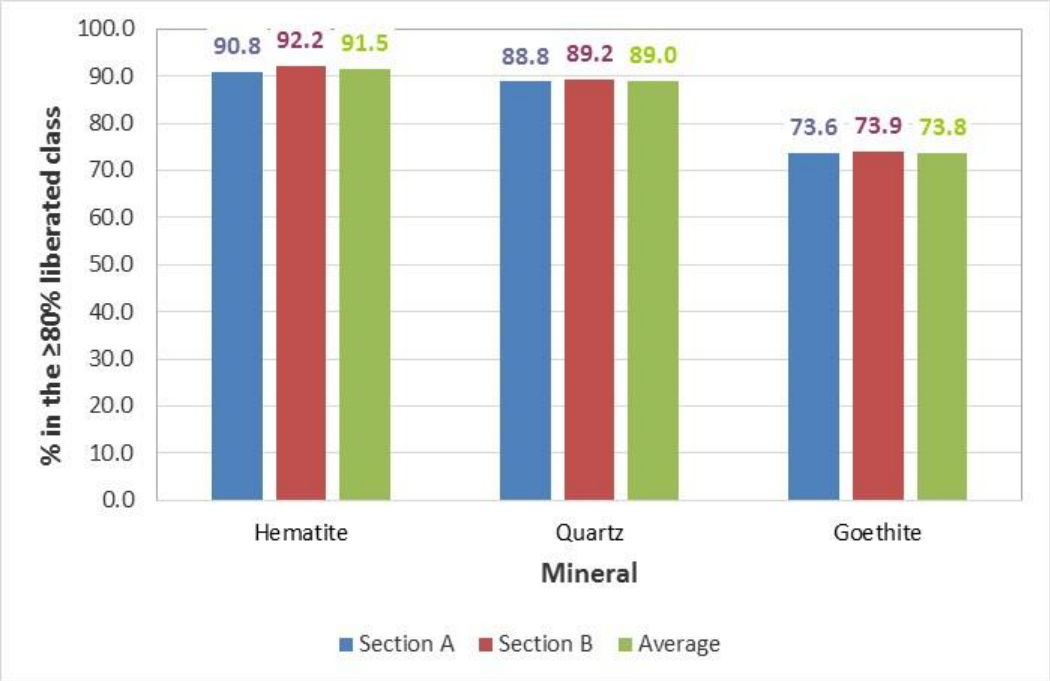


Figure 3.6: Proportion of the dominant minerals in the greater than 80% liberated class (liberation by area)

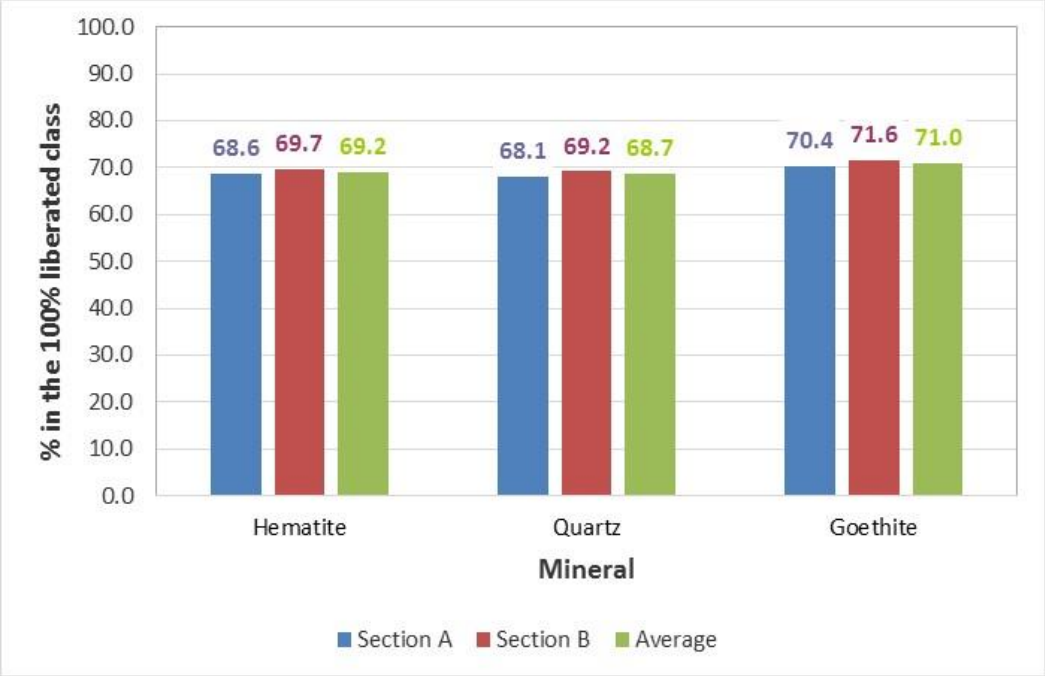


Figure 3.7: Proportion of the dominant minerals in the completely (100%) liberated class (liberation by area)

The false colour images in Figure 3.8 reveal hematite attachments to quartz for both coarse and fine particles. Figure 3.9 presents the cumulative mass% liberated for hematite for each size class and confirmed that as the particle size decreases an increases in liberation is observed with approximately 80% of the -12 µm size class being completely liberated. The proportion of completely liberated hematite (69.2%) is lower than expected and will affect the concentrate grade and recovery for both magnetic and gravity separation.

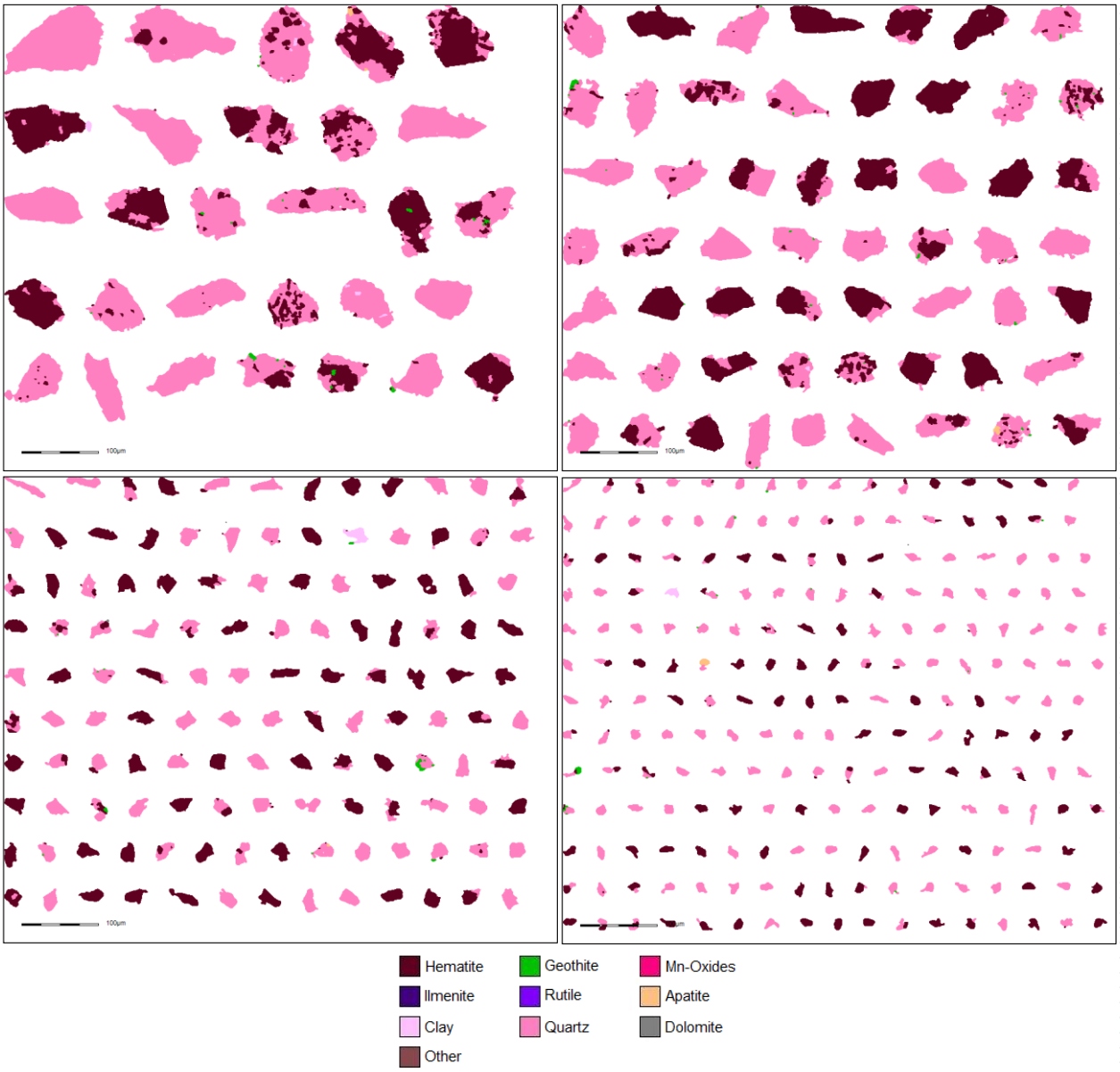


Figure 3.8: False Colour Images of the feed showing hematite and quartz attachments for various particle sizes (100 µm scale bar included for reference purposes)

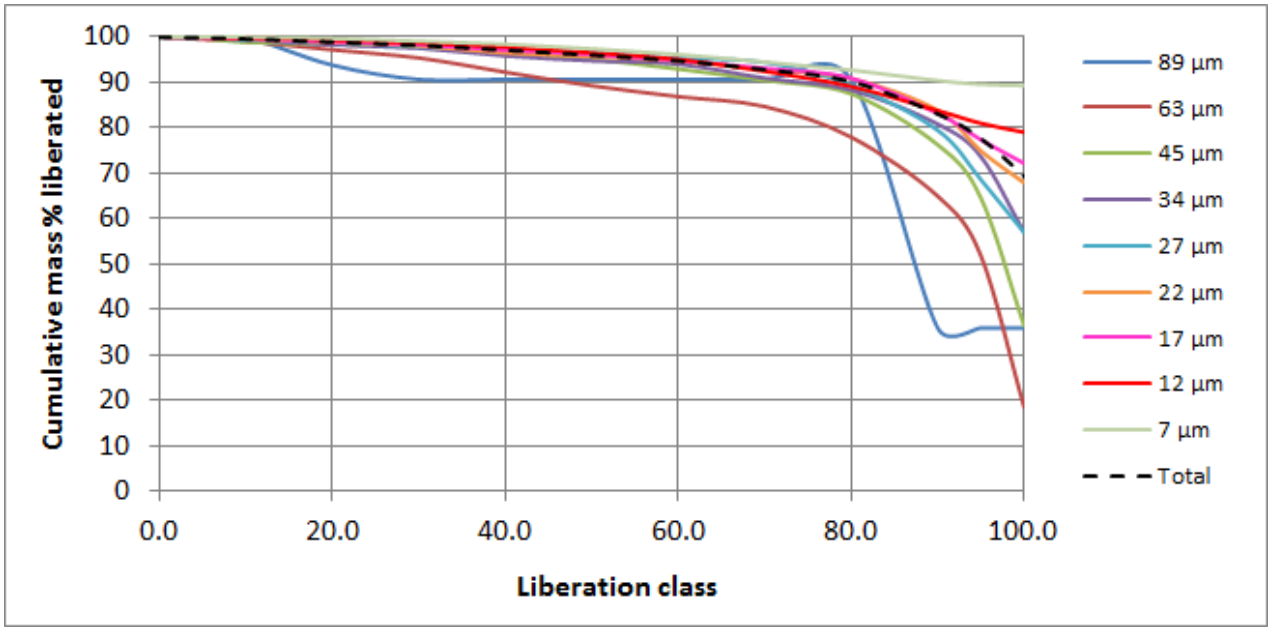


Figure 3.9: The cumulative mass per cent liberated by size for Hematite

Data Reconciliation Check

The mineral abundances and liberation characteristics for the polished section A and section B are similar as indicated in Table 3.8 and Figure 3.6 in the preceding sections. The low standard deviations at 95% confidence limit indicate the results are precise.

In addition to quantifying the confidence limits for the two polished sections, the chemical analysis by mineralogy (MNL) and chemical methods (Analytical Services Division, ASD) was compared for quality assurance. Figure 3.10 indicates a similar trend for both methods with better correlation observed at higher Fe grades. The good correlation for the analysis of the feed sample by both methods is further supported by Table 3.9 indicating a good correlation for Fe and slightly lower correlation for SiO_2.

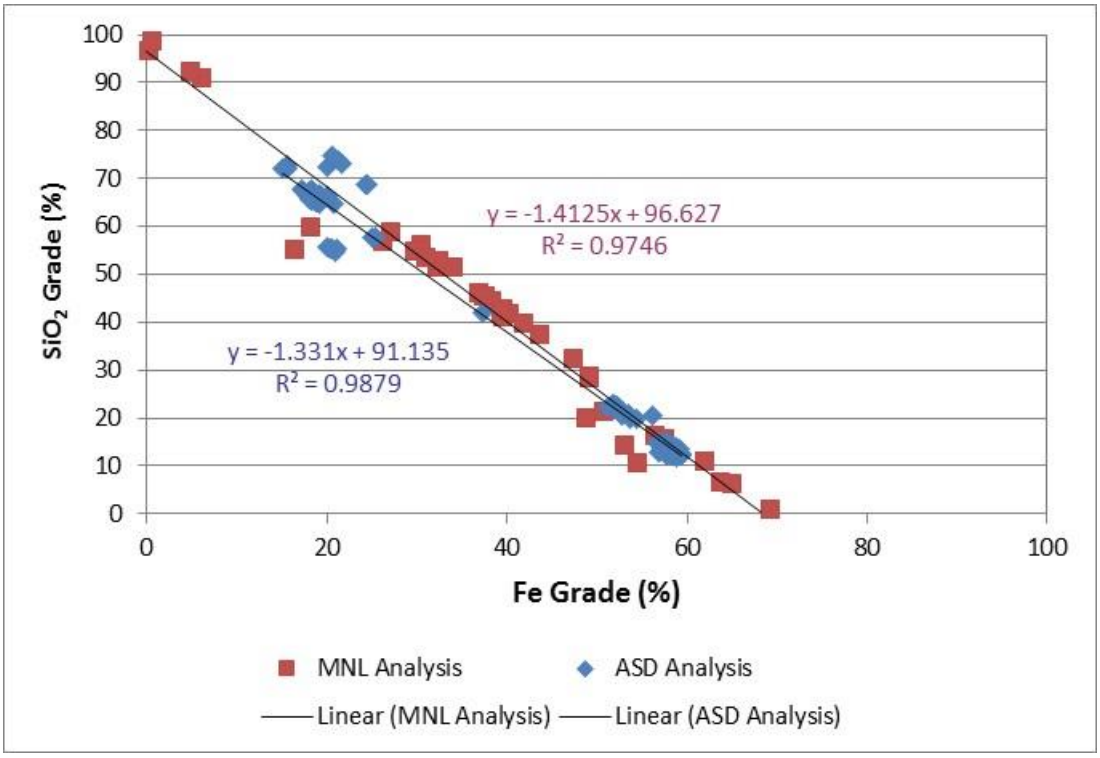


Figure 3.10: Data reconciliation check for mineralogical and chemical analysis

Table 3.9: Analysis of feed sample by chemical and mineralogical methods

Sample	Discrete Grade (%)			
	Fe	SiO_2	Al_2O_3	CaO
Chemical Analysis - Average of three aliquots	37.34	41.78	0.98	0.38
Mineralogical Analysis - Average of two sections	37.19	45.60	0.24	0.30
Difference	0.15	3.82	0.74	0.09

3.4.2.3 Size-By-Assay

3.4.2.3.1 SBA from Sieving

Two aliquots of the feed were independently sized and each size fraction chemically analysed. Figure 3.11 and Figure 3.12 indicates a similar discrete mass and Fe deportment for the two aliquots. The majority of the mass and Fe reported to the -25+10 µm size fraction at an average of 56.8% and 54.4% respectively.

In general, the discrete Fe grade across the size classes are similar for the two aliquots except for the -150+106 µm size fraction where a large discrepancy is noted (47.00% Fe vs 26.14% Fe). This can be attributed to the low mass pull in this size fraction making the Fe deportment and Fe grade discrepancy insignificant. It is observed that there is no preferential Fe upgrade to the discrete size fractions with the cumulative Fe grade ranging from 33.14% to 37.21% Fe (Figure 3.13).

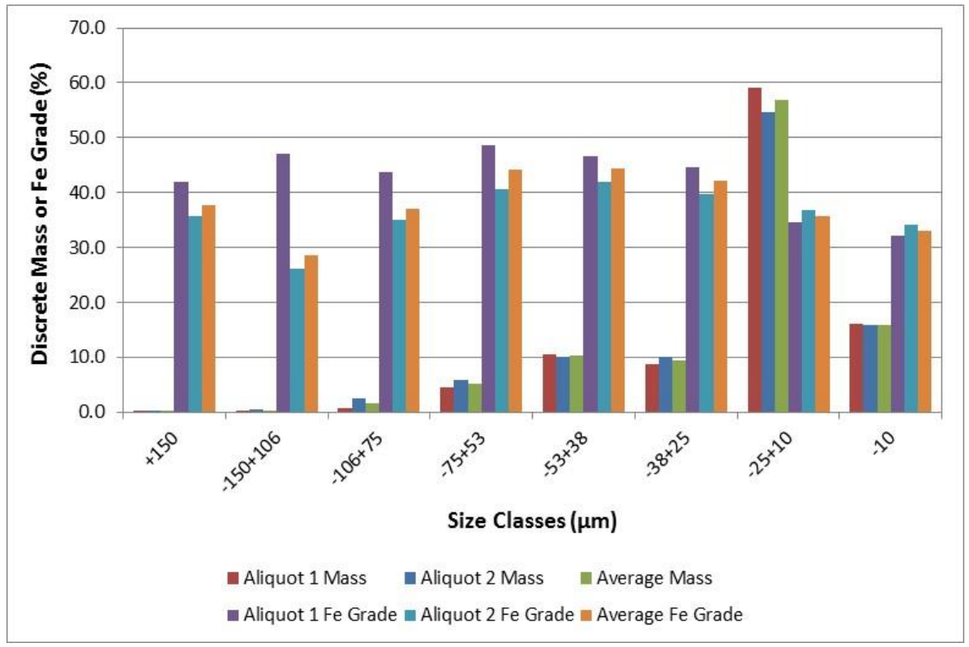


Figure 3.11: Discrete Mass and Fe Grade Distribution of the Feed

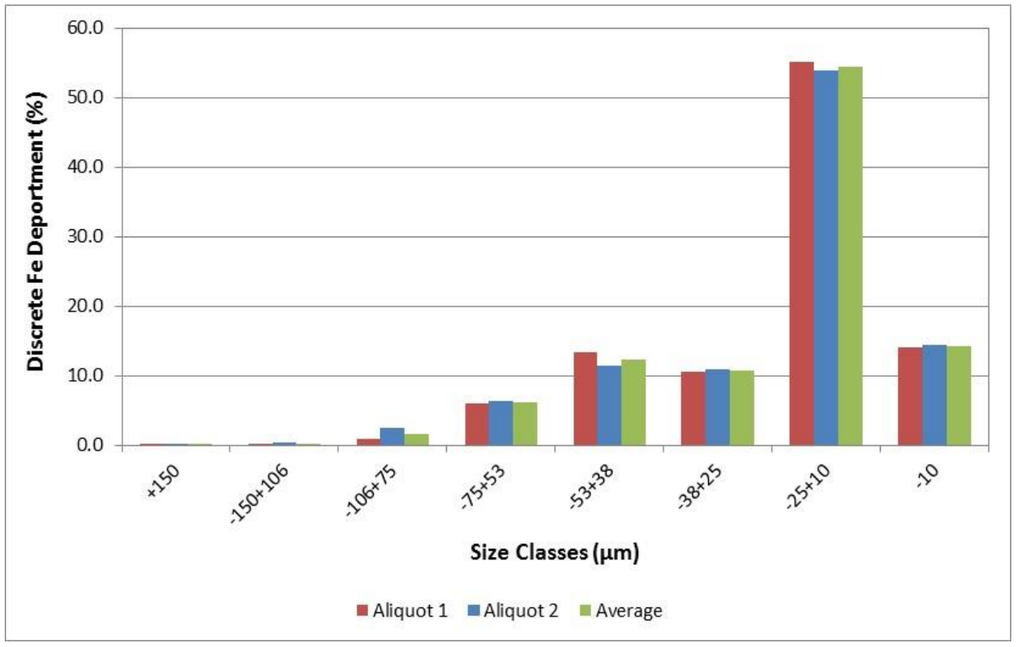


Figure 3.12: Discrete Fe Deportment of the Feed

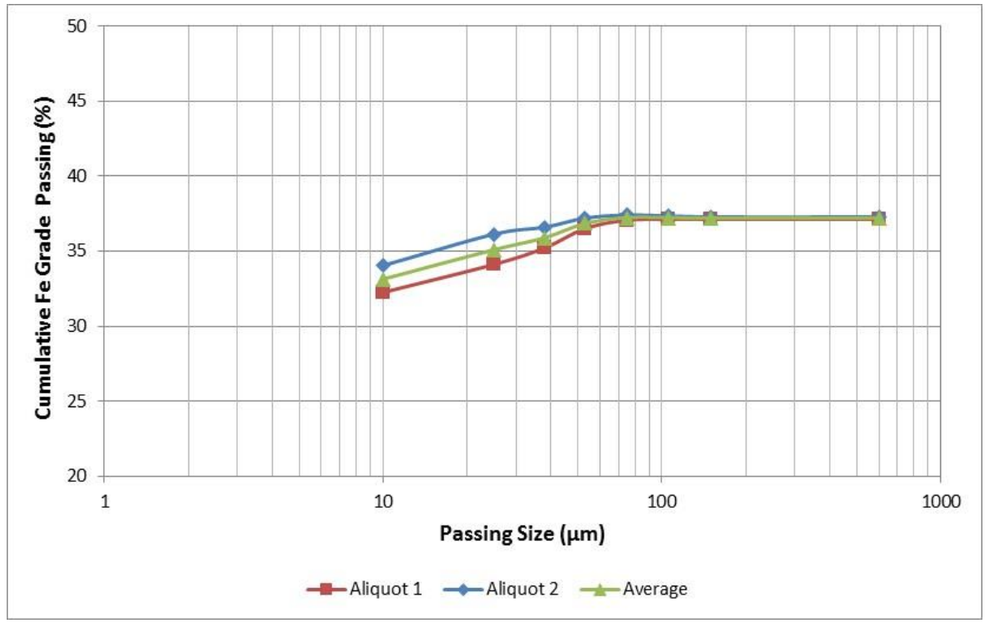


Figure 3.13: Cumulative Fe Grade of the Feed

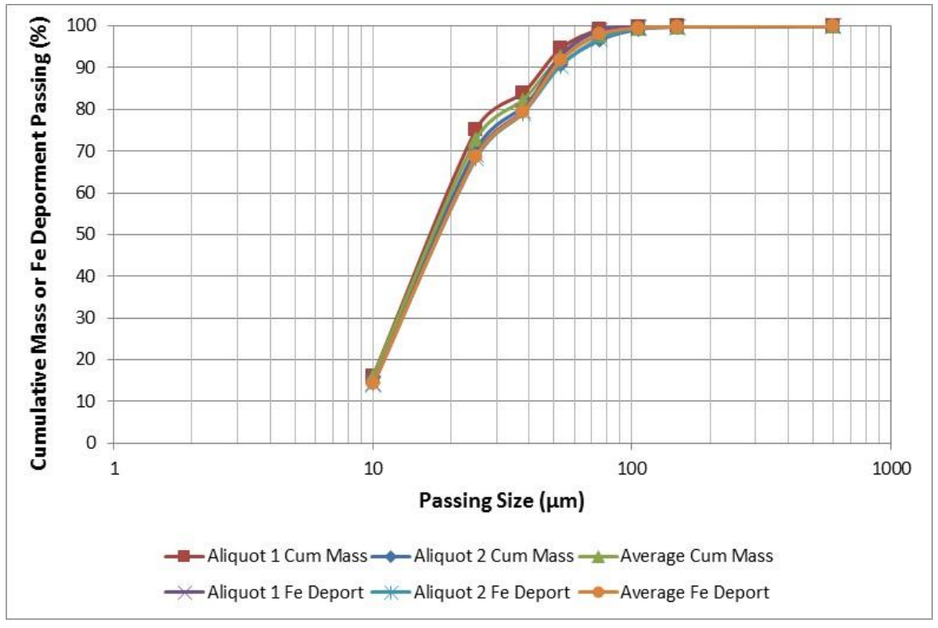


Figure 3.14: Cumulative Mass and Fe Deportment of the Feed

3.4.2.3.2 SBA from Particle Tracking Analysis

For both polished sections A and B the discrete mass, grade and deportment are similar for each size fraction except for the -106+75 µm fraction where section B reported higher Fe levels and lower Si levels (Figure 3.15 to Figure 3.16). This discrepancy may be attributed to the small mass proportion of this size fraction, and thus fewer grains were measured contributing to poorer confidence in the results for this particular size fraction.

A bimodal size distribution is observed with peaks at -53+38 µm and -10+5 µm. The sample is 85% -38 µm with the majority (~63%) of the mass reporting to the -20 µm size fraction (Figure 3.18). The deportment shows a similar trend to the mass distribution with ~60% Fe and ~66% Si reporting to this size fraction.

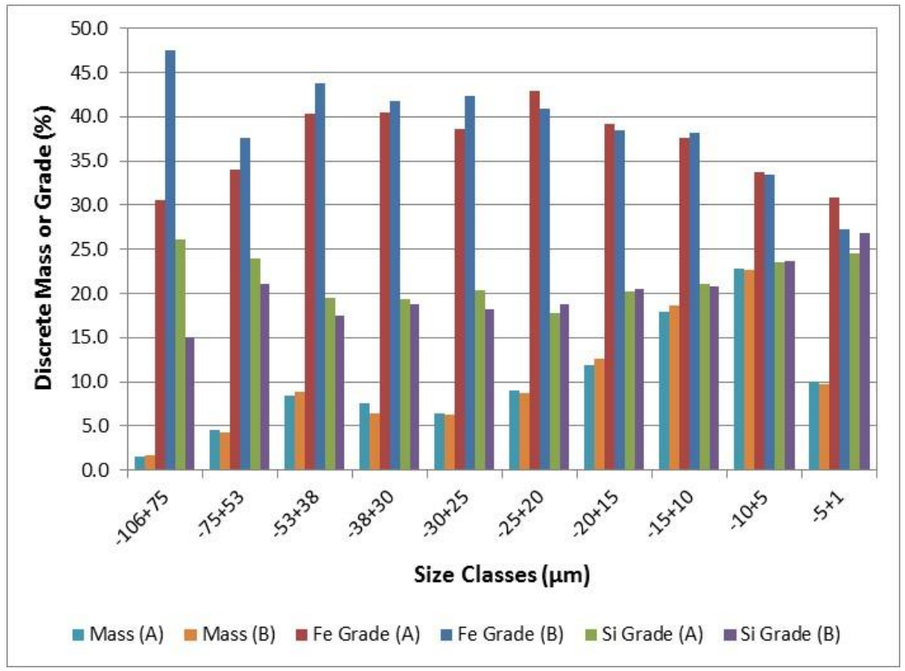


Figure 3.15: PTA Discrete Mass and Grade Distribution of the Feed

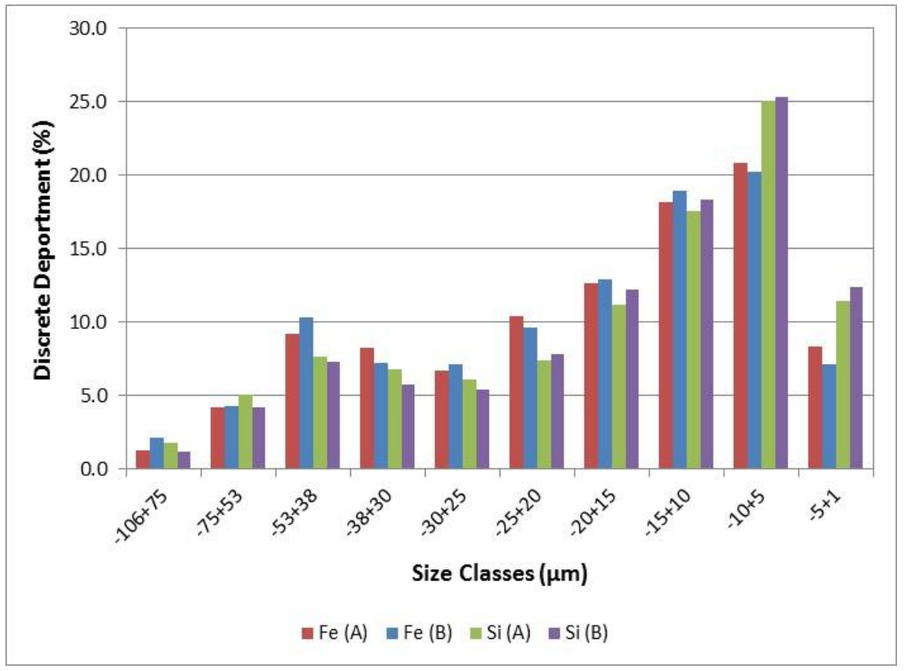


Figure 3.16: PTA Discrete Grade Deportment of the Feed

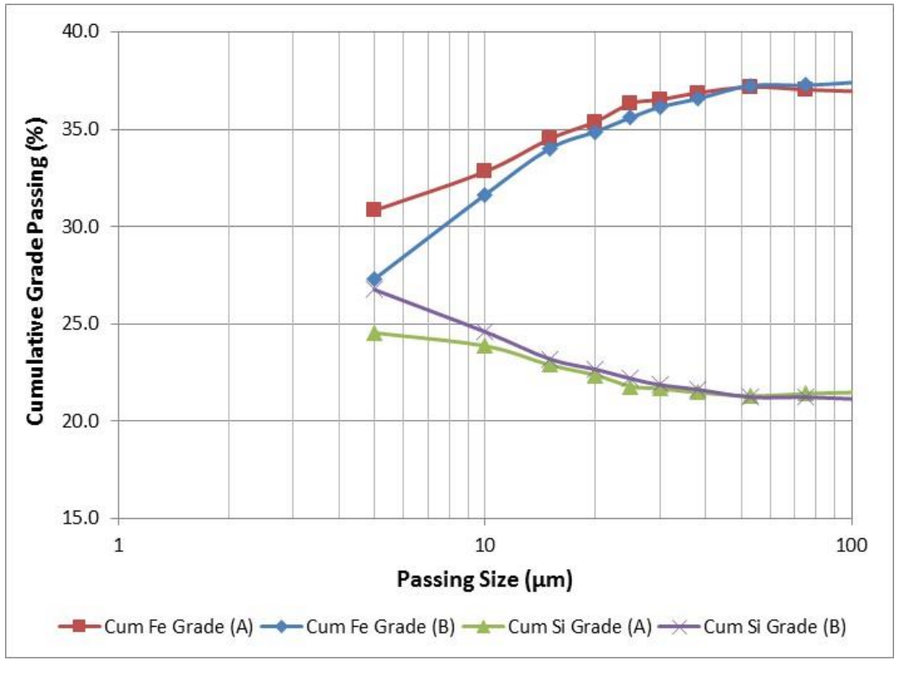


Figure 3.17: PTA Cumulative Grade Distribution of the Feed

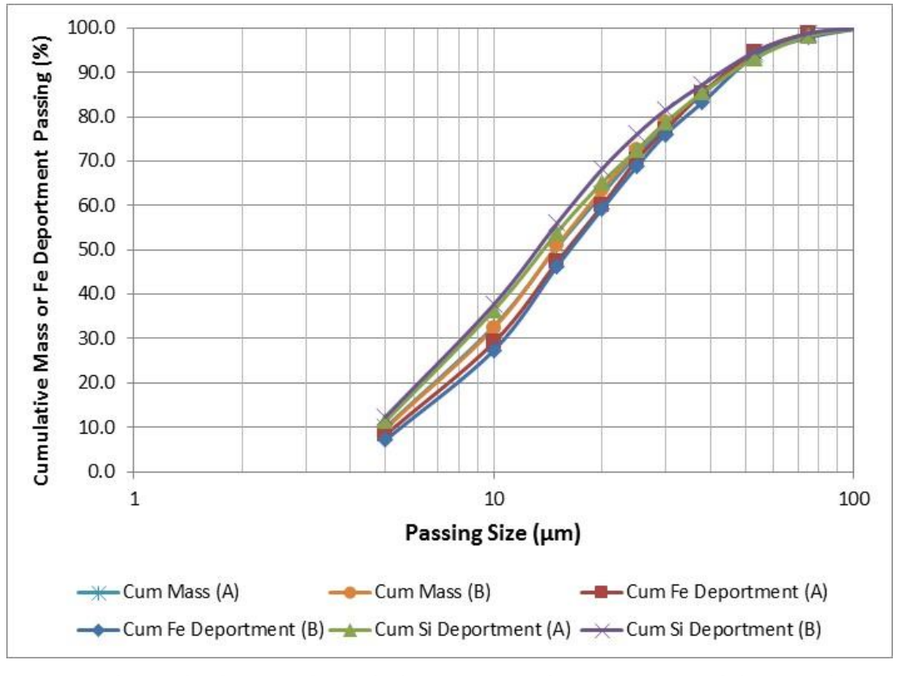


Figure 3.18: PTA Cumulative Mass and Deportment of the Feed

3.4.2.3.3 Comparative SBA results

The weighted SBA averages from sieving and PTA presented in Figure 3.19 to Figure 3.20 indicate in general a similar trend for the discrete mass and Fe grade between the sieving and PTA methods. The Fe grade indicates a flat trend resulting in Fe deportment closely following mass pull. The major discrepancies between the sieving and PTA results are located in the -25 µm size fraction with the SBA reporting 13% more Fe in the -25+10 µm and the PTA reporting double the amount of Fe in the -10 µm size fraction. The PTA results indicate a finer particle size distribution with considerably more -10 µm material than sieving. Agglomeration of the -10 µm fraction along with section preparation and measurement may have distorted the PTA results. During section preparation, a part of the particle may have been cut and appears as a particle of smaller diameter when measured on the MLA resulting in a cumulative error at the finer sizes as graphically illustrated in Figure 3.23.

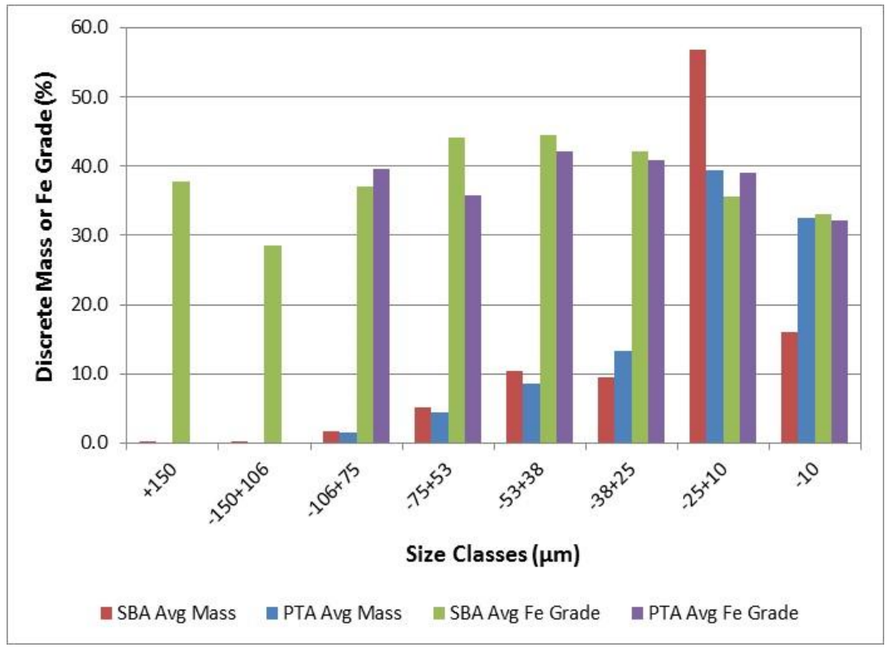


Figure 3.19: Comparative Discrete Mass and Fe Grade Distribution of the Feed via Sieving and PTA

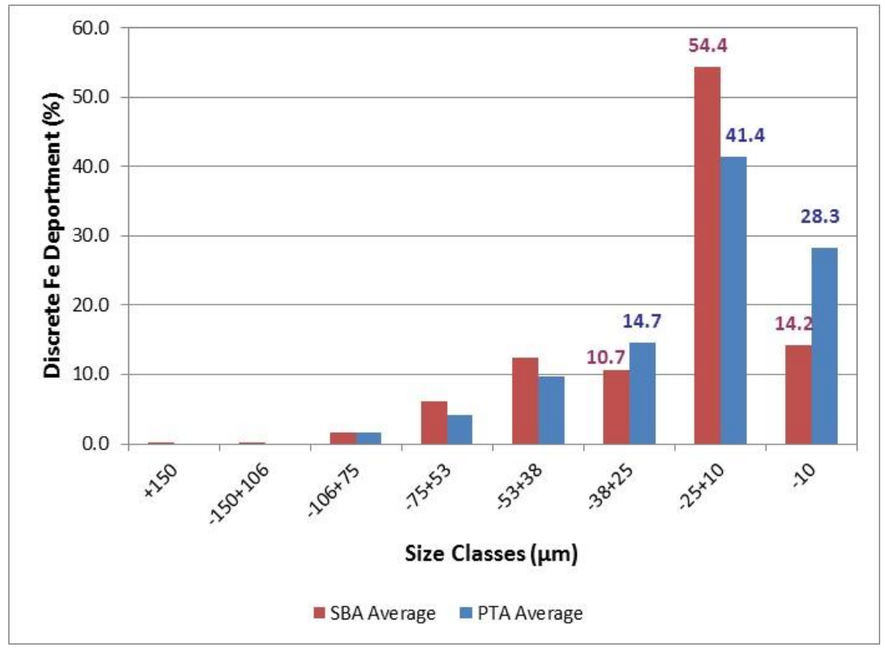


Figure 3.20: Comparative Discrete Fe Deportment of the Feed via Sieving and PTA

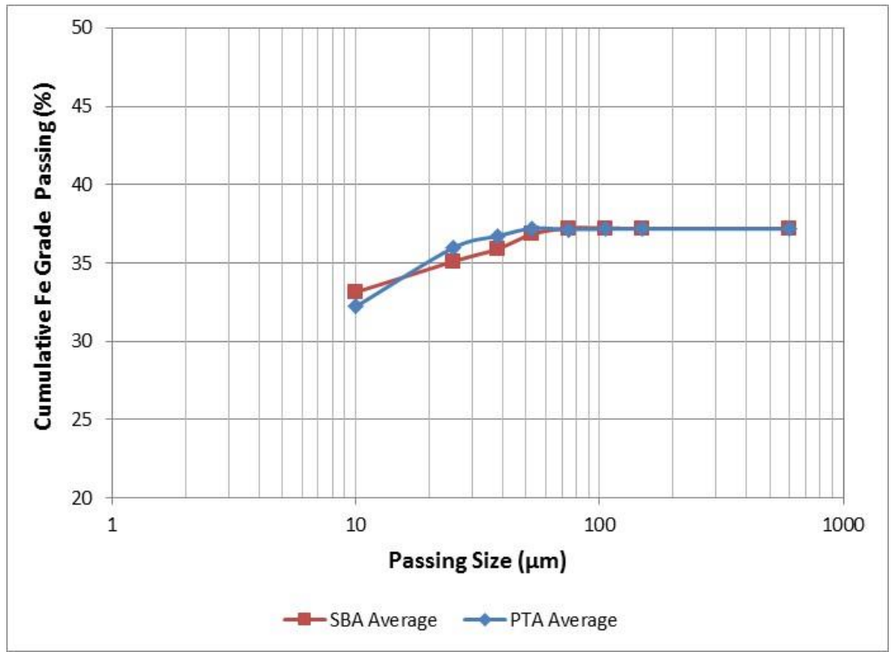


Figure 3.21: Comparative Cumulative Fe Grade Distribution of the Feed via Sieving and PTA

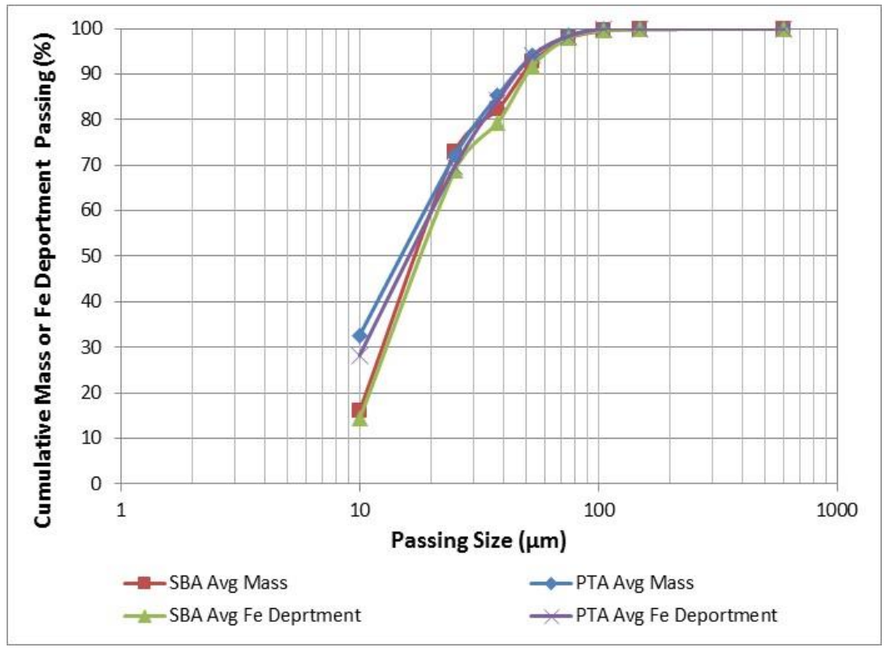


Figure 3.22: Comparative Cumulative Mass and Fe Deportment of the Feed via Sieving and PTA

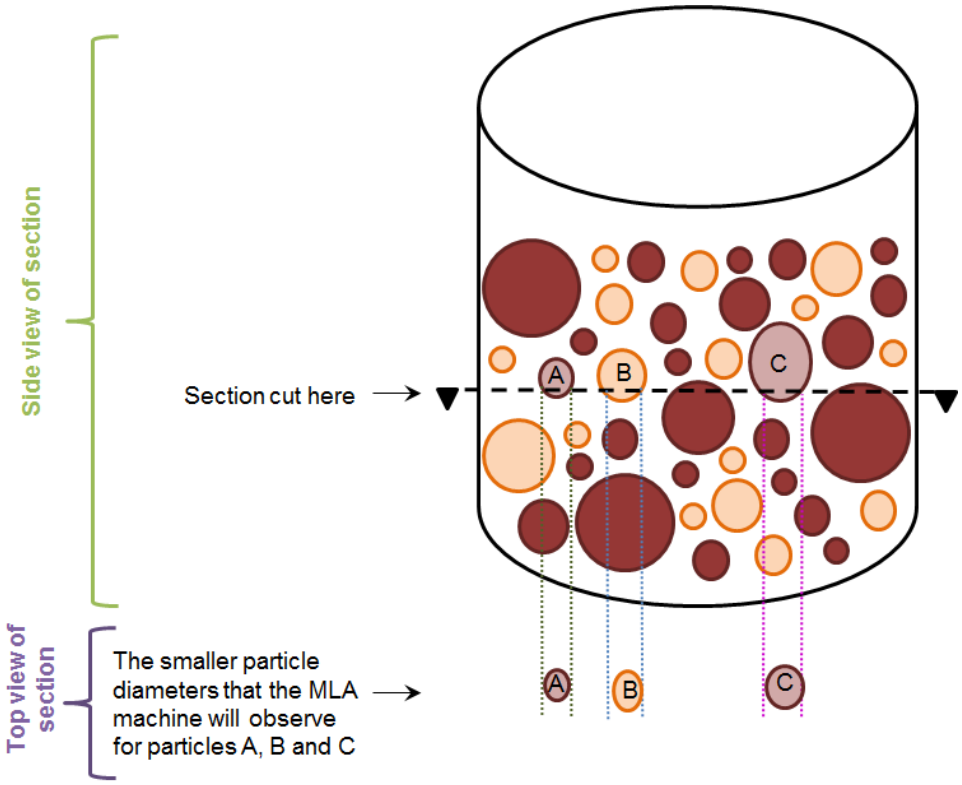


Figure 3.23: Section preparation and the reduction in particle size during measurement on the MLA

3.5 Conclusion

The simple mineralogy and good hematite liberation characteristics indicate the sample, prepared to 80% passing 35 µm, was well suited to the selective flocculation study. Mineralogy indicated that hematite was the major Fe bearing mineral (51.2%) with quartz (45.5%) as the dominant gangue mineral. The hematite is well liberated (91.5% in the >80% liberation class and 69.2% completely liberated) with the mineral chemistry indicating the sample can be upgraded from 37.34% Fe to the maximum Fe grade of 69.65% assuming perfect separation.

Approximately half of the sample by mass and Fe deportment reported to the -25+10 µm size fraction. No preferential Fe upgrade was observed to the discrete size fractions, and thus no potential for barren waste rejection exists.

The fine, liberated and simple nature of the sample made it a suitable candidate for selective flocculation and thus was used to establish the baseline conditions (Chapter 4) and later the optimised selective flocculation conditions (Chapter 5).

CHAPTER 4 : BASELINE TESTS

4.1 Introduction

The baseline tests covered in this chapter are tests that determine the preconditions required before optimisation of the selective flocculation conditions. The preconditions are the dispersant and pH studies from the first stage of Song et al. 's (2002) Floc Magnetic Separation (FMS) process defined in Figure 4.1 below. Figure 4.1 is Figure 2.14 from Chapter 2 and is repeated here for convenient reference.

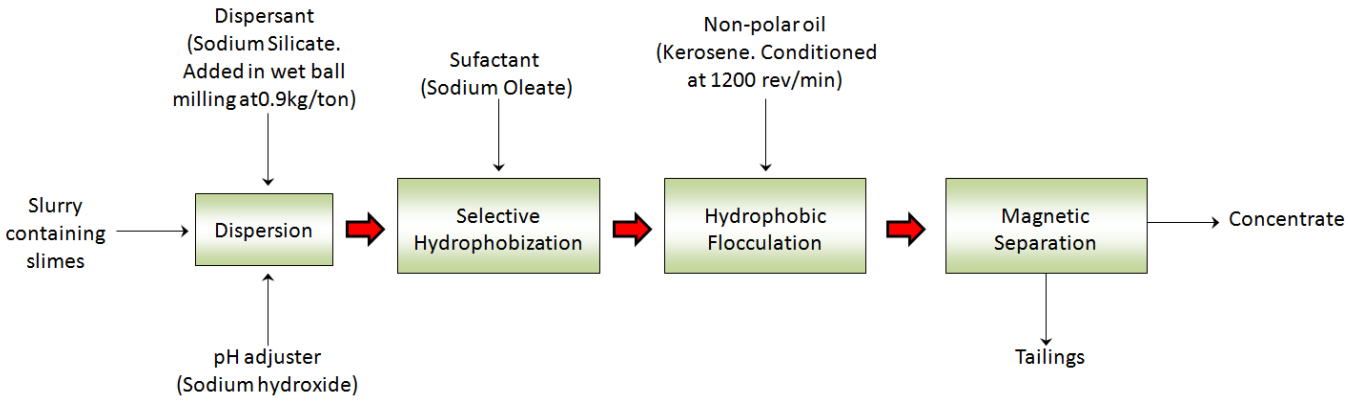


Figure 4.1: Schematic representation of the Floc Magnetic Separation (FMS) process applied to hematite (Song et al., 2002)

The critical first stage of the FMS process is dispersion, and the investigations presented in this chapter determines the effect of dispersant dosage and pulp density on dispersion using rheological analysis. An important output of the rheology tests is the calculation of the yield stress. The yield stress indicates the amount of force required to overcome the attractive forces between the solids thereby allowing for adequate dispersion. A yield stress of zero indicates a well-dispersed slurry (Wang et al., 2014).

Another aspect of the dispersion studies is to investigate the effect of pH, which has an impact on the hydrophobicity of the second stage (selective flocculation) and the size of flocs generated. The bigger the flocs, the more dominant the magnetic and gravity separation forces become over the hydrodynamic drag force. It is thus necessary to determine the particle size distribution of the sample before and after

selective flocculation at various pHs to determine the effect of pH on floc size. The flocculation conditions used for this stage were the centre point conditions for the selective flocculation tests. However floc size does not provide information regarding the effect of pH on the selectivity of the flocculation process and thus the pH tests needed to be coupled with a solid-solid separator to determine the effect of pH on the response variables separation efficiency, Fe grade and recovery. Due to the small mass requirements per a test, the SLon-100 (magnetic separator) was selected as the solid-solid separator. This coupling effect would also be applied for the second and third stages of the FMS process described in Chapter 5. However, to determine the best operating conditions for the SLon-100, intensity variation testwork without selective flocculation would first need to be conducted to establish the intensity that would optimise the response variables separation efficiency, Fe grade and recovery.

Since magnetic separation will be incorporated in the baseline tests for the first stage (dispersion), this chapter will first determine the optimum conditions for magnetic separation without selective flocculation. These optimum conditions will thereafter be applied to pH selection tests after the dispersant dosage selection tests.

The best conditions for the baseline tests will be fixed when the effect of the other factors on selective flocculation are explored in Chapter 5.

The raw data pertaining to this chapter is presented in Appendix B.

4.2 Base Case SLon-100 Intensity Variation Testwork

4.2.1 Methodology

4.2.1.1 Selection of Equipment

Mintek has two laboratory scale wet high intensity magnetic separators, namely the SLon-100 (Figure 4.2) and the Eriez laboratory scale L-4 Wet High Intensity Magnetic Separator (WHIMS) that can be used for the separation of paramagnetic minerals from gangue or other valuable minerals. The reason the SLon-100 was selected over the Eriez laboratory scale L-4 Wet High Intensity Separator (WHIMS) presented in Figure

4.3 is twofold. Firstly, reducing gangue entrainment in the floc structures was a requirement as this would improve the Fe grade of the final product. The pulsating mechanism of the SLon-100 (discussed in the following section) would reduce gangue entrainment. Secondly, Svoboda & Fujita (2003) indicated that at 1.06 Tesla hematite particles smaller than 25 µm cannot be recovered as the drag forces dominate magnetic forces. However, the pulsation mechanism of the SLon-100 allows for multiple chances in the recovery of ultrafines.



Figure 4.2: SLon-100 Pulsating WHIMS

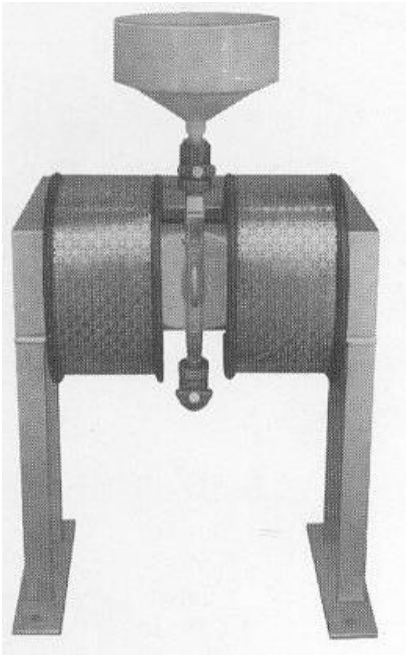


Figure 4.3: Eriez Laboratory scale L4 WHIMS (Eriez, 2016)

In this study, the SLon-100 was used to separate hematite (the target mineral) from silica (the gangue).

4.2.1.2 Working Principle of the SLon-100 Pulsating WHIMS

The SLon-100 is designed for laboratory testing; processing sample sizes typically in the 100-300g range depending on the density of the sample and the proportion of magnetics.

The laboratory scale SLon operates similarly to the conventional Wet High Intensity Magnetic Separator (WHIMS) with one distinguishing factor which is the pulsating mechanism. The pulsating mechanism (pulsating frequency and amplitude) drives the slurry up and down within the separating zone keeping the particles in the matrix in a loose state thus facilitating the capture of magnetic particles by the matrix and reducing entrainment of non-magnetic particles. A cross-sectional view of the SLon-100 is presented in Figure 4.4.

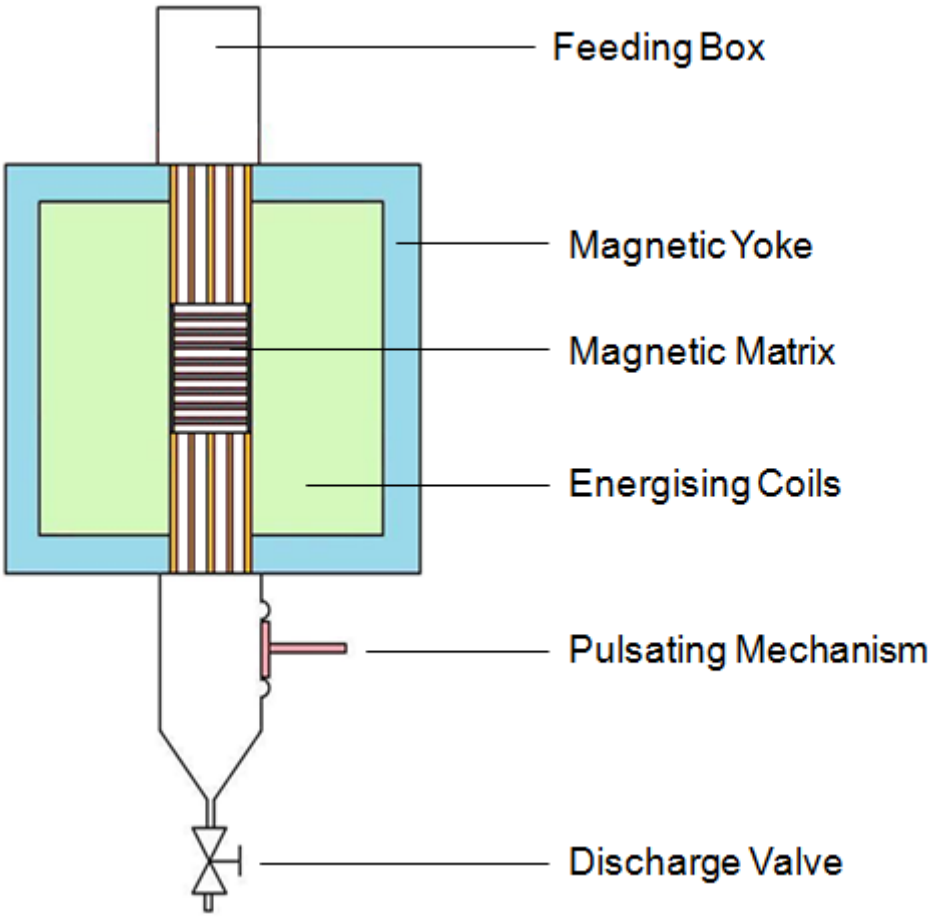


Figure 4.4: Cross-sectional view of the SLon-100 (Adapted from Outotec, 2012)

For each test, the SLon is filled with water so that the pulsating energy can be transmitted to the separating zone containing the magnetic matrix. Water continuously flows into the SLon at 600 L/hr, and the discharge valve is adjusted until the desired water level is maintained at the selected pulsation frequency and amplitude. The flow of direct current through the energising coils induces a magnetic field in the separation zone. The sample is then fed into the feeding box and enters the matrix. Expanded round bars made of magnetic stainless steel are used as a matrix and are referred to as rod matrices. Magnetic particles are attracted from the slurry onto the surface of the matrix. Non-magnetic particles pass through the matrix and flow with the water under the combined forces of gravity and hydrodynamic drag. The pulsating mechanism is arranged under the lower magnetic pole which drives a rubber diaphragm forth and back driving the slurry up and down as illustrated in Figure 4.5, with the dark blue representing water and brown the slurry.

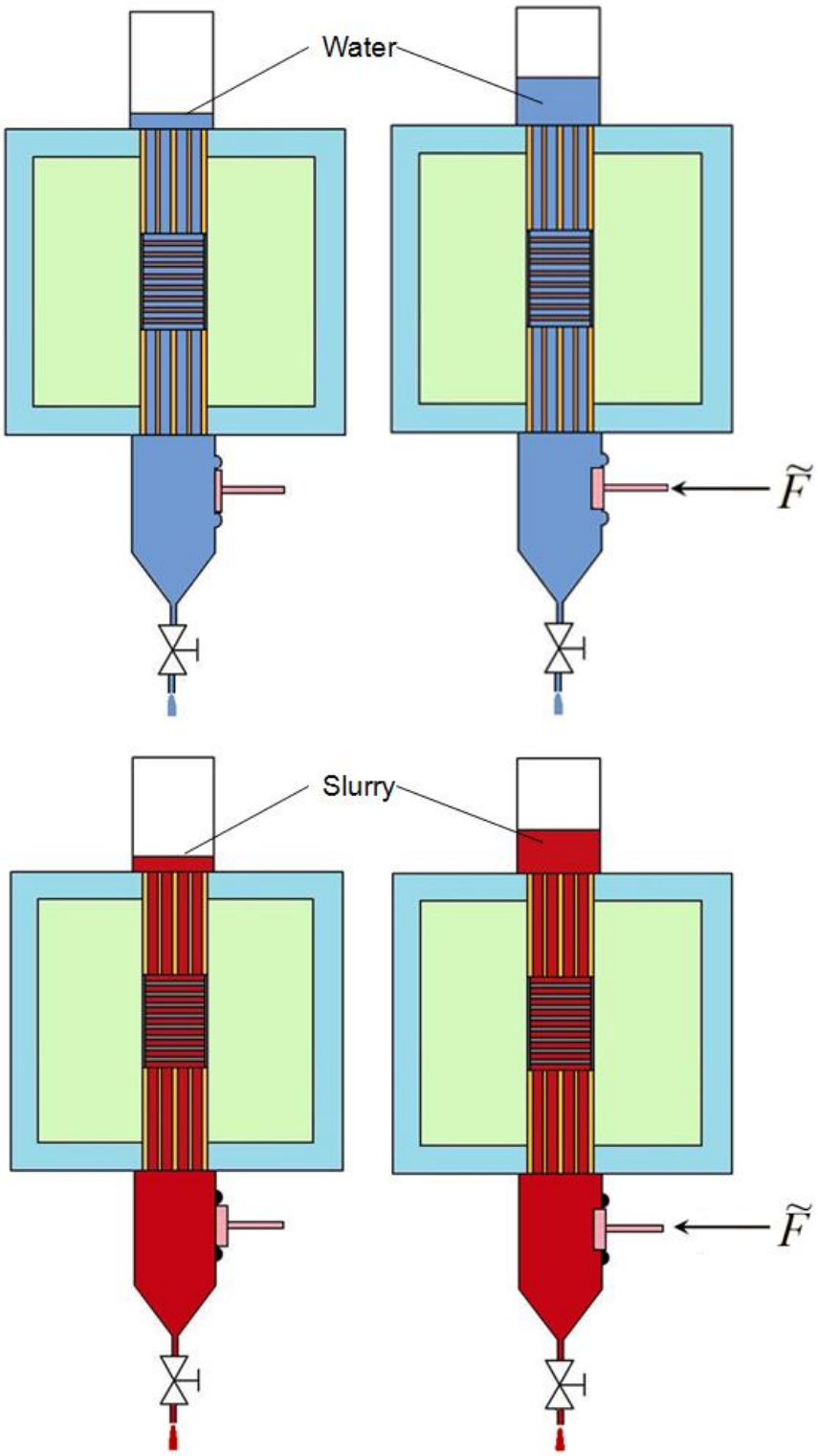


Figure 4.5: Pulsating Mechanism for the SLon-100 (Adapted from Outotec, 2012)

4.2.1.3 Selection of Operating Parameters

According to Outotec (2012) the variable operating parameters on the SLon-100 are:

- Feed Mass
- Matrix Type
- Matrix Size
- Background Magnetic Field Intensity
- Pulsation Frequency and
- Pulsation Amplitude

The selection of the various operating parameters and their ranges are explained below.

Feed Mass

Outotec (2010) recommended 200-300 g feed aliquots for ferrous minerals and based on this recommendation 200 g feed batches were processed on the Slon-100.

Matrix Selection

Outotec has both rod matrices and mesh matrices of various sizes. Due to the difficulty in effectively cleaning mesh matrices, rod matrices were selected for testwork purposes. The different rod matrices available for the SLon-100 are presented in Figure 4.6. The recommended top size for each matrix presented in Table 4.1 indicates a 1 mm rod matrix would be suitable for treating -0.6 mm fines. However, from a practical perspective, the 2 mm rod matrix was selected for testwork purposes as the finer matrices possess a higher wear rate and tend to warp under high intensities.

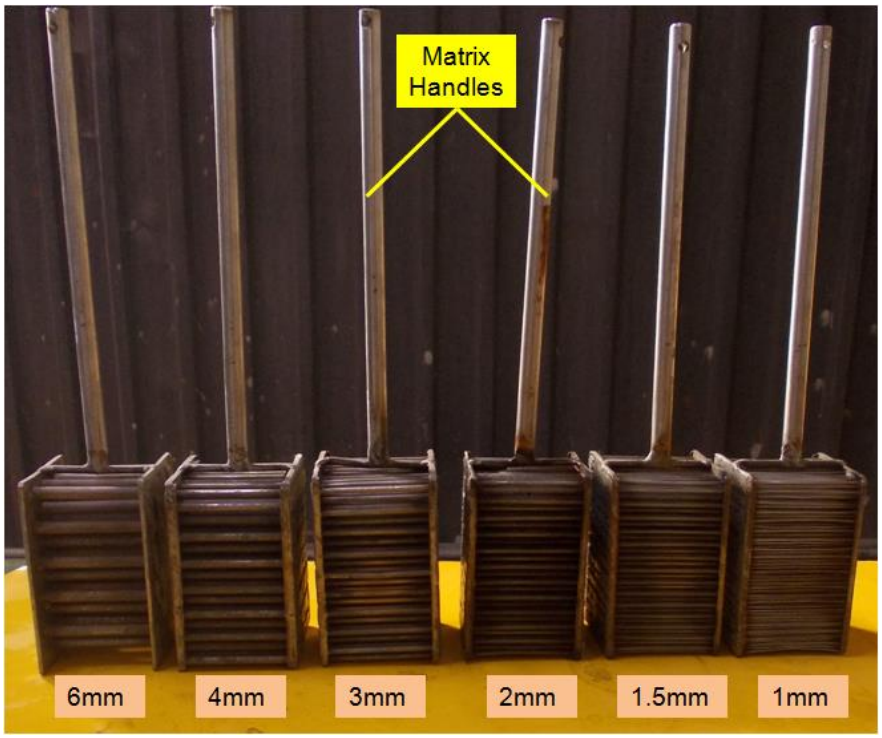


Figure 4.6: Rod Matrices with rod diameter indicated. The outer plates and handle of the matrices are a 300 series stainless (not magnetic) while rods are 400 series stainless (magnetic)

Table 4.1: Rod Matrices available (Outotec, 2012)

Rod Diameter (mm)	Maximum Particle Size (mm)
1	0.6
1.5	0.8
2	1.2
3	1.5
4	2
6	3

Background Magnetic Field Intensity

To determine the sensitivity of the various operating parameters on the product grade and recovery of two size fractions, Mintek conducted an ANOVA study on an iron ore sample of similar mineralogy to the sample used for the current investigation (Da Corte et al., 2015). The results from the previous study was used to isolate the most important operating condition for Fe recovery for the current study. Table 4.2 summarises the mineralogy and grades of the sample used by Da Corte et al. (2015) and that used in the current study. Table 4.2 shows that the -38 µm fractions of both studies have similar mineralogy and Fe grades and the -38 µm findings from the previous study should provide a good foundation for SLon testwork in the current study.

Table 4.2: Comparison of the mineralogy and grade of the samples used in the Da Corte et al. (2015) study and the current study

	Sample used in Da Corte et al.'s study (2015)	Sample used in Current Study
Mineralogy - Mineral Abundance	**-38µm**	**-38µm**
Hematite	63.7	51.3
Quartz	33.3	45.1
Chlorite	1.4	-
Goethite	-	2.4
Total	**98.5**	**98.8**
Chemical Assay	**-38µm**	**-38µm**
Fe Grade (%)	37.71	37.34
SiO_2 Grade (%)	25.29	41.78

Da Corte et al. (2015) investigated background magnetic field intensity, pulsation frequency and pulse amplitude at the selected ranges depicted in Table 4.3 on two size fractions: -1.18 mm+38 µm and -38 µm. The matrix and water feed rate remained fixed at 2 mm and 600 L/hr for each size fraction.

Table 4.3: Variation of Intensity, Pulsation Frequency and Pulse Amplitude for each Size Fraction (Da Corte et al., 2015)

Size Fraction	Background Magnetic Field Intensity (Gauss)	Pulse Frequency (rpm)	Pulse Amplitude (mm)
-1180+38µm	4 000, 6 000, 8 000	200, 250 , 300	10, 15, 20
-38µm	4 000, 6 000, 8 000	200, 250 , 300	5, 8, 10

A 3 parameter-3 level factorial design was applied in the previous study, and multivariate ANOVA was conducted on the results obtained from each size fraction. Table 4.4 indicates that the factors affecting Fe grade for the -38 µm fraction differ from those for Fe recovery. The factors significantly affecting Fe grade in the order of significance are pulse amplitude, pulse frequency, intensity and finally the pulse amplitude-pulse frequency interaction. As expected the most significant factor affecting Fe recovery for the -38 µm fraction is intensity followed by pulse amplitude, pulse frequency and the intensity-pulse amplitude interaction. Since a rougher application was tested in the current investigation and recovery is typically the main driver for rougher stages, intensity variation testwork was selected as recovery was most sensitive to this factor. It is well known that increasing the magnetic field intensity, and thus the magnetic field gradient, increases recovery. Although the study by Da Corte et al. (2015) tested a magnetic field intensity of 8 000 Gauss, a lower range of intensities was selected as higher intensities require higher energy inputs and to contain costs a maximum of 6 000 Gauss was selected. The range of intensities selected was 3 000 Gauss, 4 000 Gauss and 6 000 Gauss.

Table 4.4: Significant Factors affecting Fe Grade and Recovery for the -1.18mm+38 µm & -38 µm size fractions (Da Corte et al., 2015)

Size Fraction:		
-1.18mm+38µm	**-38µm**	
Fe Grade & Recovery	**Fe Grade**	**Fe Recovery**
Pulse Amplitude > Intensity>Pulse Frequency	Pulse Amplitude>Pulse Frequency>Intensity>Pulse Amplitude-Pulse Frequency Interaction	Intensity>Pulse Amplitude>Pulse Frequency>Intensity-Pulse Amplitude Interaction

Pulsation Frequency and Pulsation Amplitude

Based on the 3 parameter-3 level factorial design applied to the -38 µm by Da Corte et al. (2015) and excluding tests with a background magnetic field intensity exceeding 6 0000 Gauss the conditions that achieved the best Fe grade and recovery respectively are presented in Table 4.5. The results indicate that Test 11 closely followed by Test 5 achieved both the best grade and recovery for the -38 µm fraction. Based on these results a pulsation frequency and amplitude of 250 rpm and 5 mm respectively were selected for this investigation.

Table 4.5: The combination of parameters that achieve the best Fe grade and recovery at the rougher stage for the -38 µm size fraction (Da Corte et al., 2015)

Target	Test	Intensity (Gauss)	Pulse Frequency (RPM)	Pulse Amplitude (mm)	Mass %	Fe Grade (%)	Fe Recovery (%)
Target Fe Grade of 63%	11	6000	250	5	46	63	77
Target High Fe Rec	2	6000	200	5	56	54	80
	11	6000	250	5	46	63	77
	5	6000	200	8	45	62	76

4.2.1.4 Tests

In consideration of Section 4.2.1.3, intensity variation testwork was conducted holding all other parameters fixed as indicated in Table 4.6.

Table 4.6: SLon-100 Operating Conditions for -38 µm sample as-is

Fixed Operating Parameters	
Feed Mass	200 g
Matrix Type	Rod
Matrix Size	2 mm
Pulsation Frequency	250 rpm
Pulsation Amplitude	5 mm
Variable Operating Parameters	
Background Magnetic Field Intensity	3 000 Gauss
	4 000 Gauss
	6 000 Gauss

At each intensity three replicate tests were conducted, and thus a total of nine tests were conducted. The tests were randomised and conducted on the same day. The products from each test were filtered, dried and prepared for chemical analysis. Based on the grade-recovery response for each test an intensity was selected for further testwork namely pH selection and selective flocculation.

4.2.1.5 Precautions

The following precautions were followed for quality assurance:

- Prior to use of the SLon-100, a sub-sample of the feed is used to clean the unit to prevent contamination. In addition, the matrices are placed in an ultrasonic bath for about an hour to remove any contaminants.
- Before feeding the sample into the SLon, the magnet remained on for at least 5 minutes to ensure steady state is achieved

- Mintek participated in Outotec's round robin for the SLon-100 units installed around the world to assess the consistency of these units. The round-robin plan included sending the same split of a taconite sample and testing procedure to every laboratory involved. Mintek's results for all tests were within the acceptable range defined by Outotec.

4.2.1.6 Limitation of the SLon-100 Testwork

- The decision of when to collect the magnetic fraction is dependent on the operator's visual inspection of the "clean" non-magnetic fraction. The non-magnetic fraction may appear to be clean but may still contain ultrafines. On the other hand, waiting too long may result in losses of magnetic particles to the non-magnetic fraction due to the pulsation mechanism.
- It has been observed that rust from the yoke holes above and below the matrices, as depicted in Figure 4.7, will contaminate the products. In some instances, thorough washing at high pulse frequencies is not sufficient to prevent contamination. Since the rust particles are typically coarser than the sample the rust can be screened out from the products before chemical analysis.

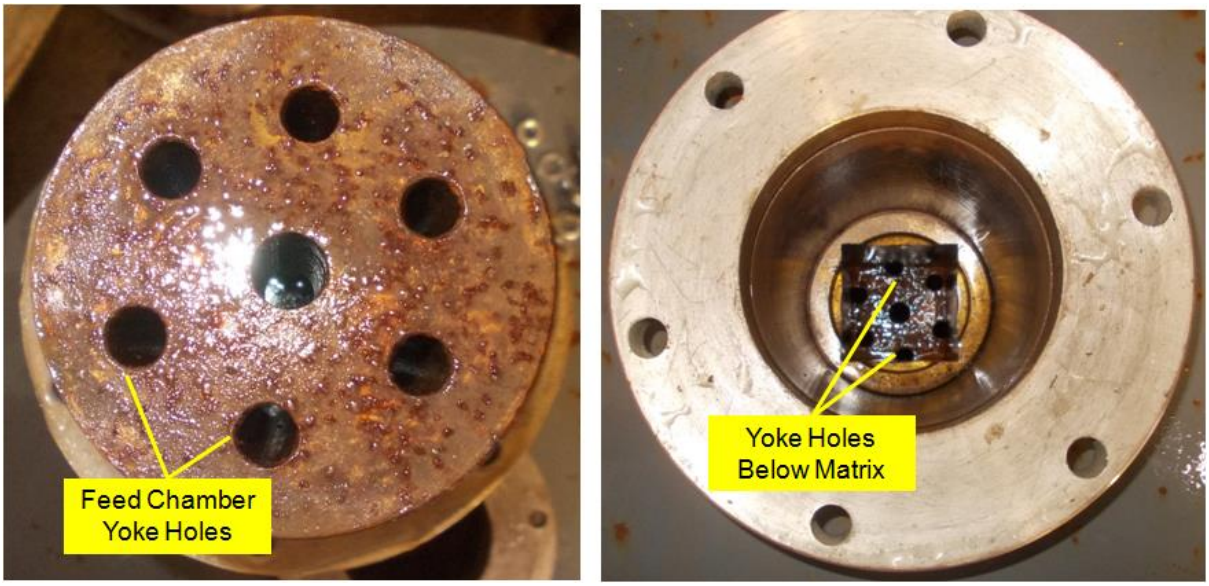


Figure 4.7: Yoke Holes in Feed Chamber and below Matrix

4.2.2 Results and Discussion

Three tests were conducted at each background magnetic field intensity with the average, and two standard deviations (indicating 95% confidence limits) of the magnetic product for the various response variables graphically illustrated in Figure 4.8. The sample followed the expected trend with increased mass pull and Fe recovery of the magnetic product as the background magnetic field intensity increased. The Fe grade of the magnetic product remained relatively constant and within the 95% confidence limits across the intensities tested.

The separation efficiency increased with increasing background magnetic field due to increasing Fe recovery and thus an intensity of 6 000 Gauss was selected for the coupled selective flocculation and magnetic separation process (FMS process).

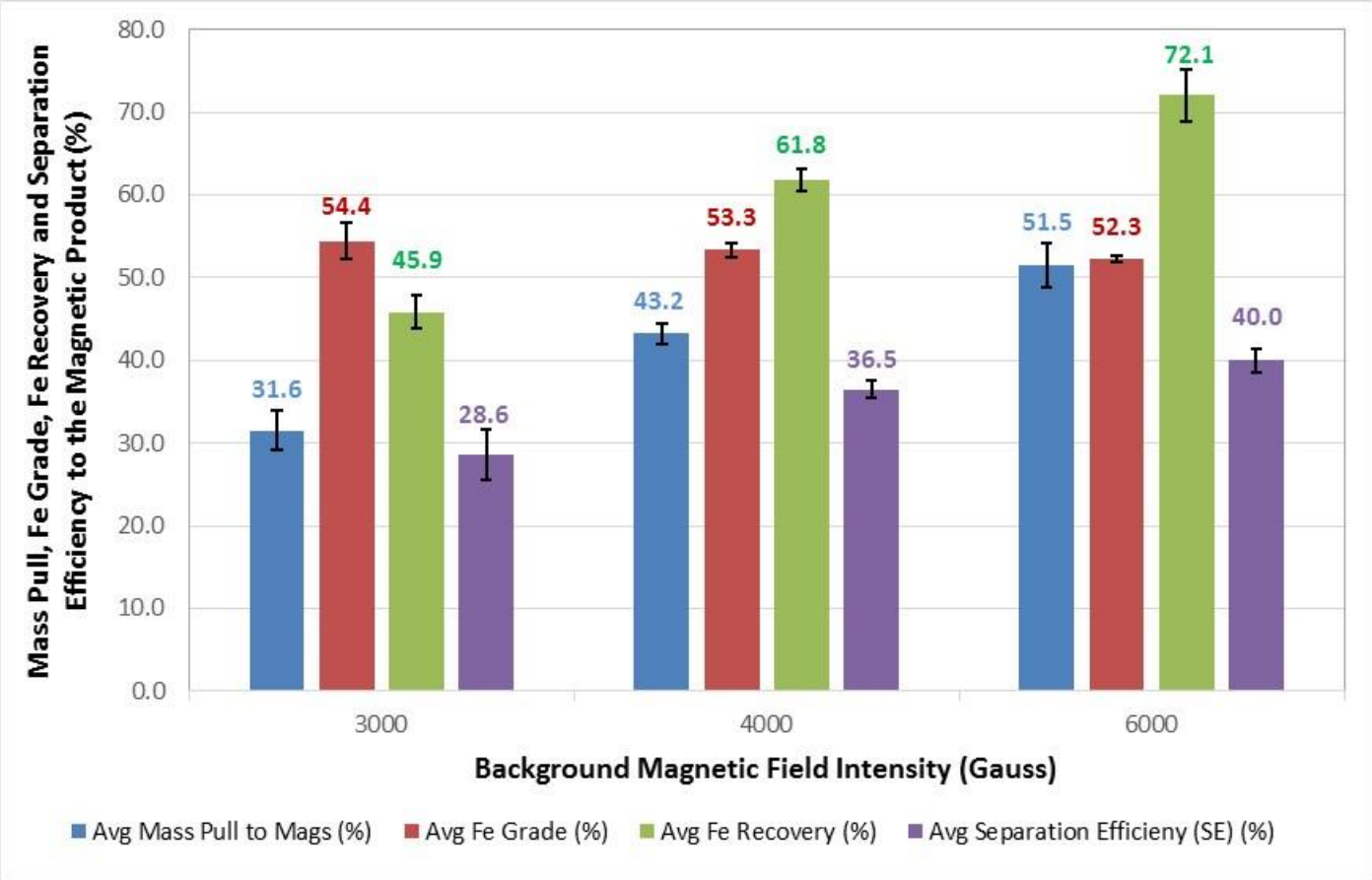


Figure 4.8: The Average Mass Pull, Fe Grade, Fe Recovery and Separation Efficiency in the Magnetic Product at three Background Magnetic Field Intensities (2 Standard deviations are depicted by the error bars)

4.3 Selection of Dispersant Dosage at Various Pulp Densities

The first critical step in the FMS process is to ensure there is adequate dispersion. In light of this and based on the mineralogy of the feed a common dispersant was selected and subjected to rheology tests at three selected dosages and three pulp densities.

4.3.1 Methodology

4.3.1.1 Selection of Dispersant

Sodium silicate is widely used in mineral flotation as a depressant, dispersant and as a controlling agent of some soluble ions. It can also interact with mineral surfaces preventing collector adsorption. Sodium silicate, with a general formula Na_2SiO_3, is produced in liquid and powder form. Sodium silicate generally consists of metasilicate (Na_2SiO_3), dimetasilicate ($Na_2Si_2O_5$) and orthosilicate (Na_4SiO_4). The chemical composition of sodium silicate can be expressed by the general formula $mNa_2O.nSiO_2$. The ratio *n/m* is referred to as the modulus of sodium silicates. Silicates whose modulus vary from 2.2 to 3.0 are frequently used in mineral flotation. According to Bulatovic (2007) sodium silicates with low moduli have a weak depressant effect and create pulps that are strongly alkaline, whilst sodium silicates with moduli exceeding 3 are insoluble in water. The modulus for the sodium silicate used in the investigation is 3.35 to 3.46 and is supplied by PQ Silicas South Africa (Pty) Ltd. Bulatovic (2007) recommends concentrations in the range 2-5% as the sodium silicate solution is most stable at these concentrations.

The function of a dispersant is to prevent aggregation of fine and clay particles and prevent slime coatings on the mineral particles by controlling the charge density at the solid-liquid interface or the electrical charges of ultrafine particles (Bulatovic, 2007). The action of sodium silicate as a dispersant is mainly associated with disassociated polysilicic acid which is partly ionised in aqueous solution. Its adsorption must lead to an increased negative charge of the solid and consequently has to stabilise mineral systems against aggregation. Some investigators have postulated that polymeric

sodium silicate adsorbs by multiple weak bonds to form hydrated layers at the mineral surface. Dispersion is a result of negative zeta potential values and hydrated layers (Bulatovic, 2007).

The sodium silicate dosages used by Song et al. (2002) and Roy (2012) ranged from 900 g/ton to 1 000 g/ton. Based on their work using the FMS process the sodium silicate dosage range was selected with 1000 g/ton the centre point and 500 g/t and 1500 g/ton the minimum and maximum dosages tested respectively. The sodium silicate used in this study was prepared to 1% concentration by mass using tap water. The matrix of tests conducted is further explained in Section 4.3.1.5.

4.3.1.2 Selection of Equipment

Wang et al. (2014) explain that when strong net repulsive interactions prevail between solids in a slurry, a stable dispersion (a dispersion that does not change its repulsive properties over an extended period) is created which results in a small change in slurry viscosity. As a result, a stable dispersion possesses no shear yield stress. However, if a strong net attractive force exists between solids in a slurry aggregation will occur resulting in a very high shear yield stress. An instrument capable of determining the yield stress was required, and thus the Physica Rheolab QC rheometer (Figure 4.9) was selected as this was the only suitable option available at the time.



Figure 4.9: Physica Rheolab QC Rheometer

4.3.1.3 Working Principle of the Rheometer

Rheology is defined as the study of the deformation and flow of fluids in response to applied forces. A rheometer measures the rheological properties of the fluid over a varied and extended range of conditions. As a diagnostic tool, rheometers indicate the level of inter-particle interaction or aggregation in a slurry and is thus an important variable for process control (Muster and Prestidge, 1995).

The Physica Rheolab QC rheometer is a rotational rheometer. In rotational rheometers, the test fluid is continuously sheared between two surfaces with either one or both surfaces rotating. The advantage of rotational rheometers is their ability to shear the sample for an extended period while monitoring the transient behaviour or equilibrium state of the fluid under controlled conditions. Rheometers are suited for the measurement of concentrated suspensions, gels and pastes but are generally less precise compared to rheometric measurements via the alternative capillary method (Hackley & Ferraris, 2001).

Hackly and Ferraris (2001) explain that rotational measurements can either be stress-controlled or rate-controlled. In stress-controlled measurements a constant torque is applied to the measuring tool to generate rotation with the resulting rotation speed determined and converted into a corresponding shear rate. In rate-controlled measurements a constant rotation speed is maintained, and the resulting torque generated by the sample is determined using a suitable stress-sensing device such as a torsion spring or gauge. Mintek's Physica Rheolab QC rheometer is a rate-controlled device.

4.3.1.4 Selection of Operating Parameters

Tool Geometry

The Physica Rheolab QC rheometer is a rotational rheometer whereby a fluid is sheared between two surfaces with the either one or both surfaces rotating at the same time. The surfaces that typically rotate are the tool geometries with the three main tool geometries; namely the cone and plate, concentric cylinder, or parallel plates; schematically presented in Figure 4.10.

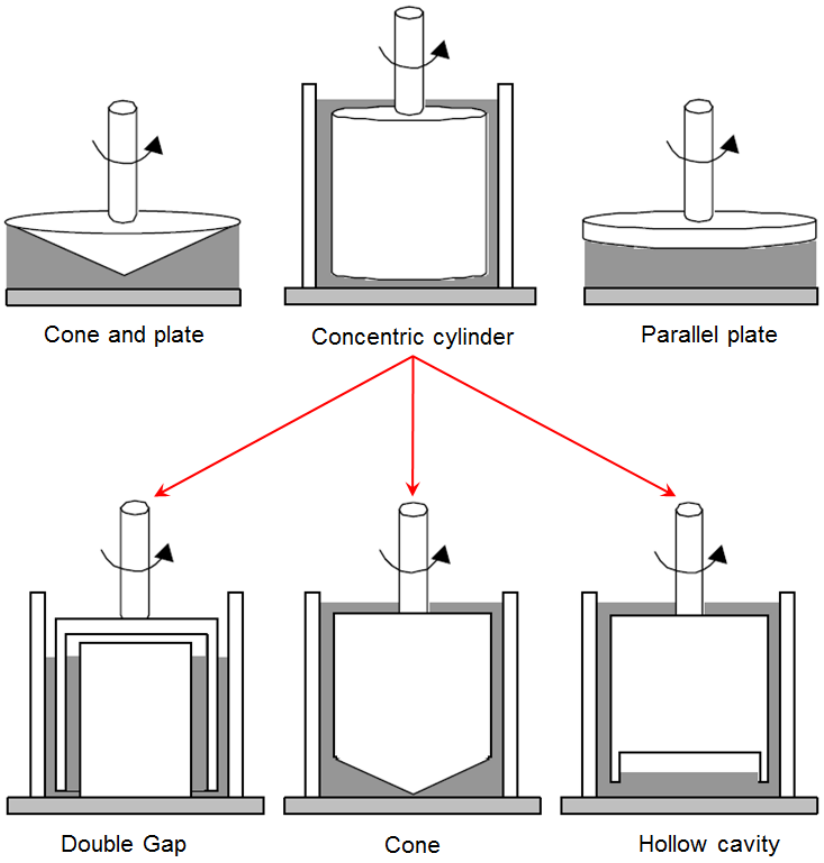


Figure 4.10: Schematic diagram of the basic tool geometries for the rotational rheometer (Hackley & Ferraris, 2001)

The cone and plate geometries consist of an inverted cone in near contact with a lower plate. The angle of the cone is typically less than 4°, and either the upper or lower surface may rotate depending on the instrument design. The parallel plate is a simplified version of the cone with an angle of 0°. In both the cone and plate geometry, the fluid is constrained in the narrow gap between the two surfaces. These two geometries are typically applied to highly viscous pastes, gels and concentrated suspensions (Hackley & Ferraris, 2001).

The concentric cylinder (also referred to as Couette or Coaxial) is typically used for fluid suspensions. In the concentric cylinder geometry, either the inner, outer or both cylinders may rotate depending on the instrument design. The fluid remains in the annulus between the cylinder surfaces and typically one of the cylinders is rotated at a set speed thereby determining the shear rate inside the annulus. The fluid tends to

drag the other cylinder round, and the force (torque) it exerts on that cylinder is measured and converted to a shear stress (Rheosys LLC, 2011).

The concentric cylinder comes in several configurations with the three most common being the double gap, cone and hollow cavity. The double gap configuration is useful for low viscosity fluids or low shear rates as it increases the total area and thus viscous drag on the rotating inner cylinder and generally increases the accuracy of the measurement. The cone and hollow cavity configurations are designed to reduce or account for end effects (Hackley & Ferraris, 2001).

Since the yield stress is the most important factor to establish the extent of dispersion, low shear rates would need to be investigated to ensure there is sufficient resolution near the yield stress. Based on this requirement and the relatively low to medium concentration of suspensions to be tested, the double gap concentric cylinder geometry was selected. The components of the double gap configuration are presented in Figure 4.11.



Figure 4.11: Double Gap tool for the Physica Rheolab QC Rheometer

Model

Rheological behaviour can be represented in the form of shear stress versus shear rate flow curves known as rheograms as shown in Figure 4.12. Rheograms for suspensions and solutions measured under equilibrium conditions may exhibit a

variety of behaviours over a limited range of shear rates. Hackley & Ferraris (2001) indicate that some materials may exhibit more than one distinct behaviour over different shear rate regions of the same flow curve. Several types of behaviour can be classified according to their characteristic shape with six of the most frequently encountered flow types presented in Figure 4.12.

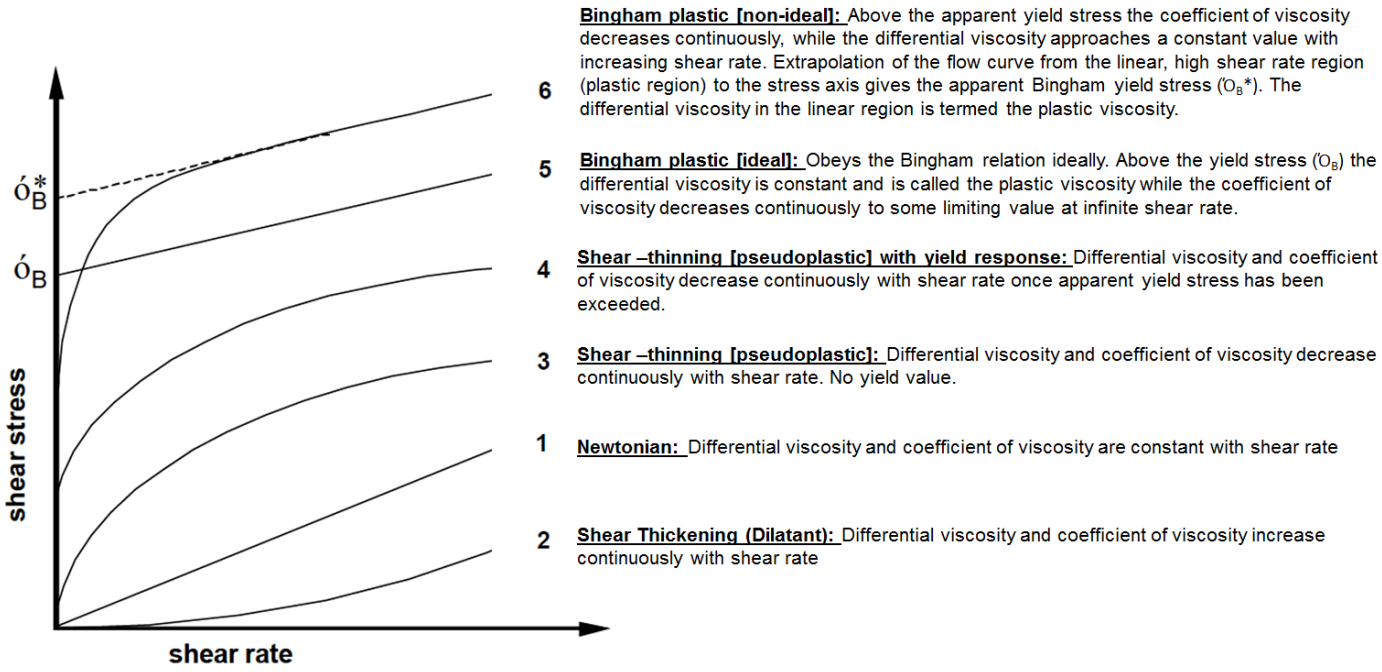


Figure 4.12: Identification of flow curves based on their characteristic shapes (Hackley & Ferraris, 2001)

Rheology is significantly affected by solids concentration, solids type, particle size distribution as well as the chemical nature of the slurry. Inter-particle forces are predominant particularly at fine particle sizes and high slurry concentrations. Dilatant and Newtonian behaviours have been reported for mineral slurries depending on the solids concentration and particle size distribution (Shi and Napier-Munn, 2002); however pseudo-plastic behaviour is often observed for dense slurries (Huynh et al., 2000; Tangsathitkulchai, 2003). Pseudo-plastic behaviour is characterised by a rapid increase of the shear stress with the shear rate followed by a change of slope and then a linear increase of the shear stress with the shear rate (Tangsathitkulchai and Austin, 1989).

Many models in literature can be used to characterise the behaviour of non-Newtonian fluids under equilibrium and steady shear flow conditions. Table 4.7 lists the various models Hackley and Ferraris (2001) considered to be important for suspensions, gels and pastes that exhibit pseudoplastic flow curves.

TA Instruments (n.d) reveals that since the models are empirical and there are no theoretical rules in the selection of a model, the selection of a model is determined by trial and error. Since the yield stress is the primary focus for dispersant selection, the Herschel-Bulkley model was selected for its simplicity and its ability to satisfactorily fit experimental data.

Table 4.7: Various models for suspensions, gels and pastes that exhibit pseudoplastic flow curves

Model	Formula	Description	Advantages	Disadvantages
Power-law [Ostwald-de Waele]	$\sigma = K\dot{\gamma}^n$	A two parameter model for describing pseudoplastic or shear-thickening behaviour of material that show a negligible yield response and a varying differential viscosity. A log-log plot of σ versus $\dot{\gamma}$ gives a slope n (the power-law exponent) where n<1 indicates pseudoplastic behaviour and n>1 indicate shear-thickening behaviour (Hackley & Ferraris, 2001).	Simple	Gives an approximate description of a real non-Newtonian fluid. For pseudoplastic fluids (n<1) the model predicts that at rest (no shear rate) the viscosity of the fluid would approach infinity and as the shear rate approaches infiity the viscosity would approach zero. In reality a fluid has a minumum and maximum viscosity and thus the power law is sufficient at shear rates to which the constants can be fitted (Sumnu and Sahin, 2008).
Herschel-Bulkley	$\sigma = \sigma_y + k\dot{\gamma}^n$	A three parameter model used to describe viscoplastic material exhibiting a yield response with a power-law relationship between shear stress and shear rate above the yield stress σ_y. A plot of log σ-σ_y versus log $\dot{\gamma}$ gives a slope *n* that differs from unity. The Herschel-Buckley relation reduces to the equation for a Bingham plastic when *n* =1 (Hackley & Ferraris, 2001).	Three parameter model (Khalili et al, 2006).	Satisfactory fit of experimental data but fit not as good as a four parameter model (Khalili et al, 2006).
Ellis	$\eta = \frac{\eta_0}{1 + \left(\sigma/\sigma_2\right)^{\alpha-1}}$	A two parameter model, written in terms of shear stress and used to represent pseudoplastic material exhibiting a power-law relationship between shear stress and shear rate, with a low shear rate asymptotic viscosity. The parameter σ_2 can be roughly identified as the shear stress value at which η has fallen to half its final asymptotic value (Hackley & Ferraris, 2001).	Easy calculation of viscosity profiles from a known stress distribution (Nguyen and Nguyen, 2012).	The reverse calculation is tedious and cumbersome (Nguyen and Nguyen, 2012).
Meter	$\eta = \eta_\infty + \frac{\eta_0 - \eta_\infty}{1 + \left(\sigma/\sigma_2\right)^{\alpha-1}}$	Expressed in terms of shear stress, this relation is used to represent a pseudoplastic material exhibiting a power-law relationship between shear stress and shear rate, with both high (η∞) and low (η0) shear rate aympototic viscosity limits. The parameter σ_2 can be roughly idenitified as the shear stress value at which η has falled to half its final amypotitc value. The Meter and Carreau-Yasuda models give equivalent representations in terms of shear stress and shear rate, respectively. If η0 and η∞ are not known independently from experiment, these quantiites may be treated as additional adjustable parameters (Hackley & Ferraris, 2001).	Simplified Meter model is similar to the Ellis Model (Lodesova and Lodes, 1983)	A four parameter model which makes the evaluation of constants difficult (Khalili et al, 2006).
Cross	$\frac{\eta - \eta_\infty}{\eta_0 - \eta_\infty} = \frac{1}{(1 + \lambda\,\dot{\gamma}^m)}$	Similar to the Carreau-Yasuda relation, this model describes pseudoplastic flow with asymmptotic viscosities ar zero (η0) and infinity (η∞)shear rates , and with no yield stress. The parameter λ is a constant with units of time, and *m* is a dimensionless constant with a typical range from 2/3 to 1. If η0 and η∞ are not known independently from experiment, these quantities may be treated as additional adjustable parameters (Hackley & Ferraris, 2001).	The Cross model can be used for data over a wide range of shear rates (Rao, 2014). The Cross model is commonly used when it is necessary to describe the viscosities at low-shear-rates	A four parameter model which makes the evaluation of constants difficult (Khalili et al, 2006).
Carreau-Yasuda	$\frac{\eta - \eta_\infty}{\eta_0 - \eta_\infty} = [1 + (\lambda\dot{\gamma})^a]^{(n-1)/a}$	Describes pseudoplastic flow with asymptotic viscosities at zero (η_0) and infinite (η_∞)shear rates and with no yield stress. The parameter λ is a constant with units of time, where 1/λ is the critical shear rate at whch viscosity begins to decrease. The power-law slope is (*n* -1) and the parameter *a* represents the width of the tranistion region between η0 and the power-law region. If η0 and η∞ are not known independently from experiment, these quanitites may be treated as additional adjustable parameters (Hackley & Ferraris, 2001).	Fits most data (Bhaskar, 2014)	Contains 5 parameters and does not give molecular insight into polymer behaviour (Bhaskar, 2014)

4.3.1.5 Tests

Sodium silicate, prepared to 1% concentration, was added to slurries of different pulp densities at three dosages of 500 g/t, 1000 g/t and 1500 g/t. The pulp densities varied from 20%, 30% and 45% by mass. Each slurry of varying sodium silicate dosage and pulp density was subjected to the Physica Rheolab QC rheometer to determine the flow curve. Table 4.8 summarises the tests conducted on the Physica Rheolab QC rheometer whereby the tests were randomised and conducted on the same day. A shear rate range between $0.1s^{-1}$ and $168s^{-1}$ was used by first pre-shearing the slurry at a constant 168 s^{-1} to prevent any settling of the solids. The shear rate was thereafter reduced from 168 s^{-1} to $0.1s^{-1}$ and the shear stress measured. A narrow shear rate range was selected to improve resolution near the yield stress.

Table 4.8: Matrix of Tests for Sodium Silicate at various dosages and pulp densities

Test	Run	% Solids	Sodium Silicate Dosage (g/t)
A	3	0	0
B	11	20	0
C	1	30	0
D	5	45	0
E	8	20	500
F	4	30	500
G	13	45	500
H	10	20	1000
I	2	30	1000
J	6	45	1000
K	7	20	1500
L	9	30	1500
M	12	45	1500

Shear stress and apparent viscosity (viscosity at a value of shear rate) data were recorded based on the set shear rate range. The shear stress versus shear rate data obtained was fitted with the Herschel-Bulkley model, which exhibited the behaviour of the slurry, to determine the viscosity and yield stress. Plots of rheograms (shear stress as a function of shear rate flow curves) and apparent viscosity as a function of shear rate for varying pulp densities and sodium silicate dosages were generated.

4.3.1.6 Precautions

The following precautions were followed for quality assurance:

- To ensure that the Physica Rheolab QC Rheometer fitted with the double gap tool is accurately measuring the shear stress, water was measured to ensure the flow curve was indeed Newtonian over the shear rates tested. This was included in the matrix of tests as test A (Run 3).
- The slurry was tapped on a table to remove air bubbles.
- To ensure a representative sample was taken the sample was stirred and a syringe (without a needle) was used to sub-sample and dispense the sample into the tool.
- Two measurements were taken per sample, and the average was reported.
- The unit is adjusted every 6 months or when required.

4.3.1.7 Limitation of the Physica Rheolab QC rheometer

- Small sample size (solution volumes of ~12mL) are used for the measurement, and this small volume may not be representative of the sample.
- It is also assumed that solutions are measured under equilibrium conditions.
- The settling of solids in the unit when the shear rate decreases is possible, thereby altering the solids concentration and biasing the rheology measurement. Unfortunately during measurement, the tool geometry does not allow for visual inspection to determine if settling is occurring.
- For quantitative results, rheometers require oil standards for calibration purposes. In this study, which did not use oil standards for calibration, a qualitative interpretation of the results will be done in order to rank the yield stress at various dispersant dosages and pulp densities. A low yield

stress indicates that a small amount of force is required to adequately disperse the solution. Since a qualitative ranking approach is used the error encountered would apply to all the tests conducted allowing for a fair comparison to take place.

4.3.2 Results and Discussion

Sodium silicate (Silichem 3379) was prepared to 1% concentration by mass and added to slurries of various pulp densities (0%, 20%, 30% and 45%) at varying dosages (0 g/t, 500 g/t, 1000 g/t and 1500 g/t). The resulting slurries were then subjected to rheology tests, in a random order, to determine the yield stress and aid in the selection of an appropriate pulp density and dispersant dosage. The rheograms (shear stress vs shear rate) for the slurries of various pulp densities and sodium silicate dosages is presented in Figure 4.13 to Figure 4.16. Similarly the apparent viscosity as a function of shear rate for the same conditions is presented in Figure 4.17 to Figure 4.20.

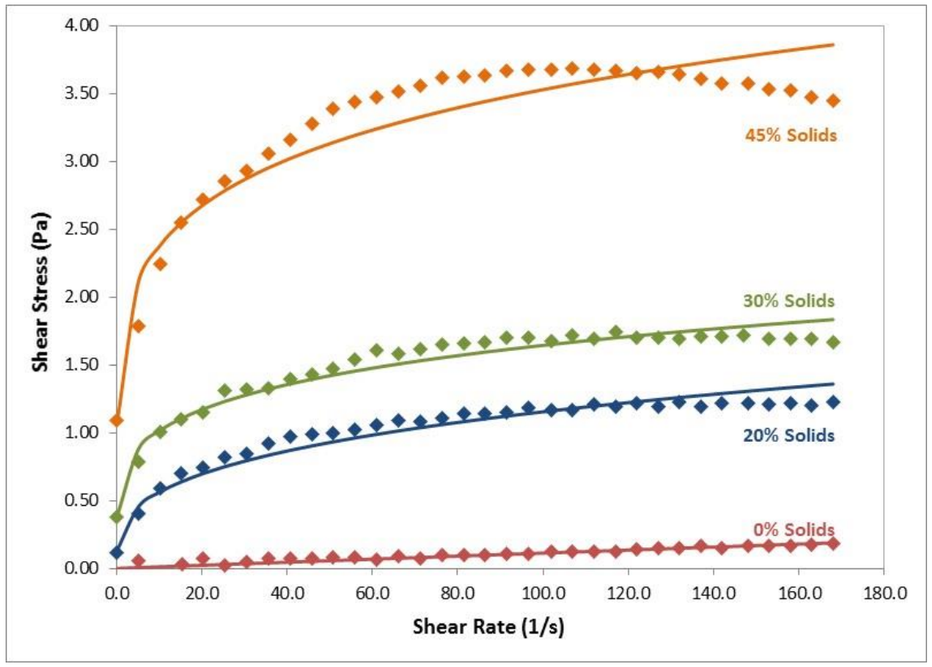


Figure 4.13: Shear Stress vs Shear Rate at 0g/t Sodium Silicate for various pulp densities

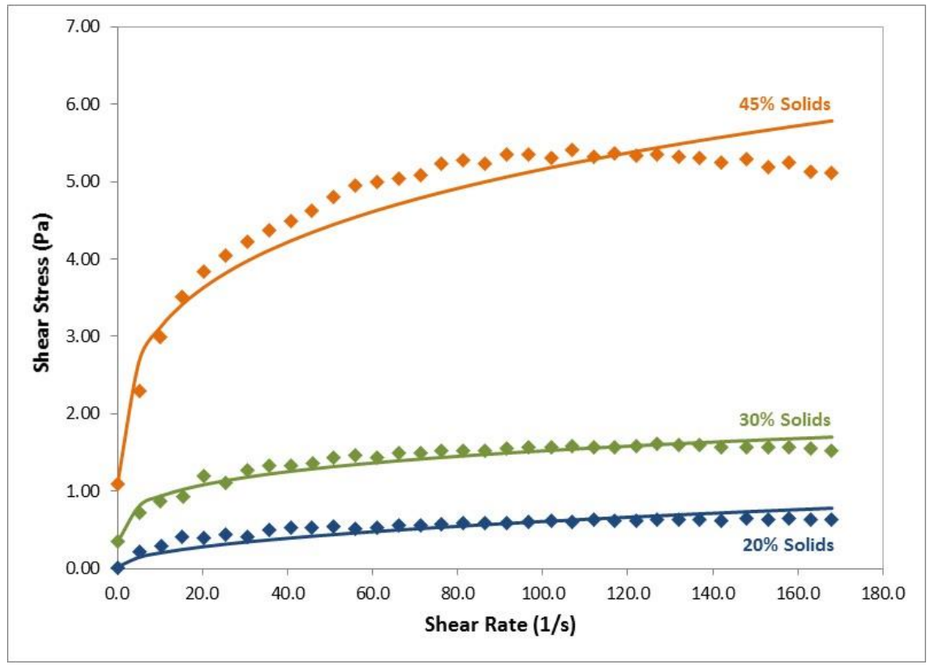


Figure 4.14: Shear Stress vs Shear Rate at 500g/t Sodium Silicate for various pulp densities

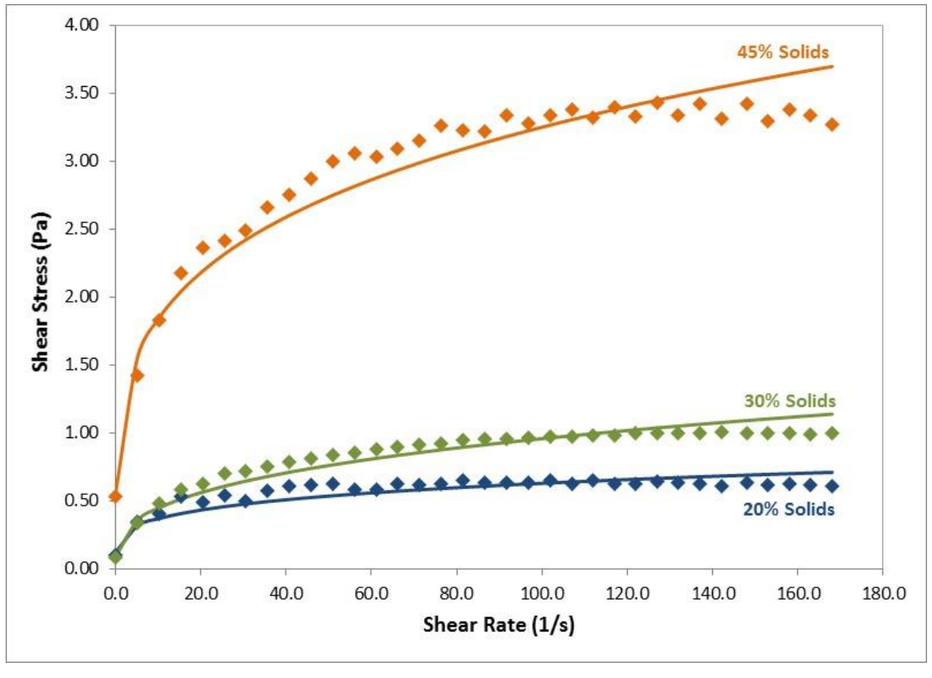


Figure 4.15: Shear Stress vs Shear Rate at 1000g/t Sodium Silicate for various pulp densities

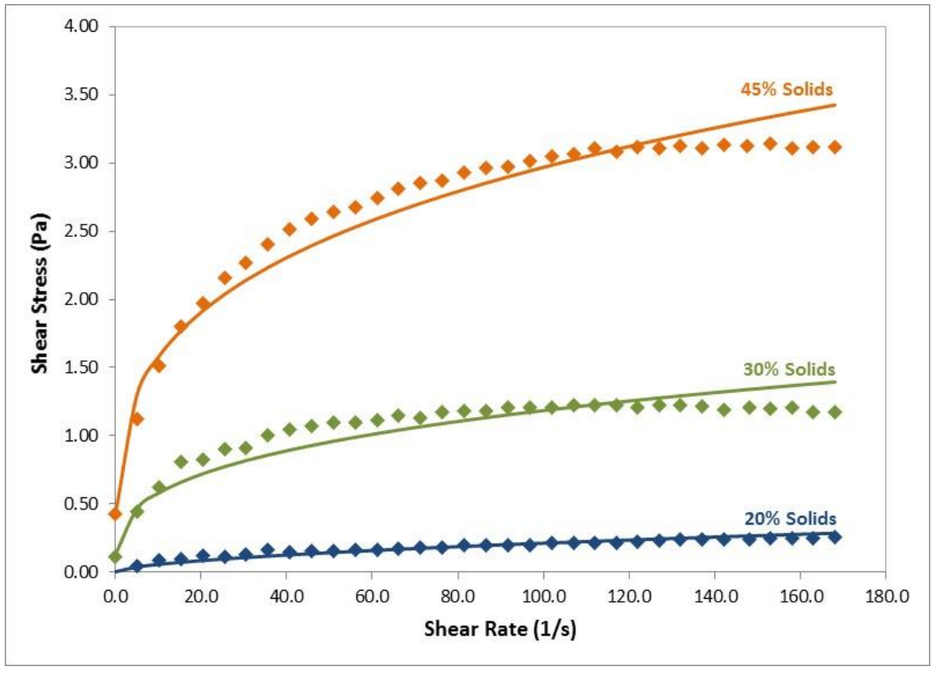


Figure 4.16: Shear Stress vs Shear Rate at 1500g/t Sodium Silicate for various pulp densities

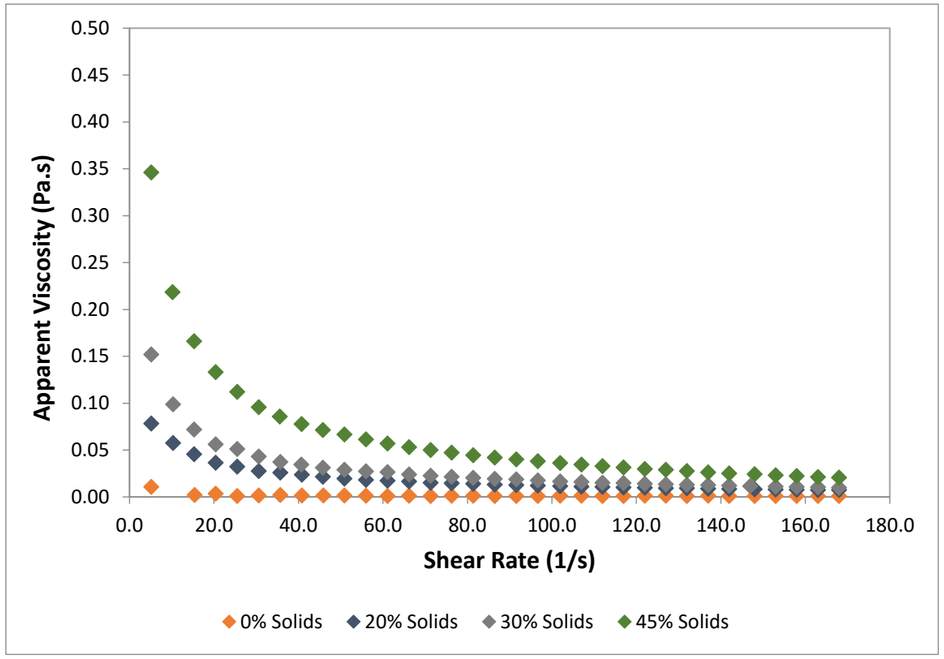


Figure 4.17: Apparent Viscosity vs Shear Rate at 0g/t Sodium Silicate for various pulp densities

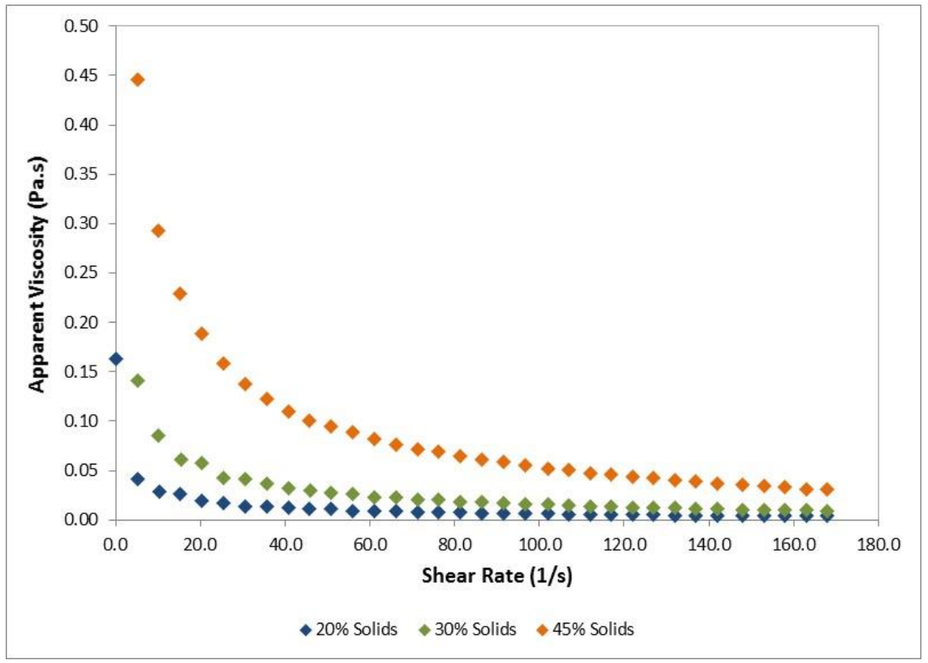


Figure 4.18: Apparent Viscosity vs Shear Rate at 500g/t Sodium Silicate for various pulp densities

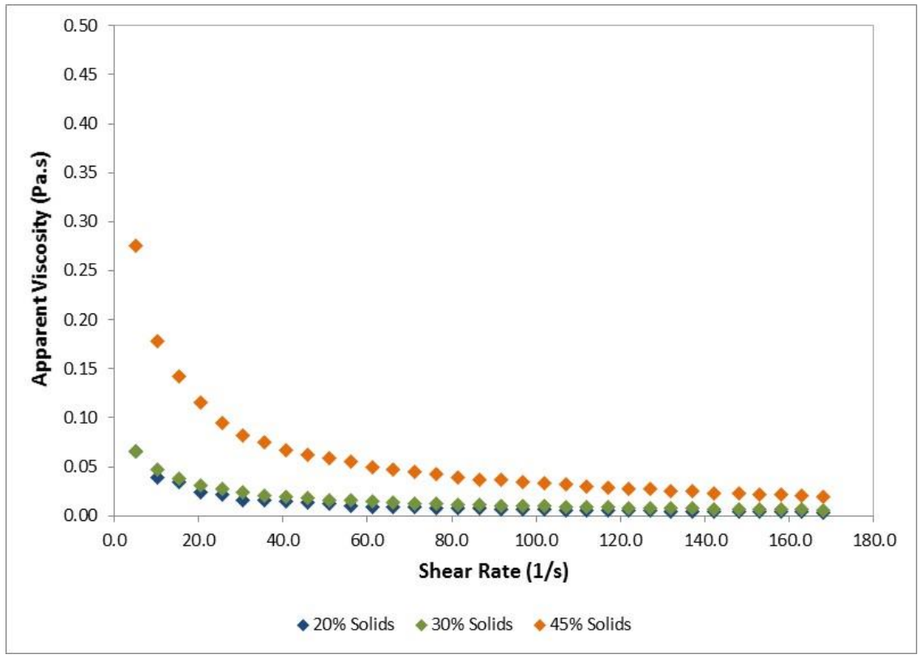


Figure 4.19: Apparent Viscosity vs Shear Rate at 1000g/t Sodium Silicate for various pulp densities

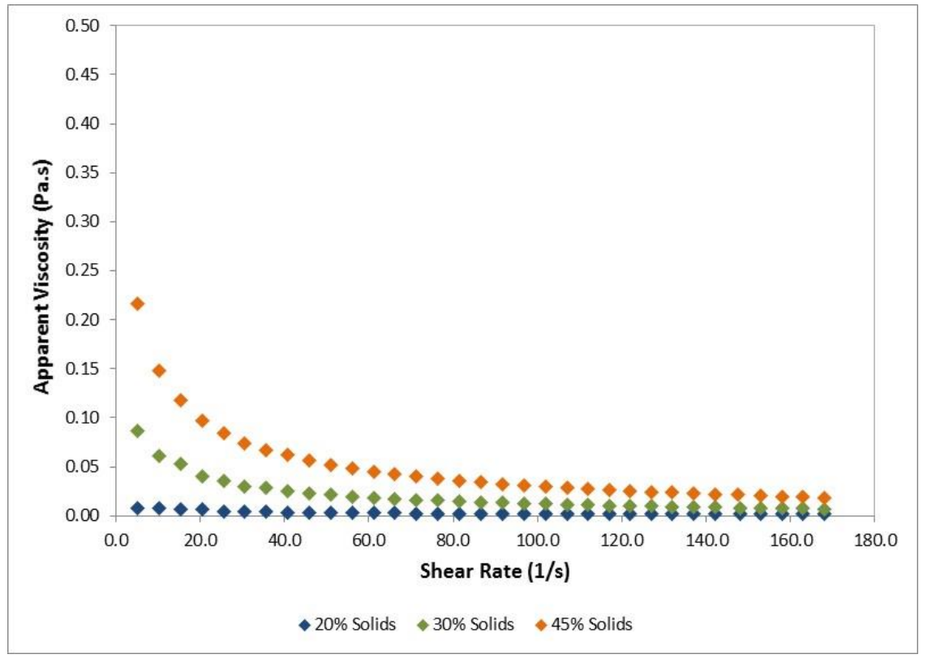


Figure 4.20: Apparent Viscosity vs Shear Rate at 1500g/t Sodium Silicate for various pulp densities

The rheology control test in which tap water without solids was tested exhibited a Newtonian flow curve as expected, and indicates the Physica Rheolab QC rheometer is generating reliable results (Figure 4.13). The rheograms (shear stress vs shear rate) presented in Figure 4.13 to Figure 4.16 indicate that all the sodium silicate dosages and pulp densities tested exhibited pseudoplastic (shear thinning) flow curves concurring with the findings of Huynh et al. (2000) and Tangsathitkulchai (2003) for dense slurries.

At each sodium silicate dosage, the apparent viscosity of the slurry increased as the pulp density increased (Figure 4.17 to Figure 4.20) agreeing with the findings by Wang et al. (2014) and Mangesana et al. (2008). Mangesana et al. (2008) attributed the increase in apparent viscosity with increasing pulp densities to the increased frequency of particle-particle interactions.

Figure 4.13 to Figure 4.16, in general, indicates the Herschel-Bulkley model provided a good fit to the experimental data with slight deviations at shear rates above 130 s^{-1} at pulp densities of 45% solids. Since the yield stress is the most important response variable for this study, it is expected that the Herschel-Bulkley model would provide valid results for this particular response variable. The interpolated yield stresses for the modelled data at all the sodium silicate dosages and pulp densities tested are presented in Table 4.9 and are ranked from smallest to largest with regard to the interpolated yield stress from the modelled data. Table 4.9 indicates that in general lower pulp densities and higher sodium silicate dosages achieve lower yield stresses with the yield stresses ranging from 0.003 Pa to 1.091 Pa. The low yield stress indicates that a force of small magnitude is required to overcome the attractive forces between the solids thereby allowing for adequate dispersion. It is expected that during the first stage of the flocculation process, namely the dispersion stage, conducted in a 1L flotation cell and stirring speed of 1200 rpm will provide sufficient force to overcome the attractive forces to ensure dispersion occurs.

Table 4.9: Interpolated Yield Stress at Various Sodium Silicate Dosages and Pulp Densities

Ranking of Yield stress from Smallest to Largest	Interpolated Yield Stress (Pa)	Sodium Silicate Dosage (g/t)	% Solids
1	0.000	0	0
2	0.003	1500	20
3	0.019	500	20
4	0.089	1000	30
5	0.120	1000	20
6	0.124	0	20
7	0.128	1500	30
8	0.337	500	30
9	0.369	0	30
10	0.420	1500	45
11	0.558	1000	45
12	1.044	0	45
13	1.091	500	45

The work of Song et al. (2002) revealed higher pulp densities of 45% solids achieved similar Fe grade and recoveries but at half the conditioning time (10 minutes) of the dilute slurry (20% solids). Since all pulp densities achieved sufficient dispersion and considering the work conducted by Song et al. (2002) the effect of sodium silicate dosage on the apparent viscosity as a function of shear rate at 45% solids is presented in Figure 4.21. Figure 4.21 indicates decreasing apparent viscosities as the sodium silicate dosage increases and thus improved dispersion. The apparent viscosity profile at 1000 g/t and 1500 g/t are similar and to contain reagent costs a lower dosage of 1 000 g/t was selected for further testwork.

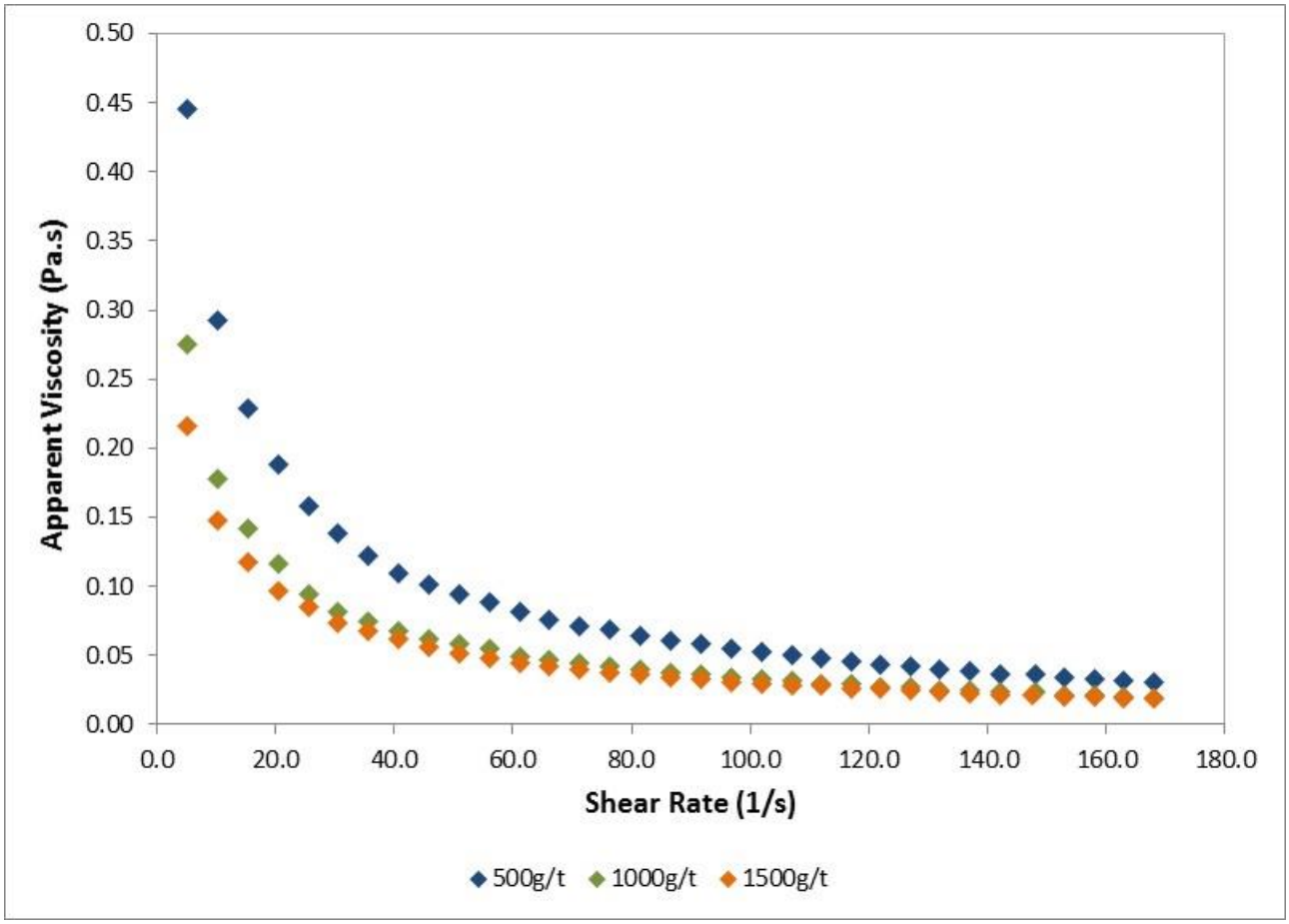


Figure 4.21: Apparent Viscosity vs Shear Rate at various Sodium Silicate Dosages for a fixed pulp density of 45% solids

4.4 pH Selection for optimum flocculation

4.4.1 Methodology

4.4.1.1 Tests

The pH of the dispersed slurry affects the hydrophobicity and floc size in the flocculation process. Tests were therefore required to find the pH that would yield big flocs that were also selective. Once the dispersant dosage and pulp density were selected a screening test for pH was conducted. Based on the work of Yin et al. (2011) a pH range of 9.5 to 11 in increments of 0.5 was selected. For pH variation testwork the centre point selective flocculation conditions for the Box-Behnken design was selected for the sodium oleate and paraffin dosages along with the conditioning time

as outlined in Table 4.10. Each pH test was conducted thrice to gain better statistical confidence in the results. The tests were randomised and conducted on the same day.

Table 4.10: Operating conditions for the pH screening tests

Fixed Operating Parameters	
Feed Mass of solids	200 g
% Solids	45 %
Sodium Silicate	1000 g/ton
Sodium Oleate	1000 g/ton
Paraffin	3000 g/ton
Stirring Time	10 min
Background Magnetic Field Intensity	6 000 Gauss
Pulsation Frequency	250 rpm
Pulsation Amplitude	5 mm
Variable Operating Parameters	
pH	9.5
	10.0
	10.5
	11.0

For each pH test, a representative 200g sample of solids was added to a 1 litre Denver flotation cell with 244.4g of tap water added to the cell to create a pulp density of 45% solids by mass as presented in Figure 4.22. The pulp was agitated at 1200rpm to ensure a homogenous pulp to which sodium silicate was added. The pH of the pulp was measured with a Knick pH meter (Figure 4.23) and the pH was adjusted to the required pH to which the sodium oleate and paraffin were added. The pH was thereafter adjusted to the required pH, and the pulp was agitated/conditioned for 10 minutes during this flocculation step. pH modifications were achieved with sodium hydroxide and sulphuric acid at solution concentrations of 1% and 0.5% by mass respectively. All solutions of reagents were prepared with tap water. High stirring speeds will produce a large amount of froth due to the presence of oleate ions, and thus the stirring speed was fixed to 1200rpm for the duration of the test. After conditioning for 10 minutes, the agitated slurry was sub-sampled with a dropper to obtain an aliquot for particle size distribution analysis using the Malvern Mastersizer.

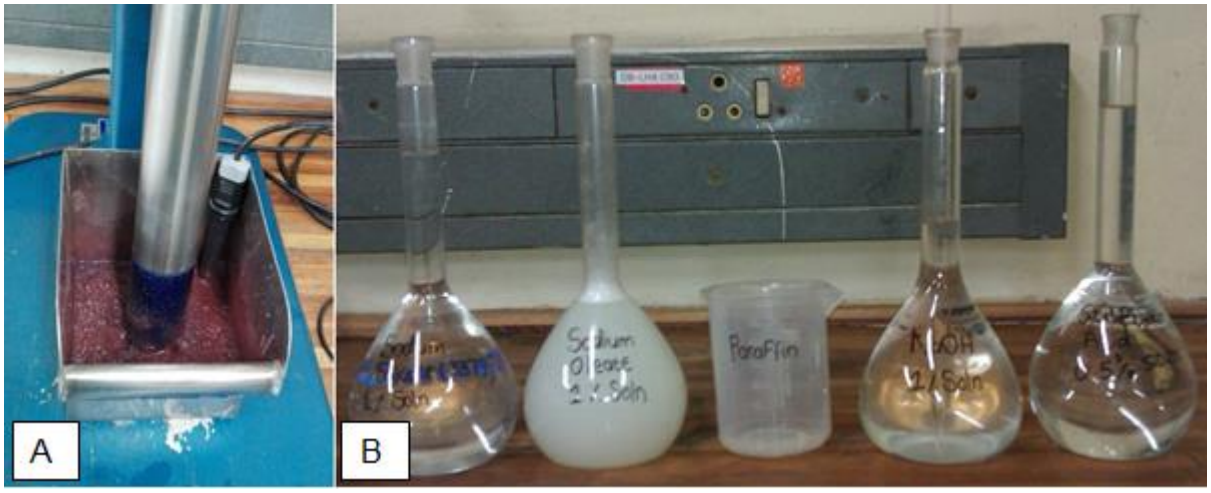


Figure 4.22: Flocculation step for pH screening tests showing (A) the Denver Float Cell with pulp at 45% solids and (B) reagents used during flocculation



Figure 4.23: Knick pH meter used during the flocculation

To determine if the flocculation stage was selective, many researchers (Drzymala and Fuerstnau, 2014; Panda et al, 2014; Abro et al, 2013; Song et al, 1999; Weissenborn, 1996; Weissenborn et al, 1994; Hanumantha Rao and Narasimhan, 1985) allowed their slurry to settle for a predetermined time after which the sediment and supernatant were collected separately. Jones (1998) listed a few limitations of this approach namely,

- settling is dependent not only on size but also on density, i.e. this method does not distinguish between the small dense aggregates which have the same settling rate as larger and lighter particles

- settling is also dependent on morphology and hence minerals of different morphologies cannot be directly compared

In light of these limitations, the selectivity of the flocculation process was determined by coupling selective flocculation with magnetic separation also referred to as FMS by Song et al. (2002). Thus subsequent to the flocculation step and sub-sampling for sizing analysis, the pulp from the Denver float cell was washed into a beaker (Figure 4.24) and processed through the magnetic separator, the SLon-100, at the optimal background magnetic field intensity, pulsation frequency and amplitude described in Section 4.2. The products from each test were filtered, dried and prepared for chemical analysis. The grade-recovery response and the separation efficiency was compared across the pH range tested, and the best pH was selected for the Box-Behnken design where the sodium oleate and paraffin dosages along with conditioning time were varied simultaneously.

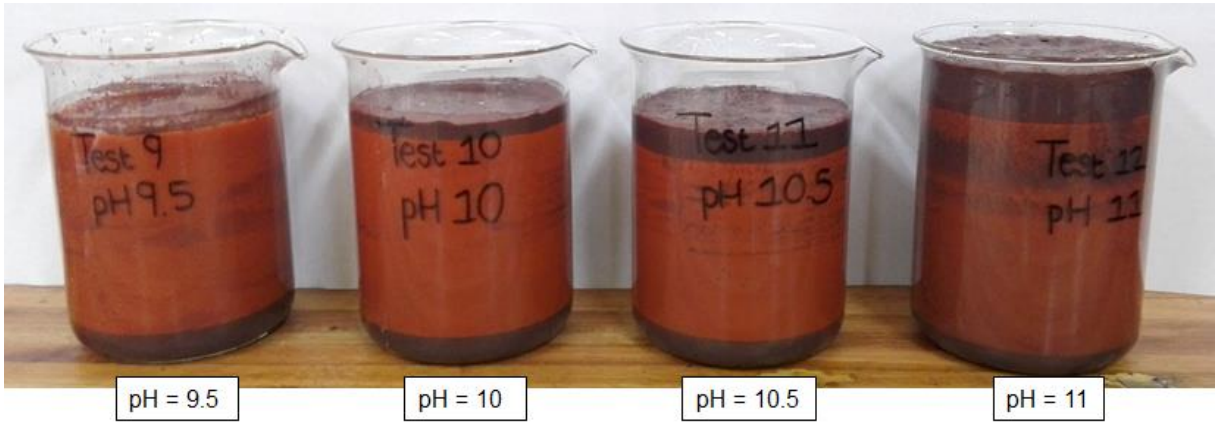


Figure 4.24: Flocculated pulp at each pH subsequent to the flocculation step and prior to magnetic separation

4.4.1.2 Reagent Preparation

For the FMS process defined by Song et al. (2002) five reagents are required for selective flocculation namely sodium silicate for dispersion, sodium oleate as the surfactant, paraffin as the non-polar oil and, sodium hydroxide and sulphuric acid as pH modifiers.

Sodium silicate (supplied by PQ Silicas South Africa (Pty) Ltd), sodium oleate (supplied by Protea Chemicals) and sodium hydroxide were prepared as solutions in concentrations of 1% by mass respectively. For easier pH modification sulphuric acid was prepared to solution concentrations of 0.5% by mass respectively.

Song et al. (1999) indicated that the positive effect of non-polar oils on hydrophobic flocculation depends on the oil's density and viscosity. They further revealed that medium density oils such as kerosene (0.78-0.81 g/cm^3) and diesel (0.83-0.84 g/cm^3) are appropriate for hydrophobic flocculation since low density oils have insufficient viscosity to pull hydrophobic particles together whilst high density oils are too viscous to be sufficiently dispersed in slurries to wet particles and cause agglomeration. Paraffin has a density of 0.80 g/cm^3 and can be categorised as a medium density oil. The required mass of paraffin (supplied by DVL Trading) was weighed out to ensure the target dosage was achieved.

To improve the solubility of sodium oleate, water was heated to 60°C on a hot plate and the pH adjusted to 10.5. Thereafter sodium oleate was added and stirred on the hot plate. Once the sodium oleate had dissolved the solution was allowed to cool down to room temperature before use. This method of sodium oleate preparation was recommended by Pascoe and Doherty (1997). These investigators recommended that fresh stock solutions of sodium oleate be prepared weekly, and thus for this study all reagents were prepared on a weekly basis. All reagent solutions were prepared with tap water to simulate industry practice.

4.4.1.3 *Particle Size Distribution by Laser Diffraction*

Yin et al. (2011) showed that pH affected the hydrophobicity and floc size of selectively flocculated material when sodium oleate is used as the surfactant/collector. The larger the floc size, the more the magnetic and gravity force dominates over the hydrodynamic drag forces thereby improving the separation efficiency of magnetic and gravity separation units. It was thus important to determine the particle size distribution of the sample without flocculation and to compare it to the selectively flocculated material at various pHs to determine what pH achieves the largest floc size. The measurement method for the floc size would need to ensure that minimal floc breakage and floc size reduction would occur and thus laser diffraction was selected for floc size measurement taking various precautions into account.

A beaker containing 800mL of tap water was positioned under the pump arm of the dispersion unit (Hydro 2000MU) of the Malvern Mastersizer. The pump/stirring speed and the ultrasonic displacement was set. The parameters selected are further presented and explained in Section 4.4.1.3.4.

Five 100g sub-samples of the feed were each prepared to 20% solids, stirred, and a sub-sample removed with a dropper and dispensed into the beaker until the required sample concentration (often referred to as obscuration, i.e. the fraction of light lost from the main beam when the sample is introduced) was achieved. Three representative slurry aliquots were also removed from each of the pH tests (Section 4.4.1.1) and similarly dispensed into the beaker until the required obscuration was achieved. Three measurements were taken for each sample, and an average reported for each sample analysed. The cumulative particle size distributions were plotted and the average D50 reported. The cumulative particle size distribution of the feed was then compared to selected samples of flocculated material from the pH tests to determine if the particle size (D50) had increased.

4.4.1.3.1 Selection of Equipment

To determine the floc size many researchers (Pascoe and Doherty, 1997; Forbes, 2011; Pascoe and Wills, 1994; Govoreanu et al., 2009) used the 50% passing by volume (D(v,0.50)) from a laser light scattering instrument as an indicator of the mean floc size. To ensure the flocs are not destroyed the ultrasonic displacement setting must be zero or switched off. Initial tests conducted on the Saturn Digisizer 5205 on the feed sample, prior to flocculation, and without ultrasonic dispersion (in preparation for the floc size determination) gave irreproducible results. The erratic results obtained can be attributed to two things. The first being the sample settling in the feed chamber presenting an inhomogeneous sample/poorly dispersed sample to the detector and secondly the pumping action that may have destroyed the flocs. Patil et al. (2001) measured the floc size distribution using a Malvern particle size analyser with a flow cell and stirred cell. They reported that the floc size distribution varied continuously due the pump used to circulate the suspension. On the other hand, the stirred cell (a small magnetic stirrer) produced a consistent floc size distribution for 30 minutes.

The Saturn Digisizer at Mintek does not have a stirred cell or sample dispersion unit. However, the Malvern Mastersizer 2000E at Mintek was installed with a sample dispersion unit called the Hydro-2000 MU. The Hydro-2000 MU allows the Mastersizer to be used for slurry particle sizing. The Hydro-2000 MU has a variable ultrasonic system to disperse particle agglomerates and a variable pump/stirrer speed to allow a wide range of particles and densities to be suspended and circulated (Malvern Instruments Ltd., 2007a). The Malvern Mastersizer 2000E used in conjunction with the Hydro-2000 MU provided reproducible results, and thus this unit was selected for particle size analysis.

4.4.1.3.2 Working Principle of the Malvern Mastersizer

Each particle size fraction will have a distinct light scattering pattern when it passes through a laser beam. The simplest of models that can be used to predict the way particles scatter and absorb light is the Fraunhofer model. This model can predict the scattering pattern created when a solid, opaque disc of a known size is passed through

a laser beam. A limitation of this model is that very few particles are disc-shaped and most particles are transparent. The Mie theory addresses this limitation as it predicts the way light is scattered by spherical particles and the way light passes through or is absorbed by the particles. This model is useful if the refractive index and absorption of the particles are known. The Malvern Mastersizer captures the light scattering pattern from a field of particles and uses the Mie theory to calculate the size of particles that created that pattern (Malvern Instruments Ltd., 2007).

The sample is prepared and dispersed to the correct concentration and delivered from the Hydro-2000 MU to the optical bench as depicted in Figure 4.25. It is important that a representative and well dispersed sample is prepared otherwise incorrect data will be obtained. The most important step in the measurement is sample preparation. Detectors within the optical bench collect the light scattering from a particular range of angles. The detectors take multiple snapshots of the scattering pattern from the particles passing through the analyser beam at that particular time. Typically over 2000 snaps are taken for each measurement with each snap taking 1ms. The snaps or raw data are then analysed by the Malvern software using the Mie theory, and the information is displayed (Malvern Instruments Ltd., 2007a). For our purposes, cumulative volume % was selected as the output. The technical specifications for the optical bench of the Malvern Mastersizer 2000E are presented in Figure 4.25.

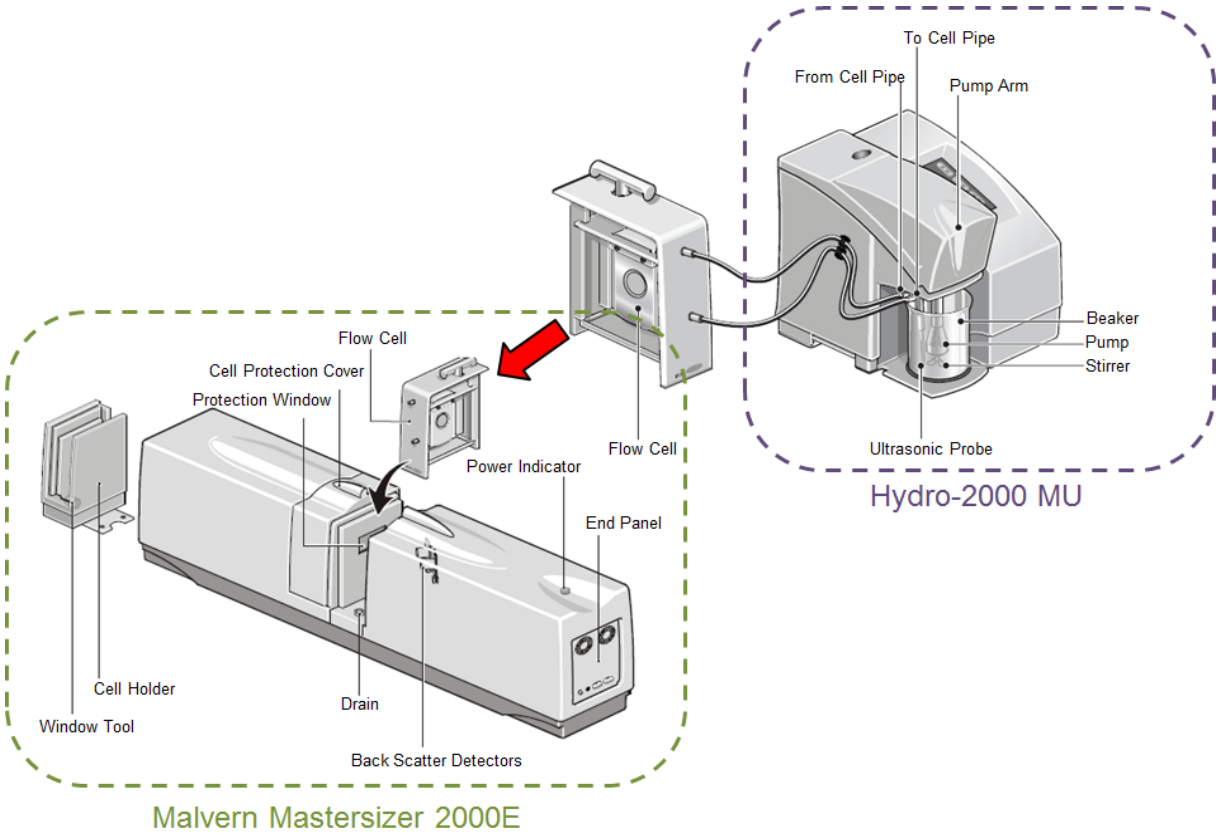


Figure 4.25: Schematic diagram of the Malvern Mastersizer 2000E with the Hydro-2000 MU as the sample dispersion unit, figure adapted from Malvern Instruments Ltd. (2007 and 2007a)

Table 4.11: Technical Specifications for the Malvern Mastersizer 2000E (Malvern Instruments Ltd., 2007)

Size range (2000E)	0.1 to 1000 microns, depending on material properties.
Measurement principle	Mie Scattering
Detection systems	Red light: Forward scattering, side scattering and back scattering. Blue light: Wide angle forward and back scattering (Mastersizer 2000 only)
Light sources	Red light: Helium neon laser. Blue light: Solid state light source (Mastersizer 2000 only)
Optical alignment system	Automatic rapid align system with dark field optical reticle and multi-element alignment detector.
Sample dispersion unit interchange system.	Sample dispersion units automatically recognised, configured and enabled on insertion of measurement cell cassettes into optical bench.

4.4.1.3.3 Selection of Operating Parameters

Four important operating parameters were identified namely sample preparation, dispersant, pump/stirrer speed and ultrasonic displacement. These parameters are further outlined below.

Sample Preparation

All samples were required to be prepared in a similar way for ease of comparison. Since the flocculated material would be in a slurry form, the feed (without flocculation) was prepared as a slurry at 20% solids by mass. All samples would be stirred, and a dropper used to sub-sample and dispense the slurry into the beaker containing the dispersant. The amount of slurry added would be determined by the required obscuration range of the Malvern Mastersizer.

Dispersant

Pascoe and Wills (1994) advised that the background measurement be conducted in the dispersant to which the sample would be added. In this case, the dispersant selected for the feed was tap water, and for the flocs tap water was prepared to the required pH (outlined in 4.4.1.1).

Pump/Stirrer Speed

To ensure that the feed and flocculated samples are adequately dispersed, flocs are not destroyed or floc growth promoted by the shearing action, the lowest pump speed of 600 rpm was selected. The solids in the beaker were monitored to ensure the sample did not settle during the test.

Ultrasonic Displacement

The ultrasonic probe is used to de-agglomerate particles and ensure an accurate particle size distribution is measured. Since the ultrasonic probe would destroy the flocs created it was essential to switch it off during testwork. The feed, without flocs, was measured with and without ultrasonic dispersion to determine the impact of the ultrasonic on the feed particle size distribution. For fair comparisons to be made the

flocculated material and feed material would need to be measured under the same conditions (no ultrasonic). For the Hydro-2000 MU unit, the control panel indicates the displacement of the tip of the ultrasonic probe in microns. The higher the value, the more powerful the ultrasonic action.

4.4.1.3.4 Tests

The Malvern Mastersizer 2000E was used in conjunction with the Hydro-2000 MU to determine the particle size distribution of the feed and flocs generated during the pH selection tests described in Section 4.4.1.1. The operating conditions for each of the tests are specified in Table 4.12.

Table 4.12: Matrix of Tests conducted on the Malvern Mastersizer 2000 E with the Hydro-2000 MU

Section	Sample	Number of Repeats	Sample Prep	Dispersant	Pump/Stirrer Speed (rpm)	Ultrasonic Displacement (µm)
Feed Characterisation	Feed	5	Slurry	Tap Water	600	Off
		1	Slurry	Tap Water	600	20
pH Selection	Flocs at pH 9.5	3	Slurry	Tap water prepared to pH 9.5	600	Off
	Flocs at pH 10	3	Slurry	Tap water prepared to pH 10	600	Off
	Flocs at pH 10.5	2	Slurry	Tap water prepared to pH 10.5	600	Off
	Flocs at pH 11	4	Slurry	Tap water prepared to pH 11	600	Off

For the pH selection section, the background measurement was taken with tap water prepared to the required pH to ensure no bias in the results. This was the method described by Pascoe and Wills (1994). The cumulative particle size distributions were reported along with the D50 for comparative purposes. For each test, three measurements were taken by the Malvern Mastersizer 2000 E and the average result

reported. A few repeats were conducted for certain tests to validate the results obtained. The tests were randomised and conducted over two consecutive days.

4.4.1.3.5 Precautions

The following precautions, outlined by Malvern Instruments Ltd. (2007), were followed for quality assurance:

- In some main water supplies bubbles may be present in the water and will bias the results as bubbles will be measured with the sample. To ensure this would not occur water was stored at room temperature and pressure for several hours before use to allow degassing to occur.
- Some samples slowly disperse when added to the beaker. A measurement was only taken once the obscuration in the required range had stabilised indicating the sample was properly dispersed.
- Fast pump/stirrer speeds will introduce air and thus bubbles into the system and can be identified by a secondary peak at 100 µm. The results were monitored to ensure no bubbles were present. This phenomenon was not observed at the low pump/stirrer speed selected (600 rpm).
- The obscuration was monitored during the test to observe if a decrease was occurring. A decrease would indicate sample agglomeration or particle settling. In the latter case, an increase in pump/stirrer speed would be required. Also the bottom of the beaker was monitored to ensure no settling had occurred. During testwork no decrease in obscuration nor particle settling was observed at a pump/stirrer speed of 600 rpm.

4.4.1.3.6 Limitations of the Malvern Mastersizer Testwork

- The Mie theory predicts the way light is scattered by spherical particles. Mineralogical images taken of the sample by the Mineral Liberation Analyser (MLA) indicates the particles are not spherical and thus the results will not be accurate.

- Gibbs and Konwar (1982) as cited by Patil et al. (2001) reported that in certain mineral flocs the use of a pipette for sampling purposes modified the floc size distribution if the pipette opening was less than 2 mm. It is assumed that the dropper does not destroy the flocs and the aperture (2 mm) is big enough to sample the flocs.
- It is assumed that the stirring and pumping does not destroy the flocs created.
- The Malvern Mastersizer 2000E equates the volume of the particle to the volume of a sphere from which the diameter (and thus particle size) is determined. Since this is a different measuring technique to sieving it cannot be directly compared, and the results would need to be modified. However, the feed (baseline) will be measured on the Malvern Mastersizer 2000E in the same way as the floc, thus allowing a direct comparison of the Malvern results.
- When measuring the particle size distribution, it is required to input the sample type. Hematite was selected and a refractive index of 2.980 was used to determine the particle size. Mineralogy indicated the majority of the sample is hematite (51%) and quartz (45%). The refractive index of quartz is much lower at an average of 1.553. The proportion of quartz and its refractive index had not been taken into consideration creating a bias in the results.
- Laser scattering is a high resolution optical method in which the detectors and windows inside the unit are an integral part of the measurement zone. Dust or smears on the windows will scatter light during measurement. The subtraction of the background will correct for this, but excessive dirt will degrade the instrument's sensitivity (Malvern Instruments Ltd., 2007).
- The geometric mean of a size band is reported as the output. However with narrow size bands and cumulative particle size distributions reported by the instrument the use of the geometric mean of a size band is not expected to skew the particle size distribution significantly.

4.4.1.4 Precautions for pH Selection

- Every week the pH meter was calibrated with buffer solutions. To ensure the pH meter was accurately reading within the range of pHs tested each time it

was used, the buffer solution at pH 10 was measured. When an incorrect pH measurement was observed the pH meter would be calibrated.

- To prevent damage to the electrode of the pH meter the electrode was stored in 3 M potassium chloride solution and if necessary, the same solution inside the electrode was topped up.

4.4.1.5 Assumptions/Limitation of this aspect

- Some investigators have conducted their flocculent tests in baffled cells to aid hydrodynamic conditions, and others have used cells without baffles as presented in Table 4.13. It is assumed that the flotation cell without baffles will not adversely affect the flocculation step. This assumption is supported by the work of Pascoe and Doherty (1997) which showed that a flocculation stage before flotation was found to be unnecessary as the process occurred quickly under the hydrodynamic conditions prevalent in a laboratory Denver D12 mechanically agitated flotation machine.

Table 4.13: Summary of hydrodynamic conditions used by various researchers

Hydrodynamic Conditions	**Reference**
Mixing tank/agitation tank/glass beakers with baffles. Impellers used vary from cross shaped impellers, paddle impellers, vertical bladed stirrers.	Panda et al (2014)
	Song et al (2002)
	Song and Lu (1994)
	Song et al (1998)
	Pascoe and Doherty (1997)
	Weissenborn (1996)
	Pascoe and Wills (1994)
Mixing tank/glass beaker with stirrer. No baffles.	Roy (2012)
	Yin et al (2011)
	Abro et al (2013)
	Ahmed and Mahran (2013)
	Hanumantha Rao and Narasimhan (1985)
	Weissenborn et al (1994)
Shaking for 24 hours	Drzymala and Fuerstenau (2014)

- It is assumed that the effect of pH on the maximum and minimum reagent dosages to be tested in the Box-Behnken design will be negligible and that the

best pH for the centre point conditions would apply to the end regions of the design.

- The effect of aged mine water or recycled reagents on the flocculation step will not be investigated and should be considered in further testwork should this process show promise.

4.4.2 Results and Discussion

The particle size distribution by volume % of the feed was measured on the Malvern Mastersizer 2000 E with the Hydro-2000 MU used as the sample dispersion unit. Five aliquots of the feed were measured without ultrasonic displacement at the lowest pump/stirring speed of 600 rpm. The results presented in Figure 4.26 indicates good reproducibility between the five aliquots. The average d80, d50 and d20 is 45 µm, 16 µm and 5 µm respectively. The average of the five aliquots was then compared to the feed prepared and measured in a similar way except an ultrasonic displacement of 20 µm was employed. The results presented in Figure 4.27 indicates a similar particle size distribution with slight differences above 30 µm. The results indicate that without ultrasonic displacement agglomeration of the ultrafines did not occur in the dispersion unit indicating the selected parameters are suitable for floc size determination.

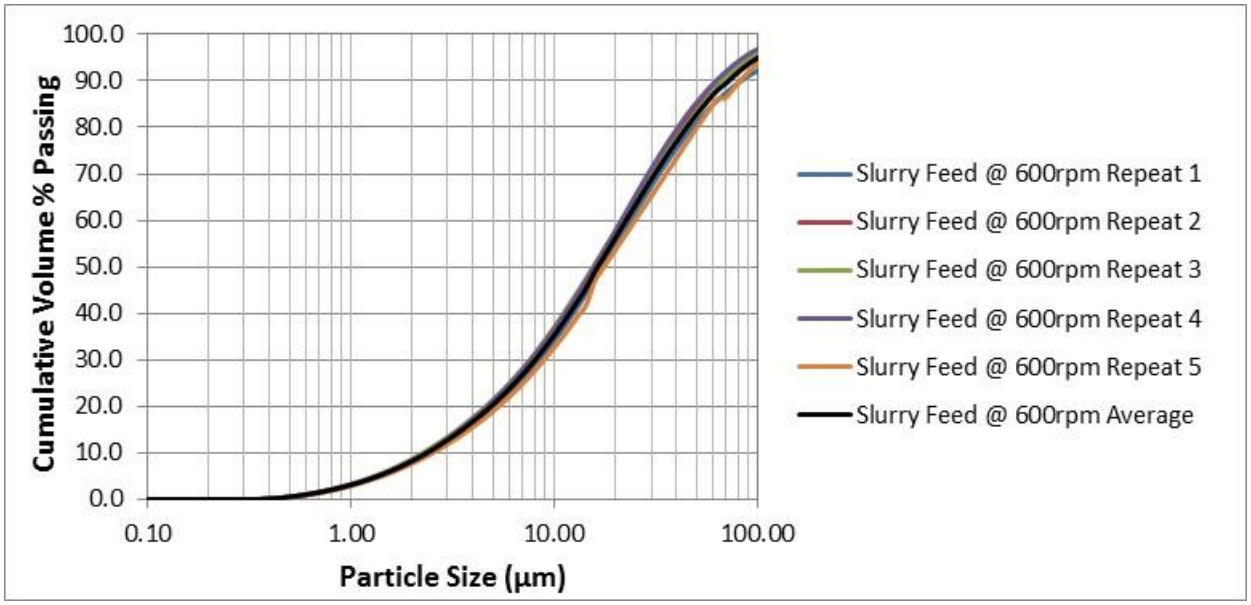


Figure 4.26: Cumulative Volume % Passing without ultrasonic displacement at a pump/stirring speed of 600 rpm

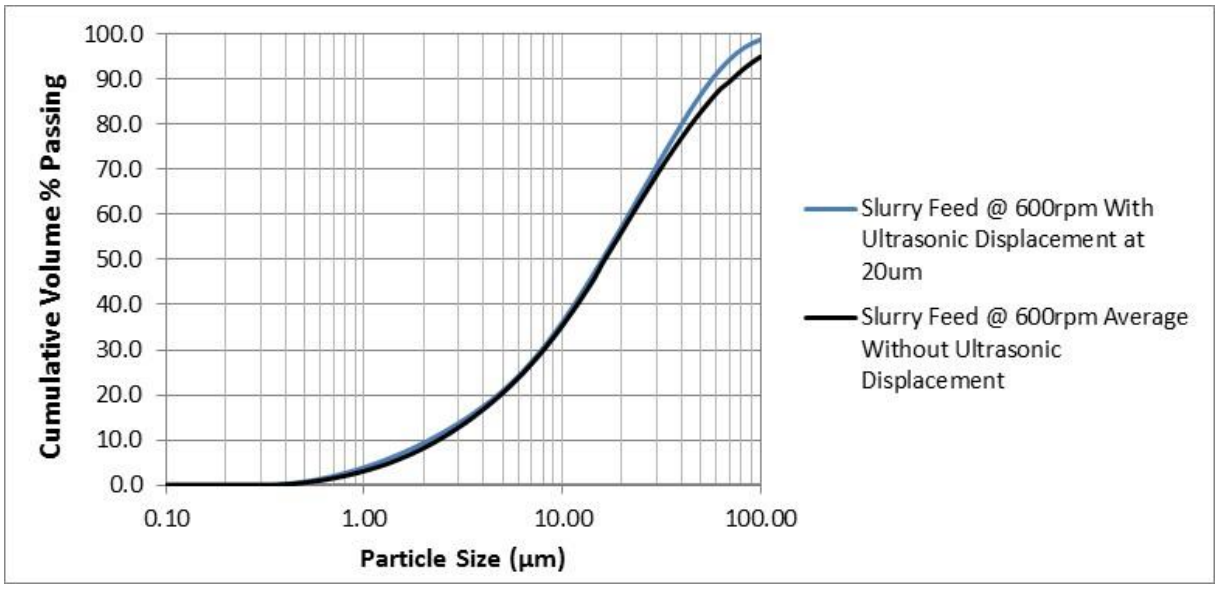


Figure 4.27: Cumulative Volume % passing with and without ultrasonic displacement at a pump/stirring speed of 600 rpm

The effect of pH on the floc size distribution was investigated with the centre points of the Box-Behnken design selected, i.e. sodium silicate and sodium oleate each at 1 000 g/ton; paraffin at 3 000 g/ton and conditioning/stirring time of 10 minutes. The cumulative particle distribution by volume presented in Figure 4.28 to Figure 4.31, in

general, shows good reproducibility for all pHs tested with slightly more variation observed at a pH of 10.5.

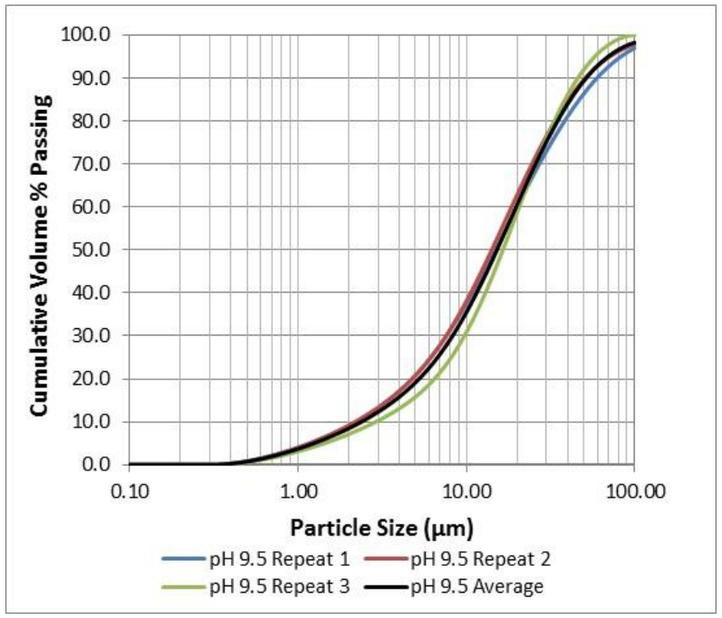


Figure 4.28: Cumulative Volume % Passing without ultrasonic displacement at a pH of 9.5 and pump/stirring speed of 600rpm

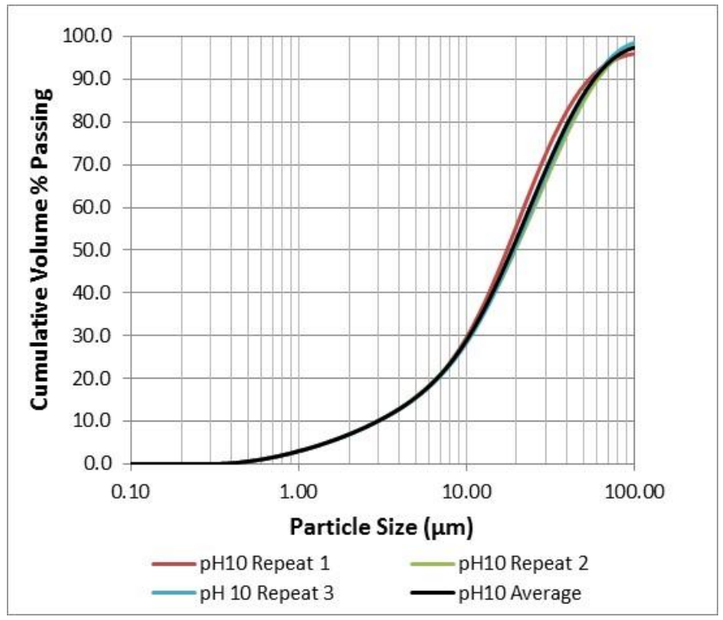


Figure 4.29: Cumulative Volume % Passing without ultrasonic displacement at a pH of 10 and pump/stirring speed of 600rpm

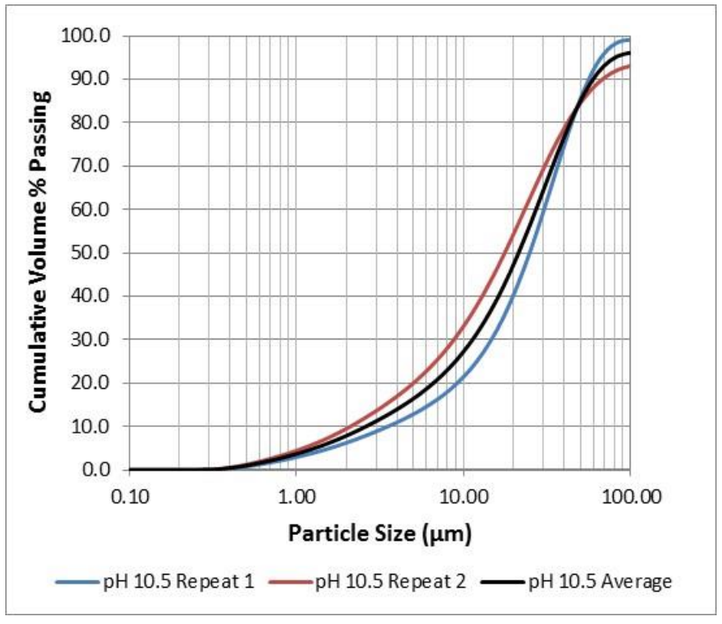


Figure 4.30: Cumulative Volume % Passing without ultrasonic displacement at a pH of 10.5 and pump/stirring speed of 600rpm

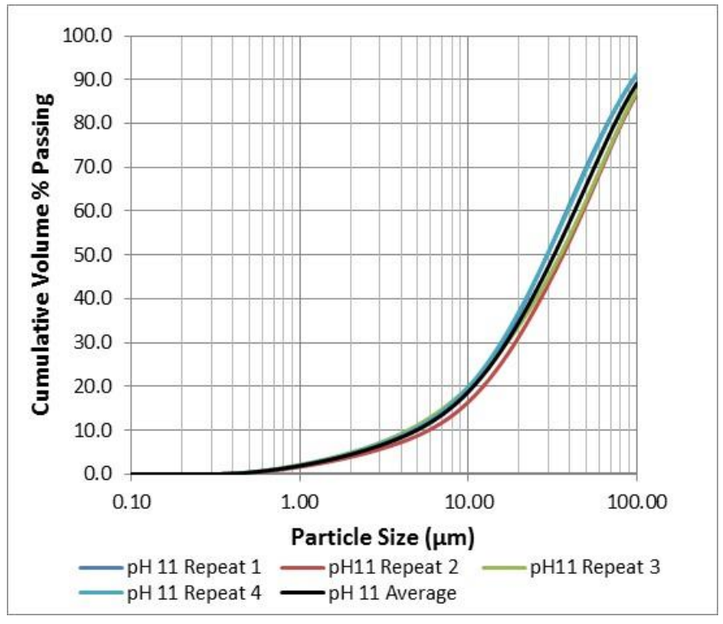


Figure 4.31: Cumulative Volume % Passing without ultrasonic displacement at a pH of 11 and pump/stirring speed of 600rpm

The average cumulative volume % passing for each pH tested presented in Figure 4.32 indicates increasing floc size distribution with increasing pH. Table 4.14 demonstrates the average Dv (0.5) for the feed, pH 9, pH 10, pH 10.5 and pH 11 are 16.75 ± 3.10 µm, 15.15 ± 2.40 µm, 18.76 ± 2.23 µm, 21.28 ± 9.23µm and 32.61 ± 7.47 µm at 95% confidence limits respectively.

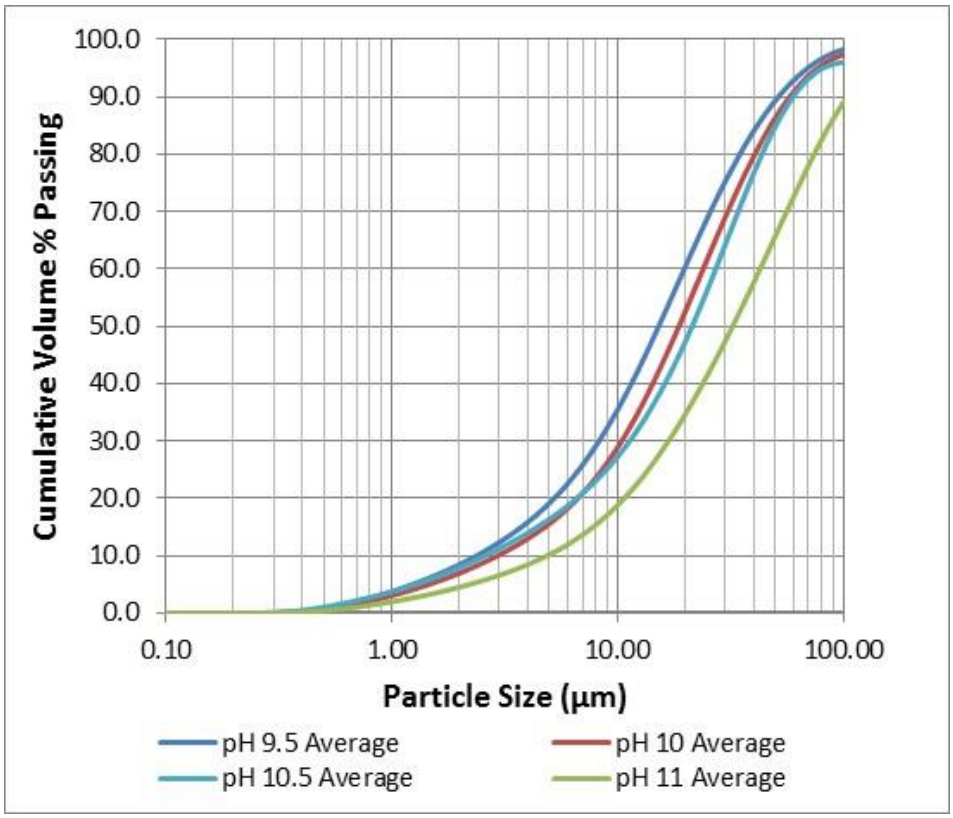


Figure 4.32: The average Cumulative Volume % Passing without ultrasonic displacement at a pH of 9.5 -11 and pump/stirring speed of 600rpm

Table 4.14: The average Dv (0.5) for each of the pHs tested compared to that of the feed (all obtained by laser diffraction)

Sample	Average D(v,0.50) (µm)		
	Average	Upper Limit @ 95% Confidence	Lower Limit @ 95% Confidence
Feed with 20µm ultrasonic displacement	15.89	-	-
Feed without ultrasonic displacement	16.75	19.85	13.65
Selective flocculation at pH 9.5	15.15	17.55	12.74
Selective flocculation at pH 10	18.76	20.99	16.53
Selective flocculation at pH 10.5	21.28	31.51	11.04
Selective flocculation at pH 11	32.61	40.08	25.14

An investigation of pH on floc size using sodium oleate as the collector was conducted by Yin et al. (2011). Their work revealed that at a pH of 8.6 an equilibrium between the molecules of oleic acid and oleate ions exist in solution resulting in maximum hydrophobicity and floc size. Their work indicated that strong alkaline conditions (pH >10) resulted in decreased floc size due to increased concentrations of OH^- that competes with RCOO- for adsorption onto the surfaces of hematite particles thereby reducing the hydrophobicity of the particle surfaces. However, this study showed the opposite of increasing floc size observed at increasing pH. The discrepancy between the two studies could be attributed to the water employed (deionised vs tap water), stirring time (20 min vs 10 min) and sodium oleate dosage (3.94×10^{-4} M vs 2.69×10^{-2} M).

Although the floc size distribution suggests the coarsest floc can be obtained at pH 11, selective flocculation coupled with magnetic separation (SLon-100) indicates that a pH of 10 yielded the best average Fe grades, recoveries and separation efficiencies as summarised in Figure 4.33. Larger standard deviations are observed at a pH of 9.5 compared to the other tests and was subsequently omitted from further comparisons. At 95% confidence, the individual response variables for the remaining pHs are within range of one another and indicate no substantial variation between pH. A pH of 10 was selected for further testwork since this pH had the lowest standard deviation and would be the cheapest from a reagent cost perspective. The Fe recovery-grade curve presented in Figure 4.34 illustrates the FMS process improved the grade and recovery compared to the base case SLon test.

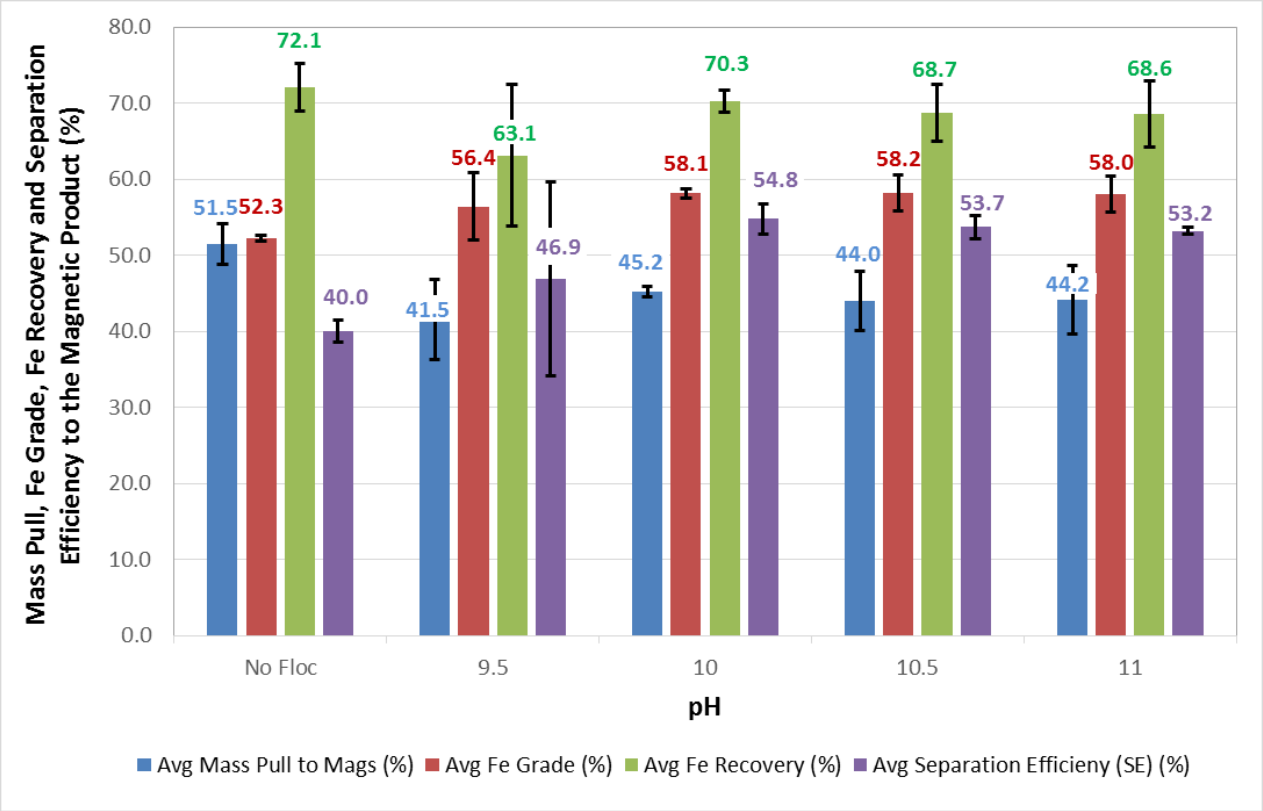


Figure 4.33: The Average Mass Pull, Fe Grade, Fe Recovery and Separation Efficiency in the Magnetic Product at three Background Magnetic Field Intensities

(2 Standard deviations are depicted by the error bars)

The comparison of the floc size distribution to the response variables obtained through the FMS process (selective flocculation coupled with the SLon) indicates that the latter is better suited to determine the effect of various process parameters on selective flocculation than sizing is and thus the FMS process was implemented in the Box-Behnken experimental design.

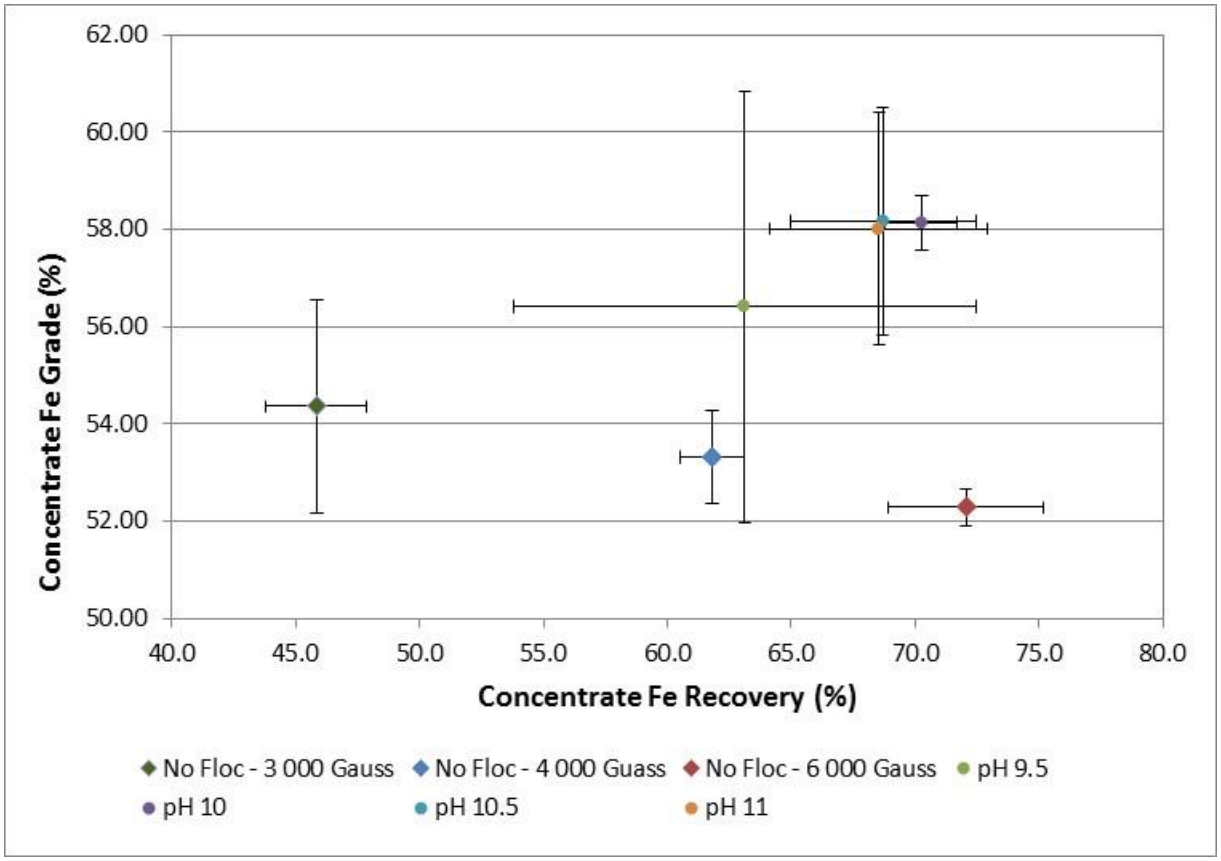


Figure 4.34: Fe Recovery-Grade Curve at the various pH conditions tested (2 Standard deviations are depicted by the error bars)

4.5 Conclusion

Increasing the magnetic field intensity from 3000 Gauss to 6000 Gauss on the SLon-100 (magnetic separator) improved the separation efficiency from 28.6±3.0% to 40±1.46% due to improved Fe recovery (45.9±2.03% to 72.1±3.15%) whilst maintaining the Fe concentrate grade at 52-54%. Thus a magnetic field intensity 6000 Gauss was selected for further testwork.

The modelled yield stress of zero was achieved at all the sodium silicate dosages (0 g/t, 500 g/t, 1000 g/t and 1500 g/t) and pulp densities (0%, 20%, 30% and 45%) tested implying a strong net repulsive interaction exists between the solids in the slurry and indicates the sample is well dispersed, satisfying one of the pre-requirements for selective flocculation. The apparent viscosity profile decreases as the sodium silicate

dosage increases. However a similar response was observed at 1000 g/t and 1500 g/t and the lower dosage, implying lower reagent costs, was selected for further testwork at a pulp density of 45% solids.

pH's of 9.5 to 11 at increments of 0.5 pH were investigated to determine the effect of pH on the floc size distribution using the centre points of the Box-Behnken design, i.e. sodium silicate and sodium oleate each at 1 000 g/ton; paraffin at 3 000 g/ton and conditioning/stirring time of 10 minutes. The floc size was determined using the Malvern Mastersizer at the lowest pump speed of 600 rpm and no ultrasonic displacement. The average cumulative volume % passing for each pH tested indicates increasing floc size distribution with increasing pH. The Dv (0.5) for the feed doubled from 16.75 ± 3.10 µm to 32.61 ± 7.47 µm at a pH of 11. Although the highest pH resulted in the biggest floc, magnetic separation coupled with selective flocculation indicated the best average Fe grades, recoveries and separation efficiencies were achieved at a lower pH of 10. These results indicate floc size should not be used to determine the efficiency of selective flocculation but rather the coupling of selective flocculation with a separation unit would be better suited to optimising the response variables. This coupling approach was used in the Box-Behnken design in Chapter 5 to determine the effect of three selective flocculation factors on the three response variables (Fe grade, Fe recovery, and separation efficiency) by fixing the dispersant conditions to 1 000g/ton of sodium silicate and pH of 10.

CHAPTER 5 : OPTIMISING SELECTIVE FLOCCULATION COUPLED WITH MAGNETIC SEPARATION

5.1 Introduction

The pre-conditions for selective flocculation were reported in Chapter 4 and involved determining the dispersant dosage and pulp density that would provide adequate dispersion along with the pH that would achieve an increase in floc size as well as improved response variables. The next stage is to optimise the selective flocculation process whilst fixing the optimum pre-conditions determined in Chapter 4. The optimisation of the selective flocculation process is necessary to reduce the operating costs of the Floc Magnetic Separation (FMS) process whilst maximising the response variables as the selective flocculation process tends to be cost prohibitive. The selective flocculation stages to be optimised in this chapter is the selective hydrophobization and hydrophobic flocculation stages presented in Figure 5.1. Figure 5.1 is Figure 2.14 from Chapter 2 and is repeated here for convenient reference.

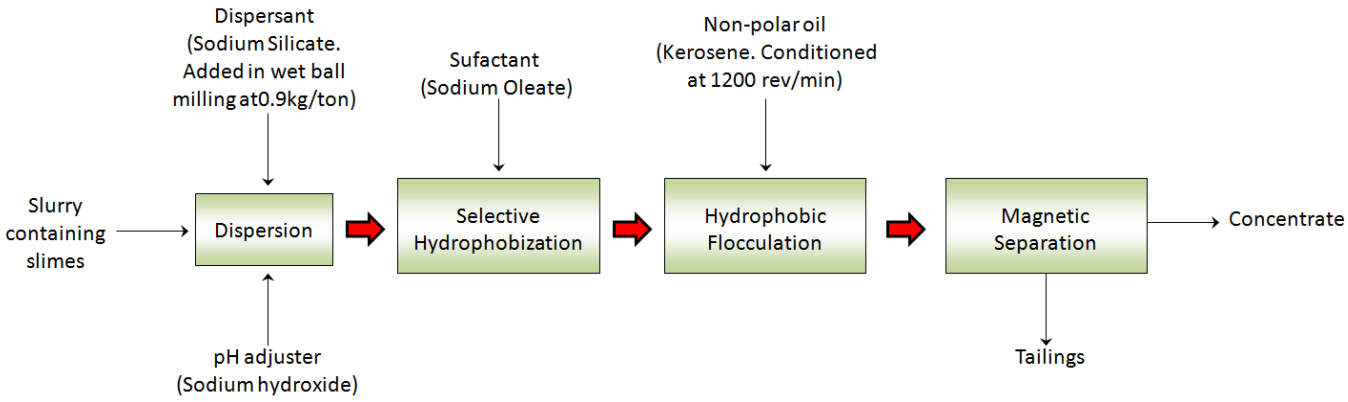


Figure 5.1: Schematic representation of the Floc Magnetic Separation (FMS) process applied to hematite (Song et al., 2002)

Based on the literature review of the FMS process in Chapter 2, three operating parameters (factors) were identified as the important parameters that influence selective flocculation. The three factors are sodium oleate dosage, paraffin dosage and conditioning time. Sodium oleate selectively hydrophobizes the hematite to create hematite flocs while the paraffin, the non-polar oil, further increases the size of the flocs. The conditioning time ensures that sufficient kinetic energy is imparted to

overcome the repulsive energy barrier between the hematite particles thereby allowing selective flocculation to occur. The influence of these three factors, at different levels, on selective flocculation will need to be established before optimisation of the selective flocculation process can be conducted.

A response surface model, namely the Box-Behnken experimental design, was used to determine the effect of the three operating variables (factors) mentioned above on the performance of selective flocculation. The Box-Behnken experimental design incorporates three levels for each operating variable (factor) allowing for the selective flocculation process to be optimised. Selective flocculation was coupled with magnetic separation to evaluate the performance of selective flocculation on the three response variables namely Fe concentrate grade, Fe concentrate recovery and separation efficiency. The experimental data was used in conjunction with Design Expert to analyse the significance of each parameter and develop empirical models that describe the response variable as a function of the factors. The models were used to generate response surface contours for each of the response variables. Thereafter the optimum operating range of each factor will be identified and experiments conducted at these optimum conditions to validate the predicted optimal selective flocculation performance.

The optimal selective flocculation conditions will be applied to gravity separation (Reflux Classifier) in Chapter 6 to determine the impact of selective flocculation on the metallurgical performance of this unit.

The raw data pertaining to this chapter is presented in Appendix C

5.2 Methodology

5.2.1 Selection of Experimental Design

According to NIST (2012), the experimental design selected is based on the objective of the experiment. NIST (2012) lists the five experimental objectives as follows:

- **Comparative Objective**

  When one or several factors are investigated, and a conclusion about one important factor in the presence of or despite the existence of other factors is the main objective of the experiment, i.e. it is to determine if there is a significant change is the response variable for the different levels of that one important factor. In these cases, a comparative design is recommended.

- **Screening Objective**

  When the primary purpose of the experiment is to select or screen out the few important main effects from the many less important ones a screening design, also referred to as the main effects design, is required.

- **Response Surface Method Objective**

  When the interaction of factors and quadratic effects, and thus the shape of the response surfaces being investigated, are to be determined a Response Surface Method Design (RSM) is recommended. Typically RSM designs are used to:

    - Determine improved or optimal process settings
    - Troubleshoot process problems and weak points
    - Make a product or process more robust (relatively insensitive) against external and non-controllable influences.

- **Optimising responses when factors are proportions of a mixture Objective**

  When factors are proportions of a mixture, and it is required to determine the "best" proportions of the factors to maximise or minimise a response then a mixture design is recommended.

- **Optimal fitting of a regression model Objective**

  NIST (2012) recommends a regression model be used when a model of a response variable as a function of a few factors is required along with good estimates of the model parameters.

The objective of the selective flocculation test is to determine the optimal process settings for the three factors within the range selected so that the best conditions can

be compared to the base case tests (without flocculation). Based on the experimental objectives listed by NIST (2012) this correlates to a response surface method objective, and the appropriate experimental design for this objective is a Central composite design or a Box-Behnken design as indicated Table 5.1.

Table 5.1: Design selection guide outline by NIST (2012)

Number of Factors	**Comparative Objective**	**Screening Objective**	**Response Surface Method Objective**
1	1-factor completely radomised design	-	-
2-4	Randomised block design	Full or fractional factorial	Central composite or Box-Behnken
5 or more	Randomised block design	Fractional factorial or Plackett-Burman	Screen first to reduce number of factors

Box and Draper (1987) as cited by NIST (2012) identified the following desirable properties for a response surface design:

- Satisfactory distribution of information across the experimental region, i.e. the design must be rotatable. A design is rotatable if the variance of the predicted response at any point depends only on the distance of that point from the design centre point. This allows the design to be rotated around its centre point without altering the variance at the said point.
- Fitted values are as close as possible to the observed values. Residual or error of prediction should be minimised.
- Good lack of fit detection.
- Internal estimate of error.
- Constant variance check.
- Transformation can be estimated.
- Suitability for blocking.
- The ability to build higher order designs with powers equal to or greater than 3 from simpler designs that are linear or quadratic.
- Good graphical representation of observed data patterns.

- Good behaviour when errors in settings of input variables occur.

In Table 5.2 NIST (2012) summarised the properties of the classical quadratic designs for RSM along with broad guidelines in the selection of an appropriate design. In addition, NIST (2012) recommends that a design with fewer runs than the allocated budget be used to ensure additional resources are available to redo runs that have processing mishaps. Since three runs will be done for each factor and level the Box-Behnken design was selected as it has the least number of runs compared to central composite designs. In addition, the combined factor extremes will be avoided as the centre points were the best operating parameters defined by Song et al. (2002) in their investigation.

Table 5.2: Summary of properties of the Classical Response Surface Designs (NIST,2012)

Design Type	Comment
Central Composite Circumscribed (CCC)	CCC designs provide high quality predictions over the entire design space, but require factor settings outside the range of the factors in the factorial part. **Note:** When the possiblity of running a CCC design is recognised before starting a factorial experiment, factor spacings can be reduced to ensure that ±α for each coded factor corresponds to feasible/reasonable levels.
	Requires 5 levels for each factor.
	For three factors 20 runs would be required containing 6 centre point runs.
Central Composite Inscribed (CCI)	CCI designs use only points within the factor ranges orginally specified, but do not provide the same high quality prediction over the entire space compared to the CCC.
	Requires 5 levels for each factor.
	For three factors 20 runs would be required containing 6 centre point runs.
Composite Face-Centred (CCF)	CCF designs provide relatively high quality predictions over the entire design space and do not require using points outide the original factor range. However, they give poor precision for estimating pure quadratic coefficients.
	Requires 3 levels for each factor.
	For three factors 20 runs would be required containing 6 centre point runs.
Box-Behnken	These designs require fewer treatment combinations than a central composite design in cases involving 3 or 4 factors.
	The Box-Behnken design is rotatable or nearly rotatable but contains regions of poor prediction quality like the CCI. It does not predict well at the corners of the design space. Its "missing corners" may be useful when the experimenter should avoid combined factor extremes. It is insensitive to outliers and missing data and is best used when the region of interest and region of operability are nearly the same.
	Requires 3 levels for each factor.
	For three factors 17 runs would be required containing 5 centre point runs.

NIST (2012) describes the Box-Behnken design as an independent quadratic design in that it does not contain an embedded factorial or fractional factorial design. In this design, the treatment combinations are at the midpoints of edges of the process space and the centre as depicted in Figure 5.2. The design incorporating three levels for each factor can be rotated. The disadvantage of the Box-Behnken design is the limited ability for orthogonal blocking which can be overcome by using the central composite designs. Orthogonal blocking occurs when the effects of the blocking can be separated from the effects of individual factors or interaction factors (NIST, 2012).

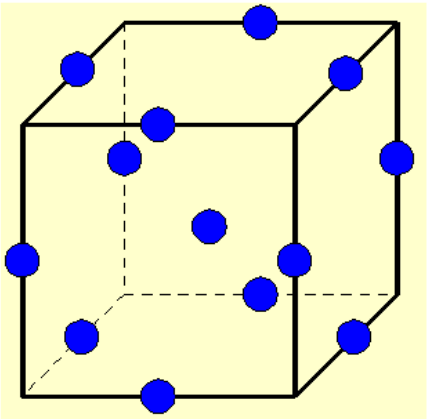


Figure 5.2: A Box-Behnken design for three factors (NIST, 2012)

5.2.2 Selection of Operating Parameters

The screening tests described in Chapter 4 allowed for the selection of pulp density, dispersant dosage and pH. The remaining three factors (sodium oleate dosage, paraffin dosage and conditioning time) were varied at three levels as presented in Table 5.3. The ranges for each factor was guided by the work of Song et al. (2002).

Table 5.3: Factors and their respective levels employed in the Box-Behnken design

Factor	Levels		
	Low (-1)	Intermediate (0)	High (1)
Factor 1: Sodium Oleate Dosage (g/t)	500	1000	2000
Factor 2: Paraffin Dosage (g/t)	2000	3000	4000
Factor 3: Conditioning Time (min)	5	10	20

5.2.3 Tests

Seventeen tests at various levels of the specified factors were conducted as outlined in Table 5.4 with the five centre points highlighted in pink. Two repeats were conducted, and thus a total of three blocks were conducted. Table 5.4 indicates that the design is orthogonal (AxB = 0; AxC = 0 and BxC = 0) and thus the effect of one factor or interaction can be estimated independently from the effect of any other factor

or interaction in the model. For each block, the runs were randomised and conducted over several days.

Table 5.4: Matrix of tests for Block 1 of the Box-Behnken Design

Block	Run	Factor A: Sodium Oleate Dosage (g/t)	Factor B: Paraffin Dosage (g/t)	Factor C: Conditioning Time (min)		Check for Orthogonal Design		
						AB	AC	BC
Block 1	1	0	1	-1		0	0	-1
Block 1	2	1	1	0		1	0	0
Block 1	3	0	-1	-1		0	0	1
Block 1	4	1	0	1		0	1	0
Block 1	5	0	0	0		0	0	0
Block 1	6	1	0	-1		0	-1	0
Block 1	7	0	0	0		0	0	0
Block 1	8	0	-1	1		0	0	-1
Block 1	9	-1	-1	0		1	0	0
Block 1	10	0	0	0		0	0	0
Block 1	11	-1	1	0		-1	0	0
Block 1	12	-1	0	1		0	-1	0
Block 1	13	0	0	0		0	0	0
Block 1	14	0	0	0		0	0	0
Block 1	15	0	1	1		0	0	1
Block 1	16	1	-1	0		-1	0	0
Block 1	17	-1	0	-1		0	1	0
					Sum	**0**	**0**	**0**

For each test, a representative 200g sample of solids was added to a 1 litre Denver flotation cell with 244.4g of tap water added to the cell to create a pulp density of 45% solids by mass. The pulp was agitated at 1200rpm to ensure a homogenous pulp to which sodium silicate at a dosage of 1kg/ton was added. The pH of the pulp was adjusted to 10 before sodium oleate and paraffin additions at the required dosage. The pH was thereafter re-adjusted to 10, and the pulp was conditioned for the required duration. pH modifications were achieved with sodium hydroxide and sulphuric acid at solution concentrations of 1% and 0.5% by mass respectively. Subsequent to the flocculation step the pulp from the Denver float cell was washed into a beaker and processed through the magnetic separator, the SLon-100, at the optimal background magnetic field intensity, pulsation frequency and amplitude described in Section 4.2. The products from each test were filtered, dried and prepared for chemical analysis to determine the Fe grade-recovery response and the separation efficiency.

5.2.4 Analysis of Results

5.2.4.1 Design Evaluation

Stat-ease (2016) recommends the following checklist for evaluating the experimental design selected. The following checklist was followed to determine if a suitable model was selected.

- The selected polynomial model used should be evaluated to ensure confounding or no aliases are present. Aliases occur when two or more variables vary together, and the effect of each variable cannot be separated from each other. Aliases indicate insufficient unique design points were selected.
- The minimum degrees of freedom for the model's for lack-of-fit and pure error should be 3 and 4 respectively.
- The standard errors for the linear coefficients should be equal. Likewise, the standard errors for the coefficients of the cross products should be equal.
- A plot of the standard error should yield a flat error profile centred in the middle of the design space. The standard error plot should appear as a circle or square of uniform precision.
- A graph of error vs Fraction of Design Space (FDS) indicates the amount of the design region that can be estimated with that precision. An FDS greater than 80% is acceptable to ensure the majority of the design space is precise enough for the objective. The standard error mean was used in this study as it is typically used when the objective of the experiment is to optimise responses using the derived model.

5.2.4.2 Analysis of Variance

Multivariate **AN**alysis **O**f **VA**riance (ANOVA) is a statistical technique used to investigate and model the relationship between a response variable and one or more independent variables also referred to as factors. Each factor may consist of two or

more levels depending on the experimental design that was selected. The three-factor analysis of variance model defined by Montgomery (2009) is given by Equation 5.1.

$$y_{ijkl} = \mu + \tau_i + \beta_j + \gamma_k + (\tau\beta)_{ij} + (\tau\gamma)_{ik} + (\beta\gamma)_{jk} + (\tau\beta\gamma)_{ijk} + \epsilon_{ijkl} \quad \begin{cases} i = 1,2,\ldots..a \\ j = 1,2,\ldots..b \\ k = 1,2,\ldots..c \\ l = 1,2,\ldots..n \end{cases}$$

Equation 5.1

Where

y : represents the response variables concentrate Fe grade, concentrate Fe recovery or separation efficiency

μ : is the overall mean effect

τ, β and γ: represents each of the factors sodium oleate dosage, paraffin dosage and conditioning time

τ_i: is the effect of the ith level of row factor A,

β_j: is the effect of the jth level of column factor B, and similarly for γ_k

$(\tau\beta)_{ij}$: is the effect of the interaction between τ_i and β_j and similarly for $(\tau\gamma)_{ik}$, $(\beta\gamma)_{jk}$, and $(\tau\beta\gamma)_{ijk}$

ϵ_{ijkl} : is the random error incorporating all sources of variability in the experiment such as measurement error and the variability of uncontrolled factors,

a : is the a number of levels for factor A and similarly for b and c

ANOVA tests the null hypothesis that the population means of each level are equal versus the alternative hypothesis that at least one of the level means are not all equal. The advantage of ANOVA is that it can simultaneously test several factors at several levels.

ANOVA was applied to the selective flocculation tests using the Box-Behnken design. The tests were randomised and thus confounding with time is not expected to be a problem. Confounding occurs when two or more variables vary together, and the effect of each variable cannot be separated from each other.

Assumptions

The probability values (p-values) obtained from the F value calculated through the ANOVA method require that the experimental data adhere to the six Fisher assumptions used in the derivation of the F distribution. Grinnel College (n.d.) lists the following six assumptions:

- The unknown true population means and thereby effect sizes of every treatment are constant.
- Each observed sample consists of a true population mean for a particular level combination plus sampling error, also referred to as the additive assumption.
- Sampling errors are normally distributed.
- Sampling errors are independent. Several residual plots should be made to validate these assumptions every time ANOVA is used.
- Every level combination has equivalent variability among its samples. When the standard deviation within any level is double that in any other level, the ANOVA may become unreliable.
- Sampling errors have a mean of 0 thus the average of the samples within a particular level should be close to the true level mean.

Other assumptions associated with multivariate ANOVA as indicated by French et al. 2008 are listed overleaf:

- Normal Distribution

  The dependent variable should be normally distributed within groups (or levels). Overall the F-test is robust to non-normality if the non-normality is caused by skewness (asymmetrical distribution of results) rather than outliers. Prior to conducting a multivariate ANOVA a test for outliers should be done and any outliers should either be transformed or omitted.

- Linearity

  Multivariate ANOVA assumes that there are linear relationships among all pairs of dependent variables, all pairs of covariates, and all dependent variable-covariate pairs in each cell. When non-linear relationships occur, the integrity of the analysis may be weakened.

- Homogeneity of Variances

  Homogeneity of variances requires that the variances for the dependent variable are equal to the variances of the predictor variable (the variable in a regression that is used to predict the response of another variable). The error variance is computed by adding the sums of squares within each group. However, when the variance in two groups differs then the within-group variance cannot be determined by simply summing up the variances in the group.

  In multivariate analysis, the intercorrelations of the multiple dependent variables (referred to as covariance) are also homogeneous across the cell of the design. The homogeneity in variances and covariances can be tested statistically.

Evaluating the selected model

Stat-ease (2016) recommends the following checklist to determine if a suitable model was selected:

- From the ANOVA table determine if the model is significant, i.e. a large F-value with $p<0.05$.

- From the ANOVA table determine if the lack-of-fit is insignificant, i.e. an F-value near one with p>0.10.
- Ensure the signal to noise ratio, i.e. precision, is greater than 4. A value of >4 indicates adequate precision.
- The predicted R-Squared is no more than 0.2 below the adjusted R-Squared.
- Ensure there are well-behaved residuals. Residuals confirm that the assumptions for the ANOVA have been met. The Pennsylvania State University (2018) lists the following characteristics of well-behaved residuals:
    - The residuals are randomly distributed around the residual line (the zero line which represents the estimated regression line). The assumption that the relationship is linear is thus considered reasonable.
    - The residuals form a rough horizontal band around the residual line which indicates the variances in the error terms are equal.
    - There are no outliers in the data set if the residuals follow the pattern of residuals.
- Plot actual versus predicted for each response to ensure points are randomly scattered along the 45-degree line. Points positioned above or below the 45-degree line indicate areas of over and underprediction respectively.

Subsequent to completing the checklists listed above the data was analysed using 3-D contour plots to determine the effect of factors on each response variable. Thereafter optimisation was conducted with constraints selected for each factor. Perturbation (trace) plots were also constructed to determine how sensitive the optimum is to changes in each factor.

5.3 Results and Discussion

5.3.1 Outlier Determination

The outliers for the average response variables over the seventeen runs are presented in Table 5.5 which indicates there are no outliers for the response variables separation efficiency and concentrate Fe grade. Although Run 17 appears to be a minor outlier

for the concentrate Fe recovery, there are no major outliers. Since the former two response variables showed no outliers, the data set can be considered to contain no outliers.

Table 5.5: Determination of outliers in the data set obtained

Test	Average Separation Efficiency (%)	Test	Average Fe Grade (%)	Test	Average Fe Recovery (%)
Run 2	56.8	Run 2	57.25	Run 12	72.4
Run 1	57.2	Run 10	57.26	Run 9	72.6
Run 10	57.3	Run 1	57.50	Run 3	73.0
Run 6	57.3	Run 6	57.54	Run 1	73.0
Run 5	57.4	Run 5	57.76	Run 2	73.1
Run 13	57.6	Run 3	57.78	Run 4	73.1
Run 14	57.7	Run 16	57.81	Run 13	73.1
Run 9	57.8	Run 13	57.85	Run 5	73.2
Run 3	57.8	Run 9	57.89	Run 14	73.3
Run 15	57.8	Run 14	57.92	Run 11	73.3
Run 11	57.9	Run 15	57.99	Run 7	73.3
Run 16	57.9	Run 7	58.17	Run 15	73.5
Run 12	57.9	Run 17	58.19	Run 8	73.5
Run 7	58.0	Run 11	58.34	Run 6	73.5
Run 4	58.3	Run 4	58.40	Run 10	73.5
Run 8	58.5	Run 8	58.72	Run 16	74.0
Run 17	58.8	Run 12	58.74	Run 17	74.4

	Average Separation Efficiency (%)	Average Fe Grade (%)	Average Fe Recovery (%)
Q1	57.3	57.7	73.1
Q2 (Median)	57.8	57.9	73.3
Q3	58.0	58.3	73.5
Interquartile Range	0.6	0.6	0.4
"Inner Fences" of the Data Set	56.4	56.7	72.4
	58.9	59.2	74.1
"Outer Fences" of the Data Set	55.5	55.8	71.8
	59.8	60.1	74.8
Are there outliers?	No outliers as data lies within the inner fences.	No outliers as data lies within the inner fences.	Minor Outliers: Run 17. No major Outliers.

5.3.2 Design Evaluation

The plot of the standard error for the design presented in Figure 5.3 to Figure 5.5 indicates a flat error profile centred in the middle of the design space with a circle of uniform precision for each of the interaction plots with the split factor at a coded value of -1. The error plots indicate a suitable design was selected with the perimeter of the design space indicating higher standard errors than near the centre. This is expected since the Box-Behnken design has five centre replicates and no replicates at the perimeter.

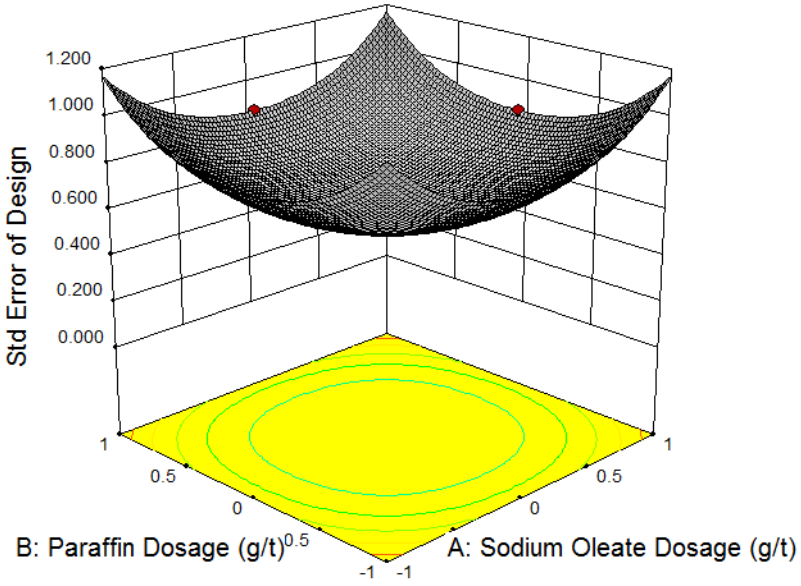


Figure 5.3: The standard error for the design for the AB interaction with the split factor C at a coded value of -1

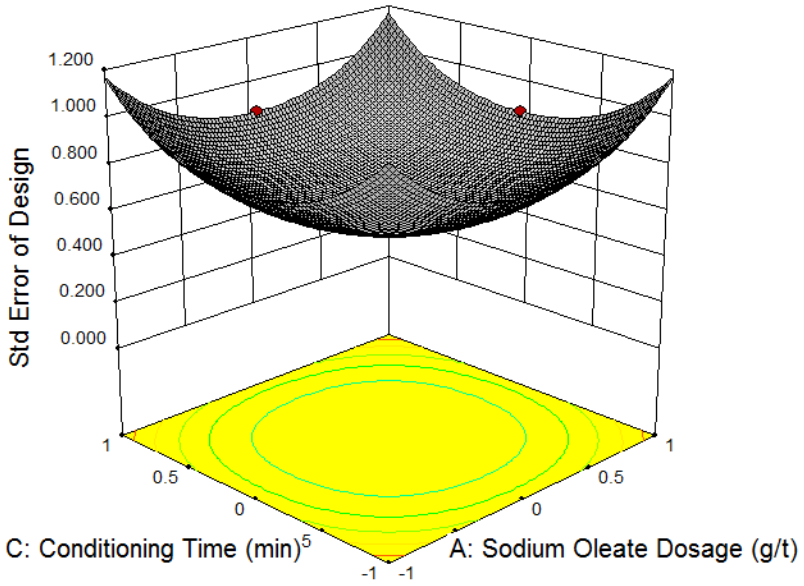


Figure 5.4: The standard error for the design for the AC interaction with the split factor B at a coded value of -1

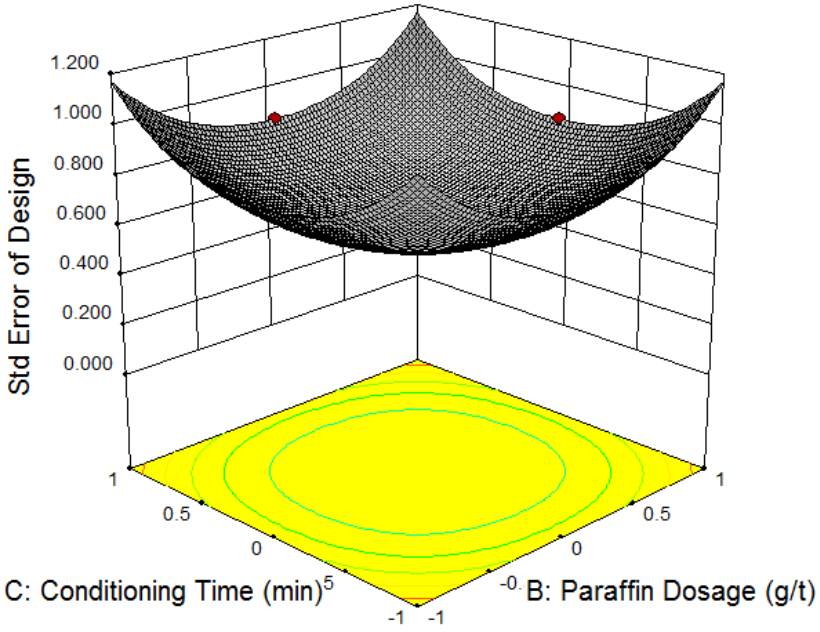


Figure 5.5: The standard error for the design for the AC interaction with the split factor B at a coded value of -1

The graph of standard error mean vs Fraction of Design Space (FDS) presented in Figure 5.6 indicates that 80% of the design region has a standard error mean of less than 0.669 and is precise enough for optimising responses using the derived models.

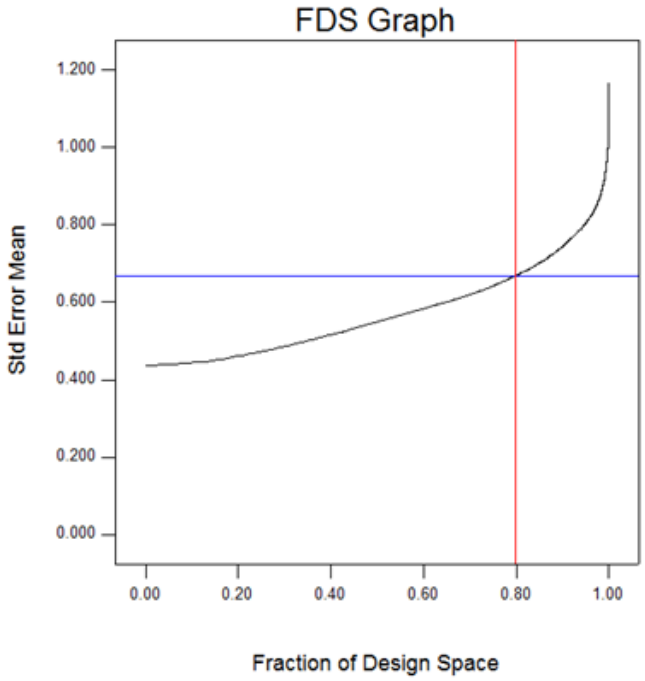


Figure 5.6: Fraction of Design Space (FDS) as a function of the standard error mean

5.3.3 Evaluating the models

The effects of three factors namely, sodium oleate dosage, paraffin dosage and conditioning time on the three response variables namely concentrate Fe grade, concentrate Fe recovery and separation efficiency was investigated. The experimental data was entered into Design Expert, and four empirical models describing the response variable as a function of the factors were evaluated as presented in Table 5.6 to Table 5.8. The cubic model was aliased for all three responses and was subsequently omitted from further comparisons. The two models that satisfy most of the criteria for a good model, except for the criterion that the predicted R-Squared is a maximum of 0.2 below the adjusted R-Squared, are the two-level factorial model (2Fl) and the quadratic models for separation efficiency and the linear and 2Fl models for Fe concentrate grade. All the models for the concentrate Fe Recovery were insignificant.

Table 5.6: Model evaluation for the Response Variable: Separation Efficiency

Type of Model	Is model significant (Large F-value with p<0.05)		Lack-of-fit is insignificant i.e. an F-value near one with p>0.10.		Precision (Target >4)	R-Squared	Adjusted R-Squared	Predicted R-Squared	Adjusted R-Squared minus predicted R-Squared (Target < 0.20)
	F-value	p-value	F-value	p-value					
Linear	2.50	0.11	3.27	0.13	5.3	0.365	0.219	-0.231	0.450
2FI	5.61	0.01	1.85	0.29	7.1	0.714	0.542	-0.067	0.609
Quadratic	4.04	0.04	1.50	0.34	8.2	0.839	0.631	-0.485	1.116
Cubic (Aliased)	1.50	0.34	-	-	-	-	-	-	-

Table 5.7: Model evaluation for the Response Variable: concentrate Fe Grade

Type of Model	Is model significant (Large F-value with p<0.05)		Lack-of-fit is insignificant i.e. an F-value near one with p>0.10.		Precision (Target >4)	R-Squared	Adjusted R-Squared	Predicted R-Squared	Adjusted R-Squared minus predicted R-Squared (Target < 0.20)
	F-value	p-value	F-value	p-value					
Linear	5.61	0.01	0.93	0.58	8.0	0.564	0.464	0.262	0.202
2FI	3.36	0.04	0.90	0.57	6.4	0.668	0.469	0.019	0.45
Quadratic	3.65	0.05	0.32	0.81	7.5	0.824	0.599	0.229	0.37
Cubic (Aliased)	0.32	0.8088	-	-	-	-	-	-	-

Table 5.8: Model evaluation for the Response Variable: concentrate Fe Recovery

Type of Model	Is model significant (Large F-value with p<0.05)		Lack-of-fit is insignificant i.e. an F-value near one with p>0.10.		Precision (Target >4)	R-Squared	Adjusted R-Squared	Predicted R-Squared	Adjusted R-Squared minus predicted R-Squared (Target < 0.20)
	F-value	p-value	F-value	p-value					
Linear	0.60	0.63	13.93	0.01	2.7	0.122	-0.081	-0.812	0.73
2FI	1.62	0.24	6.79	0.04	4.6	0.492	0.188	-1.420	1.61
Quadratic	0.80	0.63	22.83	0.01	3.1	0.508	-0.125	-6.482	6.36
Cubic (Aliased)	13.35	0.02	-	-	-	-	-	-	-

The models for the separation efficiency and concentrate Fe grade were selected by comparing the coefficient of determination (R^2) from the actual versus predicted. The higher the R^2 value, the better the model fits the set of data. The coefficient of determination was higher for the quadratic and 2FI models for the separation efficiency and concentrate Fe grade respectively as illustrated in Figure 5.7 to Figure 5.8 and was thus selected.

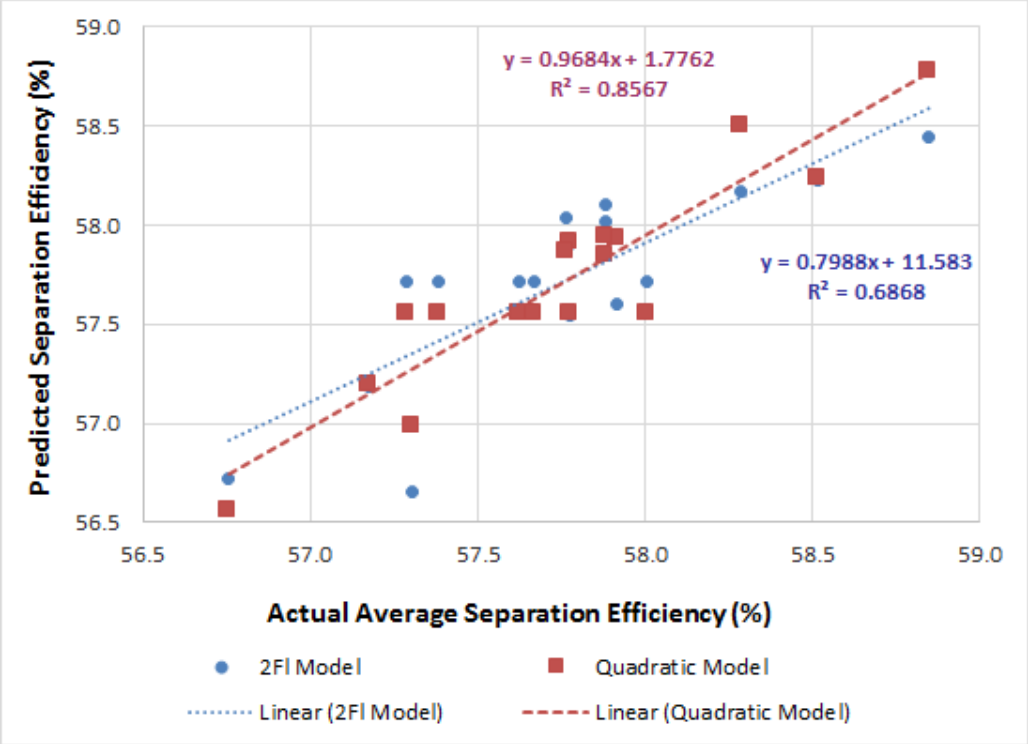


Figure 5.7: The relationship between the actual and predicted separation efficiency for the 2Fl and Quadratic Models

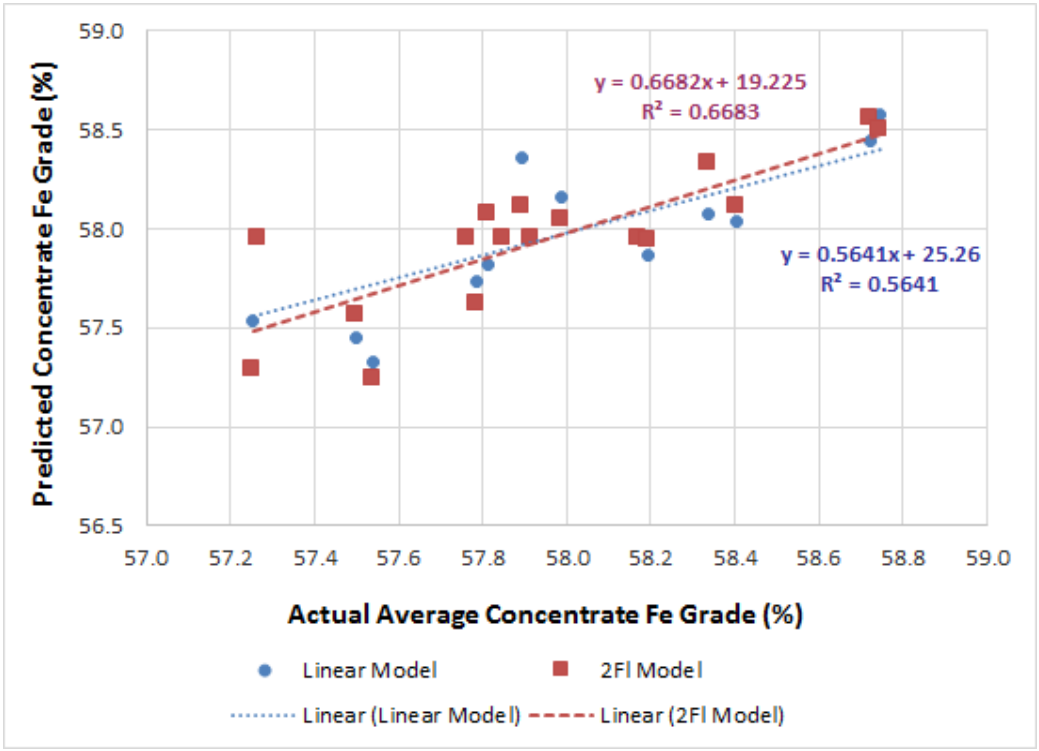


Figure 5.8: The relationship between the actual and predicted concentrate Fe grade for the linear and 2Fl Quadratic Models

Joglekar and May (1987) indicate a coefficient of at least 0.80 indicates a good fit of the model to the data. The quadratic model for the separation efficiency satisfies this requirement, but the 2Fl model does not. However the predicted separation efficiency and concentrate Fe grade lies within 95% confidence limits for each run as illustrated in Figure 5.9 to Figure 5.10 indicating an adequate fit of the data and the models are adequate to predict the response variables within experimental constraints.

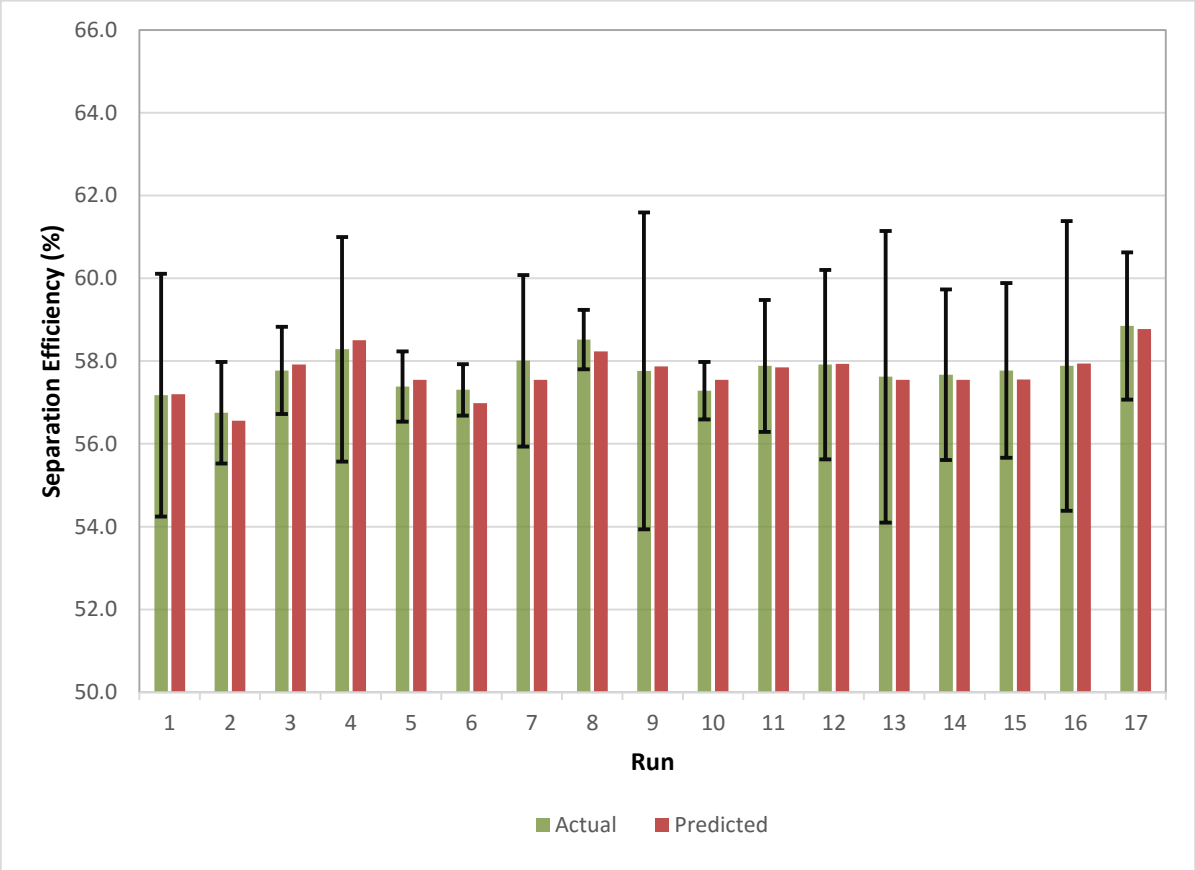


Figure 5.9: The actual and predicted separation efficiency using the Quadratic Model at 95% Confidence limits

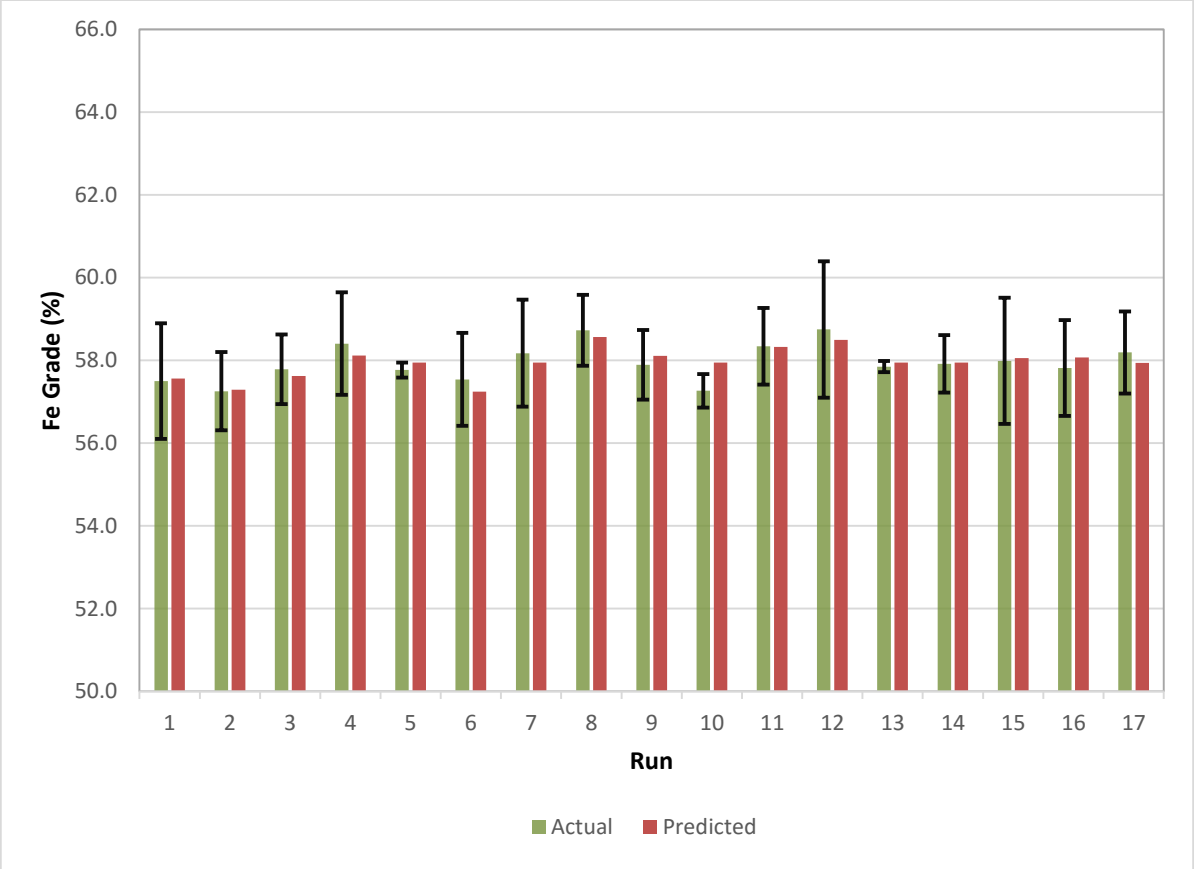


Figure 5.10: The actual and predicted concentrate Fe Grade using the 2Fl Model at 95% Confidence limits

The residuals for the selected models presented in Figure 5.11 to Figure 5.14 have a normal distribution and are randomly scattered with run number indicating the residuals for both models are well behaved and fulfil the ANOVA assumptions.

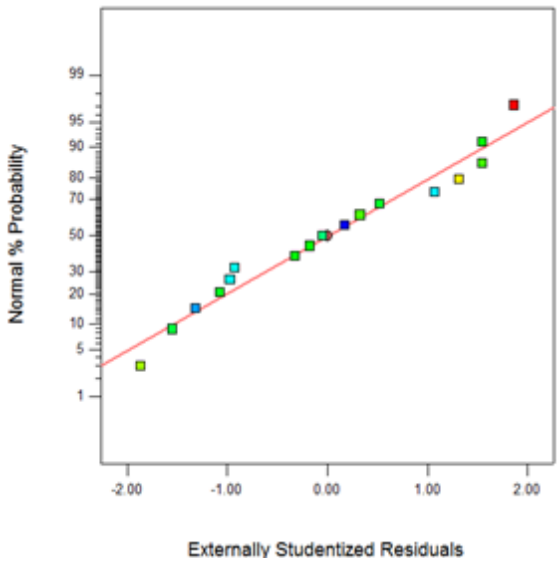


Figure 5.11: Normal plot of residuals for the response variable: Separation Efficiency

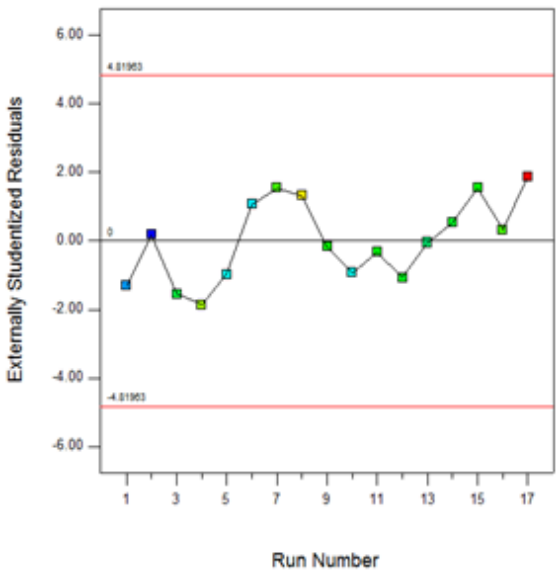


Figure 5.12: Externally studentized residuals for the response variable: Separation Efficiency

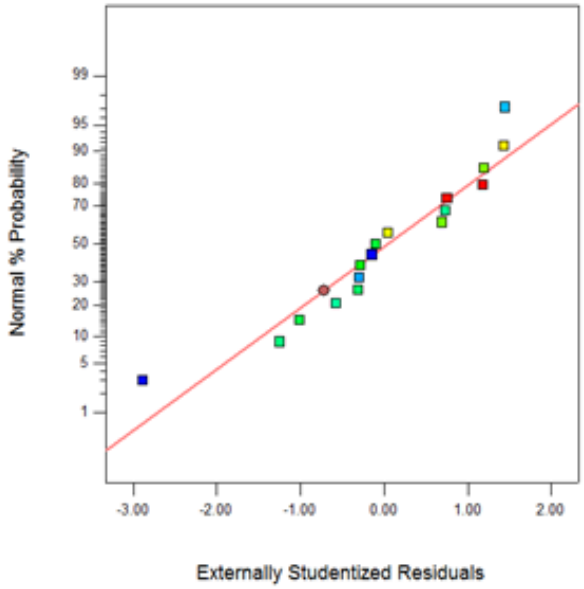


Figure 5.13: Normal plot of residuals for the response variable: concentrate Fe Grade

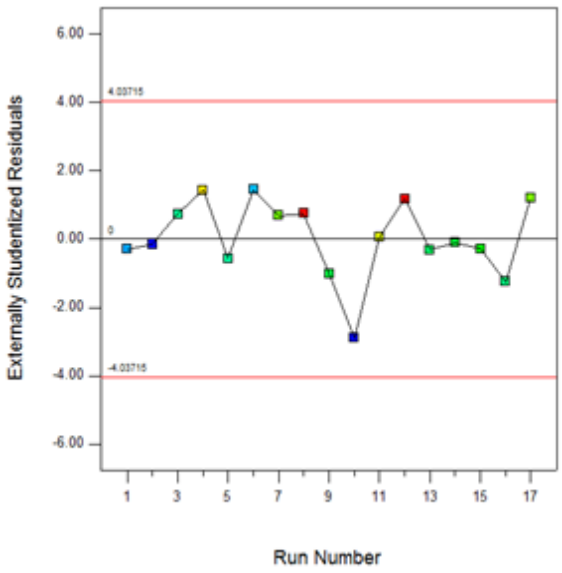


Figure 5.14: Externally studentized residuals for the response variable: concentrate Fe Grade

5.3.4 Analysis of Variance

ANOVA is typically used in the minerals processing industry to evaluate the significance of factors and their interactions on response variables (Angadi et al., 2012, Murty et al., 2013). A total of 17 runs in triplicate were performed as per the Box-Behnken experimental design to determine the effect of factors on the response variables separation efficiency, concentrate Fe grade and concentrate Fe recovery. The quadratic and 2FI model was used to predict the separation efficiency and concentrate Fe grade respectively while the models for concentrate Fe recovery were deemed to be insignificant (Section 5.3.3). For the response variables separation efficiency and concentrate Fe grade, the significance of each factor and their interactions were determined by Fisher's test (F test) and its corresponding p values at 95% confidence level.

Separation Efficiency

According to Table 5.9 separation efficiency is most sensitive to the interaction between the sodium oleate dosage and conditioning time (F=11.32) followed by the paraffin dosage (F=7.90) and finally by sodium oleate dosage (F=6.04). This order of sensitivity applies to the ranges for each factor tested in this thesis, and it may change for other studies depending on the ranges tested. The model developed for this response variable using these factors and interactions is given by Equation 5.2. The model developed is significant as suggested by the high F value and low p-value.

Table 5.9: ANOVA Table for the Quadratic model for the response variable: separation efficiency

Source	Sum of Squares	df	Mean Square	F Value	p-value Prob > F
Model	4.51	9	0.50	4.04	0.039
A-Sodium Oleate Dosage	0.75	1	0.75	6.04	0.044
B-Paraffin Dosage	0.98	1	0.98	7.90	0.026
C-Conditioning Time	0.24	1	0.24	1.93	0.208
AB	0.47	1	0.47	3.79	0.092
AC	1.40	1	1.40	11.32	0.012
BC	0.00	1	0.00	0.00	0.959
A^2	0.11	1	0.11	0.90	0.374
B^2	0.10	1	0.10	0.77	0.408
C^2	0.47	1	0.47	3.79	0.092
Residual	0.87	7	0.12		
Lack of Fit	0.46	3	0.15	1.50	0.343
Pure Error	0.41	4	0.10		
Cor Total	5.38	16			

$$Separation\ Efficiency = 57.6 - 0.306A - 0.350B + 0.173C - 0.343AB + 0.592AC + 0.09BC + 0.163A^2 - 0.151B^2 + 0.334C^2$$

Equation 5.2

Individual Effects

Stat-ease (2016) recommends perturbation plots (silhouette views of the response surfaces for all the factors) be used to determine the influential factors to plot on a 3D response surface plot. The factor that produces relatively small effects on the response variable will be set as a constant and will not be plotted as one of the axes in the 3D response surface plot. The perturbation plot for separation efficiency is presented in Figure 5.15 and indicates that at the centre point all the factors produce a small effect as they change from the reference point with factor C (conditioning time) the least significant factor as indicated in the ANOVA table, Table 5.9.

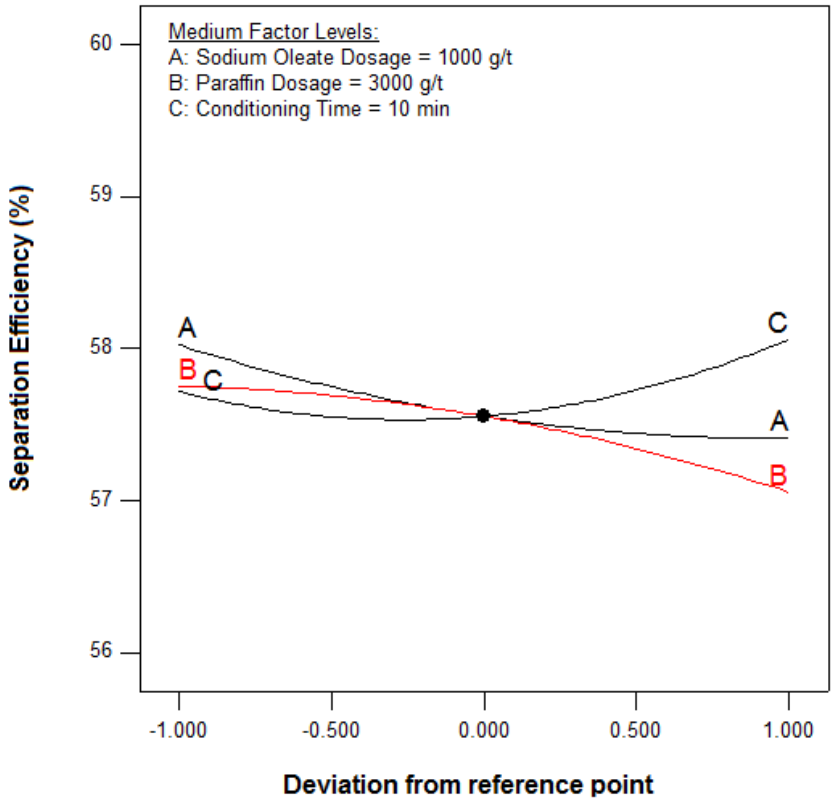


Figure 5.15: Perturbation plot for Separation Efficiency at the centre point

The calculated separation efficiency as a function of the two significant factors determined from the ANOVA analysis, namely paraffin dosage and sodium oleate dosage is presented in Figure 5.16. With the remaining factors fixed to the centre level, it is observed that both paraffin dosage and sodium oleate dosage follow a similar trend with a slight decrease in separation efficiency as the dosage increases. It is envisaged that as the dosage of the collector and non-polar oil increases the stronger the adsorption of the oleate ions onto the hematite surfaces as well as the creation of oil bridges which both contribute to an increase in hydrophobicity. The stronger adsorption may have resulted in a slight increase in the entrainment of gangue thereby reducing the separation efficiency. The results obtained in this study correlate well with those obtained by Roy (2012) as presented in Figure 5.17 with the separation efficiency relatively constant at sodium oleate dosages below 2 kg/ton and decreasing separation efficiency as the collector dosage increases. The results indicate that the range selected for the collector dosage in this study was appropriate.

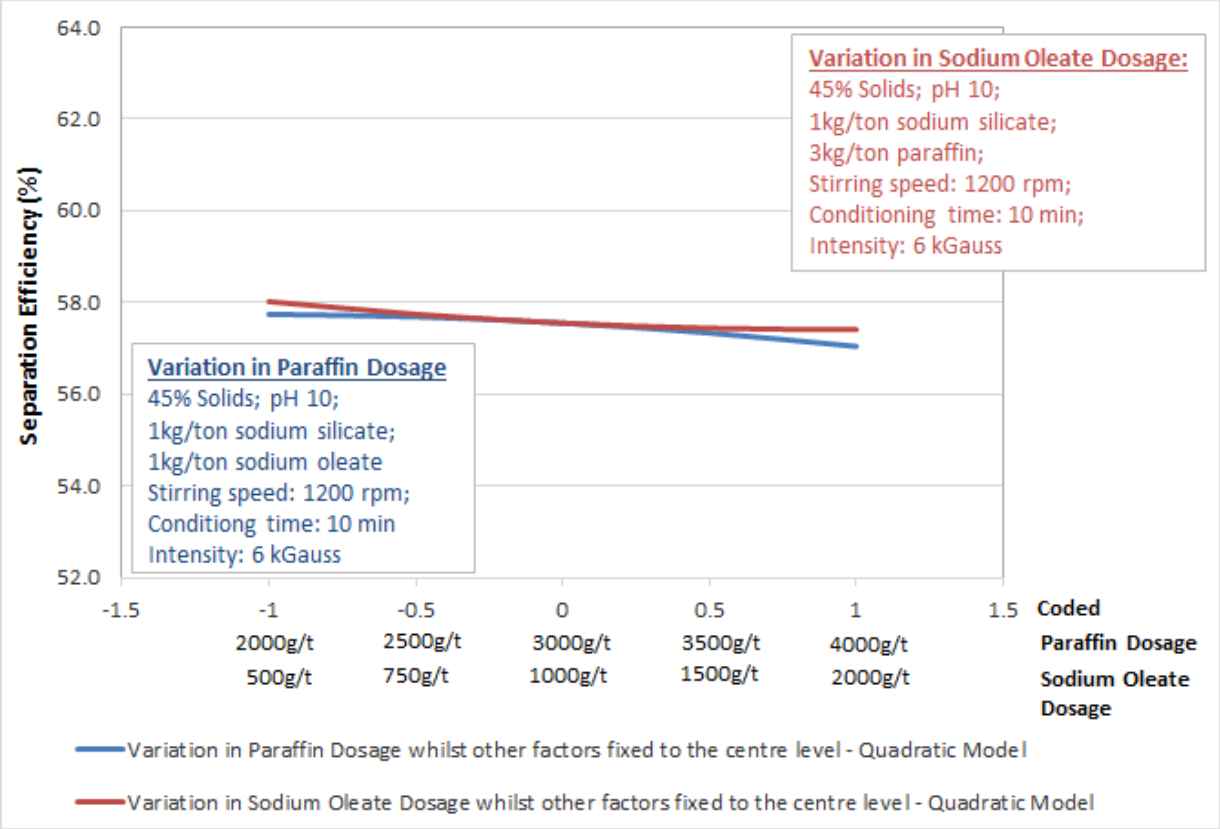


Figure 5.16: Separation efficiency as a function of paraffin and sodium oleate dosage within the range of levels tested

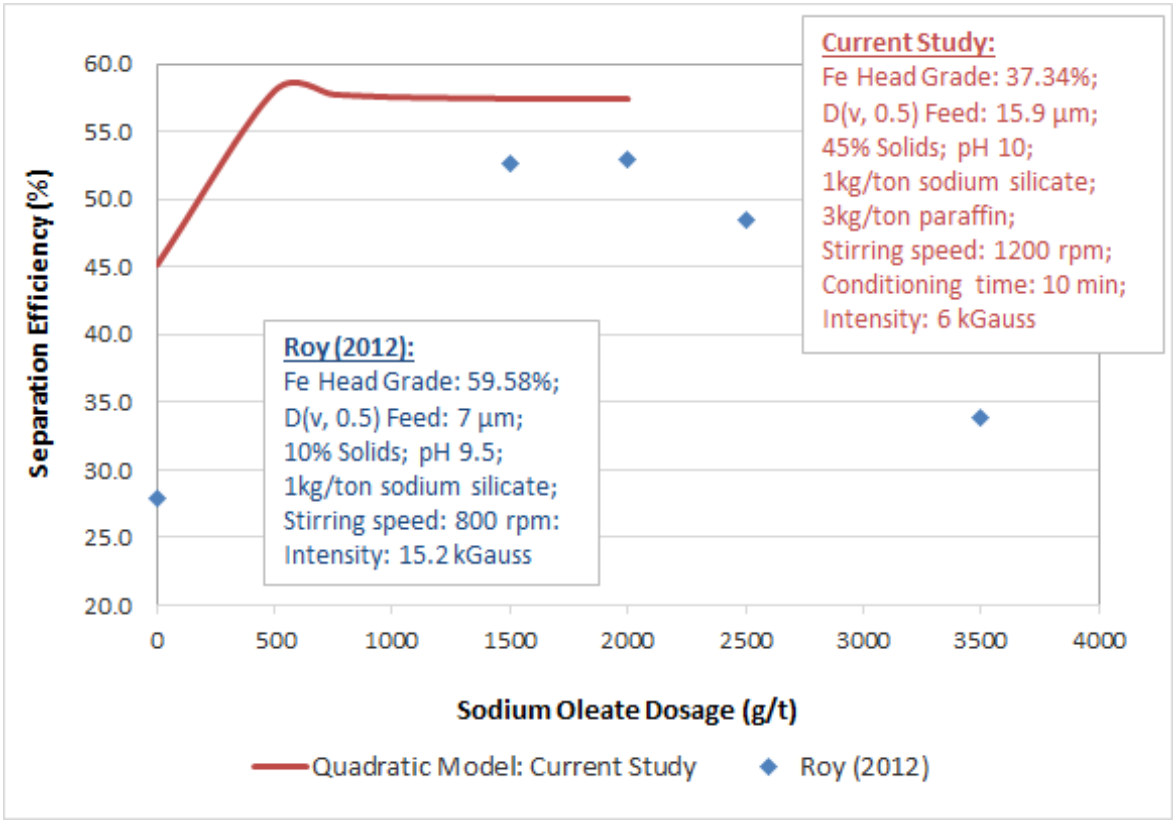


Figure 5.17: Separation efficiency as a function of sodium oleate dosage for the current study as compared to the findings of Roy (2012)

Interactional Effects

The ANOVA results indicated separation efficiency to be the most sensitive to the interaction of sodium oleate dosage and conditioning time, and this interaction is presented in Figure 5.18 and Figure 5.19. The significant interaction of these two factors yield a relatively flat response curve with maximum separation efficiency at the two extremes of the range tested namely:

- 2000g/t sodium oleate and 20 minutes of conditioning time;
- 500g/t sodium oleate and 5 minutes of conditioning time.

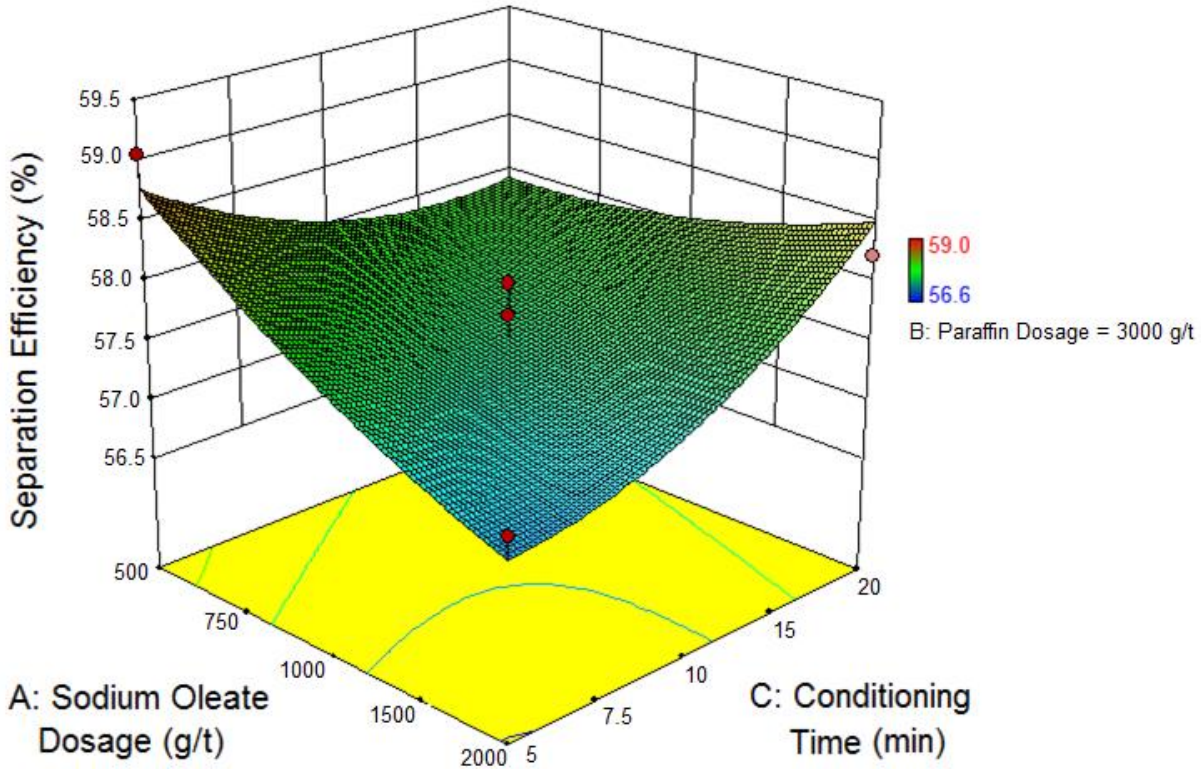


Figure 5.18: Interactive effect of sodium oleate dosage and conditioning time on separation efficiency – View A

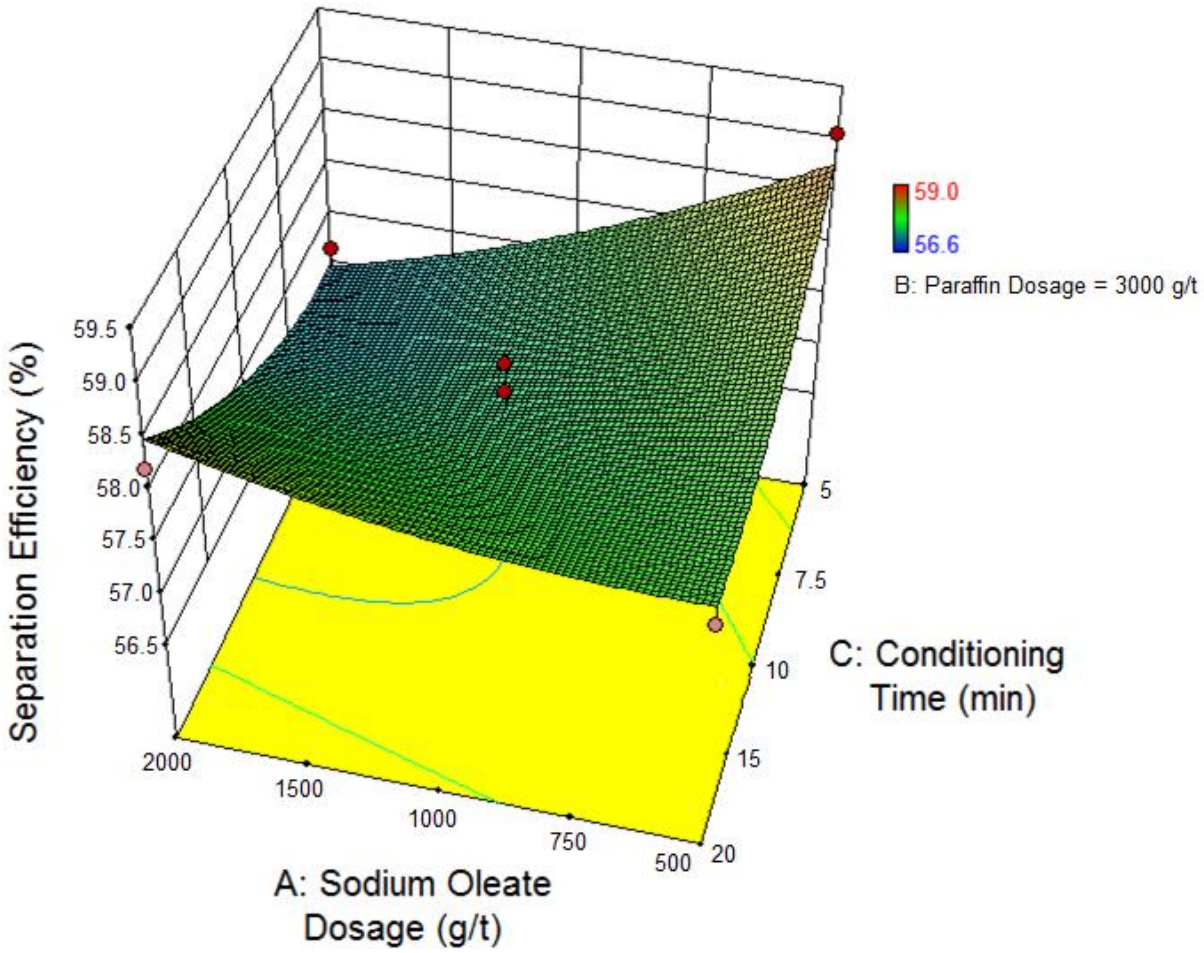


Figure 5.19: Interactive effect of sodium oleate dosage and conditioning time on separation efficiency – View B

Minimum separation efficiency was achieved at the highest sodium oleate dosage and lowest conditioning time. Williams and Arbiter (1968) as cited by Quast (2015) indicated that there are several micro-processes that may occur during the conditioning stage of hematite flotation using fatty acids such as oleic acid and tall oil, namely

- Removal of alteration films from mineral surfaces
- Dispersion of undissolved collector and insoluble hydrocarbon oil
- Mineral/collector interaction
- Mineral/hydrocarbon oil interaction
- Desorption of collector from gangue minerals
- Flocculation of floatable mineral in micron and submicron sizes

The work of Laskowski and Nayamekye (1994) as cited by Quast (2015) however suggests that at alkaline conditions the oleate is in soluble form and equilibrium is established fairly quickly and thus conditioning time has little impact on the transportation of the collector species to the mineral surfaces. Since this study was conducted at alkaline conditions (10 pH), the observation of decreasing separation efficiency with decreasing conditioning time at sodium oleate dosages exceeding 1000 g/ton can be attributed to:

- lower collision probability between the collector and mineral surfaces,
- lower application of shear stresses to the initially formed aggregates and expulsion of mechanically entrained gangue, and
- insufficient time for the desorption of the collector from gangue minerals.

Concentrate Fe Grade

Unlike separation efficiency, the concentrate Fe grade is most sensitive to conditioning time followed by sodium oleate dosage as indicated by the high F value and low p-value in Table 5.10. This order of sensitivity applies to the ranges for each factor tested in this thesis, and it may change for other studies depending on the ranges tested. The 2Fl model for the concentrate Fe grade is significant and is given by Equation 5.3.

Table 5.10: ANOVA Table for the Quadratic model for the response variable: Concentrate Fe Grade

Source	Sum of Squares	df	Mean Square	F Value	p-value Prob > F
Model	2.09	6	0.35	3.36	0.044
A-Sodium Oleate Dosage	0.58	1	0.58	5.65	0.039
B-Paraffin Dosage	0.16	1	0.16	1.56	0.240
C-Conditioning Time	1.01	1	1.01	9.80	0.011
AB	0.25	1	0.25	2.42	0.151
AC	0.02	1	0.02	0.24	0.637
BC	0.05	1	0.05	0.49	0.501
Residual	1.04	10	0.10		
Lack of Fit	0.60	6	0.10	0.90	0.568
Pure Error	0.44	4	0.11		
Cor Total	3.12	16			

$$Concentrate\ Fe\ Grade = 57.95 - 0.270A - 0.142B + 0.356C - 0.250AB + 0.078AC - 0.112BC$$

Equation 5.3

Individual Effects

The perturbation plot for concentrate Fe grade at the centre points presented in Figure 5.20 indicates that conditioning time has a significant effect on this response variable followed by sodium oleate dosage. Paraffin dosage has a minimal effect correlating to the ANOVA table, Table 5.10.

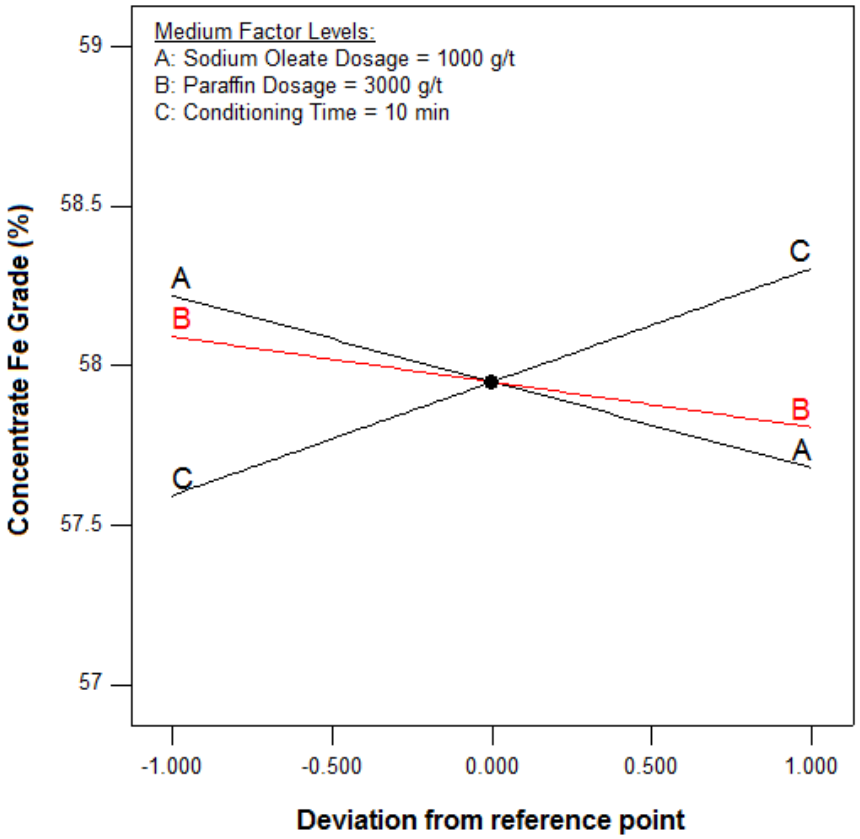


Figure 5.20: Perturbation plot for Concentrate Fe grade at the centre point

The effect of conditioning time on the concentrate Fe grade with the remaining factors fixed to their centre levels including a comparison to literature is presented in Figure 5.21. The results show similar trends to that of Song et al. (2002) with increasing conditioning time increasing the concentrate Fe grade, although the effect is not as prominent as that of Song et al. (2002). In the current study, the concentrate Fe grade reaches a plateau after 5 minutes indicating further conditioning provides no significant additional benefit.

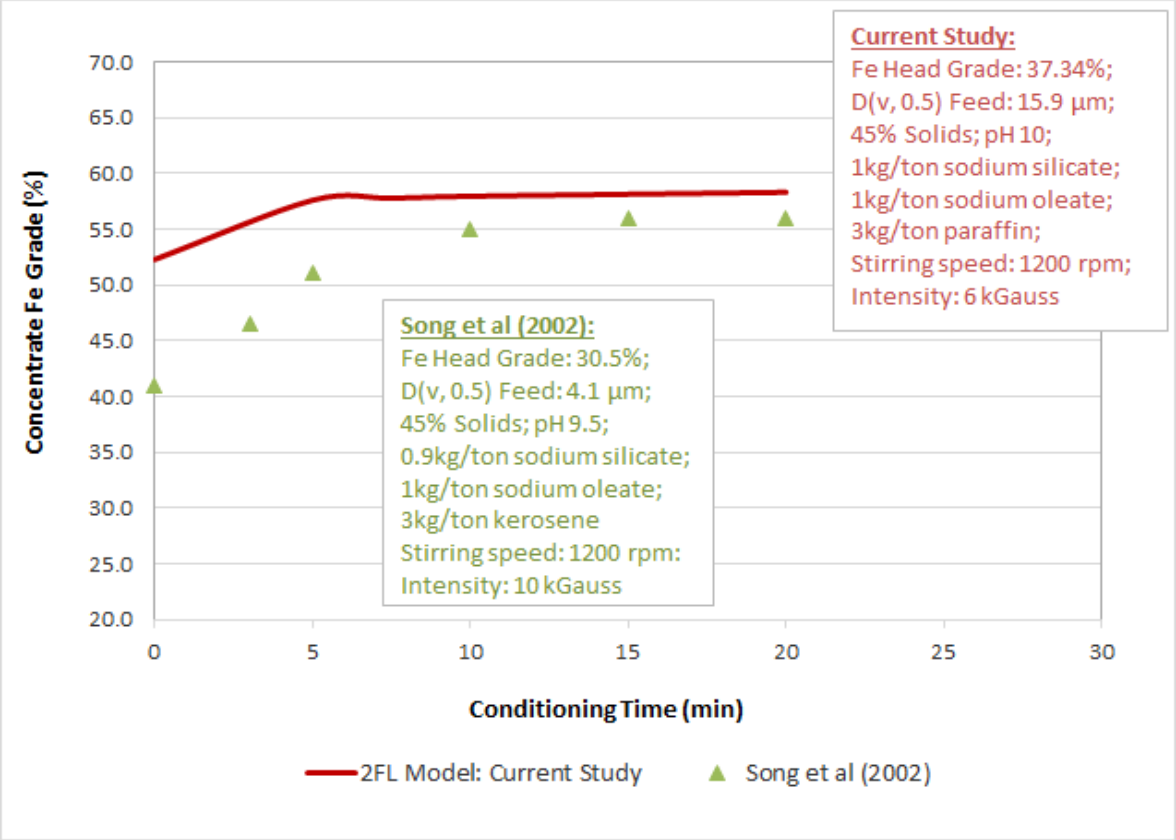


Figure 5.21: Concentrate Fe grade as a function of conditioning time for the current study as compared to the findings of Song et al. (2002)

As observed with separation efficiency, in Figure 5.22 the concentrate Fe grade slightly decreases with increasing sodium oleate dosages. Interestingly the work conducted by Song et al. (2002) at a similar Fe head grade indicates the concentrate Fe grade plateaus in the same region as that for the current study. A comparison to the work of Roy (2012) indicates that higher Fe concentrate grades can be achieved at higher Fe head grades, albeit without considering the impact of mineralogical differences.

With separation efficiency and concentrate Fe grade closely relating to one another, the reasons for the effects of sodium oleate dosage and conditioning time on Fe concentrate grade are similar to those given for separation efficiency.

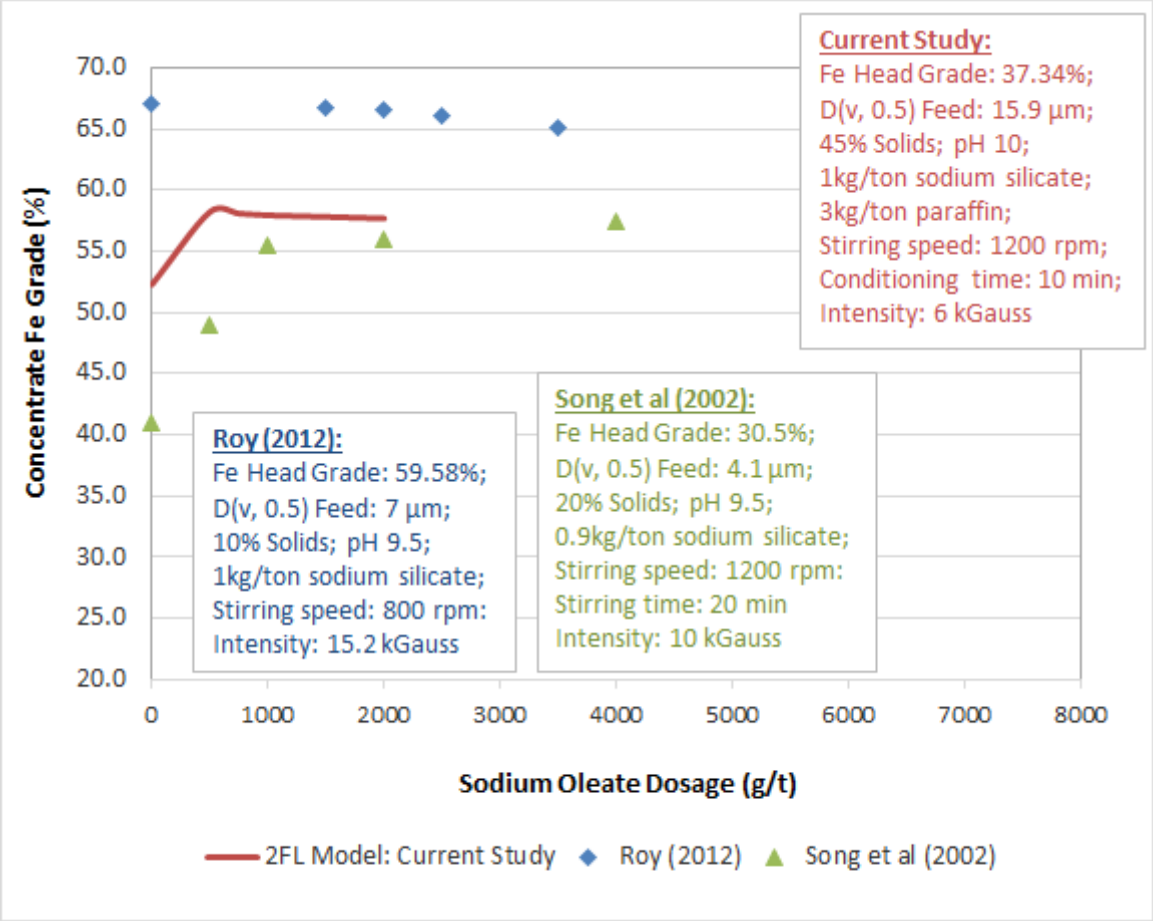


Figure 5.22: Concentrate Fe grade as a function of sodium oleate dosage for the current study as compared to the findings of Roy (2012) and Song et al. (2002)

5.3.5 Optimisation

Optimisation of the selective flocculation process was conducted by simultaneously maximising separation efficiency and concentrate Fe grade whilst minimising sodium oleate dosage, paraffin dosage and conditioning time. The objective was to remove silicates from the concentrate thereby increasing the Fe grade by using the least amount of reagents and kinetic energy. The constraints used for the optimisation are given by Table 5.11, and the best solutions obtained are presented in Table 5.12.

Table 5.11: Constraints and objectives for optimisation of the selective flocculation process

Factor or Reponse Variable	Goal	Model Used	Lower Limit	Upper Limit	Importance
A:Sodium Oleate Dosage	minimize	-	-1	0	5
B:Paraffin Dosage	minimize	-	-1	0	5
C:Conditioning Time	minimize	-	-1	0	3
Separation Efficiency	maximize	Quadratic	56.6	59.1	4
Concentrate Fe Grade	maximize	2FI	57.25	58.74	5
Concentrate Fe Recovery	none	-	-	-	-

Variable Parameters	Sodium Oleate (g/ton)	Paraffin (g/ton)	Conditioning Time (min)
Low (-1)	500	2000	5
Intermediate (0)	1000	3000	10
High (1)	2000	4000	20

Table 5.12: Optimised solutions within the defined constraints

Optimisation Run	Sodium Oleate Dosage (g/t)	Paraffin Dosage (g/t)	Conditioning Time (min)	Separation Efficiency (%)	Concentrate Fe Grade (%)	Desirability
1	500.0	2000.0	5.0	58.6	57.72	0.74
2	500.0	2000.0	5.0	58.6	57.72	0.74
3	499.9	2000.0	5.0	58.6	57.72	0.74
4	500.0	2000.0	4.9	58.6	57.73	0.74
5	500.0	1970.1	5.0	58.6	57.72	0.74
6	500.0	1999.9	4.8	58.6	57.74	0.74
7	500.0	1945.4	5.0	58.7	57.73	0.74
8	500.0	2000.0	4.7	58.6	57.74	0.74
9	500.0	2000.0	4.6	58.6	57.75	0.74
10	500.0	2000.0	4.6	58.5	57.76	0.74
11	492.7	2000.0	5.0	58.6	57.72	0.7
12	500.0	1908.0	4.9	58.6	57.74	0.74
13	500.0	1890.1	5.0	58.7	57.73	0.74
14	500.0	2000.0	4.4	58.5	57.77	0.74
15	500.0	1849.4	5.0	58.7	57.74	0.74
16	500.0	2000.0	4.3	58.5	57.77	0.74
17	500.0	1805.1	5.0	58.7	57.74	0.73
18	500.0	1774.7	5.0	58.7	57.75	0.73
19	500.0	1736.2	5.0	58.7	57.75	0.73
20	500.0	2000.0	3.8	58.4	57.82	0.73
21	500.0	2000.0	3.7	58.4	57.82	0.73
22	500.0	2000.0	3.5	58.3	57.84	0.72
23	500.0	2000.0	3.2	58.3	57.86	0.72
24	500.0	1431.1	4.6	58.6	57.81	0.71
25	500.0	1226.0	5.0	58.7	57.81	0.70
26	500.00	2000.00	2.4	58.2	57.92	0.69

The optimised conditioning time ranges from 2.4 min to 5 min and agrees well with Natarajan's (1978) findings. As cited by Quast (2015) Natarajan (1978) found that the maximum grade and recovery of hematite from a low-grade ore after flotation using sodium oleate and pine oil was 4.6 min. However, it should be noted that conditioning time is affected by particle size and the physical chemistry of the oleic acid/hydrocarbon oil system (Quast, 2015).

Four of the twenty-six solutions, namely optimisation run 11, 23 to 25 were selected, based on lower energy and reagent consumption, for model validation purposes. Each run was conducted five times to obtain statistical confidence in the results. The actual versus predicted for the selected runs are presented in Figure 5.23 and Figure 5.24 for the two response variables, separation efficiency and concentrate Fe grade

respectively. In general, the predicted separation efficiency and concentrate Fe grade lies within the 95% confidence limits and justifies the use of the selected models.

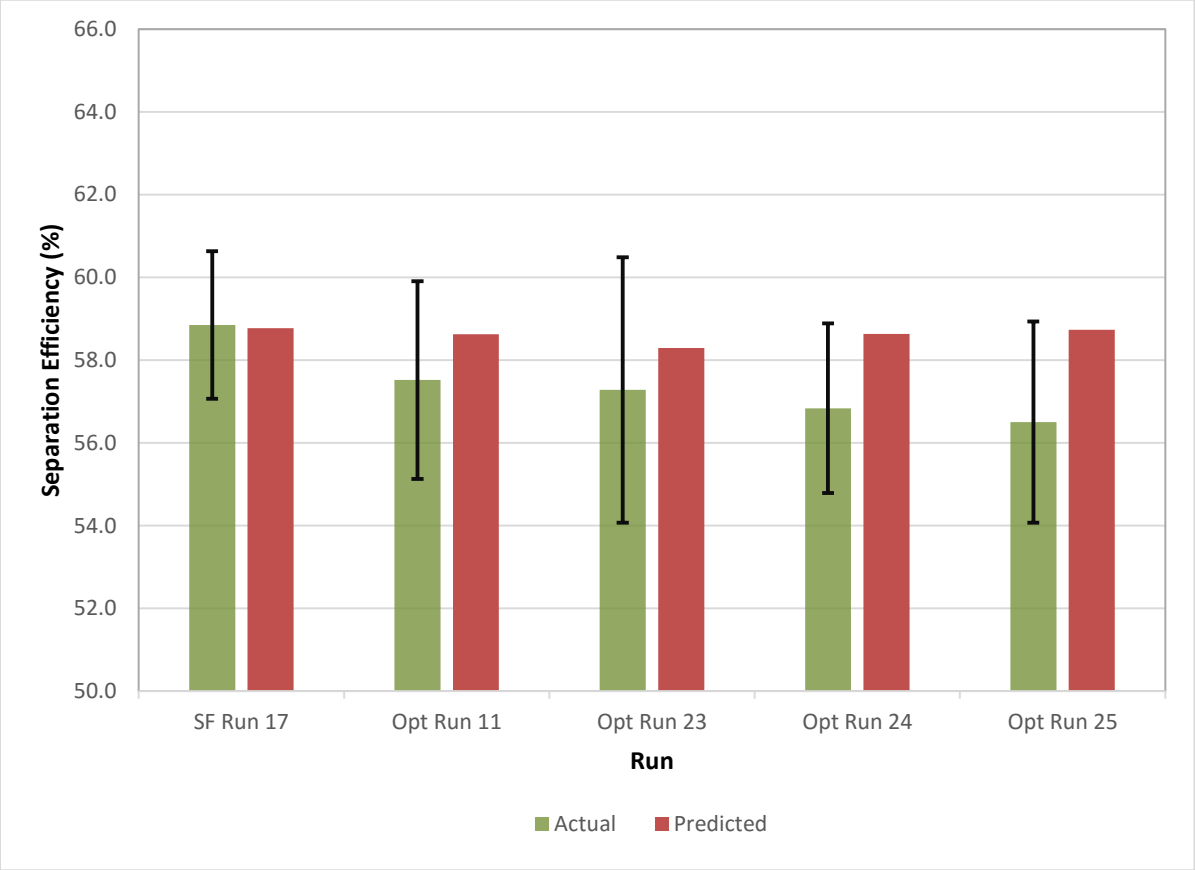


Figure 5.23: The actual and predicted separation efficiency for the optimisation runs using the Quadratic Model at 95% Confidence limits

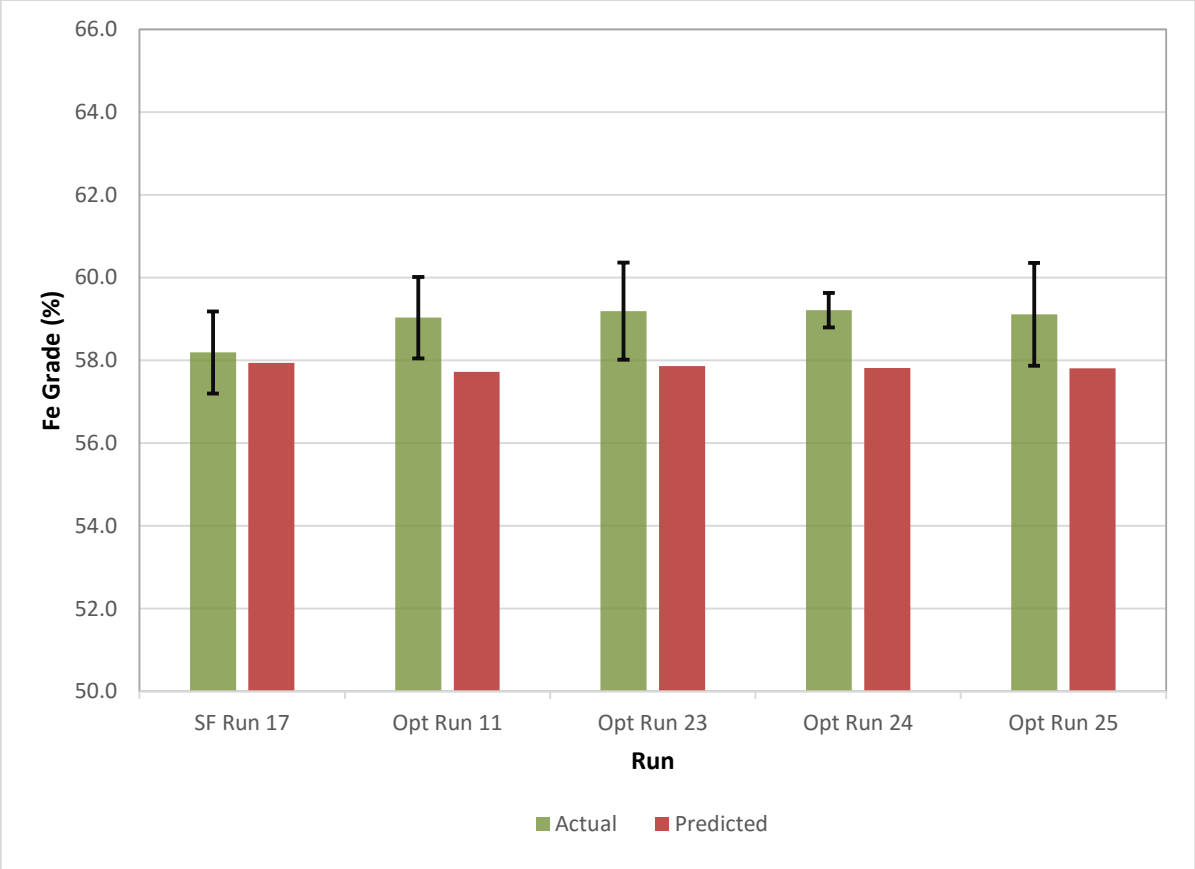


Figure 5.24: The actual and predicted concentrate Fe Grade for the optimisation runs using the 2Fl Model at 95% Confidence limits

Of the optimised tests conducted, optimisation run 24 had the least variation in both response variables (separation efficiency and concentrate Fe grade). The perturbation plots for run 17 (un-optimised) and optimisation run 24 are presented in Figure 5.25 to Figure 5.28 to determine how sensitive the optimum is to changes in each factor. For both run 17 and run 24 the optimal separation efficiency is most sensitive to sodium oleate dosage (factor A) followed by the conditioning time (factor C) with paraffin dosage (factor B) having a negligible effect. In contrast to the separation efficiency, the optimal concentrate Fe grade for both runs is sensitive to all factors. For run 17 the concentrate Fe grade is most sensitive to sodium oleate dosage followed by conditioning time and paraffin dosage. For run 24 the concentrate Fe grade is most sensitive to the variation in conditioning time followed by paraffin dosage and finally sodium oleate dosage.

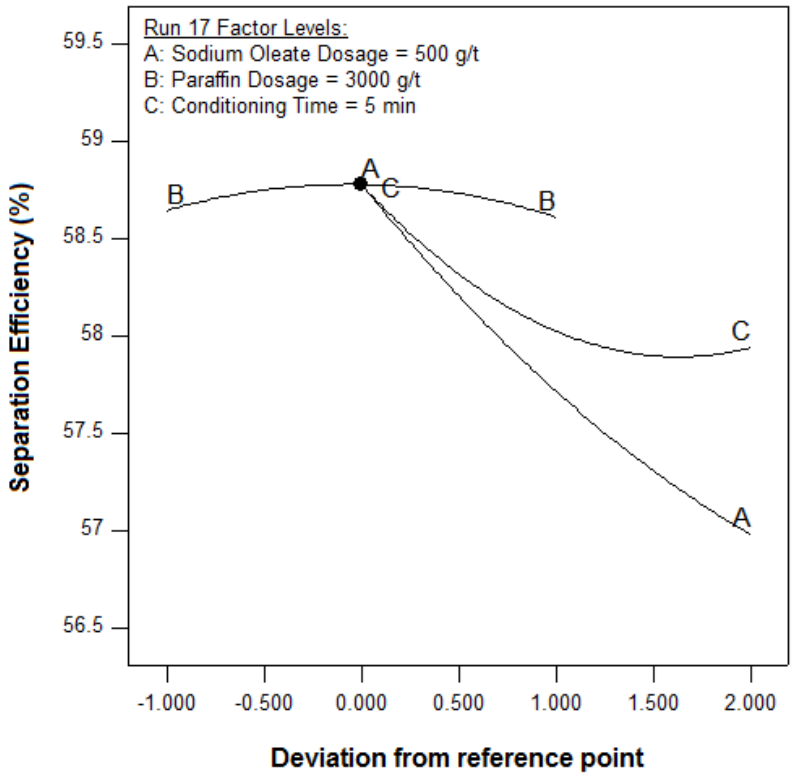


Figure 5.25: Perturbation plot for Separation Efficiency for Run 17 (un-optimised)

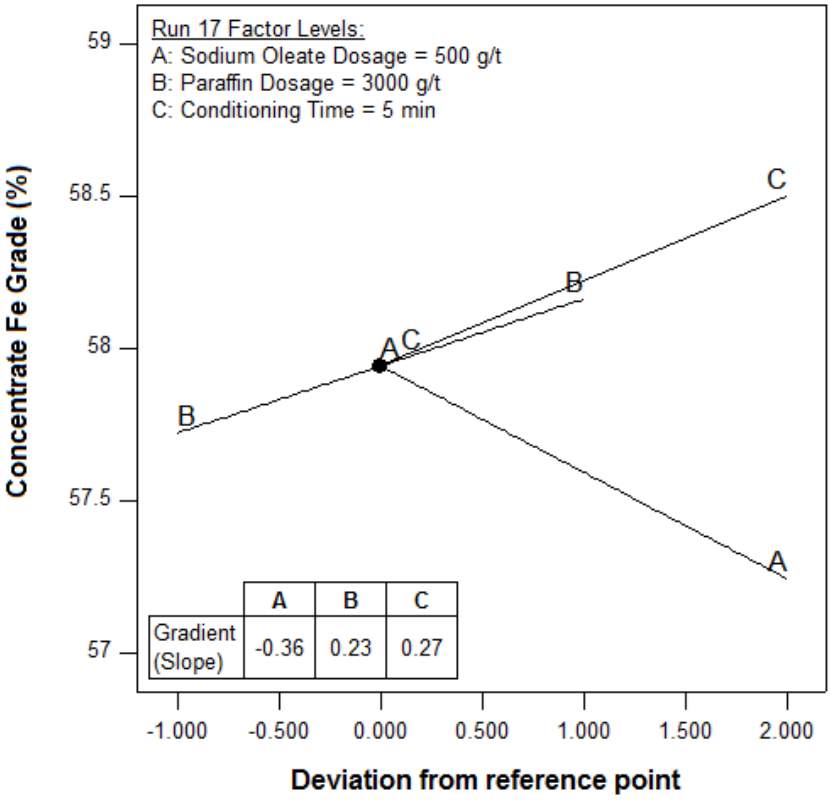


Figure 5.26: Perturbation plot for Concentrate Fe Grade for Run 17 (un-optimised)

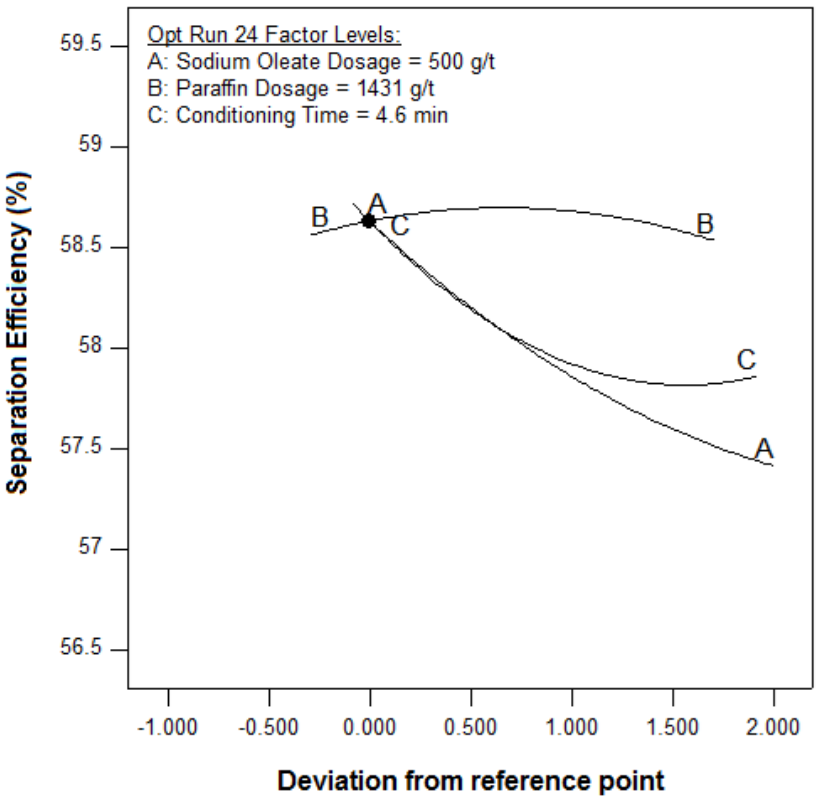


Figure 5.27: Perturbation plot for Separation Efficiency for Optimisation Run 24

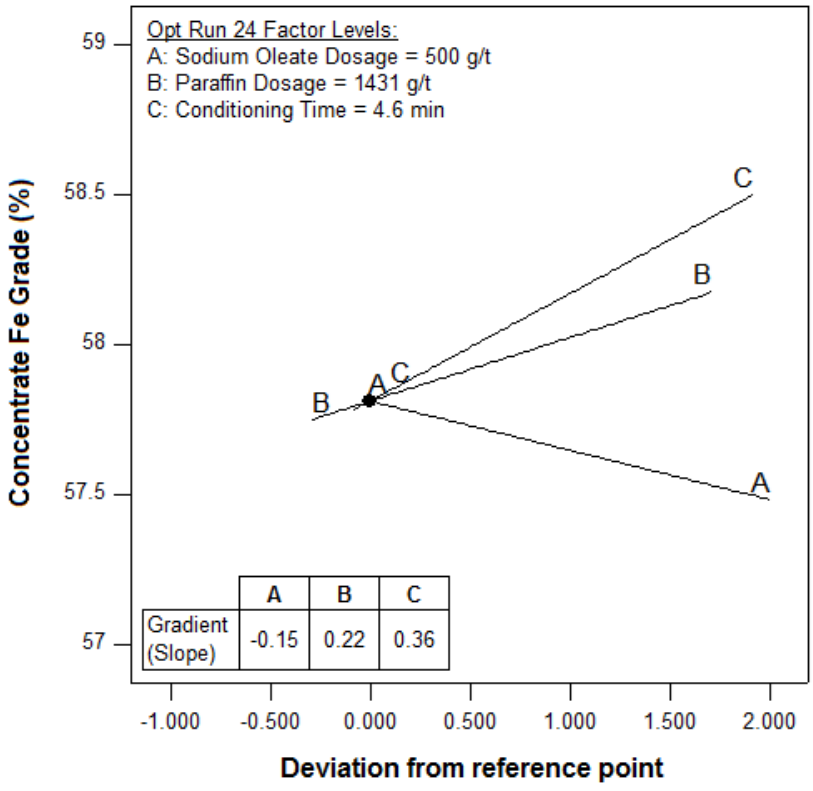


Figure 5.28: Perturbation plot for Concentrate Fe Grade for Optimisation Run 24

5.4 Conclusion

The models for the concentrate Fe recovery were insignificant whilst the models for the remaining two response variables concentrate Fe grade and separation efficiency were significant. Although the model for concentrate Fe grade had a low coefficient of determination (0.66), the predicted concentrate Fe grade lies within 95% confidence limits for each run indicating an adequate fit of the data. The models for both response variables were deemed adequate to predict the response variables within the experimental constraints.

The ANOVA results indicated separation efficiency is most sensitive to the interaction between the sodium oleate dosage and conditioning time followed by the paraffin dosage and finally by sodium oleate dosage. Maximum separation efficiency occurred at the two extremes of the interaction range tested (2000 g/t sodium oleate and 20 minutes conditioning time; 500 g/t sodium oleate and 5 minutes conditioning time). The concentrate Fe grade, on the other hand, is most sensitive to conditioning time followed by sodium oleate dosage with increasing conditioning time and sodium oleate dosages positively and adversely affecting the concentrate Fe grade respectively.

Optimisation of the selective flocculation process was conducted by simultaneously maximising separation efficiency and concentrate Fe grade while minimising sodium oleate dosage, paraffin dosage and conditioning time. The optimal run (run 24) achieved a separation efficiency of 56.8±2.0%, and Fe concentrate grade of 59.21±0.42% at a reagent dosage of 500g/t sodium oleate; 1431.1g/t paraffin; 4.6 min conditioning time. Compared to the best unoptimised run (run 17) that achieved similar separation efficiencies and concentrate Fe grades, the optimal test reduced the paraffin reagent consumption by half and the conditioning time by 7.6%. A sensitivity analysis of the optimal run (run 24) indicated separation efficiency is most sensitive to variation in the sodium oleate dosage followed by the conditioning time with paraffin dosage having a negligible effect. The concentrate Fe grade for the optimal run is most sensitive to the variation in conditioning time followed by paraffin dosage and finally sodium oleate dosage.

The optimal conditions for selective flocculation coupled with magnetic separation was used in conjunction with the Reflux Classifier in the following chapter, Chapter 6 to establish if gravity separation could achieve better results when coupled with selective flocculation.

CHAPTER 6 : OPTIMISED SELECTIVE FLOCCULATION COUPLED WITH THE REFLUX CLASSIFIER

6.1 Introduction

The best preconditions allowing for adequate dispersion prior to selective flocculation (discussed in Chapter 4) was used to optimise the selective flocculation process in Chapter 5. The optimum selective flocculation conditions were selected based on the response variables measured by coupling the selective flocculation process with magnetic separation. Chapter 4 and Chapter 5 indicated that the best dispersing conditions at a pulp density of 45% solids was sodium silicate at a dosage of 1000 g/ton and pH of 10 while the optimal selective flocculation conditions were 500g/t sodium oleate and 1431.1g/t paraffin at a conditioning time of 4.6 min.

In this chapter, the optimal selective flocculation conditions will be applied to a different solid-solid separator. The solid-solid separator will be the Reflux Classifier, a gravity separation unit instead of a magnetic separator used in the preceding chapters. The objective is to determine if selective flocculation can improve the metallurgical performance of the Reflux Classifier (RC). A base case Reflux Classifier test, without selective flocculation, will be conducted to determine the effect of increasing water fluidisation rates on the response variables namely Fe concentrate grade, Fe concentrate recovery and separation efficiency. A similar approach was applied to the optimised selective flocculation process coupled with the RC in order to compare to the response variables of the RC with and without selective flocculation.

The raw data pertaining to this chapter is presented in Appendix D.

6.2 Methodology

6.2.1 Selection of Equipment

In the Floc Magnetic Separation (FMS) process described by Song et al. (2002), a solid-solid separator is required. To prevent the destruction of the flocs, it was necessary to select a gravity separation unit operation capable of treating ultrafines

and yet gentle enough to effect solid-solid separation without destroying the flocs. With this in mind, size classifiers were considered as these would exploit the size differences of the fine gangue particles and flocculated hematite.

Size classifiers can be categorised into two categories depending on the separation medium used in these devices. Pneumatic classifiers use air whilst hydraulic classifiers use water as the separating medium. Hydraulic classifiers are widely used in industry (Tripathy et al., 2015) and comprise of a column in which particles settle down against a rising vertical current of water. These classifiers are further categorised into either hindered bed separators or fluidised bed separators as graphically illustrated in Figure 6.1. Mintek currently has on-site two types of laboratory scale hydraulic classifiers namely the Teeter Bed Separator (TBS) and the Reflux Classifier (RC-100). Although Tripathy et al. (2015) indicate the optimal particle size for the RC to be -8+0.075 mm, Hunter et al. (2015) have successfully applied the RC to ultrafine iron ore with a particle size distribution of 59% passing 38 µm.

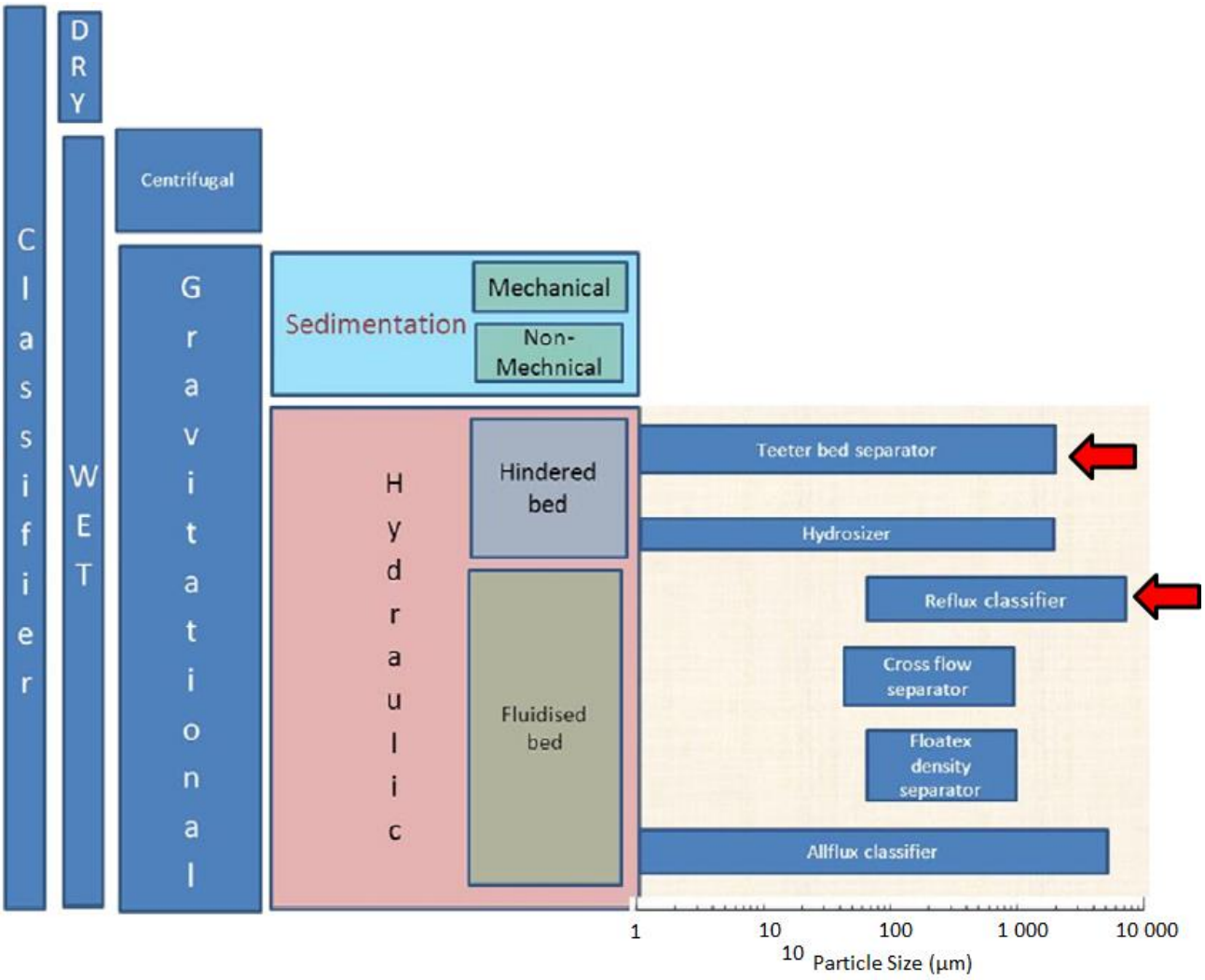


Figure 6.1: Hydraulic classifiers with their optimum particle size range (Tripathy et al., 2015)

The Reflux Classifier (RC) is a relatively new device that was introduced in 2001 and incorporates a fluidised bed with inclined plates spanning the entire cross-section of the fluidised bed. Figure 6.2 adapted from Tripathy et al. (2015) shows the major developments of the RC with regards to iron ore subsequent to 2012. The RC has been applied mainly in the coal industry and is now receiving attention in other mineral industries such as iron ore, mineral sands, chromite and manganese. Orupold et al. (2014) report that over 40 units of the RC^{TM}2020, redesigned and replaced by the RC^{TM}2000 illustrated in Figure 6.3, have been sold in the last 3 years. In addition over 24 RC^{TM}300 units, Figure 6.4, are in current use in six countries in coal and mineral applications.

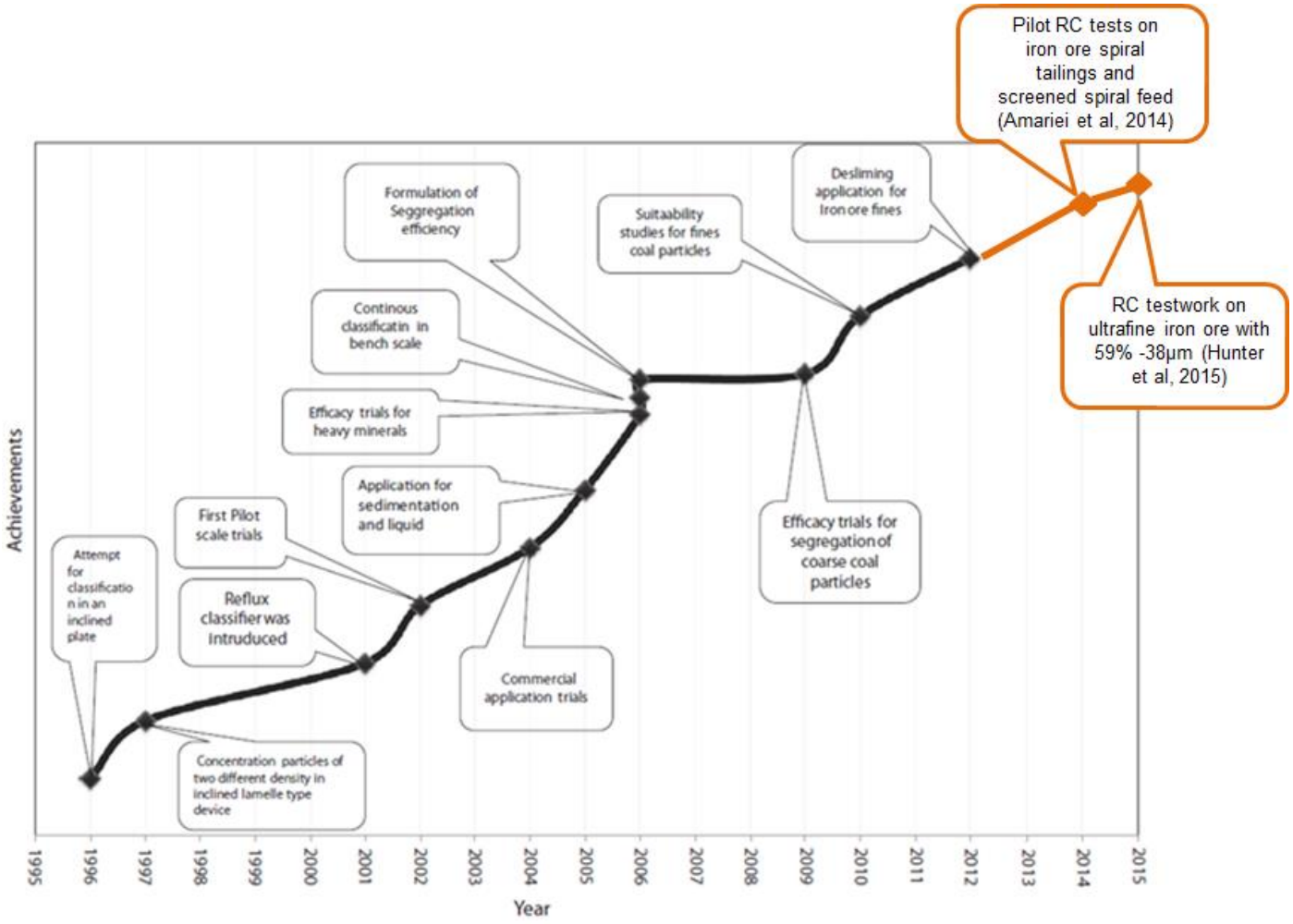


Figure 6.2: The development and applications of the Reflux Classifier until 2012, figure adapted from Tripathy et al. (2015, p. 215)



Figure 6.3: RCTM2000 Reflux Classifier (Orupold et al., 2014)



Figure 6.4: RC^{TM}300 Pilot Scale Reflux Classifier (Orupold et al., 2014)

Tripathy et al. (2015) indicate the major disadvantage of the TBS is the design of the underflow discharge. The underflow discharge is flat and the inclined teeter plate results in a low solid concentration of the underflow which allows for the entrainment of ultrafine particles. This entrainment will be detrimental to the current study, and hence the RC was selected for gravity separation coupled with selective flocculation.

Considering the RC is a relatively new device a significant amount of research has been published, and the advantages of this unit over conventional fluidised beds are presented below.

- The inclined plates in the RC increase throughput due to the Boycott phenomenon. The Boycott phenomenon indicates the segregation rate of particles from a liquid in an inclined channel is much more rapid than within a vertical channel (Nguyentranlam and Galvin, 2004). In pilot comparative trials of the RC and TBS, Galvin et al. (2002) indicated that the RC capacity was three times higher than that of the TBS. For dilute conditions in the RC, Zhou et al (2006) demonstrated that at Re_t (particle Reynolds number using the terminal velocity of the particle defining the separation) of 0.75, a high aspect ratio (length of inclined plates to the spacing of the inclined planes) of 200 and inclination angle of 70° the expected RC throughput advantage over a conventional fluidised bed is calculated to be 7 times higher as presented in Figure 6.5.

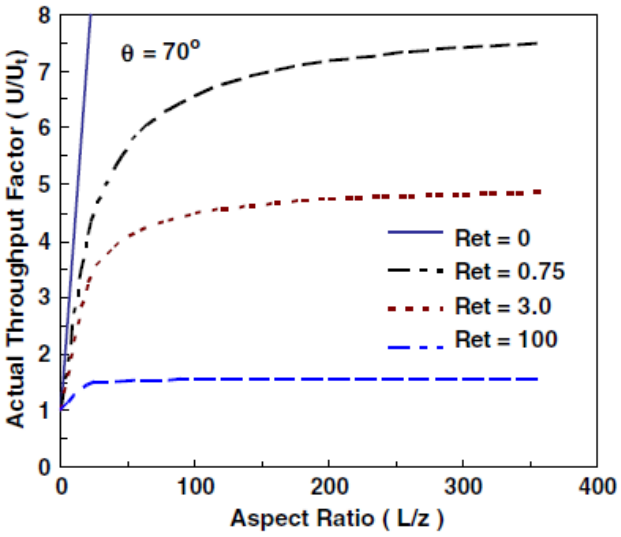


Figure 6.5: Dependence of the actual throughput advantage on the aspect ratio of the inclined channels for different particle Reynolds numbers. The angle of inclination is fixed at 70° for all the data (Zhou et al., 2006)

- From a size classification perspective, the RC is more robust in dealing with fluctuations in the feed solids concentration or feed rate as the mixing zone in the RC self-adjusts to changes in these feed characteristics. This self-adjusting maintains a relatively stable separation condition without the need to change the underflow rate. Conventional fluidised beds, on the other hand, require underflow rate adjustment to ensure a relatively fixed separation size (Nguyentranlam and Galvin, 2004).
- Separating particles based on a density differential can be achieved if a high suspension density is achieved. This is usually achieved in fluidised beds through increasing the suspension concentration by utilising low fluidisation rates. In the RC, however, the high solids concentration can be maintained at a high fluidisation rate due to the presence of the inclined plates (Nguyentranlam and Galvin, 2004).
- Galvin et al. (2002) investigated pilot scale density classification of -2 mm coal and mineral matter. In general, their investigations indicated considerably less variation in the density cut point as a function of size in the RC as compared to the TBS. In their work Galvin et al. (2002) also indicated the potential for running the RC at low feed pulp densities thereby making preconcentration by cyclones,

which is typically required for TBS operations, potentially obsolete. Supporting this claim Hunter et al. (2015) indicate that both gravity separation and desliming can simultaneously occur in the RC within a single stage of separation.

The major disadvantage of the RC is the price of a unit compared to a TBS at the same capacity. Table 6.1 indicates at a capacity of 100 t/h the capital costs of the RC 2000 or RC 2020 is an order of magnitude more expensive than the TBS and 5 times more expensive than the TBS combined with a spiral circuit.

Table 6.1: Capital and Operating Costs for the RC, TBS and TBS combined with spirals for a capacity of 100 t/h (Da Corte et al., 2016)

Equipment	**Capacity**	**Capital Cost (Capex)**
RC2000/ RC2020	100 t/h	R 5 600 000
XF 1800 TBS	115 t/h	R 530 000
XF 1200 TBS + Spirals	115 t/h	R 1 103 875

6.2.2 Working Principle of the Reflux Classifier

The Reflux Classifier (RC) is a new gravity separation device that can separate particles based on density and size.

The device combines a conventional fluidised bed (vertical part) with sets of parallel inclined plates, as shown in Figure 6.6. In the vertical part of the RC hindered settling dominates and thus the terminal settling velocity, closely related to particle size, is important. The inefficiencies of the vertical part with regards to separating fine dense particles from coarse light particles of similar terminal velocities is compensated by the inclined plates.

Feed slurry enters below the inclined plates while fluidisation water is introduced through a distribution plate in the base. The slurry feed moves downwards into the vessel, forming a bed of particles that is fluidised from below. High-density particles settle into the lower portion of the bed, and light and fine particles are transported

upward towards the inclined plates in the lamella settler. The high hydraulic load carries the suspension up into the parallel inclined plates. The particles in the inclined plates whose terminal velocities are lower than the velocity of the fluidisation water will pass through the region between the plates and report to the overflow. Faster settling particles settle onto the upward facing surfaces of the inclined channels and form a sediment layer. The sediment layer rapidly slides down the inclined channel and returns to the fluidised zone below where it is mixed with the suspension and returned to the inclined plates as a result of the fluidisation water. The internal self-recycling effect, referred to as the reflux action, is an interaction between the suspended particles and the inclined channels. The reflux action also referred to as the autogeneous dense media zone, further pushes coarse light particles from the feed directly into the overflow (Amariei et al., 2014). Laskovski et al. 2006 indicate that the transport of particles through water up an inclined plane is dependent mainly on density with particle size being less dominant.

Nguyentranlam and Galvin (2004) indicate three layers form in an inclined channel, namely a clear liquid zone below the downward facing wall as result of particles settling into the sediment layer, a layer of sediment on the upward facing wall and a suspension of particles in-between as illustrated in Figure 6.7.

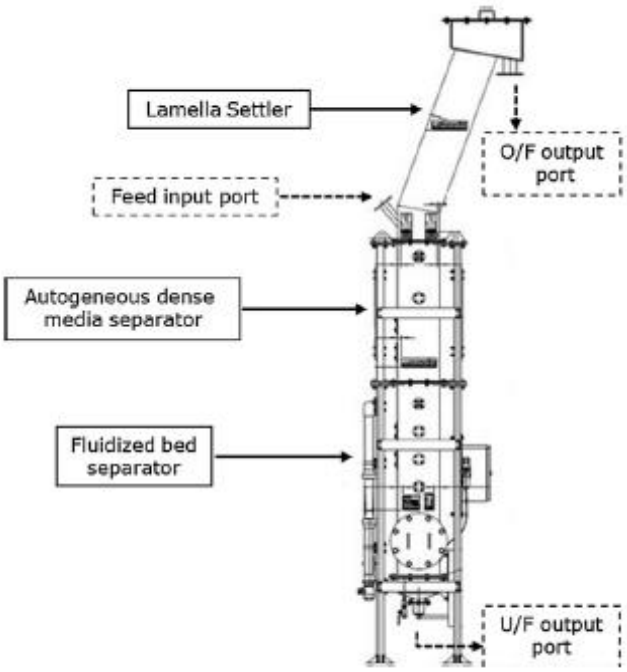


Figure 6.6: Schematic diagram of a Reflux Classifier-100 (Amariei et al., 2014)

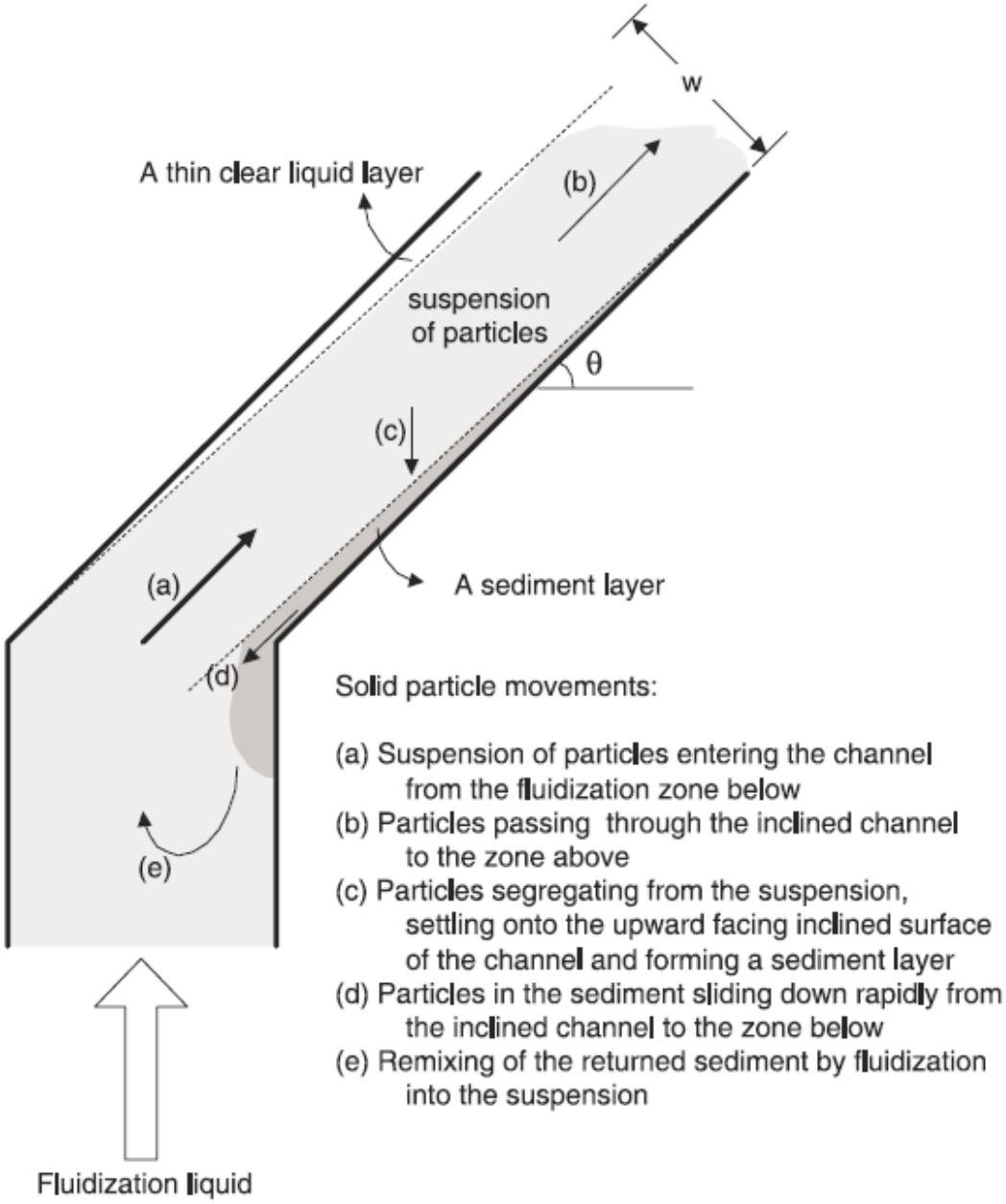


Figure 6.7: Flow conditions within an inclined channel between two parallel plates, reproduced from Nguyentranlam and Galvin (2004, p. 85)

At the bottom of the inclined section and in the autogeneous dense media zone a pressure transducer senses the high-density suspension and upon exceeding the set point the underflow discharge valve is opened.

6.2.3 Design of Mintek's PVC Reflux Classifier

At the time of this study, the RC-100 at Mintek received significant interest from industry with many requests for testwork. In light of this and the long duration expected for the tests in this study, a Polyvinyl chloride (PVC) unit was built at Mintek based on the RC-100 design. In their review of various hydraulic classifiers, Tripathy et al. (2015) listed both the design and process variables for the RC as presented in Table 6.2. Each design variable as it pertains to the PVC RC constructed at Mintek is further explained.

Table 6.2: Design and Process Variables for the RC (Tripathy et al., 2015)

Design Variables	Process Variables	Salient Features	Area of Application
Inclined plates angle, inclined plate height, inclined section height, column length, cone angle. Height of the conical and cylindrical section, feed introduction point	Fluidization water flowrate, bed density, feedrate, feed pulp density, feed particle size distribution	Introduction of parallel inclined plates, effective separation at coarser particle size as well as employed for desliming. Square type sorting chamber, pipe or teeter water distribution, DP cell based density measurement system and pinch valve based underflow discharge	Heavy minerals, coal, hematite, cenosphere

Inclined plates angle

In developing a generalised empirical relationship for the RC, Laskovski et al. (2006) investigated the effect of the angle of inclination of the channels. Angles of 45°, 60° and 70° were investigated for sand and PVC particles. The separation efficiency defined by the researchers presented in Equation 6.1 was used to compare the separation efficiencies at varying inclination angles using a similar design and operating variables. The results extracted from Laskovski et al. (2006) and presented in Table 6.3 indicate similar separation efficiencies at varying angles of inclination.

$$\eta = \frac{1}{1 + 0.133 cos\theta {Re_t}^{1/3} (L/z)}$$

Equation 6.1

Where η = separation efficiency;

Re_t = particle Reynolds number

L = channel length;

z = channel gap spacing;

Table 6.3: Separation efficiencies at varying inclination angles and similar design and operating variables (Data extracted from Laskovski et al., 2006)

Commodity	Angle of Inclination	Re_t	L/z	Separation Efficiency
Sand	70	12.2	124	0.04
	70	13.14	124	0.04
	70	6.55	124	0.05
	70	3.2	124	0.06
	45	1.26	152	0.08
PVC	70	212.88	124	0.02
	70	34.3	124	0.03
	45	57.03	152	0.02

In determining the appropriate angle of inclination for constructing a laboratory scale RC, Rakgase (2012) conducted settling tests for a -300+53 µm size range of silica sand. The angle of inclination investigated varied from 50° to 80° at intervals of 10°. Their investigations indicated that maximum settling occurred at angles of 60°to 80°.

Based on these findings the angle of inclination was selected to be 70° in line with that of the RC-100.

Length of the inclined plates

In their experience of downscaling the RC, Galvin (2016) recommends the channel length be maintained at 1m. With shorter channel lengths considerable loss in performance has been experienced. In addition Zhou et al. (2006) also indicated that the higher the aspect ratio, the higher the throughput capacity although at some point

this effect levels off. The aspect ratio is the ratio of the length of the lamellae plates to the channel spacing.

Channel spacing

Laskovski et al. (2006) discovered that denser particles required many more channels compared to lighter particles to produce an increase in the separation size. Denser particles do not exhibit the same tendency to hydraulically convey to the overflow thereby increasing the potential for separation of dense and light particles. Both Laskovski et al. (2006) and Galvin (2009) agree that high channel aspect ratios (L/z = Length/ channel spacing) promote separation on the basis of density. With the length of the channels fixed to 1 m, the aspect ratio could be increased by reducing the channel spacing.

With a narrow channel spacing of 1.7 mm, Galvin et al. (2009) discovered that the effects of particle size were suppressed and the effect of particle density promoted for PVC (sg of 1.4), silica (sg of 2.6) and ilmenite (sg of 4.5) when particle diameters exceeded 0.1 mm. Thus at very low solid concentrations experienced in the channels, the RC is capable of density separation. Galvin et al. (2009) describe two advantages of narrow 1.7 mm channel spacings, firstly the higher shear rates produced in narrow channels prevent particle blockage and secondly narrower channels produce a higher pressure drop across the device and promotes uniform flow through each channel. In their work Galvin et al. (2009) proposed a theory that revealed the importance of the fluid velocity profile and the ratio of particle diameter to channel spacing. Further to this work Walton et al. (2010) examined the potential of fractionating samples based on density by varying channel spacing. Coal and mineral matter was processed in two discrete size fractions namely -2+0.25 mm and -250+38 µm size fractions. For the latter size fraction, a channel spacing of 1.77 mm produced results in close agreement to heavy liquid separation and outperformed the 4.2 mm channels and is consistent with their earlier work. For optimal performance, Walton et al. (2010) recommend a particle top size to be less than a third of the channel spacing. Thus for the application of this study investigating a sample with a top size of 425 µm a channel spacing of approximately 1.28 mm would be required.

Galvin et al. (2009) admit that although a narrow channel spacing of 1.7 mm would be suitable for laboratory fractionation, fabricating an industrial separator with uniform narrow channels such as this would prove to be difficult. In 2009 the RC was redesigned to incorporate this separation mechanism by reducing the channel spacing to 6 mm for all industrial units. These narrow channels were used to efficiently beneficiate iron ore (Amariei et al., 2014). Subsequently, laboratory testwork conducted by Hunter et al. (2015) and Galvin et al. (2016) employed reflux classifiers with channel lengths of 1 m and channel spacings of 6mm and 5.3mm respectively.

The plastic welders at Mintek were constrained by their equipment and could not produce channel spacings of less than 5 mm and this channel spacing was selected due to construction constraints and recent testwork conducted by Hunter et al. (2015) and Galvin et al. (2016a).

Overflow weir

To promote equal flow velocities in each of the channels Galvin et al. (2009) recommend the plates that form the inclined channels extend above the level of the overflow weir. Zhou et al. (2006) recommend that the flow in each of the inclined channels be very similar. If not, reverse flow through one channel and an increased flow through another can arise. By increasing the aspect ratio and improving the design of the overflow outlet a uniform flow through the inclined channels should be possible (Zhou et al., 2006). To ensure equal flow velocities in each channel, the channels were designed to extend past the overflow weir as illustrated in Figure 6.8.

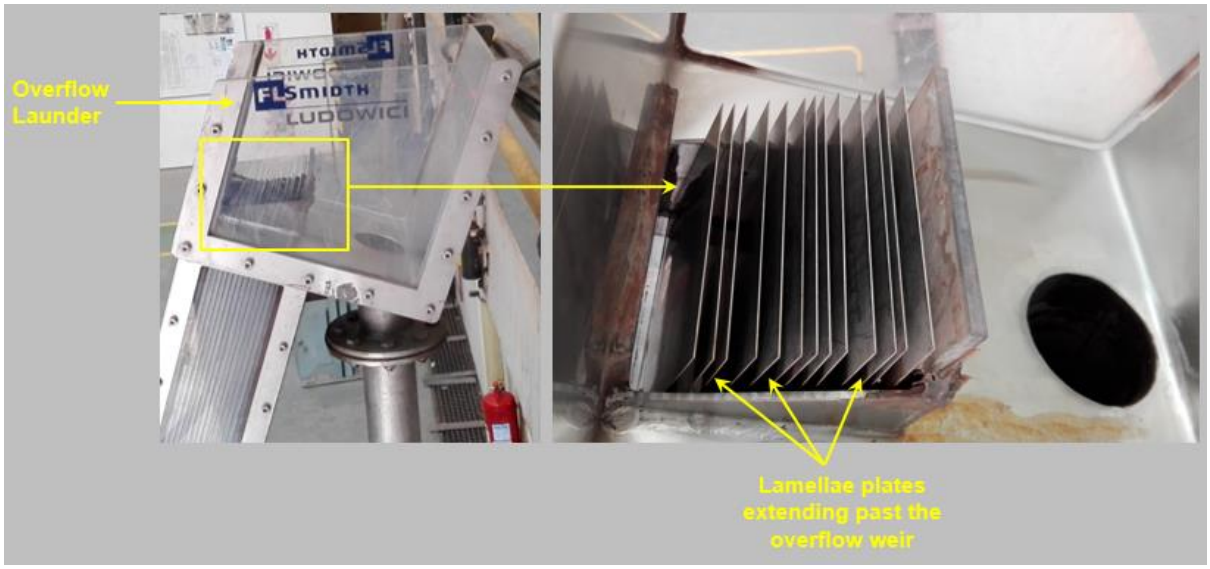


Figure 6.8: The lamellae plates of the RC-100 extending past the overflow weir to ensure equal flow velocities in each channel

Distributor for the fluidisation water

The first RC constructed by Mintek had an L-shaped pipe with exit facing downwards for the distribution of the fluidisation water as depicted in Figure 6.9. It was observed that compaction and rat-holing were occurring since the fluidisation rate was very low and not dispersed.

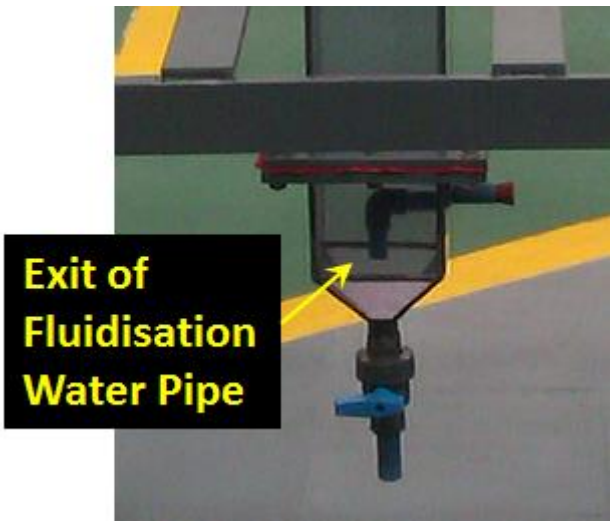


Figure 6.9: Fluidisation water distributor for the first RC built at Mintek

On review of the testwork conducted by other investigators, it was noted that Zhou et al. (2006) and Doroodchi et al. (2006) used a distributor like an inverted pyramid containing 100 0.5mm holes for an RC of cross section 0.1 m x 0.06 m. Galvin et al. (2016a) also used an inverted pyramid of height 90mm with four 0.75mm diameter holes on each of the triangular faces totalling 16 holes. Mintek's second design of the distributor was based on the design described by Galvin et al. (2016a). The angle of the holes was not specified, and two designs were tested as depicted in Figure 6.10 and Figure 6.11.

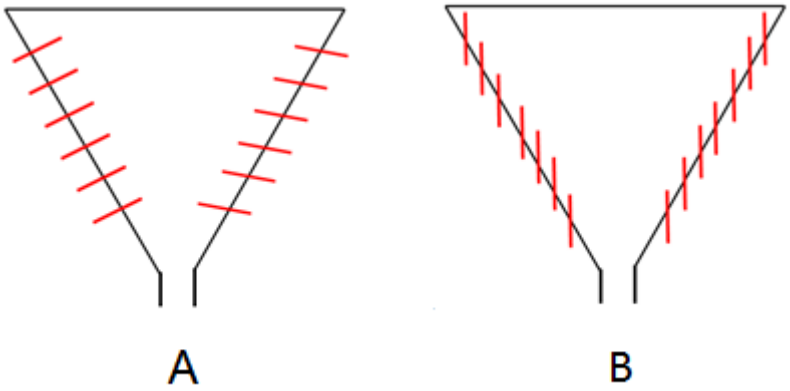


Figure 6.10: Schematic diagram of the angles of holes in the distributor for the fluidisation water

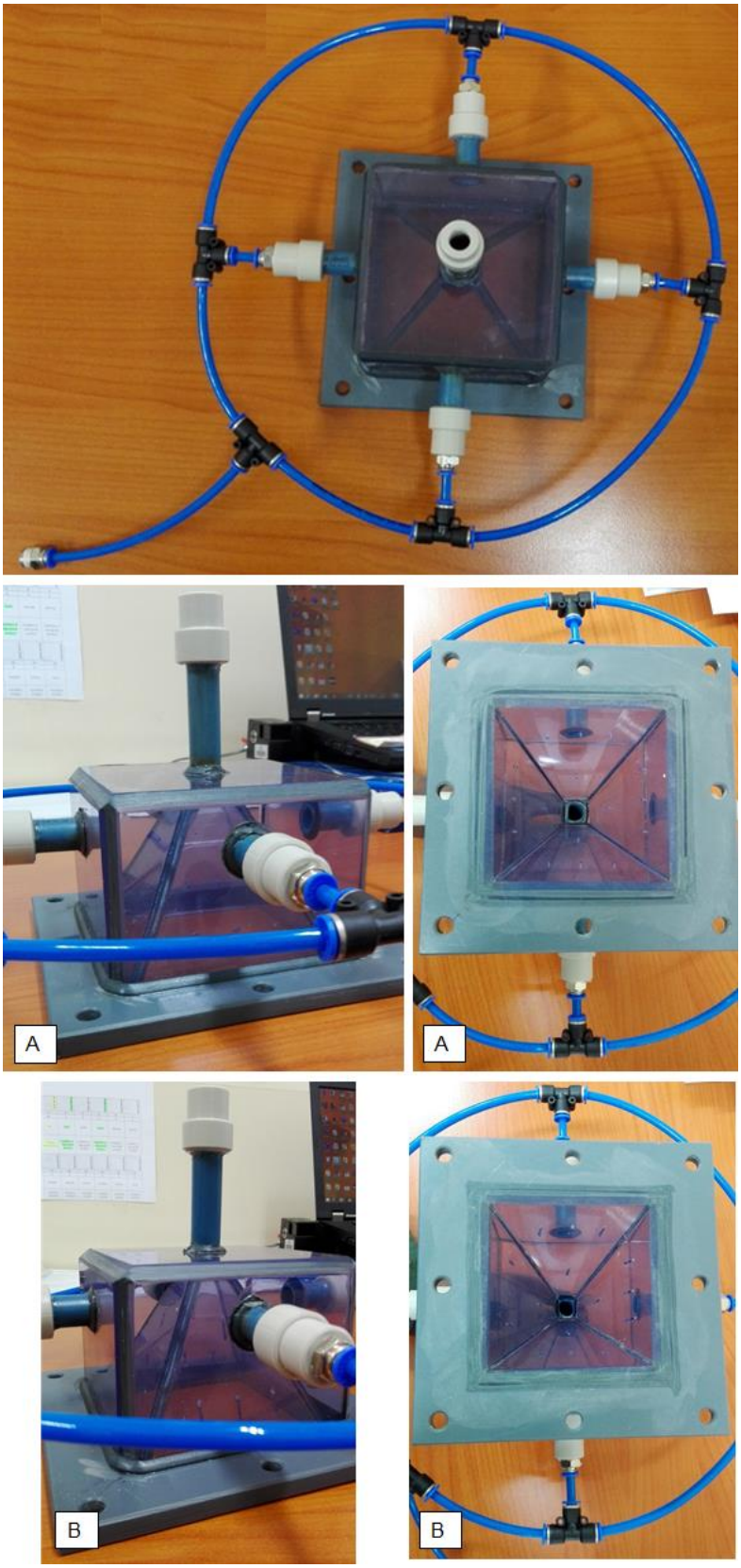


Figure 6.11: Angles of holes in the distributor for the fluidisation water

Tests were conducted with both distributors and distributor A was selected since this design allowed for an even distribution of water along the cross-sectional area of the RC. In addition the RC-100 has a similar design to that of distributor A as presented in Figure 6.12.

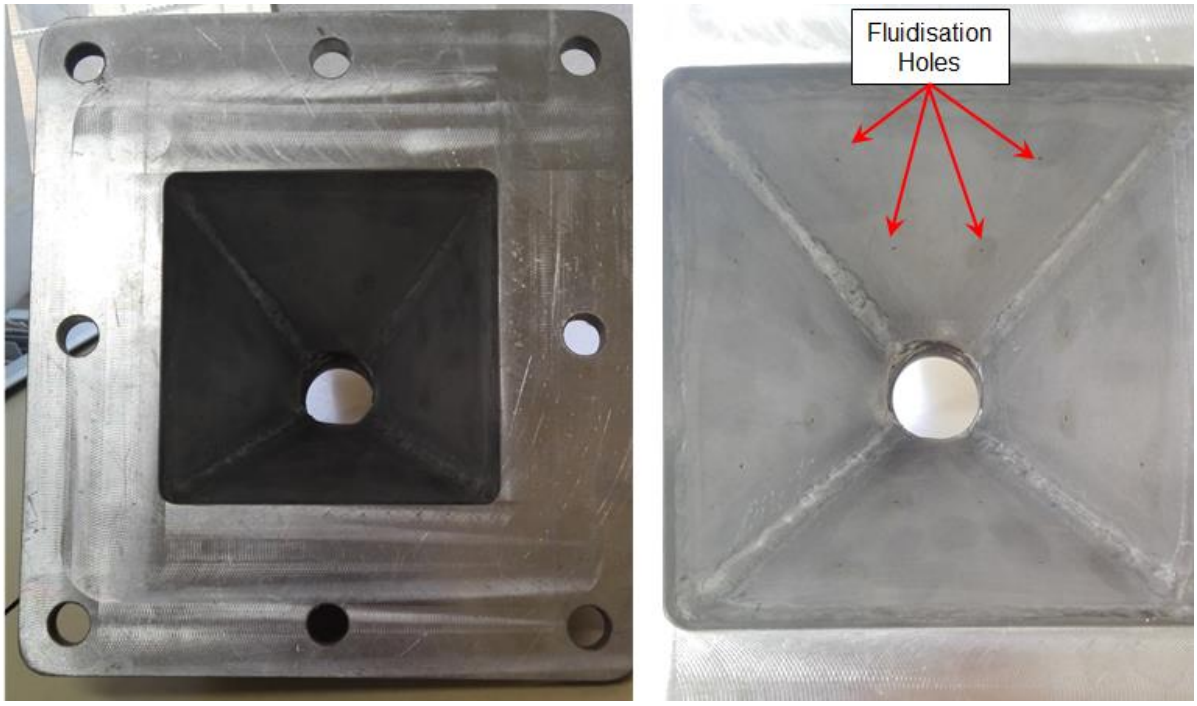


Figure 6.12: Fluidisation water distributor for the RC-100

Final RC design

The reflux classifier incorporating all the design features outlined above and presented in Figure 6.13 was used for this study. The lamellae plates presented in Figure 6.14 were made such that each plate was positioned in a specific sequence and slotted into the lamellae settler chamber. This design facilitated cleaning of the chamber and lamellae plates with a total of 16 plates slotted into the chamber.

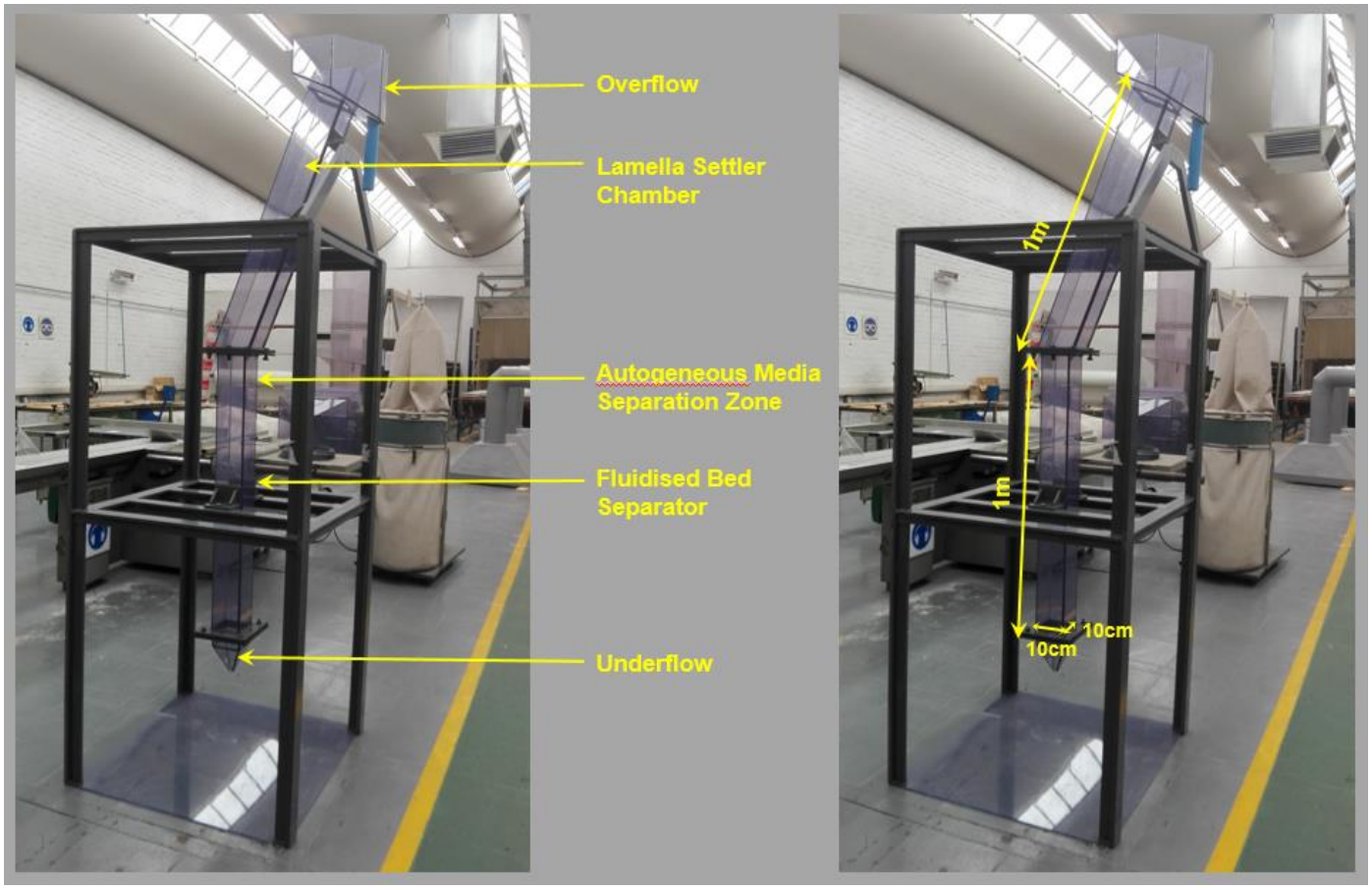


Figure 6.13: Reflux Classifier employed for this study which was made from PVC plastic

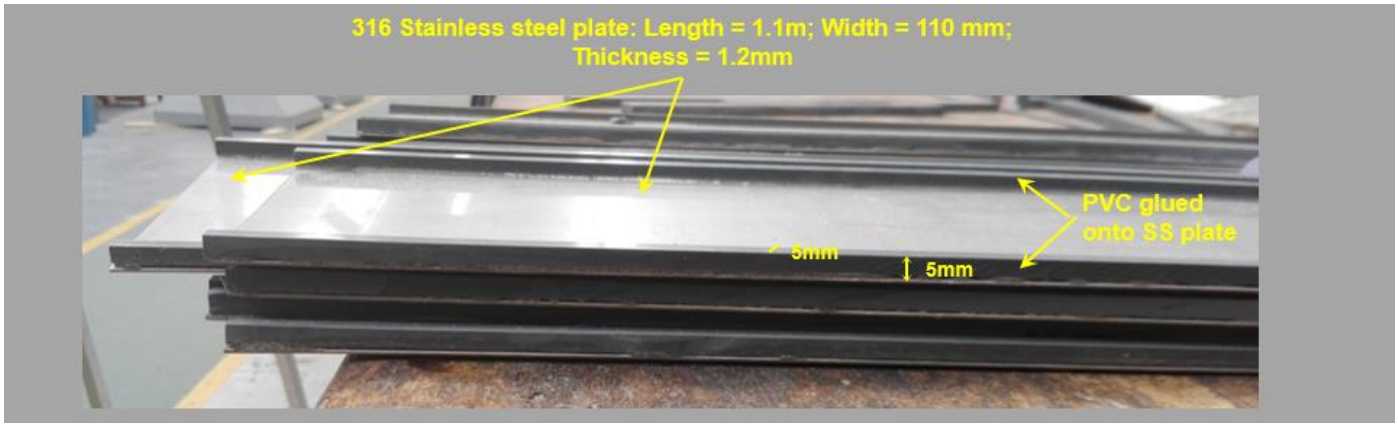


Figure 6.14: Lamellae plates made from 316 Stainless Steel with PVC plastic used to achieve a gap spacing of 5mm

6.2.4 Selection of Operating Approach

Two approaches for conducting the RC testwork were identified namely, continuous operation and semi-batch mode, and are further detailed below.

For ultrafine separation on the RC, Galvin (2016) recommended running continuously for an entire day to allow the ultrafine dense iron ore to transport downwards and achieve steady state. Galvin (2016) also recommended that sampling of the overflow and underflow occur over a significant period. This approach requires a considerable amount of sample as indicated by the work of Hunter et al. (2015) and Doroodchi et al. (2006).

Through a double stage approach to their laboratory experiments on -500 µm silica sand, Doroodchi et al. (2006) waited a total of 3.5 hours for the RC to achieve steady state and before sub-sampling. The underflow and overflow volumetric flowrates and solids flowrates were monitored over this period. The system was considered to reach steady state when the underflow and overflow volumetric flowrates and solids flowrates remained steady over a 30 minute period. At the lowest feed rate tested of 0.74 kg/m^{2}s, approximately 70 kg of material was required to achieve steady state. Hunter et al (2015) treated iron ore slimes (59% -38 µm) through the RC-100 and achieved a product of 61% Fe at a recovery of 80.2% at a solids feed rate of 15 kg/h (1.5 t/m^{2}h) and fluidisation water flowrate of 9 kg/h (0.90 m^3/m^{2}h). To achieve steady state over a three hour period a minimum sample mass of 45 kg would be required. Sample constraints and the requirement for repeat tests prohibited the application of the continuous approach in this study.

An alternative approach to continuous operation is the semi-batch process referred to as water-based fractionation. Water-based fractionation was first conducted on the RC by Laskovski et al. (2006) in which the separation of particles at a nominal particle size was investigated for one component samples of a specific density. Galvin (2009) further expanded on this approach by treating mixed samples (coal and mineral matter) of a broad particle size distribution and densities with the objective of developing a suitable substitute for sink-float analysis. The double fractionation results used in conjunction with the fractionation algorithm provided similar results to that of the sink-float analysis. The method for water-based fractionation investigated by

Laskovski et al. (2006), Galvin (2009), Walton et al. (2010) and Hunter et al. (2014) are similar. An initial charge of sample is placed into the vertical section of the laboratory reflux classifier, and the fluidisation rate increased incrementally. The fluidisation rate is held fixed until the rate of particle elutriation became insignificant. A screen of appropriate size was selected to determine this insignificance. At low elutriation flowrates, low-density particles and fine slimes were conveyed to the overflow. With increasing flowrates denser and larger particles were elutriated and reported to the overflow. The overflows at each fluidisation rate were collected separately, weighed and assayed. The reminder in the vertical section of the column was also weighed and assayed. In semi-batch mode, no further feed addition or underflow removal occurred for the duration of the test. The advantages of the semi-batch mode described above are listed below:

- Hunter et al. (2014) reveal the dilute conditions present in the semi-batch mode reduces the autogenous dense-medium effect and particle size has a larger effect. This effect is ideal in this study where the separation of flocculated hematite from finer siliceous gangue is size dependent.
- Low sample mass requirements (typically 3.5kg for coal). This allows for repeat tests to be conducted for the constrained sample mass in this study.
- In continuous operations, a peristaltic pump is typically used to feed a sample into the laboratory RC. It is envisaged that the pumping action of the peristaltic pump could destroy the flocs created and thus the semi-batch process is better suited to this study.
- Should testwork not be completed within an 8 hour work day, the remaining flowrates can be tested the following day once the elutriation rate for the current test is negligible.

The one anticipated challenge with the semi-batch mode for this study is the washability profile from the RC cannot be compared to sink-float analysis, a standard approach used by researchers. The current sink-float analysis method at Mintek cannot treat -38 µm material. At these fine particle size ranges centrifugal sink-float analysis can be conducted but only at a medium density of the separating fluid, tetrabromoethane, of 2.96 g/cm^3.

6.2.5 Selection of Operating Parameters

Tripathy et al. (2015) summarised both the design and process variables that affect separation on the TBS and RC as presented in Table 6.4. The process parameters that can be investigated on the RC for a continuous test are fluidisation water flowrate, bed density, feed pulp density and feed particle size distribution. However, based on the semi-batch mode that was implemented two operating parameters were identified namely feed mass of the sample and fluidisation water flowrates.

Table 6.4: Process Variables for the TBS and RC (Tripathy et al., 2015)

Hydraulic Classifier	Design Variables	Process Variables	Salient Features	Area of Application
Teeter Bed Separator	Height of conical and cylindrical section. Diameter of the perforated plate and the layout. Feed slurry distribution point and size	Teeter water flowrate, set point/teeter bed pressure, particle size and density distribution of feed, feed pulp density and feedrate	Higher throughput, classification at lower cut desnity, flat bottom, circular sorting chamber, water distribution using perforated plate, dart valve arrangement	Coal, placer minerals, hematite, silica sand
Reflux Classifier	Inclined plates angle, inclined plate height, inclined section height, column length, cone angle. Height of the conical and cylindrical section, feed introduction point	Fluidization water flowrate, bed density, feedrate, feed pulp density, feed particle size distribution	Introduction of parallel inclined plates, effective separation at coarser particle size as well as employed for desliming. Square type sorting chamber, pipe or teeter water distribution, DP cell based density measurement system and pinch valve based underflow discharge	Heavy minerals, coal, hematite, cenosphere

Feed Mass

The solids volume fraction used in the semi-batch tests of Hunter et al. (2014), Walton et al. (2010) and Laskovski et al. (2006) range from 0.15 to 0.19 for coal and 0.05 to 0.07 for ilmenite as presented in Table 6.5. Laskovski et al. (2006) tested different one component systems (sand, PVC, and ilmenite) and selected feed masses to yield similar solid volume fractions of 0.05. In line with their approach, a solid volume fraction of 0.05 in the Mintek PVC RC would require a solids feed mass of 3.3 kg, and this was the feed mass selected for testwork purposes.

Table 6.5: Summary of semi-batch operating conditions and sample characteristics for coal and ilmenite

	Hunter et al (2014)	Walton et al (2010)	Laskovski et al (2006)	
RC Dimensions				
Length of inclined channels (m)	1	1	1	2
Channel spacing (mm)	6.3	4.2		
Height of fluidised bed (m)	1	1	1	1
Width (m)	0.1	0.06	0.06	0.06
Breadth (m)	0.08	0.1	0.1	0.1
Volume of inclined section (m^3)	0.008	0.006	0.006	0.012
Volume of vertical section (m^3)	0.008	0.006	0.006	0.006
Total volume of RC (m^3)	0.016	0.012	0.012	0.018
Sample Characteristics				
Mineral	Coking coal	Coking coal	Ilmenite	Ilmenite
Size Fraction (mm)	-2+0.25	-0.25+0.038	Mean diameter: 0.175	Mean diameter: 0.175
Average density of coal (kg/m^3)	1165.8	1937.5	4820	4820
Mass of solids (kg)	3.5	3.5	4	4
Volume of coal in RC (m^3)	0.003	0.002	0.001	0.001
Solids volume fraction = Volume of coal / total RC volume	**0.19**	**0.15**	**0.07**	**0.05**

Note: Width of lamellae plates ignored in the calculation of the volume of the inclined section.

Fluidisation Water Flowrates

Hunter et al. (2015) achieved a product of 61% Fe at a recovery of 80.2% through one RC stage. The excellent results were obtained for an iron ore slime sample with 59% -38 µm and 31.9% -20 µm at a solids feed rate of 15 kg/h (1.5 t/m^2h) and fluidisation water flowrate of 9 kg/h (0.90 m^3/m^2h). Hunter et al. (2015) however did show that only 57% of the -20 µm size fraction was recovered whilst 87-95% was recovered for the coarser size fractions. Their results indicate that a sample containing significantly more -20 µm would require a lower fluidisation water flowrate. The Fe ore sample in this study contained 70.9% -20 µm material and thus a fluidisation water flowrate, lower than that of Hunter et al. (2015), of 8.2 kg/h was set as the minimum fluidisation flowrate. The ranges of the water fluidisation rates used for the testwork are outlined in Section 6.2.6 and were based on the visual inspection of the overflow products and mass proportion.

6.2.6 Tests

The semi-batch process described by Laskovski et al. (2006), Galvin (2009), Walton et al. (2010) and Hunter et al. (2014) was followed for the sample as-is and the flocculated sample.

Approximately a quarter of the RC was filled with water. Solids weighing 3.3kg was wetted and prepared to a solids concentration of 70% and added to the RC. This ensured the sample was adequately wetted. The remainder of the slurry in the bucket and sides of the RC were washed into the RC. Additional water was added to the RC such that the entire volume was filled. The solids were allowed to settle and thereafter the water fluidisation rate was increased incrementally. The fluidisation rate was held constant until the rate of particle elutriation became insignificant. To determine if the particle elutriation was insignificant a sub-sample of the overflow was filtered with a 2 µm filter paper and the filter paper visually inspected to determine if any solids remained. When a negligible amount of +2 µm material was observed the fluidisation water was increased and the process repeated. The collection period for each overflow varied from 26 hours to 1.5 hours depending on the water fluidisation rate. Longer collection periods were required for the initial flowrates with shorter periods for higher flowrates. The experimental set-up for the PVC RC tests is presented in Figure 6.15.



Figure 6.15: Experimental set-up for the PVC RC testwork at Mintek

The fluidisation water was administered by a peristaltic pump. A calibration curve of the pump speed and water flowrate in kg/h was obtained to facilitate testwork. Eleven fluidisation rates, given in Table 6.6, were tested and each overflow was collected separately filtered, dried, weighed and prepared for chemical analysis. The remainder in the vertical section of the column (referred to as column remainder) was filtered, dried, weighed and prepared for sizing and chemical analysis. For the duration of the test no further feed addition or underflow removal occurred.

Table 6.6: RC Operating Conditions for the -38 µm sample as-is and for the flocculated sample

Fixed Operating Parameters	
Feed Mass	3.3kg
Further Feed Addition	N/A
Underflow discharge rate	N/A
Variable Operating Parameters	
Water Fluidisation Rate	8.2 kg/h
	12.5 kg/h
	16.8 kg/h
	21.0 kg/h
	25.3 kg/h
	31.5 kg/h
	50.5 kg/h
	67.3 kg/h
	100.9 kg/h
	121.1 kg/h
	146.4 kg/h

Triplicates of each water fluidisation flowrate were conducted to gain statistical confidence in the results. The column remainder of the average of the base case test and flocculated test were sized as per the screen fractions are given in Table 3.5 in Chapter 3, Section 3.4.1.3. The +38 µm and -38 µm fractions of the underflow from the two sized samples were subjected to PTA (described in Chapter 3, Section 3.4.1.2.2) to determine the differences between the two tests.

6.2.7 Precautions

The following precautions were followed for quality assurance:

- A calibration curve for the peristaltic pump was generated. At each pump setting, three samples were taken and an average used in the calibration curve. The same pump was used for all RC testwork. A peristaltic pump was selected as easier control of the fluidisation water could be attained compared to a water rotameter where fluctuations or no supply would detrimentally affect the testwork.

- The -38 µm sample as-is was wetted prior to addition to the RC. The flocculated material was already wet and at 45% solids.
- To remove any bubbles entrapped in the sample very low water fluidisation rates were used to flush out trapped bubbles prior to testwork commencement.
- Material that collected below the water distributor upon feeding of the sample was collected separately as this material was not subjected to the fluidisation water and would bias the results of the column remainder.

6.2.8 Limitations of the Reflux Classifier Testwork

- Amariei et al. (2014) recommended that testwork on -45µm iron ore slimes be conducted but raised concerns that pulp rheology, surface chemistry and coagulation (aggregation) may hinder efficient separation.
- Zajdela et al. (2008) studied the effect of floc porosity and permeability in suspensions of biological water treatment plants. Their findings confirmed those of Huang (1993) and Lee et al. (1996), cited by Zajdela et al. (2008), in which floc porosity increased with an increase in floc size, and subsequently the floc density would decrease. The floc porosity may negatively affect its density thereby reducing the separation efficiency of the RC. However, this effect may appear to be insignificant as the semi-batch approach reduces the autogenous dense-medium effect where particle size has a larger effect on separation.

6.3 Results and Discussion

Semi-batch tests were conducted on the RC whereby the unit was charged with 3.3-3.4 kg of solids and the fluidisation water varied from 8.2 kg/hr to 146.4 kg/hr. The solids were either charged as-is (base case) or selectively flocculated before addition to the RC. Both tests were conducted in triplicate with the average and 95% confidence limits reported in this section.

The effect of increasing the fluidisation water rate on the underflow Fe grade, recovery and separation efficiency is presented in Figure 6.16 to Figure 6.18 for both the base case test and the selective flocculation test at 95% confidence limits. The results show a similar trend with or without selective flocculation, namely increasing water fluidisation rates increases the underflow Fe grade and separation efficiency with a trade-off in Fe recovery.

As the water fluidisation rate increases, light fine particles report to the overflow with dense finer particles allowed to settle in the channels and slide back into the RC until the flow velocity in the channels exceeds the particle's terminal velocity resulting in fine Fe ore reporting to the overflow. At water fluidisation rates below 120 kg/hr, the Fe grade and separation efficiency profiles with and without flocculation lie within the 95% confidence limits. Increasing the water fluidisation rate above 120 kg/hr suggests lower Fe grades and separation efficiencies are achieved with selective flocculation. It is assumed that coarse silicates entrapped in the floc structures, that have otherwise been fluidised and reported to the overflow in the base case test, are not readily removed from the floc structure at high fluidisation water rates.

Huang (1993) and Lee et al. (1996), cited by Zajdela et al. (2008), found that increasing floc size resulted in increased floc porosity and thus lower floc densities. Low floc densities would result in higher Fe losses if a density separation were to occur in the RC. However, since the semi-batch RC tests were conducted at low solids concentration (0.05 solid volume fraction) a size separation as opposed to density separation would have occurred, and the effect of floc density would be negligible. The negligible effect of floc density is confirmed by the higher Fe recoveries attained in the test whereby the RC was coupled with selective flocculation.

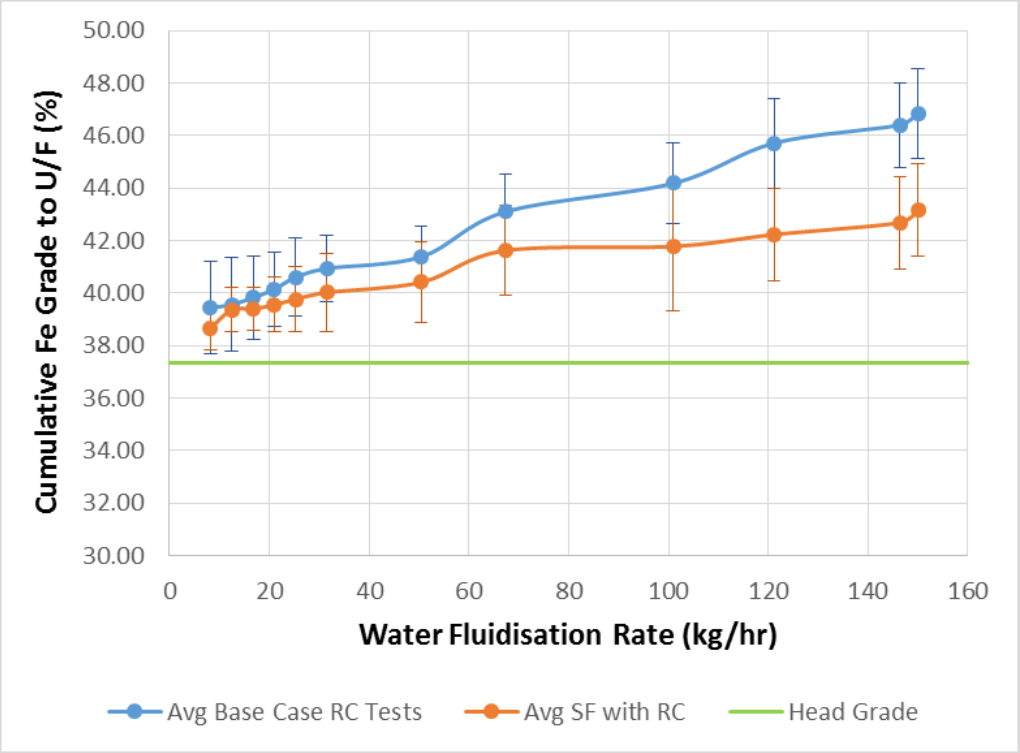


Figure 6.16: Effect of Water Fluidisation rate on the Cumulative Fe Grade of the RC U/F with and without selective flocculation (at 95% Confidence limits)

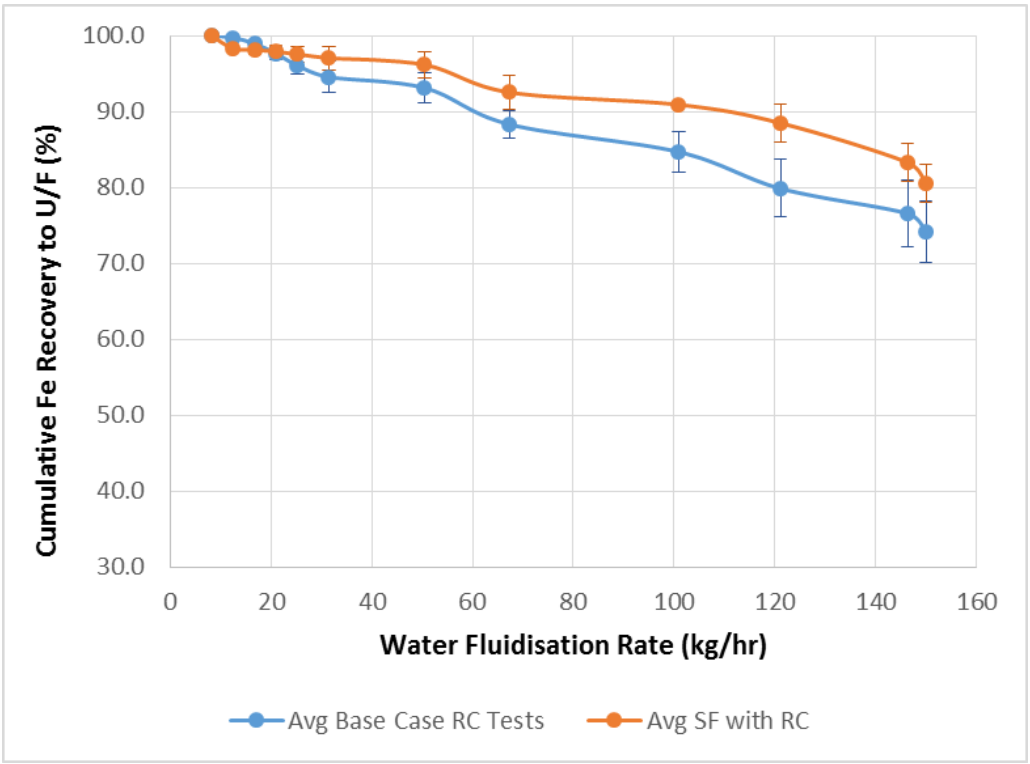


Figure 6.17: Effect of Water Fluidisation rate on the Cumulative Fe Recovery of the RC U/F with and without selective flocculation (at 95% Confidence limits)

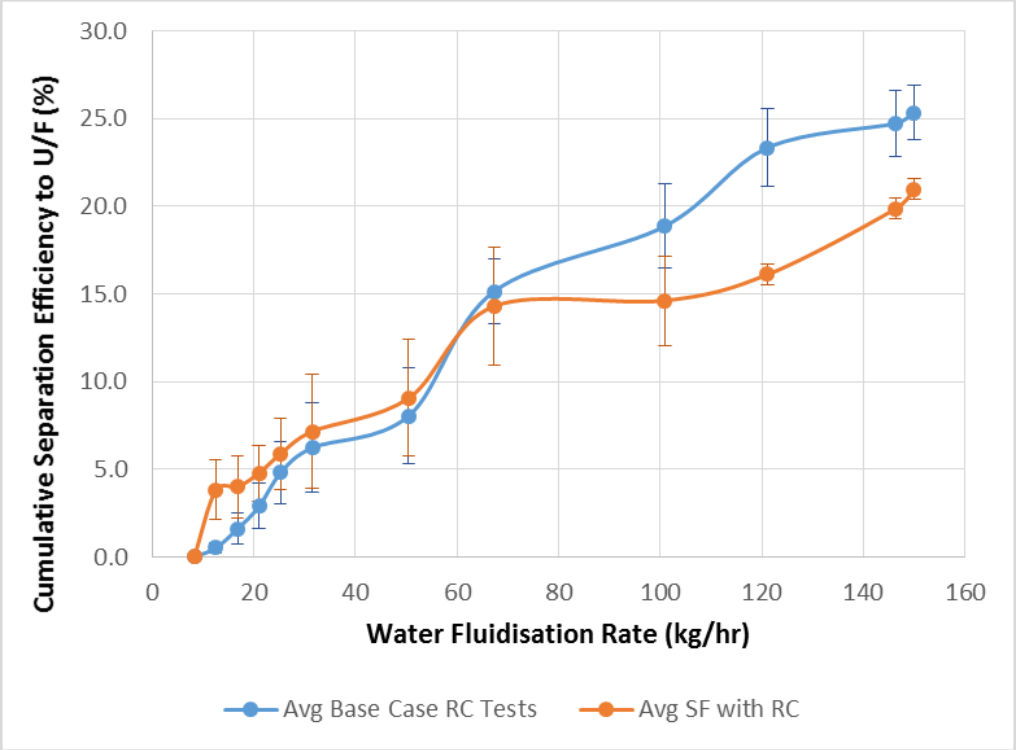


Figure 6.18: Effect of Water Fluidisation rate on the Cumulative Separation Efficiency of the RC U/F with and without selective flocculation (at 95% Confidence limits)

The lower Fe grades and separation efficiencies for the selective flocculation tests can be attributed to:

- The presence of entrapped gangue within the floc structure. The discrete size-by-assay results obtained by PTA presented in Figure 6.19 indicate similar Fe deportment across size for both the base case test and the selective flocculation test. However, the -15+10 µm fraction for the selective flocculation test has 7.8% more Si than the base case test which implies silicate entrapment within the floc structure which is not alleviated through increasing the water fluidisation rate. It is unlikely that the result is an outlier since the number of particles analysed in the -15+10 µm size class is similar for the base case test (26 166 particles) and selective flocculation coupled with the RC (27 461 particles).

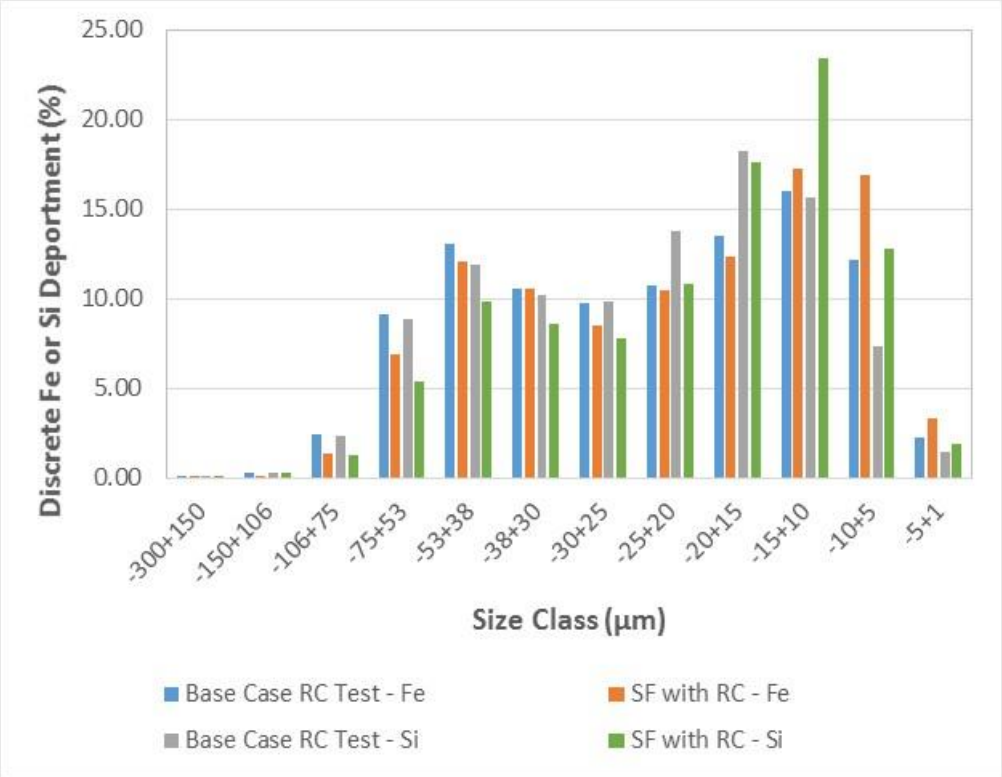


Figure 6.19: Discrete Fe and Si Deportment of the RC U/F with and without selective flocculation

- The fluidisation water pH may adversely affect the floc size as indicated in Chapter 4, Section 4.4.2 with floc size increasing with pH.
- The long residence times of the semi-batch tests may affect the floc characteristics and its selectivity.
- The optimised floc conditions for the SLon may not be the best floc conditions for the RC.

The grade-recovery curve (Figure 6.20) of the base case test and with flocculation indicate both tests lie within range of each other although the base case test achieved the best underflow Fe grade and recovery of 46.85% and 74.1% respectively. The Fe upgrade is marginal at 1.17 whilst the SLon with and without flocculation achieved an upgrade ratio of 1.39 and 1.59 respectively.

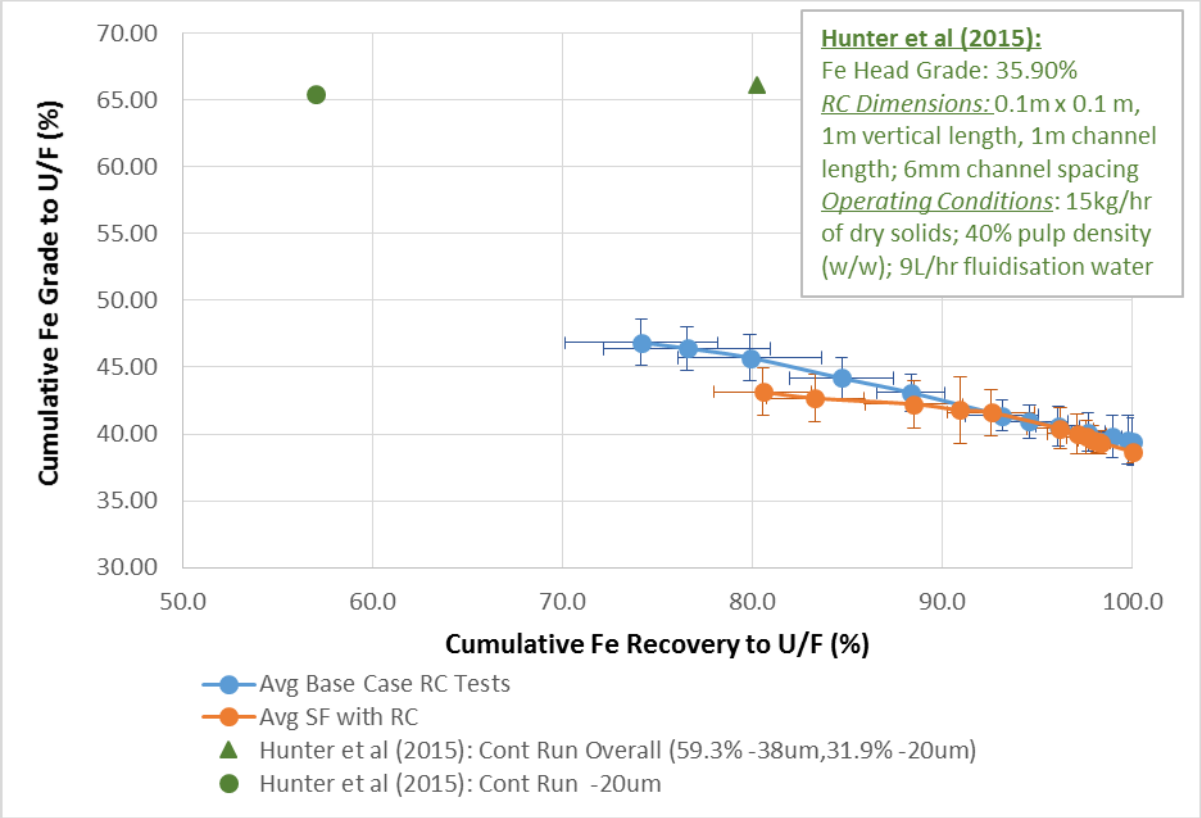


Figure 6.20: Fe grade-recovery curve for the current semi-batch study and the continuous run conducted by Hunter et al. (2015) on fine Fe ore of similar head grade

Figure 6.20 also presents the current semi-batch study in context with the continuous run on a sample of similar head grade (35.90%) and slightly coarser particle size distribution (59.3% -38 µm vs 85.4% -38 µm) conducted by Hunter et al. (2015). Disregarding the mineralogical difference between the two studies Hunter et al (2015) impressively demonstrated that an overall product of 66.1% Fe at a recovery of 80.2% could be attained running continuously on the RC-100 at a pulp density of 40% solids (w/w), slow feed (15 kg/h) and slow water fluidisation rate (9 L/h) using a gap spacing of 6 mm. However, the discrete Fe recovery of the -20 µm fraction was much lower at 57% at a similar product grade, and improved recovery of this fraction is expected with a smaller gap spacing. The work of Hunter et al. (2015) demonstrates that a continuous run could potentially achieve better results by activating the autogenous media separation zone. It is recommended that should sufficient feed be available a continuous run with and without flocculation be conducted to validate these findings before the RC is conclusively ruled out.

6.4 Conclusion

The semi-batch Reflux Classifier (RC) tests with and without selective flocculation achieved lower Fe grades and recoveries compared to the base case SLon test (magnetic separation without selective flocculation). The base case RC test achieved the best Fe grade of 46.85±1.71% at a recovery and separation efficiency of 74.1±4.0% and 25.3±1.6% respectively.

The low solids concentration in the semi-batch RC tests (0.05 solid volume fraction) facilitate a size separation as opposed to density separation and it is expected that a continuous run would improve the results through the activation of the autogenous media separation zone. It is recommended that should sufficient feed be available a continuous run with and without flocculation be conducted with a smaller gap spacing to validate these findings before the RC is conclusively ruled out.

CHAPTER 7 : COMPARISON OF SELECTIVE FLOCCULATION COUPLED WITH MAGNETIC SEPARATION AND THE RC

7.1 Introduction

Having established the optimal conditions for selective flocculation in Chapter 5, this chapter serves to determine if selective flocculation improves the response variables (separation efficiency, concentrate Fe grade and recovery) of magnetic and gravity separators. The base case tests for magnetic and gravity separation (tests without selective flocculation) will be compared to tests whereby selective flocculation was coupled with these same separators. This comparison is needed to establish which process achieved the best metallurgical performance with regards to the above-mentioned response variables.

7.2 Comparative Results

The concentrate Fe grades and recoveries for the SLon and RC with and without flocculation are compared in Figure 7.1 with the theoretical grade-recovery curve determined by mineralogy which assumes an ideal separation. The theoretical grade-recovery curve was extracted from the hematite liberation characteristics in the feed.

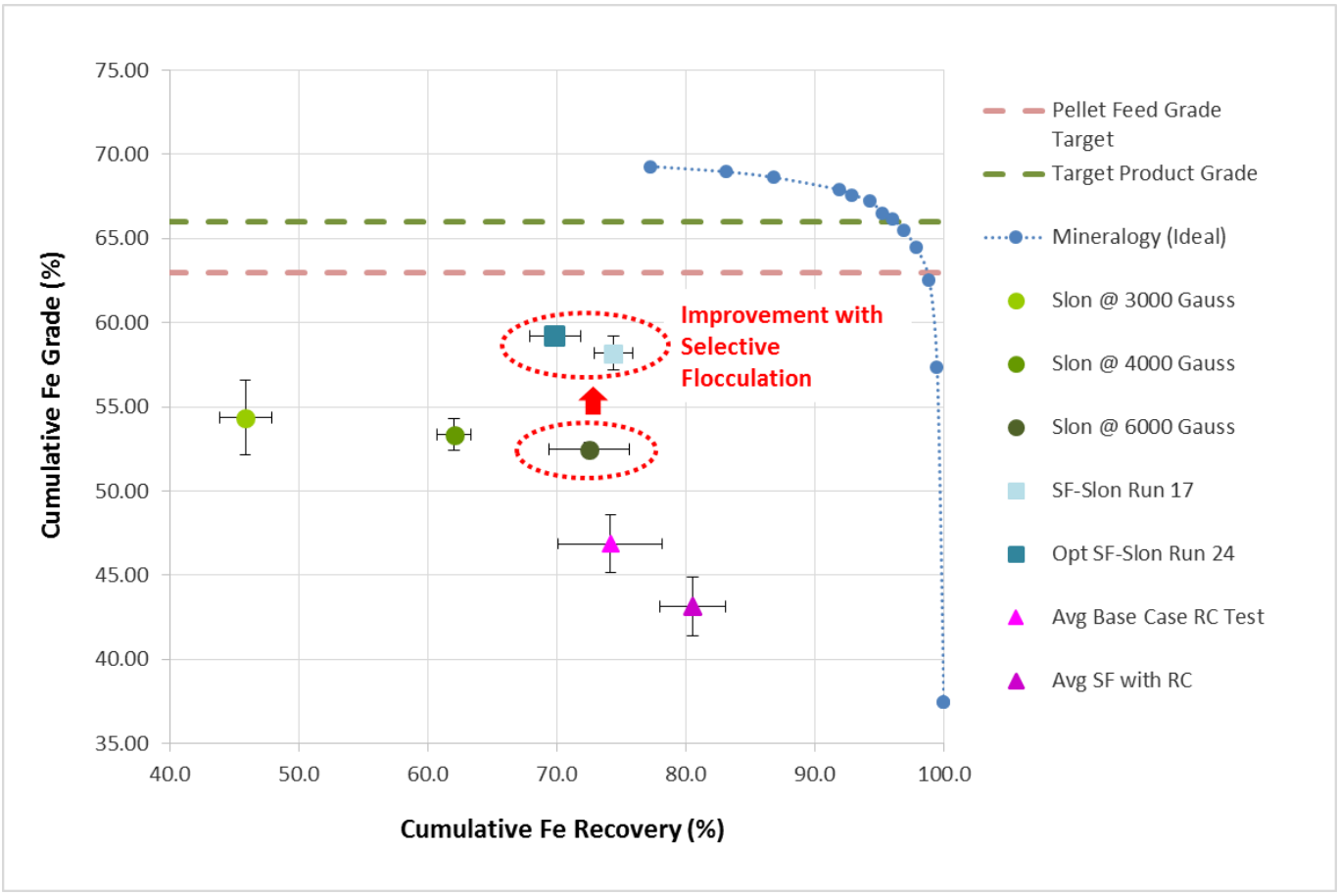


Figure 7.1: Fe Grade-Recovery curve for the SLon and RC concentrates with and without selective flocculation (at 95% Confidence limits)

Figure 7.1 indicates that for the rougher stage selective flocculation shifted the SLon Fe grade-recovery curve up towards the theoretical and ideal grade-recovery curve determined by mineralogy. The optimised selective flocculation factors (Opt Run 24) achieved similar Fe grades and recoveries to the unoptimised factors (Run 17) in one stage. The semi-batch RC tests achieved lower Fe grades and recoveries compared to the SLon, but it is anticipated that a continuous RC run would achieve better results as demonstrated by Hunter et al. (2015).

Figure 7.2 is a plot of the two significant variables (Fe Grade and Separation Efficiency) for the SLon product at the same background magnetic field intensity of 6000 Gauss with and without selective flocculation. Figure 7.2 indicates the optimised and unoptimised selective flocculation factors achieved similar Fe grades and separation efficiencies.

Optimised selective flocculation improved the product Fe grade from 52.28% to 59.20% Fe and simultaneously improved the separation efficiency from 45.1% to 56.8%.

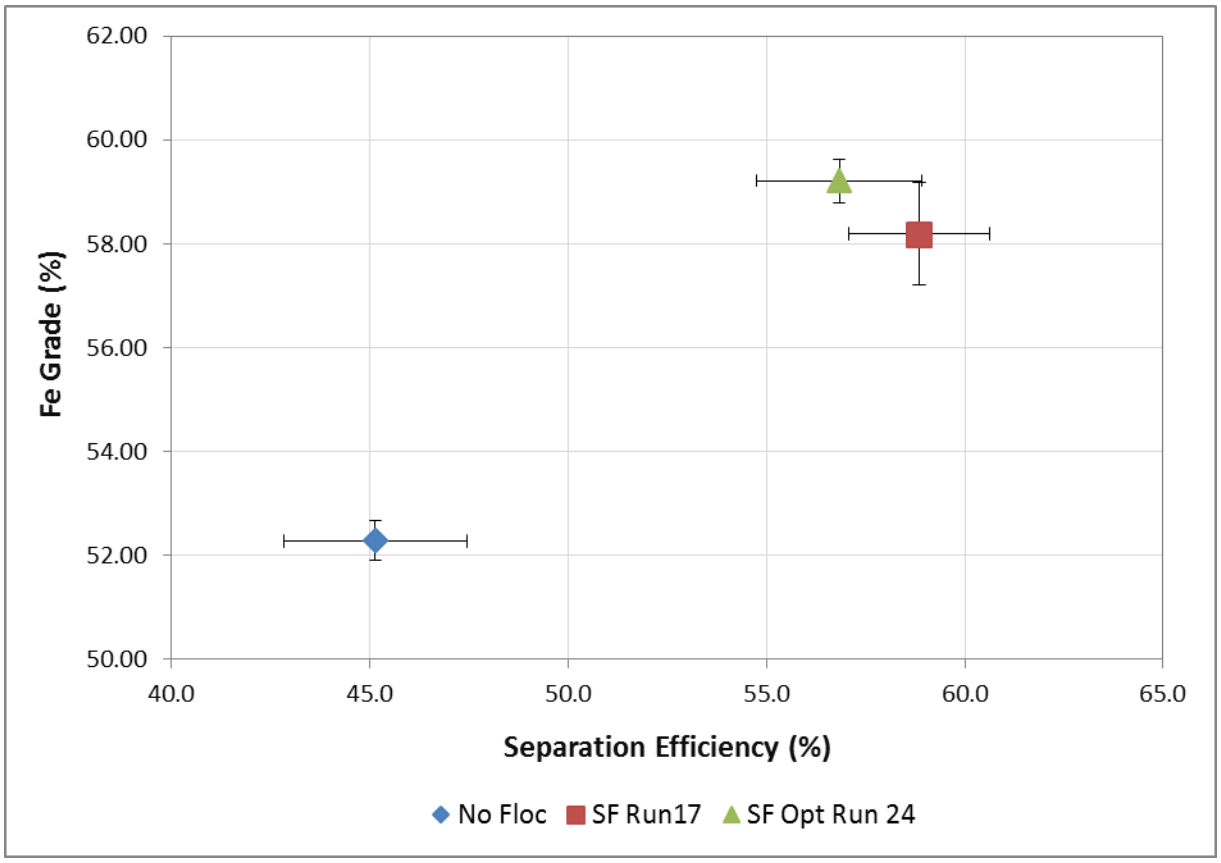


Figure 7.2: A plot of the two significant factors for the SLon product at 6 000 Gauss with and without selective flocculation (at 95% Confidence limits)

7.3 Conclusion

Magnetic separation with and without selective flocculation achieved superior metallurgical results to when the Reflux Classifier (RC) is used as the solid-solid separator in semi-batch mode. It is recommended that a continuous RC run with and without selective flocculation be conducted before the RC is conclusively ruled out.

When selective flocculation is coupled with magnetic separation (SLon-100), the Fe product grade was improved from 52.28±0.38% to 59.21±0.42% Fe while simultaneously improving the separation efficiency from 40±1.46% to 56.8±2.0% at a

background magnetic field intensity of 6000 Gauss. The Fe concentrate recovery remained constant within the 95% confidence limits and showed that at a laboratory scale selective flocculation can improve the separation efficiency of magnetic separators.

CHAPTER 8 : IMPLICATIONS OF THE FINDINGS FROM THE STUDY

8.1 Introduction

Chapter 7 conclusively showed that selective flocculation coupled with magnetic separation (also referred to as the Floc Magnetic Separation [FMS] process) achieved superior metallurgical results to magnetic separation without selective flocculation. The objective of this chapter was to determine if the reagent cost associated with the FMS process justifies its application in industry. A reagent operating cost trade-off study was conducted to compare the revenue generated from the concentrate produced without flocculation to the revenue after reagent costs for the concentrate produced by the optimised Floc Magnetic Separation (FMS) process. The reagent operating cost trade-off study does not take into account the other operating costs associated with the FMS process such as energy requirements for reagent preparation (heating of sodium oleate), stirring, pumping; labour costs; maintenance costs etcetera. The simplified comparative study is based on various assumptions that will be defined in this chapter.

8.2 Price of Fine Iron Ore

Due to increased demands and fluctuations in demands, the market or method of pricing iron ore has recently changed from an annual figure to a monthly spot price (Blas, 2010). Figure 8.1 shows the trend of iron ore prices per ton over the past 46 years as well as forecasted prices of iron ore over the next 14 years (also given in Table 8.1). Figure 8.2 focuses on the iron ore prices over the last ten years in comparison to the price of base metals. The prices indicated are spot prices of iron ore fines C.F.R. (cost and freight to China) at a grade of 62% Fe. Under the C.F.R. agreement, the shipper arranges and pays for transportation to the destination port specified by the receiver. The Fe ore price peaked at ~US$150/tonne between 2008 and 2010 and had fallen to ~US$58/tonne in 2016, similar to the prices observed before 2008. The trend of the iron ore prices correlates to the international market trends.

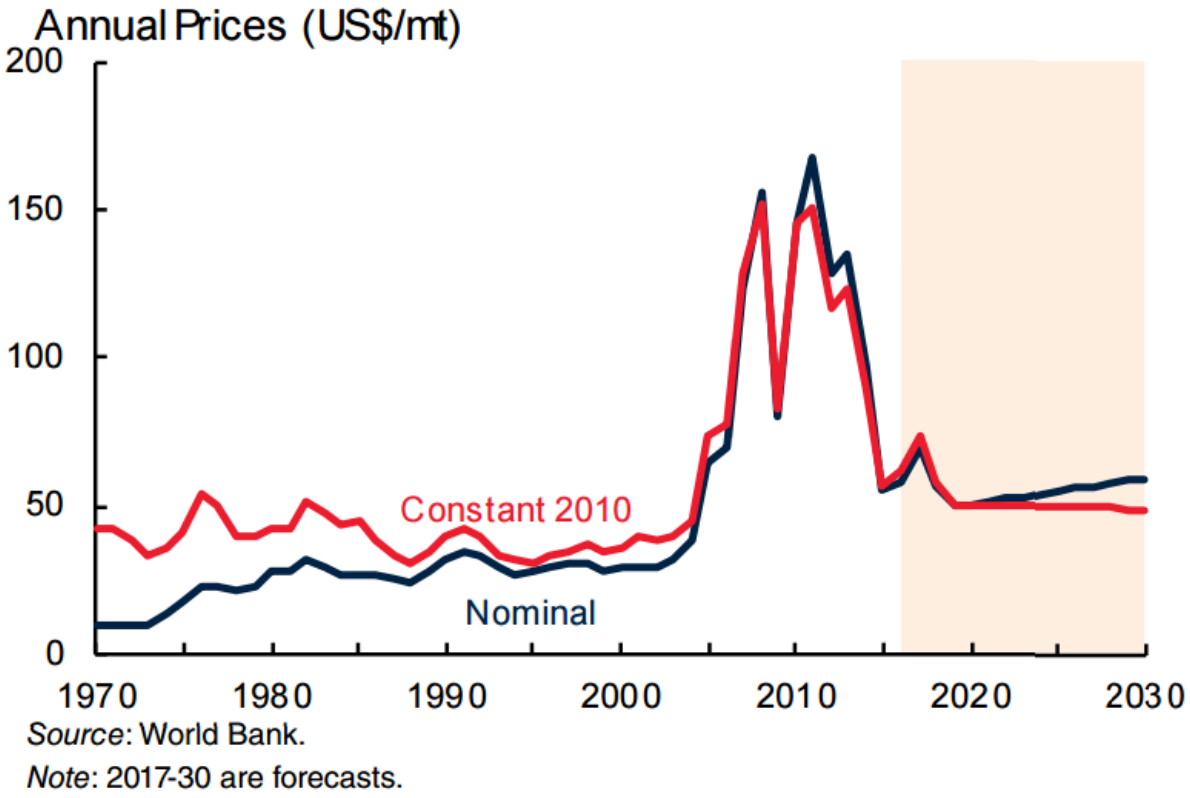
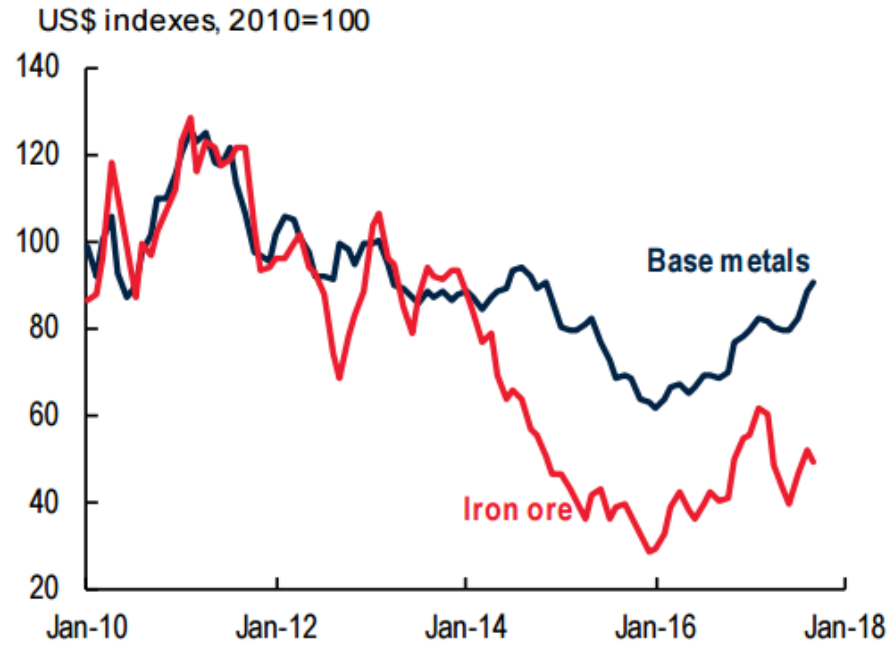


Figure 8.1: Historical and forecasted prices for iron ore fines C.F.R (cost and freight) to China at a grade of 62% Fe (World Bank Group, 2017)

Table 8.1: Historical and forecasted prices for iron ore fines C.F.R (cost and freight) to China at a grade of 62% Fe (World Bank Group, 2017)

Commodity	Unit				Forecasts					
		2014	2015	2016	2017	2018	2019	2020	2025	2030
Metals and Minerals										
Aluminum	$/mt	1,867	1,665	1,604	1,950	1,968	1,987	2,005	2,100	2,200
Copper	$/mt	6,863	5,510	4,868	6,050	6,118	6,187	6,257	6,618	7,000
Iron ore	$/dmt	97.0	55.9	58.4	70.0	57.0	50.0	50.8	55.2	60.0
Lead	$/mt	2,095	1,788	1,867	2,300	2,500	2,483	2,465	2,381	2,300
Nickel	$/mt	16,893	11,863	9,595	10,100	10,559	11,039	11,541	14,413	18,000
Tin	$/mt	21,899	16,067	17,934	20,225	20,426	20,629	20,834	21,890	23,000
Zinc	$/mt	2,161	1,932	2,090	2,900	3,000	2,945	2,890	2,634	2,400



Source: World Bank.
Note: Last observation is September 2017.

Figure 8.2: Historical Prices for iron ore fines [C.F.R China at a grade of 62% Fe] and base metals over the last 10 years (World Bank Group, 2017)

A product grade of 52.28% Fe and 59.21% Fe was generated in one stage by the SLon without and with selective flocculation respectively. The prices of fine Fe ore at similar product grades (52% Fe and 58% Fe) to that produced by the SLon are presented in Table 8.2 and indicates a price difference of R207 per dry metric ton between the two product grades. A 62% Fe fine iron ore product in 2016 was priced at US$58.4 (C.F.R. China) as shown in Table 8.1 indicates that the prices presented in Table 8.2 appear reasonable and thus were used in the following section (Section 8.3).

Table 8.2: Price of 52%Fe and 58%Fe iron ore fines [C.F.R China] in June 2016 (Platts, 2016)

Iron Ore Fines. Target Grade (%)	Platt Code	Quality	Dimensions	Location	Price (US$/dry metic ton) in June 2016	Average US$ to Rand Exchange Rate in June 2016	Price (R/dry metic ton) in June 2016
52% Fe	IONC520: The daily 52% Fe Iron Ore price assessment (IONC520) discontinued from 1 July 2016.	52%Fe	-	CFR main Chinese ports, normalized to Qingdao	26.48	0.07	400
58% Fe	IODFE00	58% Fe, 10% moisture, 5% SiO_2, 4% Al_2O_3, 0.05% phosphorus	Granular size of up to 10 mm for up to 90% of cargo		40.20		607

8.3 Reagent Operating Costs

The reagent operating cost for the optimised selective flocculation process is presented in Table 8.3 and the cheaper reagent suite (option B) comprising of sodium silicate, oleic acid, sulphuric acid, lime and paraffin was used in Table 8.4 to compare the revenue subsequent to reagent costs to the base case SLon test without selective flocculation.

The following assumptions were made in the reagent operating cost trade-off study:

- There is a market for both a 52% Fe and 59% Fe product and the price for each product excludes shipping costs from South Africa to Qingdao China.
- The plant capacity is 100 t/hr with 24-hour operation
- The plant will treat slimes from current arisings and not slimes from old tailings dams whereby weathering of particle surfaces may have occurred thereby changing the particle surface properties and the efficacy of selective flocculation.
- The energy requirements for the conditioning time and associated additional ancillaries required for the selective flocculation stage is negligible in comparison to the SLon's energy requirements when operated at a background magnetic field intensity of 6000 Gauss.

Thus the energy requirements for both options are similar and have been omitted in the operating cost trade-off study.

- According to Protea Chemicals (2017), sodium oleate is not as readily available as oleic acid, so the latter reagent was used in the reagent operating cost. Sodium hydroxide reacts with oleic acid to form sodium oleate and water as per the reaction given by Equation 8.1. The amount of sodium hydroxide required for the conversion is assumed to be negligible compared to the amount required for pH modification.

$$NaOH + CH_3(CH_2)_7CH = CH(CH_2)_7COOH \rightarrow CH_3(CH_2)_7CH = CH(CH_2)_7COONa + H_2O$$

Equation 8.1

- The largest Fe producer in South Africa is Kumba's Sishen mine located in the Northern Cape. For reagent costs, delivery to Sishen was assumed.
- A more expensive alternative to sulphuric acid, namely HCl was also considered in the reagent costs with the latter requiring double the dosage compared to sulphuric acid. It is assumed that HCl would have no adverse or beneficial effect on selective flocculation.
- Cheaper alternatives to sodium hydroxide namely lime and sodium carbonate were also considered in the reagent costs, and it is assumed these reagents require the same dosage. It is assumed that the alternatives would also have no adverse or beneficial effect on selective flocculation.
- Tilden used sodium hexametaphosphate to precipitate calcium and magnesium metaphosphates enabling the removal of $CaOH^+$ and $MgOH^+$ from the particle surfaces thereby ensuring adequate dispersion. It is assumed that water modifiers would not be required for this application.

- It is typical for the response variables to change upon scaling up from laboratory scale to pilot/industrial scale. For purposes of this study, it is assumed that pilot results will exactly coincide with laboratory scale tests.

Table 8.3: Reagent operating costs for magnetic separation coupled with selective flocculation assuming a plant capacity of 100t/hr (Protea Chemicals, 2017)

Reagent Operating Cost	Reagent									
	Sodium Silicate: Silchem 3379	Oleic Acid	HCL	Sulphuric Acid	Sodium Hydroxide	Lime	Sodium Carbonate	Paraffin	Total for Option A (Sodium Silicate, Oleic Acid, Sulphuric Acid, Sodium Hydroxide, Paraffin)	Total for Option B (Sodium Silicate, Oleic Acid, Sulphuric Acid, Lime, Paraffin)
Capacity of plant (t/hr)	100	100	100	100	100	100	100	100	400.00	400.00
Dosage of Reagent (kg/t)	1	0.464	0.147	0.073	0.2133	0.2133	0.2133	1.4311	2.18	2.18
Dosage of Reagent (kg/hr)	100	46.39	14.67	7.33	21.33	21.33	21.33	143.11	218.17	218.17
Assume 24hour operation thus Reagent Dosage (kg/week)	16800	7793.57	2464.00	1232.00	3584.00	3584.00	3584.00	24042.48	36652.05	36652.05
Assume 24hour operation thus Reagent Dosage (kg/month)	67200	31174.30	9856.00	4928.00	14336.00	14336.00	14336.00	96169.92	146608.22	146608.22
Assume 24hour operation thus Reagent Dosage (L/month) for Paraffin	-	-	-	-	-	-	-	120212.40	120212.40	120212.40
Cost of Reagent delivered to Sishen (R/kg) or R/L	R 4.82	R 23.91	R 7.00	R 5.01	R 9.97	R 3.30	R 6.13	R 5.48	R 44.37	R 37.70
Cost of Reagent delivered to Sishen (thousands of R/month)	R 323.90	R 745.38	R 68.99	R 24.69	R 142.93	R 47.31	R 87.88	R 527.25	R 1 764.16	R 1 668.53

Table 8.4: Revenue for magnetic separation with and without selective flocculation using reagent Option B and excluding all other operating costs

Option	Avg Mass Pull to Mags (%)	Avg Mags Fe Grade (%)	Avg Mags Fe Recovery (%)	Price of Product at specified Grade (R/ton)*	Mass of Product (t/month) based on 100t/hr=67 200 t/month capacity	Revenue from Product (R/month)	Reagent Costs (R/month)	Remaining Revenue after Reagent costs (R/month)
As-Is Slon	51.5	52.28	72.1	R 400	48424.28	R 19 364 739	0	R 19 364 739
SF Slon Opt Run 24	44.0	59.21	69.9	R 607	46953.54	R 28 505 255	R 1 668 534	R 26 836 721

*Platts, 2016; X-Rates, 2017.

Table 8.4 indicates the monthly cost for reagent option B delivered to Sishen would be R1.7 million. Assuming the base case SLon product grading at 52% Fe could be sold a revenue of R19 million per month (excluding all other operating costs) could be generated. Assuming a product grade of 59% Fe derived from selective flocculation coupled with magnetic separation could be sold then the revenue after reagent costs would be R27 million per month which is 39% higher than the revenue generated from the base case SLon. The simplified reagent operating cost trade-off study indicates that the additional cost for reagents required for selective flocculation is justified. However, a thorough techno-economic study is recommended to accurately capture all the costs involved in the process. In addition alternative processes could be considered to reduce reagent costs further, for example pre-concentrating the ore to a grade of 52% Fe with magnetic separation and then applying selective flocculation with a second magnetic stage to increase the grade further may reduce reagent consumption.

8.4 Conclusion

Assuming a magnetic concentrate grade of 52% Fe and 59% Fe generated without and with selective flocculation respectively could be sold, the revenue for the FMS process after reagent costs would be R27 million per month which is 39% higher than the revenue generated from magnetic separation without selective flocculation. The simplified reagent operating cost trade-off study indicates that the additional reagent cost required for selective flocculation is justified. However, a thorough techno-economic study is recommended to accurately capture all the costs involved in the process. In addition alternative processes could be considered to reduce reagent costs further, for example pre-concentrating the ore to a grade of 52% Fe with magnetic separation and then applying selective flocculation with a second magnetic stage to increase the concentrate grade further, may reduce reagent consumption.

CHAPTER 9 : CONCLUSIONS

The objective of the study was to determine the extent to which selective flocculation can improve the separation efficiency, concentrate Fe grade and recovery of conventional gravity and magnetic separation units in the beneficiation of iron ore slimes.

Selective Flocculation (SF) utilises the differences between physical and chemical properties of the various mineral species in a mixed suspension and involves the aggregation of the desired mineral from a mixture of minerals by the bridging mechanism using either surfactants (collectors) or polymers. Collectors produce more competent flocs that can withstand shearing forces during materials handling and processing, and therefore this study focused on this method of selective flocculation rather than polymers. The selective flocculation process comprises of four stages namely dispersion of particles, selective adsorption of the collector/flocculent on the desired mineral surface with the subsequent formation of flocs, the growth of flocs through conditioning at low shear and finally solid-solid separation.

The study, therefore, had to carefully investigate a large number of technical aspects that needed to be addressed to find the appropriate conditions that within the defined parameter constraints would achieve the best selective flocculation results.

The first step in the investigation was to select an appropriate sample for selective flocculation. The sample was prepared by crushing and milling to 80% passing 35µm to generate artificial slimes for this study. The feed characteristics of the sample that were important for the SF process was the head grade, mineralogy and particle size distribution. A sample low in Fe content was required to demonstrate the impact of selective flocculation as well as to compare the findings to similar studies at similar head grades. The sample selected graded at 37.34±0.47% Fe and was similar to the head grades of Song et al. (2002) and Hunter et al. (2015) which ranged between 30% and 36% Fe. Selective flocculation has had limited success at industrial scale due in part to complex ore mineralogy and thus the sample selected needed to be mineralogically simple and well liberated. The principal mineral of the sample selected was hematite which was well liberated from the dominant gangue quartz. The particle size distribution of the feed determined by laser diffraction revealed that 50% of the

sample passes 16.75 ± 3.10 µm by volume (Dv (0.5)) indicating the sample contains a considerable proportion of slimes. All the feed characteristics indicated this sample was well suited to selective flocculation.

The next aspect that needed to be addressed was the selection of an appropriate dosage for the dispersant sodium silicate. Selective flocculation requires adequate dispersion of particles in the primary step of the process to prevent heteroflocculation. In order to determine if adequate dispersion was occurring prior to selective flocculation, rheology testwork was conducted on the as-is slurry to determine the yield stress. A yield stress of zero indicates a net repulsive force exists between particles and thereby the particles are well dispersed. Rheology tests were conducted on solutions of varying sodium silicate dosages, and pulp densities at low shear rates of 0.1s-1 and 168s-1 and the shear stress was measured accordingly. The raw data was modelled using the Herschel-Bulkley model in order to calculate the yield stress. The calculated yield stresses ranged from 0.003 Pa to 1.091 Pa with lower yield stresses achieved at lower pulp densities and higher sodium silicate dosages. The work of Song et al. (2002) revealed that higher pulp densities of 45% solids achieved similar results to that of a dilute slurry (20% solids) at half the conditioning time. In light of this, a pulp density of 45% solids was selected to minimise flocculation residence times. The lower the viscosity, the better the separation efficiencies of process units and at a pulp density of 45% solids the dispersant dosage that provided the lowest apparent viscosity was 1-1.5kg/ton. From these results, a pulp density and sodium silicate dosage of 45% solids and 1kg/ton was selected respectively as these conditions achieved a low calculated yield stress of 0.558Pa as well as lower viscosities compared to the other ranges tested. The low yield stress indicates that a force of small magnitude is required to overcome the attractive forces between the solids thereby allowing for adequate dispersion. It is expected that during the first stage of the flocculation process, namely the dispersion stage, conducted in a 1L flotation cell and stirring speed of 1200 rpm will provide sufficient force to overcome the attractive forces to ensure dispersion occurs.

The bottom size limitation of current process equipment; ranging from gravity separation, magnetic separation, electrostatic separation to flotation; prevents the application of these units to slimes beneficiation. Below 20 µm matrix magnets and

froth flotation are the only units capable of treating low-value high throughput commodities like iron ore. In South Africa, gravity and magnetic separation are the primary equipment used for the beneficiation of iron ore. For gravity and magnetic separation, the dominant competing force in these units is hydrodynamic drag with this latter force dominating for small particles. However, the gravity and magnetic separation forces can be increased through increasing particle sizes. Increasing the particle size can be achieved through selective flocculation with researchers establishing a link between floc size and pH. By analysing the zeta potential of hematite, Yin et al. (2011) found its hydrophobicity increased in the pH range 9-11. Increased hydrophobicity was demonstrated to yield bigger flocs, and thus pH selection was the next critical aspect to be addressed in the selective flocculation process. The pH was varied from 9 to 11 at increments of 0.5 with the selective flocculation conditions maintained at the centre point conditions of the optimisation study that was to follow (45% pulp density; 1 kg/ton of sodium silicate and sodium oleate; 3 kg/ton paraffin and conditioning time of 10 minutes). The floc size at each pH was measured using the Saturn Digisizer and Malvern Mastersizer. The latter unit had a sample dispersion unit that yielded reproducible results as opposed to the Saturn Digisizer. The laser diffraction results from the Malvern Mastersizer indicated increasing floc size with increasing pH with the Dv (0.5) of the feed doubling at a pH of 11.

Although an increase in floc size was achieved the selectivity of the flocculation stage as a function of pH needed to be established and thus the selective flocculation process was coupled with magnetic separation. Prior to the coupling process, it was important to determine which magnetic field intensity would achieve the best metallurgical performance and thus without selective flocculation the magnetic field intensity was varied from 3 000 Gauss to 6000 Gauss. The results showed that increasing the magnetic field intensity without selective flocculation improved both the separation efficiency and Fe recovery (maximum 40±1.46% and 72.1±3.15% respectively) while maintaining the Fe grade at 52-54%. The selectively flocculated material at each of the five pHs was subjected to magnetic separation at a magnetic field intensity of 6 000 Gauss to determine the effect of pH on selectivity. Despite increased floc sizes with increasing pH, the magnetic separation results indicated similar separation efficiency, concentrate Fe grade, and recoveries were achieved

across the pH range of 10-11 with the least deviation occurring at a pH of 10. These results indicated a pH of 10 was suitable and that the coupling of selective flocculation with magnetic separation would provide more information regarding the important response variables, i.e. separation efficiency, concentrate Fe grade and recovery. This coupling approach was also applied to the next aspect investigated namely the optimisation of the process conditions in selective flocculation.

The final aspect of the selective flocculation process was to determine the optimum selective flocculation parameters in the FMS process to achieve the best results for the response variables within defined parameter constraints. Song et al. (2002) and Yin et al. (2011) defined the critical parameters that affect selective flocculation when sodium oleate is used as the flocculating agent/collector. These critical parameters are pH, stirring speed and time, % solids and dosages of dispersants, collectors and non-polar oils. With the pH, % solids and sodium silicate dosage defined in the previous aspects, the remaining three parameters were investigated in this aspect. At the best sodium silicate dispersant dosage at 45% solids and a pH of 10, a Box-Behnken design matrix was employed whereby selective flocculation was coupled with magnetic separation. Seventeen runs in triplicate were employed to study the effect of three factors (sodium oleate dosage, paraffin dosage and conditioning time each at three levels) on the response variables separation efficiency, concentrate Fe grade and recovery. The ANOVA results indicated the models for separation efficiency and concentrate Fe grade were significant whereas the models for Fe recovery were insignificant. Using the models for the significant response variables optimisation of the three factors was conducted by simultaneously maximising separation efficiency and concentrate Fe grade whilst minimising sodium oleate dosage, paraffin dosage and conditioning time. The optimised factors (500g/t sodium oleate; 1431.1g/t paraffin; 4.6 min conditioning time) achieved similar results to the best selective flocculation test but at half the paraffin dosage.

The optimised selective flocculation parameters, determined by coupling selective flocculation with magnetic separation, was applied to the Reflux Classifier (RC) to determine if selective flocculation would improve the metallurgical performance of the RC. As a baseline test, a semi-batch RC test without selective flocculation was conducted in which the water fluidisation rate was varied. A similar approach was

applied to the test in which selective flocculation was coupled with the RC. In this latter test selective flocculation of the feed sample at the optimised flocculation parameters was conducted before the RC semi-batch test. The results indicated that optimised selective flocculation did not improve the RC separation efficiency, concentrate Fe grade and concentrate recovery when compared to the baseline test (RC without selective flocculation). Potential reasons for the poor performance on the RC could be attributed to the long residence times for the test and pH of the fluidisation water affecting the floc's characteristics and its selectivity. In addition the optimised floc conditions for the SLon may not be the best floc conditions for the RC. The low solids concentration in the semi-batch tests (0.05 solid volume fraction) facilitate a size separation as opposed to density separation and it is expected that a continuous run would improve the results through the activation of the autogenous media separation zone. It is recommended that should sufficient feed be available a continuous run with and without flocculation be conducted with a smaller gap spacing to validate these findings before the RC is conclusively ruled out.

The results from this study showed promising results for selective flocculation coupled with magnetic separation (SLon) confirming the positive findings from literature. At a background magnetic field intensity of 6000 Gauss, optimised selective flocculation coupled with magnetic separation improved the magnetic product Fe grade from 52.28±0.38% to 59.21±0.42% Fe whilst simultaneously improving the separation efficiency from 40.0±1.5% to 56.8±2.0% and maintaining the Fe concentrate recovery within the 95% confidence limits (69.9±2.0%).

A reagent operating cost trade-off study was conducted to compare the revenue generated from the concentrate produced without flocculation to the revenue after reagent costs for the concentrate produced by the optimised Floc Magnetic Separation (FMS) and to determine if the reagent cost associated with the FMS process justifies its application in industry. Assuming the concentrates from either process could be sold the revenue for the FMS process after reagent costs would be R27 million per month which is 39% higher than the revenue generated from magnetic separation without selective flocculation. The simplified reagent operating cost trade-off study indicates that the additional reagent cost required for selective flocculation is justified. However a thorough techno-economic study is recommended to accurately capture

all the costs involved in the process, and if economical it is recommended that the FMS process is piloted first with artificial slimes and then slimes from a metallurgical plant to confirm the improved performance.

The conditions for the laboratory testwork were somewhat idealized and in practice conditions could be different thereby affecting the end result. The limitations of the study and factors influencing selective flocculation is presented in Sections 3.2.2 and 2.5.3 respectively. Figure 9.1 graphically shows the complexity between the multiple aspects of the FMS process and the interrelations between factors and the subsequent impact on the separation performance. The practical application of the FMS process is dependent on the various interactions and stating what impact more practical conditions would have on the conclusions presented above would be rather speculative without an appropriate and much wider investigation than was envisaged for this study. The application of the FMS process would need to be preceded by a careful experimental programme due the complexity and interrelationship between the ore characteristics, selective flocculation and the solid-solid separator.

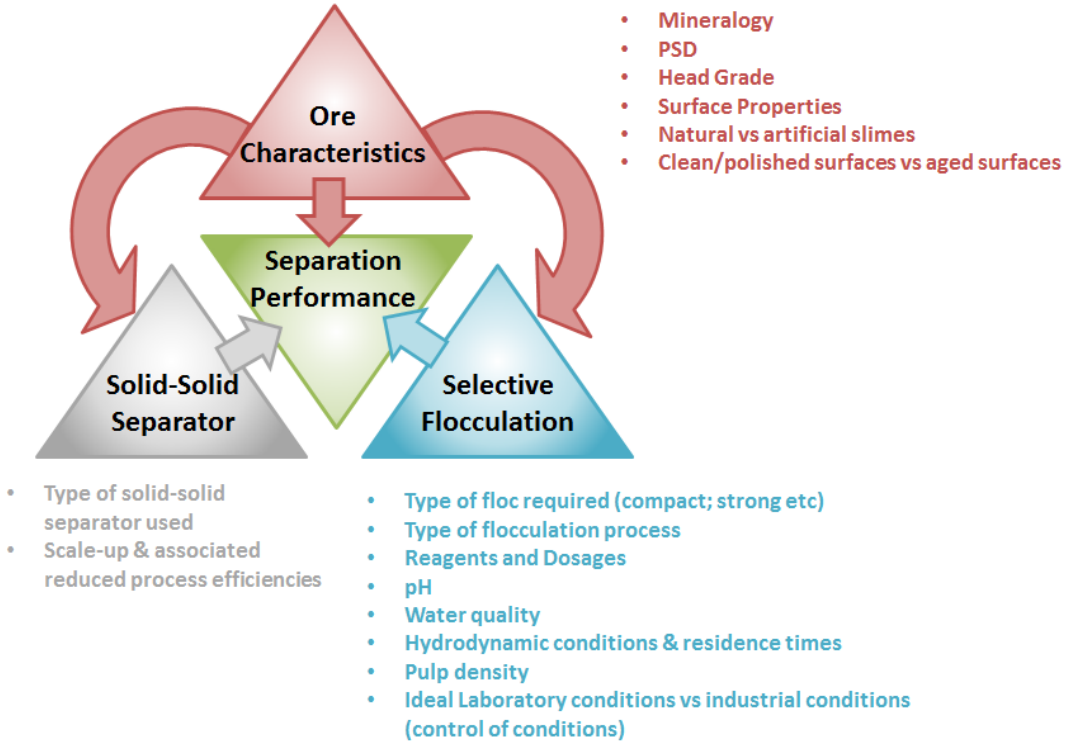


Figure 9.1: A graphical representation of the interrelationships between ore characteristics, selective flocculation and the solid-solid separator

REFERENCES

1. Abro, M.I., 2009. Upgradation of Dilband Iron Ore. PhD thesis. Mehran University of Engineering & Technology, Pakistan [online]. Available at: http://prr.hec.gov.pk/thesis/554s.pdf [accessed: January 2015]
2. Abro, M.I., Pathan, A.G., Memon, A.R., Sirajuddin, 2013. Dual polymer flocculation approach to overcome activation of gangue minerals during beneficiation of complex iron ore. *Powder Technology* [online]. 245 p. 281-291. Available at: http://www.sciencedirect.com/science/article/pii/S0032591013003240 [accessed: October 2014.
3. Ahmed, H.A.M. & Mahran, G.M.A., 2013. Processing of Iron ore fines from Alswaween Kingdom of Saudi Arabia. Physiochemical Problems of Mineral Processing. 49 (2), p. 419-430. Available at: http://www.minproc.pwr.wroc.pl/journal/pdf/ppmp49-2.419-430.pdf [accessed: October 2014]
4. Aljazeera, 2015. *Dam burst at mining site devastates Brazilian town* [online]. Available at: http://www.aljazeera.com/news/2015/11/dam-burst-mining-site-devastates-brazilian-town-151106022548631.html [accessed: 11 January 2016]
5. Allwood, J.M. Cullen, J.M., Carruth M.A., Milford, R.L., Patel, A.C.H., Moynihan, M., Cooper, D.R., MaBrien, M., 2011. *Going on a metal diet, Using less liquid metal to deliver the same services in order to save energy and carbon* [online]. United Kingdom: University of Cambridge. Available at: http://www.uselessgroup.org/files/wellmet2050-going-on-a-metal-diet.pdf [accessed: 21 August 2014]
6. Amariei, D., Michaud, D., Paquet, G., Lindsay M., 2014. The use of a Reflux Classifier for iron ores: Assessment of fine particles recovery at pilot scale. *Minerals Engineering* [online]. 62, p. 66-73. Available at: http://www.sciencedirect.com/science/article/pii/S0892687513003828 [accessed: July 2015]
7. Angadi, S. I, Ho-Seok J., Mohanthy.S, Prakash. S and Das, S., 2012. Analysis of Wet High-Intensity Magnetic Separation of Low-Grade Indian Iron Ore using Statistical Technique, *Separation Science and Technology*, [online]. 47 (8),

p.1129-1138. Available at: http://www.tandfonline.com/doi/abs/10.1080/01496395.2011.644020 [accessed: 24 August 2017]

8. Ansari, M., 1997. Fine particle processing – A difficult problem for mineral engineers. *Proceedings of National Seminar on Processing of Fines*, Jamshedpur, India, 9-10 January 1997. NML, Jamshedpur. pp.93-102.
9. Araujo, A.C., Viana, P.R.M, Peres, A.E.C., 2005. Reagents in iron ores flotation. *Minerals Engineering*. 18, p. 219-224.
10. Arol, A.I. & Aydogan., A., 2004. Recovery enhancement of magnetite fines in magnetic separation. *Colloids and Surfaces A: Physiochemical Engineering Aspects* [online]. 232, p. 151-154. Available at: http://www.sciencedirect.com/science/article/pii/S0927775703006113 [accessed: May 2014]
11. Astrup, J., Hammerbeck, E.C.I., van den Berg, H., 1998. Iron. In M.G.C Wilson and C.R. Anhaeusser, eds. *The Mineral Resources of South Africa, 6th ed.* South Africa: Council for Geosciences, 16, p.402-416
12. BBC, 2015. *Brazil dam collapse death toll rises to 17, BHP says* [online]. Available at: http://www.bbc.com/news/business-35158646 [accessed: 11 January 2016]
13. Bhaskar, R., 2014. *Introduction to rheology. [O*nline].R. C. Patel Institute of Pharmaceutical Education & Research. Available at: http://www.slideshare.net/RajveerBhaskar/introduction-to-rheology-34896958 [accessed: May 2016]
14. Birdi, K.S., 2002. *Handbook of Surface and Colloid Chemistry*, 2nd ed. New York: CRC Press
15. Blas, J., 2010. Annual Iron ore contract system collapses [online]. Available at: https://www.ft.com/content/e8a78a74-3c21-11df-b40c-00144feabdc0 [accessed: 17 August 2017]
16. Bulatovic, S.M., 2007. *Handbook of Flotation Reagents: Chemistry, Theory and Practice: Flotation of Sulphide ores.* [e-book]. Oxford: Elsevier Science & Technology Books. Available at:http://msface.webs.com/documents/Handbook%20of%20Flotation%20Reagents_%20Elsevier%20%282007%29_%200444530290.pdf [accessed: June 2014]

17. Chandraprabha, M.N., Natarajan, K.A., Modak, J.M., 2004. Selective separation of pyrite and chalcopyrite by biomodulation. *Colloids and Surfaces B: Biointerfaces* [online]. 37, p. 93-100. Available at: http://www.sciencedirect.com/science/article/pii/S0927776504001894 [accessed: August 2014]
18. Chemicool Dictionary, 2017. *Definition of van der Waals forces* [online]. Available at: https://www.chemicool.com/definition/van_der_waals_forces.html [accessed: 27 March 2018]
19. Creamer Media, 2017. *Iron Ore Report, April 2017* [online]. Available at: http://www.creamermedia.co.za/article/iron-ore-2017-a-review-of-the-iron-ore-sector-pdf-report-2017-04-11 [accessed: 24 May 2017]
20. Da Corte, C., Nembudani, P., Marape, G., Dayal, D.P., Moloane, T., Sehlotho, N., Erwee, M., Maphutha, P., Bergmann, C., 2016*. FMO2 Physical beneficiation of fines for ore, Internal Report 42619*. South Africa: Mintek
21. Da Corte, C., Sindane, Z., Sehlotho, N., Thiele, H., Bryson, M.,2015*. Fine Fe Ore Processing by Gravity, Magnetic and Flotation Techniques, Internal Report 42023*. South Africa: Mintek
22. Dey, S., Pani, S., Mohanta, M.K., Singh, R., 2012. Utilization of Iron Ore Slimes: A future perspective. *Separation Science and Technology* [online], 47. p. 769-776. Available at: http://www.tandfonline.com/doi/abs/10.1080/01496395.2011.621501 [accessed: 21 February 2016]
23. Doroodchi, E., Zhou, J., Fletcher, D.F., Galvin, K.P., 2006. Particle size classification in a fluidised bed containing parallel inclined plates. *Minerals Engineering* [online]. 19, p. 162-171. Available at: http://www.sciencedirect.com/science/article/pii/S0892687505002827 [accessed: January 2015]
24. Drzymala, J. & Fuerstenau, D.W., 2014. Selective flocculation of hematite in quartz-hematite-ferric-ion-polyacrylic acid system. Part 2. Effect of grinding and a hydrofluoric treatment on selectivity of flocculation. *International Journal of Mineral Processing* [online]. 129, p. 1-5. Available at: http://www.sciencedirect.com/science/article/pii/S0301751614000544 [accessed: November 2014]

25. Dworzanowski, M., 2014. Maximising haematite recovery within a fine and wide particle size distribution using wet high intensity magnetic separation. *The Journal of The Southern African Institute of Mining and Metallurgy*. 114, p. 559-567.
26. Elmhurst College, 2003. *Hydrogen Bonding* [online]. Available at: http://chemistry.elmhurst.edu/vchembook/161Ahydrogenbond.html [accessed: 27 March 2018]
27. Eriez, 2016. High Intensity Wet Magnetic Separator, Series L Model 4 Laboratory Separator. USA: Eriez
28. Filippov, L.O., Severov, V.V., Filippova, I.V., 2014. An overview of the beneficiation of iron ores via reverse cationic flotation. *International Journal of Mineral Processing,* [online]. Available at:http://ac.els-cdn.com/S0301751614000155/1-s2.0-S0301751614000155-main.pdf?_tid=fb3cbe70-9861-11e3-a0b5-00000aab0f02&acdnat=1392703414_b03aecd893c3d670a33e164aa8a42480 [accessed: June 2014].
29. Fluent Inc., 2006. Viscosity for Non-Newtonian Fluids [online]. Available at: https://www.sharcnet.ca/Software/Fluent6/html/ug/node340.htm [accessed: May 2016]
30. Forbes, E., 2011. Shear, selective and temperature responsive flocculation: A comparison of fine particle flotation techniques. *International Journal of Minerals Processing* [online]. 99, p. 1-10. Available at: http://www.sciencedirect.com/science/article/pii/S0301751611000226 [accessed: February 2015]
31. Franks, D.M., Boger, D.V., Cote, C.M., Mulligan, D.R., 2011. Sustainable development principles for the disposal of mining and mineral processing wastes. *Resources Policy* [online]. 36, p. 114-122. Available at: http://www.sciencedirect.com/science/article/pii/S0301420710000747 [accessed: 23 February 2015].
32. French, A., Macedo, M., Poulsen, J., Waterson, T., and Yu, A., 2008. *Multivariate Analysis of Variance (MANOVA)* [online]. Available at: http://userwww.sfsu.edu/efc/classes/biol710/manova/manovanewest.htm [accessed: 13 January 2015]

33. Galvin, K.P., 2009. Water based fractionation of particles. *Chemical Engineering Research and Design* [online]. 87, p. 1085-1099. Available at: http://www.sciencedirect.com/science/article/pii/S0263876209000136 [accessed: January 2015]
34. Galvin, K.P., 2016. *Request assistance with RC operating conditions for Fe ore slimes* [E-mail]. Message to C. Da Corte (carlad@mintek.co.za). Sent 26 February 2016, 12:35 pm.
35. Galvin, K.P., Doroodchi, E., Callen, A.M., Lambert, N., Pratten, S.J., 2002. Pilot plant trial of the Reflux Classifier. *Minerals Engineering* [online]. 15, p. 19-25. Available at: http://www.sciencedirect.com/science/article/pii/S0892687501001935 [accessed: January 2015]
36. Galvin, K.P., Walton K., Zhou, J., 2009. How to elutriate particles according to their density. *Chemical Engineering Science* [online]. 64, p. 2003-2010. Available at: http://www.sciencedirect.com/science/article/pii/S0009250909000554 [accessed: January 2015]
37. Galvin, K.P., Zhou, J., Dickinson, J.E., Ramadhani, H., 2012. Desliming of dense minerals in fluidized beds. *Minerals Engineering* [online]. 39, p. 9-18. Available at: http://www.sciencedirect.com/science/article/pii/S0892687512002518 [accessed: January 2015]
38. Galvin, K.P., Zhou, J., Price, A.J., Agrwal, P., Iveson, S.M., 2016a. Single-stage recovery and concentration of mineral sands using a REFLUX Classifier. *Minerals Engineering* [online]. 93, p. 32-40. Available at: http://www.sciencedirect.com/science/article/pii/S0892687516301029 [accessed: 30 April 2016]
39. Govoreanu, R., Saveyn, H., Van der Meeren, P., Nopens, I., Vanrolleghem, P.A., 2009. A methodological approach for direct quantification of the activated sludge floc size distribution by using different techniques. *Water Science & Technology*. p. 1857-1867.
40. Gregory, J. & Barany, S., 2011. Adsorption and flocculation by polymers and polymer mixtures. *Advances in Colloid and Interface Science* [online]. 169, p. 1-12. Available at:

http://www.sciencedirect.com/science/article/pii/S0001868611001229 [accessed: May 2015]

41. Grinnel College, n.d. *ANOVA: Full factorial Designs* [online]. Available at: http://web.grinnell.edu/individuals/Kuipers/stat2labs/Handouts/DOE%20Introductionh.pdf [accessed: 13 January 2015]
42. Hackley, V.A., Ferraris, C.F. *NIST Special Publication 946, Guide to Rheological Nomenclature for Liquid-Based Particulate Systems* [online]. USA National Institute of Standards and Technology. Available at: http://ciks.cbt.nist.gov/~garbocz/SP946/ [accessed: May 2016]
43. Hanumantha Rao, K., and Narasimhan, K.S., 1985. Selective flocculation applied to Barsuan Iron Ore tailings. *International Journal of Mineral Processing* 14, p. 67-75. Netherlands: Elsevier Science Publishers B.V
44. Haselhuhn, H.J., Carlson, J.J., Kawatra, S.K., 2012. Water chemistry analysis of an industrial selective flocculation dispersion hematite ore concentrator plant. *International Journal of Mineral Processing* [online]. 102-103, p. 99-106.
45. Helmenstine, A., 2017. *Intermolecular Force Definition in Chemistry* [online]. Available at: https://www.thoughtco.com/definition-of-intermolecular-force-605252 [accessed: 28 March 2018]
46. Hunter, D.M., Iveson, S.M., Galvin, K.P., 2014. The role of viscosity in the density fractionation of particles in a laboratory-scale Reflux Classifier. *Fuel* [online]. 129, p. 188-196. Available at: http://www.sciencedirect.com/science/article/pii/S0016236114003147 [accessed: January 2015]
47. Hunter, D.M., Zhou, J., Iveson, S.M., Galvin, K.P., 2015. Gravity Separation of Ultra-fine Iron Ore in the Reflux Classifier. In, AusIMM and CSIRO, *Iron Ore Conference*. Perth, Australia 13-15 July 2015. AusIMM: Australia
48. Huynh, L., Jenkins, P., Ralston, J., 2000. Modification of the rheological properties of concentrated slurries by control of mineral-solution interfacial chemistry. *International Journal of Mineral Processing* [online]. 59 (4), p. 305-325. Available at: http://www.sciencedirect.com/science/article/pii/S0301751699000824 [accessed: 12 June 12016]

49. IUPAC, 2002. *Chemisorption and physisorption* [online]. Available at: http://old.iupac.org/reports/2001/colloid_2001/manual_of_s_and_t/node16.html [accessed: 24 November 2015]
50. Joglekar, A. M. and May, A.T., 1987. Product excellence through design of experiments. *Cereal Foods World*. 2, p 857-868.
51. Jones, F., 1998. *The Mechanism of Bayer Residue Flocculation*. PhD. Thesis. Curtin University of Technology: School of Applied Chemistry. Online. Available at: http://espace.library.curtin.edu.au/R/?func=dbin-jump-full&object_id=10520&local_base=GEN01-ERA02 [accessed: 14 September 2015]
52. Kar, B., Sahoo, H., Rath, S.S., Das, B., 2013. Investigations on different starches as depressants for iron ore flotation. *Minerals Engineering* [online]. 49, p. 1-6. Available at:http://ac.els-cdn.com/S0892687513001453/1-s2.0-S0892687513001453-main.pdf?_tid=3c8ce642-9863-11e3-8574-00000aab0f02&acdnat=1392703953_42d40af7ae4b746b90d81daf9a88e8dd [accessed: June 2014]
53. Khalili, A., Mostoufi, N., Sadeghi, F., Hosseinzadeh, M., Fatourechi, H., Sarrafzadeh, M.H., Mehrnia, M.R., 2011. Comparison between different models for rheological characterisation of activated sludge. Iranian Journal of Environmental Health Science & Engineering [online]. 8 (3), p. 255-264. Available at: https://www.researchgate.net/publication/236898350_Comparison_between_different_models_for_rheological_characterization_of_activated_sludge [accessed: May 2016]
54. Kumba, 2007. *Kumba Iron Ore, Annual Report 2007* [Online]. Available at: http://www.kumba.co.za/reports/kumba_ar07/or_sishen.php [accessed: 26 May 2014].
55. Laskovski, D., Duncan, Stevenson, P., Zhou, J., Galvin, K.P., 2006. Segregation of hydraulically suspended particles in inclined channels. *Chemical Engineering Science* [online]. 61, p. 7269-7278. Available at: http://www.sciencedirect.com/science/article/pii/S000925090600515X [accessed: January 2015]
56. Levay, G. & Schumann, R., 2006. A systematic approach to water quality management in the minerals processing industry. In, The Australasian Institute

of Mining and Metallurgy, *Water in Mining Conference*. Brisbane, Australia, 14-16 November 2006, The Australasian Institute of Mining and Metallurgy: Australia.

57. Li, C., Sun, H., Bai, J., Li, L., 2010. Innovative methodology for comprehensive utilization of iron ore tailings Part 1. The recovery of iron from iron ore tailings using magnetic separation after magnetizing roasting. *Journal of Hazardous Materials*. [online]. Available at: http://www.sciencedirect.com/science/article/pii/S0304389409014642 [accessed: February 2015].
58. Lodesova, D., Lodes, A., 1983. Rheological behaviour of the fiber-forming mixture viscose hydroxyethylcellulose. Rhelogica Acta [online]. 22 (4), p. 396-401. Available at: http://link.springer.com/article/10.1007/BF01333770 [accessed: June 2016]
59. Lumen, n.d. *Functional Group Names, Properties and Reactions* [online]. Available at: https://courses.lumenlearning.com/boundless-chemistry/chapter/functional-group-names-properties-and-reactions/ [accessed: 27 March 2018]
60. Ma, M., 2011. The dispersive effect of sodium silicate on kaolinite particles in process water: implication for iron-ore processing. *Clays and Clay Minerals*. 59 (3), p.233-239.
61. Ma, M., 2012. The significance of dosing sequence in the flocculation of hematite. *Chemical Engineering Science* [online]. 73, p. 51-54. Available at: http://www.sciencedirect.com/science/article/pii/S0009250912000401 [accessed: September 2014].
62. Malvern Instruments Ltd., 2007. *Mastersizer 2000 User Manual*.UK: Malvern Instruments Ltd.
63. Malvern Instruments Ltd., 2007a. *Hydro 2000MU User Manual*.UK: Malvern Instruments Ltd.
64. Mangesana, N., Chikuku, R.S., Mainza, A.N., Govender, I., van der Westhuizen, A.P., Narashima, M., 2008. The effect of particles sizes and solids concentration on the rheology of silica sand based suspensions. *The Journal of The Southern African Institute of Mining and Metallurgy* [online]. 108, p. 237-243. Available at: https://www.saimm.co.za/Journal/v108n04p237.pdf [accessed: 21 September 2016]

65. Mathur, S., Singh, P., Moudgil, B.M., 2000. Advances in selective flocculation technology for solid-solid separations. *International Journal of Minerals Processing* [online]. 58, p. 201-222. Available at: http://www.sciencedirect.com/science/article/pii/S0301751699000721 [accessed: February 2015]
66. Montgomery, D., 2009. Design and Analysis of Experiments. 7th Ed. United States: John Wiley & Sons, Inc
67. Murty, V.G.K, Murthy, V.R, JaiSankar, N, Bhavya Manjeera, P and Kumar, P., 2013. Operation and optimization of silliminite beneficiation from beach sands, *International Journal of Advanced Research* [online]. 1, p 347-355. Available at: http://www.journalijar.com/article/195/operation-and-optimization-of-sillimanite-beneficiation-from-beach-sands/ [accessed: 24 August 2017]
68. Muster T. H., Prestidge C. A., (1995). Rheological investigation of sulphide mineral slurries. *Minerals Engineering*. 8, p. 1541 – 1555.
69. Nguyen, Q., and Ngoc-Diep Nguyen, N., 2012. Incompressible Non-Newtonian Fluid Flows, Continuum Mechanics - Progress in Fundamentals and Engineering Applications, Dr. Yong Gan (Ed.), ISBN: 978-953-51-0447-6, InTech. Available from: http://www.intechopen.com/books/continuum-mechanics-progress-infundamentals-and-engineering-applications/non-newtonian-fluid-flows [accessed: June 2016]
70. Nguyentranlam, G., Galvin, K.P., 2004. Applications of the Reflux Classifier in solid-liquid operations. *International Journal of Minerals Processing* [online]. 73, p. 83-89. Available at: http://www.sciencedirect.com/science/article/pii/S0301751603000656 [accessed: January 2015]
71. NIST, 2012. *e-Handbook of Statistical Methods.* [e-book]. USA: NIST (U.S. Department of Commerce. Available at: http://www.itl.nist.gov/div898/handbook [accessed: July 2015]
72. Orupold, T., Starr, D., Kenefick, T., 2014. The lamella high shear rate Reflux Classifier. *Journal of the Southern African Institute of Mining and Metallurgy*. 114 (7), p. 511-518.
73. Outotec, 2010. *SLon 100 Procedure and Test Parameter Guidelines*. USA: Outotec

74. Outotec, 2012. *Installation, Operation and Maintenance Manual. Equipment Name: SLon Model 100.* USA: Outotec
75. Panda, L., Banerjee, P.K., Biswal, S.K., Venugopal, R., Mandre, N.R., 2014. Modelling and optimisation of process parameters for beneficiation of ultrafine chromite particles by selective flocculation. *Separation and Purification Technology* [online], 132 p. 666-673. Available at: http://www.sciencedirect.com/science/article/pii/S1383586614003190 [accessed: September 2015]
76. Parsaei, R., Alamdari. A., Jahanmiri, A., Rajabzadeh, 2006. Preconcentration of low grade sedimentary phosphate ore using selective flocculation. *The Pacific Journal of Science and Technology* [online]. 7, p.77-83. Available at: http://www.akamaiuniversity.us/PJST7_1_77.pdf [accessed: September 2015]
77. Pascoe, R.D. & Doherty, E., 1997. Shear flocculation and flotation of hematite using sodium oleate. *International Journal of Mineral Processing*. 51, p. 269-282.
78. Pascoe, R.D. & Wills, B.A., 1994. Selective aggregation of ultrafine hematite and quartz under high shear conditions with conventional flotation collectors. *Minerals Engineering*. 7, p. 647-656.
79. Patil, D.P., Andrews, J.R.G, Uhlherr, P.H.T., 2001. Shear flocculation-kinetics of floc coalescence and breakage. *International Journal of Mineral Processing*. 61, p. 171-188.
80. Patra, P., & Natarajan, K.A., 2003. Microbially-induced flocculation and flotation for pyrite separation from oxide gangue minerals. *Minerals Engineering* [online]. 16, p. 965-973. Available at: http://www.sciencedirect.com/science/article/pii/S0892687503002681 [accessed: August 2014]
81. Patra, P., & Natarajan, K.A., 2004. Microbially induced flotation and flocculation of pyrite and sphalerite. *Colloids and Surfaces B: Biointerfaces* [online]. 36, p. 91-99. Available at: http://www.sciencedirect.com/science/article/pii/S0927776504001419 [accessed: August 2014]
82. Patra, P., & Natarajan, K.A., 2008. Role of mineral specific bacterial proteins in selective flocculation and flotation. *International Journal of Mineral Processing* [online]. 88, p. 53-58. Available at:

http://www.sciencedirect.com/science/article/pii/S0301751608001002 [accessed: August 2014]

83. Pennsylvania State University, 2018. *A residual vs. fits plot* [online]. Available at: https://onlinecourses.science.psu.edu/stat501/node/36 [accessed: 29 January 2018]
84. Platts, 2016. *Platts Market Data – Metals Sample, June 2016* [online]. Available at: https://www.platts.com/ [accessed: 17 August 2017]
85. Poorni, S., & Natarajan, K.A., 2013. Microbially induced selective flocculation of hematite from kaolinite. *International Journal of Mineral Processing* [online]. 125, p. 92-100. Available at: http://www.sciencedirect.com/science/article/pii/S0301751613001981 [accessed: August 2014]
86. Pradhan., N., Das., B., Gahan., C.S., Kar., R.N., Sukla, L.B., 2006. Beneficiation of iron ore slime using bacteria. *Bioresource Technology* [online]. 97. p. 1876-1879. Available at: http://www.sciencedirect.com/science/article/pii/S0960852405004001 [accessed: May 2014]
87. Protea Chemicals, 2017. *Request Reagent Prices* [E-mail]. Message from Q. Vikisi (queeneth.vikisi@proteachemicals.co.za) to C. Da Corte (carld@mintek.co.za). Sent Thursday 26 January 2017, 15:00. Available at: C:\Users\carlad\Documents\Outlook Files\ArchivedInboxItems [accessed: 30 October 2017]
88. Quast, K., 2015. Use of conditioning time to investigate the mechanisms of interactions of selected fatty acids on hematite. Part 1: Literature Review. *Minerals Engineering* [online]. 79, p. 295-300. Available at: http://www.sciencedirect.com/science/article/pii/S0892687515001430 [accessed: April 2016]
89. Rakgase, K., 2012. Applications of the Reflux Classifier on SA coals. In, Coaltech, Coaltech research association annual colloquium. South Africa, 31 August 2012. Coaltech: South Africa
90. Rao, M. A., 2014. *Rheology of Fluid, semisolid and solid Foods Principles and Applications.* 3rd ed. New York: Springer Science & Business Media
91. Rheosys LLC, 2011. A Basic Introduction to Viscometers & Viscometry [online]. Available at: http://www.rheosys.com/intro.html [accessed: May 2016]

92. Roy, S., 2012. Recovery improvement of fine magnetic particles by floc magnetic separation. *Mineral Processing & Extractive Metallurgy. 33,* p.170-179.
93. Santhiya, D., Subramanian, S., Natarajan, K.A., Hanumantha Rao, K., Forssberg, K.S.E., 2001. Bio-modulation of galena and sphalerite surfaces using Thibacillus Thiooxidans. *International Journal of Mineral Processing* [online]. 62, p. 121-141. Available at: http://www.sciencedirect.com/science/article/pii/S030175160000048X [accessed: August 2014]
94. Santhiya, D., Subramanian, S., Natarajan, K.A., Hanumantha Rao, K, 2000.Surface chemical studies on galena and sphalerite in the presence of Thiobacillus Thiooxidans with reference to mineral beneficiation. *Minerals Engineering* [online]. 13 (7), p. 747-763. Available at: http://www.sciencedirect.com/science/article/pii/S0892687500000595 [accessed: August 2014]
95. Shi F. N., Napier-Munn T. J., 2002. Effects of slurry rheology on industrial grinding mill performance. *International Journal of Minerals Processing*. 65, p.125 – 140.
96. Singh, S., Sahoo, H., Rath, S.S., Sahu, A.K. Das, B., 2015. Recovery of iron minerals from Indian iron ore slimes using colloidal magnetic coating. *Powder Technology* [online]. 269, p.38-45. Available at: http://www.sciencedirect.com/science/article/pii/S0032591014007797 [accessed: September 2015]
97. Sivamohan, R., 1990. The problem of recovering very fine particles in Mineral Processing - A review. *International Journal of Mineral Processing.* 28, p. 247-288.
98. Skosana, D.J., 2011. Upgrading of Sishen thickener underflow slimes using the SLon high gradient magnetic separator (HGMS). In The Southern African Institute of Mining and Metallurgy, *Iron Ore and Manganese Ore Metallurgy Conference*. Muldersdrift, South Africa, 5-7 September 2011. The Southern African Institute of Mining and Metallurgy: South Africa.
99. Somasundaran, P., 1978. Selective flocculation of fines. *The Physical Chemistry of Mineral-Reagent Interactions in Sulfide Flotation.* U.S. Bureau of Mines.

100. Somasundaran, P., Runkana, V., 2003. Modelling flocculation of colloidal mineral suspensions using population balances. *International Journal of Minerals Processing* 72. P. 33-55. Available at: http://www.sciencedirect.com/science/article/pii/S0301751603000863 [accessed: March 2015]

101. Song, S., & Lu., S., 2000. Theory and applications of hydrophobic flocculation technology. In, Massacci, P.(Ed.), *Proceedings of the XXI International Mineral Processing Congress*. Rome, Italy. Elsevier: Amsterdam. p. C3-34-C3-41

102. Song, S., Lopez-Valdivieso, A., Ding, Y., 1999. Effects of nonpolar oil on hydrophobic flocculation of hematite and rhodochrosite fines. *Powder Technology*. 101, p. 73-80

103. Song., S., Lu., S. & Lopez-Valdivieso. A., 2002. Magnetic separation of hematite and limonite fines as hydrophobic flocs from iron ores. *Minerals Engineering* [online]. 15, p. 415-422. Available at: http://www.sciencedirect.com/science/article/pii/S0892687502000547 [accessed: May 2014]

104. Stat-ease, 2016. Handbook for Experimenters. [e-book]. Minneapolis (USA): Stat-ease. Available at: www.statease.com/pubs/handbk_for_exp_sv.pdf [accessed: July 2016]

105. Sumnu, S.G. and Sahin, S., 2008. *Advances in Deep-Fat Frying of Foods*. United States of America: CRC Press.

106. Svoboda, J. & Fujita, T., 2003. Recent developments in magnetic methods of material separation. *Minerals Engineering* [online]. 16, p. 785-792. Available at: http://www.sciencedirect.com/science/article/pii/S0892687503002127 [accessed: May 2014]

107. TA Instruments, n.d. Rheology Applications Note [online]. Available at: http://www.tainstruments.com/pdf/literature/RN9.pdf [accessed: June 2016]

108. Tangsathitkulchai C., 2003. The effect of slurry rheology on fine grinding in a laboratory ball mill, *International Journal of Minerals Processing*. 69, p. 29 – 47.

109. Tangsathitkulchai C., Austin L. G., 1989. Slurry density effects on ball milling in a laboratory ball mill. *Powder Technology*. 59, p. 285 – 293.

110. Tripathy, S. K., Bhoja, S.K., Kumar, C.R., Suresh, N., 2015. A short review on hydraulic classification and its development in mineral industry. *Powder Technology* [online]. 270, p. 205-220. Available at: http://www.sciencedirect.com/science/article/pii/S0032591014008493 [accessed: July 2015].

111. Ucbeyiay Sahinkaya, H., Ozkan, A., 2011. Investigation of shear flocculation behaviours of colemanite with some anionic surfactants and inorganic salts. *Separation and Purification Technology* [online]. 80, p.131-139. Available at: http://www.sciencedirect.com/science/article/pii/S1383586611002449 [accessed: September 2015].

112. Umadevi, T., Singh, A.P., Abhishek, K., Suresh, B., Sah, R., 2013. Recovery of Iron Bearing Minerals from Beneficiation Plant 2 Thickener Underflow of JSW Steel Limited. *Journal of Minerals and Materials Characterization and Engineering* [online]. 1, p. 55-60. Available at: http://file.scirp.org/Html/6-2710039_29411.htm [accessed: 21 February 2016]

113. University "Federico II" of Naples, n.d. *Micelles* [online]. Available at: http://www.whatischemistry.unina.it/en/micella.html [accessed: 27 March 2018]

114. Verma, S.R., Chaudhari, P.R., Singh, R.K., Wate, S.R. 2013. Environmental modelling studies on impacts of tailing ponds on groundwater quality at iron ore mines, India. *International Research Journal of Science and Engineering* [online]. 1 (2), p. 31-40. Available at: http://files.cluster2.hostgator.co.in/hostgator121656/file/2.irjse_0102_31-40.pdf [accessed: 23 March 2015]

115. Walton, K. Zhou, J., Galvin, K.P., 2010. Processing of fine particles using closely spaced inclined channels. *Advanced Powder Technology* [online]. 21, p. 386-391. Available at: http://www.sciencedirect.com/science/article/pii/S0921883110000300 [accessed: January 2015]

116. Wang, C., Hartbottle, D., Liu, Q., Xu, Z., 2014. Current state of fine mineral tailings treatment: A critical review on theory and practice. *Minerals Engineering,* 58, P. 113-131. Available at: http://www.sciencedirect.com/science/article/pii/S0892687514000284 [accessed: February 2015]

117. Wang, Y., Sun, D., Wang, L., Zhou, Y., 2011. Effects of sodium tripolyphosphate and sodium carbonate on the selective flocculation of diasporic-bauxite in the presence of calcium and magnesium ions. *Minerals Engineering* [online]. 24 p. 1031-1037. Available at: http://www.sciencedirect.com/science/article/pii/S0892687511001737 [accessed: September 2015]

118. Weissenborn, P.K., 1996. Behaviour of amylopectin and amylose components of starch in the selective flocculation of ultrafine iron ore. *International Journal of Mineral Processing* [online]. 47, p. 197-211.

119. Weissenborn, P.K., Warren, L.J. Dunn, J.G., 1994. Optimisation of selective flocculation of ultrafine iron ore. *International Journal of Minerals Processing* [online]. 42, p. 191-213.

120. Wills, B.A. & Napier-Munn, T.J., 2006. *Wills' Mineral Processing Technology: An introduction to the practical aspects of ore treatment and mineral recovery.* 7th Ed. p. 16. Oxford: Butterworth-Heinemann

121. Wong, M.H., 1981. Environmental impacts of Iron Ore Tailings – The case of Tolo Harbour, Hong Kong [online]. *Environmental Management* [online]. 5 (2), p.135-145. Available at: https://link.springer.com/article/10.1007/BF01867333 [accessed: 17 March 2015].

122. World Bank Group, 2017. Commodity Markets Outlook, October 2017 [online], Washington, DC: World Bank. Available at: http://pubdocs.worldbank.org/en/743431507927822505/CMO-October-2017-Full-Report.pdf [accessed: 02 November 2017]

123. X-Rates, 2017. Monthly average exchange rate for ZAR to USD for year 2016 [online]. Available at: http://www.x-rates.com/average/?from=ZAR&to=USD&amount=1&year=2016 [accessed: 17 August 2017]

124. Yin, W., Yang, X., Zhou, D., Li, Y., Lu, Z., 2011. Shear hydrophobic flocculation and flotation of ultrafine Anshan hematite using sodium oleate. *Transaction of Nonferrous Metals Society of China* [online]. 21, p. 652-644. Available at: http://www.sciencedirect.com/science/article/pii/S1003632611607620 [accessed: 25 August 2015]

125. Zajdela, B., Hribersek, M., Hribernik, A., 2008. Experimental Investigations of Porosity and Permeability of Flocs in the Suspensions of Biological Water Treatment Plants. *Journal of Mechanical Engineering*. 54, p. 547-556. Available at: https://www.sv-jme.eu/?ns_articles_pdf=/ns_articles/files/ojs3/1350/submission/1350-1-2093-1-2-20171103.pdf&id=4731 [accessed: February 2016]

126. Zhan, Y., 1999. Latices as flocculants in selective flocculation of mineral suspensions, PhD. *The University of British Columbia* [online]. Available at: https://circle.ubc.ca/bitstream/id/24937/ubc_1999-464555.pdf [accessed: February 2015]

127. Zhao, Y., Deng, Y., Zhu, J.Y., 2004. Roles of Surfactants in Flotation Deinking. *Progress in Paper Recycling*, [online]. 14(1). Available at: https://www.researchgate.net/publication/228852362_Roles_of_surfactants_in_flotation_deinking. [accessed: 28 March 2018]

128. Zhou, J., Walton, K., Laskovski, D., Duncan, P., Galvin, K.P., 2006. Enhanced separation of mineral sands using the Reflux Classifier. *Minerals Engineering* [online]. 19, p. 1573-1579. Available at: http://www.sciencedirect.com/science/article/pii/S0892687506002147 [accessed: January 2015]

APPENDIX A: RAW DATA FOR SAMPLE PREPARATION AND FEED CHARACTERISATION

Table A.1: Particle size distribution of the HPGR product (-1.18mm)

Size Fraction (µm)	Unit Discrete Mass (%)
-1180+850	13.3
-850+600	16.3
-600+425	11.3
-425+300	11.3
-300+212	8.2
-212+150	6.6
-150+106	5.2
-106+75	4.3
-75+53	3.6
-53+38	3.7
-38+25	2.5
-25+10	11.3
-10+5	0.3
-5	2.1
Total (Calculated)	**100.0**

Table A.2: Milling Curve Raw Data

	Time: 35 min	Time: 40 min	Time: 45 min	Time: 50 min
Size Fraction	**Mass %**	**Mass %**	**Mass %**	**Mass %**
+38µm	27.7	23.9	19.8	16.6
-38µm	72.3	76.1	80.2	83.4
Total	**100.0**	**100.0**	**100.0**	**100.0**

Table A.3: Data reconciliation check for Fe and SiO_2 chemical analysis of testwork products

Unit	Grade (%)		Unit	Grade (%)		Unit	Grade (%)	
	Fe	SiO_2		Fe	SiO_2		Fe	SiO_2
Head	37.41	41.75	SF	57.87	14.00	SF	17.50	67.40
	37.54	41.90		18.47	66.80		57.69	14.20
	37.08	41.70		58.03	13.90		18.38	66.60
SBA	37.72	34.69		18.73	65.80		57.25	14.20
	28.56	50.10		58.43	13.50		18.19	65.70
	37.03	41.65		18.06	66.50		57.53	13.90
	44.07	31.09		58.41	13.60		18.47	66.30
	44.43	32.47		18.03	66.50		56.93	14.90
	42.07	35.89		58.33	12.30		18.06	66.10
	35.65	44.55		18.22	66.70		57.77	13.60
	33.16	44.59		57.07	14.40		17.79	66.70
	33.14	44.61		18.30	66.20		57.52	14.45
Base Case Slon Tests	53.13	21.34		58.59	13.90		17.95	66.70
	55.23	18.51		18.29	67.60		56.80	14.80
	54.73	19.18		59.44	12.60		19.02	65.60
	52.82	21.76		19.39	66.20		56.84	14.50
	53.77	20.48		57.88	14.70		18.86	65.10
	53.35	21.04		19.22	64.80		57.63	13.90
	52.27	22.50		58.16	14.00		18.24	65.20
	52.48	22.22		19.17	65.80		57.47	14.80
	52.10	22.73		58.86	13.70		18.28	66.30
pH Slon Tests	56.10	17.33		18.08	66.80		57.19	14.70
	54.37	19.67		57.91	14.80		18.71	65.40
	58.77	13.72		18.36	66.80		57.65	14.30
	58.42	14.20		58.73	13.60		18.39	65.90
	57.87	14.94		18.49	67.00		57.47	14.60
	58.10	14.63		59.21	13.50		18.50	65.90
	59.29	13.02		18.55	66.30		57.43	14.50
	56.96	16.17		58.62	13.90		18.60	66.00
	58.24	14.45		18.62	66.90		57.49	14.40
	59.33	12.97		58.65	13.80		18.22	66.90
	57.00	16.12		18.12	67.10		57.74	14.65
	57.70	15.17		57.84	13.95		18.57	65.90
SF	58.19	13.55		18.90	65.50		57.80	14.20
	18.20	66.50		57.86	14.00		18.60	66.40
	57.16	14.50		19.22	64.90		57.50	14.50
	18.94	65.90		57.75	13.60		18.36	66.30
	58.27	13.10		17.22	67.70		58.09	14.00
	18.60	66.10		58.05	13.50		18.38	66.80
	59.12	12.80		18.61	65.50		58.05	14.30
	18.02	66.90		58.33	13.30		18.26	66.50

Table A.3: Data reconciliation check for Fe and SiO2 chemical analysis of testwork products (Contd.)

Unit	Grade (%)		Unit	Grade (%)		Unit	Grade (%)	
	Fe	SiO_2		Fe	SiO_2		Fe	SiO_2
SF	58.95	13.00	Optimised SF	20.09	64.40	Base Case RC	26.75	56.95
	18.61	66.20		58.65	16.76		25.71	59.98
	57.89	13.90		21.02	66.77		25.03	63.90
	18.02	66.90		59.41	14.87		27.76	61.10
	58.07	13.80		20.11	69.02		27.62	61.30
	18.08	66.80		58.26	13.44		32.55	54.00
	57.77	14.20		19.70	64.91		35.59	48.90
	18.52	66.20		59.49	13.57		47.10	34.00
	58.55	13.30		20.05	64.45		40.21	42.67
	18.43	66.10		59.73	13.52		19.34	65.40
	57.55	14.35		20.01	64.51		27.31	54.79
	18.08	65.60	Base Case RC	16.05	60.85	Floc RC	16.32	69.41
Optimised SF	59.44	13.41		20.98	57.22		16.05	69.77
	19.02	69.76		23.64	53.80		17.62	67.68
	59.17	15.77		23.57	58.74		21.77	62.17
	19.98	68.48		25.87	58.76		25.20	57.59
	59.19	14.66		21.53	59.61		42.05	35.17
	19.65	67.84		23.18	67.35		20.16	64.30
	58.17	14.17		27.34	61.20		28.28	53.50
	19.49	65.19		28.67	60.50		14.30	72.10
	59.19	14.08		33.71	53.60		15.88	70.00
	18.84	66.06		36.71	49.00		18.43	66.60
	59.18	12.37		45.90	33.40		18.10	67.05
	19.33	69.34		38.49	43.42		19.64	65.00
	59.61	14.62		17.92	58.72		29.78	51.50
	19.77	66.98		22.47	55.73		33.38	46.70
	59.14	15.15		24.33	56.73		42.85	39.30
	19.99	64.52		26.71	56.50		17.55	67.77
	58.26	13.80		27.43	56.47		19.58	65.07
	20.39	63.99		25.22	61.21		19.02	65.82
	59.77	13.27		23.64	65.30		15.03	71.12
	19.19	65.59		27.27	61.70		17.20	68.24
	59.05	12.54		28.95	59.80		18.50	66.52
	20.00	68.59		35.24	51.50		24.35	58.73
	59.28	14.72		35.45	50.80		31.50	49.21
	20.19	68.05		47.55	34.50		28.40	53.33
	59.09	13.39		39.62	44.32		28.00	53.87
	18.90	65.98		18.03	58.32		32.40	48.01
	59.09	14.47		22.02	55.11		43.15	33.70
	20.95	63.26		27.36	54.04			
	59.55	13.46		21.98	58.36			

Table A.4: EPMA raw data of 100 randomly selected Fe oxide grains (15 kV, 20 nA, spot size 5 µm)

Point	O	Mg	Al	Si	Fe	MgO	Al_2O_3	SiO_2	FeO	Total
1	30.43	0.12	0.17	0.26	69.58	0.19	0.32	0.56	99.48	100.55
2	30.39	-	-	0.20	70.20	-	-	0.42	100.37	100.79
3	30.23	0.02	0.05	0.37	69.25	0.04	0.09	0.78	99.01	99.92
4	29.98	0.05	-	0.42	68.57	0.08	-	0.90	98.03	99.01
5	30.42	0.02	0.06	0.20	70.12	0.03	0.11	0.43	100.25	100.81
6	30.43	-	-	0.05	70.67	-	-	0.12	101.03	101.15
7	30.18	-	0.04	0.28	69.39	-	0.08	0.61	99.20	99.89
8	30.52	0.08	0.05	0.43	69.66	0.13	0.10	0.92	99.59	100.74
9	30.18	-	-	0.19	69.74	-	-	0.40	99.70	100.10
10	30.23	-	0.05	0.07	70.05	-	0.10	0.16	100.15	100.41
11	30.23	0.01	-	0.30	69.56	0.02	-	0.63	99.44	100.10
12	30.42	0.04	-	0.09	70.48	0.07	-	0.19	100.77	101.03
13	29.68	-	0.24	0.09	68.35	-	0.45	0.19	97.73	98.36
14	30.25	0.01	-	0.05	70.23	0.02	-	0.11	100.41	100.54
15	29.79	-	-	0.11	69.01	-	-	0.24	98.67	98.91
16	30.58	0.02	-	0.41	70.04	0.03	-	0.88	100.14	101.05
17	30.27	-	-	0.06	70.26	-	-	0.14	100.46	100.59
18	29.94	-	-	0.16	69.25	-	-	0.35	99.00	99.35
19	30.24	-	0.07	0.32	69.37	-	0.14	0.69	99.18	100.01
20	29.98	-	0.04	0.13	69.34	-	0.08	0.27	99.14	99.49
21	30.26	0.02	-	0.30	69.58	0.03	-	0.65	99.49	100.16
22	29.97	0.04	-	0.10	69.40	0.07	-	0.22	99.23	99.52
23	30.44	-	-	0.17	70.40	-	-	0.35	100.65	101.01
24	30.23	0.03	-	0.08	70.08	0.05	-	0.17	100.19	100.42
25	30.18	0.05	-	0.23	69.53	0.09	-	0.49	99.42	99.99
26	30.31	-	-	0.26	69.84	-	-	0.55	99.85	100.40
27	30.29	0.03	-	0.26	69.75	0.04	-	0.56	99.72	100.33
28	30.26	0.04	-	0.23	69.75	0.07	-	0.49	99.73	100.29
29	30.34	0.02	-	0.73	68.64	0.03	-	1.56	98.14	99.73
30	30.36	-	0.06	0.10	70.26	-	0.11	0.22	100.45	100.78
31	30.69	-	-	0.60	69.83	-	-	1.28	99.84	101.12
32	30.30	0.07	-	0.43	69.26	0.12	-	0.92	99.03	100.07
33	30.24	0.03	0.05	0.20	69.70	0.06	0.09	0.43	99.65	100.22
34	29.96	0.02	0.06	0.18	69.11	0.03	0.11	0.38	98.80	99.32
35	30.29	0.03	-	0.24	69.82	0.05	-	0.51	99.82	100.37
36	29.97	-	0.20	0.49	68.04	-	0.37	1.04	97.28	98.69
37	29.94	0.03	-	0.21	69.08	0.05	-	0.45	98.77	99.26
38	30.03	0.02	0.06	0.10	69.46	0.03	0.11	0.21	99.30	99.66
39	30.28	-	-	0.07	70.29	-	-	0.14	100.49	100.63
40	30.08	-	-	0.33	69.12	-	-	0.71	98.82	99.53

Table A.4: EPMA raw data of 100 randomly selected Fe oxide grains (15 kV, 20 nA, spot size 5 µm) (Contd.)

Point	O	Mg	Al	Si	Fe	MgO	Al_2O_3	SiO_2	FeO	Total
41	30.30	-	-	0.26	69.82	-	-	0.56	99.83	100.39
42	30.52	-	0.05	0.46	69.70	-	0.09	0.99	99.66	100.74
43	30.34	0.02	-	0.34	69.65	0.04	-	0.74	99.58	100.35
44	30.36	-	-	0.22	70.05	-	-	0.48	100.15	100.63
45	30.17	-	-	0.06	70.05	-	-	0.13	100.15	100.28
46	30.20	-	-	0.07	70.09	-	-	0.15	100.21	100.36
47	30.04	-	-	0.06	69.73	-	-	0.13	99.69	99.83
48	30.17	0.04	-	0.13	69.83	0.06	-	0.27	99.83	100.16
49	29.91	-	-	0.14	69.23	-	-	0.30	98.98	99.28
50	30.27	-	-	0.06	70.29	-	-	0.13	100.49	100.62
51	30.12	-	-	0.18	69.62	-	-	0.38	99.54	99.92
52	30.14	-	-	0.27	69.43	-	-	0.57	99.27	99.84
53	30.19	0.04	0.20	0.45	68.58	0.06	0.39	0.96	98.06	99.46
54	30.09	-	-	0.03	69.92	-	-	0.07	99.97	100.05
55	30.13	0.03	-	0.33	69.21	0.04	-	0.70	98.95	99.70
56	30.39	0.09	-	0.40	69.52	0.15	-	0.86	99.40	100.41
57	29.91	0.04	-	0.15	69.14	0.07	-	0.32	98.86	99.24
58	30.53	0.05	-	0.25	70.30	0.09	-	0.54	100.51	101.14
59	30.26	0.01	0.04	0.19	69.79	0.02	0.08	0.41	99.79	100.30
60	30.30	-	-	0.11	70.20	-	-	0.24	100.37	100.61
61	30.16	-	0.04	0.07	69.93	-	0.08	0.14	99.97	100.20
62	29.91	0.02	-	0.09	69.32	0.04	-	0.20	99.11	99.35
63	30.10	0.02	0.07	0.21	69.32	0.03	0.13	0.45	99.12	99.73
64	30.38	0.03	-	0.18	70.15	0.05	-	0.39	100.30	100.75
65	30.14	0.01	-	0.48	68.84	0.02	-	1.04	98.43	99.48
66	30.19	-	0.05	0.10	69.88	-	0.10	0.21	99.91	100.22
67	30.34	-	-	0.04	70.48	-	-	0.10	100.77	100.86
68	30.36	-	-	0.05	70.50	-	-	0.11	100.80	100.91
69	30.17	-	-	0.26	69.51	-	-	0.56	99.38	99.94
70	30.28	0.03	-	0.22	69.84	0.04	-	0.46	99.86	100.36
71	30.17	0.02	-	0.33	69.30	0.03	-	0.71	99.08	99.81
72	30.29	-	-	0.20	69.95	-	-	0.43	100.01	100.45
73	30.44	0.05	-	0.45	69.55	0.09	-	0.96	99.44	100.49
74	30.29	-	-	0.05	70.34	-	-	0.11	100.57	100.68
75	29.97	0.03	0.23	0.48	67.95	0.04	0.44	1.03	97.15	98.67
76	30.25	0.02	-	0.20	69.83	0.03	-	0.43	99.84	100.30
77	30.61	0.02	-	0.25	70.54	0.04	-	0.54	100.85	101.43
78	29.92	-	-	0.17	69.18	-	-	0.36	98.91	99.27
79	30.56	0.02	-	0.38	70.09	0.03	-	0.81	100.21	101.05
80	30.55	0.03	-	0.25	70.38	0.05	-	0.54	100.63	101.21

Table A.4: EPMA raw data of 100 randomly selected Fe oxide grains (15 kV, 20 nA, spot size 5 µm) (Contd.)

Point	O	Mg	Al	Si	Fe	MgO	Al_2O_3	SiO_2	FeO	Total
81	30.18	0.01	-	0.22	69.62	0.02	-	0.47	99.54	100.03
82	30.42	-	-	0.08	70.59	-	-	0.16	100.93	101.09
83	30.61	0.08	0.08	0.63	69.27	0.13	0.15	1.35	99.03	100.66
84	30.39	-	-	0.54	69.29	-	-	1.16	99.07	100.23
85	30.20	-	-	0.34	69.39	-	-	0.73	99.20	99.93
86	30.40	0.06	0.05	0.27	69.85	0.09	0.09	0.58	99.86	100.62
87	30.01	0.02	-	0.05	69.67	0.03	-	0.11	99.61	99.76
88	30.54	0.10	-	0.49	69.63	0.16	-	1.05	99.55	100.76
89	30.18	-	0.15	0.39	68.86	-	0.29	0.84	98.46	99.59
90	30.32	-	-	0.10	70.28	-	-	0.22	100.48	100.70
91	30.32	-	-	0.30	69.76	-	-	0.65	99.74	100.39
92	30.36	0.08	-	0.52	69.15	0.13	-	1.12	98.86	100.11
93	30.42	0.11	-	0.48	69.35	0.19	-	1.03	99.15	100.37
94	30.30	-	-	0.07	70.32	-	-	0.15	100.54	100.68
95	30.19	0.02	-	0.09	69.99	0.04	-	0.19	100.06	100.28
96	30.31	0.12	0.10	0.64	68.44	0.20	0.19	1.37	97.85	99.61
97	30.05	-	-	0.41	68.85	-	-	0.88	98.43	99.31
98	30.13	-	-	0.07	69.92	-	-	0.16	99.97	100.12
99	30.40	-	-	0.30	69.95	-	-	0.64	100.01	100.65
100	30.20	-	0.07	0.31	69.33	-	0.12	0.67	99.12	99.91

Table A.5: PTA raw data – Density Distribution of Section A and B

	Section		Std Dev
	A	B	
Average s.g. s.g.	Mass %	Mass %	Mass %
2.50	0.0	0.0	0.0
2.70	35.9	35.2	0.5
2.90	5.8	5.9	0.1
3.10	1.7	2.4	0.5
3.30	1.7	1.5	0.1
3.50	1.4	1.0	0.3
3.70	1.0	0.8	0.2
3.90	2.7	2.9	0.1
4.10	1.3	1.0	0.2
4.30	1.2	0.8	0.3
4.55	3.0	3.2	0.1
4.80	2.7	2.2	0.4
5.00	2.6	3.2	0.5
5.20	38.9	39.9	0.7
Total	**100.0**	**100.0**	

Table A.6: PTA raw data – Mineral Abundance for Section A and B

		Section		Std Dev
		A	B	
Mineral name	**S.G.**	**Mass %**	**Mass %**	**Mass %**
Hematite	5.30	51.2	51.5	0.5
Goethite	5.30	2.1	2.6	0.7
Mn-Oxides	3.80	0.0	0.0	0.0
Ilmenite	4.55	0.1	0.0	0.1
Rutile	4.25	0.1	0.1	0.0
Apatite	2.60	0.4	0.5	0.1
Clay	3.04	0.2	0.3	0.0
Quartz	2.71	45.5	44.8	1.1
Dolomite	2.63	0.1	0.1	0.0
Other	2.62	0.2	0.2	0.0
Total		**100.0**	**100.0**	

Table A.7: Raw Data for the average hematite cumulative mass per cent liberated by size

Top size (µm)	Bottom size (µm)	Average size (µm)	% Liberated													
			0	0	5	10	20	30	40	50	60	70	80	90	95	100
106	75	89	100.0	100.0	100.0	100.0	93.8	90.7	90.7	90.7	90.7	90.7	90.7	35.9	35.9	35.9
75	53	63	100.0	100.0	99.4	99.0	97.2	95.4	92.2	89.3	86.9	84.7	78.0	65.0	51.8	18.5
53	38	45	100.0	100.0	99.6	98.9	98.3	97.9	96.5	95.1	92.9	90.4	87.5	76.3	64.5	36.5
38	30	34	100.0	100.0	99.8	99.4	98.2	97.5	95.8	94.8	94.0	90.9	88.3	80.8	73.6	57.0
30	25	27	100.0	100.0	99.7	99.4	98.8	97.8	97.3	96.6	95.2	94.4	89.3	79.5	68.6	57.0
25	20	22	100.0	100.0	99.8	99.5	98.8	98.0	96.5	95.7	94.7	92.8	90.9	83.8	74.9	67.9
20	15	17	100.0	100.0	99.9	99.6	98.9	98.3	97.1	96.1	94.8	93.1	90.9	83.1	77.4	72.2
15	10	12	100.0	100.0	100.0	99.8	99.3	98.6	97.8	96.5	95.1	92.4	89.1	83.8	81.0	79.0
10	5	7	100.0	100.0	100.0	100.0	99.6	99.1	98.4	97.4	96.1	94.5	92.7	90.4	89.6	89.3
5	1	2	100.0	100.0	100.0	100.0	100.0	99.9	99.7	99.5	99.2	98.8	98.5	98.4	98.3	98.3
		Total	**100.0**	**100.0**	**99.9**	**99.6**	**98.9**	**98.2**	**97.1**	**96.0**	**94.7**	**92.8**	**90.2**	**83.0**	**77.5**	**69.2**

Table A.8: Proportion of the dominant minerals in the greater than 80% liberated class and the completely (100%) liberated class (liberation by area)

Mineral	Section A		Section B		Average	
	% in 80-100% Liberation class	% in 100% Liberation class	% in 80-100% Liberation class	% in 100% Liberation class	% in 80-100% Liberation class	% in 100% Liberation class
Hematite	90.8	68.6	92.2	69.7	91.5	69.2
Quartz	88.8	68.1	89.2	69.2	89.0	68.7
Goethite	73.6	70.4	73.9	71.6	73.8	71.0

Table A.9: PTA Size-By-Assay for Section A

Size Fraction (µm)	Passing Size (µm)	Discrete Mass (%)	Cum Mass (%) Passing	Discrete Grade (%)									Cumulative Grade Passing (%)								
				Fe	Si	Al	Ba	C	Ca	Cl	F	H	Fe	Si	Al	Ba	C	Ca	Cl	F	H
-106+75	106	1.5	100.0	30.61	26.11	0.09	0.00	0.00	0.11	0.01	0.00	0.00	36.94	21.49	0.12	0.05	0.01	0.20	0.01	0.01	0.03
-75+53	75	4.5	98.5	34.07	23.91	0.08	0.00	0.00	0.01	0.00	0.00	0.01	37.04	21.42	0.12	0.05	0.01	0.20	0.01	0.01	0.03
-53+38	53	8.5	94.0	40.32	19.50	0.07	0.00	0.00	0.03	0.00	0.00	0.00	37.18	21.30	0.13	0.05	0.01	0.21	0.01	0.01	0.03
-38+30	38	7.6	85.5	40.46	19.39	0.08	0.00	0.06	0.15	0.00	0.00	0.01	36.87	21.48	0.13	0.06	0.02	0.23	0.01	0.01	0.03
-30+25	30	6.4	77.9	38.66	20.41	0.07	0.00	0.00	0.20	0.01	0.01	0.00	36.52	21.68	0.14	0.06	0.01	0.24	0.01	0.01	0.04
-25+20	25	9.0	71.6	42.94	17.73	0.11	0.00	0.03	0.17	0.01	0.00	0.01	36.33	21.79	0.14	0.07	0.01	0.24	0.01	0.01	0.04
-20+15	20	11.9	62.6	39.13	20.16	0.11	0.09	0.00	0.19	0.01	0.01	0.01	35.39	22.38	0.15	0.08	0.01	0.25	0.01	0.01	0.04
-15+10	15	17.9	50.7	37.58	21.11	0.12	0.03	0.01	0.25	0.01	0.01	0.02	34.50	22.90	0.16	0.08	0.01	0.26	0.01	0.01	0.05
-10+5	10	22.8	32.8	33.70	23.58	0.13	0.01	0.02	0.26	0.01	0.01	0.05	32.83	23.87	0.18	0.10	0.02	0.27	0.01	0.01	0.07
-5+1	5	10.0	10.0	30.83	24.54	0.29	0.33	0.01	0.29	0.02	0.01	0.11	30.83	24.54	0.29	0.33	0.01	0.29	0.02	0.01	0.11
	Total	**100.0**		**36.94**	**21.49**	**0.12**	**0.05**	**0.01**	**0.20**	**0.01**	**0.01**	**0.03**									

Size Fraction (µm)	Passing Size (µm)	Discrete Mass (%)	Cum Mass (%) Passing	Discrete Deportment (%)									Cumulative Deportment (%)								
				Fe	Si	Al	Ba	C	Ca	Cl	F	H	Fe	Si	Al	Ba	C	Ca	Cl	F	H
-106+75	106	1.5	100.0	1.2	1.8	1.1	0.0	0.0	0.8	0.9	0.9	0.2	100.0	100.0	100.0	100.0	100.0	100.0	100.0	100.0	100.0
-75+53	75	4.5	98.5	4.2	5.0	3.0	0.0	0.0	0.3	0.0	0.0	0.9	98.8	98.2	98.9	100.0	100.0	99.2	99.1	99.1	99.8
-53+38	53	8.5	94.0	9.2	7.7	4.6	0.0	0.0	1.4	0.8	0.8	0.9	94.6	93.1	95.9	100.0	100.0	98.9	99.1	99.1	98.9
-38+30	38	7.6	85.5	8.3	6.8	4.7	0.0	31.3	5.5	1.7	1.7	1.9	85.3	85.4	91.3	100.0	100.0	97.5	98.3	98.3	98.0
-30+25	30	6.4	77.9	6.7	6.1	3.4	0.0	0.0	6.4	7.2	7.2	0.9	77.1	78.6	86.6	100.0	68.7	91.9	96.6	96.6	96.1
-25+20	25	9.0	71.6	10.4	7.4	7.9	0.0	19.9	7.8	5.9	5.9	2.1	70.4	72.6	83.2	100.0	68.7	85.5	89.4	89.4	95.1
-20+15	20	11.9	62.6	12.6	11.2	10.4	21.0	0.0	11.5	13.0	13.0	4.1	60.0	65.2	75.4	100.0	48.8	77.7	83.5	83.5	93.0
-15+10	15	17.9	50.7	18.2	17.6	18.0	11.0	9.1	22.1	24.2	24.2	12.5	47.3	54.0	65.0	79.0	48.8	66.1	70.5	70.5	88.9
-10+5	10	22.8	32.8	20.8	25.0	23.2	3.1	29.5	29.5	30.4	30.4	37.8	29.1	36.4	47.0	67.9	39.8	44.1	46.2	46.2	76.4
-5+1	5	10.0	10.0	8.3	11.4	23.8	64.8	10.3	14.6	15.9	15.9	38.6	8.3	11.4	23.8	64.8	10.3	14.6	15.9	15.9	38.6
	Total	**100.0**		**100.0**	**100.0**	**100.0**	**100.0**	**100.0**	**100.0**	**100.0**	**100.0**	**100.0**									

Table A.10: PTA Size-By-Assay for Section B

Size Fraction (µm)	Passing Size (µm)	Discrete Mass (%)	Cum Mass (%) Passing	Discrete Grade (%)									Cumulative Grade Passing (%)								
				Fe	Si	Al	Ba	C	Ca	Cl	F	H	Fe	Si	Al	Ba	C	Ca	Cl	F	H
-106+75	106	1.7	100.0	47.47	14.99	0.08	0.00	0.00	0.02	0.00	0.00	0.00	37.44	21.13	0.13	0.05	0.01	0.22	0.01	0.01	0.03
-75+53	75	4.2	98.3	37.67	21.14	0.07	0.00	0.00	0.34	0.02	0.01	0.00	37.26	21.24	0.13	0.05	0.01	0.23	0.01	0.01	0.04
-53+38	53	8.8	94.1	43.74	17.45	0.08	0.00	0.00	0.02	0.00	0.00	0.01	37.25	21.24	0.13	0.05	0.01	0.22	0.01	0.01	0.04
-38+30	38	6.5	85.2	41.78	18.76	0.08	0.00	0.00	0.02	0.00	0.00	0.01	36.57	21.63	0.14	0.06	0.01	0.24	0.01	0.01	0.04
-30+25	30	6.3	78.7	42.28	18.16	0.13	0.00	0.04	0.13	0.00	0.00	0.01	36.14	21.87	0.14	0.06	0.01	0.26	0.01	0.01	0.04
-25+20	25	8.8	72.4	40.88	18.78	0.08	0.00	0.00	0.27	0.01	0.01	0.01	35.61	22.19	0.14	0.07	0.01	0.27	0.01	0.01	0.05
-20+15	20	12.6	63.6	38.42	20.48	0.12	0.05	0.01	0.33	0.02	0.01	0.01	34.87	22.67	0.15	0.07	0.01	0.27	0.01	0.01	0.05
-15+10	15	18.6	51.0	38.12	20.78	0.11	0.00	0.01	0.25	0.01	0.01	0.02	34.00	23.21	0.16	0.08	0.01	0.26	0.01	0.01	0.06
-10+5	10	22.6	32.4	33.50	23.67	0.13	0.01	0.01	0.26	0.01	0.01	0.06	31.63	24.60	0.18	0.13	0.01	0.26	0.01	0.01	0.08
-5+1	5	9.8	9.8	27.32	26.77	0.31	0.41	0.01	0.25	0.01	0.01	0.13	27.32	26.77	0.31	0.41	0.01	0.25	0.01	0.01	0.13
	Total	**100.0**		**37.44**	**21.13**	**0.13**	**0.05**	**0.01**	**0.22**	**0.01**	**0.01**	**0.03**									

Size Fraction (µm)	Passing Size (µm)	Discrete Mass (%)	Cum Mass (%) Passing	Discrete Deportment (%)									Cumulative Deportment (%)								
				Fe	Si	Al	Ba	C	Ca	Cl	F	H	Fe	Si	Al	Ba	C	Ca	Cl	F	H
-106+75	106	1.7	100.0	2.2	1.2	1.0	0.0	0.0	0.2	0.0	0.0	0.1	100.0	100.0	100.0	100.0	100.0	100.0	100.0	100.0	100.0
-75+53	75	4.2	98.3	4.3	4.2	2.3	0.0	0.0	6.5	7.2	7.2	0.5	97.8	98.8	99.0	100.0	100.0	99.8	100.0	100.0	99.9
-53+38	53	8.8	94.1	10.3	7.3	5.6	0.0	0.0	0.7	0.0	0.0	1.4	93.6	94.6	96.7	100.0	100.0	93.3	92.8	92.8	99.4
-38+30	38	6.5	85.2	7.2	5.8	4.0	0.0	0.0	0.5	0.0	0.0	1.2	83.3	87.3	91.1	100.0	100.0	92.6	92.8	92.8	98.0
-30+25	30	6.3	78.7	7.2	5.4	6.4	0.0	30.7	3.8	1.4	1.4	1.9	76.0	81.5	87.1	100.0	100.0	92.1	92.8	92.8	96.8
-25+20	25	8.8	72.4	9.6	7.8	5.3	0.9	0.0	10.7	11.6	11.6	1.9	68.9	76.1	80.7	100.0	69.3	88.2	91.4	91.4	94.9
-20+15	20	12.6	63.6	12.9	12.2	12.2	12.6	8.8	18.8	20.1	20.1	4.1	59.2	68.2	75.3	99.1	69.3	77.6	79.8	79.8	93.0
-15+10	15	18.6	51.0	19.0	18.3	16.7	0.0	26.2	21.2	20.9	20.9	12.0	46.3	56.0	63.1	86.5	60.4	58.7	59.8	59.8	89.0
-10+5	10	22.6	32.4	20.2	25.3	22.7	3.7	21.9	26.6	27.6	27.6	41.1	27.4	37.7	46.5	86.5	34.2	37.5	38.8	38.8	76.9
-5+1	5	9.8	9.8	7.1	12.4	23.8	82.8	12.3	10.9	11.2	11.2	35.8	7.1	12.4	23.8	82.8	12.3	10.9	11.2	11.2	35.8
	Total	**100.0**		**100.0**	**100.0**	**100.0**	**100.0**	**100.0**	**100.0**	**100.0**	**100.0**	**100.0**									

Table A.11: PTA Average Size-By-Assay for Section A and B

Size Fraction (µm)	Passing Size (µm)	Discrete Mass (%)	Cum Mass (%) Passing	Discrete Grade (%)									Cumulative Grade Passing (%)							
				Fe	Si	Al	Ba	C	Ca	Cl	F	H	Fe	Si	Al	Ba	C	Ca	Cl	F	H
-106+75	106	1.6	100.0	39.56	20.21	0.08	0.00	0.00	0.06	0.00	0.00	0.00	37.19	21.31	0.13	0.05	0.01	0.21	0.01	0.01	0.03
-75+53	75	4.4	98.4	35.81	22.57	0.08	0.00	0.00	0.17	0.01	0.00	0.01	37.15	21.33	0.13	0.05	0.01	0.21	0.01	0.01	0.03
-53+38	53	8.7	94.0	42.07	18.46	0.07	0.00	0.00	0.03	0.00	0.00	0.00	37.21	21.27	0.13	0.05	0.01	0.22	0.01	0.01	0.03
-38+30	38	7.0	85.4	41.07	19.10	0.08	0.00	0.03	0.09	0.00	0.00	0.01	36.72	21.56	0.13	0.06	0.01	0.24	0.01	0.01	0.04
-30+25	30	6.4	78.3	40.47	19.29	0.10	0.00	0.02	0.17	0.01	0.00	0.01	36.33	21.78	0.14	0.06	0.01	0.25	0.01	0.01	0.04
-25+20	25	8.9	72.0	41.92	18.25	0.09	0.00	0.02	0.22	0.01	0.01	0.01	35.97	22.00	0.14	0.07	0.01	0.26	0.01	0.01	0.04
-20+15	20	12.3	63.1	38.77	20.32	0.12	0.07	0.00	0.27	0.01	0.01	0.01	35.13	22.52	0.15	0.08	0.01	0.26	0.01	0.01	0.05
-15+10	15	18.2	50.8	37.86	20.94	0.12	0.02	0.01	0.25	0.01	0.01	0.02	34.25	23.05	0.16	0.08	0.01	0.26	0.01	0.01	0.06
-10+5	10	22.7	32.6	33.60	23.62	0.13	0.01	0.01	0.26	0.01	0.01	0.06	32.23	24.23	0.18	0.12	0.01	0.26	0.01	0.01	0.08
-5+1	5	9.9	9.9	29.09	25.64	0.30	0.37	0.01	0.27	0.01	0.01	0.12	29.09	25.64	0.30	0.37	0.01	0.27	0.01	0.01	0.12
	Total	**100.0**		**37.19**	**21.31**	**0.13**	**0.05**	**0.01**	**0.21**	**0.01**	**0.01**	**0.03**									

Size Fraction (µm)	Passing Size (µm)	Discrete Mass (%)	Cum Mass (%) Passing	Discrete Deportment (%)									Cumulative Deportment (%)							
				Fe	Si	Al	Ba	C	Ca	Cl	F	H	Fe	Si	Al	Ba	C	Ca	Cl	F	H
-106+75	106	1.6	100.0	1.7	1.5	1.1	0.0	0.0	0.5	0.4	0.4	0.1	100.0	100.0	100.0	100.0	100.0	100.0	100.0	100.0	100.0
-75+53	75	4.4	98.4	4.2	4.6	2.6	0.0	0.0	3.6	3.9	3.9	0.7	98.3	98.5	98.9	100.0	100.0	99.5	99.6	99.6	99.9
-53+38	53	8.7	94.0	9.8	7.5	5.1	0.0	0.0	1.1	0.4	0.4	1.2	94.1	93.8	96.3	100.0	100.0	95.9	95.7	95.7	99.2
-38+30	38	7.0	85.4	7.7	6.3	4.4	0.0	18.7	2.9	0.8	0.8	1.5	84.3	86.3	91.2	100.0	100.0	94.9	95.3	95.3	98.0
-30+25	30	6.4	78.3	6.9	5.8	4.9	0.0	12.4	5.0	4.1	4.1	1.5	76.5	80.1	86.9	100.0	81.3	92.0	94.5	94.5	96.5
-25+20	25	8.9	72.0	10.0	7.6	6.6	0.4	11.9	9.3	9.0	9.0	2.0	69.6	74.3	81.9	100.0	68.9	87.0	90.5	90.5	95.0
-20+15	20	12.3	63.1	12.8	11.7	11.3	16.9	3.6	15.4	16.8	16.8	4.1	59.6	66.7	75.3	99.6	57.1	77.6	81.5	81.5	93.0
-15+10	15	18.2	50.8	18.6	17.9	17.3	5.6	16.0	21.6	22.4	22.4	12.2	46.8	55.0	64.0	82.7	53.5	62.2	64.7	64.7	88.9
-10+5	10	22.7	32.6	20.5	25.2	22.9	3.4	26.4	28.0	28.9	28.9	39.6	28.3	37.1	46.7	77.0	37.5	40.6	42.2	42.2	76.7
-5+1	5	9.9	9.9	7.7	11.9	23.8	73.7	11.1	12.6	13.3	13.3	37.1	7.7	11.9	23.8	73.7	11.1	12.6	13.3	13.3	37.1
	Total	**100.0**		**100.0**	**100.0**	**100.0**	**100.0**	**100.0**	**100.0**	**100.0**	**100.0**	**100.0**									

Table A.12: Fe and SiO_2 Data reconciliation check for mineralogical analysis

Fe Grade (%)	SiO_2 Grade (%)
30.61	55.87
34.07	51.16
40.32	41.74
39.64	42.50
38.32	44.23
32.34	51.47
36.94	45.99
0.00	100.03
0.70	98.42
6.16	90.88
16.44	55.02
27.27	58.62
32.57	52.69
39.64	40.96
53.20	14.16
49.22	28.64
50.83	21.31
56.62	16.29
62.10	10.90
63.86	6.44
69.29	0.84
36.94	45.99
47.47	32.08
37.67	45.24
43.74	37.35
42.03	39.51
38.28	44.09
29.94	54.72
37.44	45.22
0.39	96.63
0.75	98.40
5.04	92.22
18.24	59.73
26.23	56.61
31.20	53.26
39.50	41.86
54.53	10.48
49.31	28.26
48.87	19.84
57.66	15.43
62.01	10.75
64.99	6.21
69.29	0.86
37.44	45.22

Table A.13: Sieving Size-By-Assay for Aliquot 1

Size Fraction (µm)	Passing Size (µm)	Aliquot 1		Discrete Grade (%)										∑ Oxides	Cumulative Grade Passing (%)									
		Discrete Mass (%)	Cum Mass (%) Passing	Fe	SiO_2	Al_2O_3	MnO	K_2O	CaO	P_2O_5	Na_2O	MgO	LOI		Fe	SiO_2	Al_2O_3	MnO	K_2O	CaO	P_2O_5	Na_2O	MgO	LOI
+150	600	0.1	100.0	41.84	36.05	1.02	1.44		0.09			0.68		98.69	37.13	41.79	0.88	0.06	0.07	0.27	0.25	0.10	0.34	0.55
-150+106	150	0.1	99.9	47.00	27.20	0.66	0.77		0.07			0.40		95.85	37.13	41.80	0.88	0.06	0.07	0.27	0.25	0.10	0.34	0.55
-106+75	106	0.7	99.8	43.82	28.20	0.44	0.06		0.07			0.14		91.12	37.12	41.81	0.88	0.06	0.07	0.27	0.25	0.10	0.34	0.56
-75+53	75	4.5	99.1	48.69	25.90	0.38	0.06	0.05	0.07	0.12	0.10	0.10	0.30	96.23	37.07	41.91	0.88	0.06	0.07	0.27	0.25	0.10	0.34	0.56
-53+38	53	10.6	94.5	46.71	29.10	0.18	0.06	0.05	0.07	0.13	0.10	0.11	0.37	96.49	36.51	42.68	0.91	0.06	0.07	0.28	0.25	0.10	0.35	0.57
-38+25	38	8.8	83.9	44.66	32.00	0.38	0.06	0.05	0.09	0.14	0.10	0.07	0.18	96.48	35.22	44.40	1.00	0.06	0.08	0.31	0.27	0.10	0.38	0.60
-25+10	25	59.0	75.2	34.63	45.80	0.76	0.06	0.05	0.26	0.24	0.10	0.27	0.51	97.23	34.12	45.84	1.07	0.06	0.08	0.34	0.28	0.10	0.42	0.65
-10	10	16.1	16.1	32.25	46.00	2.23	0.06	0.18	0.61	0.44	0.10	0.96	1.15	97.53	32.25	46.00	2.23	0.06	0.18	0.61	0.44	0.10	0.96	1.15
Total (Calculated)		**100.0**		**37.13**	**41.79**	**0.88**	**0.06**	**0.07**	**0.27**	**0.25**	**0.10**	**0.34**	**0.55**	**97.05**										
Total (Measured)				**37.34**	**41.78**	**0.98**	**0.05**	**0.07**	**0.38**	**0.26**	**0.10**	**0.31**	**0.86**	**97.82**										
% Relative Error				***0.56***	***0.03***	***9.70***	***24.51***	***1.06***	***29.18***	***6.88***	***0.93***	***9.67***	***35.55***											

Size Fraction (µm)	Passing Size (µm)	Aliquot 1		Discrete Deportment (%)										Cumulative Deportment (%)									
		Discrete Mass (%)	Cum Mass (%) Passing	Fe	SiO_2	Al_2O_3	MnO	K_2O	CaO	P_2O_5	Na_2O	MgO	LOI	Fe	SiO_2	Al_2O_3	MnO	K_2O	CaO	P_2O_5	Na_2O	MgO	LOI
+150	600	0.1	100.0	0.1	0.1	0.1	2.9	0.0	0.0	0.0	0.0	0.3	0.0	100.0	100.0	100.0	100.0	100.0	100.0	100.0	100.0	100.0	100.0
-150+106	150	0.1	99.9	0.1	0.0	0.1	0.9	0.0	0.0	0.0	0.0	0.1	0.0	99.9	99.9	99.9	97.1	100.0	100.0	100.0	100.0	99.7	100.0
-106+75	106	0.7	99.8	0.9	0.5	0.4	0.7	0.0	0.2	0.0	0.0	0.3	0.0	99.8	99.8	99.8	96.2	100.0	99.9	100.0	100.0	99.7	100.0
-75+53	75	4.5	99.1	6.0	2.8	2.0	4.4	3.2	1.2	2.3	4.6	1.4	2.5	98.9	99.4	99.4	95.5	100.0	99.8	100.0	100.0	99.4	100.0
-53+38	53	10.6	94.5	13.3	7.4	2.2	10.2	7.3	2.6	5.6	10.7	3.3	7.0	92.9	96.5	97.5	91.1	96.8	98.6	97.7	95.4	98.0	97.5
-38+25	38	8.8	83.9	10.6	6.7	3.8	8.5	6.1	2.8	4.9	8.9	1.9	2.8	79.6	89.2	95.3	80.9	89.5	96.0	92.1	84.7	94.7	90.6
-25+10	25	59.0	75.2	55.1	64.7	50.7	56.9	42.7	56.8	58.3	59.6	47.2	54.3	69.1	82.4	91.6	72.4	83.4	93.2	87.2	75.9	92.8	87.8
-10	10	16.1	16.1	14.0	17.8	40.9	15.6	40.7	36.4	29.0	16.3	45.6	33.5	14.0	17.8	40.9	15.6	40.7	36.4	29.0	16.3	45.6	33.5
Total (Calculated)		**100.0**		**100.0**	**100.0**	**100.0**	**100.0**	**100.0**	**100.0**	**100.0**	**100.0**	**100.0**	**100.0**										

Table A.14: Sieving Size-By-Assay for Aliquot 2

Size Fraction (µm)	Passing Size (µm)	Aliquot 2		Discrete Grade (%)										∑ Oxides	Cumulative Grade Passing (%)									
		Discrete Mass (%)	Cum Mass (%) Passing	Fe	SiO_2	Al_2O_3	MnO	K_2O	CaO	P_2O_5	Na_2O	MgO	LOI		Fe	SiO_2	Al_2O_3	MnO	K_2O	CaO	P_2O_5	Na_2O	MgO	LOI
+150	600	0.3	100.0	35.64	34.00	0.94	0.93		3.42			0.58		90.46	37.28	41.69	0.99	0.05	0.08	0.19	0.26	0.10	0.36	0.56
-150+106	150	0.6	99.7	26.14	53.10	0.74	0.06		0.60			0.25		91.87	37.28	41.70	0.99	0.05	0.08	0.18	0.26	0.10	0.36	0.56
-106+75	106	2.6	99.2	35.14	45.40	0.61	0.05	0.06	0.13	0.19	0.10	0.23	0.58	97.24	37.35	41.64	0.99	0.05	0.08	0.18	0.26	0.10	0.36	0.57
-75+53	75	5.9	96.6	40.51	35.10	0.51	0.05	0.05	0.08	0.18	0.10	0.22	0.25	94.07	37.41	41.54	1.00	0.05	0.08	0.18	0.26	0.10	0.36	0.57
-53+38	53	10.1	90.7	42.04	36.00	0.55	0.05	0.05	0.08	0.18	0.10	0.23	0.53	97.48	37.21	41.96	1.03	0.05	0.08	0.19	0.26	0.10	0.37	0.59
-38+25	38	10.1	80.6	39.83	39.25	0.52	0.05	0.05	0.10	0.19	0.10	0.20	0.44	97.45	36.60	42.70	1.09	0.05	0.08	0.20	0.28	0.10	0.39	0.59
-25+10	25	54.6	70.5	36.74	43.20	0.93	0.05	0.05	0.17	0.25	0.10	0.29	0.44	97.64	36.13	43.20	1.17	0.05	0.09	0.22	0.29	0.10	0.42	0.62
-10	10	15.8	15.8	34.05	43.20	2.02	0.05	0.21	0.38	0.43	0.10	0.86	1.22	96.83	34.05	43.20	2.02	0.05	0.21	0.38	0.43	0.10	0.86	1.22
Total (Calculated)		**100.0**		**37.28**	**41.69**	**0.99**	**0.05**	**0.08**	**0.19**	**0.26**	**0.10**	**0.36**	**0.56**	**97.20**										
Total (Measured)				**37.34**	**41.78**	**0.98**	**0.05**	**0.07**	**0.38**	**0.26**	**0.10**	**0.31**	**0.86**	**97.82**										
% Relative Error				***0.16***	***0.24***	***1.14***	***4.52***	***6.59***	***50.38***	***2.78***	***0.80***	***15.68***	***34.69***											

Size Fraction (µm)	Passing Size (µm)	Aliquot 2		Discrete Deportment (%)										Cumulative Deportment (%)									
		Discrete Mass (%)	Cum Mass (%) Passing	Fe	SiO_2	Al_2O_3	MnO	K_2O	CaO	P_2O_5	Na_2O	MgO	LOI	Fe	SiO_2	Al_2O_3	MnO	K_2O	CaO	P_2O_5	Na_2O	MgO	LOI
+150	600	0.3	100.0	0.2	0.2	0.2	4.5	0.0	4.5	0.0	0.0	0.4	0.0	100.0	100.0	100.0	100.0	100.0	100.0	100.0	100.0	100.0	100.0
-150+106	150	0.6	99.7	0.4	0.7	0.4	0.6	0.0	1.8	0.0	0.0	0.4	0.0	99.8	99.8	99.8	95.5	100.0	95.5	100.0	100.0	99.6	100.0
-106+75	106	2.6	99.2	2.5	2.9	1.6	2.5	2.0	1.8	2.0	2.6	1.6	2.7	99.4	99.1	99.3	94.9	100.0	93.7	100.0	100.0	99.2	100.0
-75+53	75	5.9	96.6	6.4	5.0	3.0	5.6	4.0	2.5	4.2	5.9	3.6	2.6	96.9	96.2	97.7	92.4	98.0	91.9	98.0	97.4	97.6	97.3
-53+38	53	10.1	90.7	11.4	8.7	5.6	9.7	6.8	4.3	7.1	10.2	6.6	9.5	90.5	91.3	94.7	86.8	94.0	89.4	93.8	91.4	93.9	94.7
-38+25	38	10.1	80.6	10.8	9.5	5.3	9.7	6.9	5.3	7.4	10.2	5.7	7.9	79.1	82.6	89.1	77.1	87.1	85.1	86.7	81.2	87.4	85.1
-25+10	25	54.6	70.5	53.8	56.6	51.3	52.3	37.0	47.7	52.9	55.1	43.5	42.8	68.3	73.0	83.7	67.4	80.3	79.8	79.3	71.0	81.7	77.2
-10	10	15.8	15.8	14.5	16.4	32.5	15.2	43.3	32.0	26.4	16.0	38.2	34.4	14.5	16.4	32.5	15.2	43.3	32.0	26.4	16.0	38.2	34.4
Total (Calculated)		**100.0**		**100.0**	**100.0**	**100.0**	**100.0**	**100.0**	**100.0**	**100.0**	**100.0**	**100.0**	**100.0**										

Table A.15: Sieving Average Size-By-Assay for Aliquot 1 and 2

Size Fraction (µm)	Passing Size (µm)	Average		Discrete Grade (%)										∑ Oxides	Cumulative Grade Passing (%)									
		Discrete Mass (%)	Cum Mass (%) Passing	Fe	SiO_2	Al_2O_3	MnO	K_2O	CaO	P_2O_5	Na_2O	MgO	LOI		Fe	SiO_2	Al_2O_3	MnO	K_2O	CaO	P_2O_5	Na_2O	MgO	LOI
+150	600	0.2	100.0	37.72	34.69	0.96	1.10		2.30			0.61		93.22	37.21	41.74	0.93	0.06	0.07	0.23	0.25	0.10	0.35	0.55
-150+106	150	0.3	99.8	28.56	50.10	0.73	0.14		0.54			0.27		92.33	37.21	41.75	0.93	0.06	0.07	0.23	0.25	0.10	0.35	0.55
-106+75	106	1.7	99.5	37.03	41.65	0.57	0.05		0.12			0.21		95.18	37.23	41.73	0.93	0.06	0.07	0.23	0.25	0.10	0.35	0.55
-75+53	75	5.2	97.8	44.07	31.09	0.45	0.05	0.05	0.08	0.16	0.10	0.17	0.27	95.01	37.24	41.73	0.94	0.06	0.08	0.23	0.25	0.10	0.35	0.56
-53+38	53	10.3	92.6	44.43	32.47	0.36	0.06	0.05	0.07	0.15	0.10	0.17	0.45	96.97	36.85	42.33	0.97	0.06	0.08	0.24	0.26	0.10	0.36	0.58
-38+25	38	9.5	82.3	42.07	35.89	0.45	0.05	0.05	0.09	0.16	0.10	0.14	0.32	97.00	35.90	43.57	1.04	0.06	0.08	0.26	0.27	0.10	0.39	0.60
-25+10	25	56.8	72.8	35.65	44.55	0.84	0.06	0.05	0.22	0.24	0.10	0.28	0.48	97.43	35.10	44.56	1.12	0.06	0.08	0.28	0.29	0.10	0.42	0.63
-10	10	16.0	16.0	33.14	44.61	2.13	0.06	0.20	0.50	0.43	0.10	0.91	1.18	97.18	33.14	44.61	2.13	0.06	0.20	0.50	0.43	0.10	0.91	1.18
Total (Calculated)		**100.0**		**37.21**	**41.74**	**0.93**	**0.06**	**0.07**	**0.23**	**0.25**	**0.10**	**0.35**	**0.55**	**97.11**										
Total (Measured)				**37.34**	**41.78**	**0.98**	**0.05**	**0.07**	**0.38**	**0.26**	**0.10**	**0.31**	**0.86**	**97.82**										
% Relative Error				***0.36***	***0.10***	***4.28***	***14.51***	***1.67***	***39.79***	***5.78***	***2.18***	***12.67***	***36.01***											

Size Fraction (µm)	Passing Size (µm)	Average		Discrete Deportment (%)										Cumulative Deportment (%)									
		Discrete Mass (%)	Cum Mass (%) Passing	Fe	SiO_2	Al_2O_3	MnO	K_2O	CaO	P_2O_5	Na_2O	MgO	LOI	Fe	SiO_2	Al_2O_3	MnO	K_2O	CaO	P_2O_5	Na_2O	MgO	LOI
+150	600	0.2	100.0	0.2	0.2	0.2	3.6	0.0	1.9	0.0	0.0	0.3	0.0	100.0	100.0	100.0	100.0	100.0	100.0	100.0	100.0	100.0	100.0
-150+106	150	0.3	99.8	0.2	0.4	0.2	0.8	0.0	0.7	0.0	0.0	0.2	0.0	99.8	99.8	99.8	96.4	100.0	98.1	100.0	100.0	99.7	100.0
-106+75	106	1.7	99.5	1.7	1.7	1.0	1.5	0.0	0.9	0.0	0.0	1.0	0.0	99.6	99.5	99.6	95.6	100.0	97.4	100.0	100.0	99.4	100.0
-75+53	75	5.2	97.8	6.2	3.9	2.5	5.0	3.6	1.7	3.3	5.3	2.5	2.6	97.9	97.8	98.5	94.1	100.0	96.5	100.0	100.0	98.4	100.0
-53+38	53	10.3	92.6	12.4	8.0	4.0	10.0	7.2	3.3	6.5	10.6	5.0	8.4	91.7	93.9	96.0	89.1	96.4	94.8	96.7	94.7	95.9	97.4
-38+25	38	9.5	82.3	10.7	8.1	4.6	9.0	6.6	3.8	6.3	9.7	3.8	5.4	79.4	85.9	92.0	79.2	89.2	91.5	90.2	84.1	90.9	89.0
-25+10	25	56.8	72.8	54.4	60.6	51.0	54.8	40.2	53.1	56.1	58.1	45.3	49.2	68.7	77.7	87.4	70.1	82.7	87.7	84.0	74.4	87.1	83.6
-10	10	16.0	16.0	14.2	17.1	36.4	15.4	42.5	34.6	27.9	16.3	41.8	34.4	14.2	17.1	36.4	15.4	42.5	34.6	27.9	16.3	41.8	34.4
Total (Calculated)		**100.0**		**100.0**	**100.0**	**100.0**	**100.0**	**100.0**	**100.0**	**100.0**	**100.0**	**100.0**	**100.0**										

APPENDIX B: RAW DATA FOR THE BASELINE TESTS

Table B.1: Raw Data for the SLon-100 Baseline Tests without Selective Flocculation

Test #	Element	Magnetic Field Intensity (Gauss)	Product	Mass Split	Discrete Grade										∑ Oxides	Fe Upgrade Ratio
					Fe	SiO_2	Al_2O_3	MnO	K_2O	CaO	P_2O_5	Na_2O	MgO	LOI		
	UNITS			%	%	%	%	%	%	%	%	%	%	%		
			HEAD	100.0	37.34	41.78	0.98	0.05	0.07	0.38	0.26	0.10	0.31	0.86	97.82	
1	Relative Error				0.20	1.82	6.35	0.00	1.66	6.75	3.47	0.00	14.08	32.00		
	Calculated Head			100.0	**37.42**	**42.54**	**1.04**	**0.05**	**0.07**	**0.36**	**0.25**	**0.10**	**0.27**	**0.58**	**98.77**	**1.00**
		3000	Mags	32.8	53.13	21.34	0.78	0.05	0.05	0.19	0.15	0.10	0.19	0.41	99.24	1.42
			N-Mags	67.2	29.75	52.89	1.16	0.05	0.08	0.44	0.31	0.10	0.31	0.67	98.54	0.80
2	Relative Error				0.48	1.49	7.33	0.00	0.79	5.37	2.70	0.00	11.77	38.09		
	Calculated Head			100.0	**37.52**	**42.41**	**0.90**	**0.05**	**0.07**	**0.36**	**0.26**	**0.10**	**0.27**	**0.53**	**98.61**	**1.00**
		3000	Mags	31.5	55.23	18.51	0.65	0.05	0.05	0.17	0.14	0.10	0.15	0.32	99.11	1.47
			N-Mags	68.5	29.39	53.38	1.02	0.05	0.08	0.45	0.31	0.10	0.33	0.63	98.38	0.78
3	Relative Error				0.28	2.41	0.46	0.00	0.41	4.69	3.11	0.00	12.48	25.17		
	Calculated Head			100.0	**37.24**	**42.79**	**0.97**	**0.05**	**0.07**	**0.36**	**0.26**	**0.10**	**0.27**	**0.64**	**98.76**	**1.00**
		3000	Mags	30.4	54.73	19.18	0.70	0.05	0.05	0.18	0.14	0.10	0.18	0.40	99.24	1.47
			N-Mags	69.6	29.59	53.10	1.09	0.05	0.08	0.45	0.31	0.10	0.31	0.75	98.55	0.79
4	Relative Error				0.33	2.46	4.85	0.00	0.13	6.10	2.85	0.00	16.54	28.90		
	Calculated Head			100.0	**37.22**	**42.81**	**0.93**	**0.05**	**0.07**	**0.36**	**0.26**	**0.10**	**0.26**	**0.61**	**98.67**	**0.99**
		4000	Mags	43.9	52.82	21.76	0.75	0.05	0.05	0.19	0.15	0.10	0.17	0.46	99.20	**1.42**
			N-Mags	56.1	25.01	59.29	1.07	0.05	0.09	0.50	0.34	0.10	0.33	0.73	98.26	0.67
5	Relative Error				0.61	1.33	22.52	0.00	0.44	6.45	4.01	0.00	12.58	18.11		
	Calculated Head			100.0	**37.57**	**42.34**	**0.76**	**0.05**	**0.07**	**0.36**	**0.25**	**0.10**	**0.27**	**0.70**	**98.63**	**1.00**
		4000	Mags	42.7	53.77	20.48	0.53	0.05	0.05	0.19	0.14	0.10	0.18	0.71	99.30	1.43
			N-Mags	57.3	25.51	58.62	0.93	0.05	0.09	0.49	0.34	0.10	0.34	0.70	98.12	0.68
6	Relative Error				0.59	2.78	20.52	0.00	2.11	5.55	5.11	0.00	3.02	20.29		
	Calculated Head			100.0	**37.12**	**42.94**	**0.77**	**0.05**	**0.07**	**0.36**	**0.25**	**0.10**	**0.30**	**0.69**	**98.62**	**0.99**
		4000	Mags	43.2	53.35	21.04	0.62	0.05	0.05	0.19	0.14	0.10	0.21	0.64	99.33	1.44
			N-Mags	56.8	24.80	59.57	0.89	0.05	0.09	0.50	0.33	0.10	0.37	0.72	98.08	0.67
7	Relative Error				0.30	2.43	9.05	0.00	3.54	6.39	3.42	0.00	7.51	19.78		
	Calculated Head			100.0	**37.23**	**42.80**	**0.89**	**0.05**	**0.07**	**0.36**	**0.25**	**0.10**	**0.29**	**0.69**	**98.73**	**0.99**
		6000	Mags	50.1	52.27	22.50	0.70	0.05	0.05	0.18	0.15	0.10	0.20	0.63	99.32	1.40
			N-Mags	49.9	22.14	63.16	1.07	0.05	0.09	0.53	0.36	0.10	0.37	0.75	98.14	0.59
8	Relative Error				0.12	2.21	8.57	0.00	1.83	6.85	4.09	0.00	18.22	31.04		
	Calculated Head			100.0	**37.30**	**42.71**	**0.89**	**0.05**	**0.07**	**0.36**	**0.25**	**0.10**	**0.25**	**0.59**	**98.61**	**1.00**
		6000	Mags	51.5	52.48	22.22	0.73	0.05	0.05	0.18	0.14	0.10	0.20	0.69	99.41	1.41
			N-Mags	48.5	21.15	64.49	1.06	0.05	0.09	0.54	0.37	0.10	0.32	0.49	97.76	0.57
9	Relative Error				0.39	1.60	6.76	0.00	3.56	8.05	5.11	0.00	19.44	27.84		
	Calculated Head			100.0	**37.48**	**42.45**	**0.91**	**0.05**	**0.07**	**0.35**	**0.25**	**0.10**	**0.25**	**0.62**	**98.66**	**1.00**
		6000	Mags	52.8	52.10	22.73	0.78	0.05	0.05	0.19	0.15	0.10	0.20	0.80	99.55	**1.39**
			N-Mags	47.2	21.15	64.49	1.05	0.05	0.09	0.54	0.37	0.10	0.31	0.42	97.66	0.56

Table B.1: Raw Data for the SLon-100 Baseline Tests without Selective Flocculation (Contd.)

Test #	Element	Magnetic Field Intensity (Gauss)	Product	Mass Split	Discrete Recovery (%)									
					Fe	SiO_2	Al_2O_3	MnO	K_2O	CaO	P_2O_5	Na_2O	MgO	LOI
	UNITS			%										
			HEAD	100.0										
1	Relative Error													
	Calculated Head			100.0	100.0	117.8	100.0	100.0	100.0	100.0	100.0	100.0	100.0	100.0
		3000	Mags	32.8	46.6	19.4	24.8	32.8	22.9	17.9	19.3	32.8	22.8	23.0
			N-Mags	67.2	53.4	98.4	75.2	67.2	77.1	82.1	80.7	67.2	77.2	77.0
2	Relative Error													
	Calculated Head			100.0	100.0	117.6	100.0	100.0	100.0	100.0	100.0	100.0	100.0	100.0
		3000	Mags	31.5	46.3	16.2	22.6	31.5	21.8	15.0	16.8	31.5	17.4	18.9
			N-Mags	68.5	53.7	101.5	77.4	68.5	78.2	85.0	83.2	68.5	82.6	81.1
3	Relative Error													
	Calculated Head			100.0	100.0	118.8	100.0	100.0	100.0	100.0	100.0	100.0	100.0	100.0
		3000	Mags	30.4	44.7	16.2	21.8	30.4	21.0	15.1	16.8	30.4	20.3	18.9
			N-Mags	69.6	55.3	102.6	78.2	69.6	79.0	84.9	83.2	69.6	79.7	81.1
4	Relative Error													
	Calculated Head			100.0	100.0	118.6	100.0	100.0	100.0	100.0	100.0	100.0	100.0	100.0
		4000	Mags	43.9	62.3	26.5	35.3	43.9	30.1	22.7	25.2	43.9	28.5	33.0
			N-Mags	56.1	37.7	92.1	64.7	56.1	69.9	77.3	74.8	56.1	71.5	67.0
5	Relative Error													
	Calculated Head			100.0	100.0	117.7	100.0	100.0	100.0	100.0	100.0	100.0	100.0	100.0
		4000	Mags	42.7	61.1	24.3	29.7	42.7	29.4	22.2	23.8	42.7	27.7	43.0
			N-Mags	57.3	38.9	93.4	70.3	57.3	70.6	77.8	76.2	57.3	72.3	57.0
6	Relative Error													
	Calculated Head			100.0	100.0	119.5	100.0	100.0	100.0	100.0	100.0	100.0	100.0	100.0
		4000	Mags	43.2	62.0	25.3	34.6	43.2	30.3	22.2	24.7	43.2	30.3	40.3
			N-Mags	56.8	38.0	94.3	65.4	56.8	69.7	77.8	75.3	56.8	69.7	59.7
7	Relative Error													
	Calculated Head			100.0	100.0	117.8	100.0	100.0	100.0	100.0	100.0	100.0	100.0	100.0
		6000	Mags	50.1	70.3	31.0	39.8	50.1	35.6	25.7	29.5	50.1	35.4	45.7
			N-Mags	49.9	29.7	86.8	60.2	49.9	64.4	74.3	70.5	49.9	64.6	54.3
8	Relative Error													
	Calculated Head			100.0	100.0	118.5	100.0	100.0	100.0	100.0	100.0	100.0	100.0	100.0
		6000	Mags	51.5	72.5	31.8	42.4	51.5	36.0	26.3	29.4	51.5	39.6	60.0
			N-Mags	48.5	27.5	86.7	57.6	48.5	64.0	73.7	70.6	48.5	60.4	40.0
9	Relative Error													
	Calculated Head			100.0	100.0	118.4	100.0	100.0	100.0	100.0	100.0	100.0	100.0	100.0
		6000	Mags	52.8	73.4	33.5	45.5	52.8	37.6	28.2	30.8	52.8	41.6	68.0
			N-Mags	47.2	26.6	84.9	54.5	47.2	62.4	71.8	69.2	47.2	58.4	32.0

Table B.2: Summary of the Raw Data for SLon-100 Baseline Tests without Selective Flocculation

Test #	Intensity (Gauss)	Current (Amps)	Pulse Frequency (Hz)	Pulse Frequency (RPM)	Mass Pull to Mags (%)	Fe Grade (%)	SiO_2 Grade (%)	Fe Recovery (%)	SiO_2 Recovery (%)	Separation Efficieny (SE) (%)
Test 1	3000	188	34.7	261.2	32.8	53.1	21.3	46.6	19.4	27.2
Test 2					31.5	55.2	18.5	46.3	16.2	30.2
Test 3					30.4	54.7	19.2	44.7	16.2	28.5
Average					**31.6**	**54.4**	**19.7**	**45.9**	**17.2**	**28.6**
Std Dev					**1.19**	**1.10**	**1.48**	**1.02**	**1.84**	**1.50**
2 Std Dev					**2.38**	**2.19**	**2.96**	**2.03**	**3.69**	**3.00**
Std Error with 95% confidence					**1.38**	**1.27**	**1.71**	**1.17**	**2.13**	**1.73**

Test #	Intensity (Gauss)	Current (Amps)	Pulse Frequency (Hz)	Pulse Frequency (RPM)	Mass Pull to Mags (%)	Fe Grade (%)	SiO_2 Grade (%)	Fe Recovery (%)	SiO_2 Recovery (%)	Separation Efficieny (SE) (%)
Test 4	4000	253	34.7	261.2	43.9	52.8	21.8	62.3	26.5	35.8
Test 5					42.7	53.8	20.5	61.1	24.3	36.8
Test 6					43.2	53.4	21.0	62.0	25.3	36.7
Average					**43.2**	**53.3**	**21.1**	**61.8**	**25.3**	**36.5**
Std Dev					**0.62**	**0.47**	**0.64**	**0.64**	**1.09**	**0.53**
2 Std Dev					**1.24**	**0.95**	**1.28**	**1.29**	**2.18**	**1.07**
Std Error with 95% confidence					**0.71**	**0.55**	**0.74**	**0.74**	**1.26**	**0.62**

Test #	Intensity (Gauss)	Current (Amps)	Pulse Frequency (Hz)	Pulse Frequency (RPM)	Mass Pull to Mags (%)	Fe Grade (%)	SiO_2 Grade (%)	Fe Recovery (%)	SiO_2 Recovery (%)	Separation Efficieny (SE) (%)
Test 7	6000	393	34.7	261.2	50.1	52.3	22.5	70.3	31.0	39.3
Test 8					51.5	52.5	22.2	72.5	31.8	40.7
Test 9					52.8	52.1	22.7	73.4	33.5	39.9
Average					**51.5**	**52.3**	**22.5**	**72.1**	**32.1**	**40.0**
Std Dev					**1.35**	**0.19**	**0.26**	**1.57**	**1.25**	**0.73**
2 Std Dev					**2.71**	**0.38**	**0.51**	**3.15**	**2.51**	**1.46**
Std Error with 95% confidence					**1.56**	**0.22**	**0.30**	**1.82**	**1.45**	**0.84**

Table B.3: The experimental and modelled yield stress as well as apparent viscosity as a function of shear rate for 0 g/t Sodium Silicate at 0% solids (w/w) [Sample 3]

Herschel-Buckley model	
n	0.989
K	0.001
HB yield stress (Pa)	0.000

Shear Rate [1/s]	Shear Stress [Pa] Experimental	Apparent Viscosity (Pa.s)	Shear Stress [Pa] Model
168.000	0.179	0.001	0.188
163.000	0.173	0.001	0.183
158.000	0.168	0.001	0.177
153.000	0.162	0.001	0.172
148.000	0.163	0.001	0.166
142.000	0.145	0.001	0.160
137.000	0.162	0.001	0.154
132.000	0.146	0.001	0.148
127.000	0.149	0.001	0.143
122.000	0.140	0.001	0.137
117.000	0.127	0.001	0.132
112.000	0.125	0.001	0.126
107.000	0.126	0.001	0.121
102.000	0.126	0.001	0.115
96.700	0.110	0.001	0.109
91.600	0.103	0.001	0.103
86.500	0.099	0.001	0.098
81.400	0.098	0.001	0.092
76.300	0.097	0.001	0.086
71.300	0.077	0.001	0.081
66.200	0.091	0.001	0.075
61.100	0.064	0.001	0.069
56.000	0.079	0.001	0.064
50.900	0.084	0.002	0.058
45.900	0.072	0.002	0.052
40.800	0.069	0.002	0.046
35.700	0.074	0.002	0.041
30.600	0.048	0.002	0.035
25.500	0.024	0.001	0.029
20.400	0.072	0.004	0.023
15.400	0.034	0.002	0.018
10.300	-0.019	-0.002	0.012
5.180	0.056	0.011	0.006
0.100	-0.004	-0.037	0.000

Table B.4: The experimental and modelled yield stress as well as apparent viscosity as a function of shear rate for 0 g/t Sodium Silicate at 20% solids (w/w) [Sample 11]

Herschel-Buckley model	
n	0.314
K	0.271
HB yield stress (Pa)	0.000

Shear Rate [1/s]	Shear Stress [Pa] Experimental	Apparent Viscosity (Pa.s)	Shear Stress [Pa] Model
168.000	1.230	0.007	1.360
163.000	1.200	0.007	1.347
158.000	1.220	0.008	1.334
153.000	1.210	0.008	1.320
148.000	1.220	0.008	1.306
142.000	1.220	0.009	1.290
137.000	1.190	0.009	1.275
132.000	1.230	0.009	1.260
127.000	1.190	0.009	1.245
122.000	1.220	0.010	1.229
117.000	1.190	0.010	1.213
112.000	1.210	0.011	1.197
107.000	1.170	0.011	1.180
102.000	1.170	0.012	1.162
96.700	1.180	0.012	1.143
91.600	1.150	0.013	1.124
86.500	1.140	0.013	1.103
81.400	1.140	0.014	1.083
76.300	1.110	0.015	1.061
71.300	1.080	0.015	1.038
66.200	1.090	0.017	1.014
61.100	1.060	0.017	0.989
56.000	1.020	0.018	0.962
50.900	0.999	0.020	0.934
45.800	0.988	0.022	0.903
40.800	0.971	0.024	0.871
35.700	0.920	0.026	0.835
30.600	0.846	0.028	0.796
25.500	0.823	0.032	0.752
20.400	0.743	0.036	0.701
15.300	0.702	0.046	0.640
10.300	0.590	0.058	0.565
5.180	0.405	0.078	0.455
0.097	0.118	1.210	0.130

Table B.5: The experimental and modelled yield stress as well as apparent viscosity as a function of shear rate for 500 g/t Sodium Silicate at 20% solids (w/w) [Sample 8]

Herschel-Buckley model	
n	0.480
K	0.067
HB yield stress (Pa)	0.000

Shear Rate [1/s]	Shear Stress [Pa] Experimental	Apparent Viscosity (Pa.s)	Shear Stress [Pa] Model
168.000	0.635	0.004	0.780
163.000	0.635	0.004	0.769
158.000	0.643	0.004	0.757
153.000	0.631	0.004	0.746
148.000	0.642	0.004	0.734
142.000	0.621	0.004	0.720
137.000	0.629	0.005	0.707
132.000	0.627	0.005	0.695
127.000	0.630	0.005	0.682
122.000	0.615	0.005	0.669
117.000	0.615	0.005	0.656
112.000	0.632	0.006	0.642
107.000	0.604	0.006	0.628
102.000	0.614	0.006	0.614
96.700	0.608	0.006	0.598
91.600	0.593	0.006	0.583
86.500	0.586	0.007	0.567
81.400	0.587	0.007	0.551
76.300	0.576	0.008	0.534
71.300	0.564	0.008	0.517
66.200	0.564	0.009	0.499
61.100	0.532	0.009	0.480
56.000	0.520	0.009	0.461
50.900	0.542	0.011	0.440
45.800	0.530	0.012	0.418
40.750	0.526	0.013	0.395
35.700	0.493	0.014	0.371
30.600	0.412	0.013	0.345
25.500	0.444	0.017	0.316
20.400	0.395	0.019	0.284
15.350	0.409	0.027	0.247
10.300	0.288	0.028	0.204
5.175	0.212	0.041	0.147
0.097	0.016	0.164	0.022

Table B.6: The experimental and modelled yield stress as well as apparent viscosity as a function of shear rate for 1 000 g/t Sodium Silicate at 20% solids (w/w) [Sample 10]

Herschel-Buckley model	
n	0.233
K	0.215
HB yield stress (Pa)	0.000

Shear Rate [1/s]	Shear Stress [Pa] Experimental	Apparent Viscosity (Pa.s)	Shear Stress [Pa] Model
168.000	0.609	0.004	0.709
163.000	0.613	0.004	0.704
158.000	0.623	0.004	0.699
153.000	0.617	0.004	0.694
148.000	0.634	0.004	0.689
142.000	0.605	0.004	0.682
137.000	0.623	0.005	0.676
132.000	0.633	0.005	0.670
127.000	0.640	0.005	0.664
122.000	0.626	0.005	0.658
117.000	0.625	0.005	0.652
112.000	0.646	0.006	0.645
107.000	0.620	0.006	0.638
102.000	0.647	0.006	0.631
96.700	0.634	0.007	0.624
91.600	0.629	0.007	0.616
86.500	0.636	0.007	0.608
81.400	0.647	0.008	0.599
76.300	0.626	0.008	0.590
71.300	0.612	0.009	0.581
66.200	0.624	0.009	0.571
61.100	0.580	0.009	0.560
56.000	0.579	0.010	0.549
50.900	0.620	0.012	0.537
45.800	0.618	0.014	0.524
40.750	0.606	0.015	0.510
35.700	0.576	0.016	0.494
30.600	0.494	0.016	0.477
25.500	0.542	0.021	0.457
20.400	0.488	0.024	0.434
15.350	0.529	0.034	0.406
10.300	0.400	0.039	0.370
5.175	0.341	0.066	0.315
0.094	0.100	1.072	0.124

Table B.7: The experimental and modelled yield stress as well as apparent viscosity as a function of shear rate for 1 500 g/t Sodium Silicate at 20% solids (w/w) [Sample 7]

Herschel-Buckley model	
n	0.569
K	0.016
HB yield stress	0.000

Shear Rate [1/s]	**Shear Stress [Pa]**	**Apparent Viscosity**	**Shear Stress [Pa]**
	Experimental	**(Pa.s)**	**Model**
168.000	0.257	0.002	0.286
163.000	0.253	0.002	0.281
158.000	0.249	0.002	0.277
153.000	0.246	0.002	0.272
148.000	0.240	0.002	0.266
142.000	0.243	0.002	0.260
137.000	0.243	0.002	0.255
132.000	0.239	0.002	0.250
127.000	0.229	0.002	0.244
122.000	0.224	0.002	0.239
117.000	0.217	0.002	0.233
112.000	0.219	0.002	0.227
107.000	0.215	0.002	0.222
102.000	0.213	0.002	0.216
96.700	0.202	0.002	0.209
91.600	0.198	0.002	0.203
86.500	0.194	0.002	0.196
81.400	0.197	0.002	0.190
76.300	0.184	0.002	0.183
71.300	0.177	0.002	0.176
66.200	0.176	0.003	0.169
61.100	0.163	0.003	0.161
56.000	0.161	0.003	0.153
50.950	0.160	0.003	0.145
45.850	0.155	0.003	0.137
40.800	0.150	0.004	0.128
35.700	0.164	0.005	0.119
30.600	0.128	0.004	0.109
25.500	0.113	0.004	0.098
20.400	0.124	0.006	0.086
15.400	0.096	0.006	0.074
10.300	0.086	0.008	0.058
5.175	0.042	0.008	0.040
0.099	-0.015	-0.143	0.004

Table B.8: The experimental and modelled yield stress as well as apparent viscosity as a function of shear rate for 0 g/t Sodium Silicate at 30% solids (w/w) [Sample 1]

Herschel-Buckley model	
n	0.211
K	0.622
HB yield stress (Pa)	0.000

Shear Rate [1/s]	Shear Stress [Pa] Experimental	Apparent Viscosity (Pa.s)	Shear Stress [Pa] Model
168.000	1.670	0.010	1.835
163.000	1.690	0.010	1.824
158.000	1.690	0.011	1.812
153.000	1.690	0.011	1.800
147.000	1.720	0.012	1.784
142.000	1.710	0.012	1.771
137.000	1.710	0.013	1.758
132.000	1.690	0.013	1.744
127.000	1.700	0.013	1.730
122.000	1.700	0.014	1.716
117.000	1.740	0.015	1.701
112.000	1.690	0.015	1.685
107.000	1.720	0.016	1.669
102.000	1.680	0.017	1.652
96.700	1.700	0.018	1.633
91.600	1.700	0.019	1.615
86.500	1.670	0.019	1.595
81.400	1.660	0.020	1.575
76.300	1.650	0.022	1.554
71.300	1.620	0.023	1.532
66.200	1.580	0.024	1.508
61.100	1.610	0.026	1.483
56.000	1.540	0.027	1.456
50.900	1.470	0.029	1.427
45.800	1.430	0.031	1.395
40.700	1.400	0.034	1.361
35.700	1.330	0.037	1.324
30.600	1.320	0.043	1.281
25.500	1.310	0.051	1.233
20.400	1.150	0.056	1.176
15.300	1.100	0.072	1.107
10.300	1.010	0.099	1.018
5.170	0.783	0.152	0.880
0.095	0.376	3.980	0.378

Table B.9: The experimental and modelled yield stress as well as apparent viscosity as a function of shear rate for 500 g/t Sodium Silicate at 30% solids (w/w) [Sample 4]

Herschel-Buckley model	
n	0.213
K	0.571
HB yield stress (Pa)	0.000

Shear Rate [1/s]	Shear Stress [Pa] Experimental	Apparent Viscosity (Pa.s)	Shear Stress [Pa] Model
168.000	1.530	0.009	1.700
163.000	1.550	0.010	1.689
158.000	1.560	0.010	1.678
153.000	1.570	0.010	1.666
148.000	1.570	0.011	1.654
142.000	1.560	0.011	1.640
137.000	1.590	0.012	1.627
132.000	1.590	0.012	1.615
127.000	1.610	0.013	1.601
122.000	1.580	0.013	1.588
117.000	1.560	0.013	1.574
112.000	1.570	0.014	1.559
107.000	1.580	0.015	1.544
102.000	1.570	0.015	1.528
96.700	1.560	0.016	1.511
91.600	1.550	0.017	1.494
86.500	1.530	0.018	1.476
81.400	1.520	0.019	1.457
76.300	1.530	0.020	1.437
71.200	1.500	0.021	1.416
66.200	1.490	0.023	1.394
61.100	1.430	0.023	1.371
56.000	1.470	0.026	1.345
50.900	1.430	0.028	1.318
45.900	1.360	0.030	1.290
40.800	1.330	0.033	1.258
35.700	1.330	0.037	1.222
30.600	1.270	0.041	1.183
25.500	1.100	0.043	1.138
20.400	1.190	0.058	1.085
15.400	0.931	0.061	1.022
10.200	0.871	0.085	0.936
5.160	0.726	0.141	0.810
0.095	0.348	3.660	0.346

Table B.10: The experimental and modelled yield stress as well as apparent viscosity as a function of shear rate for 1 000 g/t Sodium Silicate at 30% solids (w/w) [Sample 2]

Herschel-Buckley model	
n	0.333
K	0.207
HB yield stress (Pa)	0.000

Shear Rate [1/s]	Shear Stress [Pa]	Apparent Viscosity	Shear Stress [Pa]
	Experimental	(Pa.s)	Model
168.000	0.996	0.006	1.138
163.000	0.993	0.006	1.127
158.000	0.994	0.006	1.115
153.000	0.997	0.007	1.103
148.000	0.995	0.007	1.091
142.000	1.004	0.007	1.076
137.000	0.999	0.007	1.063
132.000	0.999	0.008	1.050
127.000	0.996	0.008	1.037
122.000	1.001	0.008	1.023
117.000	0.985	0.008	1.009
112.000	0.985	0.009	0.994
107.000	0.976	0.009	0.979
102.000	0.973	0.010	0.964
96.700	0.966	0.010	0.947
91.600	0.954	0.010	0.930
86.500	0.952	0.011	0.912
81.400	0.945	0.012	0.894
76.300	0.922	0.012	0.875
71.250	0.909	0.013	0.855
66.200	0.900	0.014	0.835
61.100	0.877	0.014	0.813
56.000	0.857	0.015	0.789
50.900	0.835	0.016	0.765
45.800	0.811	0.018	0.738
40.750	0.782	0.019	0.710
35.650	0.749	0.021	0.679
30.600	0.718	0.023	0.645
25.500	0.698	0.027	0.607
20.400	0.626	0.031	0.564
15.350	0.586	0.038	0.513
10.300	0.480	0.047	0.449
5.175	0.339	0.065	0.357
0.095	0.080	0.849	0.094

Table B.11: The experimental and modelled yield stress as well as apparent viscosity as a function of shear rate for 1 500 g/t Sodium Silicate at 30% solids (w/w) [Sample 9]

Herschel-Buckley model	
n	0.312
K	0.281
HB yield stress (Pa)	0.000

Shear Rate [1/s]	Shear Stress [Pa] Experimental	Apparent Viscosity (Pa.s)	Shear Stress [Pa] Model
168.000	1.175	0.007	1.395
163.000	1.175	0.007	1.381
158.000	1.210	0.008	1.368
153.000	1.195	0.008	1.354
148.000	1.210	0.008	1.340
142.000	1.190	0.008	1.323
137.000	1.215	0.009	1.308
132.000	1.220	0.009	1.293
127.000	1.220	0.010	1.278
122.000	1.205	0.010	1.262
117.000	1.220	0.010	1.246
112.000	1.220	0.011	1.229
107.000	1.220	0.011	1.211
102.000	1.210	0.012	1.193
96.700	1.205	0.013	1.174
91.600	1.205	0.013	1.154
86.500	1.180	0.014	1.133
81.400	1.185	0.015	1.112
76.300	1.170	0.015	1.090
71.300	1.135	0.016	1.067
66.200	1.150	0.017	1.043
61.100	1.115	0.018	1.017
56.000	1.095	0.020	0.989
50.900	1.095	0.022	0.960
45.800	1.073	0.023	0.929
40.750	1.046	0.026	0.896
35.700	1.006	0.028	0.860
30.600	0.909	0.030	0.819
25.500	0.901	0.035	0.774
20.400	0.825	0.040	0.722
15.300	0.806	0.053	0.660
10.300	0.625	0.061	0.583
5.175	0.448	0.087	0.470
0.093	0.111	1.185	0.134

Table B.12: The experimental and modelled yield stress as well as apparent viscosity as a function of shear rate for 0 g/t Sodium Silicate at 45% solids (w/w) [Sample 5]

Herschel-Buckley model	
n	0.173
K	1.593
HB yield stress (Pa)	0.000

Shear Rate [1/s]	Shear Stress [Pa]	Apparent Viscosity	Shear Stress [Pa]
	Experimental	(Pa.s)	Model
168.000	3.445	0.021	3.862
163.000	3.470	0.021	3.842
158.000	3.525	0.022	3.821
153.000	3.535	0.023	3.800
148.000	3.575	0.024	3.778
142.000	3.580	0.025	3.751
137.000	3.610	0.026	3.728
132.000	3.640	0.028	3.704
127.000	3.660	0.029	3.680
122.000	3.650	0.030	3.654
117.000	3.670	0.031	3.628
112.000	3.675	0.033	3.601
107.000	3.690	0.035	3.572
102.000	3.680	0.036	3.543
96.700	3.675	0.038	3.510
91.600	3.670	0.040	3.478
86.500	3.635	0.042	3.444
81.400	3.630	0.045	3.408
76.300	3.615	0.047	3.370
71.300	3.555	0.050	3.330
66.200	3.520	0.053	3.288
61.100	3.470	0.057	3.243
56.000	3.440	0.062	3.194
50.900	3.390	0.067	3.142
45.800	3.275	0.071	3.085
40.750	3.160	0.078	3.024
35.600	3.055	0.086	2.954
30.600	2.930	0.096	2.877
25.500	2.855	0.112	2.788
20.400	2.720	0.133	2.683
15.300	2.550	0.166	2.553
10.200	2.240	0.219	2.380
5.160	1.785	0.346	2.116
0.097	1.090	11.260	1.064

Table B.13: The experimental and modelled yield stress as well as apparent viscosity as a function of shear rate for 500 g/t Sodium Silicate at 45% solids (w/w) [Sample 13]

Herschel-Buckley model	
n	0.220
K	1.873
HB yield stress (Pa)	0.000

Shear Rate [1/s]	Shear Stress [Pa]	Apparent Viscosity	Shear Stress [Pa]
	Experimental	(Pa.s)	Model
168.000	5.115	0.031	5.787
163.000	5.130	0.032	5.749
158.000	5.245	0.033	5.710
153.000	5.185	0.034	5.670
148.000	5.295	0.036	5.628
142.000	5.250	0.037	5.577
137.000	5.310	0.039	5.533
132.000	5.325	0.040	5.488
127.000	5.345	0.042	5.442
122.000	5.340	0.044	5.394
117.000	5.360	0.046	5.344
112.000	5.330	0.048	5.293
107.000	5.410	0.051	5.240
102.000	5.310	0.052	5.185
96.700	5.355	0.055	5.125
91.600	5.345	0.058	5.064
86.500	5.235	0.061	5.001
81.400	5.275	0.065	4.934
76.300	5.235	0.069	4.864
71.300	5.085	0.071	4.792
66.200	5.040	0.076	4.715
61.100	5.000	0.082	4.632
56.000	4.945	0.088	4.544
50.900	4.810	0.095	4.450
45.800	4.630	0.101	4.347
40.750	4.490	0.110	4.237
35.600	4.370	0.123	4.113
30.600	4.220	0.138	3.978
25.500	4.045	0.159	3.822
20.400	3.835	0.188	3.638
15.300	3.510	0.229	3.415
10.200	2.995	0.293	3.123
5.160	2.300	0.446	2.688
0.097	1.085	11.150	1.121

Table B.14: The experimental and modelled yield stress as well as apparent viscosity as a function of shear rate for 1 000 g/t Sodium Silicate at 45% solids (w/w) [Sample 6]

Herschel-Buckley model	
n	0.248
K	1.037
HB yield stress (Pa)	0.000

Shear Rate [1/s]	Shear Stress [Pa] Experimental	Apparent Viscosity (Pa.s)	Shear Stress [Pa] Model
168.000	3.270	0.020	3.699
163.000	3.340	0.021	3.671
158.000	3.380	0.021	3.643
153.000	3.300	0.022	3.614
148.000	3.420	0.023	3.584
142.000	3.310	0.023	3.548
137.000	3.420	0.025	3.516
132.000	3.340	0.025	3.484
127.000	3.430	0.027	3.451
122.000	3.330	0.027	3.416
117.000	3.400	0.029	3.381
112.000	3.320	0.030	3.345
107.000	3.380	0.032	3.307
102.000	3.340	0.033	3.268
96.700	3.280	0.034	3.225
91.600	3.340	0.037	3.182
86.500	3.220	0.037	3.137
81.400	3.230	0.040	3.090
76.300	3.260	0.043	3.041
71.300	3.150	0.044	2.990
66.200	3.090	0.047	2.935
61.100	3.030	0.050	2.877
56.000	3.060	0.055	2.816
50.900	3.000	0.059	2.750
45.900	2.870	0.063	2.680
40.800	2.750	0.067	2.603
35.600	2.660	0.075	2.516
30.600	2.490	0.081	2.424
25.500	2.410	0.094	2.316
20.400	2.360	0.116	2.192
15.300	2.180	0.142	2.041
10.200	1.830	0.178	1.845
5.160	1.420	0.275	1.558
0.094	0.535	5.680	0.577

Table B.15: The experimental and modelled yield stress as well as apparent viscosity as a function of shear rate for 1 500 g/t Sodium Silicate at 45% solids (w/w) [Sample 12]

Herschel-Buckley model	
n	0.276
K	0.834
HB yield stress (Pa)	0.000

Shear Rate [1/s]	Shear Stress [Pa] Experimental	Apparent Viscosity (Pa.s)	Shear Stress [Pa] Model
168.000	3.120	0.019	3.425
163.000	3.120	0.019	3.397
158.000	3.110	0.020	3.368
153.000	3.140	0.021	3.338
147.500	3.125	0.021	3.304
142.000	3.130	0.022	3.270
137.000	3.105	0.023	3.238
132.000	3.125	0.024	3.205
127.000	3.105	0.024	3.171
122.000	3.115	0.026	3.136
117.000	3.085	0.026	3.100
112.000	3.105	0.028	3.063
107.000	3.065	0.029	3.025
102.000	3.045	0.030	2.985
96.700	3.015	0.031	2.941
91.600	2.975	0.032	2.898
86.500	2.965	0.034	2.852
81.400	2.925	0.036	2.805
76.300	2.870	0.038	2.755
71.250	2.855	0.040	2.704
66.200	2.810	0.043	2.650
61.100	2.745	0.045	2.592
56.000	2.675	0.048	2.530
50.900	2.640	0.052	2.464
45.800	2.590	0.057	2.394
40.700	2.515	0.062	2.317
35.700	2.400	0.067	2.235
30.600	2.265	0.074	2.142
25.500	2.160	0.085	2.037
20.400	1.970	0.097	1.915
15.300	1.805	0.118	1.769
10.250	1.510	0.148	1.584
5.165	1.120	0.217	1.312
0.095	0.431	4.535	0.436

Table B.16: Malvern Mastersizer sizing results for the as-is feed in slurry form with and without ultrasonic displacement

Dry Sample/ Slurry	Slurry	Slurry	Slurry	Slurry	Slurry	Slurry	Slurry
Pump Speed (rpm)	600	600	600	600	600	600	600
Ultrasonic	Off	Off	Off	Off	Off	Off	On (20)
Water	Distilled Water	Distilled Water	Distilled Water	Distilled Water	Distilled Water	Distilled Water	Distilled Water
Specific Surface Area (m^2/g)	0.989	1.04	1.06	1.05	0.946	1.02	1.11
d(0.1) (µm)	2.431	2.339	2.256	2.322	2.528	2.38	2.131
d(0.5) (µm)	17.283	15.988	15.509	15.726	19.234	16.75	15.894
d(0.9) (µm)	82.599	67.5	66.836	62.302	81.657	72.18	56.88
File Name	Repeat 1	Repeat 2	Repeat 3	Repeat 4	Repeat 5	Average Repeat 1-5	First Test

Particle Diameter (µm)	**Cumulative Vol % Passing**	**Cumulative Vol % Passing**	**Cumulative Vol % Passing**	**Cumulative Vol % Passing**	**Cumulative Vol % Passing**	**Cumulative Vol % Passing**	**Cumulative Vol % Passing**
100.000	92.25	95.62	96.24	96.86	93.79	94.95	98.77
91.201	91.24	94.48	95.20	95.93	92.23	93.82	98.03
83.176	90.09	93.23	93.92	94.73	90.40	92.47	97.04
75.858	88.80	91.88	92.41	93.38	88.34	90.96	95.77
69.183	87.35	90.41	90.69	91.89	86.34	89.34	94.21
63.096	85.77	88.83	88.79	90.24	86.09	87.94	92.38
57.544	84.02	87.13	86.72	88.43	83.70	86.00	90.28
52.481	82.12	85.29	84.52	86.46	81.21	83.92	87.95
47.863	80.05	83.30	82.23	84.32	78.64	81.71	85.43
43.652	77.84	81.15	79.86	82.02	76.02	79.38	82.74
39.811	75.47	78.84	77.43	79.56	73.39	76.94	79.93
36.308	72.97	76.37	74.95	76.96	70.74	74.40	77.02
33.113	70.34	73.73	72.42	74.23	68.09	71.76	74.04
30.200	67.60	70.96	69.85	71.38	65.45	69.05	71.03
27.542	64.78	68.06	67.24	68.44	62.82	66.27	67.99
25.119	61.89	65.07	64.57	65.44	60.19	63.43	64.94
22.909	58.97	62.01	61.86	62.39	57.56	60.56	61.90
20.893	56.02	58.92	59.11	59.32	54.95	57.66	58.87
19.055	53.09	55.82	56.31	56.26	52.33	54.76	55.85
17.378	50.17	52.74	53.49	53.23	49.74	51.87	52.86
15.849	47.30	49.72	50.66	50.25	47.16	49.02	49.91
14.454	44.50	46.77	47.85	47.34	42.10	45.71	47.00
13.183	41.77	43.91	45.06	44.51	39.64	42.98	44.15
12.023	39.13	41.17	42.33	41.77	37.24	40.33	41.38
10.965	36.60	38.54	39.68	39.14	34.92	37.78	38.70
10.000	34.17	36.03	37.11	36.62	32.68	35.32	36.13
9.120	31.89	33.64	34.64	34.21	30.54	32.98	33.68
8.318	29.68	31.38	32.29	31.91	28.49	30.75	31.35
7.586	27.61	29.24	30.06	29.73	26.54	28.64	29.16
6.918	25.67	27.21	27.95	27.66	24.70	26.64	27.11
6.310	23.83	25.28	25.95	25.70	22.95	24.74	25.19
5.754	22.11	23.46	24.08	23.83	21.30	22.96	23.41
5.248	20.49	21.74	22.31	22.07	19.74	21.27	21.76
4.786	18.96	20.11	20.64	20.40	18.27	19.68	20.21
4.365	17.52	18.56	19.07	18.81	16.88	18.17	18.77
3.981	16.16	17.09	17.58	17.31	15.56	16.74	17.43
3.631	14.87	15.70	16.18	15.88	14.31	15.39	16.16
3.311	13.65	14.38	14.84	14.53	13.12	14.10	14.96
3.020	12.49	13.12	13.58	13.26	12.00	12.89	13.83
2.754	11.40	11.94	12.38	12.05	10.94	11.74	12.75
2.512	10.36	10.82	11.24	10.92	9.93	10.65	11.72
2.291	9.38	9.77	10.17	9.85	8.98	9.63	10.74
2.089	8.45	8.79	9.17	8.86	8.09	8.67	9.80

Table B.16: Malvern Mastersizer sizing results for the as-is feed in slurry form with and without ultrasonic displacement (Contd.)

Dry Sample/ Slurry	Slurry	Slurry	Slurry	Slurry	Slurry	Slurry	Slurry
Pump Speed (rpm)	600	600	600	600	600	600	600
Ultrasonic	Off	Off	Off	Off	Off	Off	On (20)
Water	Distilled Water	Distilled Water	Distilled Water	Distilled Water	Distilled Water	Distilled Water	Distilled Water
Specific Surface Area (m^2/g)	0.989	1.04	1.06	1.05	0.946	1.02	1.11
d(0.1) (µm)	2.431	2.339	2.256	2.322	2.528	2.38	2.131
d(0.5) (µm)	17.283	15.988	15.509	15.726	19.234	16.75	15.894
d(0.9) (µm)	82.599	67.5	66.836	62.302	81.657	72.18	56.88
File Name	Repeat 1	Repeat 2	Repeat 3	Repeat 4	Repeat 5	Average Repeat 1-5	First Test

Particle Diameter (µm)	**Cumulative Vol % Passing**	**Cumulative Vol % Passing**	**Cumulative Vol % Passing**	**Cumulative Vol % Passing**	**Cumulative Vol % Passing**	**Cumulative Vol % Passing**	**Cumulative Vol % Passing**
1.905	7.59	7.87	8.22	7.93	7.26	7.77	8.92
1.738	6.78	7.02	7.34	7.07	6.48	6.94	8.07
1.585	6.03	6.24	6.53	6.28	5.76	6.17	7.27
1.445	5.33	5.51	5.77	5.55	5.09	5.45	6.52
1.318	4.69	4.85	5.07	4.88	4.48	4.79	5.81
1.202	4.10	4.23	4.43	4.27	3.91	4.19	5.14
1.096	3.55	3.67	3.84	3.70	3.39	3.63	4.51
1.000	3.05	3.16	3.29	3.19	2.91	3.12	3.92
0.912	2.59	2.69	2.80	2.72	2.47	2.65	3.37
0.832	2.18	2.26	2.35	2.28	2.07	2.23	2.86
0.759	1.80	1.87	1.94	1.89	1.71	1.84	2.39
0.692	1.45	1.52	1.57	1.54	1.38	1.49	1.95
0.631	1.15	1.20	1.24	1.22	1.09	1.18	1.56
0.575	0.88	0.93	0.95	0.94	0.83	0.91	1.21
0.525	0.65	0.68	0.70	0.69	0.61	0.67	0.90
0.479	0.45	0.48	0.49	0.49	0.42	0.47	0.64
0.437	0.29	0.31	0.32	0.32	0.26	0.30	0.43
0.398	0.17	0.18	0.18	0.18	0.15	0.17	0.25
0.363	0.08	0.08	0.08	0.09	0.06	0.08	0.12
0.331	0.03	0.03	0.03	0.03	0.01	0.03	0.04
0.302	0.00	0.00	0.00	0.00	0.00	0.00	0.00
0.275	0.00	0.00	0.00	0.00	0.00	0.00	0.00
0.251	0.00	0.00	0.00	0.00	0.00	0.00	0.00
0.229	0.00	0.00	0.00	0.00	0.00	0.00	0.00
0.209	0.00	0.00	0.00	0.00	0.00	0.00	0.00
0.191	0.00	0.00	0.00	0.00	0.00	0.00	0.00
0.174	0.00	0.00	0.00	0.00	0.00	0.00	0.00
0.158	0.00	0.00	0.00	0.00	0.00	0.00	0.00
0.145	0.00	0.00	0.00	0.00	0.00	0.00	0.00
0.132	0.00	0.00	0.00	0.00	0.00	0.00	0.00
0.120	0.00	0.00	0.00	0.00	0.00	0.00	0.00
0.110	0.00	0.00	0.00	0.00	0.00	0.00	0.00
0.100	0.00	0.00	0.00	0.00	0.00	0.00	0.00

Table B.17: Malvern Mastersizer sizing results at the Box-Behnken centre points for Selective Flocculation and at a pH of 9.5

Dry Sample/ Slurry	Slurry	Slurry	Slurry	Slurry
Pump Speed (rpm)	600	600	600	600
Ultrasonic	Off	Off	Off	Off
Water	pH 9.5 Tap Water	pH 9.5 Tap Water	pH 9.5 Tap Water	pH 9.5 Tap Water
Specific Surface Area (m^2/g)	1.13	1.13	0.946	1.07
d(0.1) (µm)	2.203	2.195	2.904	2.43
d(0.5) (µm)	14.833	14.133	16.475	15.15
d(0.9) (µm)	59.496	50.681	45.853	52.01
File Name	First Test	Repeat 1	Repeat 2	Average First Test and Repeats

Particle Diameter (µm)	**Cumulative Vol % Passing**	**Cumulative Vol % Passing**	**Cumulative Vol % Passing**	**Cumulative Vol % Passing**
100.000	97.03	97.91	100.00	98.31
91.201	96.16	97.31	99.88	97.78
83.176	95.13	96.6	99.39	97.04
75.858	93.94	95.75	98.67	96.12
69.183	92.58	94.75	97.70	95.01
63.096	91.06	93.58	96.46	93.70
57.544	89.37	92.21	94.94	92.17
52.481	87.52	90.65	93.14	90.44
47.863	85.51	88.87	91.07	88.48
43.652	83.35	86.88	88.70	86.31
39.811	81.04	84.69	86.05	83.93
36.308	78.59	82.28	83.12	81.33
33.113	76.01	79.69	79.70	78.47
30.200	73.31	76.91	76.43	75.55
27.542	70.51	73.98	72.74	72.41
25.119	67.6	70.9	68.84	69.11
22.909	64.61	67.7	64.81	65.71
20.893	61.56	64.4	60.67	62.21
19.055	58.47	61.04	56.51	58.67
17.378	55.35	57.63	52.37	55.12
15.849	52.23	54.22	48.31	51.59
14.454	49.13	50.82	44.38	48.11
13.183	46.09	47.48	40.64	44.74
12.023	43.11	44.22	37.11	41.48
10.965	40.22	41.07	33.83	38.37
10.000	37.44	38.06	30.80	35.43
9.120	34.79	35.2	28.05	32.68
8.318	32.26	32.51	25.55	30.11
7.586	29.88	29.99	23.32	27.73
6.918	27.64	27.66	21.31	25.54
6.310	25.54	25.5	19.53	23.52
5.754	23.59	23.51	17.94	21.68
5.248	21.78	21.69	16.52	20.00
4.786	20.11	20.02	15.25	18.46
4.365	18.55	18.48	14.09	17.04
3.981	17.11	17.07	13.04	15.74
3.631	15.78	15.76	12.08	14.54
3.311	14.54	14.55	11.18	13.42
3.020	13.39	13.41	10.34	12.38
2.754	12.32	12.35	9.55	11.41
2.512	11.32	11.36	8.80	10.49
2.291	10.38	10.42	8.09	9.63
2.089	9.5	9.53	7.42	8.82

Table B.17: Malvern Mastersizer sizing results at the Box-Behnken centre points for Selective Flocculation and at a pH of 9.5 (Contd.)

Dry Sample/ Slurry	Slurry	Slurry	Slurry	Slurry
Pump Speed (rpm)	600	600	600	600
Ultrasonic	Off	Off	Off	Off
Water	pH 9.5 Tap Water	pH 9.5 Tap Water	pH 9.5 Tap Water	pH 9.5 Tap Water
Specific Surface Area (m^2/g)	1.13	1.13	0.946	1.07
d(0.1) (µm)	2.203	2.195	2.904	2.43
d(0.5) (µm)	14.833	14.133	16.475	15.15
d(0.9) (µm)	59.496	50.681	45.853	52.01
File Name	First Test	Repeat 1	Repeat 2	Average First Test and Repeats

Particle Diameter (µm)	**Cumulative Vol % Passing**	**Cumulative Vol % Passing**	**Cumulative Vol % Passing**	**Cumulative Vol % Passing**
1.905	8.67	8.7	6.77	8.05
1.738	7.9	7.9	6.16	7.32
1.585	7.16	7.15	5.58	6.63
1.445	6.47	6.45	5.02	5.98
1.318	5.81	5.78	4.50	5.36
1.202	5.18	5.14	4.00	4.77
1.096	4.59	4.54	3.52	4.22
1.000	4.03	3.97	3.08	3.69
0.912	3.5	3.44	2.66	3.20
0.832	3	2.93	2.27	2.73
0.759	2.53	2.46	1.90	2.30
0.692	2.1	2.03	1.56	1.90
0.631	1.7	1.63	1.25	1.53
0.575	1.34	1.27	0.98	1.20
0.525	1.01	0.95	0.73	0.90
0.479	0.73	0.68	0.52	0.64
0.437	0.5	0.45	0.35	0.43
0.398	0.3	0.27	0.20	0.26
0.363	0.16	0.13	0.10	0.13
0.331	0.06	0.05	0.04	0.05
0.302	0	0	0.00	0.00
0.275	0	0	0.00	0.00
0.251	0	0	0.00	0.00
0.229	0	0	0.00	0.00
0.209	0	0	0.00	0.00
0.191	0	0	0.00	0.00
0.174	0	0	0.00	0.00
0.158	0	0	0.00	0.00
0.145	0	0	0.00	0.00
0.132	0	0	0.00	0.00
0.120	0	0	0.00	0.00
0.110	0	0	0.00	0.00
0.100	0	0	0.00	0.00

Table B.18: Malvern Mastersizer sizing results at the Box-Behnken centre points for Selective Flocculation and at a pH of 10

Dry Sample/ Slurry	Slurry	Slurry	Slurry	Slurry
Pump Speed (rpm)	600	600	600	600
Ultrasonic	Off	Off	Off	Off
Water	pH 10	pH 10	pH 10	pH 10
Specific Surface Area (m^2/g)	0.918	0.904	0.899	0.907
d(0.1) (µm)	2.959	2.936	2.977	2.957
d(0.5) (µm)	17.488	19.569	19.221	18.759
d(0.9) (µm)	54.007	60.547	57.458	57.337
File Name	Repeat 1	Repeat 2	Repeat 3	Average Repeats 1-3

Particle Diameter (µm)	**Cumulative Vol % Passing**	**Cumulative Vol % Passing**	**Cumulative Vol % Passing**	**Cumulative Vol % Passing**
100.000	95.99	97.76	98.52	97.42
91.201	95.65	96.93	97.89	96.82
83.176	95.17	95.87	96.97	96.00
75.858	94.51	94.52	95.72	94.92
69.183	93.64	92.89	94.14	93.56
63.096	92.52	90.96	92.24	91.91
57.544	91.13	88.73	90.04	89.97
52.481	89.44	86.22	87.55	87.74
47.863	87.46	83.44	84.82	85.24
43.652	85.16	80.42	81.85	82.48
39.811	82.56	77.21	78.68	79.48
36.308	79.66	73.84	75.34	76.28
33.113	76.48	70.35	71.84	72.89
30.200	73.06	66.78	68.24	69.36
27.542	69.42	63.18	64.55	65.72
25.119	65.61	59.57	60.81	62.00
22.909	61.69	55.98	57.05	58.24
20.893	57.70	52.46	53.32	54.49
19.055	53.70	49.01	49.66	50.79
17.378	49.75	45.67	46.09	47.17
15.849	45.90	42.46	42.66	43.67
14.454	42.20	39.39	39.39	40.33
13.183	38.68	36.48	36.30	37.15
12.023	35.38	33.73	33.41	34.17
10.965	32.32	31.15	30.73	31.40
10.000	29.50	28.74	28.27	28.84
9.120	26.94	26.51	26.01	26.49
8.318	24.63	24.45	23.95	24.34
7.586	22.54	22.55	22.08	22.39
6.918	20.68	20.81	20.37	20.62
6.310	19.01	19.21	18.83	19.02
5.754	17.51	17.74	17.41	17.55
5.248	16.17	16.40	16.12	16.23
4.786	14.95	15.17	14.93	15.02
4.365	13.84	14.03	13.84	13.90
3.981	12.83	12.99	12.82	12.88
3.631	11.88	12.01	11.86	11.92
3.311	11.00	11.10	10.97	11.02
3.020	10.18	10.25	10.13	10.19
2.754	9.40	9.45	9.33	9.39
2.512	8.65	8.69	8.58	8.64
2.291	7.95	7.98	7.87	7.93
2.089	7.28	7.30	7.19	7.26

Table B.18: Malvern Mastersizer sizing results at the Box-Behnken centre points for Selective Flocculation and at a pH of 10 (Contd.)

Dry Sample/ Slurry	Slurry	Slurry	Slurry	Slurry
Pump Speed (rpm)	600	600	600	600
Ultrasonic	Off	Off	Off	Off
Water	pH 10	pH 10	pH 10	pH 10
Specific Surface Area (m^2/g)	0.918	0.904	0.899	0.907
d(0.1) (µm)	2.959	2.936	2.977	2.957
d(0.5) (µm)	17.488	19.569	19.221	18.759
d(0.9) (µm)	54.007	60.547	57.458	57.337
File Name	Repeat 1	Repeat 2	Repeat 3	Average Repeats 1-3

Particle Diameter (µm)	**Cumulative Vol % Passing**	**Cumulative Vol % Passing**	**Cumulative Vol % Passing**	**Cumulative Vol % Passing**
1.905	6.64	6.66	6.55	6.62
1.738	6.03	6.05	5.95	6.01
1.585	5.46	5.47	5.38	5.44
1.445	4.91	4.92	4.84	4.89
1.318	4.39	4.40	4.33	4.37
1.202	3.90	3.91	3.85	3.89
1.096	3.44	3.45	3.40	3.43
1.000	3.01	3.02	2.98	3.00
0.912	2.60	2.61	2.57	2.59
0.832	2.21	2.22	2.20	2.21
0.759	1.86	1.87	1.85	1.86
0.692	1.53	1.54	1.53	1.53
0.631	1.23	1.24	1.23	1.23
0.575	0.96	0.97	0.97	0.97
0.525	0.72	0.73	0.73	0.73
0.479	0.52	0.53	0.53	0.53
0.437	0.35	0.36	0.36	0.36
0.398	0.21	0.21	0.21	0.21
0.363	0.10	0.11	0.11	0.11
0.331	0.04	0.04	0.04	0.04
0.302	0.00	0.00	0.00	0.00
0.275	0.00	0.00	0.00	0.00
0.251	0.00	0.00	0.00	0.00
0.229	0.00	0.00	0.00	0.00
0.209	0.00	0.00	0.00	0.00
0.191	0.00	0.00	0.00	0.00
0.174	0.00	0.00	0.00	0.00
0.158	0.00	0.00	0.00	0.00
0.145	0.00	0.00	0.00	0.00
0.132	0.00	0.00	0.00	0.00
0.120	0.00	0.00	0.00	0.00
0.110	0.00	0.00	0.00	0.00
0.100	0.00	0.00	0.00	0.00

Table B.19: Malvern Mastersizer sizing results at the Box-Behnken centre points for Selective Flocculation and at a pH of 10.5

Dry Sample/ Slurry	Slurry	Slurry	Slurry
Pump Speed (rpm)	600	600	600
Ultrasonic	Off	Off	Off
Water	pH 10.5	pH 10.5	pH 10.5
Specific Surface Area (m^2/g)	0.812	1.140	0.976
d(0.1) (µm)	3.530	2.105	2.818
d(0.5) (µm)	24.895	17.655	21.275
d(0.9) (µm)	56.221	67.863	62.042
File Name	Repeat 1	Repeat 2	Average Repeats 1-2

Particle Diameter (µm)	**Cumulative Vol % Passing**	**Cumulative Vol % Passing**	**Cumulative Vol % Passing**
100.000	99.08	93.06	96.07
91.201	98.94	92.67	95.81
83.176	98.43	92.09	95.26
75.858	97.41	91.29	94.35
69.183	95.83	90.25	93.04
63.096	93.64	88.96	91.30
57.544	90.81	87.40	89.11
52.481	87.39	85.57	86.48
47.863	83.45	83.48	83.47
43.652	79.08	81.12	80.10
39.811	74.40	78.52	76.46
36.308	69.54	75.70	72.62
33.113	64.60	72.67	68.64
30.200	59.72	69.49	64.61
27.542	54.97	66.19	60.58
25.119	50.43	62.81	56.62
22.909	46.16	59.41	52.79
20.893	42.19	56.02	49.11
19.055	38.55	52.69	45.62
17.378	35.23	49.45	42.34
15.849	32.24	46.33	39.29
14.454	29.55	43.35	36.45
13.183	27.15	40.53	33.84
12.023	25.01	37.87	31.44
10.965	23.10	35.38	29.24
10.000	21.40	33.05	27.23
9.120	19.87	30.88	25.38
8.318	18.50	28.86	23.68
7.586	17.26	26.98	22.12
6.918	16.13	25.23	20.68
6.310	15.09	23.60	19.35
5.754	14.14	22.08	18.11
5.248	13.25	20.66	16.96
4.786	12.43	19.32	15.88
4.365	11.65	18.07	14.86
3.981	10.91	16.89	13.90
3.631	10.21	15.76	12.99
3.311	9.53	14.69	12.11
3.020	8.89	13.66	11.28
2.754	8.26	12.67	10.47
2.512	7.66	11.72	9.69
2.291	7.08	10.80	8.94
2.089	6.52	9.93	8.23

Table B.19: Malvern Mastersizer sizing results at the Box-Behnken centre points for Selective Flocculation and at a pH of 10.5 (Contd.)

Dry Sample/ Slurry	Slurry	Slurry	Slurry
Pump Speed (rpm)	600	600	600
Ultrasonic	Off	Off	Off
Water	pH 10.5	pH 10.5	pH 10.5
Specific Surface Area (m^2/g)	0.812	1.140	0.976
d(0.1) (µm)	3.530	2.105	2.818
d(0.5) (µm)	24.895	17.655	21.275
d(0.9) (µm)	56.221	67.863	62.042
File Name	Repeat 1	Repeat 2	Average Repeats 1-2

Particle Diameter (µm)	**Cumulative Vol % Passing**	**Cumulative Vol % Passing**	**Cumulative Vol % Passing**
1.905	5.98	9.09	7.54
1.738	5.47	8.30	6.89
1.585	4.99	7.55	6.27
1.445	4.53	6.84	5.69
1.318	4.09	6.18	5.14
1.202	3.69	5.55	4.62
1.096	3.30	4.97	4.14
1.000	2.94	4.42	3.68
0.912	2.59	3.90	3.25
0.832	2.26	3.42	2.84
0.759	1.95	2.96	2.46
0.692	1.66	2.52	2.09
0.631	1.38	2.11	1.75
0.575	1.12	1.73	1.43
0.525	0.88	1.38	1.13
0.479	0.66	1.06	0.86
0.437	0.47	0.77	0.62
0.398	0.30	0.53	0.42
0.363	0.16	0.33	0.25
0.331	0.06	0.17	0.12
0.302	0.00	0.07	0.04
0.275	0.00	0.02	0.01
0.251	0.00	0.00	0.00
0.229	0.00	0.00	0.00
0.209	0.00	0.00	0.00
0.191	0.00	0.00	0.00
0.174	0.00	0.00	0.00
0.158	0.00	0.00	0.00
0.145	0.00	0.00	0.00
0.132	0.00	0.00	0.00
0.120	0.00	0.00	0.00
0.110	0.00	0.00	0.00
0.100	0.00	0.00	0.00

Table B.20: Malvern Mastersizer sizing results at the Box-Behnken centre points for Selective Flocculation and at a pH of 11

Dry Sample/ Slurry	Slurry	Slurry	Slurry	Slurry	Slurry
Pump Speed (rpm)	600	600	600	600	600
Ultrasonic	Off	Off	Off	Off	Off
Water	pH 11	pH 11	pH 11	pH 11	pH 11
Specific Surface Area (m^2/g)	0.623	0.553	0.655	0.656	0.622
d(0.1) (µm)	4.966	5.816	4.374	4.646	4.951
d(0.5) (µm)	29.346	36.479	35.141	29.475	32.610
d(0.9) (µm)	95.401	112.542	109.494	94.701	103.035
File Name	Repeat 1	Repeat 2	Repeat 3	Repeat 4	Average Repeats 1-4

Particle Diameter (µm)	**Cumulative Vol % Passing**	**Cumulative Vol % Passing**	**Cumulative Vol % Passing**	**Cumulative Vol % Passing**	**Cumulative Vol % Passing**
100.000	91.08	86.78	87.36	91.27	89.12
91.201	88.91	83.92	84.43	89.06	86.58
83.176	86.51	80.80	81.30	86.57	83.80
75.858	83.88	77.48	78.01	83.82	80.80
69.183	81.06	74.02	74.61	80.88	77.64
63.096	78.08	70.47	71.14	77.76	74.36
57.544	74.95	66.90	67.66	74.52	71.01
52.481	71.70	63.34	64.20	71.18	67.61
47.863	68.35	59.84	60.78	67.78	64.19
43.652	64.94	56.41	57.45	64.35	60.79
39.811	61.48	53.08	54.21	60.93	57.43
36.308	58.00	49.84	51.08	57.52	54.11
33.113	54.52	46.70	48.08	54.16	50.87
30.200	51.06	43.67	45.20	50.86	47.70
27.542	47.66	40.74	42.45	47.63	44.62
25.119	44.34	37.92	39.83	44.48	41.64
22.909	41.10	35.20	37.33	41.43	38.77
20.893	37.99	32.60	34.96	38.49	36.01
19.055	35.01	30.11	32.70	35.66	33.37
17.378	32.18	27.74	30.56	32.96	30.86
15.849	29.52	25.51	28.52	30.39	28.49
14.454	27.04	23.42	26.59	27.98	26.26
13.183	24.73	21.46	24.77	25.71	24.17
12.023	22.61	19.65	23.05	23.60	22.23
10.965	20.67	17.98	21.42	21.65	20.43
10.000	18.90	16.45	19.89	19.85	18.77
9.120	17.30	15.07	18.46	18.21	17.26
8.318	15.86	13.81	17.12	16.71	15.88
7.586	14.55	12.68	15.87	15.36	14.62
6.918	13.38	11.66	14.70	14.13	13.47
6.310	12.32	10.74	13.61	13.02	12.42
5.754	11.36	9.91	12.60	12.01	11.47
5.248	10.49	9.16	11.67	11.09	10.60
4.786	9.69	8.47	10.79	10.25	9.80
4.365	8.96	7.84	9.98	9.49	9.07
3.981	8.28	7.26	9.23	8.78	8.39
3.631	7.65	6.72	8.52	8.13	7.76
3.311	7.06	6.22	7.87	7.51	7.17
3.020	6.51	5.74	7.25	6.94	6.61
2.754	5.98	5.29	6.67	6.40	6.09
2.512	5.49	4.87	6.13	5.89	5.60
2.291	5.02	4.47	5.62	5.41	5.13
2.089	4.58	4.08	5.14	4.95	4.69

Table B.20: Malvern Mastersizer sizing results at the Box-Behnken centre points for Selective Flocculation and at a pH of 11 (Contd.)

Dry Sample/ Slurry	Slurry	Slurry	Slurry	Slurry	Slurry
Pump Speed (rpm)	600	600	600	600	600
Ultrasonic	Off	Off	Off	Off	Off
Water	pH 11	pH 11	pH 11	pH 11	pH 11
Specific Surface Area (m^2/g)	0.623	0.553	0.655	0.656	0.622
d(0.1) (µm)	4.966	5.816	4.374	4.646	4.951
d(0.5) (µm)	29.346	36.479	35.141	29.475	32.610
d(0.9) (µm)	95.401	112.542	109.494	94.701	103.035
File Name	Repeat 1	Repeat 2	Repeat 3	Repeat 4	Average Repeats 1-4

Particle Diameter (µm)	**Cumulative Vol % Passing**	**Cumulative Vol % Passing**	**Cumulative Vol % Passing**	**Cumulative Vol % Passing**	**Cumulative Vol % Passing**
1.905	4.17	3.72	4.68	4.51	4.27
1.738	3.77	3.37	4.26	4.10	3.88
1.585	3.40	3.05	3.85	3.71	3.50
1.445	3.06	2.74	3.47	3.34	3.15
1.318	2.73	2.45	3.11	2.99	2.82
1.202	2.42	2.17	2.77	2.66	2.51
1.096	2.13	1.91	2.45	2.35	2.21
1.000	1.85	1.66	2.15	2.05	1.93
0.912	1.60	1.43	1.86	1.78	1.67
0.832	1.36	1.21	1.59	1.52	1.42
0.759	1.13	1.01	1.34	1.27	1.19
0.692	0.93	0.82	1.10	1.05	0.98
0.631	0.74	0.65	0.89	0.85	0.78
0.575	0.57	0.50	0.70	0.66	0.61
0.525	0.42	0.36	0.53	0.50	0.45
0.479	0.29	0.24	0.38	0.36	0.32
0.437	0.18	0.15	0.25	0.24	0.21
0.398	0.10	0.07	0.16	0.15	0.12
0.363	0.03	0.01	0.08	0.07	0.05
0.331	0.00	0.00	0.02	0.02	0.01
0.302	0.00	0.00	0.00	0.00	0.00
0.275	0.00	0.00	0.00	0.00	0.00
0.251	0.00	0.00	0.00	0.00	0.00
0.229	0.00	0.00	0.00	0.00	0.00
0.209	0.00	0.00	0.00	0.00	0.00
0.191	0.00	0.00	0.00	0.00	0.00
0.174	0.00	0.00	0.00	0.00	0.00
0.158	0.00	0.00	0.00	0.00	0.00
0.145	0.00	0.00	0.00	0.00	0.00
0.132	0.00	0.00	0.00	0.00	0.00
0.120	0.00	0.00	0.00	0.00	0.00
0.110	0.00	0.00	0.00	0.00	0.00
0.100	0.00	0.00	0.00	0.00	0.00

Table B.21: Raw Data of the SLon-100 tests at the Box-Behnken centre points for Selective Flocculation and at a pH of 9.5; 6 000 Gauss and 261.2 rpm

Test #	Element	Product	Mass Split	Discrete Grade										∑ Oxides
				Fe	SiO_2	Al_2O_3	MnO	K_2O	CaO	P_2O_5	Na_2O	MgO	LOI	
	UNITS		%	%	%	%	%	%	%	%	%	%	%	
		HEAD	**100.0**	37.34	41.78	0.98	0.05	0.07	0.38	0.26	0.10	0.31	0.86	97.82
Test 9	**Relative Error**			2.07	0.43	6.58	0.00	4.43	6.94	4.06	0.00	13.50	31.31	
	Calculated Head		**100.0**	**38.11**	**41.61**	**0.91**	**0.05**	**0.08**	**0.36**	**0.25**	**0.10**	**0.27**	**0.59**	**98.71**
		Mags	43.3	56.10	17.33	0.62	0.05	0.05	0.20	0.15	0.10	0.18	0.50	99.41
		N-Mags	56.7	24.37	60.15	1.13	0.05	0.10	0.48	0.33	0.10	0.34	0.66	98.18
Test 13	**Relative Error**			3.70	6.53	3.17	0.00	1.49	1.50	1.85	0.00	8.89	4.82	
	Calculated Head		**100.0**	**35.96**	**44.51**	**0.94**	**0.05**	**0.07**	**0.39**	**0.27**	**0.10**	**0.28**	**0.90**	**98.94**
		Mags	38.5	54.37	19.67	0.57	0.05	0.05	0.24	0.18	0.10	0.19	0.60	99.40
		N-Mags	61.5	24.45	60.05	1.18	0.05	0.09	0.48	0.32	0.10	0.34	1.09	98.66
Test 17	**Relative Error**			0.19	2.30	2.33	0.00	0.76	6.75	3.05	0.00	13.92	20.40	
	Calculated Head		**100.0**	**37.27**	**42.74**	**1.00**	**0.05**	**0.07**	**0.36**	**0.26**	**0.10**	**0.27**	**0.68**	**98.82**
		Mags	42.8	58.77	13.72	0.79	0.05	0.05	0.17	0.14	0.10	0.18	0.49	99.74
		N-Mags	57.2	21.19	64.44	1.15	0.05	0.09	0.50	0.34	0.10	0.33	0.83	98.13

Test #	Element	Product	Mass Split	Discrete Recovery (%)									
				Fe	SiO_2	Al_2O_3	MnO	K_2O	CaO	P_2O_5	Na_2O	MgO	LOI
	UNITS		%										
		HEAD	**100.0**										
Test 9	**Relative Error**												
	Calculated Head		**100.0**	**100.0**	**100.0**	**100.0**	**100.0**	**100.0**	**100.0**	**100.0**	**100.0**	**100.0**	**100.0**
		Mags	43.3	63.7	18.0	29.7	43.3	28.5	23.9	26.4	43.3	28.6	36.7
		N-Mags	56.7	36.3	82.0	70.3	56.7	71.5	76.1	73.6	56.7	71.4	63.3
Test 13	**Relative Error**												
	Calculated Head		**100.0**	**100.0**	**100.0**	**100.0**	**100.0**	**100.0**	**100.0**	**100.0**	**100.0**	**100.0**	**100.0**
		Mags	38.5	58.2	17.0	23.1	38.5	26.0	24.0	25.7	38.5	26.4	25.6
		N-Mags	61.5	41.8	83.0	76.9	61.5	74.0	76.0	74.3	61.5	73.6	74.4
Test 17	**Relative Error**												
	Calculated Head		**100.0**	**100.0**	**100.0**	**100.0**	**100.0**	**100.0**	**100.0**	**100.0**	**100.0**	**100.0**	**100.0**
		Mags	42.8	67.5	13.7	34.0	42.8	29.1	20.6	23.1	42.8	28.8	30.6
		N-Mags	57.2	32.5	86.3	66.0	57.2	70.9	79.4	76.9	57.2	71.2	69.4

Table B.22: The average raw data of the SLon-100 Mags at the Box-Behnken centre points for Selective Flocculation and at a pH of 9.5; 6 000 Gauss and 261.2 rpm

Test #	pH	Intensity (Gauss)	Pulse Frequency (RPM)	Mass Pull to Mags (%)	Fe Grade (%)	SiO_2 Grade (%)	Fe Recovery (%)	SiO_2 Recovery (%)	Separation Efficieny (SE) (%)
Test 9	9.5	6000	261.2	43.3	56.10	17.33	63.7	18.0	45.7
Test 13				38.5	54.37	19.67	58.2	17.0	41.2
Test 17				42.8	58.77	13.72	67.5	13.7	53.7
Average				**41.5**	**56.41**	**16.91**	**63.1**	**16.3**	**46.9**
Std Dev				**2.6**	**2.22**	**3.00**	**4.7**	**2.2**	**6.4**
2 Std Dev				**5.3**	**4.44**	**5.99**	**9.3**	**4.5**	**12.7**
Std Error with 95% confidence level				**3.1**	**2.56**	**3.46**	**5.4**	**2.6**	**7.3**

Table B.23: Raw Data of the SLon-100 tests at the Box-Behnken centre points for Selective Flocculation and at a pH of 10; 6 000 Gauss and 261.2 rpm

Test #	Element	Product	Mass Split	Discrete Grade										∑ Oxides
				Fe	SiO_2	Al_2O_3	MnO	K_2O	CaO	P_2O_5	Na_2O	MgO	LOI	
	UNITS		%	%	%	%	%	%	%	%	%	%	%	
		HEAD	**100.0**	37.34	41.78	0.98	0.05	0.07	0.38	0.26	0.10	0.31	0.86	97.82
Test 10	**Relative Error**			0.20	1.82	5.64	0.00	9.15	11.29	9.92	0.00	21.46	28.59	
	Calculated Head		**100.0**	**37.42**	**42.54**	**0.92**	**0.05**	**0.07**	**0.34**	**0.24**	**0.10**	**0.24**	**0.61**	**98.62**
		Mags	45.3	58.42	14.20	0.72	0.05	0.05	0.18	0.14	0.10	0.17	0.39	99.53
		N-Mags	54.7	20.00	66.05	1.09	0.05	0.08	0.48	0.32	0.10	0.30	0.80	97.86
Test 14	**Relative Error**			0.01	2.07	27.87	0.00	8.79	2.60	2.93	0.00	13.84	16.45	
	Calculated Head		**100.0**	**37.34**	**42.65**	**0.70**	**0.05**	**0.08**	**0.37**	**0.26**	**0.10**	**0.27**	**0.72**	**98.59**
		Mags	44.8	57.87	14.94	0.48	0.05	0.05	0.19	0.15	0.10	0.19	0.50	99.40
		N-Mags	55.2	20.67	65.14	0.88	0.05	0.10	0.52	0.35	0.10	0.33	0.90	97.94
Test 18	**Relative Error**			0.18	1.85	9.88	0.00	1.36	6.75	3.74	0.00	14.23	9.93	
	Calculated Head		**100.0**	**37.41**	**42.56**	**0.88**	**0.05**	**0.07**	**0.36**	**0.25**	**0.10**	**0.27**	**0.77**	**98.80**
		Mags	45.4	58.10	14.63	0.66	0.05	0.05	0.19	0.15	0.10	0.18	0.48	99.56
		N-Mags	54.6	20.17	65.82	1.06	0.05	0.09	0.50	0.34	0.10	0.34	1.02	98.17

Test #	Element	Product	Mass Split	Discrete Recovery (%)									
				Fe	SiO_2	Al_2O_3	MnO	K_2O	CaO	P_2O_5	Na_2O	MgO	LOI
	UNITS		%										
		HEAD	**100.0**										
Test 10	**Relative Error**												
	Calculated Head		**100.0**	**100.0**	**100.0**	**100.0**	**100.0**	**100.0**	**100.0**	**100.0**	**100.0**	**100.0**	**100.0**
		Mags	45.3	70.8	15.1	35.2	45.3	34.2	23.5	26.9	45.3	32.0	28.8
		N-Mags	54.7	29.2	84.9	64.8	54.7	65.8	76.5	73.1	54.7	68.0	71.2
Test 14	**Relative Error**												
	Calculated Head		**100.0**	**100.0**	**100.0**	**100.0**	**100.0**	**100.0**	**100.0**	**100.0**	**100.0**	**100.0**	**100.0**
		Mags	44.8	69.4	15.7	30.8	44.8	28.3	23.1	25.5	44.8	31.0	30.9
		N-Mags	55.2	30.6	84.3	69.2	55.2	71.7	76.9	74.5	55.2	69.0	69.1
Test 18	**Relative Error**												
	Calculated Head		**100.0**	**100.0**	**100.0**	**100.0**	**100.0**	**100.0**	**100.0**	**100.0**	**100.0**	**100.0**	**100.0**
		Mags	45.4	70.6	15.6	34.2	45.4	30.8	23.6	26.2	45.4	30.1	28.2
		N-Mags	54.6	29.4	84.4	65.8	54.6	69.2	76.4	73.8	54.6	69.9	71.8

Table B.24: The average raw data of the SLon-100 Mags at the Box-Behnken centre points for Selective Flocculation and at a pH of 10; 6 000 Gauss and 261.2 rpm

Test #	pH	Intensity (Gauss)	Pulse Frequency (RPM)	Mass Pull to Mags (%)	Fe Grade (%)	SiO_2 Grade (%)	Fe Recovery (%)	SiO_2 Recovery (%)	Separation Efficieny (SE) (%)
Test 10	10	6000	261.2	45.3	58.42	14.20	70.8	15.1	55.6
Test 14				44.8	57.87	14.94	69.4	15.7	53.7
Test 18				45.4	58.10	14.63	70.6	15.6	55.0
Average				**45.2**	**58.13**	**14.59**	**70.3**	**15.5**	**54.8**
Std Dev				**0.3**	**0.28**	**0.37**	**0.7**	**0.3**	**1.0**
2 Std Dev				**0.7**	**0.55**	**0.74**	**1.5**	**0.6**	**1.9**
Std Error with 95% confidence level				**0.4**	**0.32**	**0.43**	**0.8**	**0.4**	**1.1**

Table B.25: Raw Data of the SLon-100 tests at the Box-Behnken centre points for Selective Flocculation and at a pH of 10.5; 6 000 Gauss and 261.2 rpm

Test #	Element	Product	Mass Split	Discrete Grade										∑ Oxides
				Fe	SiO_2	Al_2O_3	MnO	K_2O	CaO	P_2O_5	Na_2O	MgO	LOI	
	UNITS		%	%	%	%	%	%	%	%	%	%	%	
		HEAD	100.0	37.34	41.78	0.98	0.05	0.07	0.38	0.26	0.10	0.31	0.86	97.82
Test 11	Relative Error			0.37	2.52	7.75	0.00	7.81	5.43	5.82	0.00	14.31	10.59	
	Calculated Head		100.0	37.20	42.84	0.90	0.05	0.08	0.36	0.25	0.10	0.27	0.77	98.81
		Mags	41.8	59.29	13.02	0.51	0.05	0.05	0.17	0.14	0.10	0.18	0.60	99.61
		N-Mags	58.2	21.36	64.21	1.18	0.05	0.10	0.50	0.33	0.10	0.33	0.89	98.23
Test 15	Relative Error			0.77	2.99	8.57	0.00	20.26	3.09	4.74	0.00	8.21	21.90	
	Calculated Head		100.0	37.05	43.03	0.89	0.05	0.09	0.37	0.25	0.10	0.28	0.67	98.73
		Mags	45.5	56.96	16.17	0.65	0.05	0.05	0.21	0.16	0.10	0.18	0.47	99.49
		N-Mags	54.5	20.44	65.46	1.09	0.05	0.12	0.51	0.33	0.10	0.38	0.84	98.10
Test 19	Relative Error			0.31	1.69	10.28	0.00	0.28	6.15	4.36	0.00	16.02	10.72	
	Calculated Head		100.0	37.46	42.49	0.87	0.05	0.07	0.36	0.25	0.10	0.26	0.77	98.79
		Mags	44.8	58.24	14.45	0.60	0.05	0.05	0.19	0.15	0.10	0.17	0.58	99.62
		N-Mags	55.2	20.61	65.22	1.10	0.05	0.09	0.49	0.33	0.10	0.33	0.92	98.12

Test #	Element	Product	Mass Split	Discrete Recovery (%)									
				Fe	SiO_2	Al_2O_3	MnO	K_2O	CaO	P_2O_5	Na_2O	MgO	LOI
	UNITS		%										
		HEAD	100.0										
Test 11	Relative Error												
	Calculated Head		100.0	100.0	100.0	100.0	100.0	100.0	100.0	100.0	100.0	100.0	100.0
		Mags	41.8	66.5	12.7	23.6	41.8	26.6	19.8	22.7	41.8	28.1	32.6
		N-Mags	58.2	33.5	87.3	76.4	58.2	73.4	80.2	77.3	58.2	71.9	67.4
Test 15	Relative Error												
	Calculated Head		100.0	100.0	100.0	100.0	100.0	100.0	100.0	100.0	100.0	100.0	100.0
		Mags	45.5	69.9	17.1	33.3	45.5	26.0	25.3	28.3	45.5	28.2	31.8
		N-Mags	54.5	30.1	82.9	66.7	54.5	74.0	74.7	71.7	54.5	71.8	68.2
Test 19	Relative Error												
	Calculated Head		100.0	100.0	100.0	100.0	100.0	100.0	100.0	100.0	100.0	100.0	100.0
		Mags	44.8	69.6	15.2	30.6	44.8	30.8	24.2	27.2	44.8	29.4	33.8
		N-Mags	55.2	30.4	84.8	69.4	55.2	69.2	75.8	72.8	55.2	70.6	66.2

Table B.26: The average raw data of the SLon-100 Mags at the Box-Behnken centre points for Selective Flocculation and at a pH of 10.5; 6 000 Gauss and 261.2 rpm

Test #	pH	Intensity (Gauss)	Pulse Frequency (RPM)	Mass Pull to Mags (%)	Fe Grade (%)	SiO_2 Grade (%)	Fe Recovery (%)	SiO_2 Recovery (%)	Separation Efficieny (SE) (%)
Test 11	10.5	6000	261.2	41.8	59.29	13.02	66.5	12.7	53.9
Test 15				45.5	56.96	16.17	69.9	17.1	52.8
Test 19				44.8	58.24	14.45	69.6	15.2	54.4
Average				**44.0**	**58.17**	**14.54**	**68.7**	**15.0**	**53.7**
Std Dev				**2.0**	**1.17**	**1.57**	**1.9**	**2.2**	**0.8**
2 Std Dev				**4.0**	**2.33**	**3.15**	**3.7**	**4.4**	**1.6**
Std Error with 95% confidence level				**2.3**	**1.35**	**1.82**	**2.2**	**2.5**	**0.9**

Table B.27: Raw Data of the SLon-100 tests at the Box-Behnken centre points for Selective Flocculation and at a pH of 11; 6 000 Gauss and 261.2 rpm

Test #	Element	Product	Mass Split	Discrete Grade										∑ Oxides
				Fe	SiO_2	Al_2O_3	MnO	K_2O	CaO	P_2O_5	Na_2O	MgO	LOI	
	UNITS		%	%	%	%	%	%	%	%	%	%	%	
		HEAD	**100.0**	37.34	41.78	0.98	0.05	0.07	0.38	0.26	0.10	0.31	0.86	97.82
Test 12	**Relative Error**			0.18	1.85	8.40	0.00	6.24	5.04	3.83	0.00	9.86	26.57	
	Calculated Head		**100.0**	**37.41**	**42.56**	**0.89**	**0.05**	**0.08**	**0.36**	**0.25**	**0.10**	**0.28**	**0.63**	**98.70**
		Mags	41.7	59.33	12.97	0.55	0.05	0.05	0.20	0.15	0.10	0.18	0.41	99.51
		N-Mags	58.3	21.72	63.73	1.14	0.05	0.10	0.48	0.33	0.10	0.35	0.79	98.12
Test 16	**Relative Error**			0.13	2.22	0.32	0.00	4.88	4.33	3.05	0.00	9.83	12.15	
	Calculated Head		**100.0**	**37.29**	**42.71**	**0.97**	**0.05**	**0.08**	**0.37**	**0.26**	**0.10**	**0.28**	**0.76**	**98.89**
		Mags	46.1	57.00	16.12	0.72	0.05	0.05	0.21	0.17	0.10	0.19	0.61	99.72
		N-Mags	53.9	20.43	65.47	1.19	0.05	0.10	0.50	0.33	0.10	0.36	0.88	98.19
Test 20	**Relative Error**			0.19	1.84	9.05	0.00	5.04	6.10	4.69	0.00	15.81	12.97	
	Calculated Head		**100.0**	**37.41**	**42.55**	**0.89**	**0.05**	**0.08**	**0.36**	**0.25**	**0.10**	**0.26**	**0.75**	**98.78**
		Mags	44.8	57.70	15.17	0.59	0.05	0.05	0.22	0.17	0.10	0.14	0.48	99.47
		N-Mags	55.2	20.98	64.73	1.13	0.05	0.10	0.48	0.32	0.10	0.36	0.97	98.22

Test #	Element	Product	Mass Split	Discrete Recovery (%)									
				Fe	SiO_2	Al_2O_3	MnO	K_2O	CaO	P_2O_5	Na_2O	MgO	LOI
	UNITS		%										
		HEAD	**100.0**										
Test 12	**Relative Error**												
	Calculated Head		**100.0**	**100.0**	**100.0**	**100.0**	**100.0**	**100.0**	**100.0**	**100.0**	**100.0**	**100.0**	**100.0**
		Mags	41.7	66.2	12.7	25.6	41.7	26.9	22.8	25.2	41.7	27.5	27.1
		N-Mags	58.3	33.8	87.3	74.4	58.3	73.1	77.2	74.8	58.3	72.5	72.9
Test 16	**Relative Error**												
	Calculated Head		**100.0**	**100.0**	**100.0**	**100.0**	**100.0**	**100.0**	**100.0**	**100.0**	**100.0**	**100.0**	**100.0**
		Mags	46.1	70.5	17.4	34.0	46.1	30.2	26.7	30.3	46.1	30.8	37.2
		N-Mags	53.9	29.5	82.6	66.0	53.9	69.8	73.3	69.7	53.9	69.2	62.8
Test 20	**Relative Error**												
	Calculated Head		**100.0**	**100.0**	**100.0**	**100.0**	**100.0**	**100.0**	**100.0**	**100.0**	**100.0**	**100.0**	**100.0**
		Mags	44.8	69.0	16.0	29.6	44.8	29.2	27.0	30.2	44.8	24.7	28.4
		N-Mags	55.2	31.0	84.0	70.4	55.2	70.8	73.0	69.8	55.2	75.3	71.6

Table B.28: The average raw data of the SLon-100 Mags at the Box-Behnken centre points for Selective Flocculation and at a pH of 11; 6 000 Gauss and 261.2 rpm

Test #	pH	Intensity (Gauss)	Pulse Frequency (RPM)	Mass Pull to Mags (%)	Fe Grade (%)	SiO_2 Grade (%)	Fe Recovery (%)	SiO_2 Recovery (%)	Separation Efficieny (SE) (%)
Test 12	11	6000	261.2	41.7	59.33	12.97	66.2	12.7	53.4
Test 16				46.1	57.00	16.12	70.5	17.4	53.1
Test 20				44.8	57.70	15.17	69.0	16.0	53.1
Average				**44.2**	**58.01**	**14.75**	**68.6**	**15.4**	**53.2**
Std Dev				**2.3**	**1.20**	**1.61**	**2.2**	**2.4**	**0.2**
2 Std Dev				**4.5**	**2.39**	**3.23**	**4.4**	**4.8**	**0.4**
Std Error with 95% confidence level				**2.6**	**1.38**	**1.86**	**2.5**	**2.8**	**0.3**

APPENDIX C: RAW DATA FOR OPTIMISING SELECTIVE FLOCCULATION COUPLED WITH MAGNETIC SEPARATION

Table C.1: Raw Data for Block 1 results of the SLon-100 coupled with Selective Flocculation using the Box-Behnken experimental Design

Test #	Factor 1: Sodium Oleate Dosage (g/t)	Factor 2: Paraffin Dosage (g/t)	Factor 3: Conditioning Time (min)	Product	Mass Split	Discrete Grade (WDXRF)								∑ Oxides
						Fe	SiO_2	Al_2O_3	MnO	CaO	P_2O_5	MgO	LOI	
					%	%	%	%	%	%	%	%	%	
				HEAD	**100.0**	37.34	41.78	0.98	0.05	0.38	0.26	0.31	0.86	97.82
Block 1 Run 1	1000	4000	5	**Relative Error**		1.11	0.18	12.77	0.00	57.06	10.09	10.84	24.97	
				Calculated Head	**100.0**	**36.93**	**41.71**	**0.85**	**0.05**	**0.16**	**0.24**	**0.28**	**0.65**	**96.73**
				Mags	**46.8**	58.19	13.55	0.37	0.05	0.05	0.12	0.10	0.39	97.85
				N-Mags	**53.2**	18.20	66.50	1.27	0.05	0.27	0.34	0.43	0.87	95.75
Block 1 Run 2	2000	4000	10	**Relative Error**		0.73	0.64	20.76	0.00	52.32	12.52	32.05	29.59	
				Calculated Head	**100.0**	**37.07**	**41.52**	**0.77**	**0.05**	**0.18**	**0.23**	**0.21**	**0.61**	**96.58**
				Mags	**47.4**	57.16	14.50	0.58	0.05	0.05	0.14	0.07	0.39	97.51
				N-Mags	**52.6**	18.94	65.90	0.95	0.05	0.30	0.31	0.34	0.80	95.73
Block 1 Run 3	1000	2000	5	**Relative Error**		1.02	0.51	0.48	0.00	56.61	11.32	6.88	30.48	
				Calculated Head	**100.0**	**36.96**	**41.57**	**0.98**	**0.05**	**0.17**	**0.23**	**0.29**	**0.60**	**96.74**
				Mags	**46.3**	58.27	13.10	0.57	0.05	0.05	0.10	0.09	0.34	97.63
				N-Mags	**53.7**	18.60	66.10	1.33	0.05	0.27	0.35	0.46	0.82	95.97
Block 1 Run 4	2000	3000	20	**Relative Error**		0.29	0.42	1.90	0.00	55.21	10.36	7.28	20.45	
				Calculated Head	**100.0**	**37.23**	**41.61**	**0.96**	**0.05**	**0.17**	**0.24**	**0.29**	**0.68**	**97.24**
				Mags	**46.8**	59.12	12.80	0.50	0.05	0.05	0.11	0.07	0.37	98.49
				N-Mags	**53.2**	18.02	66.90	1.36	0.05	0.28	0.35	0.48	0.96	96.13
Block 1 Run 5	1000	3000	10	**Relative Error**		2.07	1.81	11.29	0.00	51.48	8.76	16.48	31.36	
				Calculated Head	**100.0**	**36.57**	**42.54**	**0.86**	**0.05**	**0.19**	**0.24**	**0.26**	**0.59**	**97.02**
				Mags	45.9	57.87	14.00	0.55	0.05	0.05	0.11	0.07	0.32	97.90
				N-Mags	**54.1**	18.47	66.80	1.13	0.05	0.30	0.35	0.42	0.82	96.28
Block 1 Run 6	2000	3000	5	**Relative Error**		0.15	1.50	8.49	0.00	54.96	14.43	23.54	39.15	
				Calculated Head	**100.0**	**37.40**	**41.16**	**0.89**	**0.05**	**0.17**	**0.23**	**0.24**	**0.52**	**96.73**
				Mags	**47.5**	58.03	13.90	0.67	0.05	0.05	0.13	0.09	0.35	98.23
				N-Mags	**52.5**	18.73	65.80	1.09	0.05	0.28	0.31	0.37	0.68	95.38
Block 1 Run 7	1000	3000	10	**Relative Error**		2.25	1.20	5.84	0.00	54.43	13.77	16.35	22.17	
				Calculated Head	**100.0**	**36.50**	**42.29**	**0.92**	**0.05**	**0.17**	**0.23**	**0.26**	**1.05**	**97.16**
				Mags	**45.7**	58.43	13.50	0.57	0.05	0.05	0.09	0.09	0.35	98.26
				N-Mags	**54.3**	18.06	66.50	1.21	0.05	0.28	0.34	0.40	1.64	96.24
Block 1 Run 8	1000	2000	20	**Relative Error**		0.42	0.89	14.95	0.00	53.14	11.42	7.68	28.62	
				Calculated Head	**100.0**	**37.18**	**41.41**	**1.12**	**0.05**	**0.18**	**0.23**	**0.29**	**0.61**	**97.07**
				Mags	**47.4**	58.41	13.60	0.66	0.05	0.05	0.09	0.08	0.33	98.38
				N-Mags	**52.6**	18.03	66.50	1.54	0.05	0.30	0.37	0.48	0.87	95.89
Block 1 Run 9	500	2000	10	**Relative Error**		1.18	0.99	8.02	0.00	46.02	13.64	12.99	29.74	
				Calculated Head	**100.0**	**36.90**	**41.37**	**1.05**	**0.05**	**0.21**	**0.23**	**0.27**	**0.60**	**96.54**
				Mags	**46.6**	58.33	12.30	0.79	0.05	0.05	0.08	0.09	0.46	97.23
				N-Mags	**53.4**	18.22	66.70	1.28	0.05	0.34	0.36	0.43	0.73	95.95
Block 1 Run 10	1000	3000	10	**Relative Error**		3.23	1.40	0.65	0.00	54.34	12.64	10.65	35.50	
				Calculated Head	**100.0**	**36.13**	**42.37**	**0.97**	**0.05**	**0.17**	**0.23**	**0.28**	**1.17**	**96.91**
				Mags	**46.0**	57.07	14.40	0.62	0.05	0.05	0.10	0.06	0.35	97.24
				N-Mags	**54.0**	18.30	66.20	1.27	0.05	0.28	0.34	0.46	1.86	96.63
Block 1 Run 11	500	4000	10	**Relative Error**		0.74	0.15	33.53	0.00	49.26	15.63	21.55	40.40	
				Calculated Head	**100.0**	**37.62**	**41.85**	**0.65**	**0.05**	**0.19**	**0.22**	**0.24**	**0.51**	**97.51**
				Mags	**48.0**	58.59	13.90	0.43	0.05	0.05	0.10	0.11	0.32	98.74
				N-Mags	**52.0**	18.29	67.60	0.85	0.05	0.33	0.33	0.36	0.69	96.37
Block 1 Run 12	500	3000	20	**Relative Error**		3.11	2.77	30.91	0.00	49.91	19.96	29.83	51.42	
				Calculated Head	**100.0**	**38.50**	**40.62**	**0.67**	**0.05**	**0.19**	**0.21**	**0.22**	**0.42**	**97.45**
				Mags	**47.7**	59.44	12.60	0.32	0.05	0.05	0.08	0.08	0.24	98.42
				N-Mags	**52.3**	19.39	66.20	1.00	0.05	0.32	0.33	0.35	0.58	96.56

Table C.1: Raw Data for Block 1 results of the SLon-100 coupled with Selective Flocculation using the Box-Behnken experimental Design (Contd.)

Test #	Factor 1: Sodium Oleate Dosage (g/t)	Factor 2: Paraffin Dosage (g/t)	Factor 3: Conditioning Time (min)	Product	Mass Split	Discrete Recovery (%)								Separation Efficieny (SE) (%)
					%	Fe	SiO_2	Al_2O_3	MnO	CaO	P_2O_5	MgO	LOI	
				HEAD	**100.0**									
Block 1 Run 1	1000	4000	5	**Relative Error**										
				Calculated Head	**100.0**	**100.0**	**100.0**	**100.0**	**100.0**	**100.0**	**100.0**	**100.0**	**100.0**	
				Mags	**46.8**	73.8	15.2	20.6	46.8	14.2	22.7	16.9	28.3	58.6
				N-Mags	**53.2**	26.2	84.8	79.4	53.2	85.8	77.3	83.1	71.7	
Block 1 Run 2	2000	4000	10	**Relative Error**										
				Calculated Head	**100.0**	**100.0**	**100.0**	**100.0**	**100.0**	**100.0**	**100.0**	**100.0**	**100.0**	
				Mags	**47.4**	73.1	16.6	35.3	47.4	13.0	29.0	16.2	30.6	56.6
				N-Mags	**52.6**	26.9	83.4	64.7	52.6	87.0	71.0	83.8	69.4	
Block 1 Run 3	1000	2000	5	**Relative Error**										
				Calculated Head	**100.0**	**100.0**	**100.0**	**100.0**	**100.0**	**100.0**	**100.0**	**100.0**	**100.0**	
				Mags	**46.3**	73.0	14.6	27.1	46.3	13.9	20.4	14.3	26.3	58.4
				N-Mags	**53.7**	27.0	85.4	72.9	53.7	86.1	79.6	85.7	73.7	
Block 1 Run 4	2000	3000	20	**Relative Error**										
				Calculated Head	**100.0**	**100.0**	**100.0**	**100.0**	**100.0**	**100.0**	**100.0**	**100.0**	**100.0**	
				Mags	**46.8**	74.2	14.4	24.3	46.8	13.6	22.2	11.9	25.3	59.9
				N-Mags	**53.2**	25.8	85.6	75.7	53.2	86.4	77.8	88.1	74.7	
Block 1 Run 5	1000	3000	10	**Relative Error**										
				Calculated Head	**100.0**	**100.0**	**100.0**	**100.0**	**100.0**	**100.0**	**100.0**	**100.0**	**100.0**	
				Mags	45.9	72.7	15.1	29.4	45.9	12.4	21.0	11.5	24.9	57.6
				N-Mags	**54.1**	27.3	84.9	70.6	54.1	87.6	79.0	88.5	75.1	
Block 1 Run 6	2000	3000	5	**Relative Error**										
				Calculated Head	**100.0**	**100.0**	**100.0**	**100.0**	**100.0**	**100.0**	**100.0**	**100.0**	**100.0**	
				Mags	**47.5**	73.7	16.0	35.8	47.5	13.8	27.3	17.6	31.8	57.7
				N-Mags	**52.5**	26.3	84.0	64.2	52.5	86.2	72.7	82.4	68.2	
Block 1 Run 7	1000	3000	10	**Relative Error**										
				Calculated Head	**100.0**	**100.0**	**100.0**	**100.0**	**100.0**	**100.0**	**100.0**	**100.0**	**100.0**	
				Mags	**45.7**	73.1	14.6	28.4	45.7	13.1	18.9	15.8	15.2	58.5
				N-Mags	**54.3**	26.9	85.4	71.6	54.3	86.9	81.1	84.2	84.8	
Block 1 Run 8	1000	2000	20	**Relative Error**										
				Calculated Head	**100.0**	**100.0**	**100.0**	**100.0**	**100.0**	**100.0**	**100.0**	**100.0**	**100.0**	
				Mags	**47.4**	74.5	15.6	27.8	47.4	13.2	17.3	12.4	25.5	58.9
				N-Mags	**52.6**	25.5	84.4	72.2	52.6	86.8	82.7	87.6	74.5	
Block 1 Run 9	500	2000	10	**Relative Error**										
				Calculated Head	**100.0**	**100.0**	**100.0**	**100.0**	**100.0**	**100.0**	**100.0**	**100.0**	**100.0**	
				Mags	**46.6**	73.6	13.8	35.1	46.6	11.3	16.6	14.7	35.4	59.8
				N-Mags	**53.4**	26.4	86.2	64.9	53.4	88.7	83.4	85.3	64.6	
Block 1 Run 10	1000	3000	10	**Relative Error**										
				Calculated Head	**100.0**	**100.0**	**100.0**	**100.0**	**100.0**	**100.0**	**100.0**	**100.0**	**100.0**	
				Mags	**46.0**	72.7	15.6	29.2	46.0	13.2	20.2	9.8	13.8	57.0
				N-Mags	**54.0**	27.3	84.4	70.8	54.0	86.8	79.8	90.2	86.2	
Block 1 Run 11	500	4000	10	**Relative Error**										
				Calculated Head	**100.0**	**100.0**	**100.0**	**100.0**	**100.0**	**100.0**	**100.0**	**100.0**	**100.0**	
				Mags	**48.0**	74.7	15.9	31.7	48.0	12.4	22.2	22.4	29.9	58.8
				N-Mags	**52.0**	25.3	84.1	68.3	52.0	87.6	77.8	77.6	70.1	
Block 1 Run 12	500	3000	20	**Relative Error**										
				Calculated Head	**100.0**	**100.0**	**100.0**	**100.0**	**100.0**	**100.0**	**100.0**	**100.0**	**100.0**	
				Mags	**47.7**	73.7	14.8	22.4	47.7	12.4	17.9	16.9	27.4	58.9
				N-Mags	**52.3**	26.3	85.2	77.6	52.3	87.6	82.1	83.1	72.6	

Table C.1: Raw Data for Block 1 results of the SLon-100 coupled with Selective Flocculation using the Box-Behnken experimental Design (Contd.)

Test #	Factor 1: Sodium Oleate Dosage (g/t)	Factor 2: Paraffin Dosage (g/t)	Factor 3: Conditioning Time (min)	Product	Mass Split	Discrete Grade (WDXRF)								∑ Oxides
						Fe	SiO_2	Al_2O_3	MnO	CaO	P_2O_5	MgO	LOI	
					%	%	%	%	%	%	%	%	%	
				HEAD	**100.0**	37.34	41.78	0.98	0.05	0.38	0.26	0.31	0.86	97.82
Block 1 Run 13	1000	3000	10	**Relative Error**		1.44	0.54	14.80	0.00	48.61	7.89	8.81	38.07	
				Calculated Head	**100.0**	**36.80**	**42.01**	**0.83**	**0.05**	**0.20**	**0.24**	**0.34**	**0.53**	**96.83**
				Mags	**45.5**	57.88	14.70	0.45	0.05	0.05	0.11	0.08	0.26	98.46
				N-Mags	**54.5**	19.22	64.80	1.15	0.05	0.32	0.35	0.55	0.76	95.47
Block 1 Run 14	1000	3000	10	**Relative Error**		1.40	1.38	20.13	0.00	42.44	9.75	0.81	35.20	
				Calculated Head	**100.0**	**36.82**	**42.36**	**0.78**	**0.05**	**0.22**	**0.24**	**0.31**	**0.56**	**97.16**
				Mags	**45.3**	58.16	14.00	0.39	0.05	0.05	0.11	0.08	0.30	98.15
				N-Mags	**54.7**	19.17	65.80	1.10	0.05	0.36	0.34	0.51	0.77	96.35
Block 1 Run 15	1000	4000	20	**Relative Error**		0.17	0.05	22.04	0.00	52.08	10.35	9.40	29.56	
				Calculated Head	**100.0**	**37.28**	**41.80**	**0.76**	**0.05**	**0.18**	**0.24**	**0.28**	**0.61**	**97.23**
				Mags	**47.1**	58.86	13.70	0.33	0.05	0.05	0.09	0.08	0.32	98.80
				N-Mags	**52.9**	18.08	66.80	1.14	0.05	0.30	0.37	0.46	0.86	95.83
Block 1 Run 16	2000	2000	10	**Relative Error**		0.44	0.38	36.94	0.00	39.84	11.82	5.99	28.71	
				Calculated Head	**100.0**	**37.51**	**41.62**	**1.34**	**0.05**	**0.23**	**0.23**	**0.33**	**0.61**	**98.05**
				Mags	**48.4**	57.91	14.80	1.09	0.05	0.10	0.13	0.18	0.35	99.51
				N-Mags	**51.6**	18.36	66.80	1.57	0.05	0.35	0.33	0.47	0.86	96.68
Block 1 Run 17	500	3000	5	**Relative Error**		0.28	0.15	2.96	0.00	39.52	11.52	9.33	43.32	
				Calculated Head	**100.0**	**37.45**	**41.85**	**1.00**	**0.05**	**0.23**	**0.23**	**0.28**	**0.49**	**97.68**
				Mags	**47.1**	58.73	13.60	0.71	0.05	0.05	0.11	0.13	0.26	98.89
				N-Mags	**52.9**	18.49	67.00	1.27	0.05	0.39	0.35	0.42	0.69	96.61

Test #	Factor 1: Sodium Oleate Dosage (g/t)	Factor 2: Paraffin Dosage (g/t)	Factor 3: Conditioning Time (min)	Product	Mass Split	Discrete Recovery (%)								Separation Efficieny (SE) (%)
						Fe	SiO_2	Al_2O_3	MnO	CaO	P_2O_5	MgO	LOI	
					%									
				HEAD	**100.0**									
Block 1 Run 13	1000	3000	10	**Relative Error**										
				Calculated Head	**100.0**	**100.0**	**100.0**	**100.0**	**100.0**	**100.0**	**100.0**	**100.0**	**100.0**	
				Mags	**45.5**	71.5	15.9	24.5	45.5	11.6	20.4	10.5	22.2	55.6
				N-Mags	**54.5**	28.5	84.1	75.5	54.5	88.4	79.6	89.5	77.8	
Block 1 Run 14	1000	3000	10	**Relative Error**										
				Calculated Head	**100.0**	**100.0**	**100.0**	**100.0**	**100.0**	**100.0**	**100.0**	**100.0**	**100.0**	
				Mags	**45.3**	71.5	15.0	22.7	45.3	10.3	20.8	11.6	24.4	56.5
				N-Mags	**54.7**	28.5	85.0	77.3	54.7	89.7	79.2	88.4	75.6	
Block 1 Run 15	1000	4000	20	**Relative Error**										
				Calculated Head	**100.0**	**100.0**	**100.0**	**100.0**	**100.0**	**100.0**	**100.0**	**100.0**	**100.0**	
				Mags	**47.1**	74.3	15.4	20.6	47.1	12.8	17.9	13.7	24.9	58.9
				N-Mags	**52.9**	25.7	84.6	79.4	52.9	87.2	82.1	86.3	75.1	
Block 1 Run 16	2000	2000	10	**Relative Error**										
				Calculated Head	**100.0**	**100.0**	**100.0**	**100.0**	**100.0**	**100.0**	**100.0**	**100.0**	**100.0**	
				Mags	**48.4**	74.8	17.2	39.3	48.4	21.3	26.7	26.9	27.6	57.5
				N-Mags	**51.6**	25.2	82.8	60.7	51.6	78.7	73.3	73.1	72.4	
Block 1 Run 17	500	3000	5	**Relative Error**										
				Calculated Head	**100.0**	**100.0**	**100.0**	**100.0**	**100.0**	**100.0**	**100.0**	**100.0**	**100.0**	
				Mags	**47.1**	73.9	15.3	33.1	47.1	10.2	21.2	21.9	25.1	58.6
				N-Mags	**52.9**	26.1	84.7	66.9	52.9	89.8	78.8	78.1	74.9	

Table C.2: Raw Data for Block 2 results of the SLon-100 coupled with Selective Flocculation using the Box-Behnken experimental Design

Test #	Factor 1: Sodium Oleate Dosage (g/t)	Factor 2: Paraffin Dosage (g/t)	Factor 3: Conditioning Time (min)	Product	Mass Split	Discrete Grade (WDXRF)								Σ Oxides
						Fe	SiO_2	Al_2O_3	MnO	CaO	P_2O_5	MgO	LOI	
					%	%	%	%	%	%	%	%	%	
				HEAD	**100.0**	37.34	41.78	0.98	0.05	0.38	0.26	0.31	0.86	97.82
Block 2 Run 52	1000	2000	20	**Relative Error**		0.06	0.36	5.23	0.00	47.95	12.10	15.70	67.44	
				Calculated Head	**100.0**	**37.32**	**41.93**	**0.92**	**0.05**	**0.20**	**0.23**	**0.36**	**0.28**	**97.34**
				Mags	46.1	59.21	13.50	0.64	0.05	0.05	0.09	0.15	0.28	99.43
				N-Mags	53.9	18.55	66.30	1.17	0.05	0.33	0.35	0.54	0.28	95.55
Block 2 Run 53	500	4000	10	**Relative Error**		1.35	2.35	0.72	0.00	49.08	10.87	7.04	37.16	
				Calculated Head	**100.0**	**36.83**	**42.77**	**0.97**	**0.05**	**0.19**	**0.23**	**0.29**	**0.54**	**97.72**
				Mags	45.5	58.62	13.90	0.55	0.05	0.05	0.10	0.10	0.84	99.42
				N-Mags	54.5	18.62	66.90	1.32	0.05	0.32	0.34	0.45	0.29	96.29
Block 2 Run 54	1000	3000	10	**Relative Error**		0.78	1.01	18.82	0.00	52.12	10.42	5.25	6.98	
				Calculated Head	**100.0**	**37.05**	**42.20**	**0.79**	**0.05**	**0.18**	**0.24**	**0.29**	**0.80**	**97.54**
				Mags	46.7	58.65	13.80	0.39	0.05	0.05	0.11	0.09	0.72	99.07
				N-Mags	53.3	18.12	67.10	1.14	0.05	0.30	0.35	0.48	0.87	96.20
Block 2 Run 55	500	3000	20	**Relative Error**		2.37	1.14	1.10	0.00	46.47	12.03	11.84	43.06	
				Calculated Head	**100.0**	**36.46**	**42.26**	**0.96**	**0.05**	**0.20**	**0.23**	**0.27**	**0.49**	**96.60**
				Mags	45.1	57.84	13.95	0.60	0.05	0.05	0.09	0.09	0.27	97.81
				N-Mags	54.9	18.90	65.50	1.26	0.05	0.33	0.35	0.42	0.67	95.62
Block 2 Run 56	500	2000	10	**Relative Error**		2.51	1.15	3.73	0.00	50.37	12.39	12.59	46.91	
				Calculated Head	**100.0**	**36.40**	**42.26**	**1.01**	**0.05**	**0.19**	**0.23**	**0.27**	**0.46**	**96.53**
				Mags	44.5	57.86	14.00	0.60	0.05	0.05	0.08	0.05	0.19	97.77
				N-Mags	55.5	19.22	64.90	1.34	0.05	0.30	0.35	0.45	0.67	95.54
Block 2 Run 57	500	3000	5	**Relative Error**		2.24	0.43	1.92	0.00	54.74	13.43	19.08	45.55	
				Calculated Head	**100.0**	**36.50**	**41.96**	**0.99**	**0.05**	**0.17**	**0.23**	**0.25**	**0.47**	**96.33**
				Mags	47.6	57.75	13.60	0.60	0.05	0.05	0.10	0.06	0.29	97.33
				N-Mags	52.4	17.22	67.70	1.35	0.05	0.29	0.35	0.43	0.63	95.42
Block 2 Run 58	2000	3000	20	**Relative Error**		2.55	0.65	1.09	0.00	50.77	14.43	8.98	32.44	
				Calculated Head	**100.0**	**36.39**	**42.06**	**0.96**	**0.05**	**0.19**	**0.23**	**0.28**	**0.58**	**96.38**
				Mags	45.1	58.05	13.50	0.58	0.05	0.05	0.09	0.06	0.29	97.63
				N-Mags	54.9	18.61	65.50	1.28	0.05	0.30	0.33	0.46	0.82	95.36
Block 2 Run 59	2000	2000	10	**Relative Error**		1.95	0.71	64.20	0.00	43.00	13.82	0.18	39.06	
				Calculated Head	**100.0**	**36.61**	**42.08**	**1.60**	**0.05**	**0.22**	**0.23**	**0.31**	**0.52**	**97.36**
				Mags	46.8	58.33	13.30	0.55	0.05	0.05	0.10	0.05	0.29	97.80
				N-Mags	53.2	17.50	67.40	2.53	0.05	0.37	0.34	0.54	0.73	96.98
Block 2 Run 60	1000	3000	10	**Relative Error**		1.30	0.44	3.75	0.00	54.25	12.03	11.03	64.36	
				Calculated Head	**100.0**	**36.86**	**41.97**	**1.01**	**0.05**	**0.18**	**0.23**	**0.28**	**0.31**	**96.72**
				Mags	47.0	57.69	14.20	0.65	0.05	0.05	0.11	0.08	0.28	97.91
				N-Mags	53.0	18.38	66.60	1.33	0.05	0.29	0.34	0.45	0.33	95.67
Block 2 Run 61	1000	3000	10	**Relative Error**		1.44	1.49	11.08	0.00	52.46	14.08	14.40	34.42	
				Calculated Head	**100.0**	**36.80**	**41.16**	**1.08**	**0.05**	**0.18**	**0.23**	**0.35**	**0.56**	**96.25**
				Mags	47.6	57.25	14.20	0.59	0.05	0.05	0.11	0.16	0.81	97.84
				N-Mags	52.4	18.19	65.70	1.53	0.05	0.30	0.33	0.53	0.34	94.81
Block 2 Run 62	1000	2000	5	**Relative Error**		2.30	0.85	5.75	0.00	50.46	13.14	15.31	38.94	
				Calculated Head	**100.0**	**36.48**	**42.14**	**0.92**	**0.05**	**0.19**	**0.23**	**0.26**	**0.53**	**96.48**
				Mags	46.1	57.53	13.90	0.57	0.05	0.05	0.10	0.10	0.80	97.84
				N-Mags	53.9	18.47	66.30	1.22	0.05	0.31	0.34	0.40	0.29	95.32
Block 2 Run 63	2000	3000	5	**Relative Error**		2.43	0.27	6.88	0.00	51.80	13.26	16.79	36.70	
				Calculated Head	**100.0**	**36.43**	**41.90**	**1.04**	**0.05**	**0.18**	**0.23**	**0.26**	**0.54**	**96.30**
				Mags	47.3	56.93	14.90	0.73	0.05	0.05	0.11	0.10	0.75	98.11
				N-Mags	52.7	18.06	66.10	1.32	0.05	0.31	0.33	0.40	0.36	94.69

Table C.2: Raw Data for Block 2 results of the SLon-100 coupled with Selective Flocculation using the Box-Behnken experimental Design (Contd.)

Test #	Factor 1: Sodium Oleate Dosage (g/t)	Factor 2: Paraffin Dosage (g/t)	Factor 3: Conditioning Time (min)	Product	Mass Split	Discrete Recovery (%)								Separation Efficieny (SE) (%)
					%	Fe	SiO_2	Al_2O_3	MnO	CaO	P_2O_5	MgO	LOI	
				HEAD	**100.0**									
Block 2 Run 52	1000	2000	20	**Relative Error**										
				Calculated Head	**100.0**	**100.0**	**100.0**	**100.0**	**100.0**	**100.0**	**100.0**	**100.0**	**100.0**	
				Mags	46.1	73.2	14.9	31.8	46.1	11.6	18.3	19.4	46.1	58.4
				N-Mags	53.9	26.8	85.1	68.2	53.9	88.4	81.7	80.6	53.9	
Block 2 Run 53	500	4000	10	**Relative Error**										
				Calculated Head	**100.0**	**100.0**	**100.0**	**100.0**	**100.0**	**100.0**	**100.0**	**100.0**	**100.0**	
				Mags	45.5	72.5	14.8	25.7	45.5	11.7	20.2	15.0	70.8	57.7
				N-Mags	54.5	27.5	85.2	74.3	54.5	88.3	79.8	85.0	29.2	
Block 2 Run 54	1000	3000	10	**Relative Error**										
				Calculated Head	**100.0**	**100.0**	**100.0**	**100.0**	**100.0**	**100.0**	**100.0**	**100.0**	**100.0**	
				Mags	46.7	73.9	15.3	23.3	46.7	12.7	21.4	13.5	42.0	58.7
				N-Mags	53.3	26.1	84.7	76.7	53.3	87.3	78.6	86.5	58.0	
Block 2 Run 55	500	3000	20	**Relative Error**										
				Calculated Head	**100.0**	**100.0**	**100.0**	**100.0**	**100.0**	**100.0**	**100.0**	**100.0**	**100.0**	
				Mags	45.1	71.5	14.9	28.2	45.1	11.0	17.0	15.3	24.9	56.6
				N-Mags	54.9	28.5	85.1	71.8	54.9	89.0	83.0	84.7	75.1	
Block 2 Run 56	500	2000	10	**Relative Error**										
				Calculated Head	**100.0**	**100.0**	**100.0**	**100.0**	**100.0**	**100.0**	**100.0**	**100.0**	**100.0**	
				Mags	44.5	70.7	14.7	26.4	44.5	11.7	16.0	8.9	18.5	56.0
				N-Mags	55.5	29.3	85.3	73.6	55.5	88.3	84.0	91.1	81.5	
Block 2 Run 57	500	3000	5	**Relative Error**										
				Calculated Head	**100.0**	**100.0**	**100.0**	**100.0**	**100.0**	**100.0**	**100.0**	**100.0**	**100.0**	
				Mags	47.6	75.3	15.4	28.8	47.6	13.7	20.7	10.8	29.5	59.8
				N-Mags	52.4	24.7	84.6	71.2	52.4	86.3	79.3	89.2	70.5	
Block 2 Run 58	2000	3000	20	**Relative Error**										
				Calculated Head	**100.0**	**100.0**	**100.0**	**100.0**	**100.0**	**100.0**	**100.0**	**100.0**	**100.0**	
				Mags	45.1	71.9	14.5	27.1	45.1	12.0	18.6	9.7	22.5	57.4
				N-Mags	54.9	28.1	85.5	72.9	54.9	88.0	81.4	90.3	77.5	
Block 2 Run 59	2000	2000	10	**Relative Error**										
				Calculated Head	**100.0**	**100.0**	**100.0**	**100.0**	**100.0**	**100.0**	**100.0**	**100.0**	**100.0**	
				Mags	46.8	74.6	14.8	15.9	46.8	10.7	19.6	7.6	25.9	59.8
				N-Mags	53.2	25.4	85.2	84.1	53.2	89.3	80.4	92.4	74.1	
Block 2 Run 60	1000	3000	10	**Relative Error**										
				Calculated Head	**100.0**	**100.0**	**100.0**	**100.0**	**100.0**	**100.0**	**100.0**	**100.0**	**100.0**	
				Mags	47.0	73.6	15.9	30.3	47.0	13.4	21.3	13.2	42.9	57.7
				N-Mags	53.0	26.4	84.1	69.7	53.0	86.6	78.7	86.8	57.1	
Block 2 Run 61	1000	3000	10	**Relative Error**										
				Calculated Head	**100.0**	**100.0**	**100.0**	**100.0**	**100.0**	**100.0**	**100.0**	**100.0**	**100.0**	
				Mags	47.6	74.1	16.4	26.0	47.6	13.1	23.0	21.2	68.4	57.7
				N-Mags	52.4	25.9	83.6	74.0	52.4	86.9	77.0	78.8	31.6	
Block 2 Run 62	1000	2000	5	**Relative Error**										
				Calculated Head	**100.0**	**100.0**	**100.0**	**100.0**	**100.0**	**100.0**	**100.0**	**100.0**	**100.0**	
				Mags	46.1	72.7	15.2	28.4	46.1	12.2	20.4	17.7	70.2	57.5
				N-Mags	53.9	27.3	84.8	71.6	53.9	87.8	79.6	82.3	29.8	
Block 2 Run 63	2000	3000	5	**Relative Error**										
				Calculated Head	**100.0**	**100.0**	**100.0**	**100.0**	**100.0**	**100.0**	**100.0**	**100.0**	**100.0**	
				Mags	47.3	73.9	16.8	33.2	47.3	12.8	23.6	18.7	65.1	57.1
				N-Mags	52.7	26.1	83.2	66.8	52.7	87.2	76.4	81.3	34.9	

Table C.2: Raw Data for Block 2 results of the SLon-100 coupled with Selective Flocculation using the Box-Behnken experimental Design (Contd.)

Test #	Factor 1: Sodium Oleate Dosage (g/t)	Factor 2: Paraffin Dosage (g/t)	Factor 3: Conditioning Time (min)	Product	Mass Split	Discrete Grade (WDXRF)								Σ Oxides
						Fe	SiO_2	Al_2O_3	MnO	CaO	P_2O_5	MgO	LOI	
					%	%	%	%	%	%	%	%	%	
				HEAD	**100.0**	37.34	41.78	0.98	0.05	0.38	0.26	0.31	0.86	97.82
Block 2 Run 64	1000	3000	10	**Relative Error**		2.07	0.06	4.10	0.00	51.73	13.29	10.19	5.81	
				Calculated Head	**100.0**	**36.57**	**41.76**	**1.01**	**0.05**	**0.18**	**0.23**	**0.34**	**0.81**	**96.68**
				Mags	47.0	57.77	13.60	0.65	0.05	0.05	0.11	0.17	0.81	98.05
				N-Mags	53.0	17.79	66.70	1.34	0.05	0.30	0.33	0.49	0.81	95.47
Block 2 Run 65	1000	3000	10	**Relative Error**		1.73	0.39	5.18	0.00	53.93	12.84	20.49	50.52	
				Calculated Head	**100.0**	**36.69**	**41.95**	**0.92**	**0.05**	**0.18**	**0.23**	**0.25**	**0.43**	**96.47**
				Mags	47.4	57.52	14.45	0.56	0.05	0.05	0.10	0.06	0.37	97.90
				N-Mags	52.6	17.95	66.70	1.25	0.05	0.29	0.34	0.41	0.48	95.19
Block 2 Run 66	1000	4000	5	**Relative Error**		2.55	1.10	1.42	0.00	53.33	13.02	15.76	28.45	
				Calculated Head	**100.0**	**36.39**	**42.24**	**0.96**	**0.05**	**0.18**	**0.23**	**0.26**	**0.62**	**96.57**
				Mags	46.0	56.80	14.80	0.61	0.05	0.05	0.12	0.10	0.41	97.37
				N-Mags	54.0	19.02	65.60	1.26	0.05	0.29	0.32	0.40	0.79	95.90
Block 2 Run 67	2000	4000	10	**Relative Error**		1.79	0.99	2.77	0.00	54.46	14.87	19.37	29.73	
				Calculated Head	**100.0**	**36.67**	**41.37**	**1.00**	**0.05**	**0.17**	**0.22**	**0.25**	**0.60**	**96.12**
				Mags	46.9	56.84	14.50	0.57	0.05	0.05	0.11	0.05	0.36	96.97
				N-Mags	53.1	18.86	65.10	1.38	0.05	0.28	0.33	0.43	0.82	95.36
Block 2 Run 68	1000	4000	20	**Relative Error**		2.34	0.77	8.55	0.00	39.34	14.46	61.03	32.72	
				Calculated Head	**100.0**	**36.47**	**41.46**	**1.06**	**0.05**	**0.23**	**0.23**	**0.50**	**0.58**	**96.25**
				Mags	46.3	57.63	13.90	0.63	0.05	0.05	0.11	0.20	0.31	97.66
				N-Mags	53.7	18.24	65.20	1.43	0.05	0.39	0.33	0.75	0.81	95.04

Test #	Factor 1: Sodium Oleate Dosage (g/t)	Factor 2: Paraffin Dosage (g/t)	Factor 3: Conditioning Time (min)	Product	Mass Split	Discrete Recovery (%)								Separation Efficieny (SE) (%)
						Fe	SiO_2	Al_2O_3	MnO	CaO	P_2O_5	MgO	LOI	
					%									
				HEAD	**100.0**									
Block 2 Run 64	1000	3000	10	**Relative Error**										
				Calculated Head	**100.0**	**100.0**	**100.0**	**100.0**	**100.0**	**100.0**	**100.0**	**100.0**	**100.0**	
				Mags	47.0	74.2	15.3	30.0	47.0	12.7	22.4	23.5	47.0	58.9
				N-Mags	53.0	25.8	84.7	70.0	53.0	87.3	77.6	76.5	53.0	
Block 2 Run 65	1000	3000	10	**Relative Error**										
				Calculated Head	**100.0**	**100.0**	**100.0**	**100.0**	**100.0**	**100.0**	**100.0**	**100.0**	**100.0**	
				Mags	47.4	74.3	16.3	28.9	47.4	13.4	21.4	12.3	40.6	57.9
				N-Mags	52.6	25.7	83.7	71.1	52.6	86.6	78.6	87.7	59.4	
Block 2 Run 66	1000	4000	5	**Relative Error**										
				Calculated Head	**100.0**	**100.0**	**100.0**	**100.0**	**100.0**	**100.0**	**100.0**	**100.0**	**100.0**	
				Mags	46.0	71.8	16.1	29.2	46.0	12.9	24.3	18.1	30.6	55.7
				N-Mags	54.0	28.2	83.9	70.8	54.0	87.1	75.7	81.9	69.4	
Block 2 Run 67	2000	4000	10	**Relative Error**										
				Calculated Head	**100.0**	**100.0**	**100.0**	**100.0**	**100.0**	**100.0**	**100.0**	**100.0**	**100.0**	
				Mags	46.9	72.7	16.4	26.9	46.9	13.5	23.0	9.8	27.9	56.2
				N-Mags	53.1	27.3	83.6	73.1	53.1	86.5	77.0	90.2	72.1	
Block 2 Run 68	1000	4000	20	**Relative Error**										
				Calculated Head	**100.0**	**100.0**	**100.0**	**100.0**	**100.0**	**100.0**	**100.0**	**100.0**	**100.0**	
				Mags	46.3	73.1	15.5	27.4	46.3	10.0	21.8	18.9	24.8	57.6
				N-Mags	53.7	26.9	84.5	72.6	53.7	90.0	78.2	81.1	75.2	

Table C.3: Raw Data for Block 3 results of the SLon-100 coupled with Selective Flocculation using the Box-Behnken experimental Design

Test #	Factor 1: Sodium Oleate Dosage (g/t)	Factor 2: Paraffin Dosage (g/t)	Factor 3: Conditioning Time (min)	Product	Mass Split	Discrete Grade (WDXRF)								Σ Oxides
						Fe	SiO_2	Al_2O_3	MnO	CaO	P_2O_5	MgO	LOI	
					%	%	%	%	%	%	%	%	%	
				HEAD	**100.0**	37.34	41.78	0.98	0.05	0.38	0.26	0.31	0.86	97.82
Block 3 Run 35	1000	3000	10	**Relative Error**		1.39	0.36	3.82	0.00	55.13	12.89	14.02	28.12	
				Calculated Head	**100.0**	**36.82**	**41.94**	**0.94**	**0.05**	**0.17**	**0.23**	**0.27**	**0.62**	**96.86**
				Mags	47.3	57.47	14.80	0.51	0.05	0.05	0.10	0.07	0.36	98.13
				N-Mags	52.7	18.28	66.30	1.32	0.05	0.28	0.34	0.45	0.85	95.73
Block 3 Run 36	2000	2000	10	**Relative Error**		1.86	0.03	1.46	0.00	53.86	14.44	12.36	62.63	
				Calculated Head	**100.0**	**36.64**	**41.77**	**0.99**	**0.05**	**0.18**	**0.23**	**0.27**	**0.32**	**96.21**
				Mags	46.6	57.19	14.70	0.58	0.05	0.05	0.10	0.07	0.30	97.63
				N-Mags	53.4	18.71	65.40	1.35	0.05	0.29	0.34	0.45	0.34	94.97
Block 3 Run 37	2000	3000	5	**Relative Error**		2.18	0.66	6.70	0.00	53.61	14.45	26.12	37.63	
				Calculated Head	**100.0**	**36.53**	**42.06**	**0.91**	**0.05**	**0.18**	**0.23**	**0.23**	**0.54**	**96.42**
				Mags	46.2	57.65	14.30	0.56	0.05	0.05	0.11	0.05	0.80	98.36
				N-Mags	53.8	18.39	65.90	1.21	0.05	0.29	0.33	0.38	0.31	94.76
Block 3 Run 38	1000	4000	20	**Relative Error**		1.99	0.72	0.88	0.00	52.78	12.37	8.85	30.73	
				Calculated Head	**100.0**	**36.60**	**42.08**	**0.98**	**0.05**	**0.18**	**0.23**	**0.28**	**0.60**	**96.74**
				Mags	46.4	57.47	14.60	0.48	0.05	0.05	0.09	0.06	0.81	98.33
				N-Mags	53.6	18.50	65.90	1.42	0.05	0.29	0.35	0.47	0.41	95.36
Block 3 Run 39	1000	3000	10	**Relative Error**		1.84	0.67	4.43	0.00	55.89	12.09	16.78	31.57	
				Calculated Head	**100.0**	**36.65**	**42.06**	**1.02**	**0.05**	**0.17**	**0.23**	**0.26**	**0.59**	**96.79**
				Mags	46.5	57.43	14.50	0.57	0.05	0.05	0.11	0.05	0.84	98.30
				N-Mags	53.5	18.60	66.00	1.41	0.05	0.27	0.34	0.44	0.37	95.48
Block 3 Run 40	500	2000	10	**Relative Error**		2.07	1.41	0.62	0.00	52.82	13.42	16.86	10.54	
				Calculated Head	**100.0**	**36.57**	**42.37**	**0.97**	**0.05**	**0.18**	**0.23**	**0.26**	**0.77**	**97.12**
				Mags	46.7	57.49	14.40	0.58	0.05	0.05	0.10	0.07	0.78	98.24
				N-Mags	53.3	18.22	66.90	1.31	0.05	0.30	0.34	0.43	0.76	96.14
Block 3 Run 41	1000	3000	10	**Relative Error**		1.04	0.15	0.72	0.00	53.23	11.94	1.57	24.34	
				Calculated Head	**100.0**	**36.95**	**41.85**	**0.97**	**0.05**	**0.18**	**0.23**	**0.31**	**0.65**	**97.08**
				Mags	46.9	57.74	14.65	0.54	0.05	0.05	0.10	0.08	0.38	98.42
				N-Mags	53.1	18.57	65.90	1.35	0.05	0.29	0.35	0.50	0.89	95.89
Block 3 Run 42	500	4000	10	**Relative Error**		1.71	1.24	8.32	0.00	49.66	10.83	9.37	35.16	
				Calculated Head	**100.0**	**36.70**	**42.30**	**0.89**	**0.05**	**0.19**	**0.23**	**0.28**	**0.56**	**96.99**
				Mags	46.2	57.80	14.20	0.54	0.05	0.05	0.11	0.07	0.31	97.99
				N-Mags	53.8	18.60	66.40	1.20	0.05	0.32	0.34	0.46	0.77	96.14
Block 3 Run 43	1000	4000	5	**Relative Error**		1.50	0.34	2.31	0.00	59.13	10.80	5.78	20.73	
				Calculated Head	**100.0**	**36.78**	**41.92**	**1.00**	**0.05**	**0.16**	**0.23**	**0.29**	**0.68**	**96.93**
				Mags	47.1	57.50	14.50	0.56	0.05	0.05	0.13	0.09	0.47	98.07
				N-Mags	52.9	18.36	66.30	1.39	0.05	0.25	0.33	0.47	0.87	95.92
Block 3 Run 44	500	3000	5	**Relative Error**		0.33	0.06	13.89	0.00	51.90	14.77	26.00	37.12	
				Calculated Head	**100.0**	**37.22**	**41.76**	**0.84**	**0.05**	**0.18**	**0.22**	**0.23**	**0.54**	**97.05**
				Mags	47.4	58.09	14.00	0.55	0.05	0.05	0.10	0.06	0.32	98.20
				N-Mags	52.6	18.38	66.80	1.10	0.05	0.31	0.33	0.39	0.74	96.00
Block 3 Run 45	2000	3000	20	**Relative Error**		2.05	1.64	7.55	0.00	50.55	13.87	14.85	31.58	
				Calculated Head	**100.0**	**36.58**	**42.47**	**0.90**	**0.05**	**0.19**	**0.23**	**0.26**	**0.59**	**96.99**
				Mags	46.0	58.05	14.30	0.48	0.05	0.05	0.10	0.07	0.27	98.32
				N-Mags	54.0	18.26	66.50	1.26	0.05	0.31	0.34	0.43	0.86	95.86
Block 3 Run 46	500	3000	20	**Relative Error**		1.82	1.46	5.57	0.00	49.25	12.42	22.88	37.87	
				Calculated Head	**100.0**	**36.66**	**42.40**	**0.92**	**0.05**	**0.19**	**0.23**	**0.24**	**0.53**	**96.99**
				Mags	44.7	58.95	13.00	0.55	0.05	0.05	0.08	0.05	0.31	98.39
				N-Mags	55.3	18.61	66.20	1.22	0.05	0.31	0.35	0.39	0.72	95.85

Table C.3: Raw Data for Block 3 results of the SLon-100 coupled with Selective Flocculation using the Box-Behnken experimental Design (Contd.)

Test #	Factor 1: Sodium Oleate Dosage (g/t)	Factor 2: Paraffin Dosage (g/t)	Factor 3: Conditioning Time (min)	Product	Mass Split	Discrete Recovery (%)								Separation Efficieny (SE) (%)
					%	Fe	SiO_2	Al_2O_3	MnO	CaO	P_2O_5	MgO	LOI	
				HEAD	**100.0**									
Block 3 Run 35	1000	3000	10	**Relative Error**										
				Calculated Head	**100.0**	**100.0**	**100.0**	**100.0**	**100.0**	**100.0**	**100.0**	**100.0**	**100.0**	
				Mags	47.3	73.8	16.7	25.8	47.3	13.8	21.4	11.9	27.6	57.1
				N-Mags	52.7	26.2	83.3	74.2	52.7	86.2	78.6	88.1	72.4	
Block 3 Run 36	2000	2000	10	**Relative Error**										
				Calculated Head	**100.0**	**100.0**	**100.0**	**100.0**	**100.0**	**100.0**	**100.0**	**100.0**	**100.0**	
				Mags	46.6	72.7	16.4	27.1	46.6	13.2	20.4	12.0	43.5	56.3
				N-Mags	53.4	27.3	83.6	72.9	53.4	86.8	79.6	88.0	56.5	
Block 3 Run 37	2000	3000	5	**Relative Error**										
				Calculated Head	**100.0**	**100.0**	**100.0**	**100.0**	**100.0**	**100.0**	**100.0**	**100.0**	**100.0**	
				Mags	46.2	72.9	15.7	28.4	46.2	13.0	22.1	10.1	68.9	57.2
				N-Mags	53.8	27.1	84.3	71.6	53.8	87.0	77.9	89.9	31.1	
Block 3 Run 38	1000	4000	20	**Relative Error**										
				Calculated Head	**100.0**	**100.0**	**100.0**	**100.0**	**100.0**	**100.0**	**100.0**	**100.0**	**100.0**	
				Mags	46.4	72.9	16.1	22.7	46.4	12.8	18.5	10.2	63.1	56.8
				N-Mags	53.6	27.1	83.9	77.3	53.6	87.2	81.5	89.8	36.9	
Block 3 Run 39	1000	3000	10	**Relative Error**										
				Calculated Head	**100.0**	**100.0**	**100.0**	**100.0**	**100.0**	**100.0**	**100.0**	**100.0**	**100.0**	
				Mags	46.5	72.8	16.0	25.9	46.5	13.8	22.1	9.2	66.4	56.8
				N-Mags	53.5	27.2	84.0	74.1	53.5	86.2	77.9	90.8	33.6	
Block 3 Run 40	500	2000	10	**Relative Error**										
				Calculated Head	**100.0**	**100.0**	**100.0**	**100.0**	**100.0**	**100.0**	**100.0**	**100.0**	**100.0**	
				Mags	46.7	73.5	15.9	28.0	46.7	12.9	20.1	11.8	47.4	57.6
				N-Mags	53.3	26.5	84.1	72.0	53.3	87.1	79.9	88.2	52.6	
Block 3 Run 41	1000	3000	10	**Relative Error**										
				Calculated Head	**100.0**	**100.0**	**100.0**	**100.0**	**100.0**	**100.0**	**100.0**	**100.0**	**100.0**	
				Mags	46.9	73.3	16.4	26.0	46.9	13.1	21.0	12.9	27.4	56.9
				N-Mags	53.1	26.7	83.6	74.0	53.1	86.9	79.0	87.1	72.6	
Block 3 Run 42	500	4000	10	**Relative Error**										
				Calculated Head	**100.0**	**100.0**	**100.0**	**100.0**	**100.0**	**100.0**	**100.0**	**100.0**	**100.0**	
				Mags	46.2	72.7	15.5	27.7	46.2	12.0	21.8	11.3	25.7	57.2
				N-Mags	53.8	27.3	84.5	72.3	53.8	88.0	78.2	88.7	74.3	
Block 3 Run 43	1000	4000	5	**Relative Error**										
				Calculated Head	**100.0**	**100.0**	**100.0**	**100.0**	**100.0**	**100.0**	**100.0**	**100.0**	**100.0**	
				Mags	47.1	73.6	16.3	26.2	47.1	15.0	25.8	14.5	32.4	57.3
				N-Mags	52.9	26.4	83.7	73.8	52.9	85.0	74.2	85.5	67.6	
Block 3 Run 44	500	3000	5	**Relative Error**										
				Calculated Head	**100.0**	**100.0**	**100.0**	**100.0**	**100.0**	**100.0**	**100.0**	**100.0**	**100.0**	
				Mags	47.4	74.0	15.9	31.1	47.4	12.9	21.8	11.4	28.1	58.1
				N-Mags	52.6	26.0	84.1	68.9	52.6	87.1	78.2	88.6	71.9	
Block 3 Run 45	2000	3000	20	**Relative Error**										
				Calculated Head	**100.0**	**100.0**	**100.0**	**100.0**	**100.0**	**100.0**	**100.0**	**100.0**	**100.0**	
				Mags	46.0	73.1	15.5	24.6	46.0	12.2	20.3	11.3	21.1	57.6
				N-Mags	54.0	26.9	84.5	75.4	54.0	87.8	79.7	88.7	78.9	
Block 3 Run 46	500	3000	20	**Relative Error**										
				Calculated Head	**100.0**	**100.0**	**100.0**	**100.0**	**100.0**	**100.0**	**100.0**	**100.0**	**100.0**	
				Mags	44.7	72.0	13.7	26.8	44.7	11.5	15.9	9.9	25.5	58.2
				N-Mags	55.3	28.0	86.3	73.2	55.3	88.5	84.1	90.1	74.5	

Table C.3: Raw Data for Block 3 results of the SLon-100 coupled with Selective Flocculation using the Box-Behnken experimental Design (Contd.)

Test #	Factor 1: Sodium Oleate Dosage (g/t)	Factor 2: Paraffin Dosage (g/t)	Factor 3: Conditioning Time (min)	Product	Mass Split	Discrete Grade (WDXRF)								Σ Oxides
						Fe	SiO_2	Al_2O_3	MnO	CaO	P_2O_5	MgO	LOI	
					%	%	%	%	%	%	%	%	%	
				HEAD	**100.0**	37.34	41.78	0.98	0.05	0.38	0.26	0.31	0.86	97.82
Block 3 Run 47	1000	3000	10	**Relative Error**		2.02	1.05	7.15	0.00	55.51	12.41	16.14	27.69	
				Calculated Head	**100.0**	**36.59**	**42.22**	**0.91**	**0.05**	**0.17**	**0.23**	**0.26**	**0.62**	**96.78**
				Mags	46.6	57.89	13.90	0.57	0.05	0.05	0.10	0.07	0.36	97.89
				N-Mags	53.4	18.02	66.90	1.20	0.05	0.28	0.34	0.42	0.85	95.81
Block 3 Run 48	1000	3000	10	**Relative Error**		1.21	0.21	7.41	0.00	56.07	13.17	9.87	28.31	
				Calculated Head	**100.0**	**36.89**	**41.87**	**0.90**	**0.05**	**0.17**	**0.23**	**0.28**	**0.62**	**96.87**
				Mags	47.0	58.07	13.80	0.52	0.05	0.05	0.10	0.08	0.41	98.06
				N-Mags	53.0	18.08	66.80	1.24	0.05	0.27	0.34	0.46	0.80	95.82
Block 3 Run 49	2000	4000	10	**Relative Error**		1.14	0.10	3.25	0.00	53.06	14.89	14.09	27.73	
				Calculated Head	**100.0**	**36.92**	**41.83**	**1.01**	**0.05**	**0.18**	**0.22**	**0.27**	**0.62**	**96.96**
				Mags	46.9	57.77	14.20	0.60	0.05	0.05	0.10	0.06	0.34	98.01
				N-Mags	53.1	18.52	66.20	1.37	0.05	0.29	0.33	0.45	0.87	96.04
Block 3 Run 50	1000	2000	20	**Relative Error**		1.68	0.61	7.18	0.00	53.51	12.23	11.41	35.37	
				Calculated Head	**100.0**	**36.71**	**42.04**	**1.04**	**0.05**	**0.18**	**0.23**	**0.27**	**0.56**	**96.87**
				Mags	45.6	58.55	13.30	0.61	0.05	0.05	0.08	0.05	0.30	98.16
				N-Mags	54.4	18.43	66.10	1.41	0.05	0.29	0.36	0.46	0.77	95.79
Block 3 Run 51	1000	2000	5	**Relative Error**		2.59	0.16	12.21	0.00	51.18	13.14	6.59	10.01	
				Calculated Head	**100.0**	**36.37**	**41.85**	**1.09**	**0.05**	**0.19**	**0.23**	**0.29**	**0.77**	**96.49**
				Mags	46.3	57.55	14.35	0.55	0.05	0.05	0.10	0.07	0.35	97.83
				N-Mags	53.7	18.08	65.60	1.56	0.05	0.31	0.34	0.48	1.14	95.33

Test #	Factor 1: Sodium Oleate Dosage (g/t)	Factor 2: Paraffin Dosage (g/t)	Factor 3: Conditioning Time (min)	Product	Mass Split	Discrete Recovery (%)								Separation Efficieny (SE) (%)
						Fe	SiO_2	Al_2O_3	MnO	CaO	P_2O_5	MgO	LOI	
					%									
				HEAD	**100.0**									
Block 3 Run 47	1000	3000	10	**Relative Error**										
				Calculated Head	**100.0**	**100.0**	**100.0**	**100.0**	**100.0**	**100.0**	**100.0**	**100.0**	**100.0**	
				Mags	46.6	73.7	15.3	29.2	46.6	13.7	21.0	12.9	27.0	58.4
				N-Mags	53.4	26.3	84.7	70.8	53.4	86.3	79.0	87.1	73.0	
Block 3 Run 48	1000	3000	10	**Relative Error**										
				Calculated Head	**100.0**	**100.0**	**100.0**	**100.0**	**100.0**	**100.0**	**100.0**	**100.0**	**100.0**	
				Mags	47.0	74.0	15.5	27.2	47.0	14.0	20.8	13.8	31.3	58.5
				N-Mags	53.0	26.0	84.5	72.8	53.0	86.0	79.2	86.2	68.7	
Block 3 Run 49	2000	4000	10	**Relative Error**										
				Calculated Head	**100.0**	**100.0**	**100.0**	**100.0**	**100.0**	**100.0**	**100.0**	**100.0**	**100.0**	
				Mags	46.9	73.4	15.9	27.7	46.9	13.0	21.5	11.1	25.6	57.4
				N-Mags	53.1	26.6	84.1	72.3	53.1	87.0	78.5	88.9	74.4	
Block 3 Run 50	1000	2000	20	**Relative Error**										
				Calculated Head	**100.0**	**100.0**	**100.0**	**100.0**	**100.0**	**100.0**	**100.0**	**100.0**	**100.0**	
				Mags	45.6	72.7	14.4	26.6	45.6	12.8	16.2	8.3	24.6	58.3
				N-Mags	54.4	27.3	85.6	73.4	54.4	87.2	83.8	91.7	75.4	
Block 3 Run 51	1000	2000	5	**Relative Error**										
				Calculated Head	**100.0**	**100.0**	**100.0**	**100.0**	**100.0**	**100.0**	**100.0**	**100.0**	**100.0**	
				Mags	46.3	73.3	15.9	23.5	46.3	12.4	21.2	11.8	21.0	57.4
				N-Mags	53.7	26.7	84.1	76.5	53.7	87.6	78.8	88.2	79.0	

Table C.4: Raw Data for Block 1-3 Mags Average results of the SLon-100 coupled with Selective Flocculation using the Box-Behnken experimental Design

Factor 1: Sodium Oleate Dosage (g/t)	Factor 2: Paraffin Dosage (g/t)	Factor 3: Conditioning Time (min)	Block 1- Mags				Block 2- Mags				Block 3- Mags				Average - Mags		
			Run	Separation Efficiency (%)	Fe Grade (%)	Fe Recovery (%)	Run	Separation Efficiency (%)	Fe Grade (%)	Fe Recovery (%)	Run	Separation Efficiency (%)	Fe Grade (%)	Fe Recovery (%)	Separation Efficiency (%)	Fe Grade (%)	Fe Recovery (%)
1000	4000	5	Run 1	58.6	58.19	73.8	Run 66	55.7	56.80	71.8	Run 43	57.3	57.50	73.6	57.2	57.5	73.0
2000	4000	10	Run 2	56.6	57.16	73.1	Run 67	56.2	56.84	72.7	Run 49	57.4	57.77	73.4	56.8	57.3	73.1
1000	2000	5	Run 3	58.4	58.27	73.0	Run 62	57.5	57.53	72.7	Run 51	57.4	57.55	73.3	57.8	57.8	73.0
2000	3000	20	Run 4	59.9	59.12	74.2	Run 58	57.4	58.05	71.9	Run 45	57.6	58.05	73.1	58.3	58.4	73.1
1000	3000	10	Run 5	57.6	57.87	72.7	Run 60	57.7	57.69	73.6	Run 41	56.9	57.74	73.3	57.4	57.8	73.2
2000	3000	5	Run 6	57.7	58.03	73.7	Run 63	57.1	56.93	73.9	Run 37	57.2	57.65	72.9	57.3	57.5	73.5
1000	3000	10	Run 7	58.5	58.43	73.1	Run 54	58.7	58.65	73.9	Run 39	56.8	57.43	72.8	58.0	58.2	73.3
1000	2000	20	Run 8	58.9	58.41	74.5	Run 52	58.4	59.21	73.2	Run 50	58.3	58.55	72.7	58.5	58.7	73.5
500	2000	10	Run 9	59.8	58.33	73.6	Run 56	56.0	57.86	70.7	Run 40	57.6	57.49	73.5	57.8	57.9	72.6
1000	3000	10	Run 10	57.0	57.07	72.7	Run 61	57.7	57.25	74.1	Run 35	57.1	57.47	73.8	57.3	57.3	73.5
500	4000	10	Run 11	58.8	58.59	74.7	Run 53	57.7	58.62	72.5	Run 42	57.2	57.80	72.7	57.9	58.3	73.3
500	3000	20	Run 12	58.9	59.44	73.7	Run 55	56.6	57.84	71.5	Run 46	58.2	58.95	72.0	57.9	58.7	72.4
1000	3000	10	Run 13	55.6	57.88	71.5	Run 64	58.9	57.77	74.2	Run 47	58.4	57.89	73.7	57.6	57.8	73.1
1000	3000	10	Run 14	56.5	58.16	71.5	Run 65	57.9	57.52	74.3	Run 48	58.5	58.07	74.0	57.7	57.9	73.3
1000	4000	20	Run 15	58.9	58.86	74.3	Run 68	57.6	57.63	73.1	Run 38	56.8	57.47	72.9	57.8	58.0	73.5
2000	2000	10	Run 16	57.5	57.91	74.8	Run 59	59.8	58.33	74.6	Run 36	56.3	57.19	72.7	57.9	57.8	74.0
500	3000	5	Run 17	58.6	58.73	73.9	Run 57	59.8	57.75	75.3	Run 44	58.1	58.09	74.0	58.8	58.2	74.4

Table C.4: Raw Data for Block 1-3 Mags Average results of the SLon-100 coupled with Selective Flocculation using the Box-Behnken experimental Design (Contd.)

Factor 1: Sodium Oleate Dosage (g/t)	Factor 2: Paraffin Dosage (g/t)	Factor 3: Conditioning Time (min)	2 Std Dev (95% Confidence) - Mags			Standard Error at 95% Confidence for Mags			Predicted for Mags			
			Separation Efficiency (%)	Fe Grade (%)	Fe Recovery (%)	Separation Efficiency (%)	Fe Grade (%)	Fe Recovery (%)	Separation Efficiency (%)	Separation Efficiency (%)	Fe Grade (%)	Fe Grade (%)
									2Fl Model	Quad. Model	Linear Model	2Fl Model
1000	4000	5	2.9	1.4	2.2	5.1	2.4	3.0	57.2	57.2	57.5	57.6
2000	4000	10	1.2	0.9	0.7	2.2	1.7	0.9	56.7	56.6	57.5	57.3
1000	2000	5	1.1	0.8	0.6	1.8	1.5	0.8	57.9	57.9	57.7	57.6
2000	3000	20	2.7	1.2	2.3	4.7	2.1	3.2	58.2	58.5	58.0	58.1
1000	3000	10	0.8	0.2	0.9	1.5	0.3	1.2	57.7	57.6	57.9	57.9
2000	3000	5	0.6	1.1	1.0	1.1	2.0	1.4	56.7	57.0	57.3	57.2
1000	3000	10	2.1	1.3	1.1	3.6	2.2	1.5	57.7	57.6	57.9	57.9
1000	2000	20	0.7	0.9	1.9	1.2	1.5	2.6	58.2	58.2	58.4	58.6
500	2000	10	3.8	0.8	3.3	6.6	1.5	4.5	58.0	57.9	58.4	58.1
1000	3000	10	0.7	0.4	1.6	1.2	0.7	2.1	57.7	57.6	57.9	57.9
500	4000	10	1.6	0.9	2.4	2.7	1.6	3.3	58.0	57.9	58.1	58.3
500	3000	20	2.3	1.6	2.3	4.0	2.8	3.1	57.6	57.9	58.6	58.5
1000	3000	10	3.5	0.1	2.8	6.1	0.2	3.9	57.7	57.6	57.9	57.9
1000	3000	10	2.1	0.7	3.1	3.6	1.2	4.2	57.7	57.6	57.9	57.9
1000	4000	20	2.1	1.5	1.5	3.7	2.6	2.1	57.5	57.6	58.2	58.1
2000	2000	10	3.5	1.2	2.2	6.0	2.0	3.0	58.1	57.9	57.8	58.1
500	3000	5	1.8	1.0	1.5	3.0	1.7	2.0	58.4	58.8	57.9	57.9

Table C.5: Raw Data of the Optimisation Validation Tests for Run 11, 23, 24 and 25 of the SLon-100 coupled with the Optimal Selective Flocculation conditions

Test #	Factor 1: Sodium Oleate Dosage (g/t)	Factor 2: Paraffin Dosage (g/t)	Factor 3: Conditioning Time (min)	Product	Mass Split	Discrete Grade (WDXRF)									∑ Oxides
						Fe	SiO_2	MnO	K_2O	CaO	P_2O_5	Na_2O	MgO	LOI	
					%	%	%	%	%	%	%	%	%	%	
				HEAD	**100.0**	37.34	42.65	0.05	0.07	0.38	0.26	0.10	0.31	0.86	97.82
Opt Run 11 A	492.67	1999.97	4.99	**Relative Error**		1.33	1.29	0.00	31.37	13.42	8.41	0.00	41.27	25.20	
				Calculated Head	**100.0**	**36.84**	**42.10**	**0.05**	**0.05**	**0.33**	**0.24**	**0.10**	**0.18**	**0.64**	**96.38**
				Mags	44.1	59.44	12.02	0.05	0.05	0.12	0.10	0.10	0.06	0.47	97.96
				N-Mags	55.9	19.02	65.83	0.05	0.05	0.50	0.35	0.10	0.28	0.78	95.13
Opt Run 23 A	500.00	1999.98	3.20	**Relative Error**		0.37	2.41	0.00	31.37	12.67	7.95	0.00	47.25	26.55	
				Calculated Head	**100.0**	**37.20**	**41.62**	**0.05**	**0.05**	**0.33**	**0.24**	**0.10**	**0.16**	**0.63**	**96.39**
				Mags	44.9	59.18	12.37	0.05	0.05	0.13	0.12	0.10	0.05	0.40	97.89
				N-Mags	55.1	19.33	65.41	0.05	0.05	0.50	0.35	0.10	0.26	0.82	95.17
Opt Run 24 A	500.00	1431.11	4.62	**Relative Error**		0.19	3.07	0.00	31.37	12.27	6.49	0.00	41.02	28.49	
				Calculated Head	**100.0**	**37.41**	**41.34**	**0.05**	**0.05**	**0.34**	**0.25**	**0.10**	**0.18**	**0.62**	**96.42**
				Mags	44.6	59.05	12.54	0.05	0.05	0.15	0.13	0.10	0.06	0.41	97.92
				N-Mags	55.4	20.00	64.52	0.05	0.05	0.49	0.34	0.10	0.29	0.78	95.21
Opt Run 25 A	500.00	1226.02	5.00	**Relative Error**		1.00	4.00	0.00	31.37	11.71	7.65	0.00	39.21	28.64	
				Calculated Head	**100.0**	**37.71**	**40.94**	**0.05**	**0.05**	**0.34**	**0.24**	**0.10**	**0.19**	**0.61**	**96.45**
				Mags	44.4	58.65	13.07	0.05	0.05	0.15	0.12	0.10	0.05	0.38	97.85
				N-Mags	55.6	21.02	63.16	0.05	0.05	0.49	0.34	0.10	0.30	0.80	95.34
Opt Run 11 B	492.67	1999.97	4.99	**Relative Error**		0.14	2.68	0.00	31.37	11.27	6.64	0.00	39.51	19.86	
				Calculated Head	**100.0**	**37.29**	**41.50**	**0.05**	**0.05**	**0.34**	**0.25**	**0.10**	**0.19**	**0.69**	**96.49**
				Mags	44.2	59.17	12.38	0.05	0.05	0.14	0.12	0.10	0.05	0.41	97.92
				N-Mags	55.8	19.98	64.54	0.05	0.05	0.50	0.35	0.10	0.29	0.91	95.36
Opt Run 23 B	500.00	1999.98	3.20	**Relative Error**		2.15	0.34	0.00	31.37	9.77	6.55	0.00	40.56	29.80	
				Calculated Head	**100.0**	**36.54**	**42.50**	**0.05**	**0.05**	**0.35**	**0.25**	**0.10**	**0.18**	**0.60**	**96.33**
				Mags	42.1	59.61	11.80	0.05	0.05	0.15	0.12	0.10	0.05	0.38	97.93
				N-Mags	57.9	19.77	64.82	0.05	0.05	0.49	0.34	0.10	0.28	0.77	95.17
Opt Run 24 B	500.00	1431.11	4.62	**Relative Error**		0.51	2.24	0.00	31.37	12.63	7.86	0.00	42.69	36.62	
				Calculated Head	**100.0**	**37.15**	**41.69**	**0.05**	**0.05**	**0.33**	**0.24**	**0.10**	**0.18**	**0.55**	**96.31**
				Mags	43.4	59.28	12.24	0.05	0.05	0.13	0.11	0.10	0.06	0.33	97.83
				N-Mags	56.6	20.19	64.27	0.05	0.05	0.49	0.34	0.10	0.27	0.71	95.15
Opt Run 25 B	500.00	1226.02	5.00	**Relative Error**		0.07	2.92	0.00	31.37	10.53	6.85	0.00	40.84	34.52	
				Calculated Head	**100.0**	**37.37**	**41.40**	**0.05**	**0.05**	**0.34**	**0.25**	**0.10**	**0.18**	**0.56**	**96.37**
				Mags	43.9	59.41	12.06	0.05	0.05	0.13	0.11	0.10	0.05	0.35	97.85
				N-Mags	56.1	20.11	64.37	0.05	0.05	0.51	0.35	0.10	0.29	0.73	95.21
Opt Run 11 C	492.67	1999.97	4.99	**Relative Error**		1.61	0.96	0.00	31.37	10.25	4.67	0.00	38.48	29.25	
				Calculated Head	**100.0**	**36.74**	**42.24**	**0.05**	**0.05**	**0.34**	**0.25**	**0.10**	**0.19**	**0.61**	**96.37**
				Mags	43.2	59.19	12.36	0.05	0.05	0.14	0.12	0.10	0.05	0.37	97.88
				N-Mags	56.8	19.65	64.98	0.05	0.05	0.50	0.35	0.10	0.30	0.79	95.21
Opt Run 23 C	500.00	1999.98	3.20	**Relative Error**		0.02	2.87	0.00	31.37	11.32	4.80	0.00	33.66	15.46	
				Calculated Head	**100.0**	**37.35**	**41.42**	**0.05**	**0.05**	**0.34**	**0.25**	**0.10**	**0.21**	**0.73**	**96.56**
				Mags	44.3	59.14	12.43	0.05	0.05	0.15	0.13	0.10	0.06	0.51	98.03
				N-Mags	55.7	19.99	64.52	0.05	0.05	0.49	0.35	0.10	0.32	0.90	95.38
Opt Run 24 C	500.00	1431.11	4.62	**Relative Error**		1.72	0.84	0.00	31.37	13.88	10.54	0.00	40.04	28.86	
				Calculated Head	**100.0**	**36.70**	**42.29**	**0.05**	**0.05**	**0.33**	**0.24**	**0.10**	**0.19**	**0.61**	**96.33**
				Mags	44.3	59.09	12.48	0.05	0.05	0.15	0.12	0.10	0.05	0.38	97.88
				N-Mags	55.7	18.90	65.98	0.05	0.05	0.47	0.33	0.10	0.29	0.80	95.10
Opt Run 25 C	500.00	1226.02	5.00	**Relative Error**		2.17	0.31	0.00	31.37	12.81	8.72	0.00	38.09	30.91	
				Calculated Head	**100.0**	**36.53**	**42.51**	**0.05**	**0.05**	**0.33**	**0.24**	**0.10**	**0.19**	**0.59**	**96.31**
				Mags	43.6	58.26	13.58	0.05	0.05	0.13	0.11	0.10	0.05	0.38	97.78
				N-Mags	56.4	19.70	64.91	0.05	0.05	0.49	0.34	0.10	0.30	0.76	95.18

Table C.5: Raw Data of the Optimisation Validation Tests for Run 11, 23, 24 and 25 of the SLon-100 coupled with the Optimal Selective Flocculation conditions (Contd.)

Test #	Factor 1: Sodium Oleate Dosage (g/t)	Factor 2: Paraffin Dosage (g/t)	Factor 3: Conditioning Time (min)	Product	Mass Split	Discrete Recovery (%)										Separation Efficieny (SE) (%)
					%	Fe	SiO_2	MnO	K_2O	CaO	P_2O_5	Na_2O	MgO	LOI		
				HEAD	**100.0**											
Opt Run 11 A	492.67	1999.97	4.99	**Relative Error**												
				Calculated Head	**100.0**	**100.0**	**100.0**	**100.0**	**100.0**	**100.0**	**100.0**	**100.0**	**100.0**	**100.0**		
				Mags	44.1	71.2	12.6	44.1	44.1	15.3	18.2	44.1	14.4	32.2		58.6
				N-Mags	55.9	28.8	87.4	55.9	55.9	84.7	81.8	55.9	85.6	67.8		
Opt Run 23 A	500.00	1999.98	3.20	**Relative Error**												
				Calculated Head	**100.0**	**100.0**	**100.0**	**100.0**	**100.0**	**100.0**	**100.0**	**100.0**	**100.0**	**100.0**		
				Mags	44.9	71.3	13.3	44.9	44.9	18.0	21.3	44.9	13.7	28.4		58.0
				N-Mags	55.1	28.7	86.7	55.1	55.1	82.0	78.7	55.1	86.3	71.6		
Opt Run 24 A	500.00	1431.11	4.62	**Relative Error**												
				Calculated Head	**100.0**	**100.0**	**100.0**	**100.0**	**100.0**	**100.0**	**100.0**	**100.0**	**100.0**	**100.0**		
				Mags	44.6	70.4	13.5	44.6	44.6	19.8	22.8	44.6	13.7	29.7		56.9
				N-Mags	55.4	29.6	86.5	55.4	55.4	80.2	77.2	55.4	86.3	70.3		
Opt Run 25 A	500.00	1226.02	5.00	**Relative Error**												
				Calculated Head	**100.0**	**100.0**	**100.0**	**100.0**	**100.0**	**100.0**	**100.0**	**100.0**	**100.0**	**100.0**		
				Mags	44.4	69.0	14.2	44.4	44.4	20.0	22.4	44.4	11.8	27.5		54.8
				N-Mags	55.6	31.0	85.8	55.6	55.6	80.0	77.6	55.6	88.2	72.5		
Opt Run 11 B	492.67	1999.97	4.99	**Relative Error**												
				Calculated Head	**100.0**	**100.0**	**100.0**	**100.0**	**100.0**	**100.0**	**100.0**	**100.0**	**100.0**	**100.0**		
				Mags	44.2	70.1	13.2	44.2	44.2	18.6	21.2	44.2	12.8	26.3		56.9
				N-Mags	55.8	29.9	86.8	55.8	55.8	81.4	78.8	55.8	87.2	73.7		
Opt Run 23 B	500.00	1999.98	3.20	**Relative Error**												
				Calculated Head	**100.0**	**100.0**	**100.0**	**100.0**	**100.0**	**100.0**	**100.0**	**100.0**	**100.0**	**100.0**		
				Mags	42.1	68.7	11.7	42.1	42.1	18.0	20.7	42.1	11.4	26.1		57.0
				N-Mags	57.9	31.3	88.3	57.9	57.9	82.0	79.3	57.9	88.6	73.9		
Opt Run 24 B	500.00	1431.11	4.62	**Relative Error**												
				Calculated Head	**100.0**	**100.0**	**100.0**	**100.0**	**100.0**	**100.0**	**100.0**	**100.0**	**100.0**	**100.0**		
				Mags	43.4	69.2	12.7	43.4	43.4	16.9	20.2	43.4	13.7	26.3		56.5
				N-Mags	56.6	30.8	87.3	56.6	56.6	83.1	79.8	56.6	86.3	73.7		
Opt Run 25 B	500.00	1226.02	5.00	**Relative Error**												
				Calculated Head	**100.0**	**100.0**	**100.0**	**100.0**	**100.0**	**100.0**	**100.0**	**100.0**	**100.0**	**100.0**		
				Mags	43.9	69.8	12.8	43.9	43.9	16.3	19.5	43.9	12.0	27.3		57.0
				N-Mags	56.1	30.2	87.2	56.1	56.1	83.7	80.5	56.1	88.0	72.7		
Opt Run 11 C	492.67	1999.97	4.99	**Relative Error**												
				Calculated Head	**100.0**	**100.0**	**100.0**	**100.0**	**100.0**	**100.0**	**100.0**	**100.0**	**100.0**	**100.0**		
				Mags	43.2	69.6	12.6	43.2	43.2	18.0	20.8	43.2	11.3	26.3		57.0
				N-Mags	56.8	30.4	87.4	56.8	56.8	82.0	79.2	56.8	88.7	73.7		
Opt Run 23 C	500.00	1999.98	3.20	**Relative Error**												
				Calculated Head	**100.0**	**100.0**	**100.0**	**100.0**	**100.0**	**100.0**	**100.0**	**100.0**	**100.0**	**100.0**		
				Mags	44.3	70.2	13.3	44.3	44.3	19.5	22.3	44.3	12.6	31.1		56.9
				N-Mags	55.7	29.8	86.7	55.7	55.7	80.5	77.7	55.7	87.4	68.9		
Opt Run 24 C	500.00	1431.11	4.62	**Relative Error**												
				Calculated Head	**100.0**	**100.0**	**100.0**	**100.0**	**100.0**	**100.0**	**100.0**	**100.0**	**100.0**	**100.0**		
				Mags	44.3	71.3	13.1	44.3	44.3	20.0	22.2	44.3	11.9	27.1		58.2
				N-Mags	55.7	28.7	86.9	55.7	55.7	80.0	77.8	55.7	88.1	72.9		
Opt Run 25 C	500.00	1226.02	5.00	**Relative Error**												
				Calculated Head	**100.0**	**100.0**	**100.0**	**100.0**	**100.0**	**100.0**	**100.0**	**100.0**	**100.0**	**100.0**		
				Mags	43.6	69.6	13.9	43.6	43.6	17.4	20.5	43.6	11.4	27.9		55.7
				N-Mags	56.4	30.4	86.1	56.4	56.4	82.6	79.5	56.4	88.6	72.1		

Table C.5: Raw Data of the Optimisation Validation Tests for Run 11, 23, 24 and 25 of the SLon-100 coupled with the Optimal Selective Flocculation conditions (Contd.)

Test #	Factor 1: Sodium Oleate Dosage (g/t)	Factor 2: Paraffin Dosage (g/t)	Factor 3: Conditioning Time (min)	Product	Mass Split	Discrete Grade (WDXRF)									Σ Oxides
						Fe	SiO_2	MnO	K_2O	CaO	P_2O_5	Na_2O	MgO	LOI	
					%	%	%	%	%	%	%	%	%	%	
				HEAD	**100.0**	37.34	42.65	0.05	0.07	0.38	0.26	0.10	0.31	0.86	97.82
Opt Run 11 D	492.67	1999.97	4.99	**Relative Error**		1.56	1.02	0.00	31.37	14.27	10.95	0.00	46.39	15.65	
				Calculated Head	**100.0**	**36.76**	**42.21**	**0.05**	**0.05**	**0.33**	**0.23**	**0.10**	**0.17**	**0.73**	**96.43**
				Mags	44.6	58.17	13.71	0.05	0.05	0.14	0.12	0.10	0.05	0.36	97.77
				N-Mags	55.4	19.49	65.19	0.05	0.05	0.48	0.33	0.10	0.26	1.02	95.35
Opt Run 23 D	500.00	1999.98	3.20	**Relative Error**		0.39	2.39	0.00	31.37	13.03	8.84	0.00	48.28	28.27	
				Calculated Head	**100.0**	**37.19**	**41.63**	**0.05**	**0.05**	**0.33**	**0.24**	**0.10**	**0.16**	**0.62**	**96.37**
				Mags	44.4	58.26	13.59	0.05	0.05	0.14	0.12	0.10	0.05	0.45	97.86
				N-Mags	55.6	20.39	63.99	0.05	0.05	0.49	0.34	0.10	0.25	0.75	95.18
Opt Run 24 D	500.00	1431.11	4.62	**Relative Error**		0.86	3.85	0.00	31.37	13.85	8.07	0.00	41.36	37.03	
				Calculated Head	**100.0**	**37.66**	**41.01**	**0.05**	**0.05**	**0.33**	**0.24**	**0.10**	**0.18**	**0.54**	**96.36**
				Mags	43.8	59.09	12.48	0.05	0.05	0.13	0.11	0.10	0.06	0.30	97.78
				N-Mags	56.2	20.95	63.26	0.05	0.05	0.49	0.34	0.10	0.28	0.73	95.25
Opt Run 25 D	500.00	1226.02	5.00	**Relative Error**		0.47	3.40	0.00	31.37	11.17	6.19	0.00	38.08	31.85	
				Calculated Head	**100.0**	**37.52**	**41.20**	**0.05**	**0.05**	**0.34**	**0.25**	**0.10**	**0.19**	**0.59**	**96.41**
				Mags	44.3	59.49	11.96	0.05	0.05	0.13	0.11	0.10	0.05	0.38	97.89
				N-Mags	55.7	20.05	64.45	0.05	0.05	0.51	0.36	0.10	0.31	0.75	95.24
Opt Run 11 E	492.67	1999.97	4.99	**Relative Error**		0.15	2.67	0.00	31.37	12.42	8.45	0.00	45.08	34.25	
				Calculated Head	**100.0**	**37.28**	**41.51**	**0.05**	**0.05**	**0.34**	**0.24**	**0.10**	**0.17**	**0.57**	**96.34**
				Mags	45.7	59.19	12.36	0.05	0.05	0.16	0.13	0.10	0.06	0.37	97.91
				N-Mags	54.3	18.84	66.06	0.05	0.05	0.49	0.34	0.10	0.26	0.73	95.02
Opt Run 23 E	500.00	1999.98	3.20	**Relative Error**		0.84	3.83	0.00	31.37	13.85	7.76	0.00	47.14	37.65	
				Calculated Head	**100.0**	**37.66**	**41.01**	**0.05**	**0.05**	**0.33**	**0.24**	**0.10**	**0.16**	**0.54**	**96.34**
				Mags	45.5	59.77	11.58	0.05	0.05	0.15	0.12	0.10	0.06	0.40	97.98
				N-Mags	54.5	19.19	65.59	0.05	0.05	0.48	0.34	0.10	0.25	0.65	94.97
Opt Run 24 E	500.00	1431.11	4.62	**Relative Error**		0.03	2.81	0.00	31.37	13.12	6.69	0.00	44.67	33.91	
				Calculated Head	**100.0**	**37.33**	**41.45**	**0.05**	**0.05**	**0.33**	**0.25**	**0.10**	**0.17**	**0.57**	**96.35**
				Mags	43.7	59.55	11.87	0.05	0.05	0.12	0.11	0.10	0.05	0.36	97.87
				N-Mags	56.3	20.09	64.40	0.05	0.05	0.50	0.35	0.10	0.27	0.73	95.17
Opt Run 25 E	500.00	1226.02	5.00	**Relative Error**		0.27	3.16	0.00	31.37	11.94	7.80	0.00	49.15	40.04	
				Calculated Head	**100.0**	**37.44**	**41.30**	**0.05**	**0.05**	**0.34**	**0.24**	**0.10**	**0.16**	**0.52**	**96.30**
				Mags	43.9	59.73	11.63	0.05	0.05	0.14	0.12	0.10	0.05	0.28	97.83
				N-Mags	56.1	20.01	64.51	0.05	0.05	0.50	0.34	0.10	0.24	0.70	95.09

Table C.5: Raw Data of the Optimisation Validation Tests for Run 11, 23, 24 and 25 of the SLon-100 coupled with the Optimal Selective Flocculation conditions (Contd.)

Test #	Factor 1: Sodium Oleate Dosage (g/t)	Factor 2: Paraffin Dosage (g/t)	Factor 3: Conditioning Time (min)	Product	Mass Split	Discrete Recovery (%)										Separation Efficieny (SE) (%)
					%	Fe	SiO_2	MnO	K_2O	CaO	P_2O_5	Na_2O	MgO	LOI		
				HEAD	**100.0**											
Opt Run 11 D	492.67	1999.97	4.99	**Relative Error**												
				Calculated Head	**100.0**	**100.0**	**100.0**	**100.0**	**100.0**	**100.0**	**100.0**	**100.0**	**100.0**	**100.0**	**100.0**	
				Mags	44.6	70.6	14.5	44.6	44.6	19.3	23.0	44.6	13.4	22.1	56.1	
				N-Mags	55.4	29.4	85.5	55.4	55.4	80.7	77.0	55.4	86.6	77.9		
Opt Run 23 D	500.00	1999.98	3.20	**Relative Error**												
				Calculated Head	**100.0**	**100.0**	**100.0**	**100.0**	**100.0**	**100.0**	**100.0**	**100.0**	**100.0**	**100.0**	**100.0**	
				Mags	44.4	69.5	14.5	44.4	44.4	18.3	21.4	44.4	14.4	32.4	55.0	
				N-Mags	55.6	30.5	85.5	55.6	55.6	81.7	78.6	55.6	85.6	67.6		
Opt Run 24 D	500.00	1431.11	4.62	**Relative Error**												
				Calculated Head	**100.0**	**100.0**	**100.0**	**100.0**	**100.0**	**100.0**	**100.0**	**100.0**	**100.0**	**100.0**	**100.0**	
				Mags	43.8	68.8	13.3	43.8	43.8	17.0	20.6	43.8	13.5	24.3	55.4	
				N-Mags	56.2	31.2	86.7	56.2	56.2	83.0	79.4	56.2	86.5	75.7		
Opt Run 25 D	500.00	1226.02	5.00	**Relative Error**												
				Calculated Head	**100.0**	**100.0**	**100.0**	**100.0**	**100.0**	**100.0**	**100.0**	**100.0**	**100.0**	**100.0**	**100.0**	
				Mags	44.3	70.2	12.9	44.3	44.3	16.7	19.7	44.3	11.5	28.7	57.4	
				N-Mags	55.7	29.8	87.1	55.7	55.7	83.3	80.3	55.7	88.5	71.3		
Opt Run 11 E	492.67	1999.97	4.99	**Relative Error**												
				Calculated Head	**100.0**	**100.0**	**100.0**	**100.0**	**100.0**	**100.0**	**100.0**	**100.0**	**100.0**	**100.0**	**100.0**	
				Mags	45.7	72.6	13.6	45.7	45.7	21.3	23.9	45.7	16.2	29.9	59.0	
				N-Mags	54.3	27.4	86.4	54.3	54.3	78.7	76.1	54.3	83.8	70.1		
Opt Run 23 E	500.00	1999.98	3.20	**Relative Error**												
				Calculated Head	**100.0**	**100.0**	**100.0**	**100.0**	**100.0**	**100.0**	**100.0**	**100.0**	**100.0**	**100.0**	**100.0**	
				Mags	45.5	72.2	12.8	45.5	45.5	20.2	23.0	45.5	15.6	33.9	59.4	
				N-Mags	54.5	27.8	87.2	54.5	54.5	79.8	77.0	54.5	84.4	66.1		
Opt Run 24 E	500.00	1431.11	4.62	**Relative Error**												
				Calculated Head	**100.0**	**100.0**	**100.0**	**100.0**	**100.0**	**100.0**	**100.0**	**100.0**	**100.0**	**100.0**	**100.0**	
				Mags	43.7	69.7	12.5	43.7	43.7	16.2	19.6	43.7	12.7	27.7	57.2	
				N-Mags	56.3	30.3	87.5	56.3	56.3	83.8	80.4	56.3	87.3	72.3		
Opt Run 25 E	500.00	1226.02	5.00	**Relative Error**												
				Calculated Head	**100.0**	**100.0**	**100.0**	**100.0**	**100.0**	**100.0**	**100.0**	**100.0**	**100.0**	**100.0**	**100.0**	
				Mags	43.9	70.0	12.4	43.9	43.9	17.6	21.0	43.9	13.9	23.8	57.7	
				N-Mags	56.1	30.0	87.6	56.1	56.1	82.4	79.0	56.1	86.1	76.2		

Table C.6: Average Raw Data of the Optimisation Validation Tests for Run 11, 23, 24 and 25 of the SLon-100 coupled with the Optimal Selective Flocculation conditions

Optimisation Run	Sodium Oleate Dosage (g/t)	Paraffin Dosage (g/t)	Conditioning Time (min)	Separation Efficiency (%)			Concentrate Fe Grade (%)			Concentrate Fe Recovery (%)	
				Predicted	Actual Average	2 Std Dev	Predicted	Actual Average	2 Std Dev	Predicted	Actual Average
SF Run 17	500.0	3000.0	5.0	58.8	58.8	1.8	57.9	58.2	1.0	71.5	74.4
Opt Run 11	492.7	2000.0	5.0	58.6	57.5	2.4	57.7	59.0	1.0	73.6	70.8
Opt Run 23	500.0	2000.0	3.2	58.3	57.3	3.2	57.9	59.2	1.2	73.2	70.4
Opt Run 24	500.0	1431.1	4.6	58.6	56.8	2.0	57.8	59.21	0.42	73.8	69.9
Opt Run 25	500.0	1226.0	5.0	58.7	56.5	2.4	57.8	59.1	1.2	74.0	69.7

APPENDIX D: RAW DATA FOR OPTIMISED SELECTIVE FLOCCULATION COUPLED WITH REFLUX CLASSIFIER

Table D.1: Raw Data for the Base case Reflux Classifier testwork without selective flocculation (Test 1)

Test 1					Discrete Grade							∑ Oxides	Cumulative Grade to Overflow						
					Fe	SiO_2	Al_2O_3	MnO	CaO	MgO	LOI		Fe	SiO_2	Al_2O_3	MnO	CaO	MgO	LOI
Stream	Pump Speed (rpm)	Fluidisation Water Flowrate (kg/hr)	Discrete Mass (%)	Cumulative Mass (%)	%	%	%	%	%	%	%		%	%	%	%	%	%	%
Overflow 1	10	8.23	0.5	0.5	16.05	60.85	7.48	0.06	1.17	2.66	4.51	99.68	16.05	60.85	7.48	0.06	1.17	2.66	4.51
Overflow 2	15	12.48	2.1	2.6	20.98	57.22	6.35	0.06	1.12	2.44	4.46	101.66	20.06	57.90	6.56	0.06	1.13	2.48	4.47
Overflow 3	20	16.84	2.4	5.0	23.64	53.80	4.40	0.06	0.98	1.81	4.24	99.10	21.77	55.94	5.53	0.06	1.06	2.16	4.36
Overflow 4	25	21.02	2.9	7.9	23.57	58.74	3.08	0.05	0.76	1.31	1.97	99.61	22.42	56.97	4.64	0.06	0.95	1.85	3.49
Overflow 5	30	25.26	2.8	10.7	25.87	58.76	1.83	0.05	0.66	0.71	1.28	100.30	23.34	57.44	3.89	0.06	0.87	1.55	2.90
Overflow 6	37.35	31.5	2.4	13.1	21.53	59.61	1.33	0.05	0.05	0.51	0.94	93.27	23.01	57.84	3.43	0.06	0.72	1.36	2.54
Overflow 7	60	50.5	6.6	19.7	23.18	67.35	0.86	0.06	0.42	0.32	0.57	102.73	23.07	61.02	2.57	0.06	0.62	1.01	1.88
Overflow 8	80	67.3	5.2	24.9	27.34	61.20	0.49	0.06	0.44	0.22	0.43	101.94	23.96	61.06	2.13	0.06	0.58	0.85	1.58
Overflow 9	120	100.9	6.8	31.7	28.67	60.50	0.42	0.06	0.42	0.17	0.47	103.03	24.97	60.94	1.77	0.06	0.55	0.70	1.34
Overflow 10	144	121.1	4.3	36.1	33.71	53.60	0.32	0.06	0.37	0.11	0.43	103.09	26.02	60.06	1.59	0.06	0.53	0.63	1.23
Overflow 11	174	146.4	2.6	38.7	36.71	49.00	0.34	0.06	0.32	0.10	0.39	102.72	26.75	59.30	1.51	0.06	0.51	0.59	1.17
Underflow (Remainder in column)	-	-	61.3	100.0	45.90	33.40	0.28	0.06	0.30	0.08	0.50	100.25	38.49	43.42	0.76	0.06	0.38	0.28	0.76
Total (Calculated)	**Total**	**Total**	**100.0**		**38.49**	**43.42**	**0.76**	**0.06**	**0.38**	**0.28**	**0.76**								
Total (Measured)					**37.34**	**41.78**	**0.98**	**0.05**	**0.38**	**0.31**	**0.86**								
% Relative Error					**3.08**	**3.92**	**22.40**	**18.83**	**0.36**	**10.16**	**11.92**								

Table D.1: Raw Data for the Base case Reflux Classifier testwork without selective flocculation (Test 1) (Contd.)

Test 1					Discrete Recovery							Cumulative Recovery to Overflow						
					Fe	SiO_2	Al_2O_3	MnO	CaO	MgO	LOI	Fe	SiO_2	Al_2O_3	MnO	CaO	MgO	LOI
Stream	**Pump Speed (rpm)**	**Fluidisation Water Flowrate (kg/hr)**	**Discrete Mass (%)**	**Cumulative Mass (%)**	**%**	**%**	**%**	**%**	**%**	**%**	**%**	**%**	**%**	**%**	**%**	**%**	**%**	**%**
Overflow 1	10	8.23	0.5	0.5	0.2	0.7	4.8	0.5	1.5	4.6	2.9	0.2	0.7	4.8	0.5	1.5	4.6	2.9
Overflow 2	15	12.48	2.1	2.6	1.2	2.8	17.8	2.3	6.2	18.6	12.5	1.4	3.5	22.7	2.8	7.7	23.3	15.4
Overflow 3	20	16.84	2.4	5.0	1.5	3.0	13.9	2.6	6.1	15.5	13.4	2.8	6.4	36.6	5.4	13.9	38.8	28.8
Overflow 4	25	21.02	2.9	7.9	1.8	3.9	11.7	2.4	5.7	13.5	7.5	4.6	10.3	48.3	7.8	19.6	52.3	36.3
Overflow 5	30	25.26	2.8	10.7	1.9	3.9	6.9	2.4	4.9	7.3	4.8	6.5	14.2	55.2	10.2	24.5	59.6	41.1
Overflow 6	37.35	31.5	2.4	13.1	1.3	3.3	4.2	2.0	0.3	4.3	3.0	7.8	17.5	59.4	12.3	24.8	63.9	44.0
Overflow 7	60	50.5	6.6	19.7	4.0	10.2	7.5	6.7	7.2	7.7	4.9	11.8	27.7	66.9	18.9	32.0	71.6	48.9
Overflow 8	80	67.3	5.2	24.9	3.7	7.3	3.4	5.3	6.0	4.0	3.0	15.5	35.1	70.3	24.2	38.0	75.6	51.9
Overflow 9	120	100.9	6.8	31.7	5.1	9.5	3.7	6.9	7.5	4.0	4.2	20.6	44.5	74.0	31.0	45.5	79.7	56.1
Overflow 10	144	121.1	4.3	36.1	3.8	5.3	1.8	4.4	4.2	1.8	2.5	24.4	49.9	75.8	35.4	49.7	81.4	58.6
Overflow 11	174	146.4	2.6	38.7	2.5	3.0	1.2	2.7	2.2	1.0	1.4	26.9	52.8	77.0	38.1	51.9	82.4	59.9
Underflow (Remainder in column)	-	-	61.3	100.0	73.1	47.2	23.0	61.9	48.1	17.6	40.1	100.0	100.0	100.0	100.0	100.0	100.0	100.0
Total (Calculated)	**Total**	**Total**	**100.0**		**100.0**	**100.0**	**100.0**	**100.0**	**100.0**	**100.0**	**100.0**							

Table D.2: Raw Data for the Base case Reflux Classifier testwork without selective flocculation (Test 2)

Test 2					Discrete Grade								Cumulative Grade to Overflow						
					Fe	SiO_2	Al_2O_3	MnO	CaO	MgO	LOI		Fe	SiO_2	Al_2O_3	MnO	CaO	MgO	LOI
Stream	**Pump Speed (rpm)**	**Fluidisation Water Flowrate (kg/hr)**	**Discrete Mass (%)**	**Cumulative Mass (%)**	%	%	%	%	%	%	%	**∑ Oxides**	%	%	%	%	%	%	%
Overflow 1	10	8.23	0.4	0.4	17.92	58.72	6.44	0.11	1.10	2.40	4.28	98.67	17.92	58.72	6.44	0.11	1.10	2.40	4.28
Overflow 2	15	12.48	1.4	1.8	22.47	55.73	5.44	0.12	1.19	2.26	3.32	100.18	21.34	56.47	5.69	0.11	1.17	2.29	3.56
Overflow 3	20	16.84	2.1	3.9	24.33	56.73	3.84	0.09	1.04	1.68	2.47	100.63	22.94	56.61	4.70	0.10	1.10	1.96	2.98
Overflow 4	25	21.02	2.2	6.1	26.71	56.50	2.63	0.09	0.87	1.20	1.83	101.30	24.30	56.57	3.95	0.10	1.01	1.69	2.56
Overflow 5	30	25.26	2.3	8.3	27.43	56.47	1.91	0.08	0.77	0.90	1.42	100.77	25.16	56.54	3.39	0.09	0.95	1.47	2.25
Overflow 6	37.35	31.5	2.4	10.8	25.22	61.21	1.33	0.06	0.76	0.64	0.99	101.06	25.17	57.60	2.93	0.09	0.90	1.28	1.97
Overflow 7	60	50.5	9.4	20.2	23.64	65.30	1.15	0.06	0.92	0.48	0.87	102.58	24.45	61.19	2.10	0.07	0.91	0.91	1.45
Overflow 8	80	67.3	5.9	26.1	27.27	61.70	0.78	0.06	1.13	0.30	0.51	103.47	25.09	61.31	1.80	0.07	0.96	0.77	1.24
Overflow 9	120	100.9	7.2	33.3	28.95	59.80	1.02	0.06	0.31	0.42	0.99	104.00	25.92	60.98	1.63	0.07	0.82	0.69	1.19
Overflow 10	144	121.1	3.7	36.9	35.24	51.50	0.36	0.06	0.46	0.12	0.42	103.32	26.84	60.05	1.51	0.07	0.79	0.64	1.11
Overflow 11	174	146.4	2.4	39.3	35.45	50.80	0.39	0.06	0.41	0.13	0.52	103.01	27.36	59.49	1.44	0.07	0.76	0.61	1.08
Underflow (Remainder in column)	-	-	60.7	100.0	47.55	34.50	0.32	0.06	0.35	0.09	0.58	103.90	39.62	44.32	0.76	0.06	0.51	0.29	0.77
Total (Calculated)	**Total**	**Total**	**100.0**		**39.62**	**44.32**	**0.76**	**0.06**	**0.51**	**0.29**	**0.77**								
Total (Measured)					**38.34**	**41.78**	**0.98**	**0.05**	**0.38**	**0.31**	**0.86**								
% Relative Error					**3.33**	**6.07**	**22.06**	**25.56**	**34.19**	**5.58**	**9.93**								

Table D.2: Raw Data for the Base case Reflux Classifier testwork without selective flocculation (Test 2) (Contd.)

Test 2					Discrete Recovery							Cumulative Recovery to Overflow						
					Fe	SiO_2	Al_2O_3	MnO	CaO	MgO	LOI	Fe	SiO_2	Al_2O_3	MnO	CaO	MgO	LOI
Stream	**Pump Speed (rpm)**	**Fluidisation Water Flowrate (kg/hr)**	**Discrete Mass (%)**	**Cumulative Mass (%)**	**%**	**%**	**%**	**%**	**%**	**%**	**%**	**%**	**%**	**%**	**%**	**%**	**%**	**%**
Overflow 1	10	8.23	0.4	0.4	0.2	0.6	3.8	0.8	1.0	3.7	2.5	0.2	0.6	3.8	0.8	1.0	3.7	2.5
Overflow 2	15	12.48	1.4	1.8	0.8	1.7	9.7	2.5	3.1	10.4	5.8	1.0	2.3	13.5	3.3	4.1	14.1	8.3
Overflow 3	20	16.84	2.1	3.9	1.3	2.7	10.5	3.0	4.2	11.9	6.6	2.2	4.9	23.9	6.3	8.3	26.0	14.9
Overflow 4	25	21.02	2.2	6.1	1.5	2.8	7.6	3.1	3.7	8.9	5.2	3.7	7.7	31.5	9.4	12.0	34.9	20.0
Overflow 5	30	25.26	2.3	8.3	1.6	2.9	5.7	2.8	3.4	7.0	4.2	5.3	10.6	37.2	12.2	15.4	41.9	24.2
Overflow 6	37.35	31.5	2.4	10.8	1.5	3.4	4.3	2.5	3.6	5.3	3.1	6.8	14.0	41.5	14.7	19.0	47.2	27.3
Overflow 7	60	50.5	9.4	20.2	5.6	13.9	14.3	9.0	16.8	15.5	10.6	12.5	27.9	55.8	23.7	35.8	62.7	37.9
Overflow 8	80	67.3	5.9	26.1	4.1	8.2	6.0	5.7	13.0	6.0	3.9	16.5	36.1	61.8	29.4	48.8	68.7	41.8
Overflow 9	120	100.9	7.2	33.3	5.2	9.7	9.6	6.8	4.4	10.1	9.1	21.8	45.8	71.4	36.2	53.2	78.9	51.0
Overflow 10	144	121.1	3.7	36.9	3.2	4.2	1.7	3.5	3.3	1.5	2.0	25.0	50.0	73.2	39.7	56.5	80.3	53.0
Overflow 11	174	146.4	2.4	39.3	2.1	2.7	1.2	2.3	1.9	1.0	1.6	27.1	52.7	74.4	42.0	58.4	81.3	54.5
Underflow (Remainder in column)	-	-	60.7	100.0	72.9	47.3	25.6	58.0	41.6	18.7	45.5	100.0	100.0	100.0	100.0	100.0	100.0	100.0
Total (Calculated)	**Total**	**Total**	**100.0**		**100.0**	**100.0**	**100.0**	**100.0**	**100.0**	**100.0**	**100.0**							

Table D.3: Raw Data for the Base case Reflux Classifier testwork without selective flocculation (Test 3)

Test 3					Discrete Grade								Cumulative Grade to Overflow						
					Fe	SiO_2	Al_2O_3	MnO	CaO	MgO	LOI		Fe	SiO_2	Al_2O_3	MnO	CaO	MgO	LOI
Stream	**Pump Speed (rpm)**	**Fluidisation Water Flowrate (kg/hr)**	**Discrete Mass (%)**	**Cumulative Mass (%)**	**%**	**%**	**%**	**%**	**%**	**%**	**%**	**∑ Oxides**	**%**	**%**	**%**	**%**	**%**	**%**	**%**
Overflow 1	10	8.23	0.7	0.7	18.03	58.32	6.90	0.10	1.09	2.59	4.41	99.19	18.03	58.32	6.90	0.10	1.09	2.59	4.41
Overflow 2	15	12.48	1.0	1.7	22.02	55.11	5.37	0.10	1.16	2.39	3.36	98.98	20.31	56.48	6.02	0.10	1.13	2.48	3.81
Overflow 3	20	16.84	1.6	3.3	27.36	54.04	2.70	0.09	0.90	1.23	1.86	99.94	23.69	55.31	4.43	0.10	1.02	1.88	2.88
Overflow 4	25	21.02	2.8	6.1	21.98	58.36	3.72	0.09	0.98	1.67	2.39	98.64	22.91	56.70	4.11	0.09	1.00	1.78	2.65
Overflow 5	30	25.26	1.5	7.6	26.75	56.95	1.93	0.08	0.80	0.93	1.36	100.29	23.66	56.75	3.68	0.09	0.96	1.62	2.40
Overflow 6	37.35	31.5	2.2	9.9	25.71	59.98	1.38	0.06	0.74	0.63	1.05	100.62	24.12	57.48	3.16	0.08	0.91	1.39	2.10
Overflow 7	60	50.5	7.7	17.6	25.03	63.90	1.04	0.06	0.73	0.45	1.06	103.04	24.52	60.30	2.23	0.07	0.83	0.98	1.64
Overflow 8	80	67.3	4.6	22.1	27.76	61.10	0.57	0.06	0.81	0.25	0.51	103.00	25.19	60.46	1.89	0.07	0.83	0.83	1.41
Overflow 9	120	100.9	6.1	28.2	27.62	61.30	0.55	0.06	0.93	0.18	0.40	102.92	25.72	60.65	1.60	0.07	0.85	0.69	1.19
Overflow 10	144	121.1	3.5	31.8	32.55	54.00	0.43	0.06	0.66	0.14	0.30	102.13	26.48	59.91	1.47	0.07	0.83	0.63	1.09
Overflow 11	174	146.4	2.9	34.7	35.59	48.90	0.32	0.06	0.41	0.10	0.41	101.09	27.25	58.98	1.37	0.07	0.79	0.58	1.03
Underflow (Remainder in column)	-	-	65.3	100.0	47.10	34.00	0.30	0.06	0.34	0.08	0.36	102.49	40.21	42.67	0.67	0.06	0.50	0.25	0.59
Total (Calculated)	**Total**	**Total**	**100.0**		**40.21**	**42.67**	**0.67**	**0.06**	**0.50**	**0.25**	**0.59**								
Total (Measured)					**38.34**	**41.78**	**0.98**	**0.05**	**0.38**	**0.31**	**0.86**								
% Relative Error					**4.87**	**2.12**	**30.99**	**24.89**	**29.66**	**18.01**	**30.96**								

Table D.3: Raw Data for the Base case Reflux Classifier testwork without selective flocculation (Test 3) (Contd.)

Test 3					Discrete Recovery							Cumulative Recovery to Overflow						
					Fe	SiO_2	Al_2O_3	MnO	CaO	MgO	LOI	Fe	SiO_2	Al_2O_3	MnO	CaO	MgO	LOI
Stream	**Pump Speed (rpm)**	**Fluidisation Water Flowrate (kg/hr)**	**Discrete Mass (%)**	**Cumulative Mass (%)**	**%**	**%**	**%**	**%**	**%**	**%**	**%**	**%**	**%**	**%**	**%**	**%**	**%**	**%**
Overflow 1	10	8.23	0.7	0.7	0.3	1.0	7.6	1.2	1.6	7.6	5.5	0.3	1.0	7.6	1.2	1.6	7.6	5.5
Overflow 2	15	12.48	1.0	1.7	0.5	1.3	7.9	1.6	2.3	9.4	5.6	0.9	2.3	15.6	2.9	4.0	16.9	11.1
Overflow 3	20	16.84	1.6	3.3	1.1	2.0	6.4	2.3	2.9	7.7	5.0	2.0	4.3	22.0	5.2	6.8	24.6	16.2
Overflow 4	25	21.02	2.8	6.1	1.5	3.8	15.5	4.0	5.5	18.4	11.3	3.5	8.2	37.5	9.2	12.4	43.0	27.4
Overflow 5	30	25.26	1.5	7.6	1.0	2.0	4.3	1.9	2.4	5.5	3.4	4.5	10.2	41.8	11.1	14.8	48.5	30.9
Overflow 6	37.35	31.5	2.2	9.9	1.4	3.1	4.5	2.3	3.3	5.5	3.9	5.9	13.3	46.3	13.4	18.1	54.0	34.8
Overflow 7	60	50.5	7.7	17.6	4.8	11.6	11.9	7.4	11.4	13.6	13.8	10.7	24.8	58.2	20.8	29.5	67.6	48.6
Overflow 8	80	67.3	4.6	22.1	3.1	6.5	3.8	4.4	7.5	4.5	3.9	13.9	31.4	62.1	25.2	37.0	72.1	52.5
Overflow 9	120	100.9	6.1	28.2	4.2	8.8	5.0	5.9	11.4	4.4	4.1	18.1	40.1	67.1	31.1	48.4	76.4	56.6
Overflow 10	144	121.1	3.5	31.8	2.9	4.5	2.2	3.4	4.7	1.9	1.8	20.9	44.6	69.3	34.4	53.1	78.4	58.4
Overflow 11	174	146.4	2.9	34.7	2.6	3.4	1.4	2.8	2.4	1.1	2.0	23.5	48.0	70.7	37.3	55.5	79.5	60.4
Underflow (Remainder in column)	-	-	65.3	100.0	76.5	52.0	29.3	62.7	44.5	20.5	39.6	100.0	100.0	100.0	100.0	100.0	100.0	100.0
Total (Calculated)	**Total**	**Total**	**100.0**		**100.0**	**100.0**	**100.0**	**100.0**	**100.0**	**100.0**	**100.0**							

Table D.4: Raw Data for the Average Base case Reflux Classifier testwork without selective flocculation (Test 1-3)

Stream	Pump Speed (rpm)	Fluidisation Water Flowrate (kg/hr)	Discrete Mass (%)					Discrete Fe Grade (%)					Discrete Fe Recovery (%)					Discrete SiO_2 Grade (%)					Discrete SiO_2 Recovery (%)				
			Test 1	Test 2	Test 3	Average	Std Dev	Test 1	Test 2	Test 3	Average	Std Dev	Test 1	Test 2	Test 3	Average	Std Dev	Test 1	Test 2	Test 3	Average	Std Dev	Test 1	Test 2	Test 3	Average	Std Dev
Overflow 1	10	8.2	0.5	0.4	0.7	0.6	0.2	16.05	17.92	18.03	17.33	1.1	0.2	0.2	0.3	0.2	0.1	60.85	58.72	58.32	59.30	1.4	0.7	0.6	1.0	0.8	0.2
Overflow 2	15	12.5	2.1	1.4	1.0	1.5	0.6	20.98	22.47	22.02	21.82	0.8	1.2	0.8	0.5	0.8	0.3	57.22	55.73	55.11	56.02	1.1	2.8	1.7	1.3	1.9	0.8
Overflow 3	20	16.8	2.4	2.1	1.6	2.0	0.4	23.64	24.33	27.36	25.11	2.0	1.5	1.3	1.1	1.3	0.2	53.80	56.73	54.04	54.86	1.6	3.0	2.7	2.0	2.5	0.5
Overflow 4	25	21.0	2.9	2.2	2.8	2.6	0.4	23.57	26.71	21.98	24.09	2.4	1.8	1.5	1.5	1.6	0.2	58.74	56.50	58.36	57.87	1.2	3.9	2.8	3.8	3.5	0.6
Overflow 5	30	25.3	2.8	2.3	1.5	2.2	0.7	25.87	27.43	26.75	26.68	0.8	1.9	1.6	1.0	1.5	0.5	58.76	56.47	56.95	57.39	1.2	3.9	2.9	2.0	2.9	0.9
Overflow 6	37.35	31.5	2.4	2.4	2.2	2.3	0.1	21.53	25.22	25.71	24.15	2.3	1.3	1.5	1.4	1.4	0.1	59.61	61.21	59.98	60.27	0.8	3.3	3.4	3.1	3.3	0.1
Overflow 7	60	50.5	6.6	9.4	7.7	7.9	1.4	23.18	23.64	25.03	23.95	1.0	4.0	5.6	4.8	4.8	0.8	67.35	65.30	63.90	65.52	1.7	10.2	13.9	11.6	11.9	1.9
Overflow 8	80	67.3	5.2	5.9	4.6	5.2	0.7	27.34	27.27	27.76	27.46	0.3	3.7	4.1	3.1	3.6	0.5	61.20	61.70	61.10	61.33	0.3	7.3	8.2	6.5	7.4	0.9
Overflow 9	120	100.9	6.8	7.2	6.1	6.7	0.5	28.67	28.95	27.62	28.41	0.7	5.1	5.2	4.2	4.8	0.6	60.50	59.80	61.30	60.53	0.8	9.5	9.7	8.8	9.3	0.5
Overflow 10	144	121.1	4.3	3.7	3.5	3.8	0.4	33.71	35.24	32.55	33.83	1.4	3.8	3.2	2.9	3.3	0.5	53.60	51.50	54.00	53.03	1.3	5.3	4.2	4.5	4.7	0.6
Overflow 11	174	146.4	2.6	2.4	2.9	2.6	0.3	36.71	35.45	35.59	35.92	0.7	2.5	2.1	2.6	2.4	0.3	49.00	50.80	48.90	49.57	1.1	3.0	2.7	3.4	3.0	0.3
Underflow (Remainder in column)		U/F	61.3	60.7	65.3	62.4	2.5	45.90	47.55	47.10	46.85	0.9	73.1	72.9	76.5	74.1	2.0	33.40	34.50	34.00	33.97	0.6	47.2	47.3	52.0	48.8	2.8
Total (Calculated)			**100.0**	**100.0**	**100.0**	**100.0**		**38.49**	**39.62**	**40.21**	**39.44**	**0.9**	**100.0**	**100.0**	**100.0**	**100.0**		**43.42**	**44.32**	**42.67**	**43.47**	**0.8**	**100.0**	**100.0**	**100.0**	**100.0**	

Stream	Pump Speed (rpm)	Fluidisation Water Flowrate (kg/hr)	Cumulative Mass to O/F (%)					Cumulative Fe Grade to O/F (%)					Cumulative Fe Recovery to O/F (%)					Cumulative SiO_2 Grade to O/F (%)					Cumulative SiO_2 Recovery to O/F (%)				
			Test 1	Test 2	Test 3	Average	Std Dev	Test 1	Test 2	Test 3	Average	Std Dev	Test 1	Test 2	Test 3	Average	Std Dev	Test 1	Test 2	Test 3	Average	Std Dev	Test 1	Test 2	Test 3	Average	Std Dev
Overflow 1	10	8.23	0.5	0.4	0.7	0.6	0.2	16.05	17.92	18.03	17.33	1.1	0.2	0.2	0.3	0.2	0.1	60.85	58.72	58.32	59.30	1.4	0.7	0.6	1.0	0.8	0.2
Overflow 2	15	12.48	2.6	1.8	1.7	2.1	0.5	20.06	21.34	20.31	20.57	0.7	1.4	1.0	0.9	1.1	0.3	57.90	56.47	56.48	56.95	0.8	3.5	2.3	2.3	2.7	0.7
Overflow 3	20	16.84	5.0	3.9	3.3	4.1	0.8	21.77	22.94	23.69	22.80	1.0	2.8	2.2	2.0	2.3	0.4	55.94	56.61	55.31	55.95	0.7	6.4	4.9	4.3	5.2	1.1
Overflow 4	25	21.02	7.9	6.1	6.1	6.7	1.0	22.42	24.30	22.91	23.21	1.0	4.6	3.7	3.5	3.9	0.6	56.97	56.57	56.70	56.75	0.2	10.3	7.7	8.2	8.7	1.4
Overflow 5	30	25.26	10.7	8.3	7.6	8.9	1.6	23.34	25.16	23.66	24.05	1.0	6.5	5.3	4.5	5.4	1.0	57.44	56.54	56.75	56.91	0.5	14.2	10.6	10.2	11.7	2.2
Overflow 6	37.35	31.5	13.1	10.8	9.9	11.2	1.7	23.01	25.17	24.12	24.10	1.1	7.8	6.8	5.9	6.9	1.0	57.84	57.60	57.48	57.64	0.2	17.5	14.0	13.3	14.9	2.2
Overflow 7	60	50.472	19.7	20.2	17.6	19.2	1.4	23.07	24.45	24.52	24.02	0.8	11.8	12.5	10.7	11.7	0.9	61.02	61.19	60.30	60.84	0.5	27.7	27.9	24.8	26.8	1.7
Overflow 8	80	67.296	24.9	26.1	22.1	24.4	2.0	23.96	25.09	25.19	24.75	0.7	15.5	16.5	13.9	15.3	1.4	61.06	61.31	60.46	60.94	0.4	35.1	36.1	31.4	34.2	2.5
Overflow 9	120	100.944	31.7	33.3	28.2	31.1	2.6	24.97	25.92	25.72	25.54	0.5	20.6	21.8	18.1	20.1	1.9	60.94	60.98	60.65	60.86	0.2	44.5	45.8	40.1	43.5	3.0
Overflow 10	144	121.1328	36.1	36.9	31.8	34.9	2.8	26.02	26.84	26.48	26.45	0.4	24.4	25.0	20.9	23.4	2.2	60.06	60.05	59.91	60.00	0.1	49.9	50.0	44.6	48.2	3.1
Overflow 11	174	146.3688	38.7	39.3	34.7	37.6	2.5	26.75	27.36	27.25	27.12	0.3	26.9	27.1	23.5	25.9	2.0	59.30	59.49	58.98	59.26	0.3	52.8	52.7	48.0	51.2	2.8
Underflow (Remainder in column)		U/F	100.0	100.0	100.0	100.0	0.0	38.49	39.62	40.21	39.44	0.9	100.0	100.0	100.0	100.0	0.0	43.42	44.32	42.67	43.47	0.8	100.0	100.0	100.0	100.0	0.0

Table D.4: Raw Data for the Average Base case Reflux Classifier testwork without selective flocculation (Test 1-3) (Contd.)

Stream	Pump Speed (rpm)	Fluidisation Water Flowrate (kg/hr)	Cumulative Mass to U/F (%)					Cumulative Fe Grade to U/F (%)					Cumulative Fe Recovery to U/F (%)					Cumulative SiO_2 Grade to U/F (%)					Cumulative SiO_2 Recovery to U/F (%)					Cumulative Separation Efficiency to U/F (%)				
			Test 1	Test 2	Test 3	Average	2 Std Dev	Test 1	Test 2	Test 3	Average	2 Std Dev	Test 1	Test 2	Test 3	Average	2 Std Dev	Test 1	Test 2	Test 3	Average	2 Std Dev	Test 1	Test 2	Test 3	Average	2 Std Dev	Test 1	Test 2	Test 3	Average	2 Std Dev
Overflow 1	10	8.23	100.0	100.0	100.0	100.0	0.0	38.49	39.62	40.21	39.44	1.7	100.0	100.0	100.0	100.0	0.0	43.42	44.32	42.67	43.47	1.7	100.0	100.0	100.0	100.0	0.0	0.0	0.0	0.0	0.0	0.0
Overflow 2	15	12.48	99.5	99.6	99.3	99.4	0.3	38.60	39.72	40.37	39.56	1.8	99.8	99.8	99.7	99.8	0.2	43.34	44.26	42.55	43.38	1.7	99.3	99.4	99.0	99.2	0.4	0.5	0.4	0.7	0.5	0.3
Overflow 3	20	16.84	97.4	98.2	98.3	97.9	1.0	38.98	39.95	40.56	39.83	1.6	98.6	99.0	99.1	98.9	0.5	43.03	44.10	42.43	43.19	1.7	96.5	97.7	97.7	97.3	1.4	2.1	1.3	1.4	1.6	0.9
Overflow 4	25	21.02	95.0	96.1	96.7	95.9	1.7	39.37	40.29	40.78	40.15	1.4	97.2	97.8	98.0	97.7	0.9	42.76	43.83	42.23	42.94	1.6	93.6	95.1	95.7	94.8	2.2	3.6	2.7	2.4	2.9	1.3
Overflow 5	30	25.26	92.1	93.9	93.9	93.3	2.1	39.86	40.61	41.34	40.60	1.5	95.4	96.3	96.5	96.1	1.2	42.26	43.53	41.75	42.52	1.8	89.7	92.3	91.8	91.3	2.8	5.7	4.0	4.7	4.8	1.7
Overflow 6	37.35	31.5	89.3	91.7	92.4	91.1	3.2	40.31	40.93	41.58	40.94	1.3	93.5	94.7	95.5	94.6	2.0	41.74	43.21	41.51	42.15	1.8	85.8	89.4	89.8	88.3	4.4	7.7	5.3	5.7	6.2	2.5
Overflow 7	60	50.472	86.9	89.2	90.1	88.8	3.4	40.83	41.36	41.97	41.39	1.1	92.2	93.2	94.1	93.1	1.9	41.25	42.72	41.05	41.67	1.8	82.5	86.0	86.7	85.1	4.5	9.6	7.2	7.4	8.0	2.7
Overflow 8	80	67.296	80.3	79.8	82.4	80.8	2.8	42.28	43.46	43.55	43.10	1.4	88.2	87.5	89.3	88.3	1.8	39.10	40.05	38.91	39.35	1.2	72.3	72.1	75.2	73.2	3.4	15.9	15.4	14.1	15.1	1.8
Overflow 9	120	100.944	75.1	73.9	77.9	75.6	4.1	43.32	44.75	44.48	44.18	1.5	84.5	83.5	86.1	84.7	2.7	37.56	38.31	37.61	37.83	0.8	64.9	63.9	68.6	65.8	5.0	19.5	19.6	17.5	18.9	2.4
Overflow 10	144	121.1328	68.3	66.7	71.8	68.9	5.2	44.77	46.45	45.91	45.71	1.7	79.4	78.2	81.9	79.9	3.8	35.28	36.01	35.59	35.63	0.7	55.5	54.2	59.9	56.5	5.9	23.9	24.0	22.1	23.3	2.2
Overflow 11	174	146.3688	63.9	63.1	68.2	65.1	5.5	45.52	47.10	46.60	46.41	1.6	75.6	75.0	79.1	76.6	4.4	34.04	35.11	34.64	34.60	1.1	50.1	50.0	55.4	51.8	6.2	25.5	25.0	23.7	24.7	1.9
Underflow (Remainder in column)		150	61.3	60.7	65.3	62.4	5.0	45.90	47.55	47.10	46.85	1.7	73.1	72.9	76.5	74.1	4.0	33.40	34.50	34.00	33.97	1.1	47.2	47.3	52.0	48.8	5.6	26.0	25.6	24.5	25.3	1.6

Table D.5: Raw Data for Optimised Selective Flocculation coupled with the Reflux Classifier (Test 4)

Test 4					Discrete Grade								Cumulative Grade to Overflow						
					Fe	SiO_2	Al_2O_3	MnO	CaO	MgO	LOI		Fe	SiO_2	Al_2O_3	MnO	CaO	MgO	LOI
Stream	**Pump Speed (rpm)**	**Fluidisation Water Flowrate (kg/hr)**	**Discrete Mass (%)**	**Cumulative Mass (%)**	%	%	%	%	%	%	%	∑ Oxides	%	%	%	%	%	%	%
Overflow 1	10.0	8.2	3.9	3.9	19.34	65.40	6.51	0.08	0.58	2.29	3.85	167.06	19.34	65.40	6.51	0.08	0.58	2.29	3.85
Overflow 2	15.0	12.5	0.3	4.2	27.31	54.79	3.78	0.08	0.57	1.84	3.17	155.08	19.89	64.66	6.32	0.08	0.58	2.26	3.80
Overflow 3	20.0	16.8	0.7	4.9	16.32	69.41	2.80	0.06	0.48	1.21	2.11	171.51	19.37	65.35	5.81	0.08	0.56	2.11	3.56
Overflow 4	25.0	21.0	0.9	5.8	16.05	69.77	2.23	0.06	0.46	1.01	1.79	171.68	18.85	66.04	5.25	0.07	0.55	1.93	3.28
Overflow 5	30.0	25.3	1.4	7.3	17.62	67.68	1.85	0.06	0.38	0.93	1.48	169.68	18.61	66.36	4.58	0.07	0.52	1.74	2.93
Overflow 6	37.4	31.5	2.0	9.3	21.77	62.17	1.75	0.06	0.51	1.14	1.13	166.02	19.30	65.44	3.96	0.07	0.51	1.61	2.53
Overflow 7	60.0	50.5	6.4	15.7	25.20	57.59	1.29	0.06	0.41	0.70	0.95	161.44	21.71	62.24	2.87	0.07	0.47	1.24	1.89
Underflow (Remainder in column)	-	-	84.3	100.0	42.05	35.17	0.49	0.06	0.08	0.27	0.44	136.63	38.85	39.42	0.87	0.06	0.14	0.42	0.67
Total (Calculated)	**Total**	**Total**	**100.0**		**38.85**	**39.42**	**0.87**	**0.06**	**0.14**	**0.42**	**0.67**								
Total (Measured)					**37.34**	**41.43**	**0.98**	**0.05**	**0.38**	**0.31**	**0.86**								
% Relative Error					**4.05**	**4.86**	**11.26**	**21.62**	**63.22**	**34.86**	**22.39**								

Test 4					Discrete Recovery							Cumulative Recovery to Overflow						
					Fe	SiO_2	Al_2O_3	MnO	CaO	MgO	LOI	Fe	SiO_2	Al_2O_3	MnO	CaO	MgO	LOI
Stream	**Pump Speed (rpm)**	**Fluidisation Water Flowrate (kg/hr)**	**Discrete Mass (%)**	**Cumulative Mass (%)**	%	%	%	%	%	%	%	%	%	%	%	%	%	%
Overflow 1	10.0	8.2	3.9	3.9	2.0	6.5	29.5	5.1	16.1	21.5	22.6	2.0	6.5	29.5	5.1	16.1	21.5	22.6
Overflow 2	15.0	12.5	0.3	4.2	0.2	0.4	1.3	0.4	1.2	1.3	1.4	2.2	6.9	30.8	5.5	17.3	22.8	24.0
Overflow 3	20.0	16.8	0.7	4.9	0.3	1.3	2.3	0.7	2.4	2.1	2.3	2.5	8.2	33.1	6.2	19.8	24.8	26.3
Overflow 4	25.0	21.0	0.9	5.8	0.4	1.6	2.4	0.9	3.0	2.2	2.5	2.8	9.8	35.5	7.1	22.8	27.0	28.7
Overflow 5	30.0	25.3	1.4	7.3	0.6	2.4	3.0	1.4	3.8	3.1	3.1	3.5	12.2	38.5	8.5	26.6	30.2	31.9
Overflow 6	37.4	31.5	2.0	9.3	1.1	3.2	4.1	2.0	7.4	5.5	3.4	4.6	15.4	42.6	10.5	34.0	35.7	35.3
Overflow 7	60.0	50.5	6.4	15.7	4.2	9.4	9.5	6.3	18.7	10.7	9.1	8.8	24.8	52.2	16.8	52.7	46.4	44.4
Underflow (Remainder in column)	-	-	84.3	100.0	91.2	75.2	47.8	83.2	47.3	53.6	55.6	100.0	100.0	100.0	100.0	100.0	100.0	100.0
Total (Calculated)	**Total**	**Total**	**100.0**		**100.0**	**100.0**	**100.0**	**100.0**	**100.0**	**100.0**	**100.0**							

Table D.6: Raw Data for Optimised Selective Flocculation coupled with the Reflux Classifier (Test 5)

Test 5					Discrete Grade								Cumulative Grade to Overflow						
					Fe	SiO_2	Al_2O_3	MnO	CaO	MgO	LOI	∑ Oxides	Fe	SiO_2	Al_2O_3	MnO	CaO	MgO	LOI
Stream	Pump Speed (rpm)	Fluidisation Water Flowrate (kg/hr)	Discrete Mass (%)	Cumulative Mass (%)	%	%	%	%	%	%	%		%	%	%	%	%	%	%
Overflow 1	10	8.23	3.0	3.0	20.16	64.30	6.68	0.08	0.95	2.17	3.92	101.54	20.16	64.30	6.68	0.08	0.95	2.17	3.92
Overflow 2	15	12.48	0.3	3.3	28.28	53.50	4.06	0.10	0.91	1.63	3.03	100.43	20.85	63.38	6.46	0.08	0.95	2.12	3.84
Overflow 3	20	16.84	1.0	4.3	14.30	72.10	2.97	0.06	0.89	1.11	1.78	102.91	19.34	65.39	5.65	0.07	0.93	1.89	3.36
Overflow 4	25	21.02	1.2	5.5	15.88	70.00	2.48	0.06	0.86	1.05	1.70	103.05	18.57	66.42	4.94	0.07	0.92	1.70	2.99
Overflow 5	30	25.26	1.4	6.9	18.43	66.60	2.19	0.06	0.92	0.95	1.44	102.65	18.54	66.46	4.40	0.07	0.92	1.55	2.68
Overflow 6	37.35	31.5	1.5	8.4	18.10	67.05	1.81	0.06	0.92	0.78	1.33	102.94	18.46	66.56	3.93	0.07	0.92	1.41	2.44
Overflow 7	60.0	50.5	5.4	13.8	19.64	65.00	1.21	0.06	0.71	0.55	1.00	102.63	18.92	65.95	2.86	0.06	0.84	1.07	1.87
Overflow 8	80	67.3	3.1	16.9	29.78	51.50	1.49	0.06	0.80	0.66	1.16	102.58	20.94	63.27	2.61	0.06	0.83	1.00	1.74
Overflow 9	120	100.9	1.8	18.7	33.38	46.70	1.63	0.06	0.76	0.73	1.38	102.26	22.12	61.70	2.51	0.06	0.82	0.97	1.71
Underflow (Remainder in column)	-	-	81.3	100.0	42.85	39.30	0.45	0.06	0.42	0.13	0.42	102.06	38.98	37.52	0.70	0.05	0.42	0.22	0.55
Total (Calculated)	**Total**	**Total**	**100.0**		**38.98**	**43.49**	**0.84**	**0.06**	**0.50**	**0.29**	**0.66**								
Total (Measured)					**37.34**	**41.78**	**0.98**	**0.05**	**0.38**	**0.31**	**0.86**								
% Relative Error					**4.38**	**4.07**	**13.95**	**21.11**	**30.33**	**7.15**	**23.19**								

Table D.6: Raw Data for Optimised Selective Flocculation coupled with the Reflux Classifier (Test 5) (Contd.)

Test 5					Discrete Recovery							Cumulative Recovery to Overflow						
					Fe	SiO_2	Al_2O_3	MnO	CaO	MgO	LOI	Fe	SiO_2	Al_2O_3	MnO	CaO	MgO	LOI
Stream	**Pump Speed (rpm)**	**Fluidisation Water Flowrate (kg/hr)**	**Discrete Mass (%)**	**Cumulative Mass (%)**	%	%	%	%	%	%	%	%	%	%	%	%	%	%
Overflow 1	10	8.23	3.0	3.0	1.6	4.4	23.9	3.7	5.7	22.6	17.8	1.6	4.4	23.9	3.7	5.7	22.6	17.8
Overflow 2	15	12.48	0.3	3.3	0.2	0.3	1.4	0.5	0.5	1.6	1.3	1.8	4.8	25.3	4.2	6.2	24.2	19.1
Overflow 3	20	16.84	1.0	4.3	0.4	1.6	3.5	1.0	1.8	3.8	2.7	2.1	6.4	28.8	5.1	8.0	28.0	21.7
Overflow 4	25	21.02	1.2	5.5	0.5	2.0	3.6	1.2	2.1	4.5	3.2	2.6	8.4	32.4	6.4	10.1	32.5	24.9
Overflow 5	30	25.26	1.4	6.9	0.6	2.1	3.5	1.3	2.5	4.5	3.0	3.3	10.5	35.9	7.7	12.6	36.9	27.9
Overflow 6	37.35	31.5	1.5	8.4	0.7	2.3	3.2	1.5	2.8	4.1	3.0	4.0	12.8	39.2	9.2	15.4	41.0	30.9
Overflow 7	60.0	50.5	5.4	13.8	2.7	8.1	7.8	5.4	7.7	10.3	8.2	6.7	20.9	47.0	14.6	23.1	51.3	39.1
Overflow 8	80	67.3	3.1	16.9	2.4	3.7	5.6	3.1	5.1	7.2	5.5	9.1	24.6	52.6	17.7	28.2	58.5	44.6
Overflow 9	120	100.9	1.8	18.7	1.5	1.9	3.4	1.8	2.7	4.5	3.7	10.6	26.5	56.0	19.4	30.9	63.0	48.3
Underflow (Remainder in column)	-	-	81.3	100.0	89.4	73.5	44.0	80.6	69.1	37.0	51.7	100.0	100.0	100.0	100.0	100.0	100.0	100.0
Total (Calculated)	**Total**	**Total**	**100.0**		**100.0**	**100.0**	**100.0**	**100.0**	**100.0**	**100.0**	**100.0**							

Table D.7: Raw Data for Optimised Selective Flocculation coupled with the Reflux Classifier (Test 6)

Test 6					Discrete Grade (ICP)								Cumulative Grade to Overflow						
					Fe	SiO_2	Al_2O_3	MnO	CaO	MgO	LOI	∑ Oxides	Fe	SiO_2	Al_2O_3	MnO	CaO	MgO	LOI
Stream	**Pump Speed (rpm)**	**Fluidisation Water Flowrate (kg/hr)**	**Discrete Mass (%)**	**Cumulative Mass (%)**	**%**	**%**	**%**	**%**	**%**	**%**	**%**		**%**	**%**	**%**	**%**	**%**	**%**	**%**
Overflow 1	10	8.23	3.3	3.3	17.55	67.77	6.59	0.09	1.15	2.75	3.85	107.30	17.55	67.77	6.59	0.09	1.15	2.75	3.85
Overflow 2	15	12.48	0.2	3.5	19.58	65.07	5.05	0.11	1.16	2.76	2.94	105.09	17.68	67.60	6.49	0.09	1.15	2.75	3.79
Overflow 3	20	16.84	0.1	3.6	19.02	65.82	4.82	0.09	1.19	3.14	4.87	107.12	17.72	67.54	6.44	0.09	1.15	2.76	3.83
Overflow 4	25	21.02	0.4	4.0	15.03	71.12	2.61	0.06	1.06	1.34	1.83	99.52	17.46	67.89	6.06	0.09	1.14	2.62	3.63
Overflow 5	30	25.26	0.5	4.5	17.20	68.24	2.51	0.06	1.03	1.25	2.03	99.72	17.43	67.93	5.67	0.09	1.13	2.47	3.46
Overflow 6	37.35	31.5	1.7	6.2	18.50	66.52	1.81	0.06	1.07	0.91	1.22	98.04	17.73	67.54	4.61	0.08	1.11	2.04	2.84
Overflow 7	60.0	50.5	6.3	12.5	24.35	58.73	1.21	0.06	0.98	0.60	0.89	97.29	21.06	63.10	2.90	0.07	1.05	1.31	1.86
Overflow 8	80	67.3	2.6	15.1	31.50	49.21	1.36	0.06	0.98	0.71	1.35	98.71	22.88	60.68	2.63	0.07	1.04	1.21	1.77
Overflow 9	120	100.9	4.5	19.6	28.40	53.33	0.83	0.06	0.88	0.43	0.69	96.84	24.14	59.01	2.22	0.07	1.00	1.03	1.52
Overflow 10	144	121.1	5.9	25.5	28.00	53.87	0.66	0.06	0.84	0.32	0.68	96.47	25.03	57.82	1.86	0.06	0.96	0.87	1.33
Overflow 11	174	146.4	3.2	28.7	32.40	48.01	0.64	0.06	0.51	0.28	0.59	96.42	25.86	56.72	1.72	0.06	0.91	0.80	1.25
Underflow (Remainder in column)	-	-	71.3	100.0	43.15	33.70	0.40	0.06	0.49	0.16	0.42	96.93	38.18	40.32	0.78	0.06	0.61	0.34	0.66
Total (Calculated)	**Total**	**Total**	**100.0**		**38.18**	**40.32**	**0.78**	**0.06**	**0.61**	**0.34**	**0.66**								
Total (Measured)					**37.34**	**41.43**	**0.98**	**0.05**	**0.38**	**0.31**	**0.86**								
% Relative Error					**2.25**	**2.70**	**20.17**	**22.50**	**59.58**	**10.09**	**23.57**								

Table D.7: Raw Data for Optimised Selective Flocculation coupled with the Reflux Classifier (Test 6) (Contd.)

Test 6					Discrete Recovery							Cumulative Recovery to Overflow						
					Fe	SiO_2	Al_2O_3	MnO	CaO	MgO	LOI	Fe	SiO_2	Al_2O_3	MnO	CaO	MgO	LOI
Stream	**Pump Speed (rpm)**	**Fluidisation Water Flowrate (kg/hr)**	**Discrete Mass (%)**	**Cumulative Mass (%)**	**%**	**%**	**%**	**%**	**%**	**%**	**%**	**%**	**%**	**%**	**%**	**%**	**%**	**%**
Overflow 1	10	8.23	3.3	3.3	1.5	5.5	27.7	5.0	6.2	26.3	19.2	1.5	5.5	27.7	5.0	6.2	26.3	19.2
Overflow 2	15	12.48	0.2	3.5	0.1	0.4	1.4	0.4	0.4	1.8	1.0	1.6	5.9	29.2	5.4	6.6	28.1	20.2
Overflow 3	20	16.84	0.1	3.6	0.1	0.2	0.8	0.2	0.2	1.1	0.9	1.7	6.1	29.9	5.6	6.8	29.2	21.1
Overflow 4	25	21.02	0.4	4.0	0.2	0.7	1.3	0.4	0.7	1.5	1.1	1.8	6.7	31.2	6.0	7.5	30.8	22.2
Overflow 5	30	25.26	0.5	4.5	0.2	0.8	1.6	0.5	0.8	1.8	1.5	2.1	7.6	32.8	6.5	8.3	32.6	23.7
Overflow 6	37.35	31.5	1.7	6.2	0.8	2.8	4.0	1.7	3.0	4.6	3.2	2.9	10.4	36.8	8.1	11.3	37.1	26.9
Overflow 7	60.0	50.5	6.3	12.5	4.0	9.2	9.8	6.2	10.1	11.0	8.5	6.9	19.6	46.6	14.3	21.5	48.2	35.4
Overflow 8	80	67.3	2.6	15.1	2.2	3.2	4.6	2.6	4.2	5.5	5.4	9.1	22.8	51.2	16.9	25.7	53.7	40.8
Overflow 9	120	100.9	4.5	19.6	3.3	5.9	4.8	4.4	6.4	5.7	4.7	12.4	28.7	56.0	21.3	32.1	59.4	45.5
Overflow 10	144	121.1	5.9	25.5	4.3	7.9	5.0	5.8	8.1	5.4	6.1	16.7	36.6	61.0	27.0	40.2	64.8	51.6
Overflow 11	174	146.4	3.2	28.7	2.7	3.8	2.7	3.2	2.7	2.7	2.9	19.5	40.4	63.6	30.2	42.9	67.4	54.5
Underflow (Remainder in column)	-	-	71.3	100.0	80.5	59.6	36.4	69.8	57.1	32.6	45.5	100.0	100.0	100.0	100.0	100.0	100.0	100.0
Total (Calculated)	**Total**	**Total**	**100.0**		**100.0**	**100.0**	**100.0**	**100.0**	**100.0**	**100.0**	**100.0**							

Table D.8: Raw Data for the Average Test for Optimised Selective Flocculation coupled with the Reflux Classifier (Test 4-6)

Stream	Pump Speed (rpm)	Fluidisation Water Flowrate (kg/hr)	Discrete Mass (%)					Discrete Fe Grade (%)					Discrete Fe Recovery (%)					Discrete SiO_2 Grade (%)					Discrete SiO_2 Recovery (%)				
			Test 4	Test 5	Test 6	Average	Std Dev	Test 4	Test 5	Test 6	Average	Std Dev	Test 4	Test 5	Test 6	Average	Std Dev	Test 4	Test 5	Test 6	Average	Std Dev	Test 4	Test 5	Test 6	Average	Std Dev
Overflow 1	10	8.2	3.9	3.0	3.3	3.4	0.5	19.34	20.16	17.55	19.02	1.3	2.0	1.6	1.5	1.7	0.2	65.40	64.30	67.77	65.82	1.8	6.5	4.4	5.5	5.5	1.0
Overflow 2	15	12.5	0.3	0.3	0.2	0.3	0.0	27.31	28.28	19.58	25.06	4.8	0.2	0.2	0.1	0.2	0.1	54.79	53.50	65.07	57.79	6.3	0.4	0.3	0.4	0.4	0.0
Overflow 3	20	16.8	0.7	1.0	0.1	0.6	0.4	16.32	14.30	19.02	16.55	2.4	0.3	0.4	0.1	0.2	0.2	69.41	72.10	65.82	69.11	3.2	1.3	1.6	0.2	1.0	0.7
Overflow 4	25	21.0	0.9	1.2	0.4	0.8	0.4	16.05	15.88	15.03	15.65	0.5	0.4	0.5	0.2	0.3	0.2	69.77	70.00	71.12	70.30	0.7	1.6	2.0	0.7	1.4	0.7
Overflow 5	30	25.3	1.4	1.4	0.5	1.1	0.5	17.62	18.43	17.20	17.75	0.6	0.6	0.6	0.2	0.5	0.2	67.68	66.60	68.24	67.51	0.8	2.4	2.1	0.8	1.8	0.8
Overflow 6	37.35	31.5	2.0	1.5	1.7	1.8	0.3	21.77	18.10	18.50	19.45	2.0	1.1	0.7	0.8	0.9	0.2	62.17	67.05	66.52	65.24	2.7	3.2	2.3	2.8	2.8	0.5
Overflow 7	60	50.5	6.4	5.4	6.3	6.0	0.5	25.20	19.64	24.35	23.06	3.0	4.2	2.7	4.0	3.6	0.8	57.59	65.00	58.73	60.44	4.0	9.4	8.1	9.2	8.9	0.7
Overflow 8	80	67.3		3.1	2.6	2.9	0.4		29.78	31.50	30.64	1.2		2.4	2.2	2.3	0.2		51.50	49.21	50.35	1.6	0.0	3.7	3.2	2.3	2.0
Overflow 9	120	100.9		1.8	4.5	3.1	1.9		33.38	28.40	30.89	3.5		1.5	3.3	2.4	1.3		46.70	53.33	50.02	4.7	0.0	1.9	5.9	2.6	3.0
Overflow 10	144	121.1			5.9	5.9				28.00	28.00				4.3	4.3				53.87	53.87		0.0	0.0	7.9	2.6	
Overflow 11	174	146.4			3.2	3.2				32.40	32.40				2.7	2.7				48.01	48.01		0.0	0.0	3.8	1.3	
Underflow (Remainder in column)		U/F	84.3	81.3	71.3	70.9		42.05	42.85	43.15	42.68		91.2	89.4	80.5	87.1		35.17	39.30	33.70	36.06		75.2	73.5	59.6	69.4	
Total (Calculated)			**100.0**	**100.0**	**100.0**	**100.0**		**38.85**	**38.98**	**38.18**	**38.67**		**100.0**	**100.0**	**100.0**	**100.0**		**39.42**	**43.49**	**40.32**	**42.22**		**100.0**	**100.0**	**100.0**	**100.0**	

Stream	Pump Speed (rpm)	Fluidisation Water Flowrate (kg/hr)	Cumulative Mass to O/F (%)					Cumulative Fe Grade to O/F (%)					Cumulative Fe Recovery to O/F (%)					Cumulative SiO_2 Grade to O/F (%)					Cumulative SiO_2 Recovery to O/F (%)				
			Test 4	Test 5	Test 6	Average	Std Dev	Test 4	Test 5	Test 6	Average	Std Dev	Test 4	Test 5	Test 6	Average	Std Dev	Test 4	Test 5	Test 6	Average	Std Dev	Test 4	Test 5	Test 6	Average	Std Dev
Overflow 1	10	8.2	3.9	3.0	3.3	3.4	0.5	19.34	20.16	17.55	19.02	1.3	2.0	1.6	1.5	1.7	0.2	65.40	64.30	67.77	65.82	1.8	6.5	4.4	5.5	5.48	1.0
Overflow 2	15	12.5	4.2	3.3	3.5	3.7	0.5	19.89	20.85	17.68	19.47	1.6	2.2	1.8	1.6	1.8	0.3	64.66	63.38	67.60	65.21	2.2	6.9	4.8	5.9	5.85	1.1
Overflow 3	20	16.8	4.9	4.3	3.6	4.3	0.7	19.37	19.34	17.72	18.81	0.9	2.5	2.1	1.7	2.1	0.4	65.35	65.39	67.54	66.09	1.3	8.2	6.4	6.1	6.88	1.1
Overflow 4	25	21.0	5.8	5.5	4.0	5.1	1.0	18.85	18.57	17.46	18.29	0.7	2.8	2.6	1.8	2.4	0.5	66.04	66.42	67.89	66.79	1.0	9.8	8.4	6.7	8.32	1.5
Overflow 5	30	25.3	7.3	6.9	4.5	6.2	1.5	18.61	18.54	17.43	18.19	0.7	3.5	3.3	2.1	2.9	0.8	66.36	66.46	67.93	66.92	0.9	12.2	10.5	7.6	10.10	2.3
Overflow 6	37.35	31.5	9.3	8.4	6.2	8.0	1.6	19.30	18.46	17.73	18.50	0.8	4.6	4.0	2.9	3.8	0.9	65.44	66.56	67.54	66.52	1.0	15.4	12.8	10.4	12.88	2.5
Overflow 7	60	50.5	15.7	13.8	12.5	14.0	1.6	21.71	18.92	21.06	20.56	1.5	8.8	6.7	6.9	7.5	1.1	62.24	65.95	63.10	63.77	1.9	24.8	20.9	19.6	21.76	2.7
Overflow 8	80	67.3	15.7	16.9	15.1	16.0	1.3	21.71	20.94	22.88	21.91	1.4	8.8	9.1	9.1	9.1	0.0	62.24	63.27	60.68	61.98	1.8	24.8	24.6	22.8	23.70	1.3
Overflow 9	120	100.9	15.7	18.7	19.6	19.2	0.7	21.71	22.12	24.14	23.13	1.4	8.8	10.6	12.4	11.5	1.3	62.24	61.70	59.01	60.35	1.9	24.8	26.5	28.7	27.62	1.6
Overflow 10	144	121.1	15.7	18.7	25.5	25.5		21.71	22.12	25.03	25.03		8.8	10.6	16.7	12.0		62.24	61.70	57.82	57.82		24.8	26.5	36.6	36.58	
Overflow 11	174	146.4	15.7	18.7	28.7	28.7		21.71	22.12	25.86	25.86		8.8	10.6	19.5	12.9		62.24	61.70	56.72	56.72		24.8	26.5	40.4	40.42	
Underflow (Remainder in column)		U/F	100.0	100.0	100.0	100.0		38.85	38.98	38.18	38.67		100.0	100.0	100.0	100.0		39.42	43.49	40.32	41.07		100.0	100.0	100.0	100.00	

Table D.8: Raw Data for the Average Test for Optimised Selective Flocculation coupled with the Reflux Classifier (Test 4-6) (Contd.)

Stream	Pump Speed (rpm)	Fluidisation Water Flowrate (kg/hr)	Cumulative Mass to U/F (%)					Cumulative Fe Grade to U/F (%)					Cumulative Fe Recovery to U/F (%)					Cumulative SiO_2 Grade to U/F (%)					Cumulative SiO_2 Recovery to U/F (%)					Cumulative Separation Efficiency to U/F (%)				
			Test 4	Test 5	Test 6	Average	2 Std Dev	Test 4	Test 5	Test 6	Average	2 Std Dev	Test 4	Test 5	Test 6	Average	2 Std Dev	Test 4	Test 5	Test 6	Average	2 Std Dev	Test 4	Test 5	Test 6	Average	2 Std Dev	Test 4	Test 5	Test 6	Average	2 Std Dev
Overflow 1	10	8.2	100.0	100.0	100.0	100.0	0.0	38.85	38.98	38.18	38.7	0.9	100.0	100.0	100.0	100.0	0.0	39.42	43.49	40.32	41.1	4.3	100.0	100.0	100.0	100.0	0.0	0.0	0.0	0.0	0.0	0.0
Overflow 2	15	12.5	96.1	97.0	96.7	96.6	0.9	39.65	39.56	38.88	39.4	0.8	98.0	98.4	98.5	98.3	0.5	38.36	42.84	39.39	40.2	4.7	93.5	95.6	94.5	94.5	2.1	4.6	2.9	4.0	3.8	1.7
Overflow 3	20	16.8	95.8	96.7	96.5	96.3	1.0	39.69	39.59	38.92	39.4	0.8	97.8	98.2	98.4	98.2	0.6	38.31	42.81	39.33	40.1	4.7	93.1	95.2	94.1	94.1	2.1	4.8	3.0	4.2	4.0	1.8
Overflow 4	25	21.0	95.1	95.7	96.4	95.7	1.3	39.86	39.85	38.95	39.6	1.0	97.5	97.9	98.3	97.9	0.8	38.07	42.51	39.29	40.0	4.6	91.8	93.6	93.9	93.1	2.3	5.7	4.3	4.4	4.8	1.6
Overflow 5	30	25.3	94.2	94.5	96.0	94.9	2.0	40.10	40.16	39.05	39.8	1.3	97.2	97.4	98.2	97.6	1.1	37.77	42.15	39.16	39.7	4.5	90.2	91.6	93.3	91.7	3.1	7.0	5.8	4.9	5.9	2.1
Overflow 6	37.35	31.5	92.7	93.1	95.5	93.8	3.0	40.44	40.48	39.16	40.0	1.5	96.5	96.7	97.9	97.1	1.5	37.31	41.79	39.01	39.4	4.5	87.8	89.5	92.4	89.9	4.7	8.8	7.2	5.5	7.2	3.2
Overflow 7	60	50.5	90.7	91.6	93.8	92.0	3.2	40.86	40.85	39.54	40.4	1.5	95.4	96.0	97.1	96.2	1.8	36.75	41.38	38.51	38.9	4.7	84.6	87.2	89.6	87.1	5.0	10.8	8.8	7.5	9.1	3.3
Overflow 8	80	67.3	84.3	86.2	87.5	86.0	3.2	42.05	42.18	40.63	41.6	1.7	91.2	93.3	93.1	92.5	2.3	35.17	39.90	37.06	37.4	4.8	75.2	79.1	80.4	78.2	5.4	16.0	14.2	12.7	14.3	3.4
Overflow 9	120	100.9	84.3	83.1	84.9	84.0	2.5	42.05	42.65	40.91	41.8	2.5	91.2	90.9	90.9	90.9	0.0	35.17	39.46	36.68	38.1	3.9	75.2	75.4	77.2	76.3	2.6	16.0	15.5	13.7	14.6	2.5
Overflow 10	144	121.1	84.3	81.3	80.4	80.8	1.3	42.05	42.85	41.61	42.2	1.8	91.2	89.4	87.6	88.5	2.6	35.17	39.30	35.75	37.5	5.0	75.2	73.5	71.3	72.4	3.1	16.0	15.9	16.3	16.1	0.6
Overflow 11	174	146.4	84.3	81.3	74.5	74.5		42.05	42.85	42.68	42.7	1.8	91.2	89.4	83.3	83.3	2.6	35.17	39.30	34.32	34.3		75.2	73.5	63.4	63.4		16.0	15.9	19.9	19.9	0.6
Underflow (Remainder in column)		150.0	84.3	81.3	71.3	71.3		42.05	42.85	43.15	43.2	1.8	91.2	89.4	80.5	80.5	2.6	35.17	39.30	33.70	33.7		75.2	73.5	59.6	59.6		16.0	15.9	21.0	21.0	0.6

Table D.9: PTA raw data – Density Distribution of the RC Underflow with and without selective flocculation

Average density (g/ml)	Mass % for Base Case RC	Mass % for SF coupled with the RC
2.50	0.0	0.0
2.70	24.3	26.4
2.90	1.8	1.9
3.10	1.2	1.2
3.30	1.0	1.0
3.50	1.0	1.1
3.70	1.7	1.6
3.90	8.3	9.0
4.10	0.8	0.8
4.30	0.8	0.7
4.55	1.7	1.6
4.80	1.6	1.4
5.00	2.5	2.1
5.25	53.3	51.2
Total	**100.0**	**100.0**

Table D.10: PTA raw data – Mineral Abundance of the RC Underflow with and without selective flocculation

Mineral name	S.G.	Mass % for Base Case RC	Mass % for SF coupled with the RC
Hematite	5.30	61.1	58.3
Quartz	2.63	28.3	30.5
Goethite	3.80	10.1	10.9
Apatite	3.19	0.2	0.2
Clay	2.60	0.1	0.1
Ilmenite	4.72	0.0	0.0
Dolomite	2.85	0.0	0.0
Rutile	4.25	0.0	0.0
Mn-Oxides	4.55	0.0	0.0
Other	3.91	0.1	0.0
Total		**100.0**	**100.0**

Table D.11: PTA Size-By-Assay for the RC Underflow without selective flocculation

Size Fraction (µm)	Passing Size (µm)	Discrete Mass (%)	Cum Mass (%) Passing	Discrete Grade (%)									Cumulative Grade Passing (%)								
				Fe	Si	Al	P	H	Ba	C	Ca	Cl	Fe	Si	Al	P	H	Ba	C	Ca	Cl
-2000+1000	2000	0.0	100.0	0.00	0.00	0.00	0.00	0.00	0.00	0.00	0.00	0.00	48.79	13.45	0.09	0.05	0.12	0.01	0.00	0.11	0.01
-1000+850	1000	0.0	100.0	0.00	0.00	0.00	0.00	0.00	0.00	0.00	0.00	0.00	48.79	13.45	0.09	0.05	0.12	0.01	0.00	0.11	0.01
-850+600	850	0.0	100.0	0.00	0.00	0.00	0.00	0.00	0.00	0.00	0.00	0.00	48.79	13.45	0.09	0.05	0.12	0.01	0.00	0.11	0.01
-600+300	600	0.0	100.0	0.00	0.00	0.00	0.00	0.00	0.00	0.00	0.00	0.00	48.79	13.45	0.09	0.05	0.12	0.01	0.00	0.11	0.01
-300+150	300	0.1	100.0	22.27	17.96	1.26	4.83	0.12	0.00	0.00	10.43	0.61	48.79	13.45	0.09	0.05	0.12	0.01	0.00	0.11	0.01
-150+106	150	0.3	99.9	49.21	13.24	0.07	0.03	0.12	0.00	0.00	0.08	0.00	48.80	13.45	0.09	0.05	0.12	0.01	0.00	0.11	0.00
-106+75	106	2.4	99.6	49.21	13.11	0.08	0.03	0.14	0.02	0.01	0.08	0.00	48.80	13.45	0.09	0.05	0.12	0.01	0.00	0.11	0.00
-75+53	75	9.1	97.2	49.06	13.18	0.09	0.05	0.14	0.02	0.00	0.09	0.00	48.79	13.46	0.09	0.05	0.12	0.01	0.00	0.11	0.00
-53+38	53	12.7	88.2	50.21	12.57	0.08	0.03	0.12	0.01	0.00	0.07	0.00	48.76	13.49	0.09	0.05	0.11	0.01	0.00	0.11	0.00
-38+30	38	10.5	75.4	49.34	13.10	0.09	0.04	0.12	0.02	0.00	0.09	0.00	48.52	13.64	0.09	0.05	0.11	0.01	0.00	0.11	0.01
-30+25	30	9.7	65.0	48.71	13.61	0.08	0.06	0.09	0.01	0.00	0.14	0.01	48.39	13.73	0.09	0.05	0.11	0.01	0.00	0.12	0.01
-25+20	25	11.6	55.2	45.22	15.99	0.08	0.05	0.08	0.02	0.00	0.10	0.00	48.33	13.75	0.10	0.05	0.12	0.01	0.01	0.11	0.01
-20+15	20	14.8	43.7	44.42	16.56	0.08	0.05	0.08	0.01	0.00	0.11	0.01	49.15	13.16	0.10	0.05	0.12	0.01	0.01	0.12	0.01
-15+10	15	15.9	28.8	49.26	13.21	0.09	0.05	0.10	0.01	0.00	0.12	0.01	51.59	11.40	0.11	0.05	0.15	0.01	0.01	0.12	0.01
-10+5	10	10.8	12.9	54.79	9.16	0.12	0.04	0.17	0.01	0.01	0.11	0.00	54.48	9.18	0.15	0.04	0.20	0.01	0.01	0.12	0.00
-5+1	5	2.1	2.1	52.84	9.25	0.29	0.05	0.37	0.04	0.04	0.17	0.01	52.84	9.25	0.29	0.05	0.37	0.04	0.04	0.17	0.01
	Total	**100.0**		**48.79**	**13.45**	**0.09**	**0.05**	**0.12**	**0.01**	**0.00**	**0.11**	**0.01**									

Table D.11: PTA Size-By-Assay for the RC Underflow without selective flocculation (Contd.)

Size Fraction (µm)	Passing Size (µm)	Discrete Mass (%)	Cum Mass (%) Passing	Discrete Deportment (%)									Cumulative Deportment (%)								
				Fe	Si	Al	P	H	Ba	C	Ca	Cl	Fe	Si	Al	P	H	Ba	C	Ca	Cl
-2000+1000	2000	0.0	100.0	0.0	0.0	0.0	0.0	0.0	0.0	0.0	0.0	0.0	100.0	100.0	100.0	100.0	100.0	100.0	100.0	100.0	100.0
-1000+850	1000	0.0	100.0	0.0	0.0	0.0	0.0	0.0	0.0	0.0	0.0	0.0	100.0	100.0	100.0	100.0	100.0	100.0	100.0	100.0	100.0
-850+600	850	0.0	100.0	0.0	0.0	0.0	0.0	0.0	0.0	0.0	0.0	0.0	100.0	100.0	100.0	100.0	100.0	100.0	100.0	100.0	100.0
-600+300	600	0.0	100.0	0.0	0.0	0.0	0.0	0.0	0.0	0.0	0.0	0.0	100.0	100.0	100.0	100.0	100.0	100.0	100.0	100.0	100.0
-300+150	300	0.1	100.0	0.0	0.1	0.9	6.3	0.1	0.0	0.0	6.0	7.7	100.0	100.0	100.0	100.0	100.0	100.0	100.0	100.0	100.0
-150+106	150	0.3	99.9	0.3	0.3	0.3	0.2	0.3	0.0	0.0	0.2	0.2	100.0	99.9	99.1	93.7	99.9	100.0	100.0	94.0	92.3
-106+75	106	2.4	99.6	2.4	2.3	2.0	1.6	2.9	3.4	7.2	1.7	1.1	99.6	99.6	98.9	93.5	99.6	100.0	100.0	93.8	92.1
-75+53	75	9.1	97.2	9.1	8.9	8.5	8.5	11.1	11.5	2.9	7.5	7.6	97.2	97.3	96.9	92.0	96.7	96.6	92.8	92.2	91.0
-53+38	53	12.7	88.2	13.1	11.9	11.6	7.6	12.9	9.8	12.9	8.3	7.0	88.1	88.4	88.4	83.5	85.5	85.1	89.8	84.7	83.5
-38+30	38	10.5	75.4	10.6	10.2	10.5	9.2	10.5	14.8	1.4	8.0	8.0	75.0	76.5	76.7	75.9	72.6	75.4	76.9	76.4	76.5
-30+25	30	9.7	65.0	9.7	9.9	8.8	11.7	7.3	5.1	2.5	11.9	13.0	64.4	66.3	66.3	66.7	62.1	60.6	75.5	68.4	68.6
-25+20	25	11.6	55.2	10.7	13.8	9.9	12.8	8.1	20.1	6.9	10.7	10.9	54.7	56.4	57.4	55.0	54.8	55.6	73.0	56.4	55.5
-20+15	20	14.8	43.7	13.5	18.3	12.1	14.9	10.2	12.5	6.2	14.4	15.2	44.0	42.7	47.6	42.1	46.7	35.5	66.0	45.7	44.6
-15+10	15	15.9	28.8	16.0	15.6	14.7	16.0	13.9	11.7	16.3	17.2	17.5	30.5	24.4	35.5	27.3	36.5	23.0	59.8	31.3	29.4
-10+5	10	10.8	12.9	12.1	7.4	14.2	8.9	16.0	6.0	22.9	10.8	9.8	14.4	8.8	20.8	11.3	22.6	11.3	43.5	14.0	12.0
-5+1	5	2.1	2.1	2.3	1.4	6.6	2.3	6.6	5.3	20.6	3.2	2.2	2.3	1.4	6.6	2.3	6.6	5.3	20.6	3.2	2.2
	Total	**100.0**		**100.0**	**100.0**	**100.0**	**100.0**	**100.0**	**100.0**	**100.0**	**100.0**	**100.0**									

Table D.12: PTA Size-By-Assay for the RC Underflow with selective flocculation

Size Fraction (µm)	Passing Size (µm)	Discrete Mass (%)	Cum Mass (%) Passing	Discrete Grade (%)									Cumulative Grade Passing (%)								
				Fe	Si	Al	Ba	C	Ca	Cl	F	H	Fe	Si	Al	Ba	C	Ca	Cl	F	H
-2000+1000	2000	0.0	100.0	0.00	0.00	0.00	0.00	0.00	0.00	0.00	0.00	0.00	47.32	14.43	0.08	0.04	0.12	0.01	0.00	0.11	0.01
-1000+850	1000	0.0	100.0	0.00	0.00	0.00	0.00	0.00	0.00	0.00	0.00	0.00	47.32	14.43	0.08	0.04	0.12	0.01	0.00	0.11	0.01
-850+600	850	0.0	100.0	0.00	0.00	0.00	0.00	0.00	0.00	0.00	0.00	0.00	47.32	14.43	0.08	0.04	0.12	0.01	0.00	0.11	0.01
-600+300	600	0.0	100.0	0.00	0.00	0.00	0.00	0.00	0.00	0.00	0.00	0.00	47.32	14.43	0.08	0.04	0.12	0.01	0.00	0.11	0.01
-300+150	300	0.1	100.0	33.91	23.56	0.05	0.11	0.05	0.00	0.00	0.24	0.01	47.32	14.43	0.08	0.04	0.12	0.01	0.00	0.11	0.01
-150+106	150	0.2	99.9	34.02	23.83	0.06	0.00	0.04	0.00	0.00	0.02	0.00	47.33	14.42	0.08	0.04	0.12	0.01	0.00	0.11	0.01
-106+75	106	1.4	99.7	48.50	13.55	0.06	0.01	0.18	0.00	0.00	0.03	0.00	47.36	14.41	0.08	0.04	0.12	0.01	0.00	0.11	0.01
-75+53	75	6.5	98.4	50.85	12.08	0.08	0.03	0.14	0.01	0.00	0.07	0.00	47.34	14.42	0.08	0.04	0.12	0.01	0.00	0.11	0.01
-53+38	53	11.4	91.9	50.33	12.46	0.08	0.03	0.12	0.01	0.00	0.08	0.00	47.10	14.58	0.08	0.05	0.12	0.01	0.00	0.11	0.01
-38+30	38	9.9	80.5	50.33	12.48	0.09	0.04	0.11	0.01	0.00	0.10	0.00	46.64	14.88	0.08	0.05	0.12	0.01	0.00	0.11	0.01
-30+25	30	8.3	70.6	48.49	13.66	0.09	0.05	0.12	0.02	0.00	0.12	0.01	46.12	15.22	0.08	0.05	0.12	0.01	0.00	0.12	0.01
-25+20	25	10.6	62.3	47.09	14.79	0.08	0.03	0.09	0.00	0.00	0.08	0.00	45.80	15.43	0.08	0.05	0.13	0.01	0.00	0.12	0.01
-20+15	20	13.9	51.7	41.90	18.28	0.07	0.03	0.08	0.00	0.00	0.08	0.00	45.54	15.56	0.08	0.05	0.13	0.01	0.00	0.12	0.01
-15+10	15	19.1	37.8	42.62	17.66	0.07	0.06	0.09	0.01	0.00	0.14	0.01	46.88	14.55	0.08	0.06	0.15	0.01	0.00	0.14	0.01
-10+5	10	15.7	18.7	50.89	11.74	0.08	0.06	0.19	0.01	0.00	0.13	0.01	51.25	11.37	0.09	0.06	0.21	0.01	0.00	0.13	0.01
-5+1	5	3.0	3.0	53.12	9.40	0.11	0.06	0.36	0.01	0.01	0.15	0.01	53.12	9.40	0.11	0.06	0.36	0.01	0.01	0.15	0.01
	Total	**100.0**		**47.32**	**14.43**	**0.08**	**0.04**	**0.12**	**0.01**	**0.00**	**0.11**	**0.01**									

Table D.12: PTA Size-By-Assay for the RC Underflow with selective flocculation (Contd.)

Size Fraction (µm)	Passing Size (µm)	Discrete Mass (%)	Cum Mass (%) Passing	Discrete Deportment (%)									Cumulative Deportment (%)								
				Fe	Si	Al	Ba	C	Ca	Cl	F	H	Fe	Si	Al	Ba	C	Ca	Cl	F	H
-2000+1000	2000	0.0	100.0	0.0	0.0	0.0	0.0	0.0	0.0	0.0	0.0	0.0	100.0	100.0	100.0	100.0	100.0	100.0	100.0	100.0	100.0
-1000+850	1000	0.0	100.0	0.0	0.0	0.0	0.0	0.0	0.0	0.0	0.0	0.0	100.0	100.0	100.0	100.0	100.0	100.0	100.0	100.0	100.0
-850+600	850	0.0	100.0	0.0	0.0	0.0	0.0	0.0	0.0	0.0	0.0	0.0	100.0	100.0	100.0	100.0	100.0	100.0	100.0	100.0	100.0
-600+300	600	0.0	100.0	0.0	0.0	0.0	0.0	0.0	0.0	0.0	0.0	0.0	100.0	100.0	100.0	100.0	100.0	100.0	100.0	100.0	100.0
-300+150	300	0.1	100.0	0.1	0.1	0.0	0.2	0.0	0.0	0.0	0.2	0.2	100.0	100.0	100.0	100.0	100.0	100.0	100.0	100.0	100.0
-150+106	150	0.2	99.9	0.1	0.3	0.1	0.0	0.1	0.0	0.0	0.0	0.0	99.9	99.9	100.0	99.8	100.0	100.0	100.0	99.8	99.8
-106+75	106	1.4	99.7	1.4	1.3	1.1	0.2	1.9	0.1	0.1	0.4	0.2	99.8	99.6	99.8	99.8	99.9	100.0	100.0	99.8	99.8
-75+53	75	6.5	98.4	6.9	5.4	6.6	3.8	7.1	6.5	8.2	4.1	3.4	98.4	98.3	98.7	99.6	98.0	99.9	99.9	99.4	99.6
-53+38	53	11.4	91.9	12.1	9.8	11.8	8.2	11.2	18.9	10.1	8.2	7.3	91.5	92.9	92.1	95.8	90.8	93.4	91.8	95.4	96.2
-38+30	38	9.9	80.5	10.6	8.6	11.0	10.1	9.0	14.0	8.6	9.6	9.4	79.4	83.0	80.3	87.6	79.6	74.5	81.7	87.2	89.0
-30+25	30	8.3	70.6	8.5	7.8	9.5	9.3	7.7	15.8	1.1	9.6	10.0	68.8	74.4	69.3	77.5	70.6	60.5	73.1	77.6	79.6
-25+20	25	10.6	62.3	10.5	10.8	10.2	6.0	7.4	2.0	20.8	7.6	6.4	60.3	66.6	59.8	68.1	63.0	44.7	72.0	68.0	69.6
-20+15	20	13.9	51.7	12.3	17.6	11.9	10.0	8.9	0.7	0.4	11.1	11.0	49.8	55.8	49.6	62.1	55.6	42.7	51.2	60.5	63.2
-15+10	15	19.1	37.8	17.2	23.4	17.5	27.3	14.5	17.0	20.0	26.1	28.0	37.5	38.1	37.7	52.0	46.7	42.1	50.8	49.4	52.1
-10+5	10	15.7	18.7	16.9	12.8	16.3	20.5	23.5	20.2	15.0	19.1	19.9	20.2	14.7	20.2	24.8	32.1	25.1	30.7	23.3	24.2
-5+1	5	3.0	3.0	3.3	1.9	3.9	4.3	8.6	4.9	15.7	4.2	4.2	3.3	1.9	3.9	4.3	8.6	4.9	15.7	4.2	4.2
	Total	**100.0**		**100.0**	**100.0**	**100.0**	**100.0**	**100.0**	**100.0**	**100.0**	**100.0**	**100.0**									